

**Organized by:**  
Faculty of Industrial Technology, Institut Teknologi Nasional (Itenas) Bandung, West Java  
Indonesia.

# Conference Proceedings

## The 2nd Faculty of Industrial Technology International Congress 2020

### International Conference

*Towards Industry 4.0: Challenges and Opportunities  
for Industrial Technology and Other Sectors*

January 28 - 30, 2020  
Faculty Building, 3<sup>rd</sup> floor  
Campus of Itenas Bandung – Indonesia

**Supported by:**



**FACULTY OF INDUSTRIAL TECHNOLOGY INTERNATIONAL CONGRESS  
(FoITIC)**

## **CONFERENCE PROCEEDINGS**

**The 2<sup>nd</sup> FoITIC 2020**

**“Toward Industry 4.0: Challenges and Opportunities  
for Industrial Technology and Other Sector”**

**ISBN 978-623-7525-37-0**



**Campus of Institut Teknologi Nasional Bandung  
West Java – Indonesia  
January 28 – 30, 2020**

**FACULTY OF INDUSTRIAL TECHNOLOGY  
INSTITUT TEKNOLOGI NASIONAL  
BANDUNG**

## **Proceedings of FoITIC 2020 – International Conference**

### **Editorial Board:**

Prof. Dr. Istvan Farkas	Szent Istvan University – Hungary
Prof. Dr. Rizalman Mamat	Universiti Malaysia Pahang – Malaysia
Prof. RNDr. Zuzana Hlavacova, CSc.	Slovak University of Agriculture in Nitra – Slovak Republic
Dr. Martino Luis	The University of Exeter – United Kingdom
Dr. Dani Rusirawan	Institut Teknologi Nasional Bandung – Indonesia
Dr. Dyah Setyo Pertiwi	Institut Teknologi Nasional Bandung – Indonesia
Dr. Fahmi Arif	Institut Teknologi Nasional Bandung – Indonesia
Dr. Marisa Widyastuti P	Telkom University – Indonesia
Dr. Achmad Ghazali	Institut Teknologi Bandung – Indonesia
Dr. Winarno Sugeng	Institut Teknologi Nasional Bandung – Indonesia

### **Cover Design and Layout of Proceedings:**

Mr. Aldrian Agusta (Cover Design)  
Mr. Liman Hartawan  
Ms. Dina Budhi Utami  
Mr. Muktiadi Akhmad Januar

**Copyright @ 2021 by the FTI – Itenas and the authors**

### **Conference Organizer:**

Faculty of Industrial Technology, Institut Teknologi Nasional Bandung - Indonesia  
Jl. PKHH. Mustapa No. 23 Bandung 40124, West Java - INDONESIA  
Email: foitic@itenas.ac.id, Website: <http://foitic.itenas.ac.id>, [www.itenas.ac.id](http://www.itenas.ac.id)

**ISBN 978-623-7525-37-0**

All rights reserved. No part of the publication may be produced, transmitted, in any form or by means of electronic, mechanical, photocopying, recording or otherwise, without the permission of the publisher, except the case in critical articles and review or where prior rights are preserved.

### **Produced by:**

Faculty of Industrial Technology  
Institut Teknologi Nasional Bandung

5 4 3 2

## COMMITTEE

### Organizing Committee:

Chairman	: Dr. Dani Rusirawan	Itenas – Indonesia
Co-chairman	: Dr. Fahmi Arif	Itenas – Indonesia
Members	: Dr. Dyah Setyo Pertiwi	Itenas – Indonesia
	Mr. Liman Hartawan	Itenas – Indonesia
	Mr. Arsyad R. darlis	Itenas – Indonesia
	Ms. Dina Budhi Utami	Itenas – Indonesia

### Steering Committee:

Dr. Imam Aschuri	Itenas Bandung – Indonesia
Prof. Dr. Meilinda Nurbanasari	Itenas Bandung – Indonesia
Ms. Yuniar	Itenas Bandung – Indonesia
Dr. Dewi Kania Sari	Itenas Bandung – Indonesia
Prof. Dr. Soegijardjo Soegijoko	Itenas Bandung – Indonesia
	IEEE Indonesia SSIT Chapter
Dr. Kusmaningrum Soemadi	Itenas Bandung – Indonesia
Prof. Dr. Isa Setiasah Toha	ITB – Indonesia
Dr. Iwan Inrawan Wiratmadja	ITB – Indonesia
Dr. Ahmad Taufik Joenoes	Indonesian Society for Reliability

### Scientific Committee:

Dr. Hendi H. Rachmat	Electrical Engineering	Itenas – Indonesia
Dr. Waluyo	Electrical Engineering	Itenas – Indonesia
Dr. Niken Syafitri	Electrical Engineering	Itenas – Indonesia
Dr. T. Kristyadi	Mechanical Engineering	Itenas – Indonesia
Dr. Agus Hermanto	Mechanical Engineering	Itenas – Indonesia
Dr. Ing. M. Alexin Putra	Mechanical Engineering	Itenas – Indonesia
Dr. Arif Imran	Industrial Engineering	Itenas – Indonesia
Dr. Caecilia S. Wahyuning	Industrial Engineering	Itenas – Indonesia
Dr. Yudha Prambudia	Industrial Engineering	Telkom University – Indonesia
Dr. Winnie Septiani	Industrial Engineering	Trisakti University – Indonesia
Dr. Jono Suhartono	Chemical Engineering	Itenas – Indonesia
Dr. Maya Ramadianti M.	Chemical Engineering	Itenas – Indonesia
Dr. rer. Nat. Riny Y. Parapat	Chemical Engineering	Itenas – Indonesia
Dr. Uung Ungkawa	Informatics Engineering	Itenas – Indonesia
Dr. Sc. Lisa Kristiana	Informatics Engineering	Itenas – Indonesia



**International Scientific Committee:**

Prof. Dr. Istvan Szabo	Szent Istvan University – Hungary
Prof. DSc. Józef Horabik	Polish of Academy of Sciences – Poland
Prof. Ing. CSc. Martin Libra	Czech University of Life Sciences Prague – Czech Republic
Prof. RNDr. Ing. Jiri Blahovec, DrSc.	Czech University of Life Sciences Prague – Czech Republic
Prof. Dr. Henrik Lund	Aalborg University – Denmark
Prof. Dr.-Ing. Klaus Günter Gottschalk	Leibniz Institute for Agricultural Engineering and Bioeconomy- Germany
Prof. R. Schomaecker	Technical University Berlin – Germany
Prof. M. Schwarze	Technical University Berlin – Germany
Dr. Istvan Seres	Szent Istvan University – Hungary
Doc. Ing. Jan Banout, Ph.D.	Czech University of Life Sciences Prague – Czech Republic
Doc. RNDr. Vlasta Vozárová, PhD.	Slovak University of Agriculture in Nitra – Slovak Republic
Dr. Agus Saptoro	Curtin University – Malaysia
Dr. Chandra Ade Irawan	University of Nottingham Ningbo – China
Ts. Gs. Dr. Othman Mohd	Universiti Teknikal Malaysia Melaka – Malaysia
PM. Ts. Dr. Mohd Faizal Abdollah	Universiti Teknikal Malaysia Melaka – Malaysia
Ts. Dr. Mohd Zaki Mas'ud	Universiti Teknikal Malaysia Melaka – Malaysia
Ts. Dr. Yahaya Abd Rahim	Universiti Teknikal Malaysia Melaka – Malaysia

## **PREFACE**

### **WELCOME FROM THE RECTOR**

#### **INSTITUT TEKNOLOGI NASIONAL BANDUNG**

Dear speakers and participants,

Welcome to Bandung and welcome to Itenas campus!

It is great pleasure for me to welcome you in campus of Itenas Bandung at the 2<sup>nd</sup> Faculty of Industrial Technology International Congress (FoITIC) 2020.

The theme for the 2<sup>nd</sup> FoITIC (FoITIC 2020) “Towards Industry 4.0: Challenges and Opportunities for Industrial Technology and Other Sectors”, is very relevant and we are sure that presently the term of “industry 4.0” is one hot issues in over the world.

We believe that scientists and researchers will hand in hand with industrial experts, to create and develop new concept/system related to technologies that enable human to make products and services more efficient in various sector.

I am deeply grateful appreciative to the Faculty of Industrial Technology Itenas, Szent Istvan University Hungary, Universiti Malaysia Pahang Malaysia, Universiti Teknikal Malaysia Melaka, Indonesian Society Reliability, delegates, organizing committee and many others who have contributed to the success of this conference.

I am confident that this event will serve to promote much valuable communication and information exchange among scientist – researcher and industrial expert.

May we have a successful, stimulating, fruitful and rewarding the conference.

Again, thank you for visiting our campus, and let’s hand in hand together to overcome the challenges today, and ready to meet the next challenges.

**Dr. Iman Aschuri**

Rector

Institut Teknologi Nasional Bandung

## **PREFACE**

### **WELCOME FROM THE DEAN OF FACULTY OF INDUSTRIAL TECHNOLOGY, INSTITUT TEKNOLOGI NASIONAL BANDUNG**

Dear distinguished Guest, Ladies and Gentlemen,

Welcome to the 2<sup>nd</sup> Faculty of Industrial Technology International Congress (FoITIC) 2020, which is organized by Faculty of Industrial Technology, Institut Teknologi Nasional (Itenas), Bandung – Indonesia, with supported by Szent Istvan University (SZIU) – Hungary, Universiti Malaysia Pahang (UMP) – Malaysia, Universiti Teknikal Malaysia Melaka (UTeM) – Malaysia and Indonesian Society for Reliability (ISR).

The main theme for the 2<sup>nd</sup> congress is ‘Towards Industry 4.0: Challenges and Opportunities for Industrial Technology and Other Sectors’.

The aim of the Congress is inviting academics, researchers, engineers, government officers, company delegates and students from the field of industrial technology and other disciplines (such as electrical, mechanical, industrial, chemical, informatics, civil, architect, physics, environment, social, economic, design and etc.), to gather, present and share the results of their research and/or work and discuss the future and impact of industry 4.0.

Taking this opportunity, I would like to convey my sincere thanks and appreciations to our keynote speakers and invited speakers from Szent Istvan University Hungary, Universiti Malaysia Pahang, ProcodeCG, Indonesian Society for Reliability, and Industrial Engineering Department Itenas, and national and international scientific committee for their support of this important event. I would also like to invite all participants in expressing our appreciation to all members of the FoITIC 2020 organizing committee for their hard work in making this conference success.

Finally, we wish you all fruitful networking during conference, and we do hope that you will reap the most benefit of it.

Do enjoy your stay in Itenas Bandung campus, and thank you very much!

**Dr. Dani Rusirawan**

Dean Faculty of Industrial Technology – Institut Teknologi Nasional Bandung  
Chairman of FoITIC 2020

## **ACKNOWLEDGEMENT**

The completion of this undertaking could not have been possible without the participation and assistance of so many people whose names may not all be enumerated. The contributions are sincerely appreciated and gratefully acknowledged. However, we would like to express our especial deep appreciation and gratitude to the following:

1. Institut Teknologi Nasional Bandung (Itenas) – Indonesia
2. Szent Istvan University (SZIU) – Hungary
3. Universiti Malaysia Pahang (UMP) – Malaysia
4. Universiti Teknikal Malaysia Melaka (UTeM) – Malaysia
5. Indonesian Society for Reliability (ISR) – Indonesia
6. ProCodeCG – Indonesia

## **KEYNOTE AND INVITED SPEAKERS INTERNATIONAL CONFERENCE**

### **Prof. Dr. Istvan Farkas (Szent Istvan University)**

Prof. Dr. Istvan Farkas is Director of Institute for Environmental Engineering System, Szent Istvan University (SZIU), Godollo – Hungary. He is also Head of Department Physics and Process Control and head of Engineering Doctoral School, at SZIU. He got Doctoral Degree from Technical University Budapest (1985). Presently, a lot of his activities devotes on International professional societies such as: International Solar Energy Societies (ISES), International Federation of Automatic Control (IFAC), European Federation of Chemical Engineering (EFChE), European Thematic Network on Education and Research in Biosystems Engineering, European Network on Photovoltaic Technologies, FAO Regional Working Group on Greenhouse Crops in the SEE Countries, Solar Energy Journal Associate Editor, Drying Technology Journal Editorial Board, etc. He was a visiting Professor in several universities: Solar Energy Applications Laboratory, Colorado University State University, Fort Collins - USA; Department of Energy, Helsinki University of Technology, Espoo - Finland; Institut for Meteorology and Physics, University of Agricultures Sciencies, Vienna - Austria; Laboratory of Bioprocess Engineering, The University of Tokyo - Japan.

### **Prof. Dr. Rizalman Mamat (Universiti Malaysia Pahang - Malaysia)**

Prof. Dr. Rizalman Mamat presently is a Professor of Faculty of Mechanical and Automotive Engineering Technology, Universiti Malaysia Pahang, Malaysia. Previously he was Dean of Faculty of Mechanical and Automotive Engineering Technology. He got Doctoral degree from University of Birmingham, United Kingdom in fuel and energy. Previously, he obtained his BSc and MSc from University Teknologi Malaysia (UTM). His field research interest is Heat transfer, Combustion, Internal Combustion Engine, Alternative Energy, Computational Fluid Dynamics, Propulsion System. Prof. Dr. Rizalman Mamat was visiting Professor at Karlsruhe University of Applied Science Germany (2017), Faculty of Engineering Universitas Abulyatama Aceh, Indonesia (2017), Faculty of Engineering Universitas Gajah Putih Aceh, Indonesia (2017), Department of Mechanical Manufacture & Automation Ningxia University, Yinchuan, China (2016), Department of Mechanical Manufacture & Automation Ningxia University, Yinchuan, China (2015).

### **Ahmad Taufik, M.Eng., Ph.D (Indonesian Society for Reliability)**

Ahmad Taufik, M.Eng, Ph.D (Graduated from Georgia Institute of Technology, USA – 1996) is a lecturer and a professional trainer and consultant. He is member of American Society for Metals (ASM) and American Society for Mechanical Engineer (ASME). He performs research in fatigue and fracture mechanics of oil and gas pipeline. Dr. Ahmad Taufik highly experienced in providing industrial training and consulting work more than 20 projects related to Pipelines Failure Analysis, Risk and

Reliability Assessment, Repair Design, Pipeline Corrosion Protection in Oil and Gas Industries. Dr. Ahmad Taufik has been chairman and speakers for many Oil and Gas International Conferences in Indonesia, (INDOPIPE, MAPREC), Malaysia (ASCOPE), Singapore and China (IPTEC) for the last five years. He is founder of Indonesian Society Reliability (ISR) and presently he is a chairman of the ISR. Since 2006, he was work as part time lecturer at Dept. of Mechanical Engineering, Itenas.

**Dr. Marisa Paryasto, ST., MT. (ProCodeCG)**

Dr. Marisa Paryasto is a profesional part-time at Electrical Engineering Department – Computer Engineering – Telkom University. She earned the bachelor degree in Electrical Engineering from ITENAS Bandung and the master and doctoral degree in Electrical Engineering from STEI – Institut Teknologi Bandung. She is a member of IEEE and actively reviewing papers for international/national journal and conferences. She is currently an active researcher at Institut Teknologi Bandung and also running several businesses. She is the founder of ProCodeCG, a start up focusing education and research on programming and Information technology, mostly for teaching kids to be able to deal with future's challenges and technology. She is very experienced in teaching and computer engineering. She is familiar and expert in programming, cryptography, security, Internet of Things, artificial intelligence, machine learning, BlockChain technology and recent technology implementations.

**Dr. Fahmi Arif, ST., MT. (Institut Teknologi Nasional Bandung)**

Dr. Fahmi Arif has received his Bachelor of Engineering in Mechanical Engineering (ITENAS Bandung, Indonesia), Master of Engineering in Industrial Engineering (ITB Bandung, Indonesia), and PhD in Industrial Computing (UTeM Melaka, Malaysia). Along with his formal education, he also earned several professional certifications. He is a Certified Data Science Professional (certification by IBM). After several years working overseas in the field of education and consultancy as well, currently, he is working in his hometown as a Head of Graduate Program in the Department of Industrial Engineering at Institut Teknologi Nasional Bandung. Along with his career, he has published various articles in some international conferences and journals. He also serves as a reviewer in some local and international journals such as the Journal of Information and Organizational Science and the editorial board for the Journal of Intelligent System. His research interest is in data science, artificial intelligence, and machine learning especially for its application in industrial automation. Currently, he is working in some research projects in the field of Industrial Information Integration and Cyber-Physical System in Industry 4.0 environment.

## LIST OF CONTENTS

<b>Committee</b>	<b>iii</b>
<b>Preface: The Rector of Itenas Bandung</b>	<b>v</b>
<b>Preface: The Dean of Faculty of Industrial Technology / Chairman of FoITIC 2020</b>	<b>vi</b>
<b>Acknowledgement</b>	<b>vii</b>
<b>Keynote and invited speaker International Conference</b>	<b>viii</b>
 <b>A. Engineering (Energy, Mechanical &amp; Chemical)</b>	 <b>1</b>
A1. Recent Achievements in Solar thermal and Photovoltaic Energy Applications ( <i>István Farkas</i> )	2
A2. Energy Management Strategy for Nickel Metal Hydride (NiMH) Battery and Proton Exchange Membrane Fuel Cell (PEMFC) on 3-wheel Hybrid Electric Car Equipped with Continuously Variable Transmission (CVT) ( <i>D. R. Harahap, Wei-Chin Chang, S. Ariyono</i> )	9
A3. Effect of Nanofluid Concentration on the Performance of PV/T Collector Under the Tropical Climate Conditions of Indonesia ( <i>Amrizal, Muhammad Irsyad, Amrul, Agung Nugroho, Miftahul Aziz</i> )	17
A4. Potential of Glycerol and Derivatives Based on Palm Oil as a Green Solvent ( <i>Syifa Tiara Saskia Mulya, Maria Agustina Rani Findriyani, Nugroho Adi Sasongko</i> )	22
A5. Feasibility Study of Thermoelectric Generator Configuration in Electricity Generation ( <i>W. Priharti, M. Ramdhani, F.R.J. Putra, A. Khansalya</i> )	28
A6. Pressure Reducing Station Design for Small Scale Business from 200 bar to 2 bar Pressure ( <i>Pratomo Setyadi</i> )	33
A7. Enhancing the Nickel Recovery of Morowali Nickel Laterite in Atmospheric Citric Acid Leaching ( <i>Feby Aryanhi, Regna Tri Jayanti</i> )	38
A8. Particle Size Analysis of Morowali Nickel Laterite on Atmospheric Citric Acid Leaching ( <i>Wirawan, Regna Tri Jayanti</i> )	43
A9. Effect of Agitation Speed and Leaching Time for Nickel Recovery of Morowali Limonite Ore in Atmospheric Citric Acid Leaching ( <i>Regna Tri Jayanti, Yusdianto</i> )	48
A10. Specimen Test Making of Polypropylene High Impact (PPHI) Polymer Composite Reinforced with Natural Fibres using Hand Lay-Up Methods ( <i>Nuha D. Anggraeni, Alfian E. Latief, Ramadhan L. Tawadha, and Rifki R. R.</i> )	53
A11. Evaporator Design with Ammonia-Water Mixture as Working Fluid for Kalina KCS34 Cycle On Electric Power Plant ( <i>Muhammad Pramuda N. S, Muhammad Ridwan, Agung Priambudi</i> )	59
A12. Pilot Plant Biodiesel from Waste Cooking ( <i>Rif'ah Amalia, Hendrik E.G.P, Achmad B. Ulum, and Eka S.N</i> )	66
A13. Ratio Optimization of Wind-Solar Hybrid System ( <i>Muhammad Haekal, Dani Rusirawan, Istvan Farkas</i> )	72

<b>B. Engineering (Electrical, Electronics, &amp; Mechatronics)</b>	<b>77</b>
B1. Measurement of Wastewater Turbidity Based on Total Dissolved Solids at Pancasila University ( <i>Muhammad Yaser , Untung Priyanto, Fauzie Busalim</i> )	78
B2. Design of Microstrip Array Antenna with Beamforming Capability for 5G Communication ( <i>Adam Tsany Magrifaghibran, Dharu Arseno, and Rizky Satria</i> )	83
B3. Automatic Location using ADS-B Mode for Ground Vehicle ( <i>Marisa Premitasari, Uung Ungkawa, Adjie Putra Perdana</i> )	89
B4. Determination of Ignition Voltage in Tank Vehicles Carrying Gasoline and LPG in Electric Field Zone ( <i>Iyus Rusmana</i> )	96
B5. Wearable Microstip Antenna with Defected Ground Structure for Breast Cancer Detection ( <i>Putri Angelia, Levy Olivia Nur, Bambang Setia Nugroho</i> )	103
B6. Design of Ultra-Wide-Band Bowtie Antenna for GPR Applications ( <i>Raeida Widyandana, Levy Olivia Nur, Heroe Wijanto</i> )	108
B7. Design of Vivaldi Antenna at 0.9 – 6 GHz for Mobile Cognitive Radio Base Station (MCRBS) ( <i>Ferialia Fitri, Heroe Wijanto, Aloysius Adya Pramudita, Yuda Nugraha</i> )	114
B8. Design of Numbering Machine Control System based on Omron CJ2M PLC with Omron NB10 Touchscreen HMI for Improving Manufacturing in Motorcycle Assembling Industry XYZ ( <i>Endang Djuana, Gunawan Tjahjadi, Qori Rohman Putra</i> )	120
B9. Haar Cascade Classifier Method for Real Time Face Detector in 2 Degree of Freedom (DOF) Robot Head ( <i>Dwi Agung Al Ayubi, Dwi Arman Prasetya, Irfan Mujahidin</i> )	130
B10. Photovoltaic's Characteristics Modelling Based on Fuzzy Time Series ( <i>Fortinov Akbar Irdam, Dani Rusirawan</i> )	136
B11. Effect of Cooling Systems on Photovoltaic Efficiency ( <i>Andika Prasetiadi, Dani Rusirawan, Lita Lidyawati</i> )	143
<b>C. Information Technology &amp; Engineering (Chemical)</b>	<b>149</b>
C1. Success Implementation of E-Voting Technology in Various Countries: A Review ( <i>Slamet Risnanto, Ts Dr Yahaya Abd.Rahim, Prof Gs Dr Nanna Suryana</i> )	150
C2. Model of Ubiquitous Precision Livestock System 4.0: A Technological Review ( <i>Irawan Afrianto, Sri Wahjuni, Taufik Djatna</i> )	156
C3. Vulnerability Assessment for Basic Data of Education Website in Regional Government X – A Black Box Testing Approach ( <i>Atho' Novian Awlarijal, Ahmad Almaarif, Avon Budiono</i> )	163
C4. Analysis of Potential Security Issues in Regional Government X Website Using Scanning Method in Kali Linux ( <i>Jelita Putri Deviarinda, Avon Budiyo, Ahmad Almaarif</i> )	169
C5. Design of Auto Height Check Machine Control System Based on PLC to Improve Quality the Complete Piston Rod Assembly Process ( <i>Syahril Ardi, Chandra Kirana Kaomu</i> )	175



C6.	The Usage of Quick Response Code and Captive Portal for Wi-Fi Security and Bandwidth ( <i>Muhammad Adam Nugraha, Nyoman Bogi Aditya Karna, Ridha Muldina Negara</i> )	180
C7.	Design of IoT-Based Manufacturing Quality Control System with Exponentially Weighted Moving Average Chart ( <i>Bintang Wibawa Mukti, Cahyadi Nugraha, Fadillah Ramadhan</i> )	186
C8.	Implementation of The Internet of Things for $\bar{X}$ and R Control Chart in Quality Control ( <i>Aldi Nahla Firdaus, Cahyadi Nugraha, Fadillah Ramadhan</i> )	193
C9.	Design of Monitoring and Control of SCADA Systems on Curing Machine using PLC and HMI Wonderware InTouch ( <i>Syahril Ardi, Nanda Indah Angger Lestari</i> )	200
C10.	Overview of Graphene-Like-Graphite (GLG) Synthesis Technology from Green Petroleum Coke (GCP) as a High-Capacity Anode Material for Lithium-Ion Batteries ( <i>Nugroho Adi Sasongko, Ulya Qonita, Riza Murniati, Cepi Kurniawan</i> )	207
<b>D.</b>	<b>Information System, Business Management &amp; Industrial Engineering, Education Technology</b>	<b>213</b>
D1.	The Role of Technology and Social Transformation Challenge in Industrial Revolution 1.0 – 4.0. ( <i>Fred Soritua Rudiyanto, Agus Sachari, Setiawan Sabana, Yannes Martinus Pasaribu</i> )	214
D2.	Design of Information System for the Protection of Indonesian Migrant Workers ( <i>Leonardi Paris Hasugian, Deden Abdul Wahab, Yeffry Handoko Putra, Rangga Sidik, and Yusrila Yeka Kerloza</i> )	228
D3.	Clustering Emotional Features Using Machine Learning in Public Opinion during the 2019 Presidential Candidate Debates in Indonesia ( <i>Agus Sasmito Aribowo, Yuli Fauziah and Siti Khomsah</i> )	234
D4.	An Innovation Capability Model to Increase Micro, Small and Medium Enterprise (MSME) Competitiveness in Indonesia: A Conceptual Model ( <i>Roosdiana Noor Rochmah</i> )	240
D5.	Determination of The Shortest Route of Electrical Scooters Maintenance Patrol in Bandung Using Nearest Neighbor and Genetic Algorithm Approaches ( <i>Sely P. Oktaviani, Rispianda</i> )	246
D6.	Economic Simulation of Indonesia's Clean Energy Policy: Shifting from LPG to Induction Stove ( <i>Dzikri Firmansyah Hakam, Meiri Triani, I Putu Wirasangka, Siti Aisyah</i> )	252
D7.	Study of Company Revenue Based on Production Planning Configuration Using Goal Programming Method ( <i>Fajar Azhari Julian, Rispianda</i> )	257
D8.	Detection of Decreased Kidney and Lung Function Through the Iris of the Eye Using the Method Convolutional Neural Network (CNN) ( <i>Juwairiah, Herry Sofyan, Vincentius Dian Asa Putra, Herlina Jayadianti</i> )	263
D9.	Decision Support System Using TOPSIS method for Smartphone Selection ( <i>Mira Musrini Barmawi, Sofia Umaroh</i> )	270
D10.	Safety Integrity Level (SIL) Study for HIPPS ( <i>Dzulfikar Ali Hafizh, Dani Rusirawan, Ahmad Taufik, Deddy Nugraha</i> )	277

## ***A. Engineering (Energy, Mechanical & Chemical)***

## Recent achievements in solar thermal and photovoltaic energy applications

István Farkas

Department of Physics and Process Control, Szent István University, Gödöllő - HUNGARY

E-mail: Farkas.Istvan@gek.szie.hu

### Abstract

This paper deals with the overview of the recent worldwide achievements and applications concerning to the solar thermal and photovoltaic (PV) technologies. Both, the technical and environmental issues are to be presented and discussed.

The worldwide situation is mainly analysed based on the recent development shown intensively at the Solar World Congresses organized by the International Solar Energy Society, and also by the ISES-Europe Unit. Moreover, the most recently published books in this topic served also a basic source to the overview statements.

The main area of solar thermal energy use covers the solar domestic hot water systems, the combined systems, the large-scale systems, the swimming pool collectors, the solar district heating systems, the process heat and the solar thermal assisted cooling systems.

The most important standpoints of the PV manufacturing and applications are as: increasing trend in energy mix, decreasing cell and module prices, cell efficiency does not increase so fast, competition between different technologies, multi-Gigawatts applications, widening feed-in tariff system. Due to the growing market demand of solar photovoltaic applications, several new issues came to the light, transparency and extra size of modules, application of new technologies.

Examples are shown for both solar thermal and photovoltaic application possibilities.

*Keywords: New solar technologies, environmental issues, thermal energy, third generation PV, passive solar*

---

## 1. Introduction

Generally saying, within the use of solar energy the solar thermal field identified at a lower innovation potential however their application shows large varieties. Especially the production of electricity from solar thermal is a preferred solution.

In spite of the recent economic situation all over the world, a significant yearly increase of photovoltaic module production and their installation were performed in last couple of year period. However, it can be observed sensitivity of the market change on the photovoltaic industry, the PV technologies still show increasingly high priority.

The worldwide situation can be analysed based on the recent development discussed intensively at the Solar World Congress events. The last one was organized by the International Solar Energy Society in Santiago, Chile during November 4-7, 2019. Within the congress beside the technical-scientific topics several forums are organized to talk on local, national and international problems of energy politics which are responsible for the wider dissemination of such technologies.

The main thematic groups were as follows:

- Solar Heating and Cooling Technologies
- Solar Heating and Cooling Applications
- Solar and Renewable Electricity
- Energy Storage for Heat and Electricity
- Solar Energy Markets and Policies

- Energy Systems and Sector Coupling
- Off-Grid & Rural Energy Access
- Solar Architecture and Building Integration
- Education and Training
- Clean Water Technologies
- Special Themes:
  - Renewable energy cities
  - Renewable energy for mobility
  - Community power programs
  - Sustainable practices in the mining industry
  - History of solar energy

The most recent solar meeting, e.g. EuroSun 2020, the 13th International Conference on Solar Energy for Buildings and Industry will be organised by the International Solar Energy Society (ISES), the Cyprus University of Technology and the University of West Attica in Athens during September 1-4, 2020 in Athens, Greece.

EuroSun 2020 will focus on all aspects of solar energy (heat and electricity), and how solar energy combines with other technologies (i.e. storage) and will be connected with different sectors (i.e., transportation, industry, buildings) as well as communities.

The conference programme will include distinguished keynote speakers in plenary sessions, specialists' meetings in breakout sessions and poster exhibitions.

This conference will give a chance to the researchers, developers and industrial and governmental actors to continue moving the world towards 100% renewable energy program.

The main thematic topics at the EuroSun 2020 will be as follows:

- Solar Buildings
- Solar Assisted District Heating and Cooling
- Solar Heat for Industrial Processes
- Domestic Hot Water and Space Heating
- PV and PVT Systems for Buildings and Industry
- Solar Thermal Collectors and Solar Loop Components
- Thermal Storage
- Testing & Certification
- Solar Resource and Energy Meteorology
- Solar Education
- Renewable Energy Strategies, Policies, Scientists for Future
- Renewable Energy Solutions for Isolated Systems (i.e. Islands)
- Renewable Energy Systems and Spatial Energy Planning

Additionally, the abovementioned international conferences and their published Proceedings, the most recently issued yearbooks, and also the easily accessible web pages serve basic sources to the overview statements and the future vision, which are listed in the reference list. That materials were also used in the course to set of this paper.

## 2. Solar thermal

There are several attempts in order to improve the different solar thermal technologies. Focusing on the recent technical and market situation a great number of publications were presented to share all the available information in the field. In this study some of them are referred as Renewables 2019 – Global Status Report; Solar Heat Worldwide – 2019 and Farkas, 2017.

Focusing the solar heat energy worldwide several comments can be drawn. The most important ones are as follows:

In the share of the total installed capacity in operation (including the glazed and unglazed water and air collectors) China is taking leading position now with 75,3%, which is going on a longer period. China is followed by Europe with about 8,1% and USA/Canada with about 2% as shown in Fig. 1 (Weiss and Spörk-Dür, M., 2019).

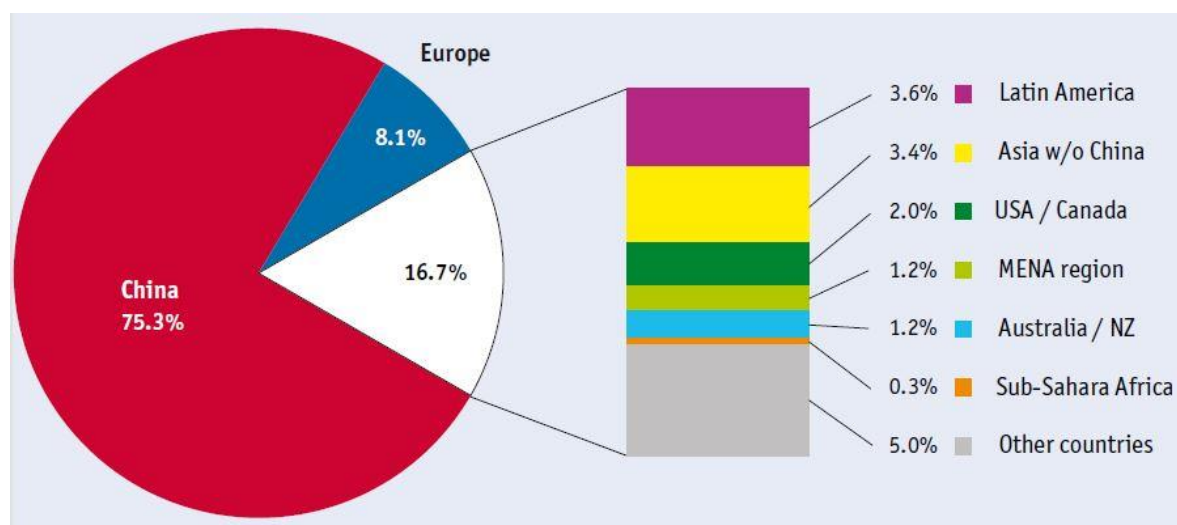


Fig. 1: Share of the solar thermal capacity by the end of 2017

The cumulated solar thermal capacity in operation by end of 2018 was 480 GW<sub>th</sub> (which equivalent with about 686 million square meters of collector area) compared to the year 2000 the installed capacity grew by a factor of 7.7.

The corresponding annual solar thermal energy yield in 2018 amounted to 396 TWh, which correlates to savings of 42.6 million tons of oil and 137.5 million tons of CO<sub>2</sub> (Fig. 2).

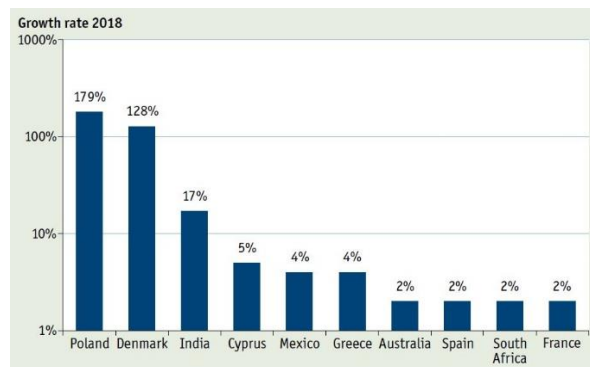


Fig. 2: Global solar thermal capacity in operation and energy yield for the period of 2000-2018

Although the global solar thermal market fell by 3.9% in 2018, there are positive growth figures in the case of the top 20 countries. Fig. 3 shows the date for the most determining 10 countries.

It is worth to mention that the Megawatt-scale solar district heating systems and the solar heating and cooling applications in the commercial and in the industrial sectors played an important role in increasing the growth in recent years. Consequently, several large-sale projects have been initiated and successfully implemented all through the world in 2018.

Nevertheless, it is a rather important fact to be mentioned that the Megawatt-scale plants still represent only about 1% of the overall global installed capacity.



**Fig. 3: Solar thermal market growth rates in the top countries in 2018**

The positive trend of solar thermal energy use discussed before, according to the recent estimation has continued in 2019, as well.

It has been observed a strange fact that the traditional mass markets for small-scale solar water heating systems for single-family houses are under market pressure from heat pumps and PV systems. The PV/T systems are also in the market.

The main issues of the use of solar thermal energy especially in Europe can be summarized along with the statements as:

- mainly solar domestic hot water systems are in use,
- growing share of combined systems,
- growing number of collective (large) systems,
- plastic absorber for swimming pool collectors,
- several solar district heating systems,
- some pilot plants for process heat,
- about 200 pilot plants for solar thermal assisted cooling system.

### 3. Solar photovoltaic

In spite of the recent economic situation all over the world a significant yearly increase of photovoltaic module production and their installation were performed in last couple of year period. However, it can be observed sensitivity of the market change on the photovoltaic industry, the PV technologies still show increasingly high priority.

In 2018, the solar photovoltaic global capacity reached 505 GW<sub>pv</sub> along with the annual additions of 100 GW<sub>pv</sub>, as can be seen in Fig. 4 showing the capacity increase for the period of 2008-2018 (Renewables 2019). It is equivalent to the production of about 40 thousand modules every hour. In 2019 it is estimated about 20% capacity addition.

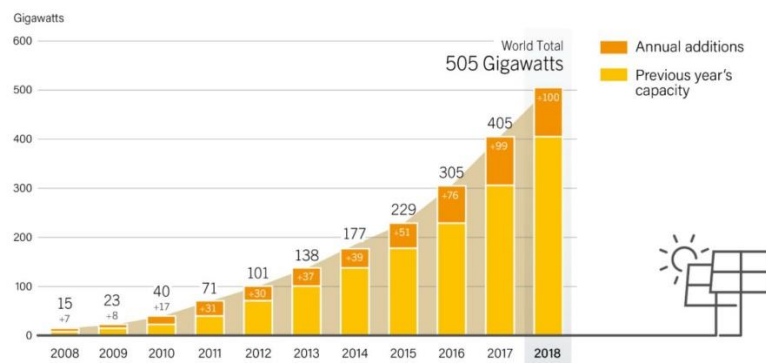


**Fig. 4: The solar PV global capacity and the annual additions for the period 2006-2018**

The Fig. 5 shows the share the solar photovoltaic global capacity in 5 top countries (China, United States, Japan, Germany and India) compared to the rest of world.

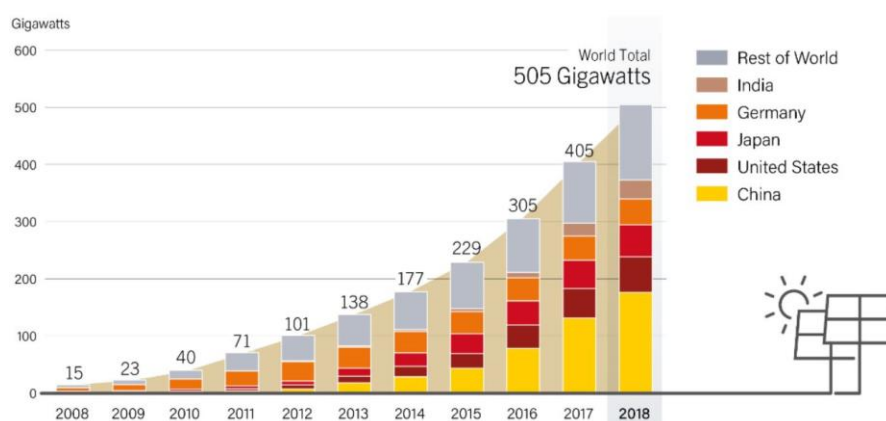


**Fig. 5: The solar PV global capacity and the annual additions for the period 2006-2018 in top countries**

In 2018 in China the annual solar photovoltaic market was declined more than 15% relative to 2017, because of the significant subsidy reductions by the central government. In spite of this fact still China is dominating in the PV productions and installations.

Just making a comparison of the different total renewable energy capacities in operation and their produced energy in 2018 is shown in Fig. 6, along with their growth rate of for the period of 2010-2018 (Fig. 7). From the referred figures it can be easily justified the increasing importance of the solar photovoltaic technology (Weiss et al., 2019).

It is an important break point in comparison of the field of solar thermal and photovoltaics is that in 2018 the PV overtook the solar thermal in the term of installed global capacity.

Concerning to the 2% growth rate of solar thermal, it is significantly less than the leading photovoltaic and the wind technologies.

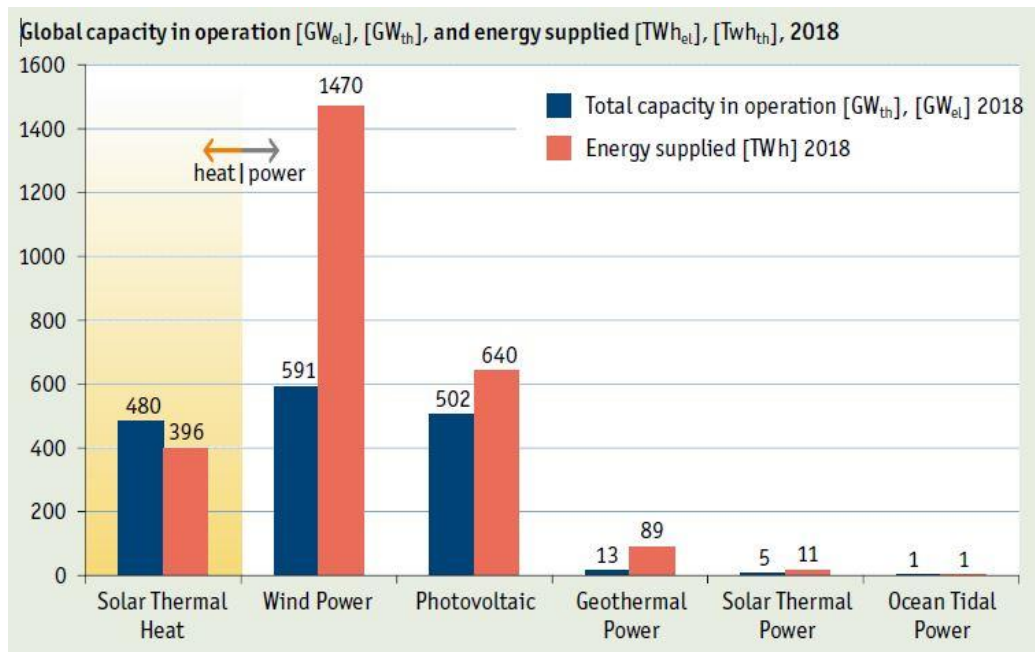


Fig. 6: The total renewable capacity and energy produced in 2018

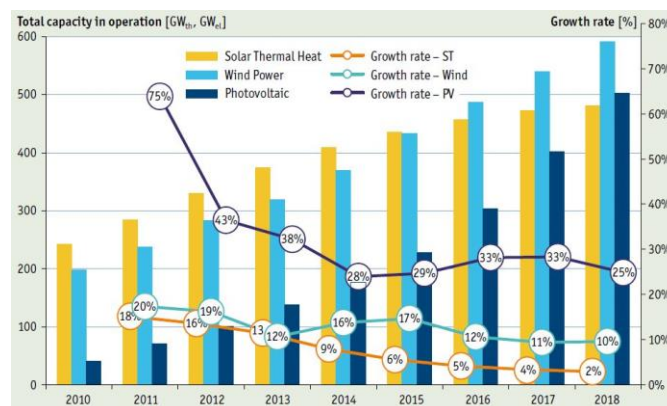


Fig. 7: The growth rate of different renewables for the period of 2010-2018

The most important standpoints, which are characterising and influencing the PV manufacturing and applications industry could be summarized as follows:

- - 20-30% of the part of renewables in the energy mix,
- at around 30-40% yearly decrease of the PV cell and module prices,
- the cell efficiency in market products does not increase in a great extent as expected,
- multi-Gigawatts applications are getting into the practice,
- widening the feed-in tariff system in several countries in worldwide,
- presence of the Chinese PV products in worldwide and especially in the European Union market.

Due to the extensive growing market demand of the solar photovoltaic applications several new issues came to the light. Among the others, such factors include the wide range of cell manufacturing technologies, colouring, transparency and extra size and concentrated type of modules along with the new type of fixation systems, as well.

Concerning to the third generation of PV cells several schemes have been suggested to increase the efficiency of PV cells above the limit of a single bandgap device. The new technologies are aiming at to reduce the losses due to the non-absorption of sub-bandgap photons and the thermalisation of above bandgap photons.

Recently, it is worth to mention the organic and perovskite type of solar cells for which several significant



scientific research and industrial investments were performed in the last couple of years as can be seen in Fig. 8 (Fraunhofer ISE, 2019). In June 2018, perovskites solar cells have reached efficiencies of 27,3% in laboratory environment.

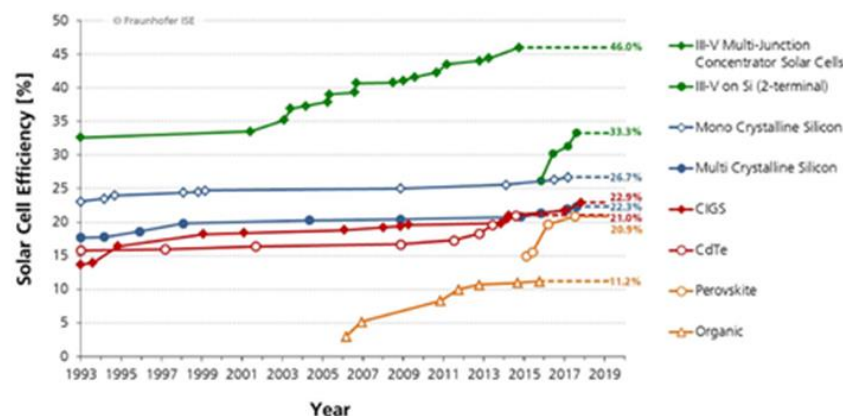


Fig. 8: The growth rate of different renewables for the period of 2010-2018

## 4. Conclusion

This paper gives an overview of both the solar thermal and photovoltaic energy applications fields worldwide. It discusses the technical developments, the market situation and also the future trends. The new technologies are also analysed and providing information on the solutions methods and approaches. Several examples are also given.

## 5. Acknowledgements

This work was supported by the Erasmus+ fund at Szent István University, Gödöllő, Hungary and Itenas, Bandung, West Java – Indonesia.

## 6. References

- Farkas I.: New trends in solar thermal and photovoltaic applications, Conference Proceedings, The 1st Faculty of Industrial Technology International Congress 2017 (FoITIC), Bandung, Indonesia, October 9-11, pp. 2-9.
- Fraunhofer ISE, Photovoltaics report, 2019
- Photovoltaic Geographical Information System - Interactive Maps,  
<http://re.jrc.ec.europa.eu/pvgis/apps4/pvest.php#>, 31.03.2020
- Renewables 2018 - Global Status Report, REN 21, Renewable Energy Policy Network for the 21th Century.
- Trends in photovoltaic applications, 2019. Report, International Energy Agency Photovoltaic Power Systems Programme
- Weiss, W., Spörk-Dür, M., 2019. Solar heat worldwide, Global market developments and trends in 2018, SHC - Solar Heating and Cooling Programme, International Energy Agency.

# **Energy Management Strategy for Nickel Metal Hydride (NiMH) Battery and Proton Exchange Membrane Fuel Cell (PEMFC) on 3-wheel Hybrid Electric Car Equipped with Continuously Variable Transmission (CVT)**

**D. R. Harahap<sup>1\*</sup>, Wei-Chin Chang<sup>2</sup>, S. Ariyono<sup>3</sup>**

<sup>1</sup> Politeknik Manufaktur Negeri Bangka Belitung (Polmanbabel), Bangka Belitung - INDONESIA

<sup>2</sup> Southern Taiwan University of Science and Technology (STUST), Tainan - TAIWAN

<sup>3</sup> Politeknik Negeri Semarang (Polines), Semarang - INDONESIA

\* Corresponding author e-mail: rdhanie84@gmail.com

## **Abstract**

Proton Exchange Membrane Fuel Cells (PEMFC) have higher energy conversion efficiencies than the internal combustion engine (ICE) which are also attractive to apply in the automotive sector, its ability to use hydrogen also become a reason why this technology is becoming popular as an alternative solution to solve the energy crisis. An objective of this research is to design the strategy to manage the energy from fuel cell and observe the energy consumption, maximum speed, and the ability of the vehicle powertrain to climb the slope. A small electric vehicle was modelled using Advanced Vehicle Simulator (ADVISOR) software which developed by the National Renewable Energy Laboratory (NREL). From this experiment, the vehicle primary power source was using a 200W small PEM fuel cell stack combined with AA-type batteries of nickel metal hydride as a backup energy source of each battery have 1.2 V and 1.9 AH. The PEM fuel cell stack and NiMH battery performance were examined using an electronic load to meet the power requirement of the hybrid vehicle. The experiment results shows that the operation range of the fuel cell maximum power was set in the range of 40%-60% to withdraw power from NiMH battery and keep the fuel cell run in its high-efficiency domain. When the vehicle power is lower than 40% of the fuel cell maximum power, the battery will supply the power for the vehicle, and the fuel cell will shut off. When the required power is bigger than the fuel cell maximum power, the battery will supply power to balance it. The car can drive on the sloping road with 3.5% gradability, the fuel consumption in 100 km about 40.6 L/100 km. In 5 seconds, the car can reach 33.9 m and reach 0.4 km need 26.1 seconds.

*Keywords: NiMH battery, PEMFC, Hybrid Electric Vehicle, Energy Management, rubber belt CVT*

## **1. Introduction**

The development technologies using renewable alternative energy such as fuel cells, solar energy, wind power, and batteries are now growing. This energy sometimes uses in some of some small portable devices such as laptops, smartphones, UAV, mobile TV, which considerable amount of energy [1-3]. In the transportation sector, PEM fuel cells are attractive to the automotive sector because of higher energy conversion efficiencies compared to internal combustion engines (ICE) and its ability to use hydrogen. Fuel cells produce only power and water and emit no harmful gas to the environment and living being. There are many different kinds of hybrid power-train structure available now. The propulsion system of a hybrid vehicle can be a load following structure or a load leveled source structure, an energy hybrid structure or a power hybrid structure [4-6]. The battery bank system that starts to producing energy was selected then to generate energy used the hydrogen by the fuel cell will be analyzed. A fuel cell/ battery hybrid small vehicle utilized a 200 W PEM fuel cell stack and 40-AA batteries of nickel metal hydride stack in series, each battery produces 1.95Wh of energy, was studied. The vehicles model, fuel cell, battery, and motor were built, the transmission in this vehicle using CVT, and the strategies to control the energy for the vehicle were established using ADVISOR 2003 software. The simulation tools are useful for the design and performance optimization of vehicles and help to optimize new and more advanced design model containing multiple power sources and drive systems.

## 2. Literature review

### 2.1 Fuel Cell

A fuel cell is like a battery because it can generate electricity from an electrochemical reaction that also convert chemical potential energy into electrical energy. as a by-product of this process also produces heat energy. However, the battery must discard when depleted or recharged by using an external electricity supply to generates the electrochemical reaction in the reverse direction so the battery can be used again as a power source [7].

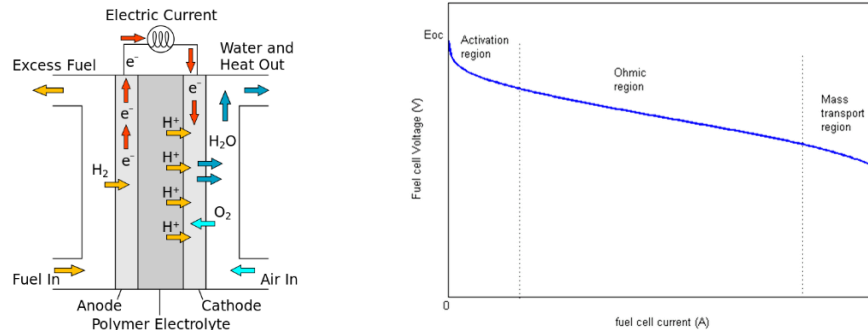


Fig. 1: The PEMFC diagram and the Voltage-Current curve

The fuel cell efficiency is ideal to the amount of power drawn from it. Drawing more power means drawing more current, this increase the losses in the fuel cell. In general rule, the more power (current) draw, the lower the efficiency. Most losses manifest themselves as a voltage drop in the cell, so the efficiency of a cell is almost proportional to its voltage.

### 2.2 Electric Vehicle

The term of ‘Electric Vehicle’ can be identified with any vehicle with an electrical propulsion system. It should encompass land, sea, and air vehicles but in fact, it has become accepted by both the scientific and industrial community that ‘Electric Vehicles’ are referenced exclusively to road vehicles unless otherwise specified. Under the term ‘Electric Vehicle’ (EV), subcategories exist. Hybrid Electric Vehicle (HEV), Fuel Cell Electric Vehicle (FCEV) and Battery Electric Vehicle (BEV) differ in specific design aspects but share the same core electrical technology. The energy source is limited, by employing multiple onboard energy systems that are specialized for the various segments become a good solution [8-9].

## 3. Research methodology

### 3.1 Methodology

This study will simulate the performance of the vehicle run by the fuel cell and NiMH battery using ADVISOR software. The simulation begins by establishing the vehicle model, driving cycle condition, power schemes, fuel converter, energy storage, motor, transmission, wheel/ axle, accessories, and powertrain then computing the parameters in the software. The relation between each component and the schematic diagram of the simulation data flow on how to configure those parameters using Matlab/Simulink program will be explain in Figure 2 [10].

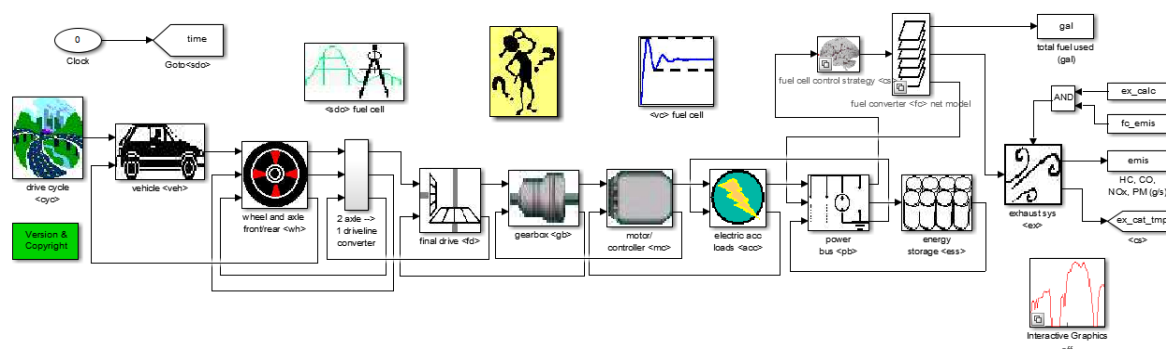


Fig. 2: Fuel cell/ battery hybrid vehicle diagram

The main parameter of this vehicle prototype is the vehicle glider mass, coefficient of drag, coefficient of rolling resistance, drag force, maximum speed/ velocity, and the drive train.

### 3.2. Drive-train configuration

The vehicle drivetrain is the group of components that distribute power to the driving wheels, not including the engine or motor that generates the power, Figure 3. The engine operating speed and the wheels are different so the correct gear ratio must be matched. The transmission system for this vehicle is Continuously Variable Transmission (CVT) which can change the transmission ratio steplessly resulting with an infinite number of effective transmission ratios between maximum to minimum values. This contrasts with other mechanical transmissions that only allow a few numbers of different discrete gear ratios to be selected. The flexibility of a CVT allows the driving shaft to maintain a constant angular velocity over a range of output velocities.

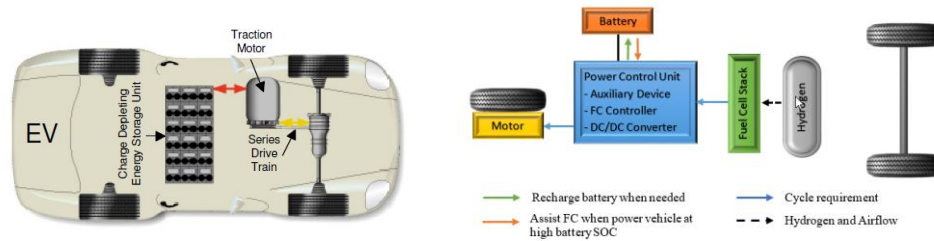


Fig. 3: Fuel cell hybrid vehicle configuration

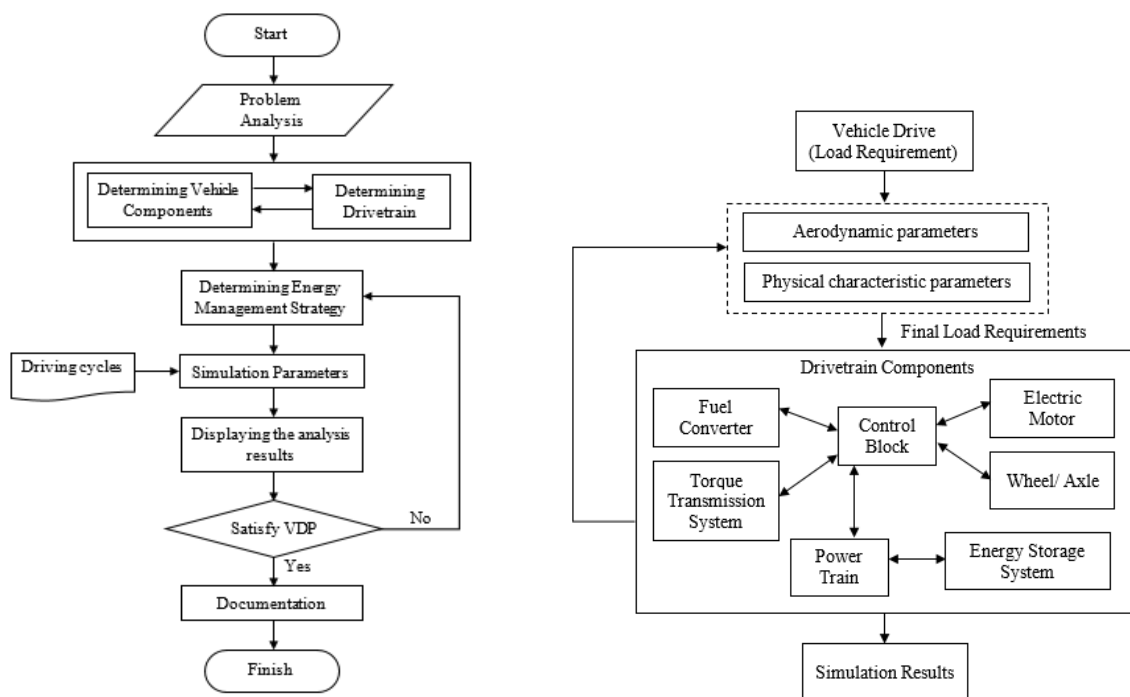
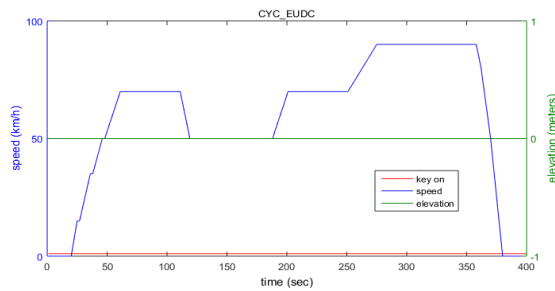


Fig. 4: Research systematic method and the Schematic diagram of simulation data flow

### 3.2. Simulation parameters

A Drive Cycle is a special test drive that duplicates the driving scenario of a person starting the car and making a short freeway trip for example while driving to the office.



Parameter	Index	unit
Duration	400	s
Simulated distance	6.61	km
Maximum speed	90	km/h
Average speed	59.48	km/h
Maximum acceleration	0.83	m/s <sup>2</sup>
Maximum deceleration	-1.39	m/s <sup>2</sup>
Idle time	41	s

Fig. 5: Extra Urban Driving Cycle (EUDC) simulation test

The driving range is one of the key electric car measurements, the longer driving range, the more useful is that car. The Extra-Urban Driving Cycle (EUDC) driving conditions were selected for this project. The chart shows that the test procedures require a constantly changing speed. The Extra-Urban Driving Cycle (EUDC) contains a large portion of extreme acceleration at very high speeds up to 80 km/h. The EUDC cycle maximum speed is 120 km/h; low-powered vehicles are limited to 90 km/h [11].

## 4. Modelling

### 4.1. Vehicle Modelling

All vehicle modeling, whether for conventional ICE vehicles, EVs, HEVs, or FCVs is derived from the basic equation of solid-body motion (Newton's Second Law), as given in Equation 1 in its scalar form.

$$F = ma \quad (1)$$

This equation can be modified with the specific forces, which are typically implemented on vehicles and can be rearranged into the form of Equation 2.

$$F = mgC_{rr} + \frac{1}{2}\rho C_d A v^2 + ma + mgsin(\theta) \quad (2)$$

### 4.2. Drive-train Component

The vehicle drivetrain is the group of components that deliver power to the driving wheels that composed of everything that makes the vehicle move includes the transmission to all the parts that allow the power from the engine to the wheels [13]. Each component configured and arranged as the vehicle drivetrain include the vehicle portion after the transmission changes depending on whether a vehicle in front-wheel, rear-wheel drive or any combination in between. The energy management control strategy is used to distribute the desired drive torque or power to make the power mechanisms work in their most efficient area [12-14].

### 4.3. Fuel Cell Modelling

A 200W Horizon Fuel Cell are used to find out the characteristic of the fuel cell stack which the open-circuit voltage was 38V. The maximum current produced by the stack was 9.5 A, and the maximum power was 200W at 24V. The system was designed with an open-cathode configuration, and the stack contains 40 cells with an active area of 19 cm<sup>2</sup> for each cell. There are two electric fans installed into the systems to supply the oxygen and remove the generating heat produced from the cell. The hydrogen fed to the system is 99.99 % purity. The fuel cell stack hydrogen pressure was 0.45 bar, the flow rate is 2.6 L/min, the fuel cell power is 200 watt, and the fuel cell efficiency is 40%. The measurement fed into a personal computer (PC) and the performance were also measured using an electronic load to see the voltage to current polarization curve, as shown in Figure 6.

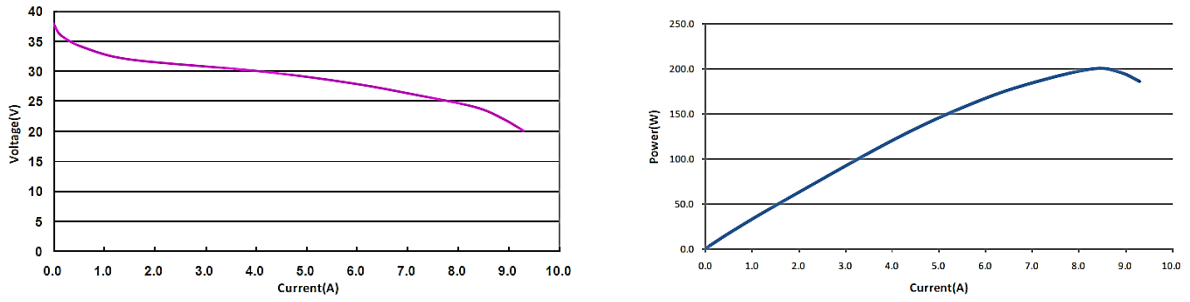


Figure 6. Fuel cell polarization curve at 0.45 bars and Power-Current curve of 200W PEMFC

Figure 6 is the fuel cell stack voltage-current polarization curve where the output voltage drop could be categorized into three regions. These phenomena can be represented by the equations.

$$V_{st} = N(E_r - V_a - V_{ohm} - V_{conc}) \quad (3)$$

where  $V_{st}$  is stack output voltage,  $N$  is the number of cells connecting in a stack;  $E_r$  is theoretical cell potential,  $V_a$  is the voltage loss due to reaction kinetic,  $V_{ohm}$  and  $V_{conc}$  are those due to the resistances and the mass transport, respectively. These losses could be calculated using the following equations. The reaction kinetic or activation voltage loss and the resistance or ohmic loss are given by empirical formula in equation (4.4) and (4.5), respectively.

$$V_a = \frac{RT}{\alpha F} \ln \left( \frac{i}{i_0} \right), \quad (4)$$

$$V_{ohm} = (R_m + r)I \quad (5)$$

Where  $\alpha$  and  $i_0$  are the transfer coefficient and the exchange current density, respectively. The exchange current density,  $i_0$ , depends on operating conditions and the properties of the catalyst and must be determined experimentally.  $R_m$  and  $r$  are a membrane and other component's resistances. The voltage and the current density obtained experimentally. The related parameters shown in the equation could be estimated where the number of cells are 40 cells, the hydrogen preassure is 0.45 bar.

#### 4.4. Transmission, Wheel/ Axle Modelling

The wheel/ axle model transmits torque and speed request by the vehicle to the final drive, includes the effects of axle losses, tire slip, wheel and axle inertia and the friction brake defined with wheel diameter 0.356 m (14 in) and 3.6 kg of the wheel mass. In this modelling the transmission is set in fix ratio (1:1 ratio), so the speed or rotation of wheel similar to the rotation of motor electric. It assumed that the power required from the wheel is provided by the power of motor electric. The fuel cell system operates some peripherals that inherently consume power as they support the reaction of gasses within the fuel cell. ADVISOR defines the standard accessory load data for use with hybrid systems based on the mechanical accessory load that was drawn from the engine and the electrical load that was drawn from the voltage/power bus. The accessory load also configures the constant torque load on the engine and also the dc-to-dc converter efficiency applied in the systems. For the electrical accessory load set at 50W to support the auxiliary power in the vehicle systems to start up and shut down.

#### 4.5. Electric Motor Modelling

This vehicle uses a MITSUBA motor model M0124D-V that usually applies for electric vehicle competition. This motor giving far greater flexibility to vehicle designers while substantially reducing drivetrain losses which mean less energy is wasted (during both acceleration and regenerative braking), causing in more of the energy from the battery pack is available to propel the vehicle.

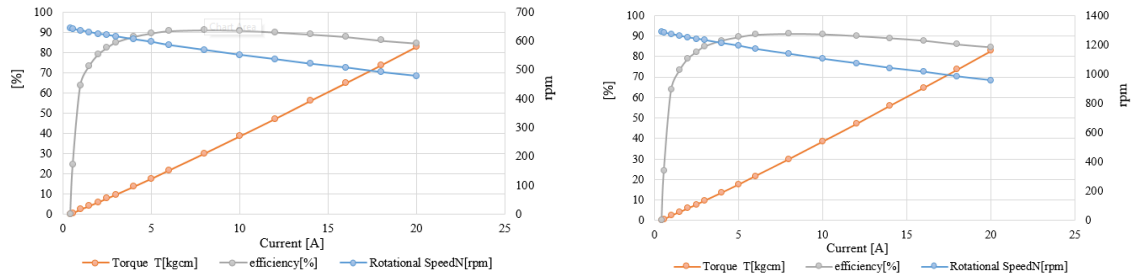


**Fig. 7: Mitsuba motor M0124D-V performance at 24V and 48V**

#### 4.6. Energy Management Strategy

The control strategy is an algorithm which determines at each sampling time the power generation split between the fuel cell systems and the energy storage system in order to fulfill the power balance between the load power and the energy sources [8, 10]. The energy consumption used by the vehicle performed by three modes; starting/normal mode, accelerating mode, and steady mode. The accelerating mode will be split into two modes, the high-speed mode, and low-speed mode. The operation range of the fuel cell maximum power was set in the range of 40%-60%, to withdraw power from NiMH battery and keep the fuel cell run in its high-efficiency domain. The maximum rate of the increasing fuel cell converter was set at 180W/s, and the maximum rate of decreasing was set at -280W/s. When the required vehicle power is lower than 40% of the fuel cell maximum power, the battery will supply all the needed power for the vehicle, and the fuel cell will shut off. When the required power is bigger than the fuel cell maximum power, the battery will supply power to balance it. The fuel cell turns on when the battery SOC reach its low limit at 40%, and the highest desired battery was set at 80%.

#### 4.7. Simulation Results

The primary outputs from the ADVISOR simulations were plots showing the velocity profile and the State of Charge as a function of time over the course of a lap in the highway fuel economy test. Figure 8 show the series of hybrid configuration results following the EUDC driving cycle test for 400 seconds and able to travel along 6.61 km with 59.48 km/h of speed. Figure 9, show the energy storage of the vehicle and the amount of fuel that consumed during the simulation in gram per kilowatt-hour is shown in Figure 11. Figure 10 show the motor torque graph that shows the motor performance during the simulation when the vehicle tries to follow the EUDC driving cycle procedure. There are inclination and declination during the 400 seconds period. The highest torque is when the vehicle attempts to reaches the maximum speed of the requirement, 90 km/h. After few second, the vehicle already decelerates and maintain the speed at 59.48 km/h in average. After 350 s, the motor going to decelerate and finished the driving cycle test. The average motor controller efficiency is above 80% of the driving performance. It is obvious to show that the simulation results are ideal. Beside those simulation results that presented by ADVISOR, below are the figure that shows the acceleration and gradability test base on EUDC driving requirement.

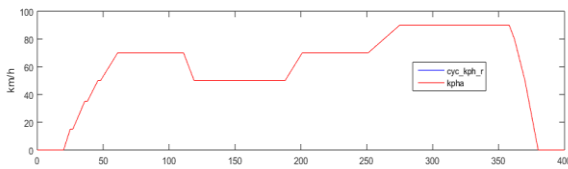


**Fig. 8: The vehicle driving test by EUDC**

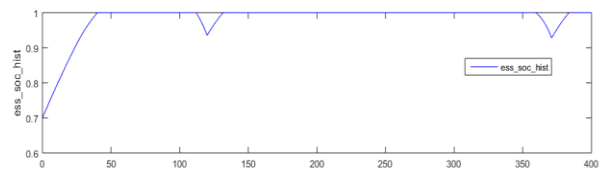


**Fig. 9: Vehicle energy storage system (ESS) SOC**



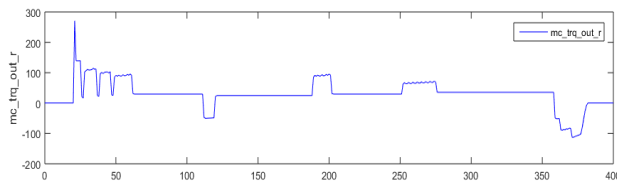


**Fig. 10: Vehicle motor torque Figure**

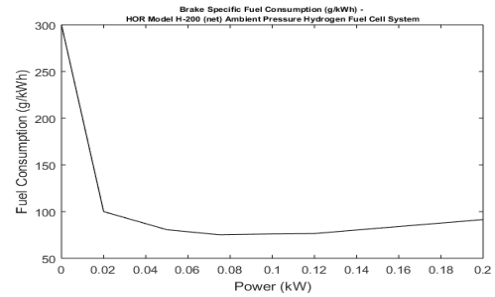


**Fig. 11: Vehicle fuel consumption**

The maximum vehicle acceleration is  $5.8 \text{ m/s}^2$ , in five seconds the vehicle able to travel along 33.9 meters. Another result shows from this simulation of acceleration test is the ability of the vehicle to reach 0.4 km in 26.1 seconds, the fuel (hydrogen) consumption in 100 km about 40.6 L/100 km equal to 2.7 liters of gasoline. The vehicle gradability is 3.5% which indicated that the vehicle ability to climb the sloping road.

## 5. Conclusions

The hybrid vehicle mode is starting mode, accelerating mode that separates into two parts, and steady mode. The Extra-Urban Driving Cycle (EUDC) was chosen for the simulation because it can use to simulate the electric vehicle driving performance to the achieved point, especially at distance, maximum speed, and average speed, then another driving cycle that available in the software. The operation range of the fuel cell maximum power was set in the range of 40%-60% to withdraw power from NiMH battery and keep the fuel cell run in its high-efficiency domain. When the vehicle power is lower than 40% of the fuel cell maximum power, the battery will supply the power for the vehicle, and the fuel cell will shut off. When the required power is bigger than the fuel cell maximum power, the battery will supply power to balance it. The car can drive on the sloping road with 3.5% gradability, the fuel consumption in 100 km about 40.6 L/100 km. In 5 seconds, the car can reach 33.9 m and reach 0.4 km need 26.1 seconds.

## 6. Acknowledgments

We would like to appreciate gratefulness to the ministry of high education for giving research grand. We also would like to appreciate gratefulness to Politeknik Negeri Semarang especially department of mechanical engineering who give us opportunity to use the laboratory to conduct the experiment. Moreover, the researcher from Polmanbabel who tries to use CVT in his research supported the Fuel Cell Laboratory of the Southern Taiwan University of Science and Technology (STUST) Taiwan.

## 7. References

- A. B. A. Alaswad, H. Achour, J. Carton, Ahmed Al Makky, A.G. Olabi, "Developments in fuel cell technologies in the transport sector," *International Journal of Hydrogen Energy*, vol. 41, pp. 16499-16508, 2016.
- M. A. H. N. Sulaiman, A. Mohamed, E.H. Majlan, W.R. Wan Daud, "A review on energy management system for fuel cell hybrid electric vehicle: Issues and challenges," *Renewable and Sustainable Energy Reviews*, vol. 52, pp. 802-814, 2015.
- Y.-J. C. Jenn-Jiang Hwang, Jenn-Kun Kuo, "The study on the power management system in a fuel cell hybrid vehicle," *International Journal of Hydrogen Energy*, vol. 37, pp. 4476-4489, 2012.
- J. P. Jingda Wu, Hongwen He, Jiayi Luo, "Comparative analysis on the rule-based control strategy of two typical hybrid electric vehicle powertrain," *Energy Procedia*, vol. 104, pp. 384-389, 2016.
- C. W. T. Himadry Shekhar Das, A.H.M. Yatim, "Fuel cell hybrid electric vehicles: A review on power conditioning units and topologies," *Renewable and Sustainable Energy Reviews*, vol. 76, pp. 268-291, 2017.
- C. C. Jean-Paul Rodrigue, Brian Slack, *The Geography of Transport Systems*, Fourth Edition ed. New York; Routledge, 2017.



- Y. L. Daniel Garraín, Cristina de la Rúa, "Polymer Electrolyte Membrane Fuel Cells (PEMFC) in Automotive Applications: Environmental Relevance of the Manufacturing Stage," *Smart Grid and Renewable Energy*, vol. 2, pp. 68-74, 2011.
- L. C. Rosario, "Power and Energy Management of Multiple Energy Storage Systems in Electric Vehicles," Ph.D. Dissertation, Department of Aerospace Power & Sensors, Cranfield University, 2007.
- G. G. Ayse Elif Sanlı, Aylin Aytac, Mahmut Mat, "Development of a power management unit for small portable direct borohydride fuel cell NiMH battery hybrid system," *International Journal of Hydrogen Energy*, vol. 37, pp. 19103-19110, 2012.
- M. S. Diego Feroldi, Jordi Riera, "Energy Management Strategies based on efficiency map for Fuel Cell Hybrid Vehicles," *Journal of Power Source*, vol. 190, pp. 387-401, 2007.
- Wikipedia. New European Driving Cycle - Wikipedia [Online]. Available: [https://en.wikipedia.org/wiki/New\\_European\\_Driving\\_Cycle](https://en.wikipedia.org/wiki/New_European_Driving_Cycle), (accessed Apr 10, 2017)
- A. B. T. Markel, T. Hendricks, V. Johnson, K. Kelly, B. Kramer, M. O'Keefe, S. Sprik, K. Wipke, "ADVISOR: a systems analysis tool for advanced vehicle modeling," *Journal of Power Source*, vol. 110, pp. 255-266, 2002.
- M. Transmission. What is a Drivetrain? [Online]. Available: <https://www.mistertransmission.com/what-is-a-drivetrain/>, (accessed Apr 14, 2017)
- P. M. Hien, "A Simulation and Experiment Study of Small Fuel Cell/ Battery Hybrid Vehicle," Master Thesis, Department of Mechanical Engineering, Southern Taiwan University of Science and Technology, Taiwan - R.O.C., 2009.

## Effect of nanofluid concentration on the performance of PV/T collector under the tropical climate of Indonesia

Amrizal<sup>1\*</sup>, Agung Nugroho<sup>2</sup>, Miftahul Aziz<sup>2</sup>, Muhammad Irsyad<sup>1</sup> and Amrul<sup>1</sup>

<sup>1</sup> Department of Mechanical Engineering, Universitas Lampung (Unila), Bandar Lampung - INDONESIA

<sup>2</sup> Magister of Mechanical Engineering, Universitas Lampung (Unila), Bandar Lampung - INDONESIA

\* Corresponding author e-mail: amrizal@eng.unila.ac.id

### Abstract

Solar energy is a very potential and most abundant source energy available and it is free of cost in consuming this type of energy. Flat plate solar collector is a device that can transform solar energy into the thermal energy and can be implemented to PV/T solar collector. In this study, a modified flat-plate PV/T solar collector was built by attaching the thermal collector underneath the PV collector surface. The application of nanofluid in the PV/T solar collector as a heat-absorbing medium needs to be developed and characterized in different environments condition. The effect of nanofluid concentration on the performance of the PV/T collector was investigated according to EN 12975-2 standard. The volume fraction of the nanoparticles used in the present study were 0.3%, 0.6% and 0.9%, respectively. The efficiency of the system was compared to the water as a base fluid performed in low latitude tropical region (Bandar Lampung climate). The experimental result shows that an increase of zero thermal efficiency up to 18% which is obtained by using nanofluid at the volume fraction of 0.9%.

*Keywords: Solar, collector, PV/T, nanofluid, PV/T, tropical*

### 1. Introduction

The sun is a renewable energy source that has several advantages such as being easily available, free of pollution and available in considerable quantities. A flat plate solar thermal collector is a device used to harness solar energy. This type collector is widely used to absorb solar radiation and transform it into heat energy which produces domestic hot water. In other applications, this type collector also can be implemented to absorb the excess heat collected on the surface of solar cell (Photovoltaic). Therefore, the attaching the two surfaces between the thermal collectors and the solar cells is a good way to solve the problem with respect to the excess heat on the solar cell surface. In particular, this type collector is called as a hybrid Photovoltaic/Thermal (PV/T) collector.

The PV/T collector can generate thermal and electricity energy simultaneously. Another advantage of using this type of collector is that the electrical efficiency remains stable even increases due to absorbing the excess heat by the working fluid on the surface temperature of the PV. Besides producing electricity, the PV/T collectors also produce hot working fluid so that they can be used for various purposes such as the heating process in industry and the health sector, household needs and other needs. Investigations have been carried out and reported over the last 25 years by several researchers (Abdelrazik et al. 2018, Amrizal et al. 2010, 2012, 2013, 2017) those are related to the evaluation of thermal and electrical output. They present experimental work, analytical, numerical models, simulation and the development of performance testing processes.

Concerning to the traditional working fluids of the PV/T solar collector, in fact, water or oil based fluids used in the PV/T collector have low thermophysical properties in term of thermal conductivity and specific heat capacity. Nanofluid shall be alternatively applied to this type collector in enhancing the performance of the collector. In this context, Das et al. (2006) introduced nanofluid that contain a small quantity of nanoparticles which have diameter usually less than 100 nm. It is mixed with conventional fluids providing more heat transfer ability. The solid particle dispersed in base fluid such as thermal oils, refrigerant, ethylene glycol or water (Yazdanifard et al. 2017, Bellos et al. 2018, Khanafer and Vafai 2018. This could be important because by implementing nanofluid, the heat transfer of the fluid can be increased significantly (Mahbubul, 2019).

Significant findings have obtained by several researchers for metal oxide nanoparticles added into different base fluids which are called it as nanofluids. Sardarabadi and Passandideh (2016) presented an experimental study and a numerical of a PV/T collector with several types of nanoparticles.  $\text{Al}_2\text{O}_3$ ,  $\text{TiO}_2$  and  $\text{ZnO}$  are used in this study were as nanofluids. The authors concluded that  $\text{ZnO}$  nanofluid and  $\text{TiO}_2$  nanofluid have the higher electrical efficiency than  $\text{Al}_2\text{O}_3$  nanofluid.

Hashim et al. (2015) conducted an experimental work of the effect of using  $\text{Al}_2\text{O}_3$  nanofluid as a cooling medium for the PVT collector system based on forced convection. Several different concentrations of  $\text{Al}_2\text{O}_3$  nanofluid were tested (0.1, 0.2, 0.3, 0.4 and 0.5%). The results show that the temperature decreased significantly to  $42.2^\circ\text{C}$  and the electrical efficiency increase 12.1% at a concentration of 0.3%.

The experimental and numerical studies of a PVT system cooled by nanofluids was introduced by Rejeb et al. (2016). Nanoparticles ( $\text{Al}_2\text{O}_3$  and  $\text{Cu}$ ) are tested by the authors at three different concentrations (0.1, 0.2, and 0.4 wt %) with fluids (ethylene glycol and water ) on the performance of the system. The results show that the thermal and electrical efficiencies of water as a base fluid is more effective than ethylene glycol.

Concerning several literatures, they studied the size, arrangement, location, and type of fluid used for cooling in PV/T collector. However, studies by using nanofluid as a coolant under the tropical climate is still limited in Indonesia, for that it is necessary to investigate the behavior of the PV/T collector in the present study since it enhances heat transfer process substantially.

## 2. Experimental methods

The collector utilized in this work was performed by attaching the solar thermal collector under the surface of PV cell as presented in Figure 1. This type collector was tested in Bandarlampung, at the Department of Mechanical Engineering, Universitas Lampung – Indonesia. Bandarlampung is the capital of the Lampung Province, Indonesia and the geographical coordinates are  $5.25^\circ\text{S}$  and  $105.17^\circ\text{E}$ . The Bandarlampung zone has a typical tropical climate which is characterized as dry and rainy seasons. The effect of nanofluid concentration on the thermal performance was investigated according to EN 12975-2 (2006) standard. The volume fraction of the nanoparticles used in the present study were 0.3%, 0.6% and 0.9%, respectively. The performance of the system was compared to the water as a traditional working fluid performed under low latitude tropical region (Bandar Lampung climate) and the average ambient temperature of  $27^\circ\text{C}$ .

### 2.1. Experimental procedures

The collector must be tested under incident radiation more than  $500\text{ W/m}^2$ . Data collection were recorded for inlet and outlet fluid temperatures, ambient temperature and incident radiation, respectively. Then, the temperatures and radiation were measured using K-type Thermocouples and Solar Power Meter SPM 1116SD, respectively. According to EN 12975-2 standard, the mass flow rate of the working fluid was regulated by using a valve at a constant flow rate of  $0.02\text{ kg/m}^2\text{s}$ . Electrical heaters were used in order to vary inlet fluid temperatures during the tests.



Fig. 1: PV/T collector

## 2.2. Characterization of PV/T solar collector

In generally, equations of solar thermal collector performance are given as follows.

$$q_u = F'[(\tau\alpha)G - U_L(T_m - T_a)] \quad (1)$$

$$q_u = \dot{m}c_p(T_m - T_a)/A_c \quad (2)$$

The above equations are based on the energy balance in which equation (1) is known as The Hottel-Whillier-Bliss equation (Dufie et al. 2006) where  $F'(\tau\alpha)$  is the zero loss efficiency,  $F'U_L$  is the overall heat loss coefficient, respectively. From equation (2)  $\dot{m}$  is the mass flow rate of fluid,  $c_p$  is the heat capacity of fluid,  $(T_m - T_a)$  is the temperature difference and  $A_c$  is the area of absorber plate. Furthermore, electrical efficiency of the PV/T collector is obtained from equation 3

$$\eta = \frac{P}{GA} \quad (3)$$

where P is electrical power given by PV/T collector during the tests ( $P = VI$ ), G is solar radiation and A is area of the collector.

## 3. Result and Discussion

Several performance tests were conducted in relation to the different nanofluid volume fraction and the inlet fluid temperature, respectively. Table 1 presents the results of the surface temperature and electrical power. Furthermore, the electrical efficiency is shown in Figure 2. Four types of working fluid were implemented such as water only and three different concentrations of TiO<sub>2</sub> nanofluid.

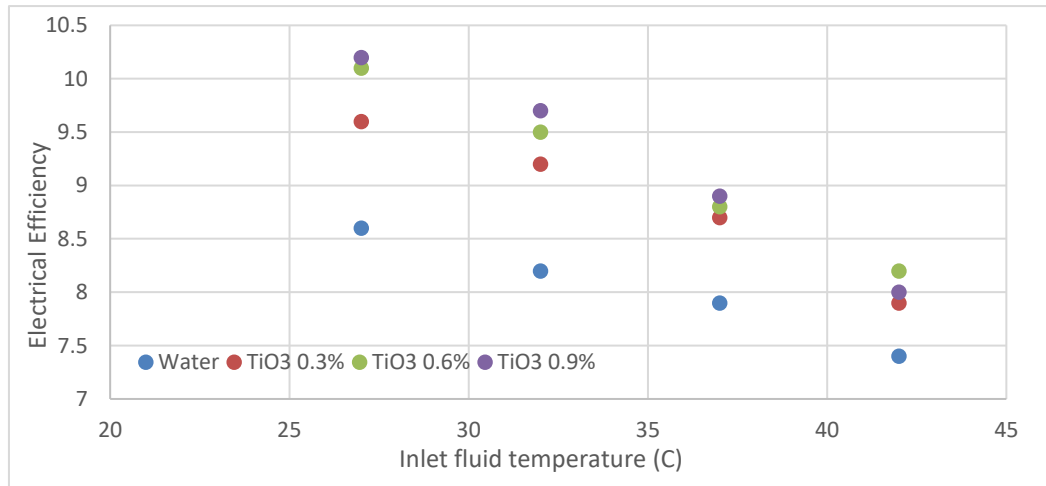


Fig. 2: Electrical efficiency versus inlet fluid temperature

Concerning the thermal performance in the current work, it describes the effect of water and TiO<sub>2</sub> nanofluid as a base fluid with different nanofluid volume fraction. The values of zero thermal efficiency parameter are 0.58, 0.71, 0.68, 0.66, 0.65 for water, TiO<sub>2</sub> nanofluid 0.3%, TiO<sub>2</sub> nanofluid 0.6%, TiO<sub>2</sub> nanofluid 0.9%, respectively. In comparison with the water only, there is an increase of zero thermal efficiency ( $F'(\tau\alpha)_e$ ) up to 18% which is obtained by using nanofluid at the volume fraction of 0,9%. The significant different between the two results with and without nanofluid because of the heat transfer can be increased as well as the thermal performance of the whole system. Consequently, the nanofluid absorb more heat than that of the conventional fluid water.

In term of the electrical performance, as shown in Figure 2 the surface temperature of PV collector with 0.9% of TiO<sub>2</sub> nanofluid has lowest value in comparison with the others. Consequently, this might give the highest value of electrical efficiency about 10.2 %. Therefore, the nanofluid implemented on the PV/T collector has better thermal performance than the water only as a base fluid. In case of increasing the concentration in the current work, it does not significantly affect the electrical efficiency of the PV/T solar collector with respect to each others. The values for electrical power from different volume fraction of the TiO<sub>2</sub> nanofluid are almost constant and a small different is given in the values for electrical efficiency.

**Table 1: average temperature of the PV surface and power based on the inlet fluid temperature different concentration of TiO<sub>2</sub> nanofluid**

Inlet Fluid Temperature (°C)	Water only		TiO <sub>2</sub> nanofluid (0,3%)		TiO <sub>2</sub> nanofluid (0,6%)		TiO <sub>2</sub> nanofluid (0,9%)	
	T <sub>s</sub> (°C)	Power (W)	T <sub>s</sub> (°C)	Power (W)	T <sub>s</sub> (°C)	Power (W)	T <sub>s</sub> (°C)	Power (W)
27	59,36	31,22	57,80	35,79	55,60	36,33	53,5	36,75
32	62,82	29,60	60,80	33,69	58,70	34,19	56,6	34,90
37	66,30	28,38	63,62	31,50	62,20	31,86	60,2	32,51
42	70,35	27,20	68,81	28,83	66,60	29,38	64,15	29,91

\*T<sub>s</sub> (C) : average temperature of the PV surface

#### 4. Conclusion

Effect of nanofluid concentration on the behavior of PV/T flat-plate solar collectors has been characterized. The parameters that characterize the PV/T collector are zero thermal efficiency, the overall heat loss coefficient, average temperature of the PV surface and electrical efficiency. The performance of the system was compared to the water as a base fluid implemented in low latitude tropical region (Bandar Lampung climate). The experimental result shows that an increase of zero thermal efficiency up to 18% which is obtained by using nanofluid at the volume fraction of 0,9%. Furthermore, the surface temperature of PV collector with 0.9% of TiO<sub>2</sub> nanofluid has lowest value in comparison with the others. The TiO<sub>2</sub> nanofluid absorbs more heat than that of the conventional fluid water. However, the values for electrical power from different volume fraction of the TiO<sub>2</sub> nanofluid are almost constant.

#### 5. Nomenclature

F'	collector efficiency factor	m <sup>2</sup>
G	solar radiation	W/m <sup>2</sup>
T	temperature	C
$\dot{m}$	mass flow rate	kg/s
q	energy gain	W
k	thermal conductivity	W/mC
c	heat specific of fluid	J/kgC
U	overall heat loss coefficient	W/m <sup>2</sup> C
A	area	m <sup>2</sup>
V	Voltage	V
I	current	Ampere
Greek letters		
$\alpha$	absorbitivity	-
$\tau$	transmissivity	-
Subscripts		
a	ambient	
m	mean	
s	surface	
u	usefull	
p	pressure	

## 6. Acknowledgements

The authors are grateful to have financial support from Research Grant (PPs-BLU) 2019, Universitas Lampung.

## 7. References

- A. S. Abdelrazik, F. A. Al-Sulaiman, R. Saidur, and R. BenMansour, 2018. "A review on recent development for the design and packaging of hybrid photovoltaic/thermal (PV/T) solar systems," *Renewable and Sustainable Energy Reviews*, vol. 95, pp. 110–129.
- Amrizal Nalis, Daniel Chemisana, J. I. Rosell, 2010. The Use of Filtering for the Dynamic Characterization of PV/T Flat-Plate Collectors. *International Conference on Solar Heating, Cooling and Buildings EuroSun*, Graz University, Austria.
- Amrizal, D. Chemisana, J.I. Rosell, J.Barrau, 2012. A dynamic model based on the piston flow concept for the thermal characterization of solar collectors. *Applied Energy*, 94, 244-250.
- Amrizal, D. Chemisana, and J. I. Rosell, 2013. Hybrid Photovoltaic-Thermal Solar Collector Dynamic Modelling. *Applied Energy*, 101, 797-807.
- Amrizal, Amrul, Ahmad Yonanda, Zulfa, 2017. Comparison Study of Solar Flat Plate Collector With Two Different Absorber Materials, *The 1<sup>st</sup> Faculty of Industrial Technology International Congress*, Itenas Bandung, ISBN 978-602-53531-8-5, 17-22 .
- A. R. A. Hashim, A. Hussien, and A. H. Noman, 2015. "Indoor investigation for improving the hybrid photovoltaic/thermal system performance using nanofluid (AL<sub>2</sub>O<sub>3</sub>-water)," *Engineering and Technology Journal*, vol. 33, no. 4, pp. 889–901,
- E. Bellos, Z. Said, and C. Tzivanidis, 2018. "The use of nanofluids in solar concentrating technologies: a comprehensive review," *Journal of Cleaner Production*, vol. 196, pp. 84–99,
- European Standard EN 12975-2:2006. CEN (European Committee for Standardisation).
- F. Yazdanifard, M. Ameri, and E. Ebrahimi-Bajestan, 2017. "Performance of nanofluid-based photovoltaic/thermal systems: a review," *Renewable and Sustainable Energy Reviews*, vol. 76, pp. 323–352,
- I. M. Mahbubul, "Preparation of nanofluid, 2019." in *Preparation, Characterization, Properties and Application of Nanofluid*, W. Andrew, Ed., p. 374, Elsevier Inc.,
- John A. Dufie, William A. Beckman. 2006. *Solar Engineering of Thermal Processes*, John Wiley & Sons, Inc.
- K. Khanafer and K. Vafai, 2018. "A review on the applications of nanofluids in solar energy field," *Renewable Energy*, vol. 123, pp. 398–406,
- M. Sardarabadi and M. Passandideh-Fard, 2016. "Experimental and numerical study of metal-oxides/water nanofluids as coolant in photovoltaic thermal systems (PVT)," *Solar Energy Materials & Solar Cells*, vol. 157, pp. 533–542,
- O. Rejeb, M. Sardarabadi, C. Ménézo, M. Passandideh-Fard, M. H. Dhaou, and A. Jemni, 2016. "Numerical and model validation of uncovered nanofluid sheet and tube type photovoltaic thermal solar system," *Energy Conversion and Management*, vol. 110, pp. 367–377
- S.K.Das, S.U.S.Choi, and H.E.Patel, 2006 "Heat transfer in nanofluids—a review," *Heat Transfer Engineering*, vol. 27, no. 10, pp. 3–19.

## Potential of Glycerol and Derivatives Based on Palm Oil as a Green Solvent

Maria Agustina Rani Findriyani<sup>1</sup>, Syifa Tiara Saskia Mulya<sup>2,\*</sup> and Nugroho Adi Sasongko<sup>3</sup>

<sup>1</sup> Department of Chemical Engineering, Universitas Negeri Semarang (UNNES), Semarang - INDONESIA

<sup>2</sup> Departement of Chemical Engineering, Universitas Negeri Semarang (UNNES), Semarang - INDONESIA

<sup>3</sup> Centre for The Assesment of The Process and Energy Industry (PPIPE), Agency for The Assesment and Application of Technology (BPPT), Semarang - INDONESIA

\* Corresponding author e-mail: syifatiarasaskia@gmail.com

### Abstract

The need for more environmentally friendly and sustainable chemicals has led to a large amount of research into the processing of renewable raw materials. Palm oil is a potential source of energy. As an agraria country, Indonesia has a great potential to play a role in the palm oil industry. Moreover, in 2007 Indonesia was recorded as the largest producer and exporter of palm oil in the world. Until 2010, the total area of oil palm plantations in Indonesia reached 7.8 million hectares. In the past 15 years the production of palm oil increased almost five times, from 4.8 million tons of crude palm oil (CPO). The increase in the production capacity of the biodiesel industry causes high production of raw glycerol because glycerol is a by-product of biodiesel, so it must be accompanied by market expansion and increase in added value so that the price of glycerol is not low. Glycerol can be used as a green solvent. Glycerol is capable of dissolving many organic and inorganic compounds, including complex metal-transitions. The use of glycerol as a solvent also has several notable disadvantages, such as high viscosity (1200 cP at 20°C) and low solubility of compounds and gases that are very hydrophobic, which limits the possibility of their use. Weakness of viscosity is usually overcome by heating above 60 °C or by using co-solvent. Glycerol with a higher level of purity (80-99%) is needed as raw material for the cosmetics industry, pharmaceutical industry, paper industry, paint and varnish industry, textile industry, food industry, tobacco processing, oleochemicals, and lubricants. Glycerol is used as a precursor for the production of various chemical commodities such as 1,2-propanediol, 1,3-propanediol, ethylene glycol, propanol, hydrocarbons, acrolein, dihydroxyacetone, glyceric acid, syngas, hydrogen, glyceril ether, glyceril ester, glycerol carbonate, 1,3-dichloro propanol, polyglycerol and glycerol acetal and ketal through several methods such as fermentation, hydrogenolysis, pyrolysis, oxidation, etherification, dehydrasesterification, carboxylation, halogenation, polymerization and glycerol acetalization.

*Keywords: Green Solvent, Glycerol, Palm Oil, Glycerol Derivatives, By-product Biodiesel.*

### 1. Introduction

The problem of decreasing air quality, environment, health and safety is becoming a serious problem in the processing of fossil-based raw materials. The need for more environmentally friendly and sustainable chemicals has led to a large amount of research into the processing of renewable raw materials.

It can be seen that domestic bioenergy consumption continues to increase because it is supported by the mandatory biodiesel policy through ESDM Regulation No. 20 of 2014. The regulation stipulates the obligation to use minimum biodiesel as a fuel mixture gradually until 2025 by 30% so that it triggers an increase in biodiesel production activities which is certainly also in line with the increase in glycerol production. The amount of glycerol produced globally has reached 1.2 million tons and will continue to increase in the future due to increasing demand for biodiesel (Zhou et al, 2008). The realization of national biodiesel industry production has reached 3.2 million kL for 2014, which means that roughly 400 thousand kL of crude glycerol is also produced (Wahyuni et al, 2016) because the biodiesel industry produces large amounts of glycerol as a by-product 10-20% of the total product volume (Darnoko et al, 2000).

Increasing the production capacity of the biodiesel industry causes an increase in crude glycerol production, so it must be accompanied by market expansion and an increase in added value so that the price of glycerol does not fall (Wahyuni et al, 2016). Can be seen in Fig. 1, glycerol has more than 2000 applications, and its derivatives are valuable starting materials for the preparation of drugs, food, drinks, chemicals and synthetic materials (Gu et al, 2010).

However, the price of glycerol is quite low, causing an unbalanced supply. At present, a proportion of these renewable chemicals are wasted. This phenomenon has produced negative feedback on the economic viability of the biodiesel industry in the future and has a negative impact on the environment due to improper disposal (Pagliaro et al, 2008). Glycerol shows high boiling point, polarity and non-flammability and is a suitable substitute for organic solvents, such as water, dimethylformamide (DMF) and dimethylsulfoxide (DMSO). Green solvent is a bio-based product that is highly sought after (Gu et al, 2013). Because to reduce the use of hazardous substances (especially volatile solvents (VOC)), it is flammable, toxic and produces waste in chemical processes. Thus, glycerol is considered a green solvent and as an important subject regarding research in green chemistry.

## 2. Palm oil

Palm oil is a potential source of energy. As a country with fertile soil, Indonesia has enormous potential to play a role in the palm oil industry. Moreover, in 2007 Indonesia was recorded as the largest producer and exporter of palm oil in the world. Until 2010, the total area of oil palm plantations in Indonesia reached 7.8 million hectares. In the past 15 years the production of palm oil increased almost five times, from 4.8 million tons of crude palm oil (CPO) in 1996 to 19.8 million tons in 2010 (Julianti et al, 2014).

**Table 1: Components and Compositions Available in Palm Oil**

Components	Compositions (%)
Trigliserida	95,62
Asam lemak bebas	4,00
Air	0,20
Phosphatida	0,07
Karoten	0,03
Aldehid	0,07

(Gunstone, 1997)

**Tabel 2. Composition and Types of Fatty Acids in Palm Oil**

Types of Fatty Acids in Palm Oil	Compositions (%)
Laurat (C12:0)	<1,2
Miristat (C14:0)	0,5-5,9
Palmitat (C16:0)	32-59
Palmitoleat (C16:0)	<0,6
Stearat (C18:0)	1,5-8
Oleat (C18:1)	27-52
Linoleat (C18:2)	5,0-14
Linolenat (C18:3)	<1,5

(Salunkhe et al, 1992)

## 3. Transesterification reaction

The predominant triglyceride content in palm oil can be converted to glycerol through transesterification. The triglyceride content reacts with alcohol (accelerated by the catalyst) and produces biodiesel, and will produce a by-product in the form of glycerol (Haryanto et al, 2015).



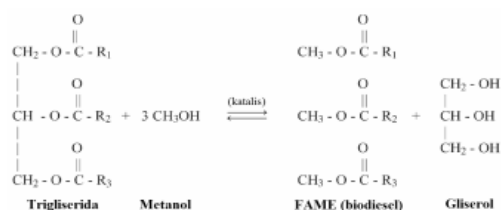


Fig. 1: Transesterification reaction

(Haryanto et al, 2015)

## 4. Glycerol

Glycerol (also known as glycerin) is polyol (1,2,3-propanetriol), which is naturally present in the structure of triglycerides, which are fatty acid esters from alcohol (Garcia et al, 2013). Glycerol, as a polyol, is capable of dissolving many organic and inorganic compounds, including complex metal-transitions. The incompatible nature of some common organic solvents, such as hydrocarbons, ethers and esters, allows easy separation of reaction products, and in the best case, the possibility of reusing the glycerol phase in subsequent reactions. This is very useful in the case of reactions catalyzed by transition metal complexes. The use of glycerol as a solvent also has several notable disadvantages, such as high viscosity (1200 cP at 20°C) and low solubility of compounds and gases that are very hydrophobic, which limits the possibility of their use. Weakness of viscosity is usually overcome by heating above 60 °C or by using co-solvent.

There are classifications of solvents derived from glycerol such as esters (such as acetone), carbonate (glycerol carbonate), acetal (formal glycerol) and ketal (solketal).

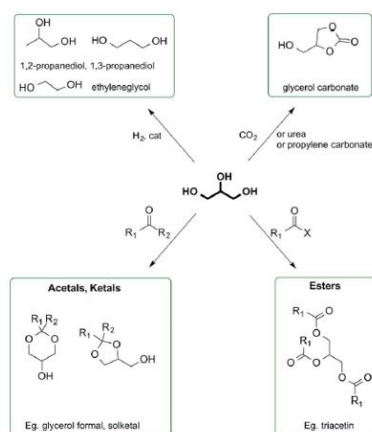


Fig. 2: Types of Green Solvent produced from Glycerol

(Moity et al, 2015)

## 5. Purification glycerol

Crude glycerol byproduct of the biodiesel industry generally has a low purity level with 40-50% glycerol content because it still contains a lot of impurities in the form of methanol residues, catalyst residues, and water. In order to be used in various industries and increase the selling value, the glycerol needs to be purified first. Glycerol with a higher level of purity (80-99%) is needed as raw material for the cosmetics industry, pharmaceutical industry, paper industry, paint and varnish industry, textile industry, food industry, tobacco processing, oleochemicals, and lubricants. One way is to use a vacuum distillation method in the hope that the purity of glycerol reaches 90% (Mulia, 2015). The choice of vacuum distillation as an advanced purification method is based on the type of impurities that are still present in 80% glycerol in the form of methanol and water that can be removed by evaporation but does not require temperatures too high as in simple distillation so as to minimize the energy used.

## 6. Glycerol derivative products methods

Glycerol is used as a precursor for the production of various chemical commodities such as 1,2-propanediol, 1,3-propanediol, ethylene glycol, propanol, hydrocarbons, acrolein, dihydroxyacetone, glyceric acid, syngas, hydrogen, glyceril ether, glyceril ester, glycerol carbonate, 1,3-dichloro propanol, polyglycerol and glycerol acetal and ketal through several methods such as fermentation, hydrogenolysis, pyrolysis, oxidation, etherification, dehydrasesterification, carboxylation, halogenation, polymerization and glycerol acetalization. Furthermore, glycerol is of great concern as a 'green solvent' in synthetic organic chemistry because of its good physical and chemical properties. Compatibility with most organic / inorganic compounds, high boiling point, negligible vapor pressure, easy dissolution and harmless properties, simple handling and storage provides an innovative way to utilize glycerol used as a green solvent.

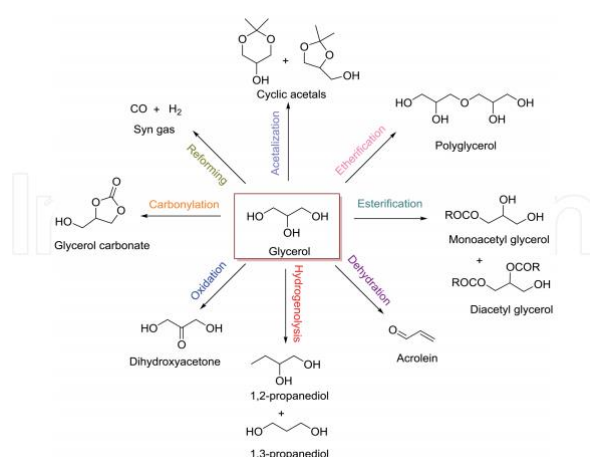


Fig. 3: Various Types of Green Solvent and Methods produced from Glycerol

### 6.1 Glycerol Hydrogenolysis

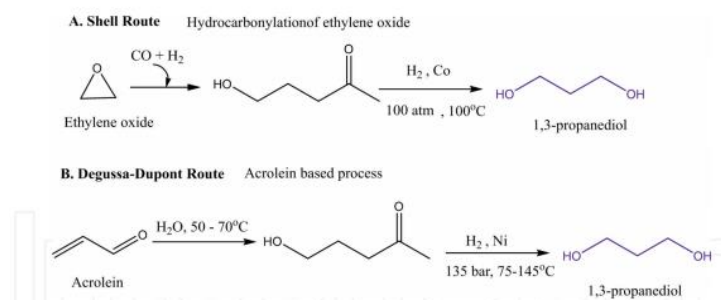
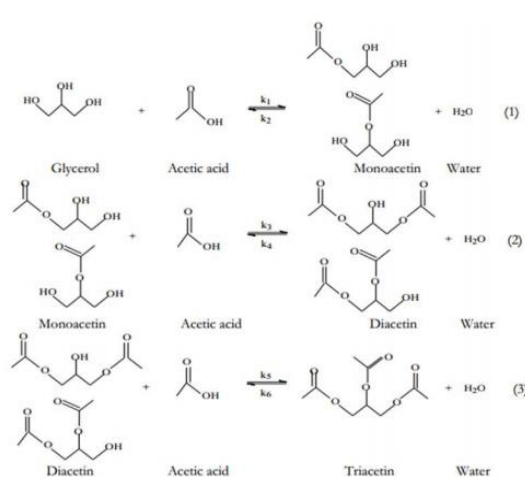


Fig. 3: Conventional Methods for Producing 1,3-Propanediol

One of the derivatives of the hydrogenolysis method is 1,3-propanediol. There are two well-known chemical methods for the synthesis of 1,3-propanediol (1,3-PDO). The first method uses ethylene oxide as a raw material and is known as the 'Shell' route is a two-step process that uses hydroformylation of ethylene oxide to 3-hydroxypropionaldehyde (3-HPA) and subsequent hydrogenation from 3-HPA to 1,3-PDO. The second 1,3-PDO synthesis method is the 'Degussa-DuPont' route and uses acrolein as a raw material. Hydration produces 3-HPA which is then hydrogenated to 1,3-PDO. However, the chemical synthesis method 1,3-PDO is a petroleum-based method and has many advantages such as high pressure, high temperature and catalyst. Support, the 1,3-PDO production cost is very high. The application of 1,3-propanediol is in the manufacture of polymethylene terephthalate (PTT) or polypropylene terephthalate (PPT), biodegradable polyester used in the manufacture of textiles and carpets, cosmetics, chemicals, chemicals, and cooling chemicals, food and beverages, cleaning fluid, water-based ink, heat transfer liquid and unsaturated polyester resin.

## 6.2 Glycerol Acetalization

Glycerol acetylation is one of the most common ways to produce monoacetin, diacetin and triacetin. Acetylation is a reaction that initiates acetyl functional groups into chemical compounds. Acetylation includes substitution of a hydrogen atom of a hydroxyl group with an acetyl group to produce an acetoxy group. The chemical used is glycerol which has a hydroxyl group and acetic acid that belongs to the acetyl functional group.



**Fig. 4: Acetalization Reaction Produced from Glycerol**

### 6.3 Glycerol Carbonylation

Glycerol carbonate (GC) is already an industrial common product, commercially available, with applications in many industrial processes. There are several general procedures to prepare glycerol carbonate from glycerol, either directly or through reactive intermediates, such as chlorohydrins or glycidol.

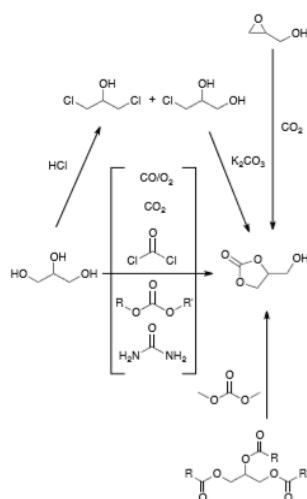


**Fig. 5: General procedures for the synthesis of glycerol carbonate from glycerol**

One of the advantages of glycerol carbonate in this context is that its ionizing and dissociating abilities are very close to those of water, preventing protein denaturation. These products are popular in the food industry as benign low hydrophilic-lipophilic balance (co)emulsifiers, rheological modifiers and dietary fat and oils.

## 6.4 Glycerol Esterification

One of the derivative products is glycerol triheptanoate which is carried out by esterification reaction between glycerol and heptanoic acid (Dakka et al., 2010). The reactions that occur as described are as follows:

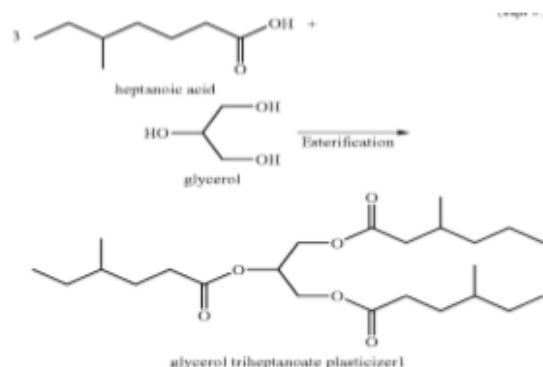


Fig. 6: Reaction of tri heptanoate ester formation

In making this glycerol derivative hexanoic acid is first made from the reaction of hexane with  $H_2$  and CO gas. The reaction will produce hexanal, which will then be oxidized to hexanoic acid. The product use of glycerol triheptanoate is an environmentally friendly plasticizer with advantages: it is phthalate free and easy to melt, low evaporation and is a glass transition (Sears & Darbey, 1982).

## 7. Conclusion

Palm oil has a lot of triglyceride content when reacted with methanol through a transesterification reaction that produces biodiesel and will produce a by-product in the form of glycerol. Glycerol has a low price value so that it has the potential to be used as a green solvent. Methods that can be used to obtain glycerol derivatives are fermentation, hydrogenolysis, pyrolysis, oxidation, etherification, dehydrasesterification, carboxylation, halogenation, polymerization and glycerol acetylation.

## 8. References

- Darnoko, D dan Cheryan, M, 2000. Kinetic of Palm Oil Transesterification in a Batch Reactor. *J. Am. Oil Chem. Soc.*, 77, 1263-1267
- Dakka, J.M., Mozeleski., E.J., Baugh, L.S., 2010. Process for Making Triglyceride Plasticizer from Crude Glycerol. US Patent Application Publication.
- Gu, Y.; Jérôme, F. 2013. Bio-based solvents: An emerging generation of fluids for the design of eco-efficient processes in catalysis and organic chemistry. *Chem. Soc. Rev.* 2013, 42, 9550–9570.
- Julianti, Wardani, Gunardi, Rosyadi. 2014. Pembuatan Biodiesel dari Minyak Kelapa Sawit RBD dengan Menggunakan Katalis Berpromotor Ganda Berpenyangga  $\gamma$ -Alumina ( $CaO/MgO/\gamma-Al_2O_3$ ) dalam Reaktor Fluidized Bed. *Jurnal Teknik POMITS*. Vol. 3, No. 2.
- Haryanto, Silviana, Triono, Prabawa. 2015. Produksi Biodiesel Daro Transesterifikasi Minyak Jelantah dengan Bantuan Gelombang Mikro: Pengaruh Intensitas Daya dan Waktu Reaksi Terhadap Rendemen dan Karakteristik Biodiesel. *Jurnal AGRITECH*. Vol. 35, No. 2. Hal 234-240.
- Moity, Laurianne, Adrien Benazzouz, Valérie Molinier, Véronique Nardello-Rataj, Mohammed Kamal Elmkaddem, Pascale de Caro, Sophie Thiébaud-Roux, Vincent Gerbaud, Philippe Marion, Jean-Marie Aubrya. 2015. *Glycerol Acetals and Ketals as Bio-based Solvents: Positioning in Hansen and COSMO-RS spaces, Volatility and Stability towards Hydrolysis and Autoxidation*.
- N. García, P. García-García, M. A. Fernández-Rodríguez, D. García, M. R. Pedrosa, F. J. Arnáiz, and R. Sanz, *Green Chem.*, 2013, 15, 999–1005.

# Feasibility Study of Thermoelectric Generator Configuration in Electricity Generation

W. Priharti\*, M. Ramdhani, F.R.J. Putra, A. Khansalya

School of Electrical Engineering, Telkom University, Bandung - INDONESIA

\* Corresponding author e-mail: wpriharti@telkomuniversity.ac.id

## Abstract

Thermoelectric generator (TEG) is a device that can directly convert heat into electrical energy based on temperature gradient. Higher temperature gradient produces higher generated energy. This study aims to analyse three different configurations of TEG in order to obtain an optimum temperature gradient. The configurations were (a) TEG only, (b) TEG attached to heat sink and (c) TEG attached to heat sink and enclosed by ceramic. TEG attached to heat sink was found to be the best configuration with the highest generated voltage and power of 0.35 V and 11.33 mW respectively. Using this configuration to store the energy, the increase of 19% capacity of 3.7 V 200 mAh LiPo battery was obtain within 300 minutes.

*Keywords: Waste heat, electricity generation, thermoelectric generator, thermoelectricity.*

## 1. Introduction

The traditional energy which sources from fossil fuels such as petroleum and coal remain a major source of electricity today. However, these sources are currently depleting and have caused several pollution problems. Thus, in the recent years, the alternative and renewable energy has become more attractive for electricity generation due to advantages towards clean environment and sustainability issues (Johar, 2017).

Various renewable energy sources such as solar, wind, hydro energy and biomass can be used to generate electricity in a large scale. Apart from that, there are a lot of research activities in the lower-level electricity generation using different physics phenomenon such as pressure (Liu et al., 2018), vibration (Wei et al., 2017), radio frequency (RF) (Aparicio et al., 2016) and thermal energy (Moreno et al., 2016).

The conversion of thermal energy into electrical energy can be generated by a device called Thermoelectric Generator (TEG). This device utilizes the thermoelectric effect known as Seebeck effect that was first discovered in 1821 by Thomas Johann Seebeck (Enescu, 2019). The effect occurs when a temperature difference across the surface of two conductors producing a voltage  $V$  between its open ends. One side of the conductors has the hot temperature  $T_h$  and another side has the cold temperature  $T_c$  (where  $T_h > T_c$ ). The value of the voltage is proportional to the temperature difference between the two surfaces that can be written as:

$$V = \alpha (T_h - T_c) \quad (1)$$

where  $V$  is the voltage across the thermoelectric module,  $\alpha$  is the Seebeck coefficient,  $T_h$  is the temperature at the hot side, and  $T_c$  is the temperature at the cold side.

A TEG consists of an array of p and n semiconductors, connected electrically in series and thermally in parallel. These conductors are connected electrically in series to increase the operating voltage and connected thermally in parallel to increase the thermal conductivity. The main characteristics of TEG is the absence of mechanical moving part, small in size, fully scalable, long lived and silent (Ahiska and Mamur, 2014). Recent studies also reported the increasing use of TEG in utilizing waste heat such as in industrial plants, automobile engines, stoves and many others (Zaman et al., 2017, Pohekar et al., 2018). Although the heat produced from waste heat is relatively small, TEG is believed to be an ideal solution in low power applications that have limited electrical grid access and require low maintenance (Dell et al., 2019).

The TEG efficiency  $\eta$  strongly depends on the temperature gradient between the hot and cold side  $\Delta T$  of the TEG, the thermoelectric figure-of-merit  $Z_T$ , and the TEG design (cross-sectional area, length and shape) (Ali et al., 2013). The temperature gradient can be obtained by manipulating the condition of TEG surrounding, for example using cooler to maintain the cold side temperature, enveloping the TEG with an insulator and so on.

This study aims to find the recommended configuration of TEG module to obtain significant temperature gradient. Three configurations will be used and a constant heat will be given. For each case, the performance of TEG will be evaluated.

## 2. Method

The TEG used in this system was Tegpro TE-MOD-22W7V-56. This TEG could give a maximum of 21.7 Watt output power with 7.2 VDC output voltage. The based material of this TEG was Bismuth Telluride ( $\text{Bi}_2\text{Te}_3$ ) with a dimension of  $(56 \times 56 \times 5)$  mm<sup>3</sup>. This TEG can operate continuously at 330°C and intermittently up to 400°C. The highly conductive graphite sheets was layered on both sides of the ceramic plates to provide low thermal resistance.

The diagram block of this system is shown in Fig.1. In this figure, the TEG was indicated by asterisk. It means that this study analysed the performance of TEG in three different configurations: (1) basic configuration of TEG (TEG only), (2) TEG attached to heat sink, (3) TEG attached to heat sink and enclosed by ceramic. The figure of these configuration are respectively shown in Fig.2 (a), (b) and (c). The heat sink was attached at the cold side of TEG and used as a passive cooler in order to dissipate heat. All of these configurations were carried out in an open circuit condition (without load).

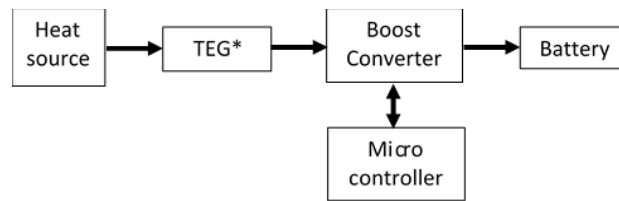


**Fig. 1:** The block diagram of the system. The asterisk symbol in TEG indicated that the experiment was carried out with three different configurations

A heater with a rating of 12V 3A was used to generate heat source on the hot side. A heater was used due to the easiness in controlling the produce heat for a laboratory environment. The TEG was exposed to a constant heat of 100°C for 60 minutes. The experiment was carried out in a room temperature of 25°C.

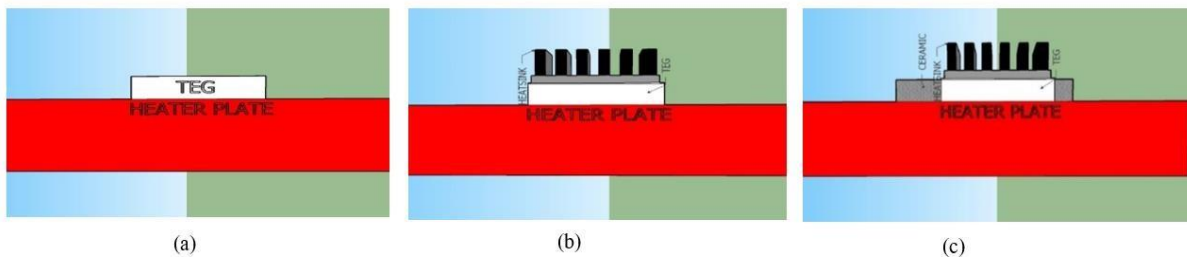


**Fig. 2:** Three different configuration of TEG used in the study: (a) basic configuration of TEG (TEG only), (b) TEG attached to heat sink, (c) TEG attached to heat sink and enclosed by ceramic

The performance of each configurations was analyzed and the best configuration were selected. The selected configuration was then used to analyses the power storage performance of the TEG. LiPo battery with a rating of 3.7 V 200 mAh (voltage range 3.1 – 4.1 V) was used as the storage. A DC-DC boost converter CE8301 was also used to stabilize and to step-up the output voltage before being storage in the battery. An Arduino Uno ATMEGA328 with 5 V operating voltage was used as the microcontroller to control the operation.

### 3. Result and Discussion

Fig.3 illustrates the variation of voltage and temperature gradient obtained from the heating of TEG for 60 minutes.  $V_1$ ,  $V_2$  and  $V_3$  indicated the output voltage for configuration: 1) basic configuration of TEG (TEG only), (2) TEG attached to heat sink, (3) TEG attached to heat sink enclosed by ceramic respectively. The same naming will be used throughout this paper for all parameter being studied, i.e.  $\Delta T_1$ ,  $\Delta T_2$ ,  $\Delta T_3$ ,  $P_1$ ,  $P_2$ ,  $P_3$  and so on.

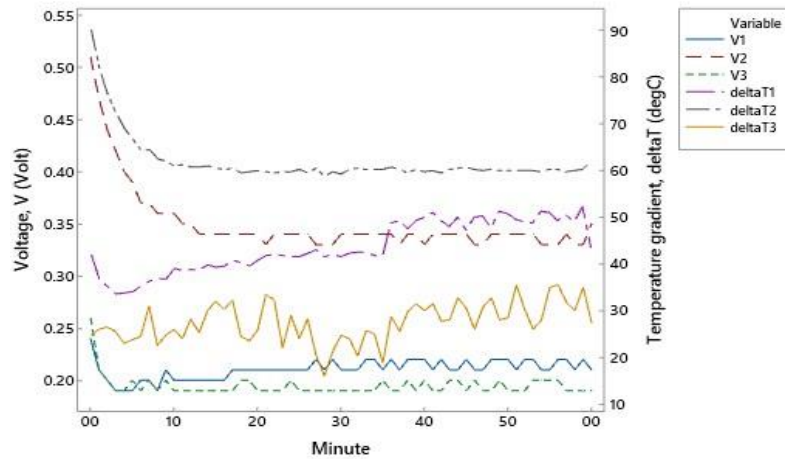


Fig. 3: The relationship between temperature gradient and the voltage generated by TEG

From this figure, it can be clearly seen that the voltage  $V$  generated by TEG is exactly proportional to the temperature gradient  $\Delta T$  between the hot side and the cold side of the TEG. The highest output voltage ( $=0.51$  V) obtain by configuration (2) with a highest temperature gradient ( $=90.19^\circ\text{C}$ ). It can also be observed that this highest output voltage was occurred within the first minute and continue to decrease until it reached an almost constant temperature gradient and output voltage. The fact that this phenomenon occurred seem to indicate that the best performance (the highest output voltage) can be obtained by TEG when the system have the largest temperature gradient. This clearly followed the  $V$  and  $\Delta T$  relationship between given by equation (1).

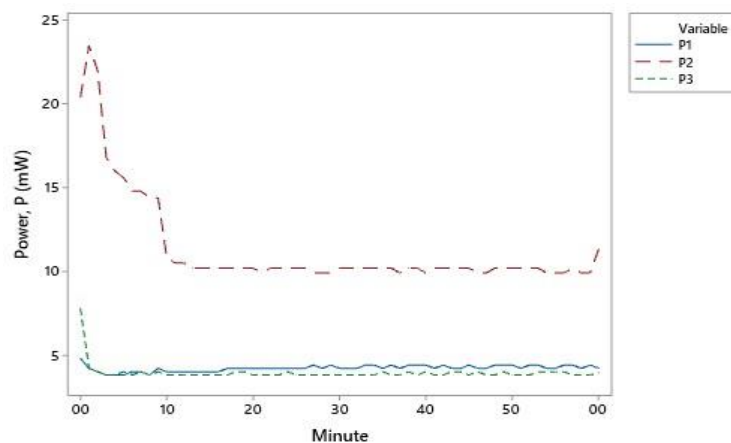


Fig. 4: The output power generated by TEG for three configurations

The output power generated by TEG for three configurations ( $P_1$ ,  $P_2$  and  $P_3$ ) is shown in Fig.4. The power  $P$  was calculated from the equation of voltage  $V$  times current  $I$  ( $P = V I$ ). For each configuration, an almost constant current of  $0.02 - 0.03$  Ampere ( $20 - 30$  mA) was produced. The highest generated power was recorded by configuration (2), followed by configuration (1) and (3). In configuration (2) where heat sink was attached to the cold side of TEG, the temperature gradient seems to be larger since the heat sink could act as the passive cooler.

However, the same phenomenon was not occurred in configuration (3) that was also attached with heat sink but with enclosed ceramic. The ceramic that originally planned as the additional cooler was actually trapped heat in the TEG. This trapped heat not only increase the temperature on the hot side but also on the cold side of the TEG. The results of this eventually yielding a lower temperature gradient thus lower generated power. The make the performance analysis of the tree configuration of TEG easier, the mean value of voltage, current and power generated by each configuration are concluded in Table 1.

**Table 1: The mean value of voltage, current and power generated by TEG using three different configurations**

Parameter	(1) <sup>a</sup>	(2) <sup>b</sup>	(3) <sup>c</sup>
Voltage (V)	0.21	0.35	0.19
Current (A)	0.02	0.03	0.02
Power (mW)	4.21	11.33	3.93

<sup>a</sup> Basic configuration of TEG (TEG only); <sup>b</sup> TEG attached to heat sink; <sup>c</sup> TEG attached to heat sink and enclosed by ceramic

Table 1 is clearly shown the best performance of TEG with number (2) configurati0n i.e TEG attached to heat sink with a generated voltage and power of 0.35 V and 11.33 mW respectively. Using the best configuration, an effort to store the generated power using a 3.7 V 200 mAh LiPo battery with a DC-DC boost converter was attempted. It was found that the initial voltage of the battery at minute 0 was 3.16 V (6% capacity) and the charging was started at minute 7 with an increase of 0.02 V (as shown in Fig. 5). The voltage was gradually increase and reach a voltage of 3.36 V (25% capacity) at minute 300. From this test, it was found that the stored power of a single TEG is low with only 19% increase of battery capacity within 300 minutes (5 hours). Several TEG connected in series and parallel could be used to maximise the generated voltage as well as the generated current.

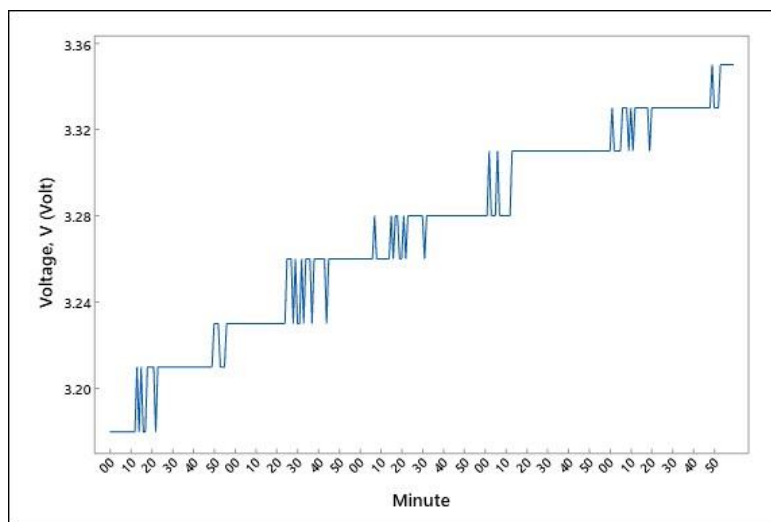


**Fig. 5: The increase of TEG generated voltage stored in the battery**

## 4. Conclusion

Feasibility study on the generation of electricity from heat was carried out using a single TEG. Three configurations of TEG were used and the configuration that given the best performance was selected i.e. TEG attached to heat sink. This configuration was used to store the power generated by TEG and the increase of 19% capacity of 3.7 V 200 mAh LiPo battery was obtain within 300 minutes. The used of several TEG connected in series and parallel are proposed in the next study to maximize the generated voltage and current.



## 5. Nomenclature

I	Current	A	T	Temperature	°C
V	Voltage	V	$\alpha$	Seebeck's coefficient	V/°C
P	Power	W	$\Delta T$	Temperature gradient	°C

## 6. Acknowledgements

The authors wish to thank Direktorat Penelitian dan Pengabdian Masyarakat (PPM) Telkom University for the financial support to attend this conference.

## 7. References

- Ahiska, R and Mamur, H. 2014. A Review: Thermoelectric Generators In Renewable Energy. *International Journal Of Renewable Energy Research*, 4, 128-136.
- Ali, H., Sahin, A.Z. and Yilbas, B.S. 2014. Thermodynamic Analysis of A Thermoelectric Power Generator Inrelation to Geometric Configuration Device Pins. *Energy Conversion and Management*, 78, 634-640.
- Aparicio, M.P., Bakkali, A. Sebastian, T., Sogorb, V. and Bou, A. 2016. Radio Frequency Energy Harvesting - Sources and Techniques, 155-169. <http://dx.doi.org/10.5772/61722>.
- Dell, R., Petralia, M.T., Pokharel, A. and Unnthorsson, R. 2019. Thermoelectric Generator Using Passive Cooling, 1-37. <http://dx.doi.org/10.5772/intechopen.85559>
- Enescu, D. 2019. Thermoelectric Energy Harvesting: Basic Principles and Applications, 1-37. <http://dx.doi.org/10.5772/intechopen.83495>.
- Johar, M. A. 2017. Feasibility Study of Thermal Electric Generator Configurations as Renewable Energy Sources. *Journal of Physics: Conference Series*, 914, 123-135.
- Liu, H., Zhong, C., Lee, S.W. and Lin, L. 2018. A Comprehensive Review on Piezoelectric Energy Harvesting Technology: Materials, Mechanisms, and Applications. *Applied Physics Reviews*. <https://doi.org/10.1063/1.5074184>.
- Moreno, R.J., Grbovic, D. and Pollman, A. 2016. Harvesting Waste Thermal Energy From Military Systems. *Proc. of the ASME 2018 Power and Energy Conference*, 1-6, June 2016.
- Pohekar, P., Alaspure, P., Punase, P. and Tikhe, S.G. 2018. Automotive Waste Heat Harvesting for Electricity Generation using Thermoelectric Generator A Review. *International Research Journal of Engineering and Technology*, 5, 477-481.
- Wei, C. and Jing, X. 2017. A Comprehensive Review on Vibration Energy Harvesting: Modelling and Realization, *Renewable and Sustainable Energy Reviews*, 74, 1-18.
- Zaman, H. Shourov, C., Mahmood, A. and Siddique, N.A. 2017. Conversion of Wasted Heat Energy into Electrical Energy Using TEG. *IEEE*, 1-5.

## Pressure Reducing Station Design for small scale business from 200 bar to 2 bar pressure

**Pratomo Setyadi**

Fire Safety Engineering

The Faculty Of Engineering, State University Of Jakarta, Indonesia

Email: pratomo\_setyadi@yahoo.com +62 8119791981

### Abstract

This research aims to create a design tool for pressure reducing station for tube cradle 200 bar where the initial temperature of the CNG is -40°C. As an environmentally friendly fuel, many advantages gained when using CNG, among others: huge gas reserves, produced in the country, it's cheap, and friendly environment. Reducing pressure from 200 bar to usable pressure at 2 bar never been easy as cheap. Small business-like restaurants and caterings are looking for fuel sources that cheap and safe in usage. CNG in distribution are tubed in 200 bar cradle and not easy to use instantly, despite its cheap price and high calorie given.

These studies are either research and development methods and the results of this research generate a pressure reducing station, which can lower the pressure to 2 bar. By discharging it into heat pump system, reducing pressure from 200 bar to 2 bar in cheap and safe way are accomplished. The reducing station has been tested as heat exchanger and volume control to maintain it safety and performance. It discusses the process of testing the pressure reducing station, which includes the maximum temperature of water, temperature of gas in the tubing before and after passing the heat exchanger, temperature of the gas in the container header, final temperature of the gas after exiting the regulator, determining the discharge of gas that comes out for 1 minute and the height of the fire. Temperature testing uses a thermocouple tool calibrated with Arduino Uno.

The results of the study are specifications of pressure reducing station equipment, as follows: Maximum temperature of water: 76.5 °C, temperature of gas in the tubing before passing through the heat exchanger for 5 stage gate opening: 34.75 °C - 35.75 °C, then after heat exchanger: 54.25 °C - 54.75 °C, gas temperature in the header: 36.78 °C, final gas temperature in the regulator: 45.75 °C, gas discharge testing for 5 stage gate opening: 13 m3 - 24 m3 and fire height testing for 5 stage gate opening : 33 cm - 56 cm.

*Key words: pressure drop, pressure reducing station, compressed natural gas, small scale business.*

---

### 1. Introduction

Gas is one of the fuels that has recently been increasingly developed in Indonesia as an alternative energy. Gas fuel itself consists of two types, namely Compressed Natural Gas (CNG) and Liquid Petroleum Gas (LPG). CNG is made by compressing CH<sub>4</sub> methane extracted from natural gas. Whereas LPG, its main components are dominated by propane C<sub>3</sub>H<sub>8</sub> and butane C<sub>4</sub>H<sub>10</sub>, with other light hydrocarbon contents such as ethane C<sub>2</sub>H<sub>6</sub> and pentane C<sub>5</sub>H<sub>12</sub>. Compressed Natural Gas or CNG is a fuel derived from natural gas with the main element of methane gas being compressed, maintained and stored in a specially designed pressure vessel. CNG contains the main components in the form of methane CH<sub>4</sub> and ethane C<sub>2</sub>H<sub>6</sub>. CNG is made by compressing methane extracted from natural gas (S. Zaini, et al., 2013). CNG has a higher hydrogen to carbon ratio than fuel oil and produces less CO<sub>2</sub> per unit of energy (L. Kirk, et al., 2014). CNG has a lower price than fuel oil, higher octane content, exhaust emissions that are cleaner and environmentally friendly compared to fuel oil. (BS and Nature, 201). The development and utilization of natural gas in Indonesia are being intensified due to the mandate of Law No. 22 of 2001, natural gas itself is divided into 2 types, namely Compressed Natural Gas (CNG) in the process of compressing CH<sub>4</sub> methane extracted from natural gas and Liquid Petroleum Gas (LPG) which is dominated by propane C<sub>3</sub>H<sub>8</sub>, butane C<sub>4</sub>H<sub>10</sub> with hydrocarbon content. Other lighter examples are ethane C<sub>2</sub>H<sub>6</sub> and pentane C<sub>5</sub>H<sub>10</sub>. Pressure Reducing Station is a device consisting of a heated pipe that is used as a pressure reducer, the gas which was originally pressurized 200 bar is changed by heating, so the pressure can be reduced to 2 bar which can then be used for industrial purposes. CNG heater or we can call this part with a heat

exchanger or gas meter. In this study the authors tested the Pressure Reducing Station tool to reduce the CNG cradle tube pressure from 200 to 2 bar in accordance with the assumptions of the calculation and design. Natural gas in Indonesia is classified as high, but the utilization of natural gas in Indonesia is still minimal, so further utilization is needed. Pressure reducing station is a tool that can reduce gas pressure from 200 bar to 2 bar, therefore researchers use a pressure reducing station for natural gas utilization and industrial stove usage from 200 bar to 2

## 2. The corner stone of the theory

### 2.1 The concept of work Pressure Reducing Station

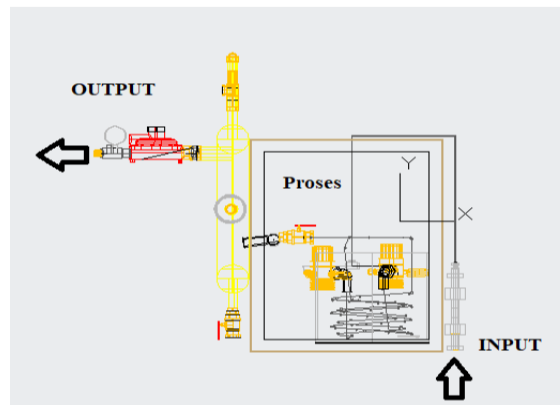


Fig. 1: the concept of work pressure reducing station

- Process input: using a hose interconnector hose with jet tube cradle cng to male conector which is already installed in the panel box to ball valve high pressure in the process fluid flows from the tube hose → → → high pressure ball valve tubing → male connector tee → opening 2 fluid lines → entry to 2 scote universal regulator to lower the pressure is high to medium. Proses : Setelah fluida mengalir dari scote regulator universal → spiral tube for heat exchange → gas heating by water transfer → medium pressure ball valve 2.
- Output: After fluid passes through the ball valve → forwarded using the connector leading into header → fluid capacity gas header → in the header there is a valve and ball valve safety → next forward towards regulators medium to low pressure → connector towards the stove.

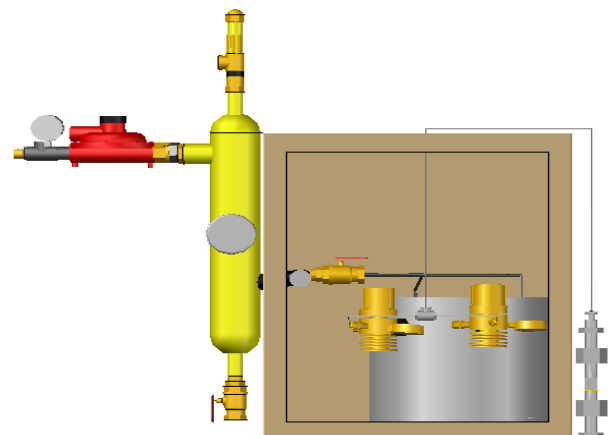
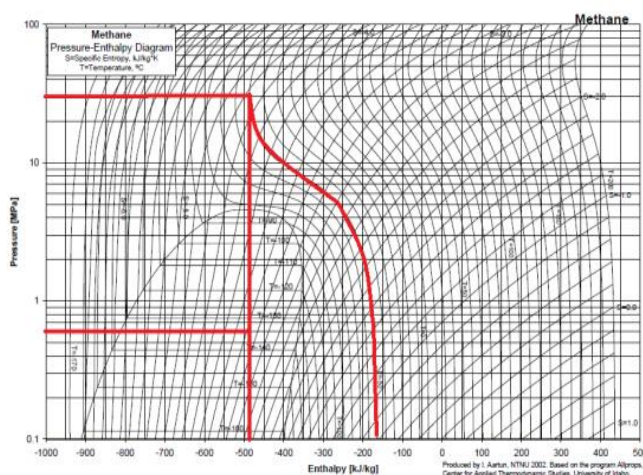


Fig. 2: Diagram p-h Methane

## 2.2 Natural gas

Natural gas is a natural resource with the third largest reserves in the world after coal and petroleum. Natural gas or gas often called Earth is material or material that consists of fossils and fossil formed in the form of gas. The main component in natural gas is methane (CH<sub>4</sub>), which is the shortest chain hydrocarbon molecules and lightest. Natural gas also contains molecules of heavier hydrocarbons such as ethane (C<sub>2</sub>H<sub>6</sub>), propane (C<sub>3</sub>H<sub>8</sub>) and butane (C<sub>4</sub>H<sub>10</sub>), as well as gases containing sulfur (sulphur).

## 3. Research methodology

The purpose of this study is to find out:

- Working temperature of the water.
- Temperature of the gas in the tubing before passing through the heat exchanger.
- Temperature of the gas in the tubing after passing the heat exchanger.
- Gas temperature in the header.
- Final temperature of the gas in the regulator.
- Discharge of gas that comes out for 1 minute.
- Height of the fire

## 4. Discussion

### 4.1 Testing the maximum temperature of the water

The results of testing the maximum water temperature are 76.5 °C for 2 hours of testing. The test was carried out using a thermocouple test instrument calibrated with Arduino Uno. So after averaging, it gets 75.25 °C. The test is done by heating water using 600 watts heating element immersed in water to give heat to be absorbed by pipe for reducing the pressure.

### 4.2 Testing the Temperature of the Gas in the Tubing Before passing the Heat Exchanger

Testing is done with the opening of the stove opening of 20%, 40%, 60%, 80%, 100% within 1 minute by using a thermocouple calibrated with Arduino Uno. Here is a table of the average results of testing the temperature of the gas in the tubing before passing through the heat exchange:

No	Pengujian	Rata-rata
1	Bukaan 20%	34°C
2	Bukaan 40%	34,25°C
3	Bukaan 60%	34,5°C
4	Bukaan 80%	34,75°C
5	Bukaan 100%	35°C

### 4.3 Testing the Gas Temperature in Tubing After Passing the Heat Exchanger

Testing is done with the opening of the stove opening of 20%, 40%, 60%, 80%, 100% within 1 minute by using a thermocouple calibrated with Arduino Uno. Here is a table of the average results of testing the temperature of the gas in the tubing before passing through the heat exchanger:

No	Pengujian	Rata-rata
1	Bukaan 20%	53,25°C
2	Bukaan 40%	53,5°C
3	Bukaan 60%	53,75°C
4	Bukaan 80%	54°C
5	Bukaan 100%	54,25°C

#### 4.4 Gas Testing on the Header

Testing the temperature of the gas in the header is done within 1 minute, using a thermocouple test instrument calibrated with Arduino Uno. After obtaining data results as in the table above, it can be averaged to 36.5 °C.

#### 4.5 Testing the final gas temperature in the regulator

Testing the final gas temperature in the regulator is done within 1 minute, using a thermocouple test instrument calibrated with Arduino Uno. After obtaining data results in the table above, it can be averaged to 41.25 °C.

#### 4.6 Gas Discharge Testing

<b>Bukaan</b>	<b>Debit gas yang keluar <math>m^3/\text{menit}</math></b>
20 %	13
40 %	16
60 %	19
80 %	21
100 %	24

This test aims to read flow of gas that comes out within 1 minute at the stove openings of 20%, 40%, 60%, 80%, 100%.

#### 4.7 Fire Height Testing

<b>Bukaan</b>	<b>Tinggi Api Cm</b>
20 %	33 cm
40 %	39 cm
60 %	45 cm
80 %	51 cm
100 %	56 cm

This test aims to determine the height of fire that comes out within 1 minute at the stove openings of 20%, 40%, 60%, 80%, 100%.

## 5. Conclusion

After testing the pressure reducing station tools the results are as followed:

- Testing the maximum temperature of water in the heat exchanger results in 75.25 °C
- The average results of testing the temperature of the gas in the tubing before passing the heat exchanger at each opening, averaging 34,2 degrees.
- The average gas temperature test in the tubing after passing the heat exchanger at each opening, averaging 53.5
- Gas temperature at the header is 36.5 °C
- Gas temperature at the regulator is 41.25 °C
- Discharge of gas that comes out at each opening, as follows:
  - Aperture of 20% = 13  $m^3/s$
  - Aperture of 40% = 16  $m^3/s$
  - Aperture of 60% = 19  $m^3/s$
  - Aperture of 80% = 21  $m^3/s$
  - Aperture of 100% = 24  $m^3/s$
- Fire height at each opening, as follows:
  - The aperture of 20% = 33 cm
  - The aperture of 40% = 39 cm
  - The aperture of 60% = 45 cm
  - The aperture of 80% = 51 cm
  - The aperture of 100% = 56 cm

These results show that pressure reducing station that being designed is suitable for small scale industry such as restaurants or catering, by having low to medium debit, low temperature operation and sufficient flame length.

## 6. References

- SAPUTRI, Z. N. (2014). Aplikasi Pengenalan Suara Sebagai Pengendali Peralatan Listrik Berbasis Arduino Uno. *Aplikasi Pengenalan Suara Sebagai Pengendali Peralatan Listrik Berbasis Arduino Uno*, 1, 8.
- Budisatriyo, C. A., Agustawan, H., &
- Aritonang, S. (2018). Meningkatkan penggunaan compressed natural gas sebagai bahan bakar angkutan umum jakarta. *Jurnal Ketahanan Energi*, 4(1), 1–25.
- Kurniaty, I. (2017). Evaluasi Aspek Finansial Penghematan Bahan Bakar Bensin Menjadi Cng (Compressed Natural Gas) Untuk Mobil Pribadi. *Jurnal Konversi*, 6(1), 43. <https://doi.org/10.24853/konversi.6.1.43-50>
- Elisabet, Y. A., E-commerce, K., Produk, P., & Cristie, A. (2014). Pengaruh perubahan laju aliran terhadap tekanan jenis aliran yang terjadi pada alat uji praktikum mekanika fluida. 2(September), 1–3. <https://doi.org/10.1080/00173139109432020>
- Prayitno, F. N. U. R. (2016). *RC GUARD P1-X: Rancang Bangun Mobile Radio Control Berbasis Arduino Nano Sebagai Pendeteksi Gas 1 FAJAR NUR PRAYITNO*. 1–6.
- Resmiyanto, R. (2014). Perumusan Model Moneter Berdasarkan Perilaku Gas Ideal. *Jurnal Riset Dan Kajian Pendidikan Fisika*, 1(1), 31. <https://doi.org/10.12928/jrkpf.v1i1.1512>
- (2015). Analisis Dampak Radiasi Sinar-X Pada Mencit Melalui Pemetaan Dosis Radiasi Di Laboratorium Fisika Medik. *Jurnal MIPA*, 38(1), 25–30.
- Ardianto, R. (2012). *Koefisien perpindahan panas pada pipa bulat skripsi*.
- Setiawan, J. A. (2016). Mencari Landasan Hukum Pembentukan Badan Penyangga (Aggregator) Gas Alam. *Jurnal Hukum Novelty*, 7(2), 237. <https://doi.org/10.26555/novelty.v7i2.a5470>

## Enhancing the Nickel Recovery of Morowali Nickel Laterite in Atmospheric Citric Acid Leaching

Feby Aryanhi<sup>1,\*</sup>, Regna Tri Jayanti<sup>2</sup>

<sup>1,2</sup>Departement of Mineral Chemical Engineering, Politeknik Industri Logam Morowali (PILM),  
Morowali- INDONESIA

\* Corresponding author e-mail: febyaryanii16@gmail.com

### Abstract

Morowali has a lot of laterite ore deposits which is one of the mineral resources containing several kinds of metal elements, consist of Iron (Fe), Silicone (Si), Nickel (Ni), Chromium (Cr), Manganese (Mn), Calcium (Ca), Phosphate (P), Zinc (Zn), Vanadium (V), and Scandium (Sc). Nickel is a metal that have high economic value because it various benefits, such as the production of stainless steel, electric plates, coins, batteries, and catalysts. There are two common nickel laterite processing that are pyrometallurgy and hydrometallurgy. In this study, hydrometallurgy method is applied to process nickel laterite of Morowali. An important step in this process line is ore leaching. This research is conducted to find a condition in atmospheric leaching of Morowali nickel laterite. This investigation work deals with varying the concentration of citric acid of 0.5 to 2.0 M and reaction time 10 to 120 minutes. The constant parameter are leaching temperature (K), stirring speed (rpm), and particle size (mesh). The results showed that the higher concentration of citric acid, the higher nickel recovery. The good conditions is obtained at concentration of citric acid 2.0 M and leaching time of 120 minutes, it proved by the amount of nickel recovery reached 1197.50 ppm.

*Keywords: laterite ore; atmospheric leaching; citric acid; hydrometallurgy; and nickel recovery*

### 1. Introduction

In nature, nickel is found in the form of sulfides and oxides. Globally, around 72% of the world's nickel reserves are in oxide rocks, commonly called laterites and the remaining sulfide rocks. However, only around 42% of total world nickel production is sourced from laterite ore (Dalvi dkk., 2004). Laterites are oxide ores widely distributed in the equatorial regions. Laterite deposits usually consist of three layers, namely the limonite, the saprolite and garnierite (Wellmer, 2002). Until now, nickel production continues to increase along with increasing world demand. However, the problem to be faced in the future is the depletion of nickel sulfide reserves. Therefore, the use of laterite as a source of nickel must be done even though the nickel content is lower than sulfide (Norgate, 2010). Nickel laterite recovery can be carried out by pyrometallurgy and hydrometallurgy process. Hydrometallurgy is a metal extraction process execute at relatively low temperatures by leaching using a chemical solution, whereas pyrometallurgy is a metal extraction process implement at high temperatures (Kyle, 2010). The processing of laterite ore in Morowali is accomplished on low-grade nickel ores namely limonite by pyrometallurgy to produce ferronickel. The hydrometallurgical process is more appropriate to be used to process laterites with low nickel content, namely limonite type (Gustiana, 2018). High pressure acid leaching (HPAL) is a type of hydrometallurgical process that is commonly used on an industrial scale. However, this process is still considered to have weaknesses in terms of environment, economy, and energy (Simate, et al., 2010). Atmospheric pressure acid leaching (APAL) requires low energy and operational costs than High pressure acid leaching (HPAL) (Kyle, 2010; Kusuma, 2012).

The APAL process can be executed using several types of acids, both inorganic acids and organic acids as leachants (McDonald and Whittington, 2008a and 2008b). Inorganic acids still cause environmental problems when the leaching treatment is not performed well. Nowadays, organic acids have been being studied as alternative leaching reagents for nickel extraction from laterite ores to address those issues and to provide environmentally acceptable techniques (McDonald and Whittington, 2008b; Tang and Valix, 2006; Tzeferis and Agatzini-Leonardou, 1994). Astuti (2015) has investigated either inorganic acids such as sulfuric, hydrochloric, and nitric acids or organic acids such as lactic and oxalic acids in the leaching of nickel laterites. It shows that citric acid



gives the best nickel extraction because of its high dissociation constant and its ability to form nickel–citrate complexes during metal dissolution. The concentration of citric acid have a significant influence in the leaching process of nickel laterite. the higher the concentration of citric acid used, the higher the recovery value of nickel obtained. This is caused by the amount of acid that will be displaced the equilibrium to the right and increase the number of  $H^+$  ions. Thus, the use of higher concentrations allows the phase of reactant diffusion, chemical reactions, and product diffusion in solids. These three phase act as controllers of the leaching process so that they have an influence that cannot be ignored in the mechanism of the leaching process of laterite nickel using citric acid solution (Wanta, 2017). The aim of this research is to determine the good concentration of citric acid in atmospheric leaching for Morowali nickel laterite.

## 2. Materials and Methods

The type of nickel laterite used in this study is limonite from Morowali, Central Sulawesi. Before the leaching process started, nickel laterite is prepared in advance by drying using an oven at temperature  $110^{\circ}C$  for 4 hours, then grinded by using a hammer mill and sieved by a shieve shaker until particle size 200 mesh. The chemical composition of Morowali nickel laterite obtained by chemical analysis using X-Ray Fluorescence (XRF) by Zetium Panalytical as listed in Table 1. The result shows that dominant chemical component of Morowali nickel laterite is iron (Fe) followed by Silicone (Si), Nickel (Ni), Chromium (Cr), Manganese (Mn), Calcium (Ca), Phosphate (P), Zinc (Zn), Vanadium (V), and Scandium (Sc).

**Table 1: Chemical Analysis of the Main Elements Present in the Laterite Ore**

Element	Si	P	Ca	Sc	V	Cr	Mn	Fe	Ni	Zn
Weight (mass %)	6.5	0.25	0.61	0.01	0.054	1.86	1.3	84.19	5.15	0.1

The leaching process is carried out in an Erlenmeyer equipped with a stirrer and thermometer, as displayed at Fig. 1. Before using the citric acid solution, the pH is measured using a pH meter by Lovibond®Water Testing, as shown at Table 2. Citric acid is taken 360 milliliters (various concentrations used are 0.5, 1.0, 1.5, 2.0 M) is heated using a hot plate until it reaches a temperature of  $70^{\circ}C$ . After the desired temperature is reached, the solution is stirred at agitation speed of 500 rpm. After that, 30 grams of nickel laterite samples with 200 mesh particle size are put into the acid solution. Entry time will be recorded as 0 minutes when the sample is added. Then, 30 milliliters sample is taken with time intervals of 10, 20, 30, 60, 90 and 120 minutes. The sample that has been taken is a suspension solution and will be separated between the liquid phase and the solid phase by filtration. The filtrate gathered is analyzed using Atomic Absorption Spectroscopy (AAS).

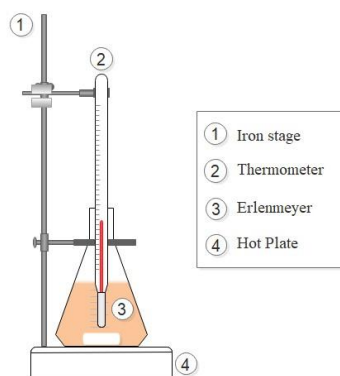


**Fig. 1: Schematic of the leaching process**



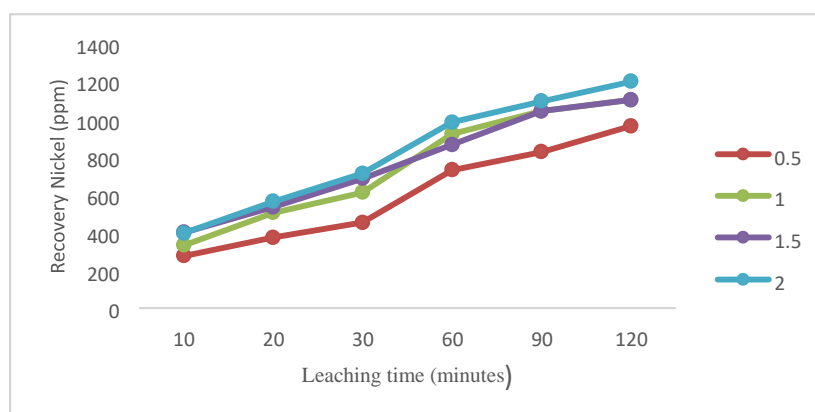
**Table 2: pH of citric acid**

Concentration (M)	pH
0.5	3.13
1.0	3.07
1.5	2.91
2.0	2.86

### 3. Results and Discussion

#### 3.1. Effect of Citric Acid Concentration

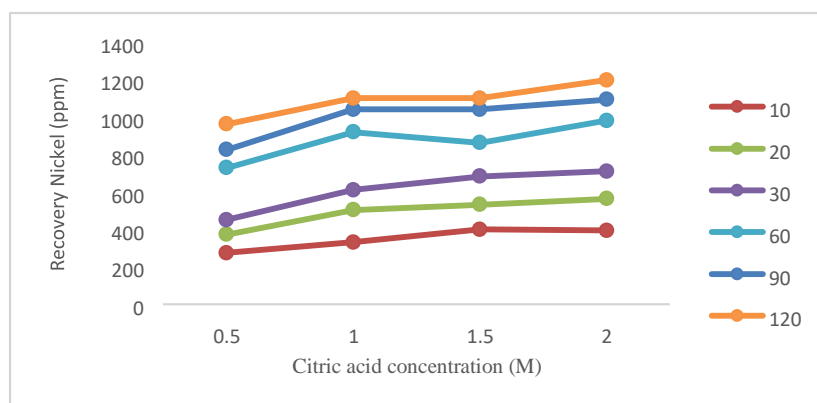
The acid concentration has main role in this investigation. As stated by Wanta (2017) Acid concentration shows the number of acid molecules in the leaching process. The results of nickel recovery by chemical analysis using Atomic Absorption Spectroscopy (AAS) are presented in Graphic. 1. The amount of nickel recovery is raised with the higher of acid concentration that is around 200 to 1200 ppm. The increasing of nickel recovery is appropriate with Le Chatelier principle where the addition of reactants will shift the direction of reaction to form the more progressive products (Solihin, 2014).



**Graphic. 1: Effect of citric acid concentration on the nickel recovery**

#### 3.2. Effect of Leaching Time

The effect of leaching time on nickel recovery is presented at Graphic. 2. The longer of leaching time implemented the higher nickel is earned. As the increasing of leaching time the frequency of intermolecular collisions rise rapidly, it causes the formation of products (nickel citrate) higher (Wanta, 2017). The improvement of nickel recovery at concentration 2.0 M very significant along leaching time of 10 to 120 minutes that is around 900 to 1200 ppm.



**Graphic. 2: Effect of Leaching Time on the Nickel Recovery**

## 4. Conclusion

Nickel laterite can recovered by atmospheric pressure acid leaching using citric acid. The acid concentration and leaching time are two influence factors on nickel leaching process. The good conditions is obtained at concentration of citric acid 2.0 M and leaching time of 120 minutes, it proved by the amount of nickel recovery reached 1197.5 ppm.

## 5. Nomenclature

AAS : Atomic Absorption Spectroscopy

APAL : Atmospheric Pressure Acid

Leaching HPAL : High pressure acid leaching

ppm : part per

million rpm :

rotation per

minutes XRF :

X-Ray Fluorescence

## 6. Acknowledgements

Authors are thankfull to Politeknik Industri Logam Morowali (PILM), Morowali, Central Sulawesi, Indonesia for supported this research.

## 7. References

Astuti W, Hirajima T, Sasaki K dan Okibe N. Comparison of Effectiveness of Citric Acid and Other Acids in Leaching of Low – Grade Indonesian Saprolitic Ores. *Minerals Engineering* 2016 ; 85: 1-16.

Dalvi AD, Bacon WG dan Osbourne RC. *The Past and the Future of Nickel Laterites*. Inco Limited, Ontario, Canada 2004; p. 27.

Gustiana et al., 2018, Pelindian Nikel dari Bijih Limonit Low-Grade Pomalaa Menggunakan Pelarut Asam Asetat, ISSN 1693-4393

Kusuma, G. D., 2012, Pengaruh Reduksi Roasting dan Konsentrasi Leaching Asam Sulfat terhadap Recovery Nikel dari Bijih Limonite, Skripsi, Universitas Indonesia.

Kyle, J., 2010, Nickel laterite processing technologies – Where to next?, ALTA 2010 Nickel/Cobalt/Copper Conference, Australia.

Levenspiel, O., 1999, *Chemical Reaction Engineering*, John Wiley & Sons, New York.

- McDonald, R., G. dan Whittington, B., I., 2008, Atmospheric acid leaching of nickel laterites review : Part I. Sulphuric acid technologies, *Hydrometallurgy*, 91, 35-55.
- McDonald, R., G. dan Whittington, B., I., 2008, Atmospheric acid leaching of nickel laterites review : Part II. Chloride and biotechnologies, *Hydrometallurgy*, 91, 56-69.
- Norgate, T dan Jahanshahi. Low Grade Ores – Smelt, Leach or Concentrate? *Minerals Engineering* 2010 ; 23:6573
- Purwanto, Hadi., Taihei SHIMADA., Reijiro TAKAHASHI., and Jun-ichiro YAGI., 2002, Recovery of Nickel from Selectively Reduced Laterite Ore by Sulphuric Acid Leaching, Vol. 43 (2003), *ISIJ International*, No. 2, pp. 181–186.
- Sitorus, Lungguk., Julius Ponte., Vandal Kamu, 2019, Analisis Beberapa Asam Organik dengan Metode High Performance Liquid Chromatography(HPLC) Grace Smart Rp18 5 $\mu$ , *JURNAL MIPA UNSRAT ONLINE* 4 (2) 148-152
- Solihin., F. Firdiyono, 2014, PERILAKU PELARUTAN LOGAM NIKEL DAN BESI DARI BIJIH NIKEL KADAR RENDAH SULAWESI TENGGARA, *Majalah Metalurgi*, V 29.2.2014, ISSN 0126-3188/ 139-144
- Sukla, L., B., Behera, S., K., dan Pradhan, N., 2014, Microbial Recovery of Nickel from Lateritic (Oxidic) Nickel Ore : A Review, dalam *Geomicrobiology and Biogeochemistry*, vol. 39, Springer Berlin Heidelberg, 137-151.
- Simate, G., S., Ndlovu, S., Walubita, L., F., 2010, The fungal and chemolithotrophic leaching of nickel laterites – Challenges and opportunities, *Hydrometallurgy*, 103, 150-157.
- Tang, JA dan Valix M. Leaching of Low Grade Limonite and Nontronite Ores by Fungi Metabolc Acids. *Minerals Engineering* 2006; 19: 1274-1279.
- Tzeferis, PG dan Agatzini-Leonardou, S. Leaching of Nickel and Iron from Greek Non-Sulphide Nickeliferous Ores by Organic Acids. *Hydrometallurgy* 1994; 36:345-360.
- Wanta, K., C., Perdana, I., Petrus, H., T., B., M., 2017, Uji Validitas Model Shrinking Core terhadap Pengaruh Konsentrasi Asam Sitrat dalam Proses Leaching Nikel Laterit, *Jurnal Rekayasa Proses* Volume 11 No. 1, 2017, hal. 30-35.
- WELLMER, F.W (2002): Leachable supergene base and precious metaldeposits worldwide.– *ERZMETALL*, **55**: 25-33.

## Particle Size Analysis of Morowali Nickel Laterite on Atmospheric Citric Acid Leaching

Wirawan<sup>1\*</sup>, Regna Tri Jayanti<sup>2</sup>

<sup>12</sup>Departement of Mineral Chemical Engineering, Politeknik Industri Logam Morowali (PILM), Morowali  
- INDONESIA

\* Corresponding author e-mail: wirawan.p10@g-mail.com

### Abstract

Atmospheric Pressure Acid Leaching (APAL) is one of nickel laterite processing which has a big potential to be applied in industry. The leaching process is significantly influenced by the particle size effect, agitation leaching speed, and leaching time. This research demonstrated that particle size has important role to determine leaching performances of nickel laterite. The main focus of this research is to study the effect of particle size of Morowali nickel laterite in order to increase nickel recovery on atmospheric citric acid leaching. Particle sizes of nickel laterite used on this experiment are 50 mesh, 100 mesh, 150 mesh, 200 mesh and range of leaching time of 10, 20, 30, 60, 90, 120 minutes. Other constant operating conditions applied in this study are concentration of citric acid (M), agitation speed (rpm), leaching temperature (°C). The results shown that the amount recovery of nickel tend to increases with smaller particle size of nickel laterite. But this research work indicated that particle size 100 mesh achieved good recovery of nickel at 2824 ppm.

*Keywords: Particle size, Atmospheric leaching, Citric acid, Nickel laterite, Hydrometallurgy.*

### 1. Introduction

In the future, hydrometallurgical methods or aqueous treatments will become the primary techniques for the recovery of nickel and other metals from nickel laterite ores, especially low-grade laterite ores, because they enable valuable metals such as nickel, cobalt, iron, magnesium, chromium, and aluminum to be extracted comprehensively (Watling et al., 2011; Liu et al., 2010; Fan and Gerson, 2013). Laterites are oxide ores widely distributed in the tropical regions. They were formed during laterization, a weathering process of ultramafic rocks that is favoured by warm climate and abundant rainfall. Lateritic deposits usually consist of three layers, namely the limonite, the saprolite and the garnierite layer. Limonite, which comprises the top lateritic layer, is a homogeneous ore consisting mainly of goethite associated with nickel (Gleeson et al., 2003; Golightly, 1981).

New, effective, energy saving, easily controlled and environmentally safe methods for nickel recovery from large quantities of low-grade laterites nickel ore are needed, since the established pyrometallurgical and hydrometallurgical industrial processes are either energy intensive or present severe engineering problems. One hydrometallurgical method that has not yet been used industrially, although its study is becoming increasingly important, is atmospheric acid leaching. Some researchers have investigated the atmospheric acid leaching of nickel laterite using inorganic acids such as sulfuric acid, hydrochloric acid, and nitric acid, and a range of organic acids (MacCarthy et al., 2014; Nosrati et al., 2014; Rice and Strong, 1974a, 1974b; Wang et al., 2012; Wang et al., 2014). The use of organic acids in dissolution of the metals in nickel laterite ores is an alternative method that has advantages in terms of environmental issues. Many researchers have confirmed that citric acid is the most effective organic acid in the leaching of nickel laterites (Mc Donald and Whittington, 2008b). According to (Mubarok et al., 2011) The use of citric acid in nickel leaching has several advantages, especially in environmental issues such as providing leaching reagents that are non-toxic and biodegradable and overcoming the problem of agricultural waste. In addition, leaching of citric acid has high effectiveness and selectivity in nickel leaching. Therefore, citric acid leaching will be a suitable alternative technique for nickel extraction from Indonesian lateritic ores.

Recently, with continuous updation of the grinding equipment, mineral particle size distribution has become possible and has been industrialized in some factories. For heterogeneous reactions, the migration rate of reactive

molecules from one phase to another must be related to the area of the interface then fine particles react faster because of the larger surface area of the former. Unfortunately, few studies have been conducted on the effects of particle size on the leaching of nickel laterite ore with citric acid. The effect of different particle sizes, after refining the mineral is undefined (Burgges et al., 2018).

## 2. Material and methods

### 2.1. Nickel laterite ore

Laterite nickel ore used in this experiment is a type of limonite from Morowali, Central Sulawesi Province. Before the leaching process is carried out, laterite nickel ore is prepared by drying in an oven at 110 ° C for 4 hours to reduce the water content, then grinded using a hammer mill. Later, the ore is heated to facilitate the shieving process by using shieve shakers. Different particle sizes are obtained by weight laterite nickel ore of 500 gram and shieve along 5 minutes. The investigation is done by 5 times shieving with persistent mass entry. The refined particle size are 50, 100, 150 and 200 mesh. The high amount of refined particle is 151,08 gram by particle size 50 mesh and the lower amount is 45,42 gram by particle size 200 mesh. The distribution of particle size by weight can be seen in Figure 1.

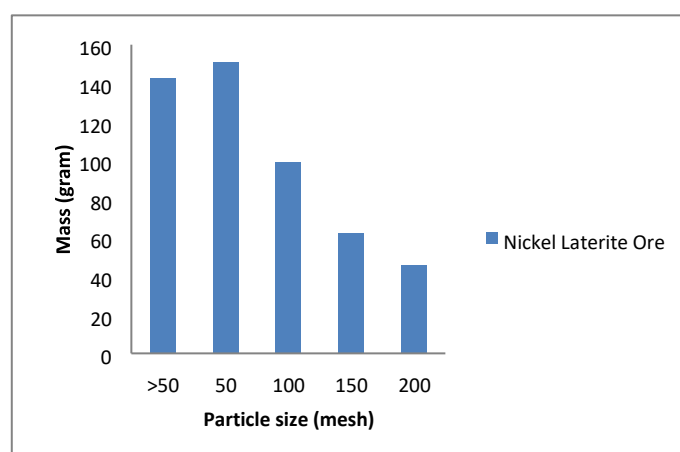


Fig. 1: Distribution particle size by weight (gr)

Sample was analyzed for its nickel content using an X-Ray Fluorescence (XRF) in the sample of 5.15% by weight. As for the metal content in nickel laterite ore can be seen in more detail in Table 1.

Table 1: Chemical analysis of the main elements present in the laterite ore

Element	Si	P	Ca	Sc	V	Cr	Mn	Fe	Ni	Zn
Weight (mass %)	6.5	0.25	0.61	0.01	0.054	1.86	1.3	84.19	5.15	0.1

Table 1 shows that iron (Fe) is the main chemical component of Morowali nickel laterite as said (Purwanto, 2002) is laterite ore with low nickel content is recommended to have an iron content of about 50% by weight.

### 2.3. Leaching and analytical methods

The methods used in this research is atmospheric pressure acid leaching. The process was conducted by pouring 360 ml of 1 M citric acid solution, heated until 70 °C and stirred by agitation speed of 1000 rpm. 30 gram nickel laterite ore was added into the erlenmeyer after the temperature is reached. The variation of particle size are 50, 100, 150 and 200 mesh. The filtrate sample is taken periodically at time of 10, 20, 30, 60, 90, 120 minutes.

### 3. Result and discussion

#### 3.1. Effect of leaching time

One of the factors that has an important role in the nickel laterite leaching process is the leaching time because the frequency of collisions between molecules increases with the leaching time. The results of the analysis using AAS are presented in Graph 2.

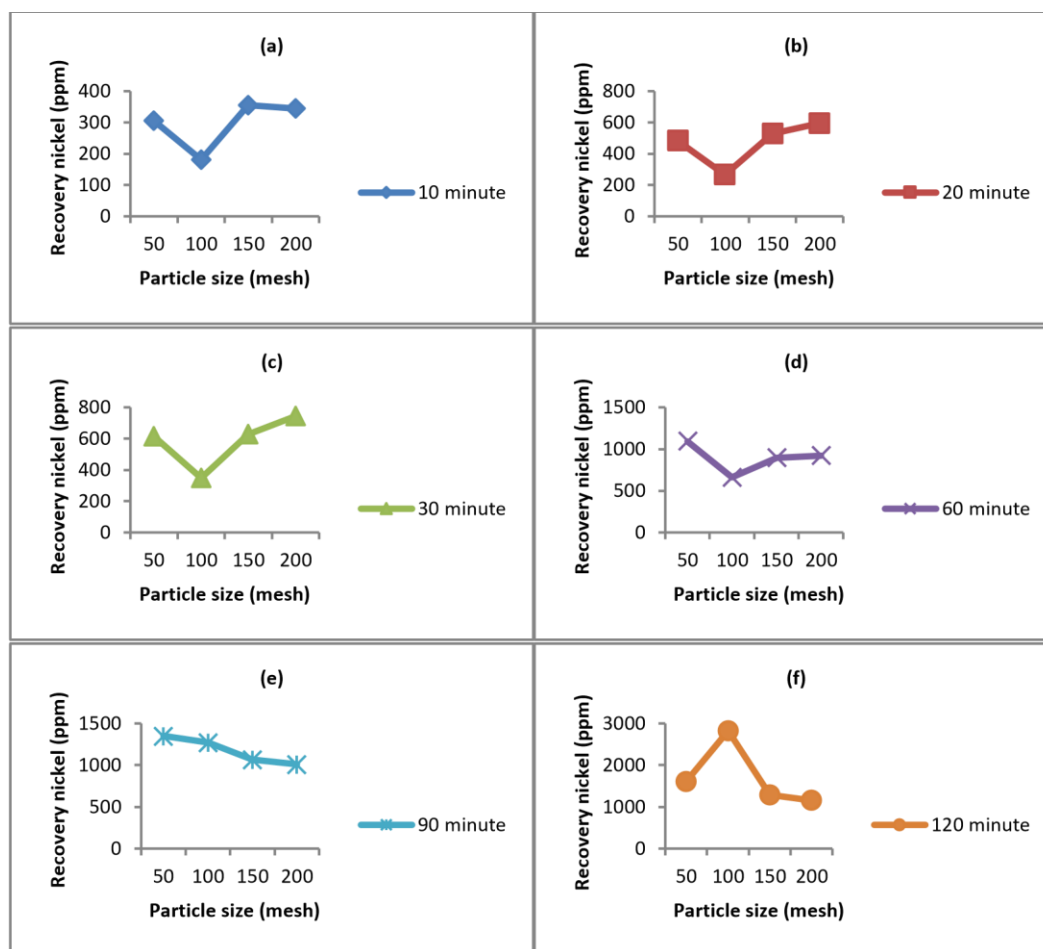


Fig. 2: Data of recovery nickel (ppm) variable of leaching time 10 minute (a), 20 minute (b), 30 minute (c), 60 minute (d), 90 minute (e) and 120 minute (f).

Figure 2 shows that the effect of particle size on atmospheric citric acid leaching of nickel laterite increases the nickel recovery. Time duration on leaching process also influence the recovery value of nickel. The longer the leaching process is carried out, the higher of nickel recovery obtained. This phenomenon can occur because the frequency of collisions between molecules increases as the leaching time increases. The dense of frequency intermolecular collisions, the higher product formed.

#### 3.2. Effect of particle size

The particle size has main role in this nickel laterite leaching process. Analysis using AAS revealed that particle size of the are presented in Figure 3.

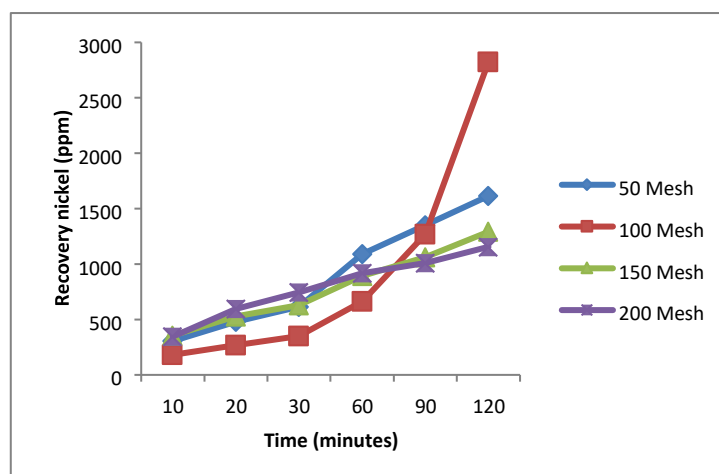


Fig. 3: Data of recovery nickel (ppm) variable of particle size

Figure 3 shows the influence of the duration of the leaching process on the concentration value of nickel recovery. According to the references, the value of nickel recovery enhanced with smaller particle size. However, in this the investigation the amount of nickel recovery show the high performance at 100 mesh that is 2824 ppm. It is probably because the particle size on the leaching process are heterogeneous reactions.

## 4. Conclusion

The nickel recovery of Morowali nickel laterite is performed using an atmospheric citric acid leaching. The results indicated that particle size and leaching time are influenced parameters to enhance nickel recovery. Based on the reference an increase in recovery value increases if the particle size gets smaller. However, in this research work nickel recovery greatly improved at particle size 100 mesh and reached 2824 ppm.

## 5. Nomenclature

T	temperature	C
M	Molarity	g/Mr
R	rotation speed	rpm

Subscripts

APAL	Atmospheric Pressure Acid Leaching
AAS	Atomic Absorption Spectrophotometry
XRF	X-Ray Fluorescence

## 6. Acknowledgements

The author would like to thank to Yudianto, S.Tp., M.Si and Ika Fitriani Juli Palupi, S.Si., M.Si for the support and assistance that have been given in this research.

## 7. References

- Burgess, W. A.; Keller, M. J.; Lekse, J. W.; Howard, B. H.; Roth, E. A.; Granite, E. J. Effect of Pre-Reaction Ball Milling on Kinetics of Lanthanum Phosphate Roasting with Sodium Carbonate. *Ind. Eng. Chem. Res.* 2018, 57, 6088–6096.
- Fan, R., Gerson, A.R., 2013. Mineralogical characterization of Indonesian laterites prior to and post atmospheric leaching. *Hydrometallurgy* 134-135, 102–109.
- Gleeson, S.A., Butt, C.R., Wllas, M., 2003. Nickel laterites: a review. *SEG Newsletter, Society of Economic Geologists*, p. 54. Available from [www.segweb.org](http://www.segweb.org).

- Golightly, J.P., 1981. Nickeliferous laterite deposits. *Econ. Geol.* 75 (1), 710–735.
- Liu, K., Chen, Q., Hu, H., Yin, Z., Wu, B., 2010. Pressure acid leaching of a Chinese laterite ore containing mainly maghemite and magnetite. *Hydrometallurgy* 104, 32–38.
- MacCarthy, J., Addai-Mensah, J., Nosrati, A., 2014. Atmospheric acid leaching of siliceous goethitic Ni laterite ore: effect of solid loading and temperature. *Miner. Eng.* 69, 154–164.
- McDonald, R.G., Whittington, B.I., 2008. Atmospheric acid leaching of nickel laterites review. Part II. Chloride and bio-technologies. *Hydrometallurgy* 91, 56–69.
- Mubarak, M.Z., Astuti, W., Chaerun, S.K., 2011. Leaching behavior of nickel from Indonesian laterite ore in some organic acids. *Proceeding of International Mineral Processing Symposium*. Turkey.
- Nosrati, A., Quast, K., Xua, D., Skinner, W., Robinson, D.J., Addai-Mensah, J., 2014. Agglomeration and column leaching behaviour of nickel laterite ores: effect of ore mineralogy and particle size distribution. *Hydrometallurgy* 146, 29–39.
- Purwanto, Hadi., Taihei SHIMADA., Reijiro TAKAHASHI., and Jun-ichiro YAGI., 2002, Recovery of Nickel from Selectively Reduced Laterite Ore by Sulphuric Acid Leaching, Vol. 43 (2003), ISIJ International, No. 2, pp. 181–186.
- Rice, N.M., Strong, L.W., 1974a. The leaching of lateritic nickel ores in hydrochloric acid. *Can. Metall. Q.* 13, 485–493.
- Rice, N.M., Strong, L.W., 1974b. The leaching of nickeliferous laterites with hydrochloric acid (optimization of process variables). In: Davies, G.A., Scuffham, J.B. (Eds.), *Hydrometallurgy, I. Chem. E. Symposium Series No 42*. The Institution of Chemical Engineers, Rugby, pp. 6.1–6.13.
- Wang, B., Guo, Q., Wei, G., Zhang, P., Qu, J., Qi, T., 2012. Characterization and atmospheric hydrochloric acid leaching of a limonitic laterite from Indonesia. *Hydrometallurgy* 129–130, 7–13.
- Wang, X., McDonald, R.G., Hart, R.D., Li, J., van Riessen, Arie, 2014. Acid resistance of goethite in nickel laterite ore from Western Australia. Part II. Effect of liberating cementations on acid leaching performance. *Hydrometallurgy* 141, 49–58.
- Watling, H.R., Elliot, A.D., Fletcher, H.M., Robinson, D.J., Sully, D.M., 2011. Ore mineralogy of nickel laterites: controls on processing characteristics under simulated heap leach conditions. *Aust. J. Earth Sci.* 58 (7), 725–744.



## Effect of Agitation Speed and Leaching Time for Nickel Recovery of Morowali Limonite Ore in Atmospheric Citric Acid Leaching

Regna Tri Jayanti<sup>1\*</sup>, Yusdianto<sup>2</sup>

<sup>12</sup>Department of Mineral Chemical Engineering, Politeknik Industri Logam Morowali (PILM),  
Morowali – INDONESIA

\* Corresponding author e-mail: regnatj@gmail.com

### Abstract

This research work deals with atmospheric citric acid leaching of limonite ore from Morowali, Central Sulawesi by applying agitation speed and leaching time parameters. The composition of limonite ore treatment was characterized by X-Ray Fluorescence (XRF) method. Its content dominated by iron 84.2 % and enrichment nickel content up to 5.15 %. The microstructure image of limonite ore was observed by Scanning Electron Microscope (SEM) whereas nickel recovery was confirmed by Atomic Absorption Spectroscopy (AAS). Leaching process was conducted by using citric acid in a flask on a magnetic heated stirrer at constant temperature. The effect of agitation speed on atmospheric leaching in citric acid indicated enhancement of nickel recovery. The agitation speed ranges employed were 100 to 1000 rpm with leaching times of 10 to 120 minutes. This study revealed that atmospheric citric acid leaching of limonite ore from Morowali under the condition temperature 70 °C, acid concentration 1 M, agitator speed 1000 rpm could recover nickel of 2824 ppm at 120 minutes of leaching time.

*Keywords: Atmospheric leaching, Limonite ore, Agitation speed, Citric Acid, Leaching time*

### 1. Introduction

Indonesia has approximately 16 % of total global nickel resources in the form of lateritic ores. They are widely distributed and spread among the islands of Kalimantan, Sulawesi, Halmahera, Gag, and Papua (Astuti *et al.*, 2016a). Central Sulawesi has big potential for mineral resources of nickel laterite deposition especially in Morowali (Hardyanto, Widodo and Nurwaskito, 2015). Indonesia applies pyro-metallurgy method to process nickel laterite rather than hydrometallurgy in order to produce nickel alloy and nickel matte (Mubarak and Hapid, 2014). Solihin and Firdiyono (2014) explained that alternative way to process nickel laterite in particular limonite is hydrometallurgy which has low operation temperature. The more applicable Hydrometallurgical processes to the limonite (high iron laterite) are ammonia-ammonium carbonate leaching (Caron process), atmospheric leaching, and high pressure acid leaching (HPAL) (Guo *et al.*, 2011).

Atmospheric pressure acid leaching has been recently receiving more attention due to higher capital cost and materials of construction problems of high-pressure acid leaching at commercial level. It involves direct leaching of nickel laterite ores either both inorganic and/or organic acids by either agitation or heap leaching (Mohammadreza, Mohammad and Ziaeddin, 2019). Acid leaching has become the primary technology for processing nickel laterite ores because of its advantage on recovering the elements such as nickel, cobalt, iron, and magnesium comprehensively (Liu, Chen and Hu, 2009). Inorganic acid utilization of leaching process ensued harmful effect to the environment that requires acid waste handling (Gustiana, 2018). Citric acid is one of organic acids that shows good mechanism as a bonding agent in metal separation from the minerals. The hydronium ion of citric acid attacks acid and metal ions to form metal-ligand compounds and dissolves the metal (McDonald and Whittington, 2008; Astuti *et al.*, 2016b). Agitation has a pronounced effect on the leaching of copper because of the increase in the rate of copper leaching with increasing the degree of stirring suggested that the reaction is either fully diffusion controlled or under mixed diffusion and chemical control (El-okazy, Zewail and Farag, 2018).

In this atmospheric citric acid leaching experiment, the effect of different parameters on agitation speed and leaching time was examined. Therefore, the aim of this study is to investigate recovery of nickel through agitation leaching and leaching time of limonite ore at atmospheric citric acid leaching.

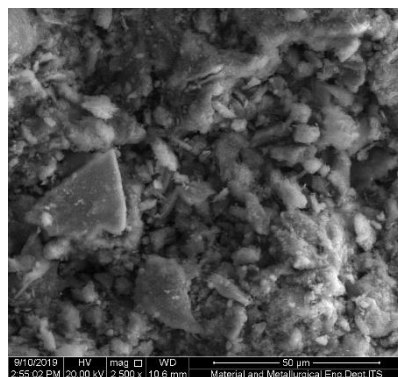
## 2. Materials and methods

### 2.1. Materials

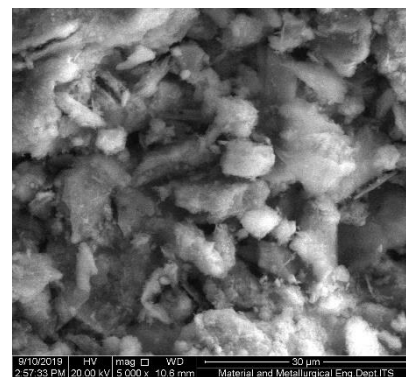
The representative samples used in this research is limonite ore type from mine area of Morowali, Central Sulawesi. Preparation of sample started by reducing water content in an oven at temperature 110°C along 4 hours, then sample was grinded by using a laboratory Jaw crusher and Hammer mill. At last, ore was sieved by sieve shaker until the particle size reach of 100 mesh. Recent study stated that the particle size of -100+200 mesh has good contribution in leaching limonite ore (Mubarok, Astuti and Chaerun, 2013). The chemical composition of sample was examined by X-Ray Fluorescence Zetium Panalytical and listed in table 1. Scanning Electron Microscope (SEM) analysis supported mineral formation, since the particles composed by metal elements. Samples consist of heterogeneous form and grain sizes are quite small (below -50  $\mu\text{m}$ ), it also has a flattened morphology (Fig.1). This is adequate a valuable increase in particle size since both the nickel and iron powders are originally <10  $\mu\text{m}$  (Fischmann and Dixon, 2009).

Table 1: Composition of Limonite ore of Morowali

Sample	Ore Composition (wt%)									
	Si	P	Ca	Sc	V	Cr	Mn	Fe	Ni	Zn
Limonite ore	6.5	0.25	0.61	0.01	0.054	1.86	1.3	84.2	5.15	0.1



(a)



(b)

Fig. 1: Microstructure of limonite ore of Morowali (a). Magnification 2500x and (b). Magnification 5000x

### 2.2. Methods

Atmospheric pressure acid leaching was performed in a flask equipped with magnetically heated stirrer and thermometer. The comparison of sample and citric acid was 8.3 % w/v. The parameters selected in this experiment were temperature (°C), type of acid, and acid concentration (M). As counted in XRF data of mineral composition, predominant element of Morowali limonite ore was iron. McDonald and Whittington, (2008) claimed that iron extraction could be controlled if the total chloride concentration is kept below 230 g/L and the initial acidity is maintained between 1 M and 2 M. Therefore, acidity of citric acid used in this work is 1 M. Citric acid was added and heated until the temperature reached 70°C. Then, limonite ore was poured gently to the opening flask and leaching time starts observed at the time of solid sample added. The effect of leaching time was determined as the sample taken after period of time 10, 20, 30, 60, 90, and 120 minutes. All the experiments were kept on for 2 h and final solutions were filtered using a paper filter. To calculate nickel recovery, filtered solution was analyzed by using Atomic Absorption Spectroscopy (AAS).

### 3. Results and discussion

#### 3.1. Influence of agitation speed

The influence of agitation speed on variation in the nickel recovery responses was evaluated. The results indicated agitation speed had convincing effect. Figure 2 shown the effect of agitation speed in the range 100 – 750 rpm on the reductive leaching of limonite ore. Moreover, slight decrease in nickel recovery was detected when agitation speed at 750 rpm. The reason of the phenomena was probably due to instabilities of the contact area between limonite ore and citric acid. Since leaching kinetics increased as the intensive mixing among them, the enhancement of nickel recovery tends to rise in the long period of reaction time and the high agitation speed of leaching. Consequently, the agitation speed of 1000 rpm was quite promising to ensure the control of chemical reaction with the mineral grains (limonite ore) in atmospheric citric acid leaching.

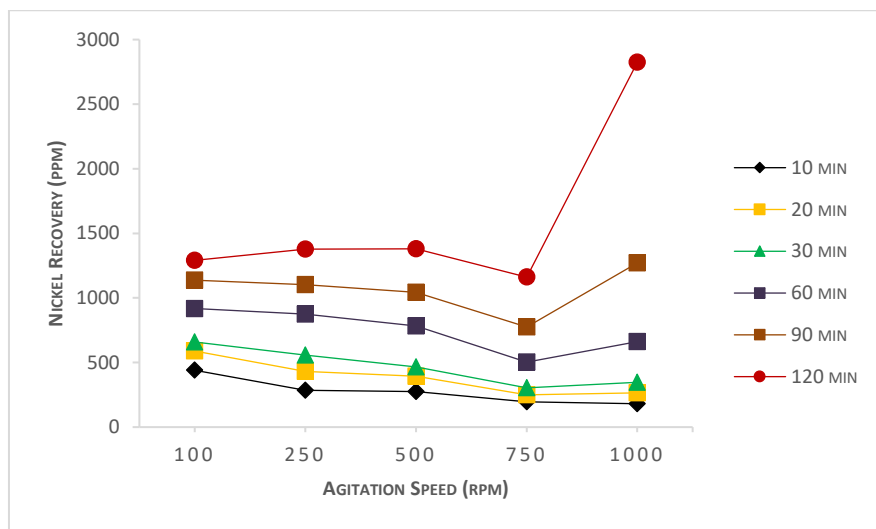


Fig. 2: Effect of agitation speed on nickel recovery

#### 3.2. Influence of leaching time

The effect of reaction time on atmospheric citric acid leaching of limonite ore is given in figure 3. The leaching efficiency of nickel recovery obtained by varying reaction time 10, 20, 30, 60, 90, and 120 minutes. At the beginning of reaction time, nickel recovery tends to decreased along the higher agitation speed. The leaching efficiency curves shows that nickel recovery increases with a slight augment in reaction time of 10 minutes to 120 minutes for agitation speed from 100 rpm to 750 rpm. Furthermore, the recovery of nickel increases dramatically at agitation speed 1000 rpm in reaction time from 30 minutes to 120 minutes.

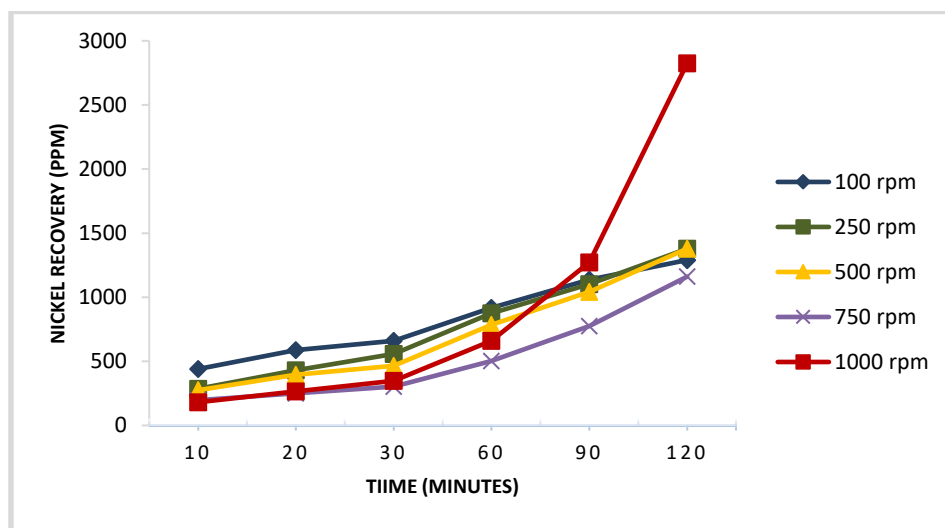


Fig. 3: Effect of leaching time on nickel recovery

## 4. Conclusion

Agitation speed and leaching time experiments showed that nickel from limonite ore could be recovered at atmospheric condition. Two factorial experimental were used to distinguish significant parameters on the process. The representative sample of nickel laterite ore assayed by XRF analysis principally consisted of Fe as a major element 84.2 %, Si 6.5 %, Ni 5.15%, Cr 1.86 %, Mn 1.3% and other metal elements below 1%.

Results analysis were done by Atomic Absorption Spectroscopy (AAS) and exhibited that atmospheric citric acid leaching could solubilize nickel. By increasing agitator speed from 100 to 1000 rpm and leaching time process from 10 to 120 minutes, the effect of agitation speed and leaching time showed the enhancement of nickel recovery indirectly.

Agitation speed enlarged the contact of limonite ore with citric acid that helped leaching reaction done well. The leaching time effected to nickel recovery by the period of interaction between limonite ore and citric acid. The results obtained from this research indicate that the agitation speed and leaching time parameters could be implemented to identify enhancement of nickel recovery on atmospheric citric acid leaching of limonite ore from Morowali under the condition temperature 70 °C, acid concentration 1 M and agitation speed 1000 rpm. The amount of nickel recovery by this reseach work reached 2824 ppm after reaction time of 120 minutes.

## 5. Nomenclature

h	hour
M	Molarity
ppm	part per millions
rpm	rotary per minutes
w/v	weight per volume

## 6. Acknowledgements

This work was funded by Politeknik Industri Logam Morowali. The authors gratefully acknowledge the Professor Isa Setiasyah Toha for valuable comments, Mineral Chemical Department Colleague for supporting many of information sources, also Feby Aryani and Wirawan for the helpful efforts.

## 7. References

- Astuti, W. et al. (2016a) 'Comparison of atmospheric citric acid leaching kinetics of nickel from different Indonesian saprolitic ores', Hydrometallurgy. Elsevier B.V., 161, pp. 138–151. doi: 10.1016/j.hydromet.2015.12.015.
- Astuti, W. et al. (2016b) 'Comparison of effectiveness of citric acid and other acids in leaching of low-grade Indonesian saprolitic ores', Minerals Engineering. Elsevier Ltd, 85, pp. 1–16. doi: 10.1016/j.mineng.2015.10.001.
- El-okazy, M. A., Zewail, T. M. and Farag, H. A. (2018) 'Recovery of copper from spent catalyst using acid leaching followed by electrodeposition on square rotating cylinder', Alexandria Engineering Journal. Faculty of Engineering, Alexandria University, 57(4), pp. 3117–3126. doi: 10.1016/j.aej.2017.12.001.
- Fischmann, A. J. and Dixon, D. G. (2009) 'Awaruite (Ni<sub>3</sub>Fe) as a nickel resource — leaching with ammoniacal – ammonium solution containing citrate and thiosulfate', Hydrometallurgy. Elsevier B.V., 99(3–4), pp. 214–224. doi: 10.1016/j.hydromet.2009.08.009.
- Guo, X. Y. et al. (2011) 'Leaching behavior of metals from limonitic laterite ore by high pressure acid leaching', Transactions of Nonferrous Metals Society of China (English Edition), 21(1), pp. 191–195. doi: 10.1016/S1003-6326(11)60698-5.
- Gustiana, H. S. E. A. (2018) 'Pelindian Nikel dari Nikel Laterit Pomalaa Menggunakan Asam Asetat', Tesis Sarjana S-2 Program Studi Teknik Kimia, Magister Teknik Proses Pengolahan Mineral, (April), pp. 1–7.

- Hardyanto, Widodo, S. and Nurwaskito, A. (2015) 'Pemodelan endapan nikel laterit, kabupaten morowali, provinsi sulawesi tengah', *Jurnal Geomine*, 02, pp. 89–96.
- Liu, K., Chen, Q. and Hu, H. (2009) 'Hydrometallurgy Comparative leaching of minerals by sulphuric acid in a Chinese ferruginous nickel laterite ore', *Hydrometallurgy*. Elsevier B.V., 98(3–4), pp. 281–286. doi: 10.1016/j.hydromet.2009.05.015.
- McDonald, R. G. and Whittington, B. I. (2008) 'Atmospheric acid leaching of nickel laterites review . Part II . Chloride and bio-technologies', 91, pp. 56–69. doi: 10.1016/j.hydromet.2007.11.010.
- McDonald, R. G. and Whittington, B. I. (2008) 'Atmospheric acid leaching of nickel laterites review. Part I. Sulphuric acid technologies', *Hydrometallurgy*, 91(1–4), pp. 35–55. doi: 10.1016/j.hydromet.2007.11.009.
- Mohammadreza, F., Mohammad, N. and Ziaeddin, S. S. (2019) 'Nickel extraction from low grade laterite by agitation leaching at atmospheric pressure International Journal of Mining Science and Technology Nickel extraction from low grade laterite by agitation leaching at atmospheric pressure', *International Journal of Mining Science and Technology*. China University of Mining & Technology, 24(4), pp. 543–548. doi: 10.1016/j.ijmst.2014.05.019.
- Mubarok, M. Z. and Hapid, A. (2014) 'PELINDIAN BIJIH NIKEL LATERIT SULAWESI TENGGARA', in *Prosiding Pemaparan Hasil Penelitian Pusat Penelitian Geoteknologi LIPI Tahun 2014*. Tangerang, pp. 527–534.
- Mubarok, Z., Astuti, W. and Chaerun, S. K. (2013) 'Effects of Individual Use , Mixed Culture and Sulfur Addition on the Effectiveness of Nickel Laterite Ore Bioelaching with *Penicillium verruculosum* and *Galactomyces geotrichum* Effects of Individual Use , Mixed Culture and Sulfur Addition on the Effectiveness', (January). doi: 10.4028/www.scientific.net/AMR.825.380.
- Solihin and Firdiyono, F. (2014) 'Perilaku pelarutan logam nikel dan besi dari bijih nikel kadar rendah sulawesi tenggara', *Majalah Metalurgi*, pp. 139–144.

# Specimen Test Making of Polypropylene High Impact (PPHI) Polymer Composite Reinforced with Natural Fibres using Hand Lay-Up Methods

Nuha D. Anggraeni<sup>1\*</sup>, Alfian E. Latief<sup>1</sup>, Ramadhan L. Tawadha<sup>1</sup>, and Rifki R. Radliya<sup>1</sup>

<sup>1</sup> Department of Mechanical Engineering, Institut Teknologi Nasional (Itenas), Bandung - INDONESIA

\* Corresponding author e-mail: nuha@itenas.ac.id

## Abstract

Pineapple and hemp are one type of natural fibre that is widely grown in Indonesia and has good mechanical properties. The use of hemp and pineapple fibres as reinforcing and high impact polypropylene (PPHI) materials that are widely used in the automotive industry as a matrix in composites for applications in the automotive field studied. In this research, the process of making bending test specimens using ASTM D 69 standard for PPHI reinforced composites and pineapple fibre uses the hand lay-up method, with meshing below 120 and 10% volume fraction. As a result, in order to make homogeneous specimen, good setting at temperature 250 °C by normalizing cooling and stirring process to enable PPHI and pineapple fibre.

*Keywords: pineapple-fibre, specimen, normalizing, homogenous, matrix*

## 1. Introduction

Plastic plays an important role in human life, such as packaging because of its superiority which is lightweight, strong, transparent, not easily broken and the price is affordable by all people and forms of lamination combined with other packaging materials and some are heat-resistant and stable (Nurminah, 2002). However, because plastic cannot be renewed, it is necessary to look for other materials that can be renewed. Materials made from natural fibres can be used to produce renewable and environmentally friendly materials.

Material development using technology that utilizes polymer composite materials with natural fibre reinforcement. The material is an alternative to meet the material needs that can function as a solution to environmental problems and the limitations of natural resources that cannot be renewed. Many researchers have developed composite polymers to use them as testing materials for polymer composites with natural fibre reinforcement (Asim, et. al, 2017; Alzebedeh, et. al, 2019, Hadi, et. al, 2016; Senthilkumar, et.al, 2019).

The composite material can be made using the hand lay-up method, namely by pouring a mixture of Polypropylene High Impact (PPHI) with natural fibre-reinforced (Mardiyati, et. al, 2017). The results of making this composite will be used to get a reference about the mechanical and physical properties of the test specimen components with a volume fraction of 10% so that later it will get the results of various tests.

## 2. Literature review

### 2.1. Composite

Composite is a material that is formed from a combination of two or more materials, where the mechanical properties of the forming material differ where one material is as a filler and the other as a reinforcing phase (Gibson, 1994). The continuous composite combination of reinforcement and other material functions as a matrix.

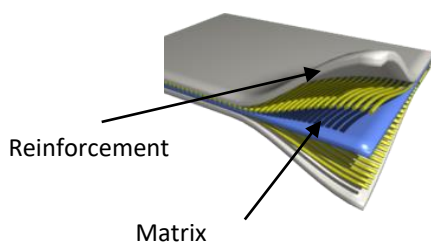


Fig. 1: Composite composition

In general, according to fibre placement, composites classification are:

- Continuous fibre composite (composite reinforced with continuous fibres)
- Woven fibre composite (composite reinforced with woven fibres)
- Chopped fibre composite (composite reinforced with short/random fibres)
- Hybrid composite (continuous and random fibre composite)

Structural composite in general:

- Composite laminate
- Composite sandwich
- Particulate composite

## 2.2. Polypropylene (PP)

Polypropylene is a hydrocarbon polymer included in thermoplastic polymers that can be processed at high temperatures. Polypropylene is derived from propylene monomers obtained from refining petroleum. Propylene molecular structure is  $\text{CH}_2 = \text{CH}-\text{CH}_3$ . Polypropylene is a type of lightweight plastic raw material, density 0.90-0.92 kg/m<sup>3</sup>, has a high hardness and friability and less stable to heat due to tertiary hydrogen.

Table 1: Plastic Material Specific Gravity

Resin	Specific Gravity
PP	0,85 - 0,90
LDPE	0,91 - 0,93
HDPE	0,93 - 0,96
Polystyrene	1,05 - 1,08
ABS	0,99 - 1,10
PVC	1,15 - 1,65
Acetyl Cellulose	1,23 - 1,34
Nylon	1,09 - 1,14
Polycarbonate	1,20
Poly acetate	1,38

## 2.3. Natural Fibre

Natural fibres derived from nature (not artificial or human engineering). Natural fibre or can be regarded as this natural fibre which is usually obtained from plant fibres (trees) such as bamboo trees, coconut trees, banana trees and other plants that have fibre on their stems or leaves (Rodiawan, et. al, 2016; Sanjay and Yagesha, 2017).

Research and use of natural fibres are growing very rapidly these days because natural fibres have many advantages compared to artificial fibres (engineering), the advantages of natural fibres such as lighter loads, easy to obtain materials, relatively inexpensive prices and most importantly environmentally friendly especially Indonesia has abundant natural wealth (Sari, 2018). In this research, the authors use natural fibres, namely hemp fibre and pineapple fibre.

**Table 2: Comparison of natural and synthetic fibres (Surdia, 1995)**

Fibre Type	Density (g/cm <sup>3</sup> )	Diameter (µm)	Tensile Strength (MPa)	Young's Modulus (GPa)	Elongation at Break (%)
Jute	1,3-1,45	20-200	393-773	13-26,5	7-8
Flax	1,5	-	345-1100	27,6	2,7-3,2
Hemp	-	-	690	-	1,6
Hemp (Rami)	1,5	-	400-938	61,4-128	1,2-3,8
Pineapple	1,45	50-200	468-649	9,4-22	3-7
PALF	-	20-80	413-1627	34,5-82,51	1,6
Cotton	1,5-1,6	-	287-800	5,5-12,6	7-8
Coir	1,15	100-450	131-175	4-6	15-40
E-Glass	2,5	-	2000-3500	70	2,5
S-Glass	2,5	-	4570	86	2,8
Aramid	1,4	-	3000-3150	63-67	3,3-3,7
Carbon	1,7	-	4000	230-240	1,4-1,8

### 3. Methods

#### 3.1. Flow Diagram

This research was conducted based on the flow chart as shown in Fig. 2:

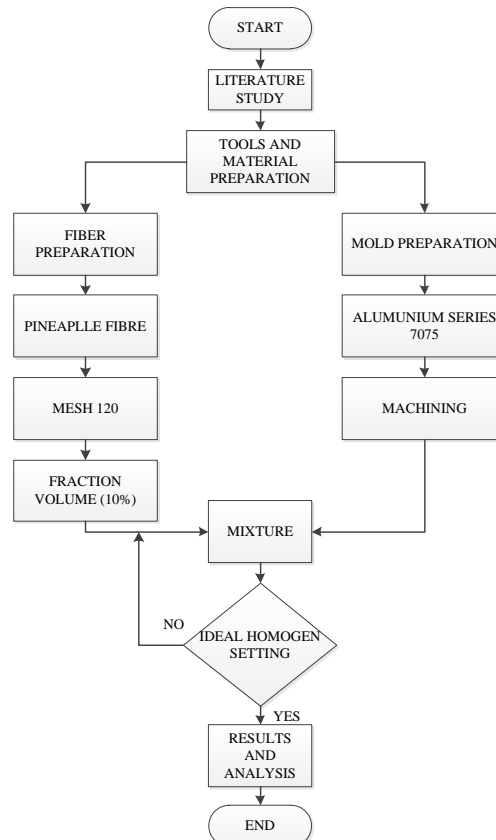


**Fig. 2: Research Methods**



1. Literature study and field survey are the first steps to find information and references relating to this research study.
2. Materials and tools preparation. Some several tools and materials support the process of specimens test making.
3. After the tools and materials needed are met. The process is continuous to specimens test making.
4. Results and discussion, after the process of making test specimens, will be seen from the physical material of the composite polymer regarding the standard.
5. Conclusions, summarizing the results of research by answering the objectives of this study.

### 3.2. Materials

Pineapple fibre and hemp fibre in this study were obtained from Sumenep, Indonesia. High impact polypropylene pellets (PPHI) obtained from PT. Chandra Asri Petrochemical Cilegon, Indonesia.

### 3.3. Preparation of Natural Fibres

The natural fibre is cut along 3 mm, then dried using an oven heater with a temperature of 200 °C and then blended and then shaken with a size below 120 mesh.




### 3.4. Manufacturing Process of PPHI composites with natural fibre reinforcement







Natural fibres that have been shaken with a mesh under 120 are mixed with PPHI pellets with a fibre volume fraction accounting for 10%. Combine PPHI fibre and pellet put in a mould that meets the test standards processed at a temperature of 250 °C after it is cooled for 3 hours.

Natural fibres that have been shaken with a mesh under 120 are mixed with PPHI pellets with a fibre volume fraction accounting for 10%. Combine PPHI fibre and pellet put in a mould that meets the test standards processed at a temperature of 250 °C after it is cooled for 3 hours.

The process of mixing PPHI and pineapple fibre with a volume fraction of 10%, is explained in the table 3:

**Table 3: Mixture process**

Process	Explanation
	Weighing to determine a 10% volume fraction
	Inserting PPHI part in to the mould
	Melt down PPHI in the furnace

Process	Explanation
	Sowing Natural Fibre and PPHI
	Mix to compact a mixture of Natural Fibre and PPHI
	This process is carried out to restore the form of a mixture of fibre and PPHI that has been mixed
	Pressing/closing the mould using a C clamp and cooling for 25 minutes at room temperature
	Finishing/final process is carried out to eliminate the results that are not needed
	Ready for testing specimen

### 3.5. Setting process

In this process the material will be seen from three important aspects when related to the level of homogeneity of the specimen using the hand lay-up method when viewed visually that is the mixing process, the stirring process, and the cooling process. These aspects are shown in table 4:

**Table 4: Specimen Homogeneity**

Parameter	Specimen Homogeneity	
	300 °C	°C
Mixing (Material Density)		
Apart	There is a gap	There is a gap
Not separated	Solid	Solid
Stirring Process (Porosity)		
Without stirring	Major porosity	Major porosity

With stirring	Minor porosity	Minor porosity
Cooling (cracks)		
Normalizing	Minor cracks	No cracks
Quenching	Major cracks	Major cracks

## 4. Conclusion

Seen from the above table 4, it can be concluded that at a temperature of 250 °C with normalizing cooling and PPHI and pineapple fibre enabling processes by stirring can increase the homogeneity of the bending test specimen. In the final product with the recommended setting found porosity defects caused by trapped gas (hydrogen) and porosity caused by shrinkage between dendrites, the gas can be removed from the specimen by stirring and cooling templates are evenly distributed, or controlled by nucleation diffusion and growth, causing a decrease in hydrogen concentration, increasing the rate of solidification so that the formation and growth of voids can be minimized.

## 5. References

- Alzebedeh, K.I., Nassar, M.M.A., Arunachalam R, 2019, Effect of fabrication parameters on strength of natural fibre polypropylene composites: Statistical assessment, Measurement 146, 195-207. (DOI: <https://doi.org/10.1016/j.measurement.2019.06.012>)
- Asim, M., Jawaid, M., Abdan, K., Ishak, M.R., 2016, Effect of Alkali and Silane Treatments on Mechanical and Fibre-matrix Bond Strength of Kenaf and Pineapple Leaf Fibres, Journal of Bionic Engineering 13, 426-435. (DOI: [https://doi.org/10.1016/S1672-6529\(16\)60315-3](https://doi.org/10.1016/S1672-6529(16)60315-3))
- ASTM D 3039, Standard Test Methods for Tensile Properties of Polymer Matrix Composites Materials
- ASTM D 6110, Standard Test for Determining the Charpy Impact Resistance of Notched Specimens of Plastics
- ASTM D 790, Standard Test Methods for Flexural Properties of Unreinforced and Reinforced Plastics and Electrical Insulating Materials
- Borrachero, B.O., Caballero, S.S., Fenollar, O., Selles, M.A., 2019, Natural-Fibre-Reinforced Polymer Composites for Automotive Parts Manufacturing, Key Engineering Materials 793, 9-16. (DOI: <https://doi.org/10.4028/www.scientific.net/KEM.793.9>)
- Gibson, R.F., 1994, Principles of Composite Materials Mechanics, Mc-Graw-Hill.
- Hadi, T.S., Jokosisworo, S., Parlindungan, M., 2016, Penggunaan Serat Daun Nanas Sebagai Alternatif Bahan Komposit Pembuatan Kulit Kapal Ditinjau Dari Kekuatan Tarik, Bending dan Impact, Jurnal Teknik Perkapalan 4, 323-331.
- Kozderka, M., Rose, B., Koci, V., Caillaud, E., Bahlouli, N., 2016, High Impact Polypropylene Recycling – Mechanical Resistance and LCA Case Study with Improved Efficiency by Preliminary Sensitivity Analysis, 12th IFIP, 541-553. (DOI: [https://doi.org/10.1007/978-3-319-33111-9\\_49](https://doi.org/10.1007/978-3-319-33111-9_49))
- Mardiyati, M., Srahputri, N., Steven, S., Suratman, R., 2017, Sifat Tarik Dan Sifat Impak Komposit Polipropilena High Impact Berpenguat Serat Rami Acak Yang Dibuat Dengan Metode Injection Molding, Mesin 26, 39-43. (DOI: <http://dx.doi.org/10.561%2FMESIN.2017.26.1.2>)
- Rodiawan, R., Suhdi, S., Rosa, F., 2017, Analisa Sifat-sifat Serat Alam Sebagai Penguat Komposit Ditinjau dari Kekuatan Mekanik, TURBO 5, 39-43. (DOI: <https://doi.org/10.24127/trb.v5i1.117>)
- Sanjay, M., Yagesha, B., 2017, Studies on Natural/Glass Fibre Reinforced Polymer Hybrid Composites: An Evolution, Materials Today: Proceeding, 2739-2747. (DOI: <https://doi.org/10.1016/j.matpr.2017.02.151>)
- Sari, N.H., 2018, Kekuatan Mekanik Komposit Diperkuat Serat Alam Selulosa, Dinamika Teknik Mesin 8, 51-56. (DOI: <https://doi.org/10.29303/dtm.v8i2.139>)
- Senthilkumar, K., Rajini, N., Saba, N., Jawaid, M., Siengchin, S., 2019, Effect of Alkali Treatment on Mechanical and Morphological Properties of Pineapple Leaf Fibre/Polyester Composites, Journal of Polymers and the Environment 27, 1191-1201. (DOI: <https://doi.org/10.1016/j.polymertesting.2018.11.011>)
- Surdia, T., Saito, S., 1995, Pengetahuan Bahan Teknik, PT. Pradnya Paramitha

## Evaporator Design With Ammonia-Water Mixture as Working Fluid for Kalina KCS34 Cycle On Electric Power Plant

Muhammad Pramuda N. S<sup>1</sup>, Muhammad Ridwan<sup>1,\*</sup> and Agung Priambudi<sup>1</sup>

<sup>1</sup> Department of Mechanical Engineering, Institut Teknologi Nasional (Itenas), Bandung - INDONESIA

\* Corresponding author e-mail: pramudasirodz@itenas.ac.id

### Abstract

Natural hot spring can be used as a heat source for generating electricity by using a Kalina Cycle KCS34 technology with ammonia-water mixture as the working fluid. An Evaporator is one component of the Kalina KCS34 cycle to change the phase of the working fluid. The purpose of this research was to obtain evaporator design for the Kalina KCS34 cycle. Simulation using cycle tempo was conducted to define the inlet and outlet temperature of the evaporator. These temperatures will be used in designing the evaporator was designed using Log Mean Temperature Difference and energy balance methods. The dimension of the evaporator was evaluated with the pressure drop, the effectiveness of the heat exchanger, and standards. The evaporator was using 4 pass shell and tube type with inlet and outlet temperature of the hot fluid (heat source) at 80 °C and 50 °C respectively and the inlet and outlet temperature of the cold fluid (working fluid) at 45 °C and 64 °C respectively. The dimension of the evaporator is 2,5 m in length, 34 tubes per pass with 19,15 diameters. This results in the capacity of the evaporator at 77,41 kW and 75% effectiveness.

*Keywords: Kalina cycle, Heat exchanger, the working fluid, ammonia-water, LMTD*

### 1. Introduction

Geothermal energy is one of the potential renewable energy to be used in generating electricity. Indonesia has 40% of geothermal potential in the world (Indonesia Investments, 2015). One of Geothermal potential indication is a natural hot spring source. Natural hot spring has a low temperature ranging from 60 °C to 80 °C. This lowtemperature heat source can be utilized for an electrical power plant using special technology such as the Kalina KCS34 cycle (Indonesia Investments, 2015).

Kalina cycle was invented by Dr. Alexander Kalina by using ammonia-water mixture as the working fluid. Ammonia-water mixture has low boiling temperature characteristics and suitable for low-temperature heat sources (Pramuda et al, 2017). The components in the Kalina KCS34 cycle are evaporator, condenser, separator, recuperator, and turbine (Figure 1).

The evaporator in the Kalina KCS34 cycle used to change the phase of the working fluid using the heat from natural hot spring water fluid. The working fluid exit the evaporator were two phases, ammonia vapor, and water mixture.

Simulation of Kalina KCS34 cycle using *Cycle Tempo* with 79% ammonia-water mixture fraction was conducted to obtain the inlet and outlet temperature of the evaporator. These temperatures will be used for designing the evaporator. The result expected from this research is the type of evaporator, dimensions, and effectiveness of the evaporator.

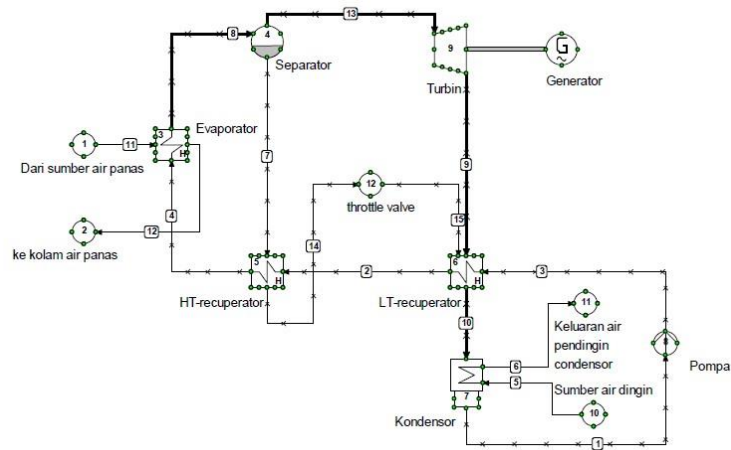


Fig. 1: Schematic Diagram of Kalina KCS34 Cycle (Pramuda et al, 2017)

## 2. Research methodology

The methodology conducted on this research was simulation using *cycle tempo* to obtain inlet and outlet temperature of the evaporator and designing the evaporator using Log Mean Temperature Difference (LMTD) method and evaluated using standards.

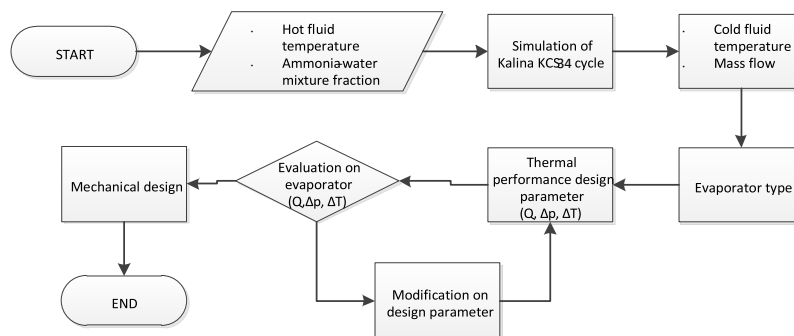


Fig. 2: Research Flow Chart

## 3. Simulation

A Simulation conducted on this research based on the field measurement conducted by Sirodz et al (2016). The temperature of natural hot spring water was 80°C. The evaporator outlet (hot side) was maintained at 50°C due to hot spring tourism requirements. With the 79% mixture fraction of ammonia-water, the simulation shows the inlet and outlet cold fluid (ammonia-water mixture) temperature ( $T_{c,i}$  &  $T_{c,o}$ ) were 45°C and 64°C (Figure 3). The operating pressure of the heat exchanger was 12 bar.

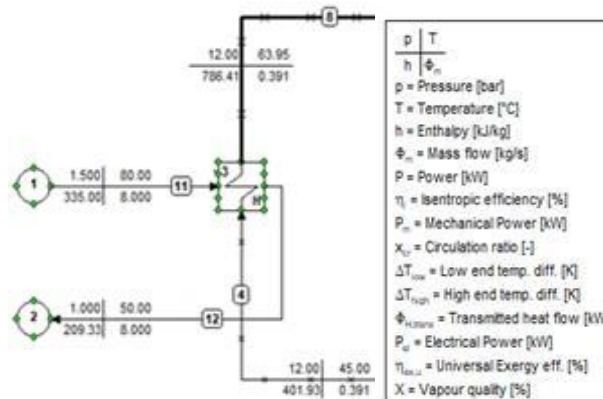


Fig. 3: Simulation results

Based on the operating pressure and operating temperature, shell and tube heat exchanger type C will be used in this research. Shell and tube heat exchanger also has another benefit which is easy for maintenance. To minimize the length of the evaporator, 2 shell passes and 4 tube passes will be used. Considering that ammonia is corrosive, therefore the working fluid will be assigned to the tube side.

## 4. Evaporator design

### 4.1 Shell and tube design

To design the heat exchanger performance, the total heat transfer rate must be related to inlet and outlet fluid temperature, overall heat transfer coefficient, and total heat transfer area. This relation can be calculated using the energy balance. In this research, energy balance was calculated to obtain the heat received by the working fluid from the heat source. The heat released by the hot spring water can be calculated with:

$$Q_h = \dot{m} \times (h_{w\ in} - h_{w\ out}) \quad (1)$$

With hot water inlet temperature ( $T_{h,i}$ ) 80 °C, outlet temperature ( $T_{h,o}$ ) maintained at 50°C, and mass flow of 8 kg/s, the heat released by the hot water was 150,54 kW.

To determine the evaporator heat transfer area, Log Mean Temperature Difference ( $\Delta LMTD$ ) method was used. The value of  $\Delta LMTD$  that has been calculated will be evaluated by a correction factor because the evaporator has multipass flow.

$$LMTD = \frac{(T_{h,i} - T_{c,o}) - (T_{h,o} - T_{c,i})}{\ln \frac{(T_{h,i} - T_{c,o})}{(T_{h,o} - T_{c,i})}} \quad (2)$$

From the calculation value of 9,45 K was obtained. The correction factor was determined by using LMTD correction factor graph with known temperature efficiency (P) and the ratio of the hot fluid temperature difference and cold fluid temperature difference (R).

$$P = \frac{T_{c,o} - T_{c,i}}{T_{h,i} - T_{c,i}} \quad (3) \quad R = \frac{T_{h,i} - T_{h,o}}{T_{c,o} - T_{c,i}} \quad (4)$$

From Figure 4 with  $P = 0,54$  and  $R = 1,54$ , the LMTD correction factor is 0,75. With this correction, the LMTD now has value of 7,09 K.

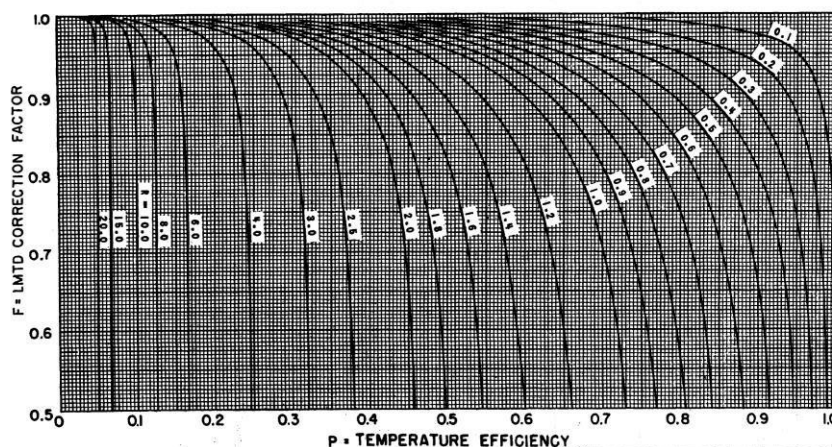


Fig. 4: LMTD Correction Factor (TEMA 8<sup>th</sup> Edition, 1999)

To determine the heat transfer area, the overall heat transfer coefficient of the ammonia-water mixture has to be known. With a 79% mixture fraction, the overall heat transfer coefficient is 952,77 W/m<sup>2</sup>K. The heat transfer area was calculated using the formula:

$$A = \frac{Q_h}{U_{mixture} \times \Delta LMTD_{corrected}} \quad (5)$$

The heat transfer area calculated is 22,28 m<sup>2</sup>. In determining the dimension of the heat exchanger, Standard of The Tubular Exchanger Manufacturer Association (TEMA) is used. The tube length is assumed to be 2,5 m for 1 pass. Copper was selected as the tube material due to high thermal conductivity. Iteration was conducted to find the optimum tube diameter with pressure drop and tube area as the parameters. From the iteration, 19,1 mm tube diameter is optimum. With this diameter, the area of the single tube (A<sup>t</sup>) is 0,149 m<sup>2</sup> therefor the number of tubes (N) required for the evaporator is calculated using:

$$N = \frac{A}{A^t} \quad (6)$$

The number of tubes required for the evaporator is 48 tubes. To facilitate maintenance activity, the square tube pitch was selected. The pitch distance (pt) is 1,25 times the outside tube diameter. With this pitch, the bundle diameter will be 393,49 mm. The bundle diameter will determine the shell inside diameter.

The shell type of the evaporator is assumed to be fixed and U tube type. From the bundle diameter value and type of the shell, using the graph in Figure 5 the clearance between shell and bundle was 13 mm. With the minimum shell thickness of 9,5 mm and shell diameter (DS) of 406,49 mm, the outside shell diameter will be 424,98 mm.

Inside the shell, there are baffles to direct the fluid stream across the tubes and improve the heat transfer rate. The evaporator was designed with segmental baffles. The distance between baffles (Bs) is 81,29 mm were calculated using formula (7) and the number of baffles (Nb) is 30 pieces were calculated using formula (8).

$$Bs = \frac{1}{5} \times Ds \quad (7)$$

$$Nb = \frac{l}{Bs} \quad (8)$$

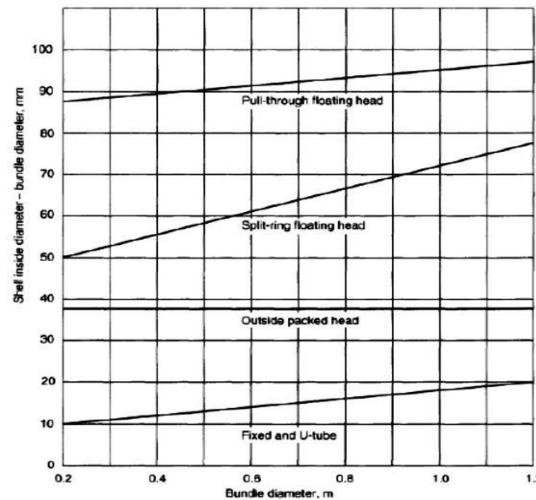


Fig. 5: Shell clearance (Sinnott, 2005)

Typical baffle clearance and tolerance from Colson & Richardson (2005) were used to determine the baffle clearance. Due to the shell diameter of 406,49 mm, the baffle diameter (Dbv) will be 404,89 mm. To allow the fluid flow between the baffles, the baffles needs to be cut. The optimum baffles cut are 25 % of the baffle diameter. This cut will give a good heat transfer rate without excessive pressure drop. From equation (9) the flow area (As) was 0,0064 m<sup>2</sup> and give shell side mass velocity (Gs) 1250,39 kg/m<sup>2</sup>s using equation (10). The shell side equivalent diameter (de) is calculated using the flow area between the tubes taken in the axial direction (parallel to the tubes) and the wetted perimeter of the tubes (equation (11)). For the square pitch arrangement, the equivalent diameter was 18,85 mm.

$$As = \frac{(pt - do) Dbv Bs}{pt} \quad (9)$$

$$Gs = \frac{\text{Shell Flow rate} \left( \frac{kg}{s} \right)}{As} \quad (10)$$

$$de = \frac{1,27}{do} (pt^2 - 0,785 do^2) \quad (11)$$



## 4.2 Pressure drop

Kern methods used to determine the pressure drop in the shell side due to the complex flow pattern. The Kern methods doesn't take account of the bypass and leakage streams. The pressure drop can be calculated using the formula :

$$\Delta p_s = 8 \times Jf \times \left(\frac{Ds}{de}\right) \times \frac{l}{Bs} \times \frac{\rho^2 u}{2} \times \left(\frac{\mu}{\mu_w}\right)^{0,14} \quad (12)$$

Where Jf is the friction factor, l is the tube length, and Bs is the baffle spacing. Arise from Reynold number of 54168,46 and using the shell side friction factors graph (Figure 6) with a 25 % baffle cut gives the friction factor of  $4 \times 10^{-1}$ . Therefore the pressure drop on the shell side is 7,033 Pa.

The pressure drop inside the tube was related to the working fluid and thermal coefficient of the tube. The number of the tube for each pass can be calculated using equation (13) with 4 number of passes. The number of

tube per pass are 37 tubes. With this number of tubes, the total heat transfer area per pass was 0,00637 m<sup>2</sup>. Therefore the flow of the working fluid was 0,00055 m<sup>3</sup>/s. This comes with the Reynold number of 2333,3 to calculate the friction factor. The friction factor (Jf) was 0,5 with considering copper as the tube material and the tube length of 2,5 m. The pressure drop calculation using equation (14) and resulting in 19378,86 Pa of pressure drop. The pressure drop in the heat exchanger is relatively low about 1,6% compared to the operating pressure.

$$N_{tpp} = \frac{Nt}{Pass} \quad (13)$$

$$\Delta p_s = \left[ Nt \left[ 2,5 \times \left( \frac{8Jf \times L}{d_i} \right) \times \left( \frac{\mu}{\mu_w} \right)^{-m} \right] \right] \frac{\rho \cdot u^2}{2} \quad (14)$$

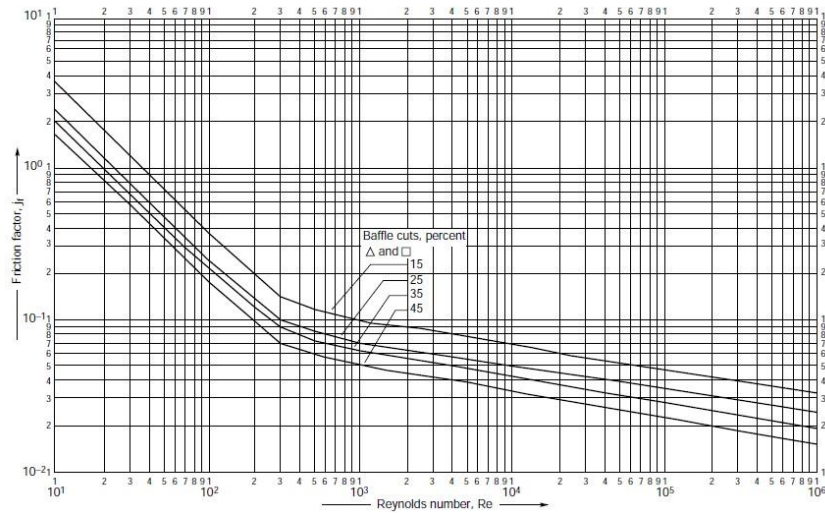


Fig. 6: Shell side friction factor (Sinnott, 2005)

## 4.3 Fouling factor

Fouling can occur in the evaporator due to the operation and condition of the fluids. Fouling factor can be calculated with the value of the overall heat transfer coefficient during the dirtiest condition and the materials to be used. The heat transfer coefficient on the tube side ( $h_i$ ) can be calculated using equation (15) with the Prandtl number of 3,55. The fluid fouling factor for ammonia-water ( $h_{di}$ ) was taken 5000 W/m<sup>2</sup>°C. The heat transfer coefficient for the shell side ( $h_o$ ) can use the equation (15) with the Reynolds number of 54168,46 and the Prandtl number of 2,71. The fluid fouling factor for the hot fluid ( $h_{do}$ ) was taken 3000 W/m<sup>2</sup>°C. The overall heat transfer coefficient during the dirtiest condition can be calculated using equation (16).

$$h_i = jh \frac{k_f}{d_i} (Re \cdot Pr)^{0,33} \left( \frac{\mu}{\mu_w} \right)^{0,14} \quad (15)$$

$$U_i = \frac{1}{\frac{1}{h_i} + \frac{1}{h_{di}} + \frac{d_i \ln\left(\frac{d_o}{d_i}\right)}{2k_w} + \frac{d_i}{d_o h_{do}} + \frac{d_i}{d_o h_o}} \quad (16)$$



The overall heat transfer coefficient during the dirtiest condition was 595,86 W/mK. During the clean condition, the overall heat transfer coefficient was 952,77 W/mK. Therefore the fouling factor was 0,00310 using equation (17). This fouling factor is acceptable.

$$R = \frac{U_i + U}{U_i \times U} = \frac{486,3 + 952,77}{486,3 \times 952,77} \quad (17)$$

#### 4.4 Heat transfer effectivity

Heat transfer effectivity represents heat exchanger performance. The value of heat transfer effectivity was affected by the mass flow and temperature of the cold and hot fluid. The heat transfer effectivity can be calculated using equation (18) .

$$\epsilon = \frac{Q_{act}}{Q_{max}} \times 100\% \quad (18)$$

The actual heat transfer ( $Q_{act}$ ) was 58063,83 W and the maximum heat transfer ( $Q_{max}$ ) was 77418,44 W.

Therefor the heat transfer effectivity was 75%.

## 5. Conclusion

The evaporator was designed with shell and tube heat exchanger type C and has the capacity of 77,41 kW and the heat transfer effectivity of 75 %. The dimension of the evaporator presented in Table 1. The general component of the evaporator presented in Figure 7.

**Table 1. Dimensions of the evaporator**

Shell		
Shell diameter	406,87	mm
number of baffles	31	baffles
baffle thickness	45	mm
shell material		carbon steel
Tube		
number of passes	4	passes
tube length (1 pass)	2500	mm
number of tubes (1 pass)	37	tubes
tube outside diameter	19,15	mm
tube inside diameter	14,82	mm
tube layout		square pitch
tube pitch	23,8	mm
tube material		copper

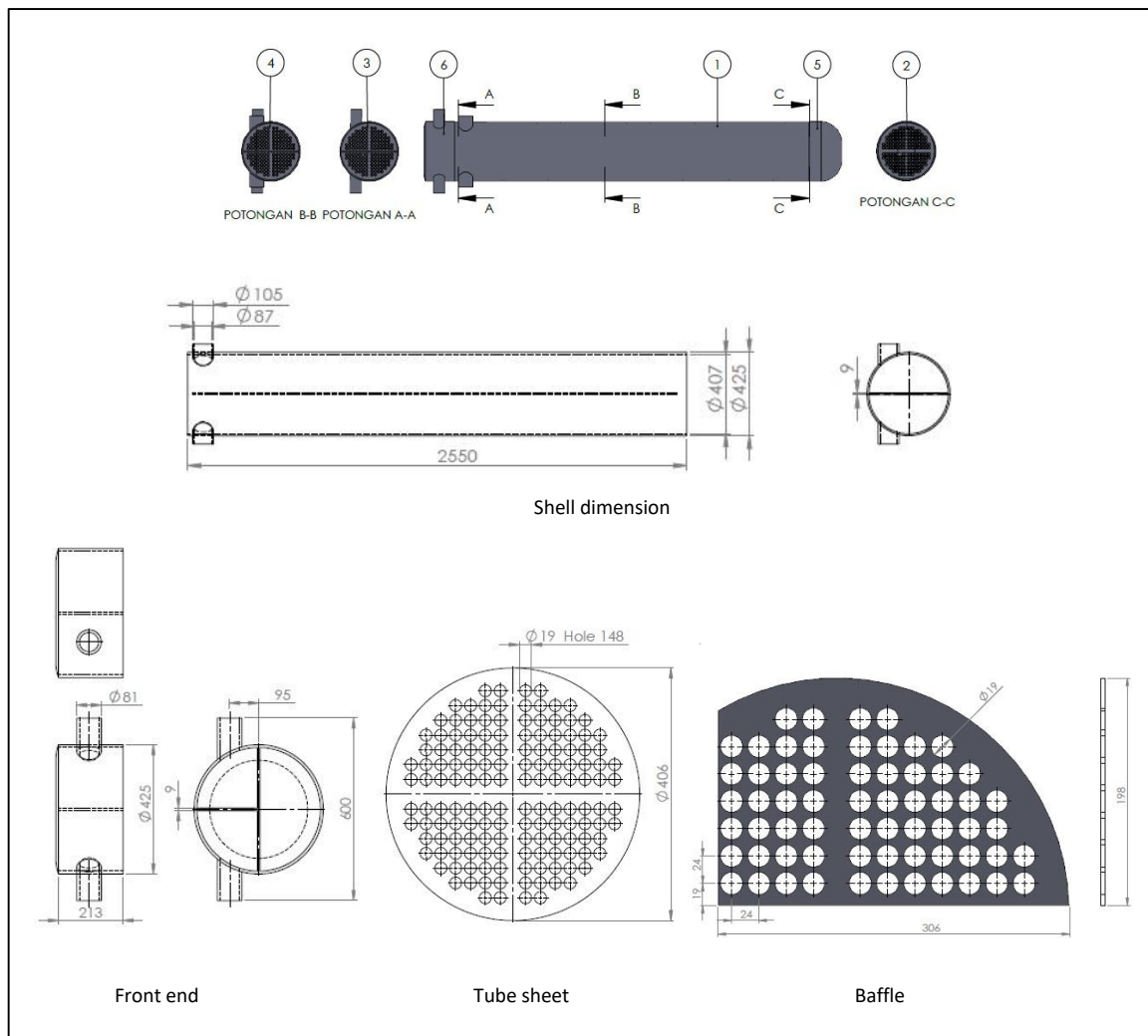


Fig. 7: Dimensions of evaporator

## 6. References

- N. S, Muhammad Pramuda., Ridwan, M., Maulana, Iqbal., 2017. Optimasi Siklus Kalina KCS34 Pada Pemanfaatan Sumber Air Panas (Natural Hot Spring) Sebagai Pembangkit Listrik. *Rekayasa Hijau*, Vol. 1, pp. 43-53.
- N. S, Muhammad Pramuda., Ridwan, M., Maulana, Iqbal., 2015. Studi Potensi Pemanfaatan Sumber Air Panas (Natural Hot Spring) Sebagai Pembangkit Listrik (Studi Kasus di Ciwidey, Jawa Barat). *Seminar Nasional XIV Rekayasa dan Aplikasi Teknik Mesin di Industri*, ISSN 1693-3168, pp. TKE 66-71.
- Kern, Donald Q., 1983. *Process Heat Transfer*. Auckland Bogota – McGraw-Hill.
- Thulukkanam, Kuppan., 2013. *Heat Exchanger Design Handbook* 2nd edition. Boca Raton – CRC Press.
- Sinnott, R. K., 2005. *Chemical Engineering Design* 4th edition. Oxford – Elsevier Butterworth-Heinemann.
- Smith, Eric M., 1997. *Thermal Design of Heat Exchanger*. Chichester – Jhon Wiley & Sons.
- Indonesia investments, Energi Panas Bumi, available at: [www.indonesiainvestments.com/id/bisnis/komoditas/energi-panas-bumi/item268?](http://www.indonesiainvestments.com/id/bisnis/komoditas/energi-panas-bumi/item268?), accessed on March 10, 2019.

## Pilot Plant Biodiesel From Waste Cooking Oil

Rif'ah Amalia<sup>1\*</sup>, Hendrik E.G.P<sup>2</sup>, Achmad B. Ulum<sup>3</sup>, and Eka S.N<sup>4</sup>

<sup>1,2,3,4</sup>Department of Power Plant Engineering, Politeknik Elektronika Negeri Surabaya, Surabaya -  
INDONESIA

\* Corresponding author e-mail: rifahamalia@pens.ac.id

### Abstract

Methyl ester or biodiesel is an alkyl ester compound that is produced through an alcoholic process (transesterification), between triglycerides methanol or ethanol with the aid of alkaline catalysts into alkyl esters and glycerol. Methyl ester is produced through a transesterification reaction between used cooking oil and methanol with a mole ratio of 6:1, the reaction is accelerated using base catalyst. The method used in the production of methyl ester is pilot plant batch scale which adopts a large scale industry with modifications according to the desired design. Base catalyst variations were carried out at 0,1% w/w, 0,3% w/w, 0,5% w/w, 0,7% w/w, and 0,9% w/w. The productions of methyl ester consists of three processes namely pre-treatment, transesterification reaction, and post-treatment. Quality test of methyl ester (post-treatment) consists of density, kinematic viscosity, total glycerol, and acid numbers. Known from the result of the research, the overall quality of methyl ester are appropriate according to the Indonesian National Standard on Biodiesel.

*Keywords: Biodiesel, Pilot Plant, Waste Cooking Oil, Transesterification*

## 1. Introduction

This 21<sup>st</sup> century life makes people increasingly consumptive in using energy. Energy needs will be a primary necessity, if no renewal or alternative energy will cause instability between the raw material and the energy requirement. Energy is the ability to perform work, the power used to perform various processes of activity. Energy has several forms and comes from anywhere e.g. electrical energy, light energy, chemical energy and others. Alternative energy is the substitute energy of energy itself. Alternative energy originated not from petroleum includes hydropower, geothermal, nuclear, solar, wind, wave, biomass, natural gas, peat, coal and natural gas. Where appropriate you should overtype the different fields with your own text. Make sure that as you do this the correct style for the current paragraph is still displayed in the style box on the menu bar. Please read through the following sections for more information on preparing your paper. However, if you use the template you do not have to worry about setting margins, page size, and column size etc. as the template already has the correct dimensions.

With the instability of energy production and consumption has changed the energy paradigm and forced the world adapt to achieve sustainable long-term energy security (Budiman, 2014). The world's consumption of petroleum diesel is 934 million tonnes per year (Atmaja, 2010). Knowing the condition of the Indonesian government began to seek alternative energy replacement of petroleum diesel by utilizing biomass from biofuels (BBN) derived from renewable natural resources such as methyl ester (biodiesel).

Methyl esters are alternative diesel fuels made from renewable biological sources such as vegetable oils and animal oils. Methyl esters can be biodegradable and nontoxic, and have low emissions as well as environmentally friendly (Atmaja, 2010). Indonesian region has a lot of potential raw materials producing methyl ester, covering oil palm, jatropha, oil, coconut oil, nyamplung oil, algae, etc (Densi, 2017).

The cooking oil is one of the raw ingredients of methyl ester. Cooking oil from the food industry and households are quite available in Indonesia. The sour oil is not good if it is reused for cooking because it contains a lot of free and radical fatty acids that can harm health. Used cooking oil can be the raw material of methyl ester but the used cooking oil has a free fatty acid content with a fairly high concentration, but the content can be reduced by reacting free fatty acids with catalysts.

Methyl esters of the barley oil are produced through the transesterification process. In the process of transesterification used cooking oil is reacted with alcohol (methanol) and a base catalyst will produce glycerol as a side product. This process has immiscible (not mixed) properties, therefore heating with heater and mixing with stirrer is necessary to homogenize the oil of the jelantah, alcohol and catalyst. The process of slurries (precipitation) occurs twice to precipitate the side products and water used to clean the methyl ester from the dirt that is still possible mixed.

The method used in this research is a pilot plant method of adopting from an industrial environment, expected the result of methyl ester close to the quality of the industry. With the advantages of production process of methyl ester through batch scale plant pilot method through transesterification reaction, it is expected to be the bridge between the transesterification process of oil in the laboratory scale and industrial scale.

## 2. Production Process of Methyl Ester

### 2.1 Methyl Ester (Biodiesel)

Methyl ester or biodiesel is an alkyl ester compound produced through the process of Alcoholis (transesterification), between triglycerides with methanol or ethanol with the help of base catalysts into methyl ester and glycerol. Excess methyl ester is among other un toxic fuels and biodegradation, high devil numbers, carbon monoxide emissions, hydrocarbons and NOx value small, phase in liquid form.

### 2.2 Raw Materials

Initially, the raw materials used for the manufacture of methyl esters are derived from vegetable oil such as edible oil, such as oil from soybeans, coconut oil, oil from sunflower seeds and many others, but gradually raises the issue Competition against the food security of a country. Therefore (Budiman 2014) the idea arises to create methyl esters from nonedible oils such as jatropha oil, nyamplung oil and castor oil. Because of pollution problems produced by nonedible material, other ideas arise to use microalgae as raw material of methyl esters that do not cause pollution and other environmental problems. In addition to the three materials above the other methyl ester material derived from low quality waste among other raw materials so it is required a long enough process to be converted to methyl ester. The use of waste cooking oil (used cooking oil) as the raw material of methyl ester aims to utilize the abundance of common oil amounts in the community.

### 2.3 Batch Scale Plant Pilot Method

The use of methods on this research is an industry adoption method. With another name of pilot plant. Pilot plant is a method of adoption of large scale factory modified according to the desired design. While the batch scale is a measure comparison in this study is intended the process of mixing oil and other materials in the manufacture of biodiesel. The molar ratio between alcohol and triglycerides is 4:1 to 20:1, but the most widely used ratio is 6:1. With operating temperatures ranging from 298 – 358K. Excess batch process is easy mixing of raw materials, efficient feeding of chemicals, and easy quality control.

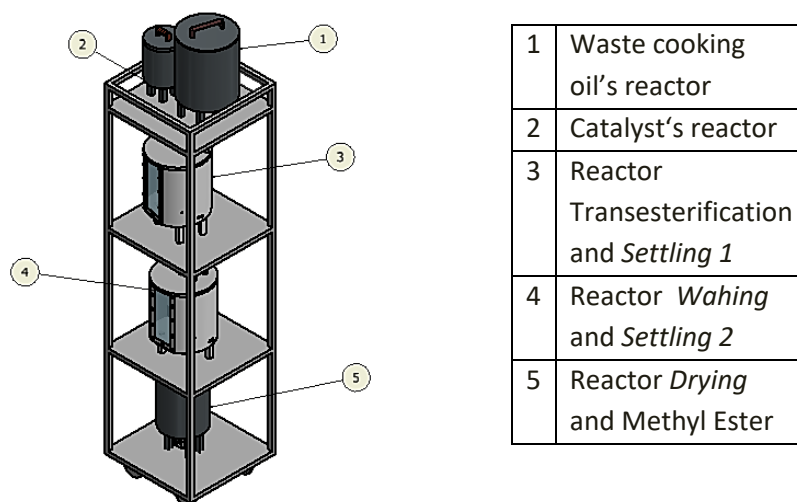


Fig. 1: Pilot Plant Biodiesel

### 2.4. Transesterification process

In this study, using a base catalyst so that the chemical reaction used was transesterification. With another sense of transesterification reaction is the reaction between alcohol and triglycerides forming methyl ester and glycerol. Step transesterification process, among others: (i) the raw material is heated and stirring in tanks up to 60°C temperature; (ii) the mixture is precipitized up to two phases between the glycerol and the crude methyl ester (process slurries 1); (iii) crude methyl ester will then be washed until normal pH (6.8-7.2) (washing process); (iv) performed re-deposition to

separate water (process slurries 2); (v) heating methyl ester at 60°C (drying process).

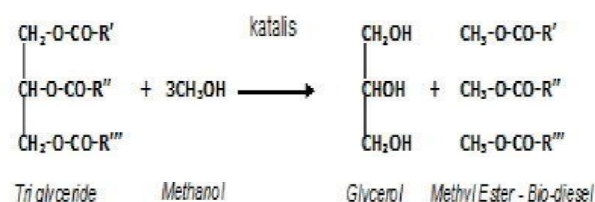


Fig. 2 : Transesterification process

### 3. Result and Discussion

Preliminary research is done by calculating the levels of free fatty acids (FFA) and the number of acids in oil. Known as FFA content of 0.5% so that it is still in terms of < 2%, then the process of transesterification is done. Density value of the equipment using the balance sheet and picnometer. Viscosity sampling is possible by the Ostward Viskometer method. Total glycerol and acid number by doing a base acid titration.

Table 1 Standard SNI Biodiesel and Solar

Parameter	SNI Biodiesel	Solar
<b>Density (kg/m<sup>3</sup>)</b>	850-890	859,9
<b>Kinematic Viscosity (cSt)</b>	2,3-6	4,17
<b>Total Glycerol (%)</b>	maks 0,05	0
<b>Acid Number (mg-NaOH/gr)</b>	maks 0,8	0

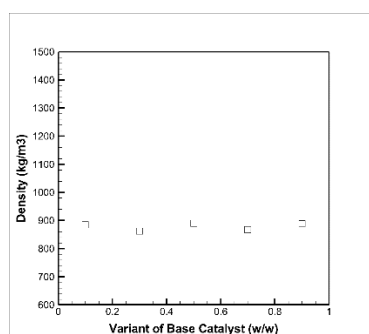
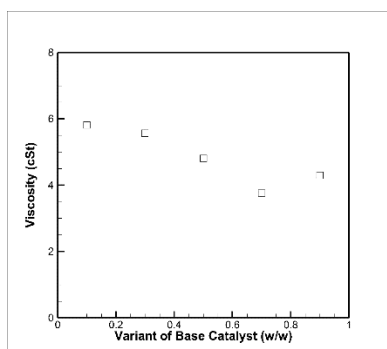


Fig. 3 : Influence of base catalyst variation on density

From Fig.3 shows the density value of methyl ester tends to increase in proportion to the increase in the concentration of the catalyst base. Factors affecting density include the concentration of basic catalysts and the purification process (washing and drying). The increase in base catalyst in the methyl ester mixture is proportional to the density, where molarity is the concentration of the solution obtained from the mole ratio of the solute to the volume of the solvent. Moles of the solute are broken down again into a ratio of the mass of the solute and the relative molar mass of a substance. Density is the ratio of mass of solute to volume. Then the density is directly proportional to the increase in base catalyst. The greater the catalyst concentration, the higher the density value will be.

Based on this study methyl esters with variations of base catalyst 0.1% w / w, 0.3% w / w, 0.5% w / w, 0.7% w / w, and 0.9% w / w value density is directly proportional to the concentration of methyl ester and the density value of methyl ester is in accordance with SNI Biodiesel, so it can be used as a diesel mixture for diesel engine fuel.



**Fig. 4 : Influence of base catalyst variation on kinematic viscosity**

It is explained in Fig. 4 that the kinematic viscosity of methyl esters towards increasing base catalyst tends to decrease. The decrease in viscosity is proportional to the increase in concentration of the base catalyst used. Based on experimental results, the kinematic viscosity value of methyl ester shows that the alkaline catalyst reaction succeeded in reducing the viscosity of the catalyst. Factors that influence the kinematic viscosity of methyl esters are the concentration of basic catalysts and the purification process. Kinematic viscosity equation is a comparison between dynamic viscosity and density. From this equation it is known that kinematic viscosity is inversely proportional to density, where density is directly proportional to the concentration of the catalyst base. Then the kinematic viscosity relationship is inversely proportional to the increase in base catalyst concentration.

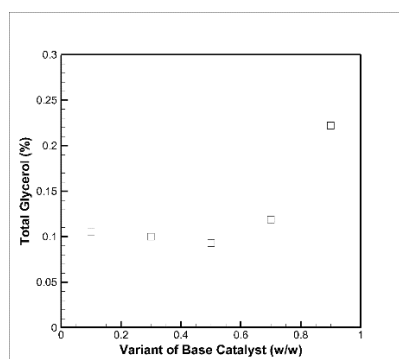


**Fig. 5 : Influence of base catalyst variation on total glycerol**

Glycerol is a byproduct of methyl esters. The total glycerol in this calculation is the glycerol methyl ester level. Glycerol is a viscous liquid, easily dissolves in water, and binds to water.

From fig.5 the glycerol content tends to increase with increasing base catalyst concentration. The volume of catalyst titration becomes the main parameter in determining the quality of methyl esters. Due to the low volume of the titration the activation energy is low. Based on the Arrhenius law where the activation energy is inversely proportional to the reaction rate constant and the reaction rate constant is directly proportional to the reaction rate. The catalyst is a substance to reduce the activation energy so that with a large catalyst concentration will decrease the activation energy and increase the reaction rate.

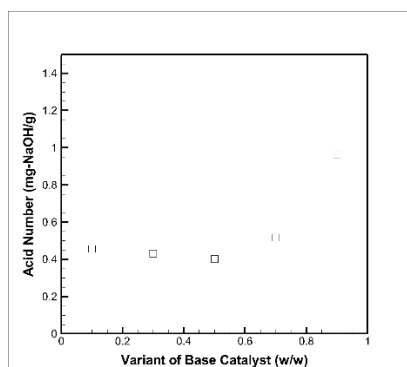


**Fig. 6 : Influence of base catalyst variation on acid number**

Acid number is the number of milligrams of catalyst needed to neutralize 1 gram of sample (methyl ester). Acid numbers are required to be as small as possible because free fatty acids are corrosive so as to cause damage to the components of diesel engines, high acid numbers can cause fuel deposits, causing pumps and filters more quickly damaged. Acid numbers indicate the acid content still present in methyl esters. Factors affecting numbers are quality of used cooking oil and base catalyst concentration. With a low acid content, the quality of methyl esters increases. This is in accordance with Arrhenius's law where the low activation energy facilitates the rate of reaction, so that the reaction of methyl ester changes will be faster and easier.

Table 2. Biodiesel Physical Properties Testing

Parameter	Waste Cooking Oil	0,1% w/w	0,3% w/w	0,5% w/w	0,7% w/w	0,9% w/w
Density (kg/m <sup>3</sup> )	928,7	855,8	858,7	863,3	865,0	<b>869,3</b>
Kinematic Viscosity (cSt)	10,55	4,80	5,18	5,51	5,55	<b>5,54</b>
Total Glycerol (%)	-	0,046	0,046	0,043	0,043	<b>0,043</b>
Acid Number (mg-NaOH/gr)	<b>1,891</b>	<b>0,565</b>	<b>0,423</b>	<b>0,413</b>	<b>0,412</b>	<b>0,363</b>



Fig. 7: Methyl Ester and Waste Cooking Oil

#### 4. Equation

Here are the equations used in working on the production of biodiesel.

$$FFA\ levels = \frac{N\ NaOH \times v\ NaOH \times 200}{w \times 1000} \times 100\% \quad (1)$$

$$\rho = \frac{m}{v} \quad (2)$$

$$\mu = \frac{\rho \times t \times \mu_0}{\rho_0 \times t_0} \quad (3)$$

$$v = \frac{\mu}{\rho} \quad (4)$$

$$glycerol = \frac{N\ NaOH \times v\ NaOH \times 92}{w \times 1000} \times 100\% \quad (5)$$

$$Acid\ number = \frac{39,9 \times v\ NaOH \times N\ NaOH}{w} \quad (6)$$

where:

- FFA levels is free fatty acid of used cooking oil,
- $N_{NaOH}$  is normality of NaOH,
- $v_{NaOH}$  is titration volumes from NaOH,
- $w$  is sample mass
- $\rho$  is the density value,
- $m$  is biodiesel sample mass,
- $v$  is biodiesel sample volume,
- $\mu$  is the dinamic viscosity value,
- $t$  is the sample time passes through fluid,
- $\mu_0$  is reference of viscosity,

- $\rho_0$  is reference of density,
- $t_0$  is reference of sample time passes through fluid
- $v$  is kinematic viscosity value,
- 92 is mass glycerol molarity, and
- 39,9 is mass fatty acid molarity.

## 5. Conclusion

Based on the analysis of the production of biodiesel pilot Plant method with a variation of alkaline catalyst can be concluded as follows: (i) Production of methyl ester pilot Plant method successfully carried out using transesterification reaction; (ii) by increasing the concentration of base catalysts on biodiesel production The pilot Plant method is known that the biodiesel quality is in accordance with SNI Biodiesel.

## 6. Nomenclature

N	Normality	N
v	titration volumes	mL
w	sample mass	gram
$\rho$	density value	gram/mL
m	biodiesel sample mass	gram
v	biodiesel sample volume	mL
$\mu$	dynamic viscosity value	cp
t	the sample time passes through fluid	second
$\mu_0$	reference of viscosity	cp
$\rho_0$	reference of density	gram/mL
$t_0$	reference of sample time passes through fluid	second
v	kinematic viscosity value	cp

## 7. Acknowledgments

The author gratefully thank you to Allah SWT and local research at Politeknik Elektronika Negeri Surabaya.

## 8. References

- Atmaja, S, 2010. Biodiesel Dari Minyak Jelantah (Waste Cooking Oil) Sebagai Solusi Sumber Energi Alternatif Ramah Lingkungan. Karya Ilmiah Teknologi Bandung.
- Budiman, A, 2014. Biodiesel Bahan Baku, Proses, dan Teknologi. Yogyakarta: Erlangga.
- Laila, L., Liatiana, O, 2017. Experiment Study Of Total Acid Number And Viscosity Of Palm Oil Based Biodiesel From PT Smart Tbk. Jurnal Teknologi Proses Dan Inovasi Industri, Vol. 2, No. 1.
- Eryilmaz, T, 2015. Design Of A Small Scale Pilot Plant Biodiesel Production Plant And Determination Of The Fuel Properties Of Biodiesel Produced With This Plant. Turkish Journal of Agriculture - Food Science and Technology, 3(2): 67-70.
- Oseni, M. I., Tuleun, M. T., & Musa, A. Development and Performance Evaluation of a Small Scale Biodiesel Production Pilot Plant. Journal of Emerging Trends in Engineering and Applied Sciences (JETEAS) 4(4): 679-685.
- Yulianingtyas, P. Kajian Proses Produksi Biodiesel Melalui Transesterifikasi In Situ Jarak Pagar (Jatropha Curcas L.) pada Skala Pilot Plant. Institut Pertanian Bogor.



## Ratio Optimization of Wind-Solar Hybrid System

Muhammad Haekal<sup>1\*</sup>, Dani Rusirawan<sup>2</sup>, and Istvan Farkas<sup>3</sup>

<sup>1</sup> Graduate Student of Mechanical Engineering, Szent Istvan University, Godollo – HUNGARY

<sup>2</sup> Department of Mechanical Engineering, Institut Teknologi Nasional (Itenas), Bandung – INDONESIA

<sup>3</sup> Department of Physics and Process Control, Szent István University, Godollo – HUNGARY

\* Corresponding author e-mail: mhaekalt@gmail.com

### Abstract

Indonesia is located in equator line which mean it has a constant period of solar radiation period throughout the year, as identified about 4.80 kWh/m<sup>2</sup>/day. The potential of wind energy is about 60,647 MW which only 0.01% is used. Therefore, in order to meets the target by 2025 and 2030 Indonesia needs to utilize renewable energy sources. Wind and solar energy appears to a prospective solution mentioned that the fast growing of both technology resulting in the decrease of its total system cost. Moreover, couple both sources energy somehow lowered the cost as well as tackle the issue of their intermittent sources. In this study, simulation of wind-solar hybrid system will be done with various capacities and will be compared with a system with 100% solar and 100% solar.

*Keywords: Hybrid, Solar, Wind, Renewable Energy*

## 1. Introduction

Traditionally, fossil fuels are used as primary sources of energy. However, harmful gas emission due to the burning of fossil fuels has challenged the future viability of the human civilization that is depending on conventional energy sources.

Moreover, under the Paris Agreement in 2015, member countries have to meet the proposed target by 2025 or 2030. Utilizing renewable energy sources come as one of the solutions to encourage the substitution for fossil fuel energy which likely result in reducing greenhouse gas (GHG) emission in the atmosphere and meet each countries target. As for Indonesia, the country sets its target to increase 23% of electricity are generated from renewable energy resources by 2025 and reduce GHG emission to 29% by 2030

Indonesia is located in the equator line, and therefore it has a constant period of solar radiation period throughout the year, as identified is about 4.80 kWh/m<sup>2</sup>/day. The potential of wind energy is about 60,647 MW, and presently only 0.01% is used. Based on this fact, it can be predicted that a hybrid renewable energy system between wind and solar energy is a potential solution to have a contribution to meet the national strategy.

**Table 1: Renewable Energy Resource Potential in Indonesia (Source: Rencana Umum Energi Nasional, 2017)**

No	Energy Sources (MW)	Potency (MW)	Installed Capacity (MW)
1	Geothermal	29,544	1,439
2	Hydro	75,091	4,827
3	Micro-Hydro	19,385	197
4	Bio Energy	32,654	1,671
5	Solar	207,898	79
6	Wind	60,647	31
7	Ocean	17,989	0
Total		443,208	

The sequences of the simulation process are as follow: fully of the photovoltaic (100% PV), fully of the wind turbine (100% WECS = wind energy conversion system), and varying of the ratio between solar and wind, as a hybrid system. The expected outcome of this study is try to find the optimal ratio between photovoltaic and wind turbine in hybrid system, in the certain area, for the predetermined of the capacity.

## 2. Hybrid Resources Energy System

(Mita Bhattacharya et al.) in their study about the effect of renewable energy on economic growth found that wind, solar PV, and hydropower are the sources having significant growth in the electricity sector. Besides, the rapid development of wind and solar has a significant contribution to the position of renewables as a vital part of the global power mix and resulting in the technical maturity and their cost.

(Mehdi Ben Jebli et al.) mentioned with the rapid reduction in the cost of the main system components including PV panels, wind turbines, and batteries, the total system cost is considerably decreased. As the result of today fast-growing rate of renewable power production based on wind and photovoltaic systems.

(Jeffy Johnson, et al) studied the feasibility of a 200 kW solar wind hybrid system in the Dehradun district (Uttarakhand, India). The study is using Homer for simulation with the model as shown in Fig. 1.



Fig. 1: Hybrid System Model (Source ....)

The model consists of solar PV system (100 kW), Wind turbine generator (100 kW), DC/AC converter (100 kW). Lead-acid battery storage, 100 kW h (1 kW h, 100 strings) and Electrical Load (193.80 kW h/day). By assuming the load profile, operation and maintenance cost, lifetime and derating factor, it was found that the yearly average electricity production was 55.56% by wind energy and 44.44%. The total net present cost or life-cycle cost (NPC) of the system is about \$1,774,269. The operating cost of the project during its entire lifetime is obtained at \$3,277 — comparison with a generator only system (considering a 200 kW diesel generator costing \$15,000). The total net present cost of a generator only system is \$7,062,077. The total operating cost will be \$267,807.

(I.A. Adejumobi et al.) studied a hybrid solar-wind power in Information Communication Center (ICT) infrastructure and communities in rural areas. The calculation of estimated load in ICT, Bank, and Hospital was done in this research. Furthermore, the model mainly consists of photovoltaic that produced direct current (DC) electricity and wind turbine system was transported to DC Disconnect before entering Mix Controller (Fig. 2)

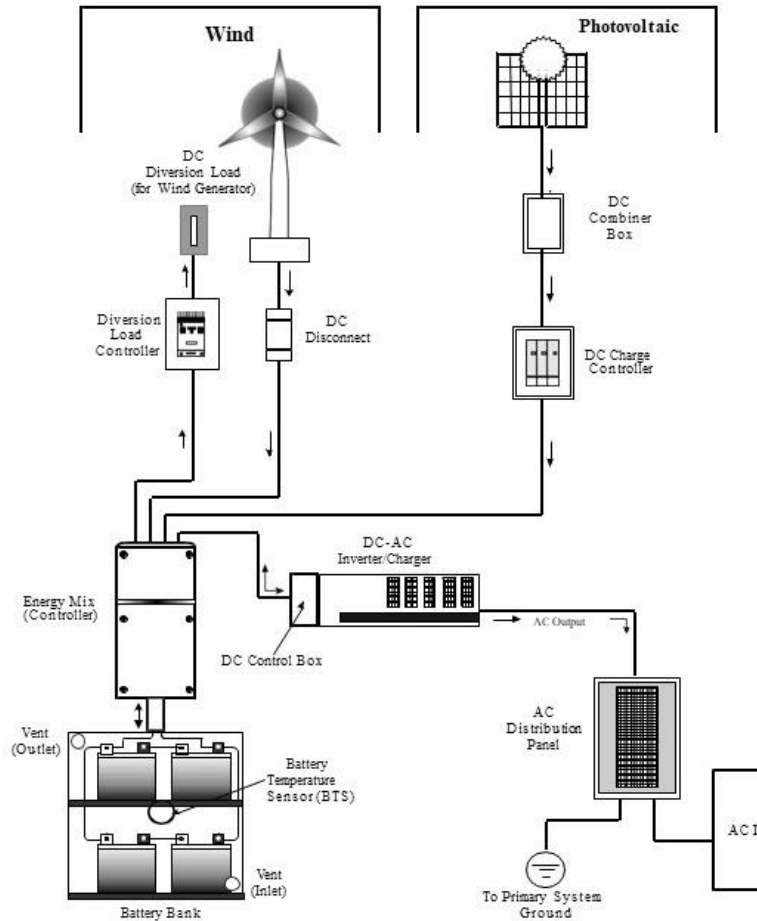


Fig. 2: Schematic Diagram of Hybrid System (Source ....)

The off-grid (stand-alone) system are suggested since there is no utility grid service in a rural area. Moreover, the off-grid system is considered economical in providing electricity at remote locations especially rural banking, hospital and ICT (Information Communication Technology) in rural environments.

### 3. Input Data

Cipatujah (West Java, Indonesia) is selected as the location of the study. Solar and wind data were obtained for the location through NASA (National Aeronautics and Space Administration) database through its site. As the latitude and longitude of which was assumed to be the same as that of Cipatujah, West Java, Indonesia.

- Latitude: -7.7294
- Longitude: 107.9152

As Figure 3 and 4 show, the simple average of the data was obtained. Direct normal irradiation is found to be 4.21 kW h/m<sup>2</sup>/day, while the average wind speed at 10 meters and 50 meters are 4.68 m/s and 5.55 m/s respectively.

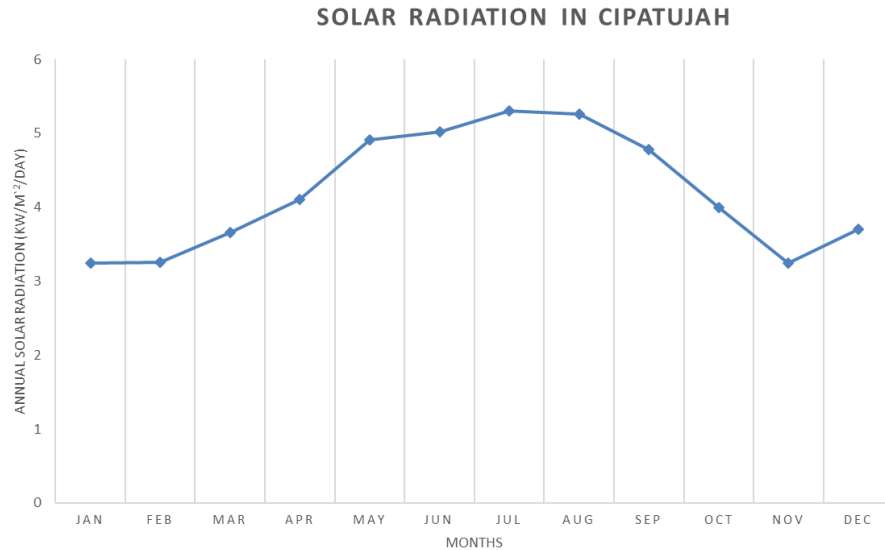


Fig. 3: Solar radiation in Cipatujah (Source: NASA Database)

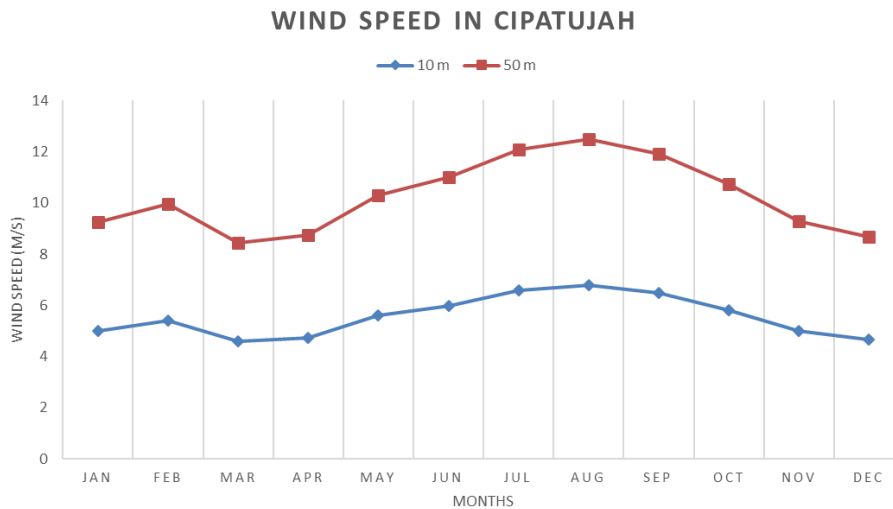


Fig. 4: Wind speed in Cipatujah (Source: NASA Database)

## 4. Simulation

In this study, the simulation will be done using HOMER (Hybrid Optimization Model for Electric Renewables) and RetScreen. HOMER simulations are performed by analyzing energy balance calculations and show all possible configurations arranged by net present cost which can be useful for comparison of system design. It also facilitates us to carry out sensitivity and optimization analysis. On the other hand, RET Screen can perform technical, financial, and economic analysis and risk and sensitivity evaluations. The proposed case is comparable with the best case to understand the plus-points.

## 5. Expected Result

The proposed study's primary goal is acquiring the optimal ratio between photovoltaic and wind turbines through. At first, the simulation will be done for fully photovoltaic, fully wind turbines, and various ratios between solar and wind hybrid systems, which the capacities of 10 KW, 50 KW, and 250 KW. Also, the long-term target is providing a method for optimized the hybrid system will be proposed as well as the differences between the existing and suggested method will be found.

## 6. References

ArcGIS Web Application, available at <https://power.larc.nasa.gov/data-access-viewer/>, accessed on January 2, 2020.

Ben Jebli, M., & Ben Youssef, S. (2015). Output, renewable and non-renewable energy consumption and international trade: Evidence from a panel of 69 countries. *Renewable Energy*, 83, 799-808. doi: 10.1016/j.renene.2015.04.061

Bhattacharya, M., Paramati, S., Ozturk, I., & Bhattacharya, S. (2016). The effect of renewable energy consumption on economic growth: Evidence from top 38 countries. *Applied Energy*, 162, 733-741. doi: 10.1016/j.apenergy.2015.10.104

Datta, U., Kalam, A., & Shi, J. (2018). Hybrid PV–wind renewable energy sources for microgrid application: an overview. *Hybrid-Renewable Energy Systems In Microgrids*, 1-22. doi: 10.1016/b978-0-08-102493-5.00001-7

I.A., A., S.G., O., F. G., A., & M.B., O. (2011). Hybrid Solar and Wind Power: An Essential for Information Communication Technology Infrastructure and People In Rural Communities. *IJRRAS*, 9(1), 130-138.

Johnson, J., Mondal, S., Mondal, A., Rana, S., & Pandey, J. (2018). Feasibility Study of a 200 kW Solar Wind Hybrid System. *Applied Solar Energy*, 54(5), 376-383. doi: 10.3103/s0003701x18050080

Rencana Umum Energi Nasional, available at <https://www.esdm.go.id/assets/media/content/content-rencana-umum-energi-nasional-ruen.pdf>, accessed on December 20, 2019.

## ***B. Engineering (Electrical, Electronics, & Mechatronics)***

## Measurement of Wastewater Turbidity Based on Total Dissolved Solids at Pancasila University

Muhammad Yaser<sup>1\*</sup>, Untung Priyanto<sup>2\*</sup>, Fauzie Busalim<sup>3</sup>.

<sup>1,2,3</sup>Faculty of Electrical Engineering, Pancasila University, Jakarta Indonesia.

\*Corresponding author Email: muhammadyaser@univpancasila.ac.id,  
untung.priyanto@univpancasila.ac.id

### Abstract

Groundwater is polluted by industry, house and laboratory disposal. It is necessary to measure the value of water turbidity quality. Application of prototype design of tool design in this study will provide solutions. It is expected that the results of the research analysis and measurement of water turbidity and do the filtering to get the quality of clean water quality and can be reused. The method is carried out by monitoring the process of Total Dissolved Solids (TDS) using Arduino-based Turbidity Sensor with digital display and using short message service (SMS) display network. Implementation steps to maintain the quality standard of water quality before being discharged into the groundwater catchment around the Engineering Department Pancasila University (FTUP) campus, the FTUP Green plan educational institution becomes the Green Campus. The results obtained show that the measuring instrument is functioning properly and it has average error value about 0.98 %.

*Keywords: Measurement, Wastewater, Turbidity, Water Quality, TDS (Total Dissolved Solids).*

## 1. Introduction

Turbidity and water filter measurement tool is designed to accommodate water quality standard around FTUP. It is stated in FTUP Development Mother Plan term 2019-2024 year, Pancasila University is expected to be a Green Campus. In this research will be designed turbidity measurement for wastewater by making the design of a tool that can monitor remotely using the IoT in conducting the filtering process to get clean water quality. Based on the Regulation of the Minister of Health No. 907 / Menkes / SK / VII / 2002, there are several conditions that must be met by water so that it becomes water that is suitable for consumption. At present most people do not know about drinking water quality standards. Drinking water is safe for health if it meets the physical, microbiological, chemical and radioactive requirements [1].

**Table 1. Requirements & supervision of drinking water quality [1].**

Parameter	Maximum allowed level	Unit
Taste & Smell	Odorless and tasteless	-
Dissolved solids (TDS)	1000	mg / l
pH	6.5 - 8.5	-
Colors	15	TCU
Turbidity	5	NTU
Temperature	Air temperature $\pm$ 3	°C

The selection of important parameters in the measurement of water in order to meet the provisions of good water that is tasteless, odorless and colorless. The first parameter is the value of turbidity of water which is a parameter that will be measured according to the conditions of changes that occur whether under ( $\leq 4$  NTU) or greater value of turbidity value ( $\geq 4$  NTU), then the tool design system will function, carry out according to the monitoring process.

## 2. Literature review.

Several studies related to water quality measurement tools have been carried out measurement of Arduino-based results reading with digital display as follow;

- Linda Handayani, Rhyann Prayuddy Reksamunandar, Lulu Brianni Puteri, and Hendro "Design of Water Turbidity Measuring Instruments using Photodiode Microcontroller-Based Light Sensor AT Mega 328" [2].
- Fauzi Amani & Kiki Prawioredjo "Measuring the quality of drinking water with parameters PH, temperature, turbidity level, and the amount of dissolved solids" [3].
- Ronaldi Zamora<sup>1</sup>, Harmadi and Wildian "Design of water dissolved solid measuring devices (TDS) with conductivity sensors in real time"[4].
- Refendi Sinaga, "a water PH meter with an arduino-based digital display", Batam State Polytechnic Electronics Engineering study program, [5].

The difference with [2],[3],[4],[5], this research will carry out the process of filtering turbidity, motoring using the internet network and improving the value of turbidity of water [1], as a further step before being discharged into the groundwater infiltration flow.

## 3. Design system

### 3.1 Block diagram of Design.

Diagram block design illustrates differences and similarities in water quality based on measurement results and water quality standards. Next, the design makes a Total Dissolved Solids (TDS) turbidity monitoring tool using an Arduino-based Turbidity Sensor with a digital display and uses a short message service display network (SMS).

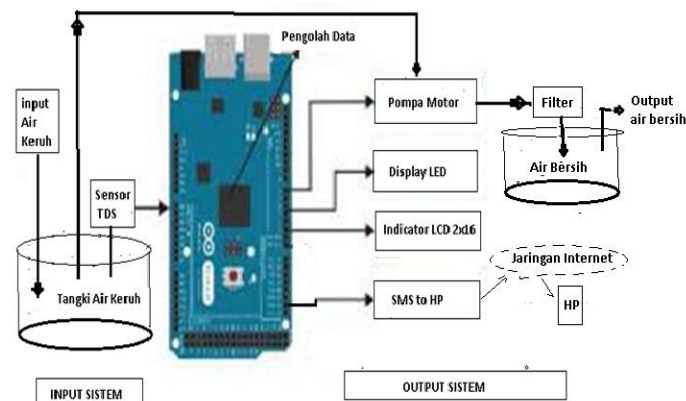


Fig. 1: Design of a turbidity tool block diagram.

### 3.2 Turbidity Sensor Circuit.

The working system of this design tool is given by changes in the data input turbidity value, which is owned by the capability of the turbidity sensor process that serves to detect turbidity in water, in the use of changes in turbidity value as the input value of the ATmega328 microcontroller system process. And the following (figure 2) is a schematic diagram of the turbidity sensor.

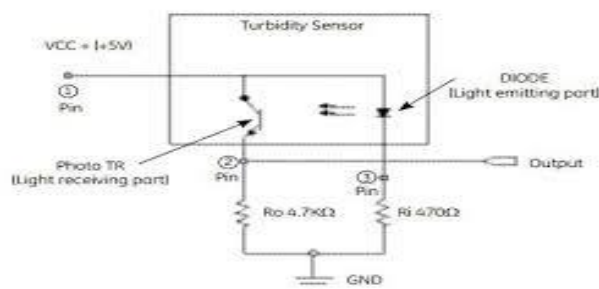


Fig. 2: Schematic diagram of the turbidity sensor.



Data is collected by performing calibration of turbidity sensor readings with the Arduino hardware program.

$$NTU = 100 - \left( \frac{V_{Terbacakeruh}}{V_{Saatjernih}} \right) \times 100\% \quad (1)$$

### 3.3 SIMA6 GSM / GPRS Module is a GSM module (Global mobile system).

GSM module (Global Mobile System) has the role of sending SMS functions according to the programming workflow (figure 3). Its module uses the UART (Universal Asynchronous Receiver Transmitter) communication protocol in communicating data with Arduino. It has 8 pins that can be used for combining with arduino (pins 0 to pin 7) 2 pins will be used as RX and TX pins which will be used in UART communication with Arduino.

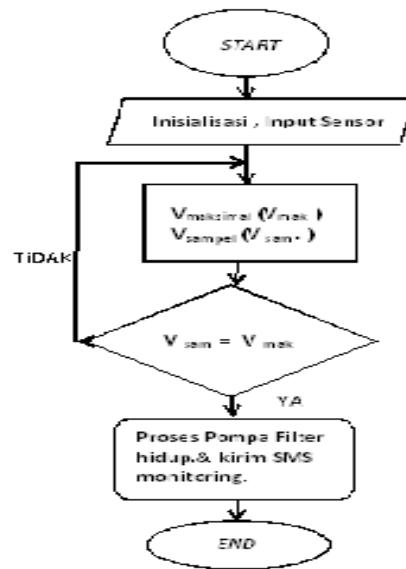


Fig. 3: Programming workflow diagram.

## 4. Simulation

The results of tool design are shown in (figure 4). The first test carried out was to measure the electrical voltage on water that has vary NTU values. The voltage is measured with the help of a color indicator on several types of LED lights (Green, Yellow, Red LED lights) shown in figure 5. It is done to find out which LED has the best linearity. The measurement results obtained are shown in table 2 and table 3,



Fig. 4: Design of turbidity measurement

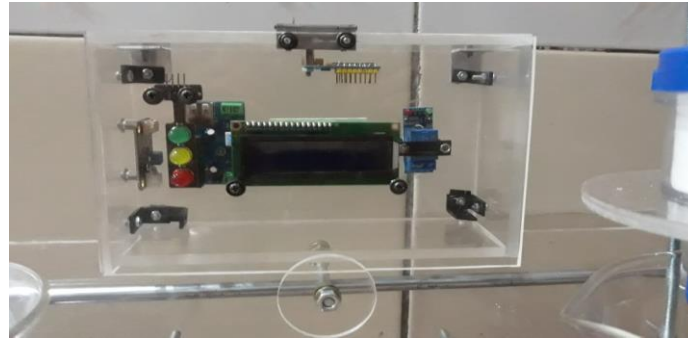


Fig. 5: LED Indicators Green, Yellow, Red.

Table 2. Test results for measuring the design tools (volts).

No	Nilai NTU	Tegangan Air terbaca oleh Sensor Turbidity (V), [volt]							
		LED Hijau		Nilai NTU	LED Kuning		Nilai NTU	LED Merah	
		V <sub>kmh</sub>	V <sub>kmh</sub>		V <sub>kmh</sub>	V <sub>kmh</sub>		V <sub>kmh</sub>	V <sub>kmh</sub>
1	= 3	3,58	3,58	= 3	3,58	3,65	= 4	3,58	3,72
2		3,58	3,59		3,58	3,66		3,58	3,73
3		3,58	3,60		3,58	3,67		3,58	3,74
4		3,58	3,61		3,58	3,68		3,58	3,75
5		3,58	3,62		3,58	3,69		3,58	3,76
6		3,58	3,63		3,58	3,70		3,58	3,77
7		3,58	3,64		3,58	3,71		3,58	3,78

Table 3. Tests of water turbidity read by means (%).

No	Nilai NTU	Uji keceruhan air terbaca oleh alat rancangan Sensor Turbidity (%).									
		LED Hijau		% kesalahan	Nilai NTU	LED Kuning		% kesalahan	Nilai NTU	LED Merah	
		V <sub>kmh</sub>	V <sub>kmh</sub>			V <sub>kmh</sub>	V <sub>kmh</sub>			V <sub>kmh</sub>	V <sub>kmh</sub>
1	= 3	3,58	3,58	0,99	= 3	3,58	3,65	0,98	= 4	3,58	3,72
2		3,58	3,59	0,99		3,58	3,66	0,98		3,58	3,73
3		3,58	3,60	0,99		3,58	3,67	0,98		3,58	3,74
4		3,58	3,61	0,99		3,58	3,68	0,98		3,58	3,75
5		3,58	3,62	0,98		3,58	3,69	0,98		3,58	3,76
6		3,58	3,63	0,98		3,58	3,70	0,98		3,58	3,77
7		3,58	3,64	0,98		3,58	3,71	0,98		3,58	3,78
Rata-rata kesalahan				0,98	Rata-rata kesalahan				0,98	Rata-rata kesalahan	
				0,98					0,98		

The water turbidity measurement test is shown in table 2. The results of the design measurement device turbidity test value increase are read by the turbidity sensor in the voltage value (volts) with a functioning design system tool. Meanwhile, It can be seen in table 3 the average error value of water turbidity is 0.98 %. At the start of the clear water reading sensor condition are shown Green LED (figure 6). This process continues until turbidity is read, the turbidity sensor is shown on the Yellow LED lights shown (Figure 7) and at the maximum level conditions are shown Red LED, the process of sending short message service (SMS) is carried out by a system that has been notification send "Detected turbidity of water carry out water purification" indicated (figure 8).

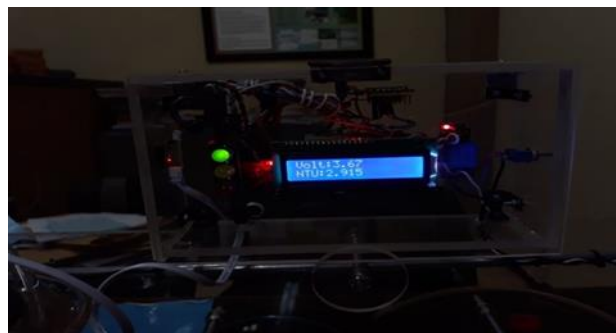


Fig. 6: The sensor reads clear water shown in Green LED.

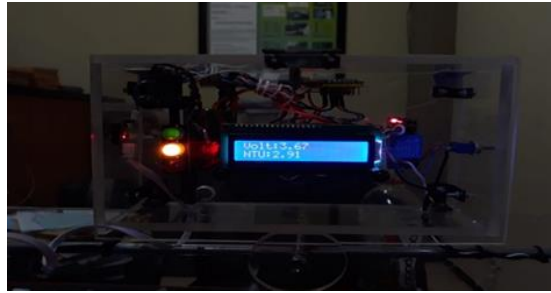


Fig. 7: the sensor reads increasing turbidity indicated the Yellow LED.



Fig. 8: Cellphone Receive short message service (SMS).

In the process of increasing the turbidity of the water shown by the Yellow LED to the red LED. Its system sends SMS according to the data of programmed phone numbers and the system starts the pump engine. It carries out the water purification process (filtering) moving turbid water from tank 1 to tank 2 through the process accordingly as shown in Programming workflow diagram of turbidity monitoring tool design in figure 3.. The results of the test data are summarized in Table 3 which the turbidity test was read by a turbidity sensor have average error value 0.98 (%).

## 5. Conclusions

- Voltage is measured with the help of a color indicator on several types of LED lights (Green, Yellow, Red LED lights), design tool is functioning properly.
- Application of design tools using TDS Turbidity sensor. The results of data testing conducted have an average error value of 0.98%.
- The device application design system can be functioned by sending the SMS program network according to the data of the HP number programmed.

## 6. References

- Regulation of the Minister of Health of the Republic of Indonesia Number: 907 / Menkes / SK / vii / 2002, 2002. Requirements and supervision of drinking water quality of the Minister of Health of the Republic of Indonesia.
- Linda Handayani, Rhyan Prayuddy Reksamunandar, Lulu Brianni Puteri, and Hendro, 2015. Design of Water Turbidity Measuring Instruments using Light Sensor Photodiode-Based Microcontroller Based AT Mega 328. Proceedings of the 2015 National Symposium on Science Innovation and Learning (SNIPS 2015)
- Fauzi Amani & Kiki Prawiroredjo, 2016. Measuring quality of drinking water with parameters ph, temperature, turbidity, and the amount of dissolved solids. JETri, Volume 14, Number 1, August 2016, Pages 49 - 62, ISSN 1412-0372.
- Ronaldi Zamora1, Harmadi, and Wildian, 2015. Design of TDS (total dissolved solid) water measuring devices with real conductivity sensors TIME "Journal of Science and Technology Vol. VII No. 1: 11-15, June 2015 ISSN: 2085-8019.
- Refendi Sinaga, 2012. A water PH meter with an arduino-based digital display, Batam State Polytechnic Electronics Engineering.

## Design of Microstrip Array Antenna with Beamforming Capability for 5G Communication

Adam Tsany Magrifaghibran<sup>1</sup>, Dharu Arseno<sup>2</sup> and Rizky Satria<sup>3</sup>

<sup>1</sup> Faculty of Electrical Engineering, Telkom University, Bandung - INDONESIA

<sup>2</sup> Faculty of Electrical Engineering, Telkom University, Bandung - INDONESIA

<sup>3</sup> Faculty of Electrical Engineering, Telkom University, Bandung - INDONESIA

e-mail: ghibranadam748@gmail.com

### Abstract

The fifth generation technology (5G) is a wireless network technology that offers access at very high data rates and greater capacity. One important element in realizing 5G technology is the antenna. Antennas with beamforming capabilities are one of the keys to 5G technology. Beamforming itself is an antenna's ability to direct the radiation patterns produced with certain characteristics. Based on previous research, antennas with beamforming capabilities can produce higher gain and wider bandwidth. In that study, antennas with high gain cause the value of SINR to increase, so that the resulting throughput is also higher. One type of antenna that can be used for 5G technology is a microstrip antenna. However, microstrip antennas have several disadvantages, including bandwidth and small gain. At present, the 28 GHz frequency is the most developed 5G frequency candidate. In this research, a microstrip antenna designed with beamforming capability can work at a frequency of 28 GHz. The antenna designed is an 8×8 MIMO array antenna arranged linearly. An array of antennas is carried out in order to increase the antenna gain. The antenna that has been designed is then performed beamforming simulation. The beamforming simulation is done by adjusting the phase difference at each antenna excitation. The desired beam characteristic is that it can point to 60 degrees with a beam width  $\leq 30$  degrees. The simulation results show that the antenna is able to work in the frequency range of 27.07 GHz - 28.77 GHz at a return loss limit of less than -10 dB with a bandwidth of 1.7 GHz and a gain value of 20.1 dB. Meanwhile, the beamforming simulation results by providing a relative phase difference between excitation of 45 degrees and 90 degrees, resulting in a radiation pattern with a beam characteristic approaching as desired. Setting the phase difference between excitation by 45 degrees produces a beam that leads to 61 degrees, with a beam width of 34.4 degrees. Meanwhile, the phase difference setting between excitation of 90 degrees produces a beam that leads to 64 degrees, with a beam width of 35.8 degrees.

*Keywords: 5G Technology, Antenna, Microstrip, Array, Beamforming.*

### 1. Introduction

The fifth-generation technology (5G) is a wireless network technology that offers access at very high data rates and greater capacities (5G Antenna White Paper on New 5G, New Antenna, 2019). The telecommunications industry around the world has done a lot of research to realize 5G technology (Yunfeng, Jiahao, & Xiaohong, 2019). In 2015, World Radio Communication (WRC), the International Telecommunications Union-Radio Communication (ITU-R) Sector officially confirmed that the official name of 5G was International Mobile Communication (IMT) -2020. IMT-2020 itself is a benchmark for the specifications of 5G communication technology. IMT-2020 has several candidate frequencies bands for 5G communication network, including the frequency range of 26.25 - 29.5 GHz, 31.8 - 33.4 GHz, 37 - 43.5 GHz, 45.5 - 50.2 GHz, 50.4 - 52.6 GHz, 66 - 76 GHz, and 81 - 86 GHz (Michael, 2019). The use of this high frequency band provides wider bandwidth for high level data communications over a short range of several hundred meters (Fatimah & Raed, 2016).

Antenna is one important element in realizing 5G technology. Antenna working frequency affects the dimensions of an antenna. The use of high frequencies causes the dimensions of an antenna to become smaller (Balanis, 2005). Based on the frequency range announced by IMT-2020, 5G Technology will use high frequencies. This causes

the antenna on the 5G technology will have a small dimension. One type of antenna that can be used for 5G technology is a microstrip antenna. Microstrip antennas are used because they have ease in the design and fabrication process, but microstrip antennas have several disadvantages, including bandwidth and small gain.

Antennas with beamforming capabilities are also one of the key 5G technologies. Beamforming itself is an antenna's ability to direct the radiation patterns produced with certain characteristics. The beamforming capability of the antenna causes the antenna gain to be higher, so the information transmitted to the user has a very low loss value (5G Antenna White Paper on New 5G, New Antenna, 2019). Based on this, we need an antenna design that is suitable for 5G wireless communication in order to achieve greater bandwidth, more directional radiation patterns, and higher antenna gain.

In a previous study, a microstrip antenna design at a working frequency of 28 GHz was carried out with a planar array arrangement using series feed rationing techniques for communication (Varum, Ramos, & Matos, 2018). The results of the study stated that the use of a 4x4 planar array with series fed rationing techniques resulted in a bandwidth of more than 1.5 GHz and a gain value ranging from 18 dBi (Varum, Ramos, & Matos, 2018). The antenna's performance can operate for a 5G communication network, but the design of the antenna has an array of shapes and complex rationing techniques. This research will design an antenna that can operate at a frequency of 5G 28 GHz. The designed antenna will be arranged 8x8 linear array. An array on the antenna is expected to obtain a higher gain value. The feed technique used in antenna design in this study uses the T-shaped microstrip line. The feed technique is chosen so that it can facilitate the unification of the microstrip channel with the antenna array (Rames, Prakash, Inder, & Apispak, 2001). The antenna that has been designed is then performed beamforming simulation. The beamforming simulation is done by adjusting the phase difference at each antenna excitation. The desired beam characteristic is that it can point to 60 degrees with a beam width <30 degrees.

## 2. Research methodology

### 2.1 Beamforming

In 5G communication, antenna with beamforming capability is one of the key technologies (Almuthanna, Ahmed, & Abdulhameed, 2015). Antennas with beamforming capabilities usually have the characteristics of a more directional radiation pattern and a higher gain. Beamforming itself is a technique or the ability of an antenna to direct a radiation pattern with certain characteristics (Balanis, 2005). In an antenna array, beamforming can be done by adjusting the phase difference for each element (or supply) (Balanis, 2005). Analysis of the radiation pattern on the antenna array can also be done by reviewing the array factor (AF). An array factor (AF) is defined as the radiation pattern of an array obtained by ignoring the radiation pattern of each element of the array antenna. An array antenna with N elements, where each element is separated by distance and has the same amplitude has a normalized array factor. Normalized element N array elements can be formulated by Equation (1) as follows (Balanis, 2005).

$$AF_n = \frac{1}{N} \times \left( \frac{\sin(\frac{N}{2} \psi)}{\sin(\frac{1}{2} \psi)} \right). \quad (1)$$

Information:

$N$  = Number of elemen antenna

$\Psi$  =  $k.d. \cos\theta + \beta$ .

The constant k is the wave constant while d is the distance between the antenna elements. The angle  $\theta$  (tetha) is the angle of direction of the signal coming to the antenna element while  $\beta$  is the phase difference given to each antenna element.

### 2.2 Microstrip Antenna Rectangular Patch

Microstrip antennas generally consist of ground plane layers, substrate, and patch.

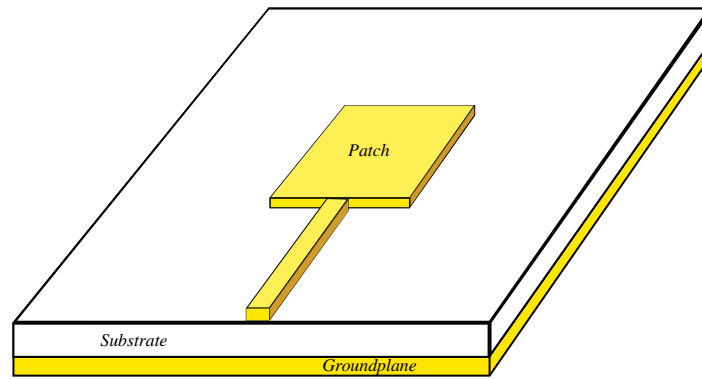


**Fig. 1: Structure of microtrip antenna.**

Groundplane is the bottom propeller layer on the microstrip antenna. The groundplane is made of conductor material and serves to reflect back unwanted irradiated signals. The substrate is a layer made of dielectric material (does not conduct electricity and serves as a place for rationing the antenna. Patch is the top layer of the microstrip antenna section which is made of conductor material and has the function of radiating electromagnetic waves. Antenna patches have a variety of shapes that can be adjusted for the purpose of the antenna. One form of patch that is most widely developed in wireless communication is rectangular patch (Balanis, 2005).

### 2.3 Antenna Specification

In this study, antennas that are designed have a working frequency range of 26.5 - 29.5 GHz, which includes the frequency most frequencies licensed by several countries, namely Japan, South Korea, Hong Kong, Uruguay, and America (GSMA Intelligence, 2019) . The antenna specifications are shown in Table 1.

**Table 1: Antenna Specification.**

Parameter	Specification
Work Frequency	28 GHz
<i>Bandiwidth</i>	> 1.2 GHz
VSWR	$\leq 1.5$
Radiation Pattern	Unidirectional
Directivity	$\geq 8$ dB
<i>Gain</i>	$\geq 8$ dB

The characteristic beamforming radiation pattern desired in this study is to be able to direct the beam towards 60 degrees with a beam width of  $\leq 35$  degrees (Trinh, Ferrero, Lizzim, Staraj, & Ribero, 2016).

The type of substrate used is Rogers RT / Duroid 5880 with a dielectric constant of 2.2 and thickness of the substrate of 0.8 mm. Duroid 5880 substrate was chosen because it can be used to produce shapes of larger dimensions and can work at high frequencies and has a small material permittivity. The material used for groundplane and patches is copper with a thickness of 0.035 mm. Copper is generally used for microstrip antennas because it is very easy to find and has quite good conductivity (Ardianto, Renaldy, Fathir, & Yunita, 2019).

### 2.4 Design and Simulation

The antenna dimension parameters for the 8×8 array antenna design are as follows.

**Table 2: Dimension Parameters of Antena Array 8×8.**

Parameter	Information	Dimension (mm)
Ht	Thickness of copper	0.035
Hs	Thickness of substrat	0.8

Wg	Width of groundplane	8.47
Lg	Length groundplane	6.096
Wp	Width of patch	4.235
Lp	Length of patch	3.048
Wf	Width of feed line 50 ohm	2.4852
Lf	Length of feed line 50 ohm	1.1067
Wf2	Width of feed line 100 ohm	0.69987
Lf2	Length of feed line 100 ohm	2.01824
Wf3	Width of feed line 70 ohm	1.405
Lf3	Length of feed line 70 ohm	1.9846
Wjunction	Connection feed	5.355
gf	Width of gap inset feed	1
fi	Length of gap inset feed	1.1067

Based on the antenna dimension parameters in Table 2. An 8×8 array antenna design is obtained as shown in Figure 2. below.

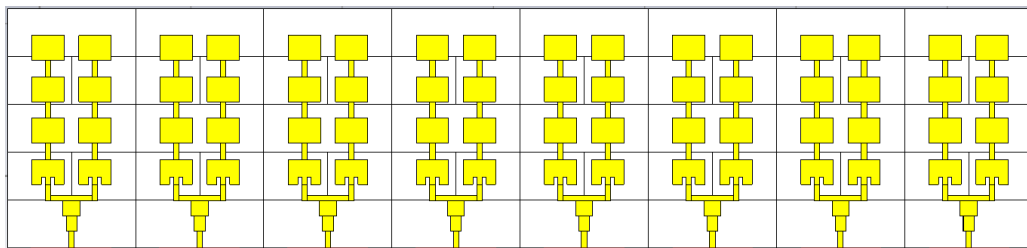


Fig. 2: Preliminary Design of Microstrip Antenna Array 8×8.

### 3. Results and Analysis

#### 3.1. Result and Analysis on Optimization Design of Antenna Array 8×8

Based on the results of the optimization that has been done on the 8×8 antenna array design, obtained the working characteristics of the antenna shown in Figure 3. and Figure 4.

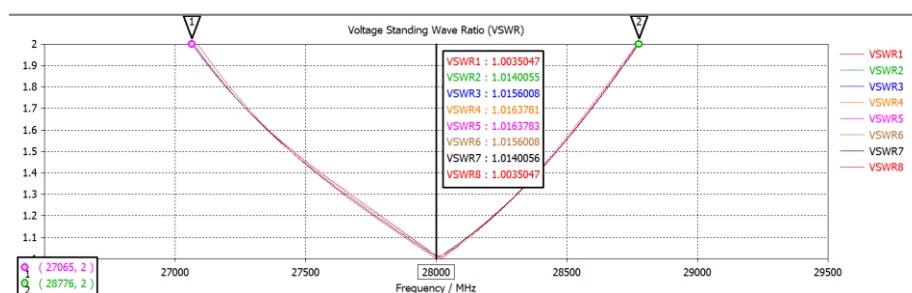


Fig. 3: VSWR of Optimization Result on Antenna Array 8×8.

Based on the analysis shown in Figure 3., the average VSWR value for the 8×8 array antenna design is 1,012 with a bandwidth of 1,698 GHz ( $\approx 1.7$  GHz).



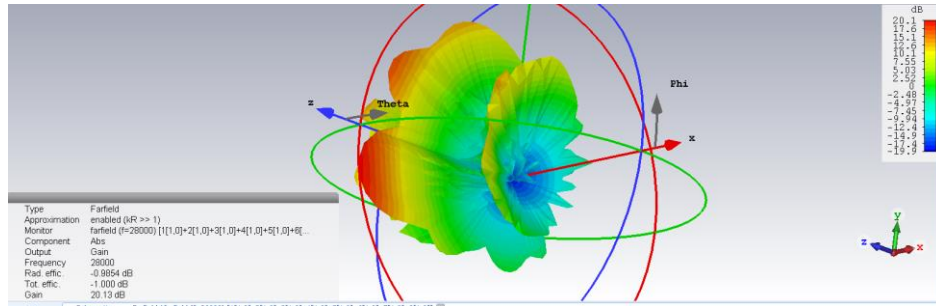


Fig. 4: Gain of Optimization Result on Antenna Array 8x8.

The gain obtained is 20.1 dB, the gain value already meets the desired antenna specifications. The resulting directivity value is 21.2 dB and the axial ratio value is 40 dB, where the value indicates that the antenna has a unidirectional radiation pattern.

### 3.2 Analysis of Beamforming Simulation Results

After the antenna is optimized to get the performance according to the desired work specifications, the antenna is then simulated beamforming by adjusting the phase difference in each array element array. The beamforming simulation results are shown in Figure 5.

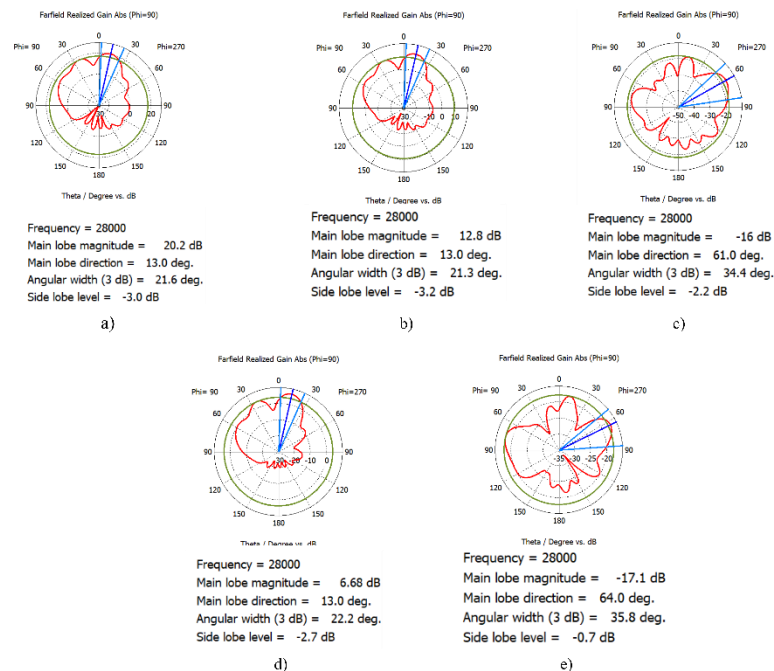


Fig. 5: Beamforming Simulation Result.

Figure 5b) shows simulation result on the first test, the relative phase difference given for each elemental supply is 30 degrees. Obtained the resulting radiation pattern has a beam direction in the direction of 13 degrees with a beam width of 21.3 degrees. The gain obtained is 12.8 dB. Figure 5c) shows beamforming result on the second test, the relative phase difference given for each elemental supply is 45 degrees. Obtained the resulting radiation pattern has a beam direction towards 61 degrees with a beam width of 34.4 degrees. The gain obtained is 16 dB. Figure 5d) shows beamforming result on the third test, the relative phase difference given for each elemental supply is 60 degrees. Obtained the resulting radiation pattern has a beam direction in the direction of 13 degrees with a beam width of 22.2 degrees. The gain obtained is 6.69 dB. Figure 5e) shows simulation result on the fourth test, the relative phase difference given for each elemental supply is 90 degrees. Obtained the resulting radiation pattern has a beam direction toward 64 degrees with a beam width of 35.8 degrees. The gain obtained is 17.1 dB.



## 4. Conclusion

Testing and analysis of 8x8 array microstrip antenna simulation at a frequency of 28 GHz has been carried out. The 8x8 array antenna simulation results in an average return loss of -40.27 dB with a bandwidth acquisition of 1,698 GHz. In the beamforming simulation results, the provision of relative phase differences between the rocks by 45 degrees and 90 degrees produces the radiation pattern that is most close to the desired characteristics. The characteristic radiation pattern that is produced when the relative phase difference given to each unit by 45 degrees produces a beam that can lead to 61 degrees, with a width of 34.4 degrees. The gain obtained is 16 dB. Meanwhile, giving a relative phase difference for each supply of 90 degrees produces a beam that can lead to 64 degrees with a beam width of 35.8 degrees and a gain obtained of 17.1 dB. Based on the simulation results, it can be concluded that the antenna has the performance according to the desired specifications. In addition, the simulation results show that the antenna designed has the potential to be used in 5G technology, because it meets the recommended standards. The next step, will be carried out the realization of the antenna that has been designed.

## 5. Acknowledgements

Thanks to friends of 3.5 years in college for giving me the opportunity to find this journal conference, the authors are also grateful for the prayers that have been given to the author in completing this journal. thank you father, mother, and also friends who always give joy to the author.

## 6. References

- 5G Americas White Paper on 5G Spectrum Recommendations. (2017). 5G Americas
- 5G Antenna White Paper on New 5G, New Antenna. (2019). Huawei Technologies Co.,Ltd.
- Balanis, C.A. (2005). Antenna Theory Analysis and Design 3<sup>rd</sup> Edition. New Jersey: John Wiley & Sons, Inc.
- Rames, G., Prakash, B., Inder, B., & Apispak, I. (2001). Microstrip Antenna Design Handbook. Canton Street: Arctech House, Inc.
- Michael J, M. (2019). 5G and IMT for 2020 and Beyond [Spectrum Policy and Regulatory Issues]. IEEE Wireless Communication, 22(4), 2 -3.
- Ardianto, F. W., Renaldy, S., Fathir, F., & Yunita, T. (2019). Desain Antena Mikrostrip Rectangular Patch Array 1x2 dengan U-Slot Frekuensi 28 GHz. Jurnal ELKOMIKA, 7(1), 43-56.
- Trinh, L. H., Ferrero, F., Lizzim L., Staraj, R., & Ribero, M. J. (2016). Reconfigurable Antenna for Future Spectrum Reallocations in 5G Communications. IEEE Antennas Wireless Propagation Letters, 15, 1297 – 1300.
- Yunfeng, N., Jiahao, L., & Xiaohong, S. (2019). Research on Key Technology in 5G Mobile Communication Network. International Conference on Intelligent Transportation, Big Data & Smart City (ICITBS).
- Varum, T., Ramos, A., & Matos, J.N. (2018). Planar Microstrip Series Fed Array for 5G Applications with Beamforming Capabilities. International Microwave Workshop Series on 5G Hardware and System Technologies (IMWS-5G).
- Almuthanna, T. N., Ahmed, I. S., & Abdulhameed, A. (2015). Radio Capacity Estimation for Millimeter Wave 5G Cellular Networks Using Narrow Beamwidth Antennas at The Base Stations. International Journal of Antennas and Propagation (IJAP). (pp 1 – 6).
- Fatimah, A., Raed, M., (2016). Millimeter Wave Mobile Communications for 5G: Challenges and Opportunities. IEEE International Symposium on Antennas and Propagation.
- GSMA Intelligence. (2019, Dec 10). Definitive Data and Analysis for The Mobile Industry. Available at: <http://gsmaintelligence.com>., Accessed on December 10, 2019.

## Automatic Location using ADS-B Mode for Ground Vehicle

Marisa Premitasari<sup>1</sup>, Uung Ungkawa<sup>2</sup>, and Adjie Putra Perdana<sup>3</sup>

<sup>1,2,3</sup> Department of Informatics, Institut Teknologi Nasional (Itenas), Bandung - INDONESIA

\* Corresponding author e-mail: marisa@itenas.ac.id

### Abstract

To increase the ground vehicle safety on landing area, Federation Aviation Administration (FAA) published some regulations for flight operation standard to implement transponder technology on aircraft by January 1st, 2020. These transponder technologies, which implemented on aircraft transmitter, aimed to transmit the aircraft position (longitude and latitude) data using Automatic Dependent Surveillance-Broadcast (ADS-B) mode as its automatic location. The aircraft will then communicate with the ground vehicle through an Air Traffic Controller (ATC) to avoid collision around landing areas. This paper presents the test results of a transmission system that simulates the ADS-B data sending through a transponder from a ground vehicle on both static and dynamic environment. The data transmission system designed by implementing HackRF, as decrypts hardware for radio data and a transmitter as the hardware for decrypting the ADS-B data. Moreover, these systems used a mini-computer called raspberry to process the ADS-B data and send the GPS data to the ground vehicle at a real-time condition. Furthermore, Pulse Position Modulation (PPM) utilised to change the digital format data-to-data radio signal. Then, the hackRF transmitter which sends ADS-B data is captured by the receiver so ground vehicle coordinate will enable to detect by a receiver or radar. Results show time delays of 1-5 second for static test and 1-20 second for the dynamic test. .

*Keywords: ADS-B, longitude, latitude, ground vehicle, transmission*

---

## 1. Introduction

The development of radar technology, especially in data transmission, has undergone sophisticated changes. For example, Primary Surveillance Radar (PSR) and Secondary Surveillance Radar (SSR), a technology that commonly used all around the world, will no longer exist and soon replaced by ADS-B. ADS-B, abbreviated from Automatic Dependent Surveillance-Broadcast is one of flight mode as navigation tools to communicate with ATC (Air Traffic Controller) or another aircraft. ADS-B mode launched as the development from the existing data transmission system, which is PSR and SSR (Devolski et Al, 2014). The previous transmission mode can only detect the location of a small object, such as military aircraft, but not its identity. SSR data transmission system operated by using 1030 MHz carrier frequency, which also requires a request to respond while transmitting the data, afterwhile the transponder answer and giving the feedback signal at 1090 MHz carrier frequency. ADS-B signal has the advantage that does not only respond to SSR interrogation but also detect aircraft distance and its location. Moreover, ADS-B also communicates with another ADS-B mode to prevent the collisions between aircraft. This ADS-B regulation will be published by January 1st, 2020 (ICAO, 2017). ADS-B mode works by using satellite technology to monitor aircraft position while it is moving and periodically it will broadcast pieces of information to navigation tools on the plane, the pilot and ATC. The information received by pilots and ATC as the replacement mode for SSR will give situation awareness and is capable of getting the data at any time (Ainnav Indonesia, 2017). At this project, the authors are building a data transmission system with ADS-B mode and testing it on a ground vehicle which Pulse Position Modulation (PPM) as the modulation technique.

## 2. Methods

These research project measured how long-time delays coming from ADS-B data signals transmission which are transmitted to a receiver. Time delays measured based on latitude and longitude comparison result and its measurement obtained from each time span on the transmitter. ADS-B signals will sent through 1090 MHz

antenna . There are five step sytem development that has been used as a method reference, namely waterfall method. First step is system requirement while this system need to analyze and design specific hardwares and softwares. For hardware devices, there were six tools implemented on these project which are Laptop Asus A43E, Smartphone One Plus X, Raspberry Pi 3 B, Rtl SDR, HackRF and GPS Module. For software devices, Phyton IDLE, Modul Phyton and Avare ADS-B has been implemented. Second Step of this methods reference is system design, illustrated on figure 1 as above

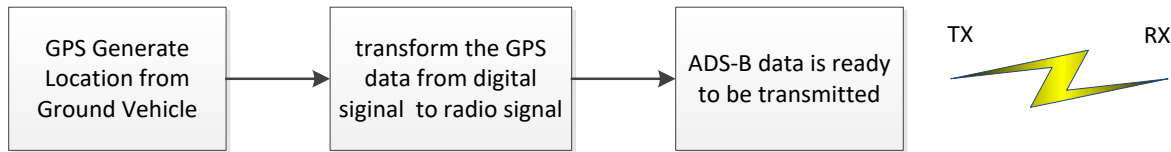


**Fig. 1: System Design**

Input coming from GPS module determine ground vehicle coordinate which generate longitude, latitude and altitude data that is ready to proceed by HackRF transmitter. This transmitter will transform digital signal data to radio signal and the signal captures by the receiver. Implementation process is the third step which illustrated on figure 2 named Diagram Block System.

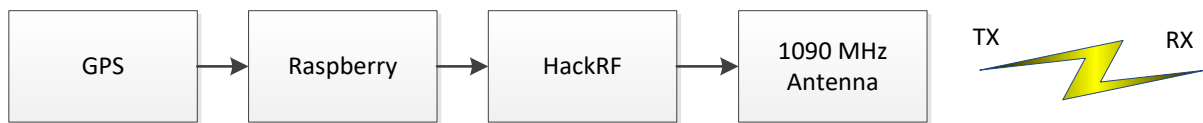


**Fig. 2: Diagram Block System**

This picture explained data transmission flow whereas the GPS module determine initial data coming from ground vehicle that has been generated three directions vehicle coordinated which updated in every second. The data converted into ADS-B file by Raspberry minicomputer whereas the data changed into DF-17 or S-mode format. Afterwhile the raspberry transformed the signal from digital signal to radio signal. Before forwarding datas to HackRF transmitter, its signal will modulated by PPM. HackRF, thats also functioned as repeater will forwarding ADS-B data which has been transformed into DF-7 or S-mode to the receiver. An antenna is sending a file with raw iq format at 1090 MHz carrier frequency so the data is ready to be received. These method step using comparasion about how long the delay occured and how accurate the transmission while sending ADS-B data format. Final step of this method is testing while the hardware built up is place on a motorcycle as the dummy ground vehicle and the specification is Honda Beat with D1B02N26L2 A/T Type, launched in 2017 with 108 CC capacity and having ABCDEF, BBBB, CCCCC call sign. The motorcycle will be running and receiver will capture its position wheter it was detected or not. This testing step revealed on how accurate data transmission using ADS-B and how the delay gap occured.

### 3. Results and Discussions

The testing results of data transmission system with these automatic location shows tables for GPS testing, Static testing and Dynamic testing as follows

#### 3.1. GPS Testing

This GPS testing was created to test the accuracy coming from GPS module on transmitter compare with GPS module on Google Maps. This testing was carried out at Ujung Berung, one of Bandung City sub-district and table 1 shown Gap results about 0.00007-0.00013 at latitude coordinate and 0.00007-0.0001 at its longitude.

**Table 1: The GPS Testing at Ujung Berung Sub-District**

GPS Transmitter		GPS Google		Gap Value	
Latitude	Longitude	Latitude	Longitude	Latitude	Longitude
-6.9100394	107.69827	-6.9101	107.69834	0.00007	0.00007
-6.91004	107.69827	-6.91011	107.69836	0.00007	0.00009

-6.91004	107.69828	-6.91013	107.69836	0.00009	0.00008
-6.910039	107.69827	-6.91014	107.69836	0.00009	0.00009
-6.910038	107.69827	-6.91014	107.69835	0.00009	0.00008
-6.9100366	107.69827	-6.91015	107.69836	0.00012	0.00009
-6.910036	107.69827	-6.91015	107.69836	0.00012	0.00009
-6.9100356	107.69827	-6.91016	107.69837	0.00013	0.0001
-6.910035	107.69827	-6.91016	107.69837	0.00013	0.0001
-6.910035	107.69827	-6.91016	107.69837	0.00013	0.0001
-6.9100347	107.69827	-6.91016	107.69837	0.00013	0.0001

### 3.2. Static Testing

.Table 2 as seen below shown result of GPS accuracy testing statically.

**Table 2: Statically Accuracy Testing**

Transmitter		Receiver		Gap Value	
Latitude	Longitude	Latitude	Longitude	Latitude	Longitude
6	107	5.999978	107.0002	0.000022	0.00002
6	107	5.999978	107.0002	0.000022	0.00002
6	107	5.999978	107.0002	0.000022	0.00002
6	107	5.999978	107.0002	0.000022	0.00002
6	107	5.999978	107.0002	0.000022	0.00002
6	107	5.999978	107.0002	0.000022	0.00002
6	107	6	107	0	0.00002
6	107	5.999978	107.0002	0.000022	0.00002
6	107	5.999978	107.0002	0.000022	0.00002
6	107	6	107	0	0.00008
8	107	8.000002	107.0002	0.000002	0.00002
8	107	8.000002	107.0002	0.000002	0.00002
8	107	8.000002	107.0002	0.000002	0.00002
8	107	8.000002	107.0002	0.000002	0.00002
8	107	8.000002	107.0002	0.000002	0.00002
8	107	8.000002	107.0002	0.000002	0.00002
8	107	8.000002	107.0002	0.000002	0.00002
8	107	8.000002	107.0002	0.000002	0.00002
6	107	5.999978	107.0002	0.000022	0.00002

Static Testing was created to test the accuracy and delay time coming from ADS-B transmission by transmit the data on ten second each at 6,8 then 4 at latitude coordinate and 107 on its longitude This test aimed to obtained how much the latitude and longitude gap coordinate on receiver and the accuracy on transmitter while doing the test statically. From table 2 above, we concluded that static testings resulted in latitude gap value both on transmitter and receiver. Meanwhile table 3, 4 and 5 is testing results for three times experiment delay with various time .

Table 3: First Experiment Testing

Time Span	Transmitter		Receiver	
	Latitude	Longitude	Latitude	Longitude
10:38:15	0	0	0	0
10:38:16	0	0	0	0
10:38:17	0	0	0	0
10:38:18	0	0	0	0
10:38:19	0	0	0	0
10:38:20	6	107	0	0
10:38:21	6	107	0	0
10:38:22	6	107	0	0
10:38:23	6	107	5.999978	107
10:38:24	6	107	0	0
10:38:25	6	107	0	0
10:38:26	6	107	0	0
10:38:27	6	107	0	0
10:38:28	6	107	5.999978	107
10:38:29	6	107	5.999978	107
10:38:30	6	107	0	0

Table 4: Second Experiment Testing

Time Span	Tranmitter		Receiver	
	Latitude	Longitude	Latitude	Longitude
10:50:20	0	0	0	0
10:50:21	0	0	0	0
10:50:22	0	0	0	0
10:50:23	0	0	0	0
10:50:24	0	0	0	0
10:50:25	8	107	0	0
10:50:26	8	107	0	0
10:50:27	8	107	0	0
10:50:28	8	107	8.000002	107
10:50:29	8	107	0	0
10:50:30	8	107	0	0
10:50:31	8	107	0	0
10:50:32	8	107	0	0
10:50:33	8	107	8.000002	107
10:50:34	8	107	0	0
10:50:35	8	107	0	0

Table 5: Third Experiment Testing

Time Span	Receiver		Gap Value	
	Latitude	Longitude	Latitude	Longitude
10:53:50	0	0	0	0

10:53:51	0	0	0	0
10:53:52	0	0	0	0
10:53:53	0	0	0	0
10:53:54	4	107	4.000001	107
10:53:55	4	107	0	0
10:53:56	4	107	0	0
10:53:57	4	107	3.999985	107
10:53:58	4	107	0	0
10:53:59	4	107	4.000001	107
10:54:00	4	107	4.000001	107
10:54:01	4	107	0	0
10:54:02	4	107	3.999985	107

ADS-B data with 6 latitude coordinates obtained gap values about Data ADS-B 0.000022 for the latitude dan 0.0000168 for its longitude coordinates, although there are some datas which doesn't have gaps on latitude coordinates. ADS-B data with 8 latitude shown some gap value about 0.000002 at latitude coordinates and the longitude shown 0.0000168. Moreover, ADS-B data with 4 latitude shown gap value about 0.000001 at latitude and 0.0000168 at longitude coordinates. Gap results from statically testing shown longitude and latitude coordinates from ADS-B data which was sent from the transmitter and captured by the receiver that is obtained gap value for the latitude around 0-0.000022 and 0.00000072-0.0000168 for the longitude. In table 3, data transmission on first trial proceeds at 6,8,4 latitude coordinates and 107 longitude coordinates which started at 10.38.15. It sent ADS-B data at 10.38.20 whereas the data just red on receiver at 10:38:23, 10:32:28 and 10:32:29. On Second experiment, given by table 4 which start at 10:50:20, ADS-B data sent at 10:50:25 and read by the receiver at 10:52:28 dan 10:50:33. Table 5 which performed third experiment just started at 10:53:50 where the data sent at 10:53:54. Receiver reading the ADS-B data at 10:53:54, 10:53:57, 10:53:59, 10:54:00, 10:54:02, 10:54:03 and 10:54:05. Results from delay testing concluded that delay time occurred from these transmissions on static testing shown around 1-5 second

### 3.3 Dynamic Testing

Dynamic testing was carried out to measure the accuracy of transmitter and receiver with moving ground vehicle. Dynamic testing showed latitude and longitude result compared by ADS-B data on receiver and transmitter whereas the data is recorded each second. Table 6 shown gap value around 0.00001-0.00034 at latitude coordinates and 0-0.00009 at the longitude

**Table 6: Dynamic Accuracy Testing**

GPS Transmitter		GPS Google		Gap Value	
Latitude	Longitude	Latitude	Longitude	Latitude	Longitude
-6.910178	107.69864	-6.91016763	107.6986431	0.00001	0
-6.910171	107.69864	-6.91016763	107.6986431	0	0
-6.9101863	107.69863	-6.91016763	107.6986431	0.00002	0.00001
-6.9102025	107.69858	-6.91021418	107.6985958	0.00001	0.00002
-6.91018	107.69858	-6.91016763	107.6985958	0.00001	0.00002
-6.910176	107.69861	-6.91017151	107.6986022	0.00001	0.00001
-6.9101725	107.698616	-6.91016763	107.6985958	0	0.00001
-6.9101715	107.698616	-6.91016763	107.6985958	0	0.00002
-6.9101477	107.69861	-6.91016763	107.6985958	0.00002	0.00002
-6.9101405	107.698616	-6.91016763	107.6985958	0.00003	0.00001
-6.910144	107.69865	-6.91012108	107.6986431	0.00002	0.00001
-6.910145	107.69863	-6.91012108	107.6986431	0.00003	0.00001

-6.9102225	107.69863	-6.91016763	107.6986431	0.00005	0.00001
-6.9102783	107.69861	-6.91026073	107.6986431	0.00002	0.00003
-6.910508	107.69866	-6.91044694	107.6985958	0.00006	0.00006
-6.9105635	107.69878	-6.91054005	107.6986905	0.00002	0.00009

Meanwhile Figure 3 as shown above mapping ground vehicle footprint for dynamic testing whereas green bullet sign describe detected signal and red cross sign describe undetected signal Figure 3 also describe the path for ground vehicle that route around Ujung Berung Residence with +- 380 meters away and took about 2 minutes.

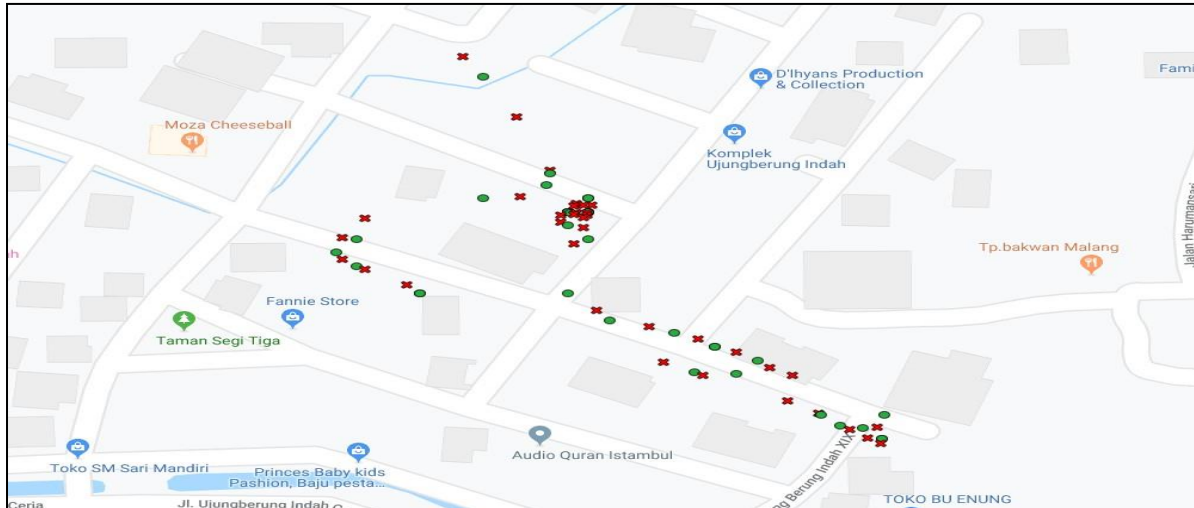


**Fig. 3: Ground Vehicle 'footprint' for Dynamic Testing**

The results for the dynamic testing shown delay around 1-20 second from transmission whereas these test start at 10:20:35 and ADS-B sytem start to send the data at 10:20:40

## 4. Conclusion

Automatic location with ADS-B mode on a ground vehicle aims to simplify ADS-B data which transmit from aircraft to communicate. The data sent to ADS-B ground vehicle only contained longitude and latitude coordinates position unlike real data on aircraft such as altitude coordinates, compass for wind directions or speed information. After doing accuracy test on coordinates between GPS transmitter and GPS Google, Gap value occurred around 0.00001-0.000015 for latitude coordinates and 0.00001-0.00011 for the longitude. For accuracy testing between static transmitter and receiver, gap value occurred around 0.000001-0.000022 at latitude coordinates and 0.0000072-0.0000168 at the longitude. On dynamic testing, data transmission accuracy between receiver and transmitter obtained gap value around 0.000001-0.000034 for longitude coordinates and around 0-0.000009 for the latitude. The static and dynamic test concluded, these ADS-B data transmission systems obtained delay time around 1-5 second for static testing and 1-20 second for the dynamic testing. Sugestion to develop this project is data transmission system with ADS-B mode are enable by using decrypt radio as translator on the receiver with more sophisticated specification to reduce delay times because of limited data input which only generate latitude and longitude coodinates . Moreover, such a project by doing an investigation at altitude coordinates on ground vehicle is needed to be developed.

## 5. References

- BS, Ali., 2016, System Spesifications for Developing an Automatic Dependent Surveillance-Broadcast (ADS-B) Monitoring System. International Journal of Critical Infrastructure Protection 15, 40-46
- Delovski, T., Werner, K., Rawlik, T., Behrens, J., Bredemeyer, J., Wendel, R., 2014. ADS-B over satellite The world's first ADS-B receiver in Space, The 4S Symposium 2014, 1-16

- Nurhayati, Y., Susanti., 2014, Implementasi Automatic Dependent Surveillance Broadcast (ADS-B) di Indonesia. *Warta Ardhia* Vol.40 No.3, 147-162
- ICAO.,2017. Automatic Dependent Surveillance-Broadcast (ADS-B) Out;Ensuring Preparedness For the 2020 Equipage Mandate, Seventh Meeting of The North American, Central American and Caribbean Directors of Civil Aviation (NACC/DCA/07), Washington, D.C., United States, 19-21 September 2017
- Murphy,T., Colles,B., 2016. The Transponder-Based Aircraft (TBAD) Overview.
- Ningsih, N., 2017. Pengembangan Simulasi Sinyal Radar dan Proses Interleaving Sebagai Inputan pada Radar Detector. *Jatisi* Volume 3 No 2, 183-195
- Sitorus,B.,Sitorus, T, I, H., 2017. Pengembangan Automatic Dependent Surveillance Broadcast untuk Peningkatan Keselamatan Penerbangan. *Jurnal Manajemen Transportasi &Logistik*, 304-312
- Xuan,Z., Jinjing, Z.,U.,Shufan,W., Qian, C., Rui, Z., 2018. Aircraft Monitoring by The Fusion of Satellite and Ground ADS-B Data. *Acta Astronautica* Volume 143, 398-405
- Couch, L. W.,2012.Digital and Analog Communication Systems Eight Edition, Pearson Education.
- Hanif,M.,2018.Analisis Sinyal Komunikasi UAV Menggunakan SDR-Fakultas Teknik Universitas Lampung at Bandar Lampung
- Purwadi, A., 2012. Penerapan Jenis Teknik Modulasi Pada Komunikasi Data . Program Studi Teknik Informatika Fakultas Teknik Matematika dan IPA Universitas Indraprasta PGRI at Jakarta
- Nugraha,B., 2014, Telekomunikasi Analog & Digital modules. Fakultas Teknik , Program Studi Teknik Elektro-Universitas Mercubuana at Jakarta
- Vehicle Movement Area Transponder (VMAT) ADS\_B Vehicle Tracking Unit available at [www.harris.com/solution/vehicle-movement-area-transponder-vmat-ads-b-vehicle-tracking-unit](http://www.harris.com/solution/vehicle-movement-area-transponder-vmat-ads-b-vehicle-tracking-unit), accessed on October 15, 2018.
- What's the difference Between ADS-B Out and ADS-B In? available at [www.thebalancecareers.com/what-s-the-difference-between-ads-b-out-and-ads-b-in-282562](http://www.thebalancecareers.com/what-s-the-difference-between-ads-b-out-and-ads-b-in-282562), accessed on October 15, 2018.
- Why is a pulse position modulation preferred in ADS-B? Available at [www.quora.com/why-is-a-pulse-position-modulation-preferred-in-ADS-B](http://www.quora.com/why-is-a-pulse-position-modulation-preferred-in-ADS-B), accessed on October 22, 2018.



## **Determination of Ignition Voltage in Tank Vehicles Carrying Gasoline and LPG in Electric Field Zone**

**Iyus Rusmana**

Prodi Teknik Elektro, Institut Teknologi Nasional Yogyakarta

E-mail: iyusrusmana@itny.ac.id

### **ABSTRACT**

This study has been conducted through computer simulations of ignition voltages, and opened-voltage on fuel tank vehicles consisted of gasoline and LPG, which is caused by the intensity of the electric field. This study reported the condition when tank vehicles consist of 5,000 liters of gasoline was passing through the electric field zone then it showed the ignition voltages was 3014.15 Volts, for tanks consist of 16,000 liters gasoline showed 2818.66 Volts. Other conditions among tanks consist of 9500 kg LPG showed ignition voltage as much as 2773.93 Volts while in the critical fields were 4040.42 Volts/meters, 2396.82 Volts/meters and 2040.55 Volts/meters, respectively. By knowing the ignition voltage result among the conditions as mentioned above, this study concluded that the tank on vehicles consisted of 5,000 liters gasoline had the most sensitivity to fire, followed by the tank on vehicles consisted of 16,000-liter gasoline and 9,500 kg LPG.

*Key words: ignition voltage, open voltage, electric field intensity, critical electric field*

---

## **1. Introduction**

### **1.1 Background**

The distribution system of fuel oil and until now is even predicted that for the next few decades, it will still use tank cars. When the vehicle passes under an extra-high-voltage air line network (SUTET) then in the metal of the tank the vehicle will accumulate an electric charge that is induced by an electric field that is under the SUTET network.

The driving factor why this research needs to be done is that most liquid fuel transport tank vehicles (including liquid, premium, Pertamina etc.) are cylindrical and space inside has the same electrical properties as a capacitor so that if there is an electric field present inside it will potentially cause capacitive spark discharge.

### **1.2 Literature Review**

A study conducted by Epri (1975) in Ultra High Voltage (UHV) transmission research project p-68, said that a fuel tank vehicle with all its skeletons could be presented as a capacitor. Thus it can be concluded that there is a relationship between the electric field (E) and the ignition voltage value owned by the tank and the liquid fuel in the tank. An electric area can trigger the ignition of liquid fuel inside the liquid fuel tank (McKinney, 1962 as quoted by Epri, 1975)

McKinney (1962) has generalized an equation model for the ignition voltage from an experimental model which displayed the relationship between the ignition voltage and the capacitance of the object. The model obtained by this experiment can determine the ignition voltage number through the magnitude of the capacitance of the object in question.

### 1.3 Basic theory

#### 1.3.1 Calculation of capacity value

The fuel tank model was represented by a horizontal-cylindrical electrode as shown below (Maruvada & Cavallius, 1975):

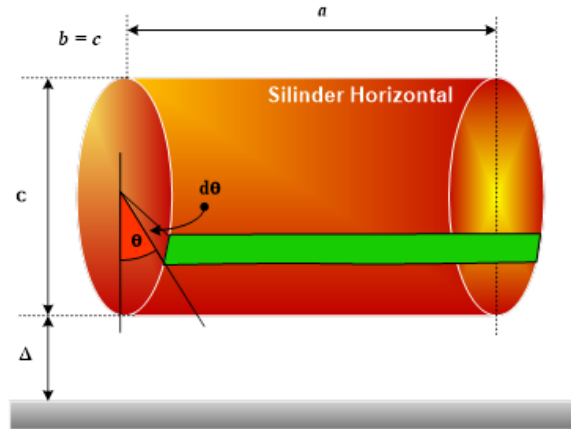


**Fig. 1: Representation of Fuel vehicle tank and Cp Value Calculation for horizontal cylindrical surfaces (Marupada and Cavallius, 1975)**

This configuration is characterized by four main dimensions:

- $a$  is the horizontal length of the fuel tank.
- $b$  is the horizontal width of the fuel tank
- $c$  fuel tank height
- $\Delta$  the smallest gap between the fuel tank and the ground

More precise way to validate the ground influence among all values and configurations as follows.  $C$  capacitance of any object is considered as being composed of two capacitance values.

$$C = C_{\infty} + C_p \quad (1)$$

Where  $C$  is the capacitance value of the object above the ground surface, the  $C_p$  value is obtained as an estimate as

$$C_p = \epsilon_0 \cdot \int_S \frac{dA}{h} \quad (2)$$

$dA$  is the elementary surface area, and  $h$  is the height above the ground. Integration is carried out on the surface area of the ground or tilted at an angle of 900 or smaller. Calculation of the value of  $C$  for horizontal cylinders,

$$C_p = 2 \cdot \epsilon_0 \cdot \int_0^{\frac{\pi}{2}} \frac{\left(\frac{c}{2}\right) \cdot a \cdot d\theta}{\Delta + \left(\frac{c}{2}\right) \cdot (1 - \cos \theta)} \quad (3)$$

And then in the next step is obtained,

$$C_p = 2 \cdot \epsilon_0 \cdot a \cdot \frac{\left\{ \pi - \arccos \left( \frac{1}{1 + \alpha} \right) \right\}}{\sqrt{(1 + \alpha)^2 - 1}} \quad (4)$$

with  $\alpha = 2 \cdot \Delta / C$

### 1.3.2 Calculation of ignition voltage of liquid fuel in the tank

The electric spark between two conductive bodies can ignite a mixture of flammable hydrocarbon vapour air (McKinney, 1962 in Epri, 1975). Three methods cause ignition, which was reviewed by McKinney (1962) in his review.

- Ignition by discharging capacitance circuit between particular electrodes as well as the closing process.
- Ignition by interference with the inductive sequence between the opening of contacts.
- Ignition by hot wire

A series of tests using real objects according to different capacitance values in the electrostatic field induced by high voltage air conductors. A fuel tank vehicle is simulated with a spout with an open container filled with liquid oil. The data shown by Figure 2 below:

A straight line was drawn through points that represent the minimum ignition voltage for a spout (which contains) oil. The formula for minimum ignition voltage:

$$V_p = 4.6 \times C^{-0.3} \text{ (Volt)} \quad (5)$$

The actual ignition voltage is obtained in the range of values from 1 to 2 times the minimum value. The rms (root means square) value for ac voltage is converted through  $(1 / \sqrt{2} = 0.707)$ .

### 1.4 Problem Identification

A liquid fuel carrier tank object has an oval-cylindrical tank that has a capacitance value for ground level, air space gap in the tank, loose bolt slit gap, and slab plate gap between the tank holder and its frame. When this vehicle enters the area SUTET, the terrain will be cut off by the presence of this vehicle.

### 1.5 Problem Formulation

Based on the description as mentioned before also by observing the electric field that is in around the SUTET-500 kV, 50 Hz network line, this study question can be described as how much the ignition voltage can be accumulated in the fuel tank installed on the vehicle and how the relationship between the electricity zone located below SUTET area and the accumulated voltage inside the fuel tank on the vehicles.

### 1.6 Research Objectives and Benefits

The objectives of this research are:

- To find out the ignition voltage for each size of the fuel tank placed on the chassis of the liquid fuel carrier.
- To know the intensity of critical electric field that is able to cause the ignition voltage in each tank with its dimensions.

## 2. Research methods

### 2.1 Research Methods

Modelled horizontal cylindrical tank truck. Modelling, as shown in Figure 3. The extra-high voltage air duct space to the ground surface is modelled as a capacitor with a dielectric medium in the form of air while the car object is modelled as a rectangular plate having an area of S.

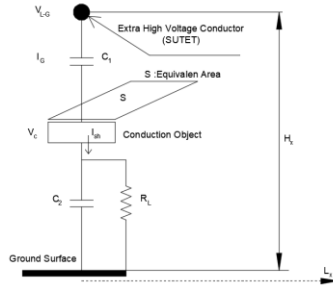


Fig. 2: One line transmission line model which has a conduction object on the below part

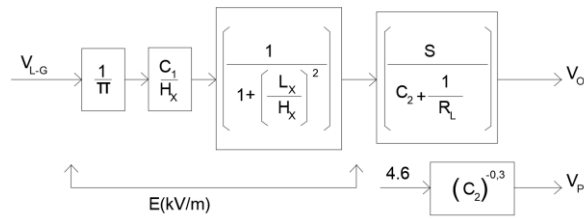


Fig. 3: The relationship between the study variables and the independent variables

Information:

- $V_o$  = open voltage on the object against the ground
- $V_p$  = object ignition voltage =  $4.6 \times (C_2)^{0.3}$ , the variable under research
- $C_2$  = Cog = value of the object's capacity to the ground
- $S$  = the surface area of the charge collector on the object
- $H_x$  = height of conductor SUTET above ground level, in meters
- $V_{L-G}$  = Voltage between one phase to neutral (to ground) in kilo-volts.
- $R_{og} = R_L$  in Ohms

Between SUTET conductor and the vehicle object which has an equivalent area of the charge collector ( $S$ ), there is an air gap that can be modelled with a capacitor  $C_1$  with a dielectric constant of relative air ( $\epsilon_r = 1$ ). While between the object of the vehicle and the surface of the earth, a capacitor appears again, which is modelled with capacitor  $C_2$ . These capacitors represent all material vehicles that are capable and have the potential to store electric charges when passing through the area under SUTET. Capacitor  $C_2$  will discharge (discharge) the charge when the voltage gradient has reached its breakdown value. The increase in the value of the gradient is triggered by the electric field generated by the conductor SUTET, which is voltage-acting against the ground by  $V_{LG}$ . RL prisoners model the condition of material objects that are resistant, including the condition of the tires of the fuel tank vehicle. This RL resistivity model is usually considered to be infinitely large which shows modelling of the physical form of a vehicle's (rubber) tires when dry (not wet).

## 1.2 Research Steps

The research was conducted as the following diagram:

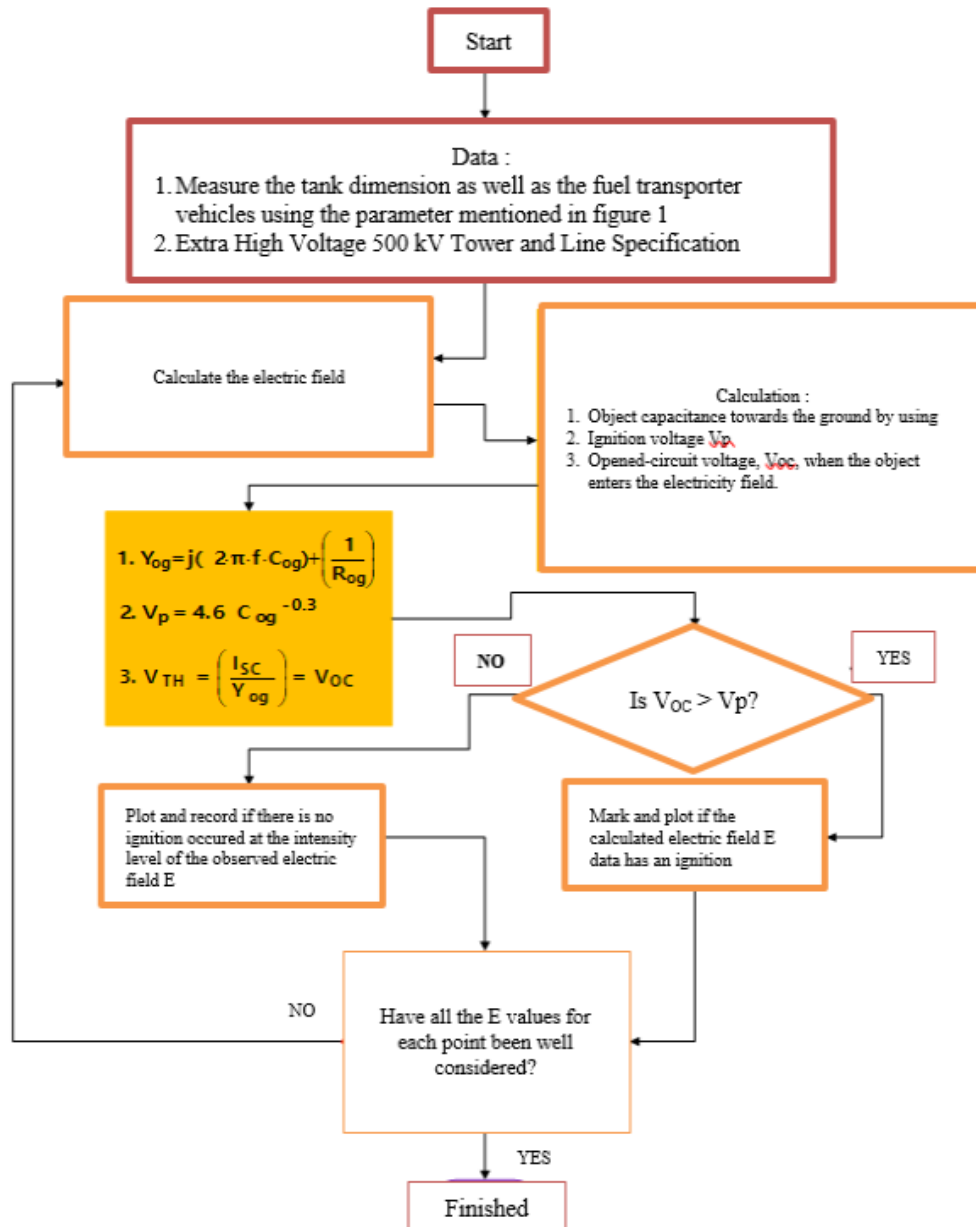


Fig. 4: Research Flow Chart

## 3. Results and analysis

The object of this research consists of three types of tank truck sizes, namely: 5000-litre premium oline tank, 9500 kg LPG tank and 16,000-litre premium petrol tank.

### 3.1. The Relationship between Opened-Voltage and Electric Field

The results of the calculation of the open-circuit voltage for the three types of armoured vehicles when entering the electric field caused by SUTET are tabulated as the table below (computer simulation results),

**Table: 1 Opened-circuit voltage (Voc) for each vehicle tank consist of 5000 litre, 16000 liter gasoline and 9500 kg LPG**

the electric field intensity (Kv/m)	Voc Cog 5000 (Farad)	Voc Cog 16000 (Farad)	Voc Cog 9500 kg (Farad)
1,528	1,140	1,796	2,075
1,618	1,207	1,902	2,198
1,715	1,279	2,016	2,329
1,820	1,357	2,138	2,471
1,932	1,440	2,270	2,623
2,053	1,530	2,412	2,787
2,182	1,627	2,565	2,963
2,322	1,731	2,728	3,152
2,471	1,842	2,904	3,355
2,630	1,961	3,091	3,571
2,799	2,087	3,290	3,801
2,979	2,221	3,501	4,045
3,168	2,362	3,723	4,302
3,366	2,510	3,956	4,571
3,572	2,663	4,198	4,850
3,782	2,820	4,445	5,136
3,996	2,979	4,696	5,426
4,208	3,137	4,945	5,714
4,415	3,292	5,188	5,995
4,611	3,438	5,419	6,262
4,792	3,573	5,632	6,507
4,950	3,691	5,818	6,722
5,081	3,789	5,972	6,900
5,179	3,862	6,086	7,032
5,239	3,907	6,157	7,114
5,260	3,922	6,182	7,142

Ignition voltage on tank consist of 5000 litre premium : 3014.15 Volt  
 Ignition voltage on tank consist of 16000 litre : 2818.66 Volt  
 Ignition voltage on tank consist of 9500 kg LPG : 2773.93 Volt

The relationship between the opened-voltage (opened-circuit) and the electric field that is under SUTET to the tank vehicle that is speeding in the region of the motor and electricity is shown in the curve below.

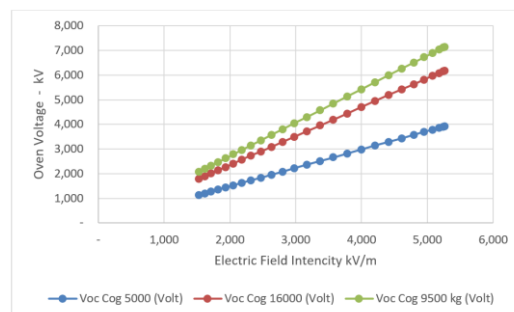


**Fig. 6: Combined graph of the three fuel tank vehicles connecting the values Open voltage (Voc) with electric fields (E) with different graph steepness.**

**5000 liters tank.** The curve (straight line) in blue has the equation of an open voltage circuit:  $Voc_5 = 0.746 E$ , the ignition voltage is = 3014.15 Volts (see table: 1) and the electric field intensity is =  $(3014.15 / 0.746) = 4040.42 \text{ V / m}$ . Thus, the critical electric field experienced by the tank is 4040.42 kV / m so that if the value of this electric field exceeds 4040.12 V / m ( $E > 4040.12$ ), then the tank has the potential to cause an electric spark or spark.

**The 9500 kg tank contains LPG** . The curve (straight line) in red has an open voltage equation:  $V_{oc95} = 1,358 E$ , ignition voltage of: 2773.93 Volts (table 4-1). and the intensity of the electric field equal to  $= (2773.93 / 1,358) = 2042.66 \text{ V / m}$ . Thus the critical electric field experienced by the tank is 2042.66 V / m so that if the value of this electric field exceeds 2042 V / m ( $E > 2042.66$ ), then the space in the tank has the potential to cause an electric spark or spark capacitive.

**16000 litters tank.** The curve (straight line) in green has an open voltage equation:  $V_{oc16} = 1.176 E$ . This vehicle with a 16000 kg tank has a rated voltage value of 2818.66 Volts (table 4-1), and the intensity of the electric field corresponding to this price is  $= (2818.66 / 1,176) = 2396.82 \text{ V / m}$ . Thus the critical electric field experienced by the tank is 2396.82 V / m so that if the value of this electric field exceeds 2396.82 V / m ( $E > 2396.82$ ), then the space in the tank has the potential to cause an electric spark or spark capacitive.

Fig. 6 shows that the LPG tank has the highest relative ignition voltage value (safer) compared to the other two tank vehicles for the number of intensity the same electric field.

#### 4. Conclusion

1. The ignition voltage for tank vehicles with a capacity of 5000 litres, 16000 litres (contents of premium gasoline) and 9500 kg (contents of LPG) are 3014.15 Volt, 2818.66 Volts, and 2773.93 Volt
2. The intensity of critical electric fields that can cause the ignition voltage values above are as follows:
  - for the ignition voltage 3014.15 Volts at 4040.42 (Volts / m)
  - for the ignition voltage of 2818.66 Volts of 2396.82 (Volts / m)
  - for the ignition voltage of 2773.93 Volts of 2042.66 (Volts / m)
3. In point 1 it is revealed that the lowest ignition voltage is an LPG tank of 2773.93 Volts with the critical electric field intensity of 2042.66 (Volt / m) = 2.04 (kV / m).

#### 5. References

- Deno, DW., 1974, "Calculating electrostatic Effects of Overhead Transmission Lines", The IEEE PES Winter Meeting, The IEEE Transmission and Distribution Committee of the IEEE Power Engineering Society, January 27 – February 1, pp. 1458 – 1471, New York, NY.
- Deno, DW., 1975, "Electrostatic Effect Induction Formulae", IEEE Trans. On PAS, Vol. PAS-94, No., Sep/Oct. 1975, pp. 1524-1536, General Electric Co., Pittsfield, Massachusetts (Mass), USA.
- Epri, 1975, "Transmission Line Reference Book 345 kV and Above", edisi ... ?, p. 248 – 273, Electric Power Research Institute, Palo Alto, California (CA), USA.
- Irvan Buchari Tamam, at al., 2017, "Analisa Pembangunan Saluran Transmisi 275 kV antara GI Kiliranjao dan GI Payakumbuh", Jurnal Energi & Kelistrikan vol. 9 no. 1, Januari - Mei 2017, p. 93 - 99
- Iskanto, E., 2000, "Pengaman pada Bahan Bakar terhadap Bahaya Kebakaran karena Api Listrik Statis", Energi dan Listrik, Vol. 10, No. 1, pp. 01 – 07.
- MacKinney, A.H., 1962, "Electrical Ignition of Combustible Atmosphere", ISA Transsactions, Vol. 1, No. 1, Januari 1962, pp. 45 – 64.
- Maruvada, P.S., Cavallius, NH., 1976, "Capacitance Calculations for some Basic High Voltage Electroda Configurations", IEEE Trans. On PAS, Vol. PAS-94, No 5, pp. 1708 – 1713, Hydro-Quebec Institute of Research Varennes, Quebec, Canada (CND)

# WEARABLE MICROSTRIP ANTENNA WITH DEFECTED GROUND STRUCTURE FOR BREAST CANCER DETECTION

Putri Angelia<sup>1</sup>, Levy Olivia Nur<sup>1</sup>, Bambang Setia Nugroho<sup>1</sup>

<sup>1</sup> School of Electrical Engineering, Telkom University, Bandung – INDONESIA

Corresponding author: levyolivia@telkomuniversity.ac.id,  
bambangsetianugroho@telkomuniversity.ac.id

## Abstract

A wearable antenna application has been spread in many fields including a solution in the medical application. One of their application in the medical field is the detection of breast cancer in the human body. This paper reports the microstrip antenna for breast cancer detection at a frequency of 2.46 GHz made from wearables material. The proximity coupled and the addition of a defected ground structure to the ground plane is used to get the wider bandwidth. Detection of breast cancer is performed by using breast modeling or breast phantom.

The dimensions of the designed antenna are 39 mm x 46.5 mm and realized using Rogers RT6006 material. Based on the results of simulations that have been done, the antenna has a return loss value  $\leq -40.28$  dB and a VSWR value  $\leq 1.01$ . The antenna can detect cancer based on the different properties of materials in the breast phantom which affects changes in the value of  $S_{11}$  parameters.

Based on the simulation, if the size of the cancer is getting bigger, then the value of return loss obtained increases or headed to 0 dB. The value of return loss caused by the differences in electromagnetic absorption of different cancer material.

*Keywords: microstrip antenna, wearable antenna, breast cancer, cancer detection, breast phantom.*

## 1. Introduction

Cancer is a disease that is caused by cells in the body's tissues that change to become malignant and divide faster than normal cells in general until out of control. Cancer cells will grow continuously, and it will not die when they are old enough. As a result, it will urge or make normal cells die in the body [1]. Several cancers have big numbers that cause die including lung cancer, liver cancer, blood cancer (leukemia), cervical cancer, tongue cancer, and breast cancer. According to the World Health Organization (WHO), breast cancer is the most common cancer among women and causes large numbers of deaths. Female deaths due to the breast cancer in 2018 is about 15% [2].

In general, cancer can be caused by genetic or genetic hereditary and unhealthy lifestyles. However, even knowledge about breast cancer is still inadequate. Therefore, self-vigilance and care are needed to detect breast cancer early to prevent or take appropriate treatment before it is too late so that it has a chance to be cured. Although early detection can be done every day by Breast Self-Examination (BSE) which is to feel the presence or absence of a lump in the breast, but this method is certainly not accurate in detecting breast cancer. To be more accurate, several methods can be performed, such as ultrasound, magnetic resonance imaging (MRI), and mammography. However, these methods are generally only available in large hospitals and require quite expensive costs. The simple and cheap method to detect early breast cancer in the human body is urgently required so that the doctor can take appropriate treatment to the patients.

Previous research has been carried out in the design and fabrication of breast cancer detection devices in the form of rectangular microstrip antennas at a working frequency of 2.4 GHz with FR4 as an antenna substrate material [3]. Other studies have made microstrip antennas with rectangular patches made by Rogers Duroid RT5880 [4] and Rogers 3003 [5]. This research will continue and develop on breast cancer detection instrument using a microstrip antenna made from Rogers Duroid 6006 which has a thickness of 1.27 mm with a working frequency of 2.46 GHz. Rogers Duroid 6006 material is used because it has a fairly high permittivity. In this study observing changes in return loss has been performed to improve the sensitivity of the sensors.



## 2. Basic concepts

### 2.1 Microstrip Antenna

Microstrip antenna is a special type of printed antenna that consists of two parts. The upper part is commonly called the 'patch', and the lower part which is usually called the 'ground' [6]. The top or patch is made by a metal material that is printed on a dielectric medium or called a substrate that serves as a source of the transmitter. Moreover, the bottom or ground has a function as a reflection of electromagnetic energy into free air. Microstrip antenna is an antenna that is simple in shape and small in size or compact [7].

### 2.2 Proximity Coupled

This study uses antenna rationing with the proximity coupled method. This method was chosen because it requires a wide bandwidth and a greater gain value. Proximity coupled uses two layers of substrate where the feed is located between substrate 1 and substrate 2 as shown in Figure 2.1 [8].

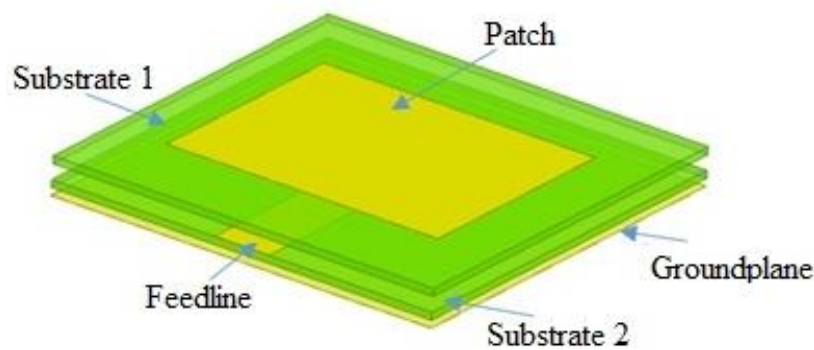


Fig. 2.1: Feedline scheme using proximity coupled.

### 2.3 Breast cancer

Breasts are organs that have tissue extending from the collarbone to the lower ribs, sternum, and armpits. Each woman's breasts have 15 to 20 glands called lobes, where milk is produced in women who are breastfeeding [9]. Breast cancer is the growth of abnormal tissue cells and become malignant in the breast. Breast cancer has many types but the most common ones are invading ductal carcinoma and invasive lobular carcinoma. In this study, the breast tissue has been modeled using the geometry size that can be seen in Table 2.1 [10].

Table 1 Geometry and Permittivity of Breast Phantom.

Item	$\epsilon_r$	Geometry (mm <sup>3</sup> )
Breast Skin	36	$96 \times 2 \times 96$
Normal Breast Tissue	9	$96 \times 96 \times 96$
Cancerous Breast Tissue	50	

## 3. System design

### 3.1 Determination of Specifications

Microstrip antenna made from Duroid 6006 as substrate and copper as patch and ground plane is designed with the following specifications.

- Frequency: 2.46 GHz
- Bandwidth:  $\geq 80$  MHz
- Radiation Pattern: Unidirectional
- Return Loss:  $\leq -10$  dB

### 3.2 Calculation of Antenna Dimensions

The following results of the calculation of the dimensions of the microstrip antenna can be seen in the Table 3.1 and the results of the microstrip antenna design can be seen in Figure 3.1 below.

**Table 2** The dimensions of microstrip antennas.

Dimensions	Value (mm)	Dimensions	Value (mm)
Width patch ( $W_p$ )	29,5	Length DGS Above	11
Length patch ( $L_p$ )	28,8	Width DGS Above	46,5
Width ground plane ( $W_g$ )	46,5	Length DGS Below	9
Length ground plane ( $L_g$ )	39	Width DGS Below	2
Width feed ( $W_f$ )	1	Slotted Patch	1,5
Length Feed ( $L_f$ )	9,5		

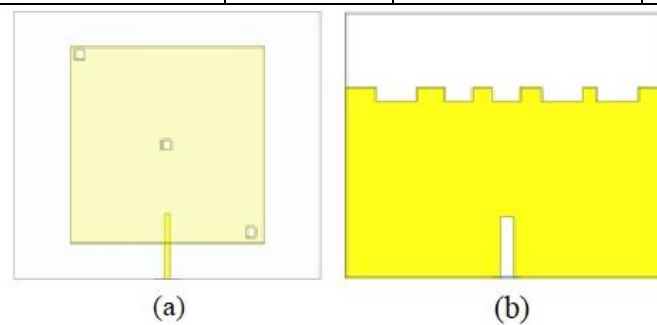


**Fig. 3.1:** Antenna design, (a) front view (b) rear view.

The antenna specification results obtained based on the simulation are a return loss of -40.2 dB at a frequency of 2.46 GHz and a bandwidth of 100 MHz. The loss is calculated from the difference between the upper frequency of 2.5 GHz with a lower frequency of 2.4 GHz, and the antenna gain of 8 dB.

## 4. Simulation and Analysis Results

### 4.1 Simulation Using Breast Phantom

In the simulation, measurements are made with the antenna placed as far as 10 mm from the breast phantom which can be seen in the following Figure 4.1.

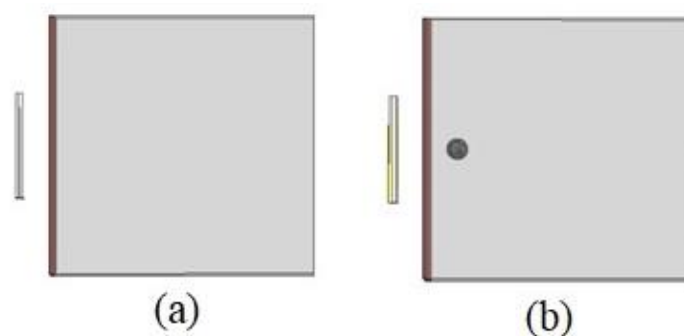


**Fig. 4.1:** Detection Antenna 10 mm away, (a) without cancer (b) with cancer.

The simulation is performed with the distance between the antenna and the breast phantom as far as 10 mm and measurements are made with different cancer sizes of 2 mm, 4 mm, 6 mm, and 8 mm. Simulation results with breast phantom can be seen in Figure 4.2 below. Based on the simulation, the result of return loss using breast phantom without cancer is -20.76 dB and measurement using breast phantom with different cancer sizes at 2 mm is -20.65 dB, at 4 mm is -20.22 dB, at 6 mm is -17.15 dB, and at 8 mm is -16.76 dB.

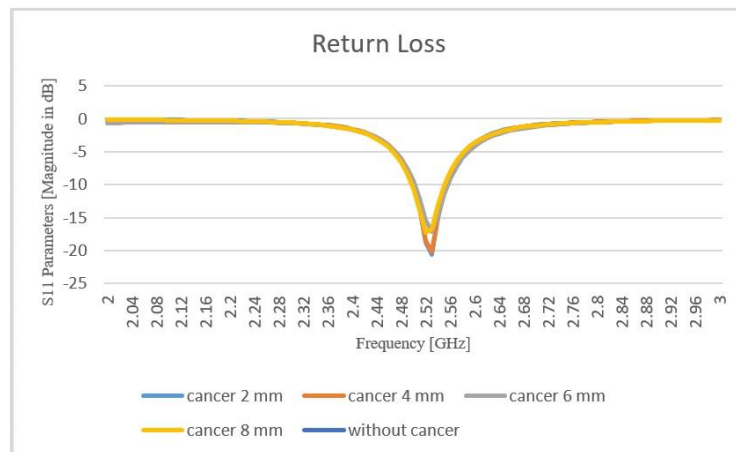


Fig. 4.2: The return loss simulation results in various size of breast cancer

## 4.2 Analysis of Simulation Results

Measurement using breast phantom without cancer obtained different return loss results, the greater the size of the cancer, the smaller the return loss produced. This change in return loss is due to additional material such as cancer that is detected, so that the value reflected back to the antenna is not the same due to partial absorption by the object.

## 5. Conclusions

Several conclusions can be drawn, viz.

- Antennas designed during simulation have met the specifications of having a return loss value of -40.28 dB and a VSWR value of 1.01.
- The use of the proximity coupled method and the addition of the antenna's defected ground structure can widen the bandwidth and increase the gain.
- Antenna can detect the presence of cancer based on changes in the value of return loss, return loss of breast phantom without cancer is used as a reference. The value of return loss without cancer is smaller than the value of return loss using cancer.
- The return loss value will increase if the size of the cancer is getting bigger

## 6. References

- Pusat Data dan Kemeneterian Kesehatan RI, "Bulan Peduli Kanker Payudara." Kementerian Kesehatan RI, 2016.
- World Health Organization, "Breast Cancer." [Online]. Available: <https://www.who.int/cancer/prevention/diagnosis-screening/breast-cancer/en/>. [Accessed on 10 October 2019, 17:52 WIB].
- M. Yumnisari, B. S. Nugroho, and P. Daud, "Perancangan dan RealisasiAntena Mikrostrip Ultra Wideband (UWB) untuk Deteksi Kanker Payudara," Telkom Univ. Bandung, 2017.
- C. Rabia, S. Sinan Gultekin, Dilek Uzer, and Ozgur Dunder, "A Microstrip Patch Antenna Design for Breast Cancer Detection," Sci. Direct, 2015.

- G. H. Arrahmah, B. S. Nugroho, and L. O. Nur, "Perancangan dan Realisasi Wearable Antena Untuk Mendeteksi Kanker Payudara," *Telkom Univ. Bandung*, vol. 6, no. 2, pp. 4587–4593, 2019.
- M. F. Iskander, *Electromagnetic Fields and Waves*. United States, 1992.
- R. Grag, P. Bhartia, I. Bahl, and A. Ittipiboon, *Microstrip Antenna Design Handbook*. Canton Street, Norwood MA: Artech House, 2001.
- S. J. Chua, P. S. Kooi, and M. S. Leong, "Increasing The Bandwidth of a Microstrip antenna by Proximity Coupling," *Electronics Letters*, vol. 23, no. 8, pp. 8–9, April 2011.
- National Breast Cancer Foundation, "Breast Anatomy and How Cancer Starts," [Online]. Available: <https://nbcf.org.au/about-national-breast-cancer-foundation/about-breast-cancer/what-you-need-to-know/breast-anatomy-cancer-starts>. [Accessed on 10 October 2019, 17:52 WIB].
- K. A. Setiaputri, "Mengenal Anatomi Payudara Wanita dan Masing-Masing Fungsinya," *Hello Sehat*, 2018. Available: <https://hellosehat.com/hidup-sehat/fakta-unik/panduan-anatomi-payudara/>. [Accessed on 13 October 2019, 16:18 WIB].
- C. A. Balanis, *Antenna Theory Analysis And Design*. Third ed. Canada: John Wiley & Sons, Inc., Hoboken, New Jersey, 2012.
- G. A. Stutzman, Warren L. Thiele, *Antenna Theory and Design*. Third ed. John Wiley & Sons, Inc., 2012.

# Design of Ultra Wide-Band Bowtie Antenna for GPR Applications

Raeida Widyananda<sup>1</sup>, Levy Olivia Nur<sup>1</sup>, Heroe Wijanto<sup>1</sup>

<sup>1</sup> School of Electrical Engineering, Telkom University, Bandung - INDONESIA

Corresponding author: levyolivia@telkomuniversity.ac.id, heroe@telkomuniversity.ac.id

## Abstract

Ground Penetrating Radar (GPR) is one technology that utilizes a radar system to determine the location of objects that are below the surface of the ground. In its current development, GPR uses an Ultra Wide-Band (UWB) radar system that works at frequencies between 10 MHz to 10 GHz [1]. The use of UWB radar systems are to get high resolution values which affect the level of accuracy in detecting objects. In general, in the implementation of the UWB radar system for GPR technology, antenna types such as bow-tie antennas, TEM Horn antennas, tapered slot antennas, spiral antennas, and vivaldi antennas are used [2]. The characteristic of antenna needed in GPR system must have wide bandwidth to examine the resolution of image. In this report, a bowtie antenna is investigated GPR applications. The bowtie antenna is used because this type of antenna has a smaller size and lightweight. The bowtie antenna design was carried out using RT-Duroid 5880 dielectric substrate with dielectric constant ( $\epsilon_r$ ) at 2.2 and thickness ( $h$ ) at 1.57 mm to get the low profile antenna dimensions. The bowtie antenna is operated in the range from 1,6 to 2,6 GHz for a VSWR  $\leq 2$ .

*Keywords: Bowtie Antenna, Ground Penetrating Radar (GPR), Ultra Wide-Band, Low-Profile Antenna, RT Duroid 5880.*

## 1. Introduction

At this time, there are many technologies that utilize radar systems. One implementation is Ground Penetrating Radar (GPR). Ground Penetrating Radar (GPR) is one of radar types technology which is used to detect the buried target into the ground with high resolution and shallow dept penetration. However, a problem that often occurs is the difficulty of finding an accurate location of objects under the ground because of the thickness of the soil. Thus, GPR requires a high resolution value to overcome these problems. GPR uses an Ultra Wide-Band (UWB) radar system that works at frequencies between 10 MHz to 10 GHz [1]. The use of UWB radar systems aims to get high resolution values. High resolution values affect the level of accuracy in detecting objects. Antenna characteristic which is needed in GPR system is an antenna with a wide bandwidth and has a narrow pulse width. Thus, UWB antennas are used to meet the needs of the GPR system. The condition of a UWB antenna is that it must have a bandwidth that is greater or equal to 25% of its center frequency [3].

In general, as an implementation of the UWB radar system for GPR technology, antenna types such as bow-tie antennas, TEM Horn antennas, tapered slot antennas, spiral antennas, and vivaldi antennas are used [2]. However, types of antennas such as TEM horn antennas and Vivaldi antennas have larger sizes and heavier masses compared to bowtie antennas which have smaller sizes and lightweight. Therefore, in this study a bowtie antenna is proposed because this type of antenna has a smaller size and lightweight. The bowtie antenna design was carried out using RT-Duroid 5880 dielectric substrate with dielectric constant ( $\epsilon_r$ ) 2.2 and thickness ( $h$ ) 1.57 mm to get the low profile antenna dimensions. The bowtie antenna is operated in the range from 1,6 to 2,6 GHz for a VSWR  $\leq 2$ .

## 2. Literature Study

### 2.1 Ground Penetrating Radar

Ground Penetrating Radar (GPR) or commonly referred as Surface Penetrating Radar (SPR) is a technology of the radar which is used to detect the buried target into the ground without having to dig it by utilizing radio waves that operate at frequency between MHz to GHz. In general, GPR is widely used in various fields of work such as the field of environment for estimating soil properties, identifikasi of soil mineral content, and measuring soil depth; archeology to study historic sites; civil engineering for borehole inspection, analysis of bridge deck conditions, strength of buildings and concrete bones, and detecting the presence of cables; military field for

detecting mines buried in the ground [1], [4], [5]. GPR performance and its ability to detect an object are influenced by several factors. These factors such as bandwidth for the level of resolution produced, the frequency of work for its application and late-time ringing that affect the received signal [6], [7].

## 2.2 Ultra-Wide Band (UWB)

According to the Federal Communication Commission (FCC), UWB is a technique that has a fractional-bandwidth (FBW) value that can be defined in the equation (1) [3] as follow:

$$\text{Fractional Bandwidth (FBW)} = \frac{2(FH-FL)}{(FL+FH)} \geq 25\% \quad (1)$$

Where  $FH$  is the highest frequency and  $FL$  is the lowest frequency. At the transmitter, UWB must have a greater fractional bandwidth or value equal to 0.25 or 25%. In addition, the impedance relative bandwidth (percent of bandwidth) can also be determined by using the equation (2), (3), (4) [3]:

$$\text{Range Frequency } (\Delta f) = FH - FL \quad (2)$$

$$\text{Frequency Center } (fc) = \left( \frac{FH+FL}{2} \right) \quad (3)$$

$$\text{Bandwidth}_{(\%)} = \left( \frac{\Delta f}{fc} \right) \times 100\% \quad (4)$$

Where  $\Delta f$  is the range of frequencies used and  $fc$  is the middle frequency.

## 3. System Design

### 3.1 Determination of Specification

The specifications for antennas in the GPR system are expected as shown in Table 1.

Table 5: Specification of bowtie antenna for GPR system.

Parameter	Value
Operated Frequency	1,6 – 2,6 GHz
Bandwidth	<i>Ultra-Wide Band</i>
Return Loss	$\leq -10 \text{ dB}$
VSWR	$\leq 2$
Ringing Level	$\leq -30 \text{ dB}$
Radiation Pattern	<i>Unidirectional</i>
	Conductor : Copper ( $t = 0,035 \text{ mm}$ )
	Substrate : RT Duroid 5880 ( $\epsilon_r = 2,2 ; h = 1,57 \text{ mm}$ )

### 3.2 Determination of Antenna Design

The antenna is designed following the standard of microstrip antenna with a curve-shaped bowtie patch. To this antenna design a parasitic element is added to the side of the feedline. The addition of this parasitic element aims to widen the bandwidth of the bowtie antenna [8]. A dielectric substrate material is used for the antenna based on the RT-Duroid 5880 which has a dielectric constant ( $\epsilon_r$ ) of 2.2 and a thickness ( $h$ ) of 1.57 mm. This antenna works at a frequency of 1.6 - 2.6 GHz for GPR system applications. The dimensions of the curve bowtie patch are obtained from the equation (5) [9] as follow:

$$y(x) = s \cdot e^{rx} \quad (5)$$

Where  $y(x)$  is the length of the side of the bowtie arm,  $s$  is the gap width on the patch and  $r$  is the diameter of the

curve. For the dimensions of the antenna substrate, an equation can be used from (6) and (7) as follow:

$$W_s \geq 6h + 2TL \quad (6)$$

$$L_s \geq 3h + TL + L_f \quad (7)$$

Where  $L_s$  is the length of the substrate,  $W_s$  is the width of the substrate,  $c$  is the speed of light,  $TL$  is length of the side of the bowtie arm and  $L_f$  is length of feedline. So from the results of calculations using equation (5), (6) and (7), the antenna dimensions are shown in Table 2 and the antenna design is shown in Figure 1.

*Table 2: Dimension of bowtie antenna.*

Parameter	Dimension (mm)	Note
$L_s$	50	Length of substrate
$W_s$	80	Width of substrate
$L_f$	37	Length of feedline
$W_f$	5,5	Width of feedline
$TL$	38	Length of the side of the bowtie arm
$g$	1	Gap between feedline
$L_c$	10	Length of parasitic element

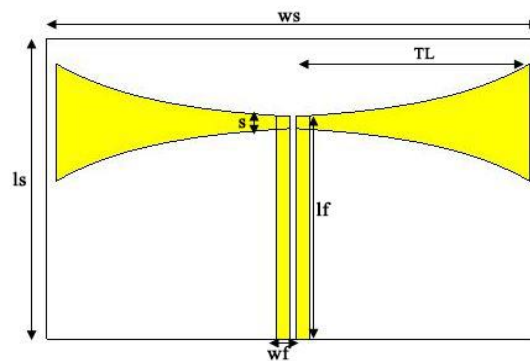


**Fig. 1: Bowtie microstrip antenna without parasitic element.**

## 4. Result and Analysis

Based on the antenna dimensions that have been designed through equations (5), (6) and (7), the bowtie antenna initiation will be carried out into the simulation software. The return loss value from the simulation results can be seen in Figure 2.

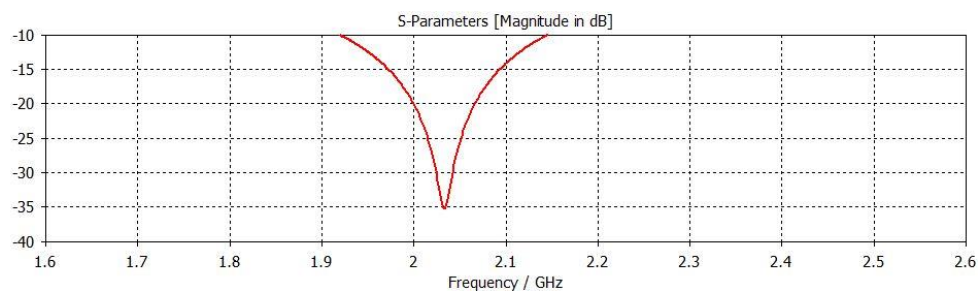


**Fig. 2: Simulation of return loss graph of bowtie antenna without parasitic element simulation.**

Return loss is the ratio of the power reflected back to the antenna with the power transmitted by the antenna. In Figure 2, it can be seen that the return loss value obtained in the simulation results is -14,15 dB at frequency 2,1 GHz. Then, the obtained bandwidth is at 226,1 MHz. However, the results of the optimization have not reached the minimum bandwidth expected because the resulting bandwidth did not reach the UWB category. So, the

parasitic elements were added to the bowtie antenna in order to widen the antenna bandwidth which can be seen in Figure 3.

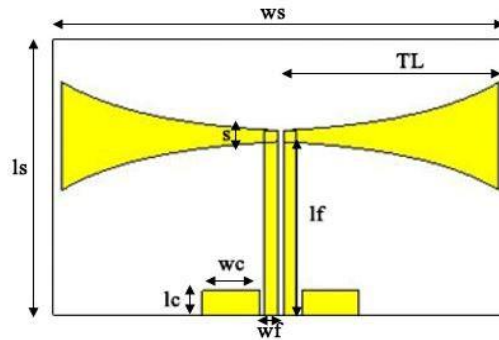


Fig. 3: Bowtie antenna with the addition of parasitic element.

The dimensions of the bowtie antenna with the addition of parasitic elements are shown in Table 3.

Table 3: Dimensions of bowtie antenna with parasitic elements.

Parameter	Dimension (mm)	Note
Ls	50	Length of substrate
Ws	80	Width of substrate
Lf	37	Length of feedline
Wf	5,5	Width of feedline
TL	38	Length of the side of the bowtie arm
g	1	Gap between feedline
Lc	10	Length of parasitic element
Wc	20	Width of parasitic element
gc	0,5	Gap between feedline and parasitic element

Based on the bowtie antenna initiation with addition of parasitic elements, the return loss value from the simulation results can be seen in Figure 4.

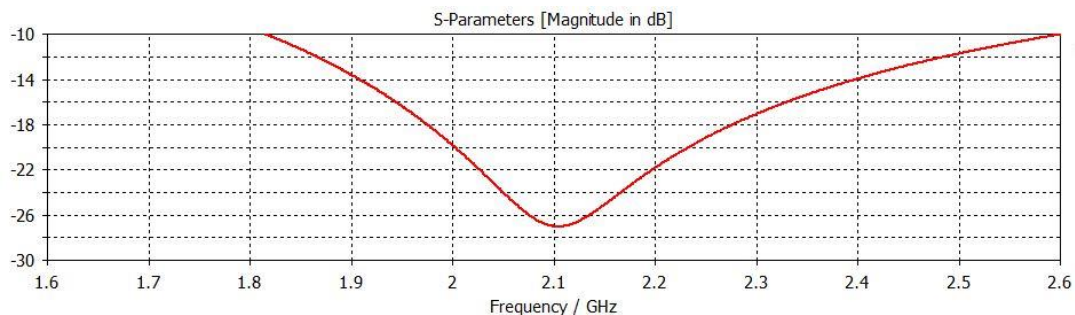
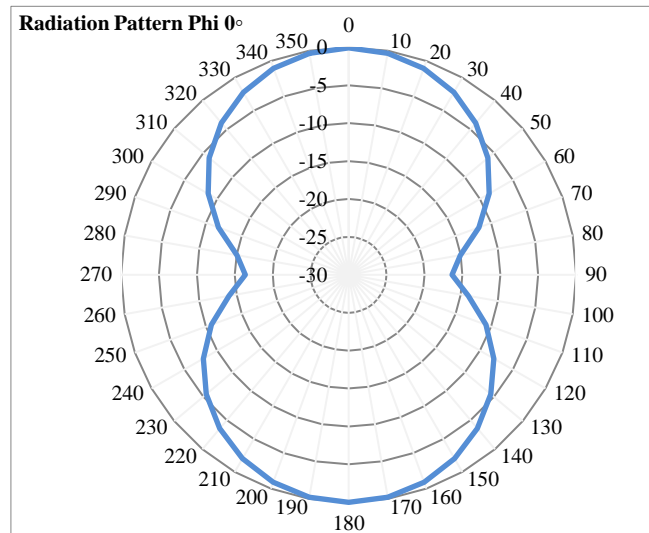


Fig. 4: Return loss graph of bowtie antenna simulation results.

In Figure 4, it can be seen that the return loss value obtained in the simulation results is -27,025 dB. Then, the obtained bandwidth is at 785 MHz from the frequency range in 1,815 – 2,6 GHz. This result clearly can meet with the UWB criteria because the fractional bandwidth value is more than the middle frequency.

Whereas VSWR is the ratio between the maximum voltage and the minimum voltage on a standing wave caused by the reflection of the wave between the transmission line and the antenna. The VSWR value for the simulation results on the bowtie curve antenna is 1,09 dB. While the radiation pattern is the antenna's radiating direction in radiating power in a certain direction. The radiation pattern is measured by azimuth direction and elevation. The depiction of the radiation pattern as an antenna beam intensity as a function of the spherical coordinate parameters ( $\theta$ ,  $\varphi$ ).





**Fig. 5: Horizontal radiation pattern (azimuth,  $\theta = 0^\circ$ )**

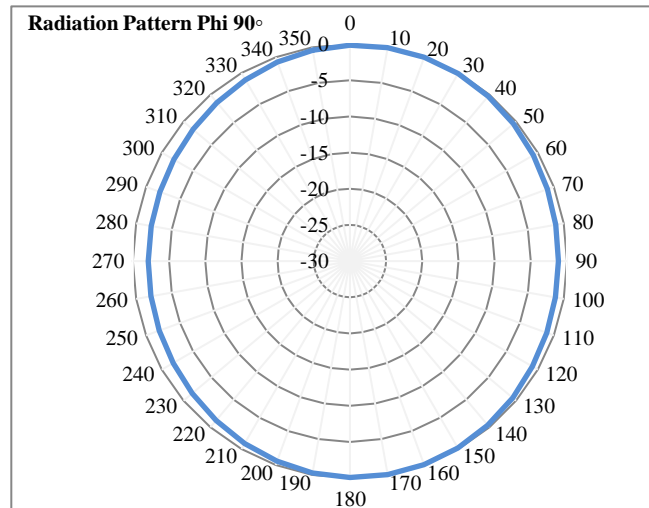


**Fig. 6: Vertical direction radiation pattern (elevation,  $\theta = 90^\circ$ )**

Based on Figure 5, the simulation results on the radiation pattern in the horizontal direction have a maximum transmit power at an angle of  $0^\circ$  and  $180^\circ$ . Thus, the position of the antenna in transferring maximum power can be done at that angle in the direction of azimuth. While the radiation pattern with vertical direction as in Figure 6 shows that the antenna has a maximum power beam at all beam angles with respect to its vertical direction. Thus, the position of the antenna can be placed in all angles of elevation direction.

While the ringing level value obtained from the simulation results is  $-32,35$  dB with a pulse width of 6 ns. Thus, the maximum limit of the ringing level meets the criteria of the GPR system specification. Moreover, the effect of adding parasitic elements on bowtie antenna is shown in Table 4.

**Table 4: Bowtie antenna comparison without parasitic elements and with parasitic elements.**

Parameter	Bowtie antenna without parasitic elements	Bowtie antenna with the addition of parasitic elements
Return Loss (dB)	-14,15	-27,025
VSWR	1,48	1,09
Bandwidth (MHz)	226,1	785
Ringing Level (dB)	-30,84	-32,35

## 5. Conclusion

In this study a bowtie antenna was designed as an antenna on the GPR system. The antenna is designed using the RT-Duroid 5880 substrate material with the addition of the parasitic element method which aims to increase the bandwidth of the antenna. Based on the simulation results, the bowtie antenna with parasitic elements has a bandwidth of 785 MHz which means the fractional bandwidth value is greater than 25%, ringing level of -32,35 dB, return loss of -27,025 dB and VSWR 1,09 for transmit power efficiency. The antenna has a radiation pattern in the bidirectional form where the maximum transmit power is at an angle of 0° and 180° in the azimuth direction and at each angle in the elevation direction. Thus, the results of the design of the bowtie antenna indicate that the bowtie antenna has met the criteria of the GPR antenna system.

## 6. References

- M. I. Skolnik, Radar Handbook, Third Edition. The McGraw-Hill, 2008.
- E. Mohd, S. Mohd, M. Yusof, J. Ali, and N. Abdullah, "Ultra-Wideband Antenna Design for GPR Applications: A Review," *Int. J. Adv. Comput. Sci. Appl.*, vol. 8, no. 7, 2017.
- Commission Federal Communications (FCC), "First Report and Order in The Matter of Revision of Part 15 of the Commission's Rules Regarding Ultrawideband Transmission System," ET Docket 98-153, 2002.
- D. J. Daniels, "Ground Penetrating Radar," in *Encyclopedia of RF and Microwave Engineering*, Hoboken, NJ, USA: John Wiley & Sons, Inc., 2005.
- Harry M. Jol, *Ground Penetrating Radar Theory and Applications*. Elsevier B.V., 2009.
- M. N. A. Karim, M. F. A. Malek, M. F. Jamlos, and N. Saudin, "Ground Penetrating Radar: Antenna for Buried Object Detection," *IEEE Symp. Wirel. Technol. Appl. ISWTA*, no. July 2014, pp. 198–201, 2013.
- A. H. Abdelgwad and T. M. Said, "Design of Ground Penetrating Radar Antenna for Detecting Soil Contamination at L-band Frequencies," *J. Microwaves, Optoelectron. Electromagn. Appl.*, vol. 16, no. 3, pp. 853–866, 2017.
- L. O. Nur, M. F. Hizbuddin, and B. S. Nugroho, "Pengembangan Antena Fleksibel Mikrostrip Bowtie Development of Flexible Microstrip Bowtie Antenna," *TELKA*, vol. 5, no. 2, pp. 130–138, 2019.
- U. S. Antenna, "Design of Vivaldi Microstrip Antenna for Ultra-Wideband Radar Applications."

## Design of Vivaldi Antenna at 0.9 – 6 GHz for Mobile Cognitive Radio Base Station (MCRBS)

Feralia Fitri<sup>1</sup>, Heroe Wijanto<sup>2,\*</sup>, Aloysius Adya Pramudita<sup>3</sup>, Yuda Nugraha<sup>4</sup>

<sup>1,2, 3,4</sup>School of Electrical Engineering, Telkom University, Bandung - INDONESIA

<sup>1</sup>[feraliaf@student.telkomuniversity.ac.id](mailto:feraliaf@student.telkomuniversity.ac.id),

<sup>2</sup> [heroe.wijanto@gmail.com](mailto:heroe.wijanto@gmail.com), <sup>3</sup> [pramuditaadya@telkomuniversity.ac.id](mailto:pramuditaadya@telkomuniversity.ac.id),

<sup>4</sup>[ynugraha@student.telkomuniversity.ac.id](mailto:ynugraha@student.telkomuniversity.ac.id) }

### Abstract

Mobile Cognitive Radio Base Station (MCRBS) is a system for disaster area. This system provides a network for an area after disaster for evacuation activities. MCRBS system works in 0.9 – 6 GHz frequency range to support the second generation of mobile communication system (2G) up to the fifth generation of mobile communication system (5G) frequency candidate. An antenna is one of MCRBS components with function to transmit and receive electromagnetic signals. To support MCRBS system, an antenna with *Ultra-Wideband* (UWB) characteristic will be needed in communication services that facilitated by MCRBS system. The Vivaldi antenna is one of UWB antennas that has wide bandwidth and high gain for UWB applications. It was invented by P. Gibson in 1979. The antipodal Vivaldi antenna which is one of Vivaldi antenna types has been designed using FR-4 material and copper. The antenna will use quarter wave transformer and array method. Based on the results of simulations conducted, the antenna has a return loss  $\leq -10$  dB, a VSWR  $\leq 2$ , with 5.1 GHz bandwidth, gain 11.13 dBi, and unidirectional radiation pattern to support MCRBS system.

*Keywords: Ultra-Wideband, Vivaldi antenna, Mobile Cognitive Radio Base Station.*

### 1. Introduction

Indonesia's geographical condition which has the potential for natural disasters greater than other regions often requires quick rescue measures[1]. In the process of searching and evacuating victims of disaster, a reliable communication system is needed to be able to support the post-disaster conditions. Mobile Cognitive Radio Base Station (MCRBS) is a technology to recover communication systems after a disaster when the main connection network is unavailable.

MCRBS is a system in the form of a Base Transceiver Station (BTS) that can be mobilized. After disaster occurred, MCRBS will provide a network that will assist the process of evacuation and search for victims by detecting the network on the victim's cell phone. MCRBS provides 2G up to 5G communication services using limited power in its application. MCRBS system requires an antenna component with a very wide bandwidth to provide services that is able to cover long distances with limited power.

In MCRBS, an antenna is needed to fulfill the standards of the system. The antennas must have wide bandwidth specification to support the frequency candidate of the communication services. To cover long distance, high gain also needed to support the MCRBS system. The Vivaldi antenna which is one of the *Ultra-Wideband* (UWB) antennas that was invented by P.J Gibson[2] is used for UWB applications[3] that has wide bandwidth and high gain [4].

This research concentrates on designing an antipodal Vivaldi antenna which is one of the types of Vivaldi antenna[5] with 5.1 GHz bandwidth using FR-4 substrate material and copper as a conductor. The quarter wave transformer method is added to reduce the return loss[6]. Array method is also added to increase the gain [7].

## 2. System Design

### 2.1 Mobile Cognitive Radio Base Station (MCRBS)

MCRBS is a device in the form of a Base Transceiver Station (BTS) that can be mobilized. MCRBS is expected to be used in emergencies such as when a natural disaster occurred. In the event of a natural disaster, the MCRBS will function as a network transmitter used to evacuate victims that are affected. This system provides 2G up to 5G communication services. Antenna is one of MCRBS components. To support MCRBS system, an antenna is needed that has wide bandwidth to support 2G up to 5G services. Also high gain is needed to cover large distances. The antipodal Vivaldi antenna is proposed to support the MCRBS system.

### 2.2 Determination of Antenna Design

The antenna designed is a Vivaldi antenna with the type of antipodal with FR-4 substrate that has a dielectric constant ( $\epsilon_r$ ) of 4.4 and thickness ( $h$ ) of 1.6 mm and copper as its conductor. This antenna works at a frequency between 0.9 to 6 GHz following the working frequency of MCRBS that serves 2G up to 5G communication with a bandwidth of 5.1 GHz, unidirectional radiation pattern, and gain  $\geq 8$  dBi. The dimensions of this antenna can be obtained from the following equation (1) [8]:

$$y(x) = s \cdot e^{rx} \quad (1)$$

Where  $y(x)$  is a function to form antipodal Vivaldi antenna,  $s$  variable is the transformer width of  $2 \times s$ , and  $r$  is the curvature of the antenna. The dimensions of the antenna's substrate are obtained from the following equation (2) [8]:

$$L_s = W_s = \frac{c}{f} \sqrt{\frac{2}{\epsilon_r + 1}} \quad (2)$$

With  $L_s$  is the length of the substrate,  $W_s$  is the width of the substrate,  $c$  is the speed of light, and  $f$  is the operating frequency, and  $\epsilon_r$  is the dielectric constant.

For the feedline dimensions, the following equation can be used (2) [7]:

$$W_o = \frac{2h}{\pi} \left[ B - 1 - \ln(2B - 1) + \frac{\epsilon_r - 1}{2\epsilon_r} \left[ \ln(B - 1) + 0.39 - \frac{0.61}{\epsilon_r} \right] \right] \quad (3)$$

For  $B$  variable, the following equation can be used (3) [7]:

$$B = \frac{60\pi^2}{Z_o \sqrt{\epsilon_r}} \quad (4)$$

$Z_o$  is a transmission impedance value of  $50 \Omega$ .

There is a quarter wave transformer in the feedline to increase matching impedance [6], [9]. From the calculation (2), (3), and (4), the dimensions of the antenna can be seen in Table 1 and antenna design as shown below in Figure 1.

Table 1. Dimensions of Antipodal Vivaldi Antenna.

Parameter	Value (mm)
Sl	40
SL2	35
r	0,037
r2	0.08
s	0.44
s2	3

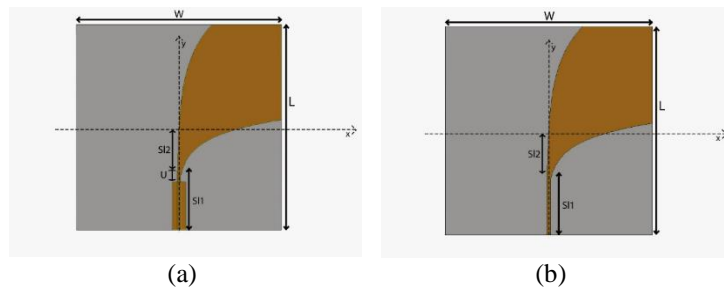


**Fig. 1: Antipodal Vivaldi Antenna, (a) Front View (b) Rear View**

Problem that occurred in antennas with single element such as low gain cannot be a solution for the developing process of communication system. To increase the gain of the antenna, array method are used [7]. With four antenna elements and the distance between elements is  $\lambda/2$ .

The results of the antipodal Vivaldi antenna with array method design can be seen in Figure 2 below.

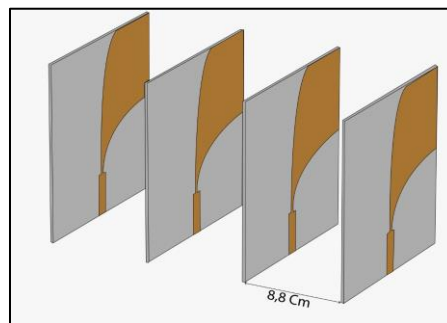


**Fig. 2: Final Antenna Design, (a) Front View (b) Rear View**

The calculation of dimensions of the antipodal Vivaldi antenna before and after using the array method can be seen in the following Table 2 below.

**Table 2. Optimization Dimensions of Antipodal Vivaldi Antenna**

Antenna Dimensions	Value before optimization (mm)	Value after optimization (mm)
W <sub>0</sub>	20	5
S <sub>1</sub>	30	40
S <sub>L2</sub>	45	35
r	0,05	0,037
r <sub>2</sub>	0.062	0.08
s	0.5	0.44
s <sub>2</sub>	5	3
q	16.65	88

### 3. Result and Analysis

In the simulation results, the parameters that have been determined at the beginning of the antenna specification are reviewed.

#### 3.1 Return Loss, VSWR, and Bandwidth

Based on the dimensions of the antenna that has been designed in simulation software with the equation, the return loss results from the simulation can be seen in Figure 4 below.

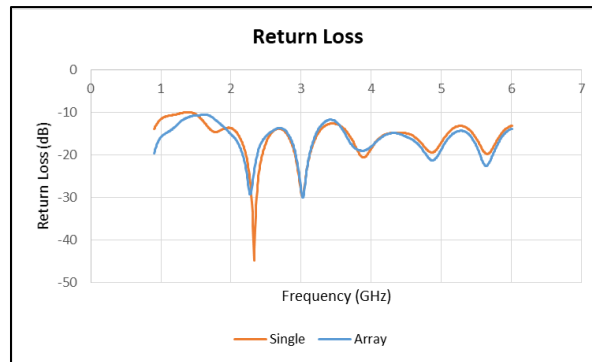


**Fig. 3: Return Loss Comparison of Single antenna and Antenna Array**

In Figure 4 the return loss value obtained in the simulation results is -10 dB on 0.9 to 6 GHz frequency range. Then the bandwidth obtained is 5.1 GHz on 0.9 - 6 GHz frequency range as seen in Figure 4. It can be concluded that the antenna designed has fulfilled the UWB requirements with a bandwidth of more than 500 MHz.

The VSWR values obtained from the simulation results on the design of antipodal Vivaldi antennas can be seen in Figure 5 below.

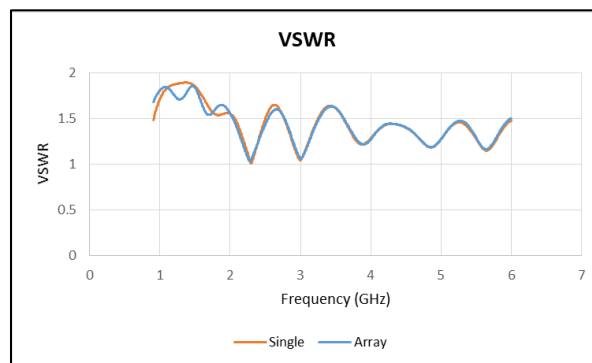


**Fig. 4: VSWR Comparison of Single Antenna and Antenna Array**

Based on Figure 5, the VSWR value for the results of the antipodal Vivaldi antenna simulation is  $\leq 2$  dB on 0.9 to 6 GHz frequency range. This means the return loss, VSWR, and bandwidth parameters already fulfilled the MCRBS requirements.

### 3.2 Gain

Gain is a comparison of how much power is emitted in a particular direction with power emitted in all directions[7]. The antenna simulation results for Gain can be seen from three sample frequencies at the frequency of 0.7 GHz, 4.35 Hz, and 8 GHz which are shown in Table 3 below.

**Table 3. Gain Comparison of Single Antenna and Antenna Array**

Frequency	Results	
	Single	Array
0,7 GHz	1,119 dB	4.017 dB
4.35 GHz	4,858 dB	11,13 dB
8 GHz	4,929 dB	11,03 dB

Based on Table 3, after the array method applied to the simulation, the gain of the antenna is increased.

### 3.3 Radiation Pattern

The radiation pattern is measured by azimuth direction and elevation. The radiation pattern simulation results are seen in three frequency samples at the frequency of 0.7 GHz, 4.35 GHz, and 8 GHz can be seen in Figure 5 – 7 below.

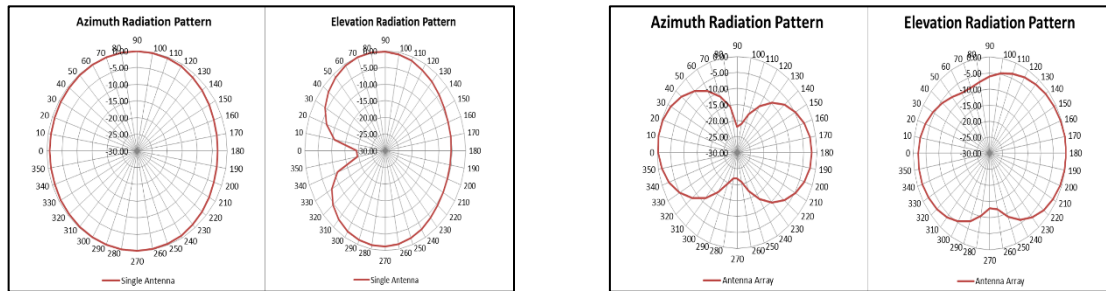


Fig. 5: Radiation Pattern of Single Antenna and Antenna Array at 0.9 GHz

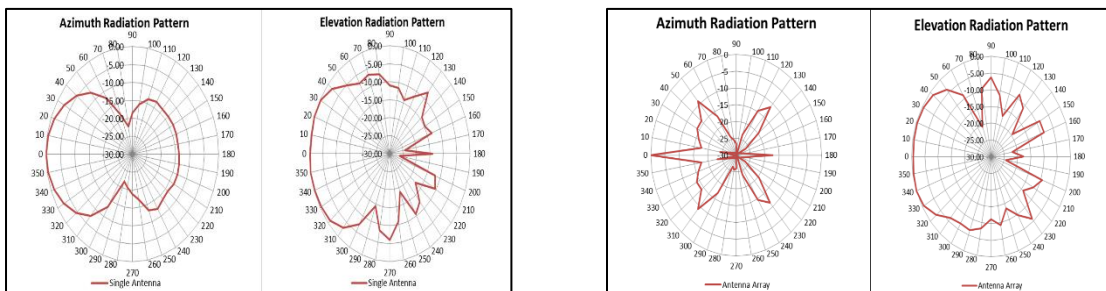


Fig. 6: Radiation Pattern of Single Antenna and Antenna Array at 3.45 GHz

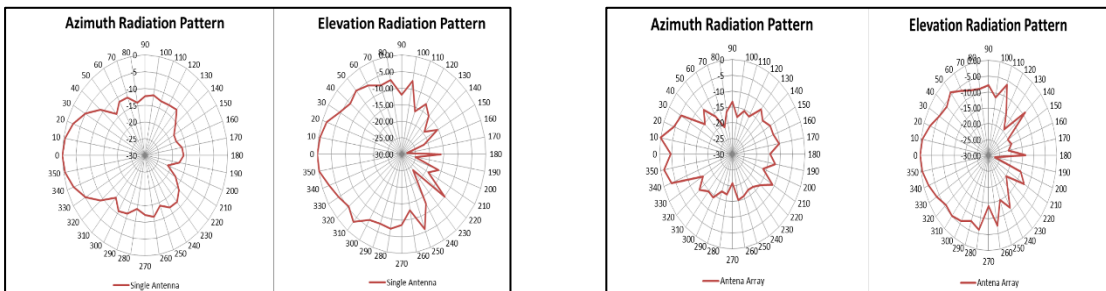


Fig. 7: Radiation Pattern of Single Antenna and Antenna Array at 6 GHz

Based on Figure 5 – 7, the radiation pattern of the simulation of a single antenna and array antenna are unidirectional.

## 4. Conclusions

The conclusion of this project entitled “Design of Vivaldi antenna at 0.9 – 6 GHz for Mobile Cognitive Radio Base Station (MCRBS)” with FR-4 as the substrate material and copper as the patch on 0.9 – 6 GHz frequency range as follows:

- The antenna simulation can work on 0.9 - 6 GHz frequency range by achieving the return loss specification  $\leq -10$  dB,  $VSWR \leq 2$  dB, 5.1 GHz bandwidth, unidirectional radiation pattern, and gain value 11.03 dBi.
- The wave quarter transformer in antenna design is used for impedance matching.
- The array method in antenna design can increase antenna gain by 3 to 7 dBi. The higher the frequency the increase of the value of the gain will be higher.

From the following conclusions, it can be shown that the antipodal Vivaldi antenna has fulfilled the standards to support the MCRBS system.

## 5. References

- Badan Nasional Penanggulangan Bencana [BNPB], "Risiko Bencana Indonesia (Disasters Risk of Indonesia)," Direktorat Pengurangan Resiko Bencana Deputi Bid. Pencegah. dan Kesiapansiagaan, pp. 9–218, 2016.
- P. J. Gibson, "The Vivaldi Aerial," 1979.
- H. C. Ba, H. Shirai, and C. D. Ngoc, "Analysis and design of antipodal Vivaldi antenna for UWB applications," 2014 IEEE 5th Int. Conf. Commun. Electron. IEEE ICCE 2014, pp. 391–394, 2014.
- B. S. Yarman, Design of Ultra Wideband Antenna Matching Network. 2008.
- F. A. Shaikh et al., "Ultra-wideband antipodal Vivaldi antenna for radar and microwave imaging application," 2017 IEEE 3rd Int. Conf. Eng. Technol. Soc. Sci. ICETSS 2017, vol. 2018-Janua, no. 2, pp. 1–4, 2018.
- S. Sharma, C. C. Tripathi, and R. Rishi, "Impedance Matching Techniques for Microstrip Patch Antenna," Indian J. Sci. Technol., vol. 10, no. 28, pp. 1–16, 2017.
- C. A. Balanis, "Antenna theory; analysis and design," in Proceedings of the IEEE, vol. 72, no. 7, 2008, pp. 989–990.
- P. MY, H. T, and Y. Wahyu, "Design of Vivaldi Microstrip Antenna for Ultra-Wideband Radar Applications," J. Phys. Conf. Ser., vol. 755, no. 1, 2016.
- I. M. Patch and A. For, "Effect of Change in Feedpoint on the Antenna Performance in Edge, Probe and Inset - Feed Microstrip Patch Antenna for 10 GHz," no. January, 2014.
- S. Wang, X. D. Chen, and C. G. Parini, "Analysis of ultra wideband antipodal vivaldi antenna design," 2007 Loughbrgh. Antennas Propag. Conf. LAPC 2007 Conf. Proc., vol. 00, no. April, pp. 129–132, 2007.
- H. B. Chu, H. Shirai, and C. N. Dao, "Effect of curvature of antipodal structure on Vivaldi antennas," IEEE Antennas Propag. Soc. AP-S Int. Symp., vol. 2015-Octob, pp. 2331–2332, 2015.



## **Design of Numbering Machine Control System based on Omron CJ2M PLC with Omron NB10 Touchscreen HMI for Improving Manufacturing in Motorcycle Assembling Industry PT XYZ**

**Qori Rohman Putra, Gunawan Tjahjadi and Endang Djuana\***

Department of Electrical Engineering, Faculty of Industrial Technology, Universitas Trisakti, Jakarta -  
INDONESIA

\* Corresponding author e-mail: edjuana@trisakti.ac.id

### **Abstract**

Engine numbering process is the earliest step in assembling a motorcycle engine and it is strictly prohibited to make slightest mistake. Because if it happens, it will disrupt the next process and / or jeopardize vehicle engine registration process required by National Police Department. However, in 2017 alone there have been no fewer than 200 engines produced with wrong number. This is because the existing machines are prone to errors, with inadequate protection system, and unavailability of human machine interface (HMI) for operator monitoring the machine. In this paper we present a new design for numbering machine control system with more reliable protection logic, so that zero mistakes can be realized. Improved protection system includes checking repetition of process for the last 100 data, better type selection protection, protection of sequential numbering process, and acknowledgment using fingerprint scanner. The programming language used was made using structured text language which making it easier for programming, monitoring and troubleshooting. An intuitive interface has also been made using HMI touchscreen. Testing all input data protection logic shows very good results with 100% success rate, so that it can fulfil zero mistake requirement. In this way this machine can be declared ready for mass production.

*Keywords: human machine interface, numbering machine, programmable logic controller,*

---

### **1. Introduction**

Engine numbering process is the most vital and critical process in assembling a motorcycle engine. It was said so, because engine number was used for the administrative process of registering a motorcycle at the National Police Vehicle Registration Department. So, it is strictly forbidden to make slightest error. Therefore, the machine numbering process must be very thorough in terms of the quality and accuracy of its processing.

The engine numbering process currently running at PT XYZ is done automatically by machine. Input data to determine the engine number to be processed by machine comes from barcode. Data is then received and processed by Programmable Logic Controller (PLC) before being forwarded to the numbering machine printing actuator. Data processing consists of three subprocesses, namely, data reception, data checking, and data sending (John and Tiegkamp, 2001).

Data received by the PLC from barcode scanner were then translated into a form that can be processed by the PLC. Furthermore, data checking process consists of, checking suitability of number with barcode, suitability of engine type that is running, checking sequence number, and checking repetition of the machine numbering process. Finally, process of sending data consists of process of separating data into two rows (according to visuals on number of the motorcycle engine) and process of translating the data so that it can be processed by the engine number printing actuator. Engine number printing is done by implementing the *scribing* method.

However, with a series of data checking processes, several printing errors were still found. The following is the error printing data collected by the PT XYZ PPIC (Production Planning Inventory Control) Department as presented in Table 1. Efforts made after printing errors occur is to analyze the problem with the *why-made* and *why-send* methods in each different case, then make improvements. The following table is result of the analysis and the efforts made by the Department as listed in Table 2.

**Table 1: Case of Incorrect Print for Case Period of January - March 2017**

Case	Case Detail	Number of Incidents
1.	Same number reprinted	47
2.	Numbers are printed out in sequence	106
3.	Numbers printed do not match the barcode entirely	28
	Total	181

**Table 2: Why-made and Why-send Analysis to Discovered Cases**

Case	Case Detail	Analysis Method	Problem Description	Improvement Efforts
1.	Same number reprinted	<i>why-made</i>	The machine only checks the repetition of number in the last 5 data	No improvement, because it's the engine's limit
		<i>why-send</i>	There is no number repetition checking	It is not possible to check number repetition
2.	Numbers are printed out in sequence	<i>why-made</i>	The machine only raises a warning when processing nonconsecutive numbers	Adding buzzer
		<i>why-send</i>	There are no sequential serial number checking procedures	Adding points of attention to the next operator SOP
3.	Numbers printed do not match the barcode entirely	<i>why-made</i>	New types have not been included in the program	Program modification for new and discontinuous types
		<i>why-send</i>	Found in the numbering machine	Found in the numbering machine

In the case of reprints and non-consecutive prints error, no further repairs can be made due to the machine's limited capabilities, so it only relies on efforts of the *why-send* analysis. But, apparently after a few months since these improvements, a new case emerged that is a print error only on the type code (initial 5 digits) of the machine number. Dept. PPIC XYZ has collected data of 23 engines with errors that have passed to become motorcycle units (presented in Appendix).

After analyzing the cause of printing errors, the main problem is programming error, which causes the type code error. Based on analysis and simulation carried out, error arises when type change is performed. The effort made of course is to improve the program. But these efforts still have potential to cause errors, because when there is an error, the PLC does not provide a warning or show error message when running the program.

After being evaluated, the existing machines are considered to be inadequate and unable to serve production demands that are very dynamic, e.g. still have potential to cause printing errors, are difficult when troubleshooting, and do not have an interface for operators on duty for these machines. For this reason, it is necessary to create a new control system for this numbering machine that can run a better inspection process, easy troubleshooting, and an intuitive interface. Therefore, in this research a new numbering machine control system has been created which is replacing the previous system and eliminate existing problems.

## 2. Problem Definition and Scope

### 2.1. Numbering Machine

Numbering machines are machines for printing machine numbers on a motorcycle. These machines print the number using the scribing method. The pin with a diamond at the end is used for scribing process on the engine. The numbering machine consists of four main components, namely barcode scanner as input, PLC as data processor, Human Machine Interface (HMI) as interface, and head marker as scribing process actuator. The display of the numbering machine is shown in Figure 1.



Fig. 1: Numbering Machine

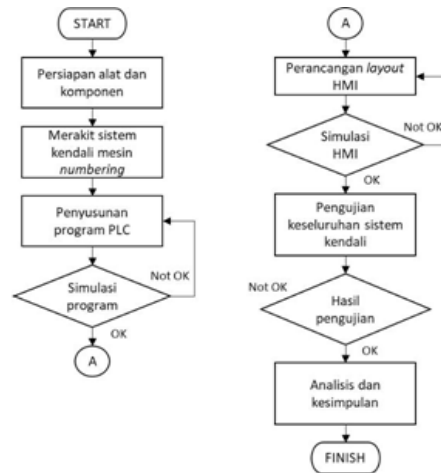


Fig. 2: Design Process Flowchart

### 2.2. Problem Definition and Objectives

In designing this numbering machine control system, the focus is to eliminate the potential causes of scribing errors. The following breakdown problems in the design of this control system:

- How to design a PLC program on this machine to translate number data from barcode scanner to numbering machine for printing.
- What is the procedure and process of checking the input number data by the machine when changing type to avoid printing error?
- What is the process of checking number input data by the machine when number repetition occurs so that data is not printed?
- What is the process of checking number input data by the machine when numbering process is not sequential, as well as the procedure for printing / not printing the number so that no errors occur?
- What is the design of PLC program on this machine when numbering process is interrupted, such as an emergency stop, so that input data that has been entered is not stored in the machine's memory?
- How to produce intuitive interface design to display information about the condition of the machine, data being processed, error status, and guidance when an error occurs.
- How to design a PLC program and HMI display that enables the machine to troubleshoot in case of error / abnormality on this machine.

With this new numbering machine control system, zero mistakes will be expected in the production numbering process. That is because the process of examining input data is more detailed with a fingerprint scanner-based acknowledgment process. In addition, there is a touch-layer HMI that makes it easy for machine operators to monitor process data. Also, program design is easy to assist troubleshooting when there is abnormality in this numbering machine since programming was made using structured text language (Antonsen, 2018).

### 2.3. Scope and Limitation

The following are the limitations of this research on the PLC Omron CJ2M-based numbering machine control system with Omron NB10 touch screen HMI (OMRON 2012, 2013):

- There are 3 number types of motorcycle engine that is processed referring to the production process carried out on the line where this engine is placed.
- Inspection of the type of machine number that has been processed is carried out on the last 100 data (according to the agreement of the meeting / discussion with related parties: Dept. of Production, Dept. of Quality Control, and Dept. of Engineering).
- The design and construction of this numbering machine has been discussed and carried out separately by the mechanical team from Dept. Engineering.

The data limit is based on the amount of machine production before changing to a different type. So that at least for 100 data there will not be an error because the type that is running is still the same, and in fact the 100th engine has been assembled and has passed the Scan-out assembly process for the next process, namely shipping. The next data limit will be accommodated in further research using a centralized database which will involve the Information Technology (IT) Department.

## 3. Methodology and Implementation

### 3.1. Design Process

Stages of implementing the Omron CJ2M PLC-based numbering machine control system with the HMI interface the Omron NB10 touch screen, contained in the form of flowchart in Figure 2.

The design of this control system starts with preparation of tools and components, where main components of this control system are barcode scanner, PLC, HMI, and scribing head marker. Furthermore, the components are assembled into a machine in construction that has been prepared previously. After assembly is complete, PLC program is compiled, then simulated to check the algorithm, if it is correct then previous process continues, if it is not correct then an improvement will be made. Next, we design the HMI layout and simulate those layouts, if it is correct, then we proceed to the next process. After the whole control system is tested on this numbering machine and the results are correct, then we perform analysis and draw the conclusion.

### 3.2. System Specification

The following system specifications of the Omron CJ2M PLC-based numbering machine control system with Omron NB10 touch screen HMI (OMRON 2012, 2013), including:

- The numbering machine control system uses the Omron CJ2M PLC as the main controller. These PLCs are used to control two pneumatic cylinders (as clasper and sliding jig) and controlling the head marker for printing engine numbers (Putra, 2014). The PLC is also used to processing barcode scanning data, until it is ready to be sent to the number printer's head marker.
- This machine has an interface in the form of Omron NB10 touchscreen HMI. With a screen size that is wide enough about 10 inches, the HMI can contain many control functions and machine performance monitoring function (Winahyu, 2015). For example, in the auto operation mode there is a barcode scanning number, last number printed, type selected, counter, sensors that are active, menu move button to recorded data menu, as well as date and time information.
- This machine is designed to store data that has been printed up to 100 data. So that barcode scan data inspection is performed on the last 100 data. If data storage has reached limit, new data will enter the FIFO (First In, First Out) system. 100 of these data can also be erased entirely through HMI by an engineer with a password.
- This machine has a fingerprint scanner, with function of running acknowledgment system. There are two cases that require this system, namely when replacing the model and when wanting to process data that is not sequential with the last data. The way it works is, when barcode is scanned, a warning will appear on the HMI indicating that the data is different (different type or not in sequence) with the last data, then the data must be checked again whether the same as the scanned data. If they are the same, the machine can process the data with approval or acknowledgment from the foreman by scanning the fingerprint.

### 3.3. System Architecture and Design

The following is the architecture of the numbering machine control system which is represented in Figure 3.

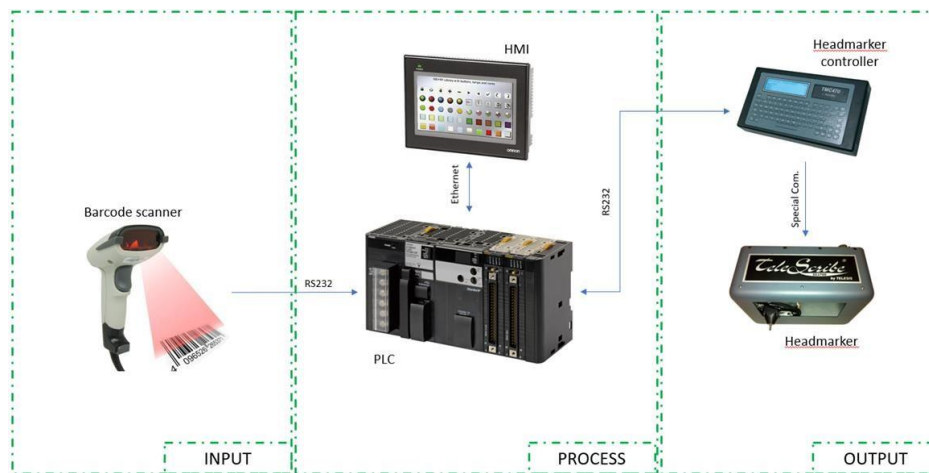


Fig. 3: Numbering Machine System Architecture

The system block diagram is also presented by dividing 3 main parts of the system, namely input, process, and output. At the input, there is a barcode scanner whose duty is of course to read the barcode. Then the data will be forwarded to the PLC to obtain. In the process section, there is a PLC for processing data and HMI Touchscreen for the system interface. Data from the barcode scanner will be processed through a series of checks and translated into data that can be read by the head marker controller. HMI Touchscreen will display the data that is being processed, the type that is running, the data that has been processed, as well as the error that is happening. In the output section, there is a head marker and its controller, which is the actuator to do the engine numbering process.

#### 3.3.1. PLC Program Design

The following is a schematic of the PLC program that flows in the form of a flowchart in Figure 4.

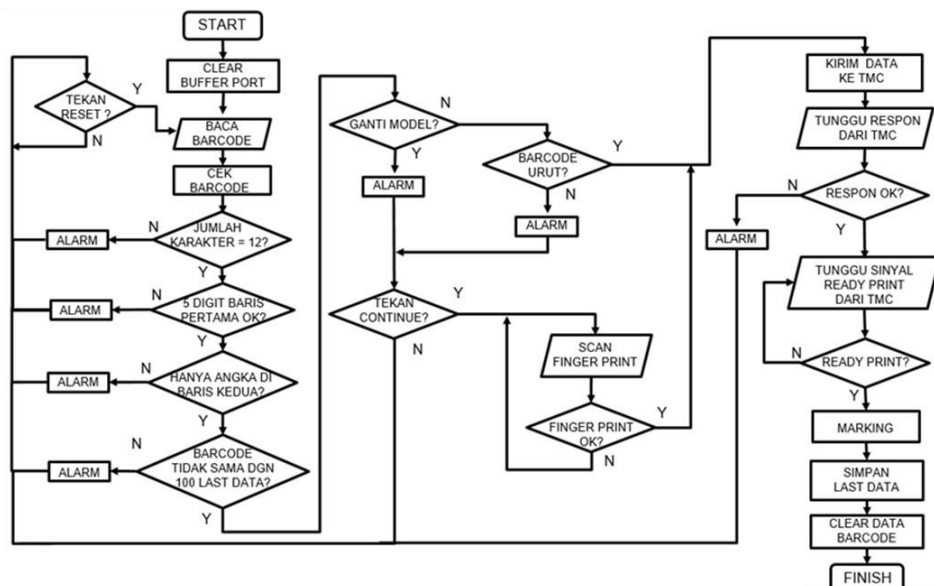


Fig. 4: PLC Program Flowchart

After pressing the start button, the program sequence starts with clear buffer port process, which ensures that no data is left on the barcode reading variable. After that, barcode is read by barcode scanner, and protection system is executed serially. The order of protection is checking the number of characters, checking the data type in the first 5 digits, checking only the numbers in the last 7 digits, and checking the repetition of data against the last

100 data. If an error is found, an alarm will appear depending on each type of protection.

Then the same data is checked whether the data is in order, if it is correct then the program will send the data to printer. Conversely, if you change the data and / or the number is not sequential, it will enter the acknowledgment logic to check the actual scan results. Data will proceed to data sending program if a fingerprint has been scanned by the registered operator.

If it has gone through previous processes according to logic designed, then data will be sent to TMC (Telesis Marking Controller). TMC feedback is needed to ensure data has been received and is ready to be printed. After print-ready feedback is provided, data will be printed, stored in memory after completion, and processing data on the PLC is deleted.

### 3.3.2. HMI Layout Design

Next is the design of the HMI layout on the numbering machine control system, divided into several pages with their respective functions:

- **Engine Initialization:** On this HMI page, a machine readiness status is displayed. Information displayed includes the status of the printer controller, the status of the wind pressure, the status of the home position for each pneumatic cylinder, the status of the emergency stop switch. If there is one that is not ready, it will appear on this page with NG status. After all are OK or ready to run, the page will switch to Auto mode operation.
- **Auto Mode Operation:** The HMI auto mode operation page is a display that will appear when the machine is in standby. There is data information that has just been scanned, the last data, counter, type selected, jig installed, also date and time. There are also buttons to switch pages to the data record page and input type code page.
- **Manual Mode Operation:** On this page there is a function to control the engine, especially pneumatic cylinders manually. There are 4 buttons, each of which functions to enter and remove the workpiece, and to grip and release stress on the workpiece. Also equipped with a light indicator that shows the status of each button.
- **Error Display:** An error is being displayed on this page, some of which are incorrect data types, the data is not sequential, and the data has been processed before. This page also provides a reset button to restore the engine to its original position or home position, and a continue button to continue the process if the error in question is the change of type and number are not sequential.
- **Warning Display:** On this page a warning is displayed for the operator to check the compatibility of the barcode with the scanning data. This warning appears when the data is not sequentially processed or will make a type change. After the operator checks the suitability of the data, the foreman of the operator must come to find out and check, then perform the acknowledgment process by scanning the fingerprint.
- **Type Code Input:** On this page is displayed a function to add the type that can run on this numbering machine. This page is password protected and can only be accessed by engineers. There are 4 types of engine provided to run on this engine, and each has 3 advanced types. The advanced type in question is the type of motorcycle color and striping.
- **Last Recorded Data:** This page displayed data that has been processed before, and a function to delete all data. Data displayed are 100 data that are divided into 4 pages which are navigated by the back and next buttons. Then on the last page there is a clear memory button to erase all data. This page can only be accessed by the responsible engineer.

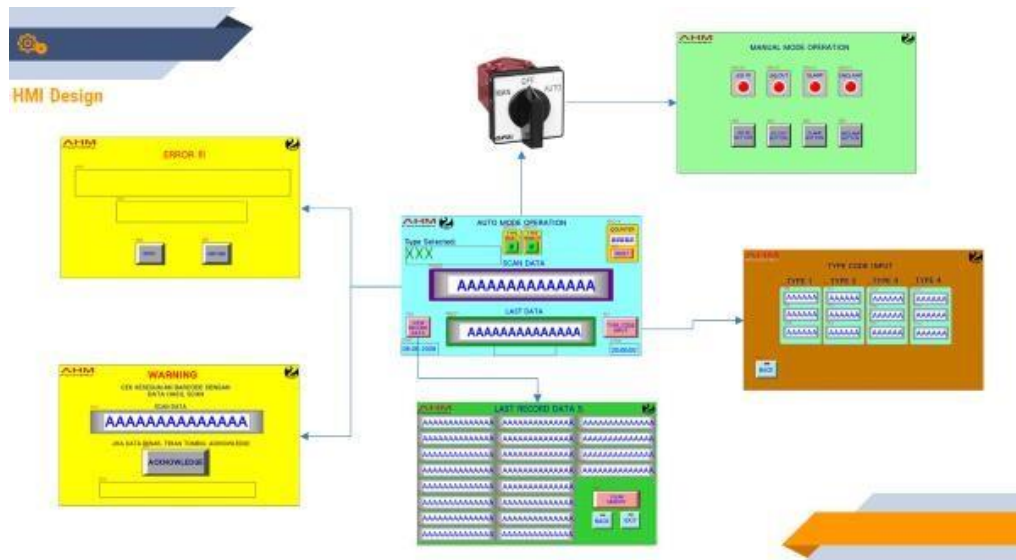


Fig. 5: HMI Layout Design

### 3.3.3. Electrical and Communication Wiring Design

The electrical design of the machine is divided into three parts of the network namely power line, control circuits, and communications cable (OMRON 2012):

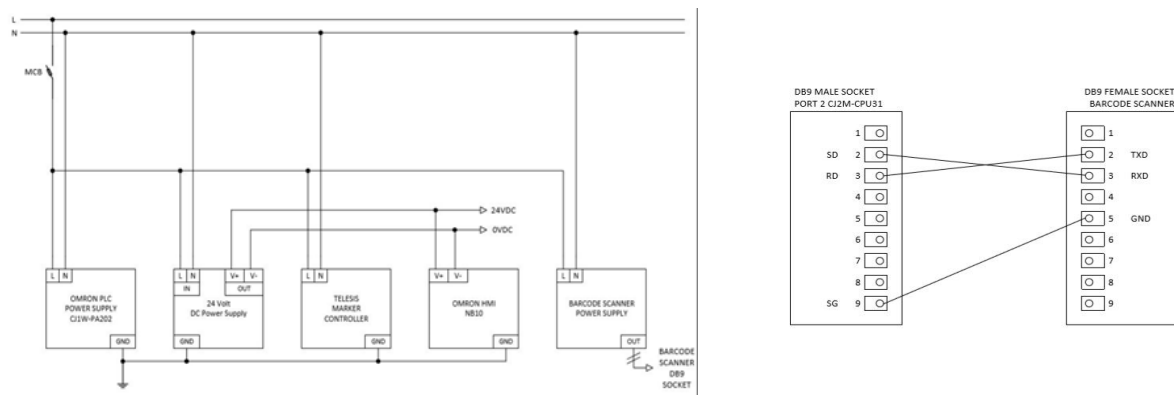


Fig. 6: Power Supply Circuit Fig. 7: PLC-Barcode Scanner Communication

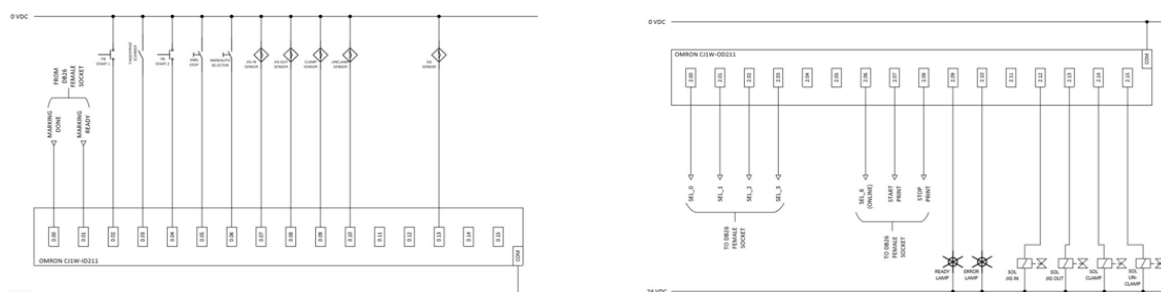


Fig. 8: Control Input Circuit Fig. 9: Control Output Circuit

- The power circuits are electrical circuits focused on providing electrical power to each of the main components of this numbering machine. Following is the illustration of the power circuit of this numbering machine shown in Figure 6. As shown in Figure 6, all major components of the system architecture are given resources according to the requirements of each component. PLC, TMC, and barcode scanner are rated 220 VAC. Whereas the HMI touch screen requires a voltage of 24 VDC, so a DC power supply was added beforehand. The 24 VDC voltage will also be a voltage source for the control circuit.

- The control circuits are electrical circuits that are focused on control function of each input and output of the machine processor which in this design is a PLC. Following is an illustration of the control circuit shown in two parts: the input circuit in Figure 8 and the output circuit in Figure 9. In the input circuit, the components used are adjusted to the specifications of the PLC input module. The module requires a voltage of 24 VDC to be active for each address. In the output circuit, the components used have also been adjusted to the specifications of the PLC output module. The module can be used at 220 VAC and 24 VDC for each address. However, the selected voltage is 24 VDC to be safer and adjusted to the availability of components on the market.
- Communication Cable Series Each communication cable used has its own special configuration according to the functions and specifications of the components that will be connected by the cable. In this design the communication cable used is RS232 with DB9 socket, I / O cable with DB26 socket, and RJ45 or Ethernet cable as shown in Figure 7.

### 3.4. Testing and Verification

Testing is carried out to determine the design of the numbering machine control system works in accordance with the expected design. Testing will be divided into two, namely testing with program simulation methods and testing by running the machine directly (OMRON 2012). Testing program simulation method will be performed on PLC programming software, CX-Programmer, by manually entering all variables to be simulated (OMRON, 2013). While testing by running the machine directly will be carried out with the type replacement method and testing each error condition.

#### 3.4.1. Testing the Machine Control System with the Program Simulation Method

The testing program simulation method is divided into 4 tests as follows:

1. Testing the engine control system under normal and ideal conditions. Normal Condition Testing: Testing is done by running a simulation program and running the machine under normal conditions or without errors. This test has the aim to test this numbering machine can run in normal and continuous production conditions and does not cause errors or printing errors.
2. Testing the engine control system when changing the machine type: Engine Control System Testing on Type Change Condition Tests are carried out by running a simulation program on the type change condition. This test has the aim to test this machine can run type changes without causing errors or print errors as has been done by the machine before. Also, to test the new system at the change of type that requires acknowledgment from the superior operator who has his fingerprint registered on this machine.
3. Testing the engine control system by providing input data that is not appropriate, such as the wrong type, the data is not sequential, the data has been processed before, and the input data is not according to the standard. This test is performed to find out the programmed protections that can filter out NG data or not. Filtering or protection in question is divided into namely, barcode data checking, number repeat checking, and number sequence checking.
  - Checking Barcode Data Checking barcode data which is simulated according to the program designed includes checking the number of characters, making sure the last 7 digits are numbers, and checking the suitability of the data type.
  - Examination Repetition of this Test Number is carried out to find out if entering the same number / has been processed in the last 100 data will cause an error or not, also on the contrary will continue the process on a number that has never been executed before.
  - Number Sequence Check Program simulation is carried out to test the success of number sequence checking protection. If the numbers are in order, the process will proceed normally, and if not, it will cause a warning.
4. Testing the machine control system when the numbering process is running, interruptions such as emergency stops. Engine Control System Testing in Interrupted Conditions This test is carried out to find out the engine response while running interruptions in the form of an emergency stop. It is expected that in accordance with the program that has been designed that is when interrupted, the data will not be sent right to the scribing / scratching machine and the data will not be stored in the machine's memory.



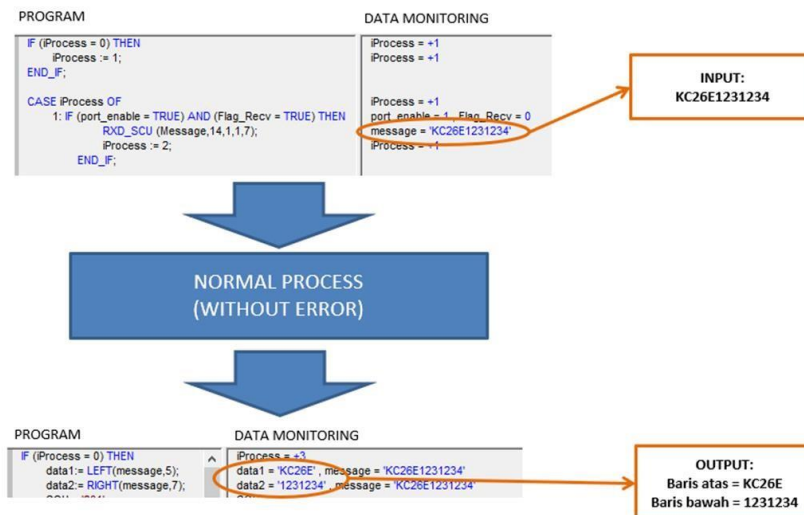


Fig. 10: The Results of Simulation Program under Normal Condition

### 3.4.2. Testing the Machine Control System Using the Running Machine Test Method

This Test is done by directly running the numbering machine. The test aims to determine the actual performance and real time on the machine that has been designed to control the system in this thesis. Tests carried out are divided into four tests, namely testing the normal conditions by changing the type twice, testing to run the type that is not in accordance with selected, testing numbers that are not sequential, and testing numbers that have been previously processed.



Fig. 11: HMI Testing for Various Scenarios

## 4. Conclusion and Further Work

The numbering engine control system that has been designed has proven to be successful in line with expectations. After passing a series of tests, the following conclusions are obtained:

- The design of the PLC program was able to successfully translate the number data from the barcode scanner to the numbering machine for printing
- When the type change was carried out successfully according to the procedures and processes designed without errors.
- When entering a number that has been processed, the machine manages to display an error in the HMI and the workpiece is not processed to print number

- In the numbering process that does not sort, there is a choice to continue or not continue the process. When not continuing the workpiece is not printed by the machine, and when proceeding, an acknowledging procedure is carried out by the responsible party whose fingerprint is registered on this machine.
- When the process is interrupted by pressing the emergency stop button, the machine does not continue the process, and the data is not stored in the memory of the machine.

Based on the results of the control system design that has been tested, here are a few suggestions to consider:

- Data checking should be carried out on more than 100 data, that is, to all engines that have been produced before. This was achieved by implementing a data inspection system that was integrated with PT XYZ data bank
- It is necessary to add workpiece sensors to eliminate the potential for double process on the same workpiece by the negligent operator.
- The further development of the machine is the addition of a camera to check the quality of prints and compatibility with the barcode.

## 5. References

- Antonsen, T. M., 2018. PLC controls with structured text (ST). Books on Demand GmbH: Copenhagen, Denmark
- John, K and Tiegelkamp, M., 2001. IEC 61131-3: Programming industrial automation systems. Springer. Berlin
- OMRON. 2012. NB-Series programmable terminals operation manual. OMRON: Kyoto, Japan
- OMRON. 2013. Sysmac CX-Programmer Ver. 9 Operation Manual. OMRON: Kyoto, Japan
- Putra, Q. R., 2014. Pemrograman kendali mesin jig boring 2½ D berbasis PLC Omron CP1H. Politeknik Manufaktur - Bandung
- Winahyu, R. K. K., 2015. Desain HMI (human machine interface) Omron NB7W-TW00B pada plant filtrasi menggunakan modul ultra filtrasi. Universitas Diponegoro, Semarang

# HAAR CASCADE CLASSIFIER METHOD FOR REAL TIME FACE DETECTOR IN 2 DEGREE OF FREEDOM (DOF) ROBOT HEAD

Dwi Agung Al Ayubi<sup>1</sup>, Dwi Arman Prasetya<sup>2</sup>, and Irfan Mujahidin<sup>3</sup>

<sup>1,2,3</sup> Electrical Engineering, University of Merdeka (UNMER), Malang - INDONESIA

dwiagung20april1995@gmail.com

## Abstract

Robotics technology is growing and advancing. The robot is a very important work for modern human life today to facilitate all human work. This era of robotics advances began to replicate the form and was able to mimic almost all human activities entirely, from robots that have a vision, deportations, and human-like movements. Research Robot Head 2 degree of freedom (DOF) for face detector in real-time use. The results obtained in the servo movement are angles to determine the detection of the captured face. For the real-time accuracy of the face detector in this study, the 3-student sample testing with the greatest precision was 95.25% with the fastest detection response time of 7 seconds.

*Keywords: Raspberry Pi, face detector, Degree of freedom, Haar Cascade classifier, Robot head*

---

## 1. Introduction

Robotics technology is growing. Robots are very important work for modern human life today to facilitate all human work. The Robot is created to replace the human role in work that requires speed and accuracy. The development of the robot world today will be focused on being a robot that has human-like features. In fact, it is hoped to have the ability to interact and behave like humanoid robots (Kumra & Kanan, 2017).

The world of robotics enters various facets of human life ranging from military, industrial, automation, entertainment, education as well as the medical field. The humanoid robot is one of the implementations in the world of robotics that can mimic various human activities. In research efforts to analyze the movement of the robot's head that detects the motion of the interlocutor and responds (Lee, 2012) (Prasetya et al., 2019a). Sensors are the senses for robots that can recognize various parameters around the environment, such as robots that can see using the camera or can be called with robot vision (Lasmono, Sari, Kuncoro, & Mujahidin, 2019).

The robotic advances to mobilize like a human being, the robot must have a human-like joint designed with a movement mechanism composed of several parts in a series that is connected to a shaft that moves and shifts that have a Degree of Freedom (DOF) (Marasco, Kim, Colgate, Peshkin, & Kuiken, 2011) (Prasetya et al., 2019b). In accordance with its function in the joint humanoid robot is very important because it uses the servo motor so it appears to resemble the human movement. The development of the robotics World Head Robot design is designed to combines branches of robotics science and computer vision with various methods used to detect or object recognition. The method to be used is the Haar Cascade Classifier for the face detector as the object captured by the camera with the 2 degree of freedom Movement on the servo motor as the control of the head movement to follow the camera's captured face (Mujahidin, Prasetya, Setywan, & Arinda, 2019) (Hidayatulail & Mujahidin, 2019). This humanoid robotic head robot's device can interact like a human in general by using face detection and implementing the Haar cascade classifier method on the robot head.

## 2. Research methods

In the design and manufacturing of robotic head tools there are several steps in testing that aims to determine the quality of the design that will be researched and in the analysis with the expectation of data on the performance of tools Useful for the future (Siswanto, Prasetya, Rachman, & Hidayatulail, 2019) (Mujahidin & Hidayatulail, 2019).

## 2.1 Block diagrams

The diagram block used for the face detection system for the design is divided into three stages as shown in Figure. The first image input was made resulting in an integral image of the new call, in the second stage of extraction characteristic was carried out using the Haar-based filter, and finally increased use for the development of the Cascade classifiers.

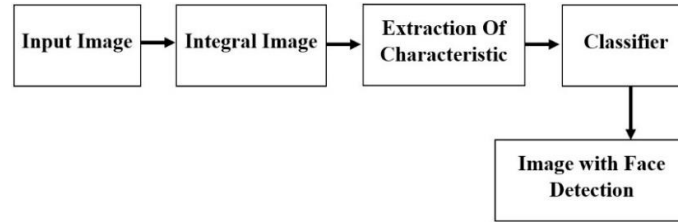


Fig. 1: Face Detection Diagram block

## 2.2 Integral Image

Integral Image is used to determine whether or not the sample exists within hundreds of features in an image quickly and with different scales efficiently.



Fig. 2: Integral Image

Figure. 2 is the x, y location, contains the number of pixels from the top left of the image and can be counted as shown below:

$$ii(x, y) = \sum_{x' \leq x, y' \leq y} i(x', y') \quad (1)$$

Where II axis (x, y) is an integral image and I axis (x, y) is an original image.

## 2.3 Feature Extraction

In the image, the characteristic of the object is extracted by applying a specific function that allows the representation and description of the object to be interesting, this filter can be efficiently calculated on an integral image. In Figure. 3, for a two-dimensional object, which consists of light and dark, the next combinations of the box-shaped combinations will be used when detecting visual objects for better (Gerber et al., 2013) (Mujahidin et al., 2019).

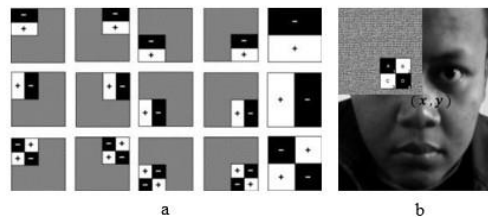


Fig. 3: (a). Haar Like Features (b). Haar Like Features with Integral Image

In Figure. 3, the Haar filter convolution with an integral image is displayed. From this operation, a characteristic can be extracted in a constant time on an integral image by adding and decreasing the vertex values for each rectangle (Sugiarto, Mujahidin, & Setiawan, 2019) (Mujahidin, Pramono, & Muslim, 2018). For greater clarity, on the image the number of pixels that make up a rectangle D can be counted as,

$$SumD = (4 + 1) - (2 + 3) \quad (2)$$

Where 1, 2, 3, 4, is the value given in the image that is integrated in that location.

## 2.4 Classifier

Analysis of an object in the form of an image in the Classifier detection stage defines a given set of characteristics this is a classification method that combines several basic classifications to form a more complex and accurate one the application of the Cascade classifications allows obtaining good results in Figure. 4, is a cascade classifications scheme.

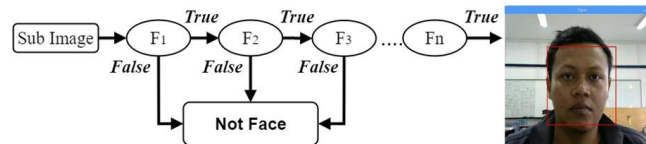


Fig. 4: Cascade Classifier

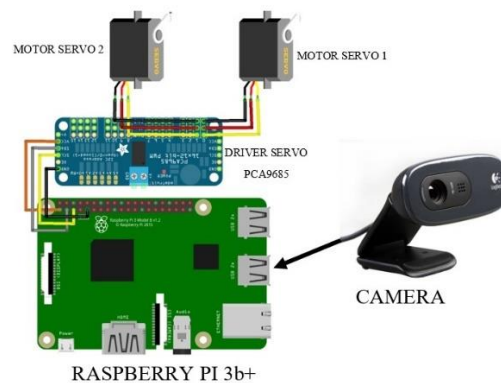
Figure. 4. is a classification process by using Cascade Classifier, the sub image is a picture image to be used will be done image detection does loop looking for a face model as much as  $F_n$  the loop process is performed as much as  $F_n$  if it is worth it Then immediately found the face model, otherwise the loop process will continue until the  $F_n$ (Otte, 2008)(Sugiarto et al., 2019).

## 2.5 Operation Planning.

In the Operation Planning that Indicates the whole system starts from the program start and initializing the Raspberry Pi port used, after which digital image data is detected by the camera, after the direct input image will be in process for determining the image detection area that has been Captured camera(Omran, Riha, & Dutta, 2013)(Mujahidin & Arinda, 2019). Object detection will be processed by face detection by using the Haar cascade classifier method to identify the object, directly after the object is detected otherwise the process repeats at determining the detection area if yes, the Raspberry Pi receives Data and sending head movement data. To move the servo part of the neck and head, on the neck if the detected object moves to the X axis if yes the servo motor moves towards the X axis and the head moves towards the left, otherwise the servo motor moves towards the x-axis and the head moves towards the right, on the head if the detected object moves to the Y axis if yes the servo motor moves towards the Y axis and the head moves towards the top otherwise the servo motor moves towards the y-axis and the head moves towards the bottom(S, Rabi', Minggu, & Mujahidin, 2019)(Kusuma, Prasetya, Kholid, & Mujahidin, 2019). The servo motor movement positions the camera that detects the object at the center position wherever the object is detected. Once the data processed output from the Raspberry Pi will be displayed on the monitor screen to display the camera captured image(Zhang, Y., Yasuno, T., D A Prasetya, 2013)(Pambudi, Maajid, Rohman, & Mujahidin, 2019).

## 2.6 Schematic Series

A network schematic that connects all the components designed in Figure 3.



Gambar. 5 Schematic Perancangan Sistem kendali Kepala Robot

Figure. 5 shows the Raspberry Pi hardware design as a mini PC, a camera connected to the available Raspberry Pi USB port, the PCA9685 motor driver for servo control connected to the GPIO pins on the Raspberry Pi and the servo motor for the drive on Humanoid robot head pre-installed on the servo driver PCA9685(Ardiansyah, Minggu, & Dirgantara, 2019)(Wibowo, Suprayogi, & Mujahidin, 2019) (D A Prasetya, T Yusano, 2012).

### 3. Results and analysis

This research performs analysis focusing on the tools implemented by retrieving data from the camera capture using the Haar Cascade Classifier method for the face detector and the position of the robot head.

#### 3.1. Results

The Data that will be used for testing detects faces in real-time using the camera with a sampling of 3 different students to detect faces in table 1.

**Table 1: Testing conducted with 3 students**

No	Sample Testing	Distance (meters)	Time	Results	Accuracy
1	1st Student	1	7	Detected	95,25%
		2	7	Detected	
		3	7,79	Detected	
		4	7,83	Detected	
		5	7,89	Detected	
		6	16,36	Not Detected	
2	2nd Student	1	7,09	Detected	80,95%
		2	7,85	Detected	
		3	7,86	Detected	
		4	8,14	Not Detected	
		5	8,67	Not Detected	
		6	20,75	Not Detected	
3	3rd Student	1	7,34	Detected	85,71%
		2	7,49	Detected	
		3	7,64	Detected	
		4	7,99	Detected	
		5	8,72	Not Detected	
		6	9,81	Not Detected	

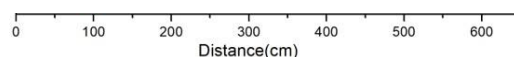


**Fig. 6: Face Detection response graph**

In Figure. 6 shows a face detection response from a table that shows the difference.

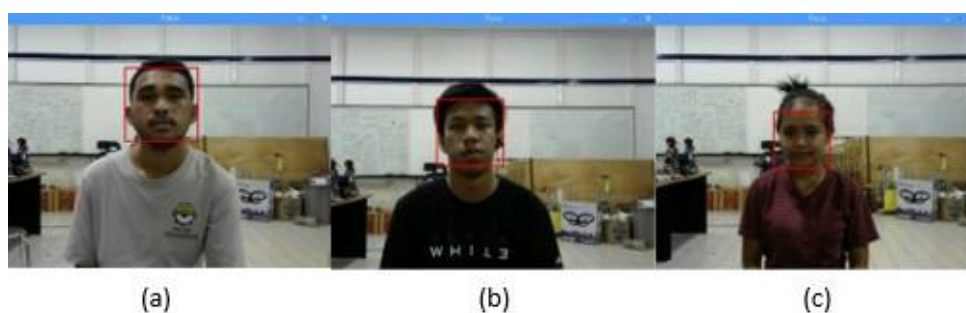


**Fig. 7: Face Detection student Testing (a) results. Student 1st (a). Student 2nd (c). 3rd Student.**

Figure. 7 is a result of facial detection on different students with the Haar cascade classifier method for robotic head detector(Kahn, Lum, Rymer, & Reinkensmeyer, 2006)(Alhamzawi, 2018)(Yuwono & Mujahidin, 2019)(D A Prasetya, EFA Phong Thanh Nguyen, Rinat Faizullin, Iswanto Iswanto, 2020)

### 3.2. Analysis

Trials of 1, 2 and 3 tests have the same high success rate that the 1st test has a face detection rate of 95.25%, the 2nd test has a face detection rate accuracy of 80.95%, and testing The 3rd has a face detection rate of 85.71%. The success rate of face detection is influenced by the face detection distance, for a 6-meters distance per student test of the 1.2, and 3 undetectable in each test. In the table, the time required to detect faces at a distance of 6 meters in each test is the longest. Failure in detection is also due to many factors Lighting, distance factor when detecting faces, and some images also have noise.

## 4. Conclusion

Based on analysis, the design and implementation of the face detection software can be concluded as follows:

- System can detect faces by using the Haar Cascade Classifier method well and quickly.
- Maximum detection rate is 6-meter with a longest face detection response of 20.75 seconds.
- The specifications the camera uses will affect the accuracy and speed of the system detecting.
- Highest accuracy rate is 90.25% of all experiments.

## 5. References

- Alhamzawi, H. A. M. (2018). Faces and eyes Detection in Digital Images Using Cascade Classifiers. *Computer Engineering and Applications Journal*. <https://doi.org/10.18495/comengapp.v7i1.222>
- Ardiansyah, N. F., Minggu, D., & Dirgantara, W. (2019). Computer Vision Untuk Pengenalan Obyek Pada Peluncuran Roket Kendaraan Tempur. *JASIEK (Jurnal Aplikasi Sains, Informasi, Elektronika Dan Komputer)*, 1(1), 28–37.
- Gerber, N., Gavaghan, K. A., Bell, B. J., Williamson, T. M., Weisstanner, C., Caversaccio, M. D., & Weber, S. (2013). High-accuracy patient-to-image registration for the facilitation of image-guided robotic microsurgery on the head. *IEEE Transactions on Biomedical Engineering*. <https://doi.org/10.1109/TBME.2013.2241063>
- Hidayatulail, B. F., & Mujahidin, I. (2019). Potential OF 77, 78 mW Red Diode Laser For Photodynamic. *JEEMCS (Journal of Electrical Engineering, Mechatronic and Computer Science)*, 2(2).
- Kahn, L. E., Lum, P. S., Rymer, W. Z., & Reinkensmeyer, D. J. (2006). Robot-assisted movement training for the stroke-impaired arm: Does it matter what the robot does? *Journal of Rehabilitation Research and Development*. <https://doi.org/10.1682/JRRD.2005.03.0056>
- Kumra, S., & Kanan, C. (2017). Robotic grasp detection using deep convolutional neural networks. *IEEE International Conference on Intelligent Robots and Systems*. <https://doi.org/10.1109/IROS.2017.8202237>
- Kusuma, D. F. C., Prasetya, D. A., Kholid, F., & Mujahidin, I. (2019). Evaluasi Database Senjata Untuk Sistem Keamanan Menggunakan Fuzzy Logic. *JASIEK (Jurnal Aplikasi Sains, Informasi, Elektronika Dan Komputer)*, 1(2), 111–116.
- Lasmono, J., Sari, A. P., Kuncoro, E., & Mujahidin, I. (2019). Optimasi Kerja Peluncur Roket Pada Robot Roda Rantai Untuk Menentukan Ketepatan Sudut Tembak. *JASIEK (Jurnal Aplikasi Sains, Informasi, Elektronika Dan Komputer)*. <https://doi.org/10.26905/jasiek.v1i1.3149>
- Lee, J. D. (2012). Image Noise. In *Brigham Young Robotic Vision Class*.
- Marasco, P. D., Kim, K., Colgate, J. E., Peshkin, M. A., & Kuiken, T. A. (2011). Robotic touch shifts perception of embodiment to a prosthesis in targeted reinnervation amputees. *Brain*. <https://doi.org/10.1093/brain/awq361>
- Mujahidin, I., & Arinda, P. S. (2019). Antena Compact Double Square Marge 2, 6GHz Dengan Output Perbedaan

Fase 90 Derajat Untuk Aplikasi LTE. *JEECAE (Journal of Electrical, Electronics, Control, and Automotive Engineering)*, 4(2), 273–278.

Mujahidin, I., & Hidayatulail, B. F. (2019). 2.4 GHz Square Ring Patch With Ring Slot Antenna For Self Injection Locked Radar. *JEEMECs (Journal of Electrical Engineering, Mechatronic and Computer Science)*, 2(2).

Mujahidin, I., Pramono, S. H., & Muslim, A. (2018). 5.5 Ghz Directional Antenna with 90 Degree Phase Difference Output. <https://doi.org/10.1109/eccis.2018.8692872>

Mujahidin, I., Prasetya, D. A., Setywan, A. B., & Arinda, P. S. (2019). Circular Polarization 5.5 GHz Double Square Margin Antenna in the Metal Framed Smartphone for SIL Wireless Sensor. *2019 International Seminar on Intelligent Technology and Its Applications (ISITIA)*, 1–6. IEEE.

Omran, Y., Riha, K., & Dutta, M. K. (2013). Automatic estimation of the arterial parameters in Ultrasound video sequence. *2013 36th International Conference on Telecommunications and Signal Processing, TSP 2013*. <https://doi.org/10.1109/TSP.2013.6614056>

Otte, M. W. (2008). A Survey of Machine Learning Approaches to Robotic Path-Planning. *International Journal of Robotics Research*. <https://doi.org/10.1109/ICALIP.2016.7846622>

Pambudi, A. E., Maajid, L., Rohman, J., & Mujahidin, I. (2019). Aplikasi Penggunaan Joystick Sebagai Pengendalian Remote Control Weapon Station (RCWS) Senjata Mesin Ringan (SMR). *JASIEK (Jurnal Aplikasi Sains, Informasi, Elektronika Dan Komputer)*, 1(2), 98–105.

Prasetya, D. A., Sanusi, A., Chandrarin, G., Roikhah, E., Mujahidin, I., & Arifuddin, R. (2019a). Community Culture Improvisation Regarding Waste Management Systems and Per Capita Income Increase. *Journal of Southwest Jiaotong University*, 54(6).

Prasetya, D. A., Sanusi, A., Chandrarin, G., Roikhah, E., Mujahidin, I., & Arifuddin, R. (2019b). Small and Medium Enterprises Problem and Potential Solutions for Waste Management. *Journal of Southwest Jiaotong University*, 54(6).

S, T. A., Rabi', A., Minggu, D., & Mujahidin, I. (2019). Frequency Hopping Video Real Time Untuk Pengamanan Data Pengintaian Operasi Intelligence TNI. *JASIEK (Jurnal Aplikasi Sains, Informasi, Elektronika Dan Komputer)*. <https://doi.org/10.26905/jasiek.v1i1.3146>

Siswanto, S., Prasetya, D. A., Rachman, N., & Hidayatulail, B. F. (2019). Pengendali Robot Beroda Berbasis Sensor Telemetri Voice Pattern Recognition. *JASIEK (Jurnal Aplikasi Sains, Informasi, Elektronika Dan Komputer)*. <https://doi.org/10.26905/jasiek.v1i1.3147>

Sugiarto, S. K., Mujahidin, I., & Setiawan, A. B. (2019). 2, 5 GHz Antena Mikrostrip Polarisasi Circular Model Patch Yin Yang untuk Wireless Sensor. *JEECAE (Journal of Electrical, Electronics, Control, and Automotive Engineering)*, 4(2), 297–300.

Wibowo, M., Suprayogi, S., & Mujahidin, I. (2019). Rancang Bangun Sistem Pengamanan Rak Senjata M16 Menggunakan Rfid Dan Fingerprint. *JASIEK (Jurnal Aplikasi Sains, Informasi, Elektronika Dan Komputer)*, 1(2), 134–142.

Yuwono, R., & Mujahidin, I. (2019). Rectifier using UWB microstrip antenna as electromagnetic energy harvester for GSM, CCTV and Wi-Fi transmitter. *Journal of Communications*. <https://doi.org/10.12720/jcm.14.11.1098-1103>

D A Prasetya, EFA Phong Thanh Nguyen, Rinat Faizullin, Iswanto Iswanto, "Resolving the Shortest Path Problem using the Harversine Algorithm," in *Journal of critical reviews* 7 (1), 62–64, 2020.

Zhang, Y., Yasuno, T., D A Prasetya, "Adaptive walking for quadrupe robot on irregular terrain by using CPG network," in *52nd Annual Conference of the Society of Instrument and Control Engineering of Japan*, Pages 1734–1737, 2013.

D A Prasetya, T Yusano, "Cooperative control of multiple mobile robot using particle swarm optimization for tracking two passive target," in *Proceeding of SICE Annual Conference (SICE)*, 1751–1754, 2012.



## Photovoltaic's characteristics modelling based on fuzzy time series

Fortinov Akbar Irdam<sup>\*1</sup>, Dani Rusirawan<sup>2</sup>

<sup>1</sup> Under Graduate Student, Department of Mechanical Engineering

<sup>2</sup> Department of Mechanical engineering

Institut Teknologi Nasional (ITENAS), Bandung – INDONESIA

\* Corresponding author e-mail: fortinovakbarirdam@yahoo.co.id

### Abstract

Recently, fulfillment of energy needs is predominated by utilization of fossil energy. Fossil energy is limited resources and less eco-friendly. Based on that, researches began to develop clean energy based on renewable resources, solar as main energy's source for humankind's live is one of them. The potential of solar energy in Indonesia is estimated 207,8 GWp, the largest around other renewable resources. Due to sunshine year-round, Indonesia become suitable place to develop solar-based energy technology, especially photovoltaic (PV). PV is device that is converted solar energy into electricity. PV has its own characteristics, such as ambient temperature, irradiation, humidity, and wind velocity as input parameters and cell temperature, voltage, current, and power as output parameters. All of characteristics can be obtained by direct measurement which need more device and waste time. To simplify in understanding all of these parameters, modelling is needed. This research will be shown PV characteristics modelling based on fuzzy time series (FTS). FTS is one of fuzzy logic method to predict future data based on historical data. The focus of modelling is output parameters, such as voltage (V), current (I), and power (P). The collected data will be divided into some classes with same intervals before fuzzy sets are created. After that, fuzzy logic processes will be done to obtain the modelling results. Margin of Error is obtained by compare of the modelling results and collected data. They are 3,9% for voltage; 24,7% for current at intervals of 0,05 and 34,8% at intervals of 0,2; 21,5% for power at intervals of 7 and 34,8% at intervals of 20.

*Keywords: Renewable Energy, Solar Energy, Photovoltaic, Fuzzy Time Series, Margin of Error*

## 1. Introduction

Fulfillment of energy needs is predominated by utilization of fossil fuel of which produces carbon emission. Fossil fuels has two big demerits, which is its limited availability and the carbon dioxide emissions from the fossil fuel combustion (Irsyad et al., 2018). Some of the solutions pushed for decreasing the carbon production are: using a better technology for combustion to reduce greenhouse gas emission, limit the usage of fossil fuels, increase efficiency of combustion, and increase the efficiency of combustion, and increase the usage of renewable energy (Irsyad et al., 2018).

One of prominent renewable energy is solar energy. The potential of solar energy in Indonesia is estimated 207,8 GWp (BPPT: Indonesia Energy Outlook, 2018), the largest around other renewable resources. Devices that can convert solar energy into electricity directly is photovoltaic (PV). PV or solar cells and their concomitant energy systems have repeatedly demonstrated extreme viability and durability over the past quarter century in thousands of earth satellites, space missions, and more recently, terrestrial applications (Jr., 1982).

PV is a source of energy very sensitive to climatic variations, such as cloud motion and surrounding weather. It can affect PV's performance to produce electricity (Severiano et al., 2017). Therefore, analyzing PV's characteristics is important to done, so that the best performances of PV can be attained. There are input parameters (irradiation, ambient temperature, humidity, wind velocity) and output parameters (cell temperature, voltage, current, power) that is needed to obtained to explain PV's characteristics. All of these parameters can be obtained by both direct measurement and modelling. To simplify researchers' work, modelling is needed.

This paper will describe PV's characteristics by Fuzzy Time Series (FTS). The modelling system with FTS captures patterns from past data, then is used to project future data, the process also does not require a complicated system as in genetic algorithms and neural networks, making it easy to develop (Haris, 2010).

This modelling will focus on output parameters of PV systems (voltage, current, and power).

## 2. Research methodology

This modelling used Chen method FTS (Chen, 1996). This method is improvement of Song method FTS which is proposed to predict number of enrollments of the University of Alabama (Song and Chissom, 1993).

Historical data is obtained by direct measurement Itenas Solar Power Plant, as can be seen in Fig. 1. It collected 721 data for each characteristics (V, I, and P) as can be seen in Table 1. The measurement is held on December 31, 2018 from 6 a.m. until 6 p.m.



Fig. 1: Itenas Solar Power Plant Instalation

Table 1: Direct Measurement on December 31 2018

Time (WIB)	Voltage /V (V)	Current/I (A)	Power/P (Watt)
06.00	111	0,151	16,761
06.01	118,9	0,157	18,6673
07.01	115,4	0,763	88,0502
08.01	119,6	2,051	245,2996
09.01	118,6	3,616	428,8576
10.01	116,8	2,07	241,776
11.01	123,2	4,25	523,6
12.01	112,7	4,65	524,055
13.01	111,5	2,839	316,5485
14.01	118,5	7,05	835,425
15.01	117,7	1,606	189,0262
16.01	118,6	0,625	74,125
17.01	136,3	0,552	75,2376
18.00	104,7	0,074	7,7478

The modelling results will be shown after modelling is done. Then, it is important to obtain Margin of Error (MoE) by comparing direct measurement data and modelling results.

### 2.1 Divison of Data

Direct measurement data is divided into several division in the same intervals. Voltage is divided into 11 divisions at intervals of 4; current is divided into 191 divisions at intervals of 0,05 and 50 divisions at intervals 0,2; power is divided into 151 divisions at intervals of 7 and 53 divisions at intervals of 20. The division of data can be seen in Table 2. This divisions will become basic of fuzzy sets division.

Table 2: Divisions of Direct Measurement Data

Voltage			Current						Power					
			Intervals 0,05			Intervals 0,2			Intervals 7			Intervals 20		
Divisions	Min.	Max.	Divisions	Min.	Max.	Divisions	Min.	Max.	Divisions	Min.	Max.	Divisions	Min.	Max.
U1	100	103	U1	0,02	0,06	U1	0	0,1	U1	3	9	U1	3	22
U2	104	107	U2	0,07	0,11	U2	0,2	0,3	U2	10	16	U2	23	42
U3	108	111	U3	0,12	0,16	U3	0,4	0,5	U3	17	23	U3	43	62
U4	112	115	U4	0,17	0,21	U4	0,6	0,7	U4	24	30	U4	63	82

U5	116	119	U5	0,22	0,26	U5	0,8	0,9	U5	31	37	U5	83	102
U6	120	123	...	...	...	...	...	...	...	...	...	...	...	...
U7	124	127	U187	9,32	9,36	U46	9	9,1	U147	1025	1031	U49	963	982
U8	128	131	U188	9,37	9,41	U47	9,2	9,3	U148	1032	1038	U50	983	1002
U9	132	135	U189	9,42	9,46	U48	9,4	9,5	U149	1039	1045	U51	1003	1022
U10	136	139	U190	9,47	9,51	U49	9,6	9,7	U150	1046	1052	U52	1023	1042
U11	140	143	U191	9,52	9,56	U50	9,8	9,9	U151	1053	1059	U53	1043	1062

## 2.2 Fuzzy Sets Division

FTS is fuzzy logic method. Therefore, it is important to define all of data into fuzzy sets. Fuzzy sets division can be seen in Table 3.

Table 3: Fuzzy Sets Division

Voltage			Current						Power					
			Intervals 0,05			Intervals 0,2			Intervals 7			Intervals 20		
Fuz zy Sets	Lingui stic Values	Cent er Valu es	Fuz zy Sets	Lingui stic Values	Cent er Valu es	Fuz zy Sets	Lingui stic Values	Cent er Valu es	Fuz zy Sets	Lingui stic Values	Cent er Valu es	Fuz zy Sets	Lingui stic Values	Cent er Valu es
A1	100	102,15	A1	0,02	0,0451	A1	0	0,1	A1	3	13,185	A1	3	13,185
A2	104,3	106,45	A2	0,0702	0,0953	A2	0,2	0,3	A2	23,37	33,555	A2	23,37	33,555
A3	108,6	110,75	A3	0,1204	0,1455	A3	0,4	0,5	A3	43,74	53,925	A3	43,74	53,925
A4	112,9	115,05	A4	0,1706	0,1957	A4	0,6	0,7	A4	64,11	74,295	A4	64,11	74,295
A5	117,2	119,35	A5	0,2208	0,2459	A5	0,8	0,9	A5	84,48	94,665	A5	84,48	94,665
A6	121,5	123,65	...	...	...	...	...	...	...	...	...	...	...	...
A7	125,8	127,95	A187	9,3572	9,3823	A46	9	9,1	A49	980,76	990,945	A147	1030,84	1034,36
A8	130,1	132,25	A188	9,4074	9,4325	A47	9,2	9,3	A50	1001,13	1011,315	A148	1037,88	1041,4
A9	134,4	136,55	A189	9,4576	9,4827	A48	9,4	9,5	A51	1021,5	1031,685	A149	1044,92	1048,44
A10	138,7	140,85	A190	9,5078	9,5329	A49	9,6	9,7	A52	1041,87	1052,055	A150	1051,96	1055,48
A11	143	-	A191	9,558	-	A50	9,8	-	A53	1062,24	-	A151	1059	-

The number of fuzzy sets division is same as the division of direct measurement data. Center values is mean between An and An+1.

## 2.3 Fuzzification

Fuzzification is process that converts numerical value into linguistic value. For example, voltage in 6 a.m is 111 Volt, this value is higher than center values between A3 and A4 and lower than center values between A4 and A5 as can be seen in Table 3, therefore fuzzification of 6 a.m data is A4. All of fuzzification can be seen in Table 4.

Table 4. Fuzzification

Time (WIB)	V (V)	Fuzzification of V	I (A)	Fuzzification of I at Intervals of 0,05	Fuzzification of I at Intervals of 0,2	P (Watt)	Fuzzification of P at Intervals of 7	Fuzzification of P at Intervals of 20
06.00	111	A4	0,151	A4	A2	16,761	A3	A2
06.01	118,9	A5	0,157	A4	A2	18,6673	A3	A2
06.02	111,5	A4	0,161	A4	A2	17,9515	A3	A2
06.03	112,1	A4	0,168	A4	A2	18,8328	A3	A2

06.04	108,1	A3	0,164	A4	A2	17,7284	A3	A2
06.05	110,6	A3	0,169	A4	A2	18,6914	A3	A2
06.06	110,4	A3	0,173	A4	A2	19,0992	A3	A2
06.07	116,7	A5	0,171	A4	A2	19,9557	A3	A2
...	...	...	...	...	...	...	...	...
17.57	113,2	A4	0,099	A3	A1	11,2068	A2	A1
17.58	105,2	A2	0,089	A2	A1	9,3628	A2	A1
17.59	112,8	A4	0,08	A2	A1	9,024	A2	A1
18.00	104,7	A2	0,074	A2	A1	7,7478	A2	A1

## 2.4 Fuzzy Logic Relationships (FLR) and Fuzzy Logic Relationship Groups (FLRG)

Relation between each time series is must be done. It is called Fuzzy Logic Relationships (FLR) as can be seen in Table 5. After that, FLR which has same current state is grouped into same Fuzzy Logic Relationships Group (FLRG) as can be seen in Table 6.

Table 5: Fuzzy Logic Relationships

Time Series	Current State V	Next State V	Current State of I at Intervals of 0,05	Next State of I at Intervals of 0,05	Current State of I at Intervals of 0,2	Next State I of at Intervals at 0,2	Current State of P at Intervals of 7	Next State of P at Intervals of 7	Current State of P at Intervals of 20	Next State of P Intervals of 20
06.00 → 06.01	A4	A5	A4	A4	A2	A2	A3	A3	A2	A2
06.01 → 06.02	A5	A4	A4	A4	A2	A2	A3	A3	A2	A2
06.02 → 06.03	A4	A4	A4	A4	A2	A2	A3	A3	A2	A2
06.03 → 06.04	A4	A3	A4	A4	A2	A2	A3	A3	A2	A2
06.04 → 06.05	A3	A3	A4	A4	A2	A2	A3	A3	A2	A2
06.05 → 06.06	A3	A3	A4	A4	A2	A2	A3	A3	A2	A2
...	...	...	...	...	...	...	...	...	...	...
17.55 → 17.56	A3	A4	A3	A3	A2	A2	A3	A2	A2	A2
17.56 → 17.57	A4	A2	A3	A3	A2	A2	A2	A2	A2	A1
17.57 → 17.58	A2	A4	A3	A3	A2	A1	A2	A2	A1	A1
17.58 → 17.59	A4	A2	A3	A2	A1	A1	A2	A2	A1	A1
17.59 → 18.00	A2	A4	A2	A2	A1	A1	A2	A2	A1	A1
17.59 → 18.00	A4	A2	A2	A2	A1	A1	A2	A2	A1	A1

Table 6: Fuzzy Logic Relationships Group

Voltage		Current				Power			
Current State	Next State	Intervals of 0,05		Intervals of 0,2		Intervals of 7		Intervals of 20	
		Current State	Next State	Current State	Next State	Current State	Next State	Current State	Next State
A2	A4	A1	A2	A1	A1 A4 A8	A1	A1 A2 A12 A24	A1	A1 A5 A9
A3	A3 A4 A5	A2	A2 A14 A29	A2	A1 A2 A3 A4	A2	A1 A2	A2	A1 A2 A3 A4
A4	A2 A3 A4 A5 A6	A3	A2 A3	A3	A2 A3 A4	A3	A2 A3 A4	A3	A2 A3 A4
A5	A3 A4 A5 A6 A7 A10	A4	A3 A4 A5	A4	A3 A4 A5	A4	A3 A4 A5	A4	A3 A4 A5
A6	A4 A5 A6 A7 A10	...	...	...	...	...	...	...	...
A7	A5 A6	A121	A168	A46	A44	A142	A135	A50	A47
A9	A4 A5 A9	A122	A94 A124	A47	A25	A145	A82 A133	A51	A29 A47
A10	A5 A6 A10	A123	A130	A49	A39	A151	A119	A53	A42

## 2.4 Defuzzification

Defuzzification is process that convert linguistic values into numerical values. It is the last step of FTS method. The modelling results is obtained on this step. On this modelling, defuzzification is mean values of next state's linguistic values on each current states. For example, next states of A7 in voltage are A5 and A6, linguistic values for each next states as can be seen in table 3 are 117,3 Volt and 121,5 Volt. Therefore, defuzzification for A7 in voltage is 119,35 Volt. All of defuzzifications can be seen in Table 7.

Table 7: Defuzzification

Voltage		Current				Power			
Current State	Defuzzification	Intervals of 1 0,05		Intervals of 0,2		Intervals of 7		Intervals of 20	
		Current State	Defuzzification	Current State	Defuzzification	Current State	Defuzzification	Current State	Defuzzification
A2	112,9	A1	0,0702	A1	0.666666667	A1	64,6	A1	64,6
A3	112,9	A2	0,7228	A2	0.3	A2	6,52	A2	6,52
A4	112,9	A3	0,0953	A3	0.4	A3	17,08	A3	17,08
A5	120,7833333	A4	0,1706	A4	0.6	A4	24,12	A4	24,12
A6	123,22	...	...	...	...	...	...	...	...
A7	119,35	A121	8,6042	A46	8.6	A142	946,36	A50	940,02
A9	121,5	A122	4,8392	A47	4.8	A145	752,76	A51	756,69
A10	125,8	A123	7,55	A49	7.6	A151	833,72	A53	838,17

## 3. Results

Comparison between direct measurement data and modelling results can be seen on Fig. 2, Fig. 3, and Fig. 4.

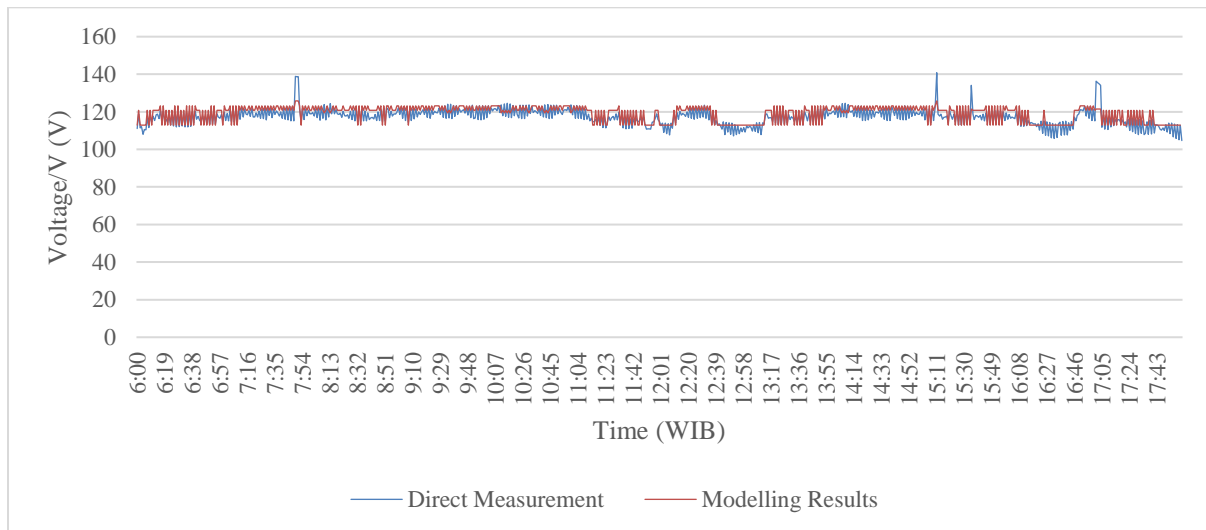
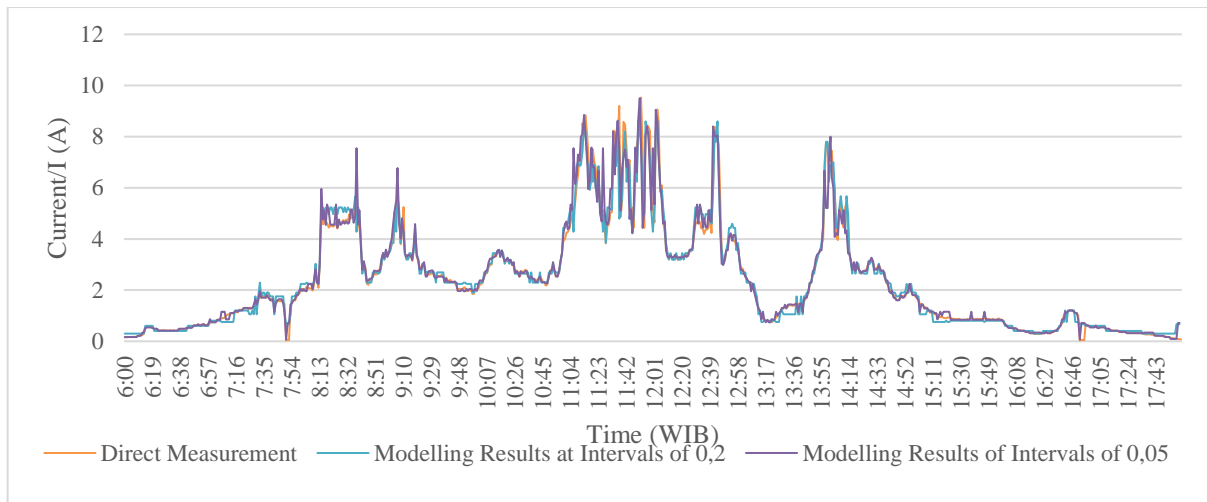
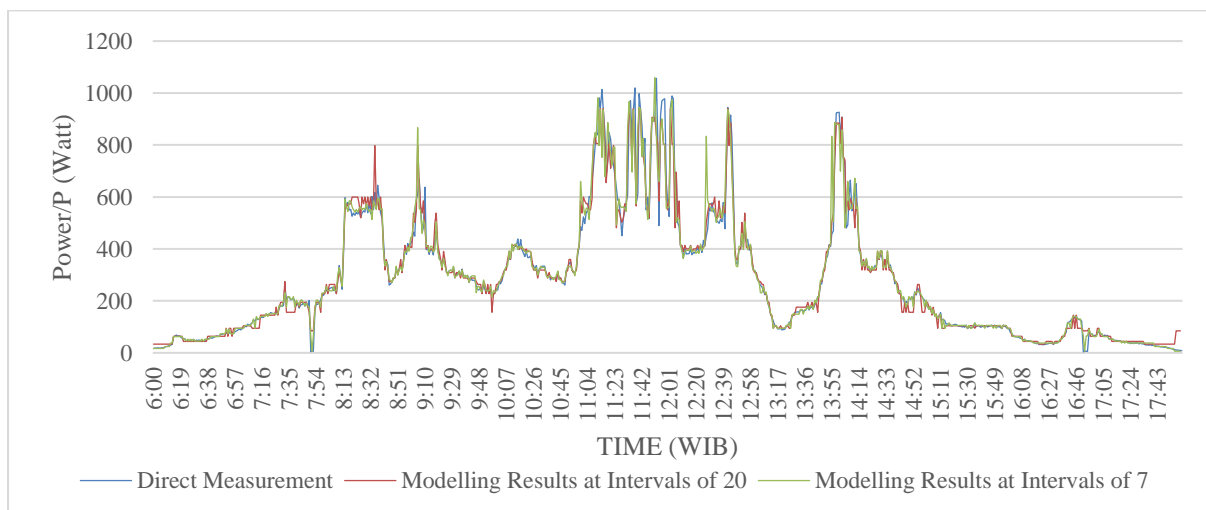


Fig. 2: Direct Measurement and Modelling Results Comparison for Voltage



**Fig. 3: Direct Measurement and Modelling Results Comparison for Current**



**Fig. 4: Direct Measurement and Modelling Results Comparison for Power**

## 4. Conclusion

Margin of Error (MoE) for each modelling is obtained by comparing the modelling results and direct measurement data. They are 3,9% for voltage; 24,7% for current at intervals of 0,05 and 33,1% at intervals of 0,2; 21,5% for power at intervals of 7 and 34,8% at intervals of 20. The modelling of voltage has the lowest MoE. It can be seen that voltage data is not as fluctuate as current and power data. It is clearly stated that the fluctuation in collected data will influence of the MoE. Narrow interval is needed in fluctuate data in order to obtain lower of MoE.

## 5. Nomenclature

I	Current	A
G	Irradiation	W/m <sup>2</sup>
P	Power	Watt
T <sub>c</sub>	Cell temperature	°C
V	Voltage	V

Subscripts

MoE Margin of Error

WIB Waktu Indonesia Barat (Western Indonesian Time)

## 6. References

- BPPT: Indonesia Energy Outlook. 2018. *Outlook Energi Indonesia 2018: Energi Berkelanjutan Untuk Transportasi Darat*. Vol. 134.
- Chen, Shyi Ming. 1996. "Forecasting Enrollments Based on Fuzzy Time Series." *Fuzzy Sets and Systems* 81:311–19.
- Haris, M. Syauqi. 2010. "Implementasi Metode Fuzzy Time Series Dengan Penentuan Interval Berbasis Rata-Rata Untuk Peramalan Data Penjualan Bulanan." (September 2017):1–8.
- Irsyad, Achmad Rofi, Byunggi Kim, Doan Hong Duc, Saiful Hasmady Bin Abu Hassan, and Kazuyoshi Fushinobu. 2018. "Numerical Study of Heat Transfer and Chemical Kinetics of Solar Thermochemical Reactor for Hydrogen Production." *AIP Conference Proceedings* 1984(August).
- Jr., Harry K. Charles. 1982. "Solar Photovoltaic Energy Systems." Pp. 663–711 in *Handbook of Energy Technology & Economics*, edited by R. A. Meyers. John Wiley & Sons.
- Severiano, Carlos A., Petrônio C. L. Silva, Hossein Javedani Sadaei, and Frederico Gadelha Guimarães. 2017. "Very Short-Term Solar Forecasting Using Fuzzy Time Series." *IEEE International Conference on Fuzzy Systems* (July).
- Song, Qiang and Brad S. Chissom. 1993. "Forecasting Enrollments with Fuzzy Time Series - Part 1." *Fuzzy Sets and Systems* 54:1–9.

## Effect of cooling systems on photovoltaic efficiency

Andika Prasetiadi<sup>1\*</sup>, Dani Rusirawan<sup>2</sup>, Lita Lidyawati<sup>3</sup>

<sup>1</sup> Under Graduate Student, Department of Mechanical Engineering

<sup>2</sup> Department of Mechanical Engineering

<sup>3</sup> Department of Electrical Engineering

Institut Teknologi Nasional (ITENAS), Bandung – INDONESIA

\* Corresponding author e-mail: Prasetiadi086@gmail.co.id

### Abstract

Solar power plant (SPP) is one of the alternative power generation systems with great potential to be developed in Indonesia because the climate is relatively constant throughout the year. The main component in the SPP is the photovoltaic (PV) system, which converts solar energy into electrical energy, directly. The ideal temperature of the PV module must be below 40 °C to maximize the power generated by photovoltaic, and to maintain this condition the cooling system should be installed in the PV system. In this research, the cooler effects on the electricity generated by the PV will have experimented. The type of PV module is monocrystalline silicon photovoltaic modules, with available in the 1000 Wp grid-connected PV system at the campus of Itenas Bandung. The PV module used 265 Wp (4 units) using 900 W of the inverter system. The results of these experiments get the difference in electricity generated by PV modules with a cooler (active cooling by spraying water) and PV modules without a cooler. Based on experiments on January 12, 2020, it was found that at 14:00, the PV modules' efficiency with and without cooler were 25.68% and 24.24%, respectively.

*Keywords: solar power plant (SPP), monocrystalline, voltage, current, power output.*

## 1. Introduction

Depletion of fossil energy today, bring humans to replace or look for another alternative energy, to meet their daily needs, especially electricity. The use of renewable energy is starting to be developed considering this situation. Renewable energy resources, such as sun, wind, water, geothermal, and biomass are essential. For Indonesia, the utilization of solar energy has the most potential due to the geographic location of Indonesia on the equator (Rusirawan, 2013). Solar energy can be converted directly into electricity by a photovoltaic (PV) system. Presently, research in the PV area is very important in the world, especially focus on how to increase the efficiencies as the progress of material technology.

In principle, the PV characteristic is affected by incoming radiation, ambient temperature, and cell temperature. The effect of cell temperature on the other parameters such as open-circuit voltage, maximum power, fill factor, and efficiency has been investigated previously by Sargunathan (2016). This research shows that all parameters will decrease with increasing temperature, and therefore is needed the cooling system.

In this research, investigated PV modules performance with and without cooling system have been performed, and the existing installation of the SPP at the campus Itenas is used as object research. The SPP system is a 100 Wp grid-connected system, with 4 pieces of PV modules @ 265 Wp.

## 2. Research Method

The electrical performance is primarily influenced by the type of PV used. A typical PV module converts 6-20% of the incident solar radiation into electricity, depending upon the type of solar cells and climatic conditions. The rest of the incident solar radiation is converted into heat, which significantly increases the temperature of the PV module and reduces the PV efficiency of the module. This heat can be extracted by flowing water or air beneath the PV module using a thermal collector, called photovoltaic thermal (PVT) collectors (Dubey, 2012).



This study modifies the PV system in Itenas, by dividing 4 PV modules into 2 (two) sections of PV systems, one system using a cooler and another without a cooler. For cooling systems using water spray, which is controlled automatically. The control system used an Arduino Uno Microcontroller, which is in the program to start the pump at a predetermined temperature. The data collection process is carried out starting at 6:00 a.m. to 6:00 p.m., with data collection intervals is once every/hour. The PV modules section as an experimental setup is shown in Fig. 1.

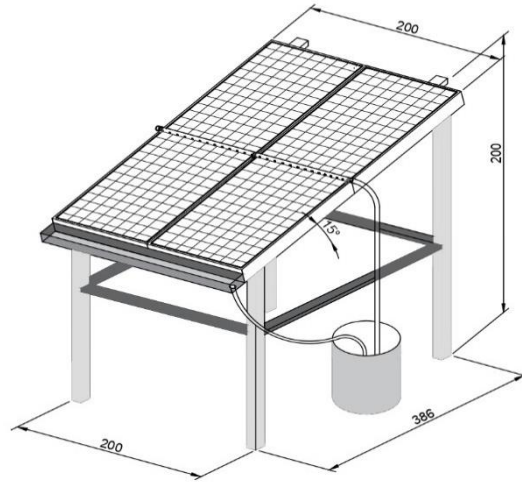


**Fig. 1: Solar Power Plant Installation**

## 2.1 Determine Operating Temperature

The cell temperature ( $T_c$ ) operation can be evaluated using the following formula (Hadiwinoto, 2018):

$$T_c = T_a + \frac{G_{\text{measured}}}{G_{\text{reference}}} + (\text{NOCT} - T_a) \quad (1)$$

where:

$T_a$  (ambient temperature): obtained from several test results and averaged to get 32°C results.

$G_{\text{measured}}$ : obtained from several test results (averaged to get 574.7 W/m<sup>2</sup>).

$G_{\text{reference}}$ : obtained from the photovoltaic specification.

NOCT: obtained from the photovoltaic specifications (in this case is 45°C)

Based on equation (1), it can be calculated the working temperature during operation, as:

$$T_c = 32 + \frac{574.7}{1000} \times (45 - 32) = 39^\circ \text{C}$$

## 2.2 Programming Control System.

The input program uses the Arduino IDE software to enter commands automatically. The commands will be sent directly to Arduino UNO, to start the cooling system and these programs require 4 cell temperature data and 2 average temperatures. The details main program control system can be seen in Figs. 2, 3, and 4, and part of the controller is shown in Fig. 5.

```

sketch_nov05a | Arduino 1.8.10
File Edit Sketch Tools Help

sketch_nov05a
//numerikal

int analogPin=A0;
int analogPin1=A1;
int analogPin2=A2;
int analogPin3=A3;

float suhu;
float suhu1;
float suhu2;
float suhu3;
float ratarataP1sP2;
float tambah;

int relayout = 10;
float batasatas = 38;
float batasbawah = 32;

void setup() {
  // put your setup code here, to run once:
  Serial.begin(9600);
  pinMode(10,OUTPUT);
}

void loop() {
  // perhitungan suhu nilai masukan dibagi 1024 * 5000
  // celcius adalah nilai diatas dibagi 10
  {suhu = analogRead(analogPin);
  suhu = suhu *0.48628125;

  {suhu1 = analogRead(analogPin1);
  suhu1 = suhu1 *0.48628125;

  {suhu2 = analogRead(analogPin2);
  suhu2 = suhu2 *0.48628125;

  {suhu3 = analogRead(analogPin3);
  suhu3 = suhu3 *0.48628125;

  Serial.print("Panel 1 : ");
  Serial.print(suhu1);
  Serial.println("C");
  delay(20);
  }

  Serial.print("Panel 2 : ");
  Serial.print(suhu2);
  Serial.println("C");
  delay(20);
  Serial.println("");
  }

  Serial.print("Panel 3 : ");
  Serial.print(suhu3);
  Serial.println("C");
  delay(20);
  Serial.println("");
  }

  {suhu3 = analogRead(analogPin3);
  suhu3 = suhu3 *0.48628125;
  Serial.print("Panel 4 : ");
  Serial.print(suhu3);
  Serial.println("");
  }

  delay(20);
  Serial.println("");
  }
  {tambah= suhu+suhu1;
  ratarata= tambah/2;

  Serial.print("rata-rata : ");
  Serial.print(ratarata);
  Serial.println("");
  }

  //program kontrol

  if (ratarata >= batasatas){
    digitalWrite(10,LOW);
  }
  else if (ratarata <= batasbawah)
    digitalWrite(10,HIGH);
  }
  //jarak waktu pengulangan program
}

```

Fig. 2: Programing (1)

```

delay(20);
Serial.println("");
}
{tambah= suhu+suhu1;
ratarata= tambah/2;

Serial.print("rata-rata : ");
Serial.print(ratarata);
Serial.println("");
}

//program kontrol

if (ratarata >= batasatas){
  digitalWrite(10,LOW);
}
else if (ratarata <= batasbawah)
  digitalWrite(10,HIGH);
}
//jarak waktu pengulangan program
}

```

Fig. 4: Programing (3)

```

sketch_nov05a | Arduino 1.8.10
File Edit Sketch Tools Help

sketch_nov05a

Serial.print("Panel 1 : ");
Serial.print(suhu1);
Serial.println("C");
delay(20);
}

{suhu1 = analogRead(analogPin1);
suhu1 = suhu1 *0.48628125;
Serial.print("Panel 2 : ");
Serial.print(suhu1);
Serial.println("C");
delay(20);
Serial.println("");
}

{suhu2 = analogRead(analogPin2);
suhu2 = suhu2 *0.48628125;
Serial.print("Panel 3 : ");
Serial.print(suhu2);
Serial.println("C");
delay(20);
Serial.println("");
}

{suhu3 = analogRead(analogPin3);
suhu3 = suhu3 *0.48628125;
Serial.print("Panel 4 : ");
Serial.print(suhu3);
Serial.println("");
}

delay(20);
Serial.println("");
}
{tambah= suhu+suhu1;
ratarata= tambah/2;

Serial.print("rata-rata : ");
Serial.print(ratarata);
Serial.println("");
}

//program kontrol

if (ratarata >= batasatas){
  digitalWrite(10,LOW);
}
else if (ratarata <= batasbawah)
  digitalWrite(10,HIGH);
}
//jarak waktu pengulangan program
}

```

Fig. 3: Programing (2)



Fig. 5: Part of controller (3)

## 2.3 Parameters of Photovoltaic

Parameters on the I (current) – V (voltage) shows that the current and voltage are changeable depending on the amount of solar intensity. The I-V characteristics of PV solar cells with load conditions or different resistance can be seen in Fig. 6.

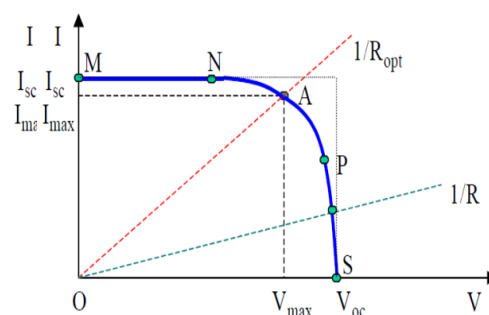


Fig. 6: Current characteristic curves and the voltage.

The parameter to determine the value Outputs on solar cells include (refer to Fig. 6):

- Short circuit current or short circuit current ( $I_{sc}$ ) is the current maximum output which is obtained from solar cells on condition there is no resistance ( $R$ ),  $V = 0$ .
- Open circuit voltage or open-circuit voltage ( $V_{oc}$ ) is output power and efficiency which can be achieved when no current.
- Maximum power ( $P_{max}$ ) is located at point A ( $V_{max}$ ,  $I_{max}$ ).
- Fill factor (FF) is a value that is close to a certain solar cell constant.

### 3. Measurement

The following data in Tables 1-2 were obtained from the experiment process on January 11-12, 2020.

Table 1: Test data for January 11<sup>th</sup>, 2020

Date :		11-Jan-20									
NO	TIME	weather conditions	PARAMETER								
			G (Radiation)	Ta (Temperature ambient)	T average 1-2	T average 3-4	Voc(Voltage 1-2)	Isc (Current 1-2)	Voc (Voltage 3-4)	Isc (Current 3-4)	the Cooler
1	06.00	Cloudy	14,2	25,65	19,925	22,788	57	0,07	57,1	0,07	OFF
2	07.00	Cloudy	76,1	27,55	51,825	39,688	59,4	0,98	60,1	0,98	OFF
3	08.00	Cloudy	338	29,1	183,55	106,33	68	2,34	68,2	2,33	OFF
4	09.00	Cloudy	345,5	28,79	187,15	107,97	68,3	3,04	68,4	3,1	OFF
5	10.00	Bright	640	30,27	335,14	182,7	68,8	4,5	67,9	4,4	ON
6	11.00	Cloudy	465,2	29	247,1	138,05	70,1	3,91	68,1	3,93	ON
7	12.00	Bright	605	31,25	318,13	174,69	71,2	5,4	69,1	5,41	ON
8	13.00	Bright	679	32,71	355,86	194,28	70,1	4,7	66,7	4,7	ON
9	14.00	Cloudy	293,5	28,32	160,91	94,615	68,2	2,83	68,1	2,81	OFF
10	15.00	Cloudy	121	26,86	73,93	50,395	60	1,2	61,4	1,21	OFF
11	16.00	Cloudy	98,5	25,86	62,18	44,02	57	0,98	57,1	0,97	OFF
12	17.00	Cloudy	64	23,93	43,965	33,948	56,4	0,68	56,3	0,68	OFF
13	18.00	Rain									

Table 2: Test data for January 12, 2020

NO	Time	weather conditions	PARAMETER								
			G (Radiation)	Ta (Temperature ambient)	T average 1-2	T average 3-4	Voc(Voltage 1-2)	Isc (Current 1-2)	Voc (Voltage 3-4)	Isc (Current 3-4)	the Cooler
1	06.00	Bright	16	21,48	21,485	20,51	60,1	0,8	60,5	0,79	OFF
2	07.00	Bright	122,2	24,9	23,685	26,61	65,2	1,3	65,1	1,31	OFF
3	08.00	Bright	613,2	27,34	28,81	37,11	70	4,9	69,3	4,83	ON
4	09.00	Bright	656	27,83	36,665	42,26	71,9	5,2	70,9	5,4	ON
5	10.00	Bright	815	29,79	32,955	45,165	71,9	5,81	70,1	5,82	ON
6	11.00	Bright	1046	32,23	35,645	50,05	72,5	7,2	69,5	7,1	ON
7	12.00	Bright	933	30,76	36,905	45,155	72,9	8,5	69,9	8,7	ON
8	13.00	Bright	875	32,71	35,15	45,655	71,6	8,2	68,9	9,1	ON
9	14.00	Bright	617	31,11	36,61	42,6	71,8	8,1	69,5	7,9	ON
10	15.00	Bright	542	33,69	34,425	39,795	71,2	71,05	68,9	7,12	ON
11	16.00	Bright	153	31,25	33,935	30,51	71	4,87	68,5	4,73	OFF
12	17.00	Bright	64	28,81	27,74	26,235	69,6	2,73	68,9	2,53	OFF
13	18.00	Bright	8,1	27,34	25,62	24,18	66,9	0,57	66,9	0,55	OFF

#### 3.1 Data processing

Furthermore, the data will be processed to obtain all PV parameters such as maximum power (P). The maximum power can be obtained using the following equation:

$$\begin{aligned}
 P_{mp} &= V_{mp} \times I_{mp} \\
 P_{mp} &= 71,6 \text{ V} \times 1,12 \text{ A} \\
 P_{mp} &= 80,192 \text{ Watt}
 \end{aligned}$$

On the other side, the maximum open-circuit power can be obtained using the following equation:

$$\begin{aligned} P_{oc} &= V_{oc} \times I_{sc} \\ P_{oc} &= 73,5 \text{ V} \times 7,2 \text{ A} \\ P_{oc} &= 522 \text{ Watt} \end{aligned}$$

The FF (fill factor) is approaching the constant value of a solar cell. The Fill Factor can be obtained using the following equation:

$$\begin{aligned} FF &= \frac{V_{mp} \times I_{mp}}{V_{oc} \times I_{sc}} \\ FF &= \frac{80,192 \text{ Watt}}{522 \text{ Watt}} = 0,15 \end{aligned}$$

Finally, based on all parameters, the efficiency of PV can be obtained using the following equation:

$$\begin{aligned} \eta &= \frac{V_{mp} \times I_{mp}}{FF \times G \times A} \\ \eta &= \frac{71,6 \text{ V} \times 1,12 \text{ A}}{0,15 \times 1046 \frac{\text{W}}{\text{m}^2} \times 3,67 \text{ m}^2} = 13,92 \% \end{aligned}$$

## 4. Results

The Tables 3-4, and Figs. 7-8 shows the comparison of the PV efficiency with and without applying the cooler.

**Table 3. The Comparison of the Efficiency**

Time	G	With The Cooler							Without The Cooler						
		V <sub>mp</sub>	I <sub>mp</sub>	P <sub>mp</sub>	V <sub>oc</sub>	I <sub>sc</sub>	P <sub>oc</sub>	η (%)	V <sub>mp</sub>	I <sub>mp</sub>	P <sub>mp</sub>	V <sub>oc</sub>	I <sub>sc</sub>	P <sub>oc</sub>	η (%)
10.00	815	71,2	1,085	77,252	71,9	5,81	417,739	13,96629946	68,9	1,09	75,101	70,1	5,82	407,982	13,64009294
11.00	1046	71,6	1,12	80,192	72,5	7,2	522	13,59792853	67,4	1,13	76,162	68,5	7,1	486,35	12,66925774
12.00	933	70,6	1,09	76,954	72,9	8,5	619,65	18,0966733	68,2	1,1	75,02	69,9	8,7	608,13	17,76023551
13.00	875	70,8	1,089	77,1012	71,6	8,2	587,12	18,28322304	68,5	1,09	74,665	68,9	9,1	626,99	19,52479564
14.00	617	68,4	0,85	58,14	71,8	8,1	581,58	25,68373823	67,1	0,86	57,706	69,5	7,9	549,05	24,24714824
15.00	542	69,7	0,84	58,548	71,2	7,05	501,96	25,23502619	67,2	0,85	57,12	68,9	7,12	490,568	24,66231638

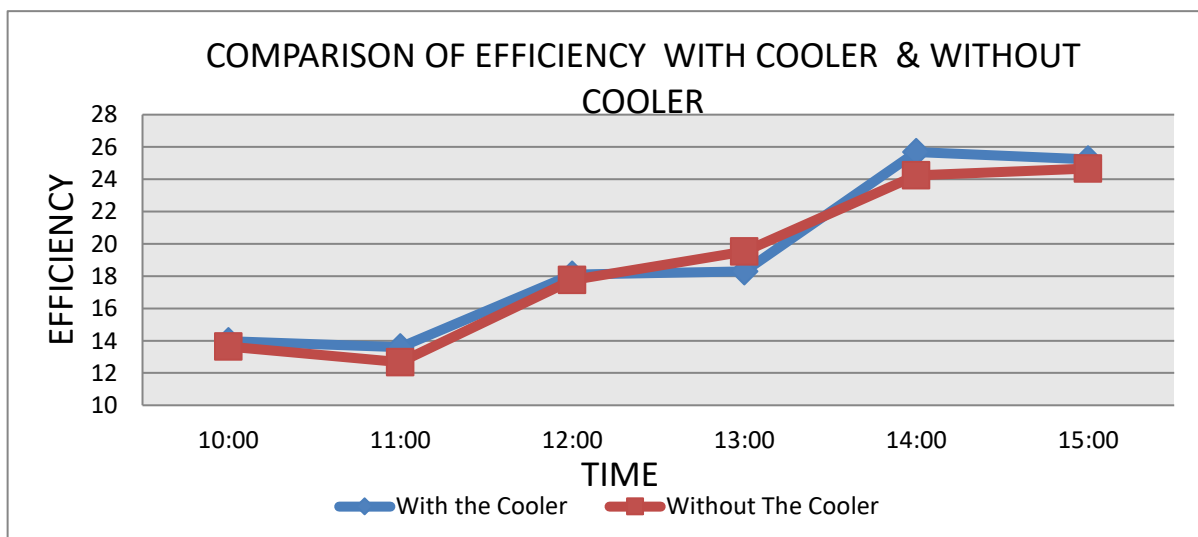
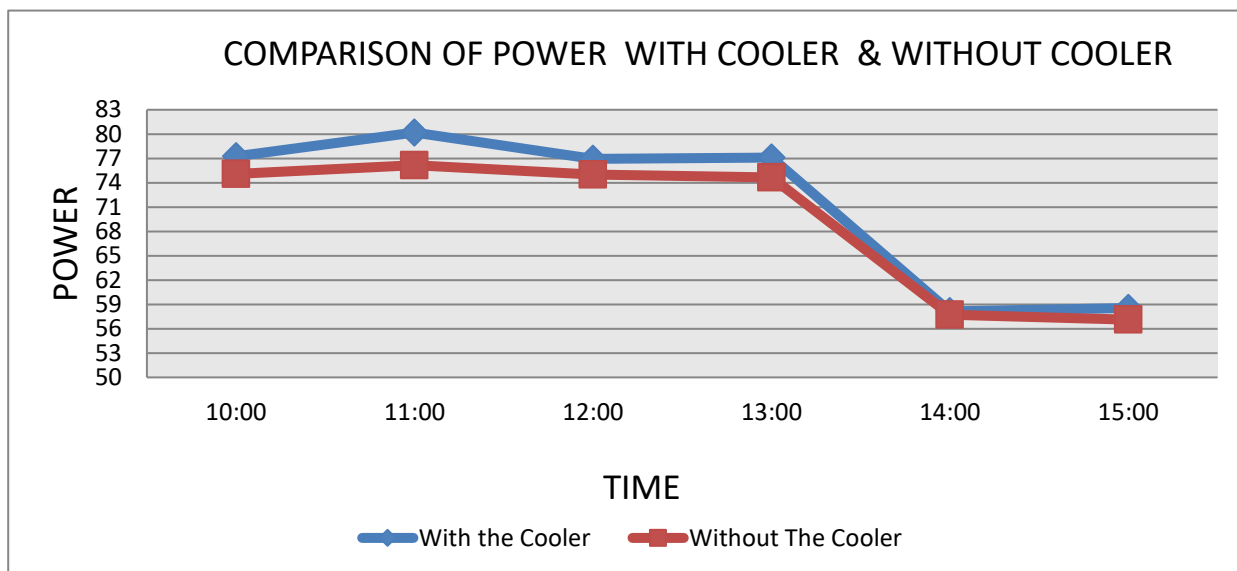


**Fig. 7: Difference of efficiency characteristic between PV module with and without a cooler**



Graph 2. The Comparison of efficiency

Fig. 8: Difference of power characteristic between PV module with and without a cooler

## 5. Conclusion

The temperature parameter can affect the PV module performance. In the high-temperature condition, the temperature of the PV module will increase and the performance of the PV module decreases. The comparison of power generated by the PV has evaluated on January 12, 2020. It is found that at 11:00 power generated by PV modules with and without cooler were 80.192 W and 76.12, respectively. There was a difference of about 4.072 W. At 14:00, there was a small difference in power generated by PV modules with and without cooler, due to the temperature differences of both PV modules were small (close to 6°C). Based on the evaluation, it is shown that in the high temperature, the voltage will decrease but the current generated by PV increased, although not significant. It is shown also that at 14:00, the PV modules' efficiency with and without cooler were 25.68% and 24.24%, respectively, and the difference was 1.44%.

## 6. Nomenclature

I	Current	A
G	Irradiation	W/m <sup>2</sup>
P	Power	Watt
T <sub>c</sub>	Cell temperature	°C
V	Voltage	V
FF	Fill Factor	-
η	Efficiency	%

## 7. References

- Rusirawan, Dani. 2013. "State Of The Art Photovoltaic Technologies And Its Challenges For Indonesia". Bandung, Institut Teknologi Nasional.
- Hadiwinoto, Ari. 2018. "Realisasi Dan Pengujian Sistem Kontrol Pendingin PLTS 1000 Wp". Bandung, Institut Teknologi Nasional.
- Dubey, Swapnil. 2012. "Temperature-Dependent Photovoltaic (PV) Efficiency and Its Effect on PV Production in the World A Review". Singapore, Nanyang Technological University.
- Sargunathan, S. 2016. "Performance enhancement of solar photovoltaic cells using effective cooling methods: A review". Tamilnadu, Institute of Road Transport Technology.

## ***C. Information Technology & Engineering (Chemical)***

## Success Implementation of E-Voting Technology In various Countries: A Review

Slamet Risnanto<sup>1</sup>, Yahaya Bin Abd Rahim<sup>2,\*</sup> and Nanna Suryana Herman<sup>3</sup>

<sup>1</sup> Department of Informatics Engineering, Universitas Sangga Buana, Bandung - INDONESIA

<sup>2,3</sup> Faculty of Information and Communication Technology, Universiti Teknikal Malaysia Melaka  
(UTeM)  
Melaka, MALAYSIA

\* Corresponding author e-mail: slamet.risnanto@usbykp.ac.id

### Abstract

Electronic voting or known as e-voting is a technology developed for voting. The use of e-voting in the general election has been widely implemented. Some countries that have successfully implemented it are India, Brazil, Estonia and the Philippines, and other countries that have unsuccessfully tried or canceled to implement it are Argentina, United States, Belgium, Canada, Japan, Mexico, France, Peru, Australia, Costa Rica, Finland, Guatemala, United Kingdom, Ireland, Italy, Kazakhstan, Netherland, Germany, Paraguay, Norway, Switzerland and others. In this study, we tried to present countries that have successfully implemented e-voting, analyzed them, and made conclusions upon the analysis. The result of this study is that the adoption of e-voting is not only about technology. Many factors are no less important that contribute to the successful implementation of e-voting in a country, so that other countries that plan to implement e-voting in the future can learn from the success of these countries.

*Keywords: e-voting, general election, election technology*

---

### 1. Introduction

Election is an activity that is prevalent in countries that adhere to a democratic system that is usually carried out to elect State leaders, regional leaders, and the representatives in parliament. By the complexity of electoral procedures, the increasing number of voters, especially if the country is an archipelagic country with many remote populations, make the things above become its own problems, such as: expensive costs, slow recapitulation of election results, security problem, etc.

Indonesia is a sample of the third largest democratic country, which in 2019 has conducted elections for members of parliament, and also its leader of the Country. According to several sources, the number of voters was 192 million, the number of polling stations was 813,350 units, and the number of committees assigned to polling stations was more than 7 million people, and also it spent more than 25 trillion rupiahs of budget. This number definitely an enormous cost for developing countries, not to mention common problems, such as: ballot distribution and tiered calculations that require a relatively long time.

Technology is the solution to the problems that arise in conventional elections and technology is the only solution (Liu and Zhao, 2018). Many countries have implemented e-voting technology, such as: Argentina, United States, Belgium, Canada, Japan, Mexico, France, Peru, Australia, Costa Rica, Finland, Guatemala, United Kingdom, Ireland, Italy, Kazakhstan, Netherland, Germany, Paraguay and others (Budurushi, Jöris and Volkamer, 2014) (Esteve, (Esteve, Goldsmith and Turner, 2012), (Goretta *et al.*, 2019). However, among those countries mentioned, only a few countries that have succeeded and successfully implemented it. Some of them ended with cancellation, only did some try-outs, did the program partially, did not continue it, and other reasons.

In this study, we tried to present the countries that have successfully implemented e-voting as an example for other countries that will implement e-voting technology in the future so that in future implementation, it does not end in failure.

## 2. Literature review

Electronic voting or e-voting is an election activity with the support of technology. The voting is not done by punching a hole in the paper, but the voters vote by machine, and the ballots are stored in digital form (Kumar *et al.*, 2011). E-voting is an election activity in which the recording and the counting of votes are carried out using electronic media (AdelekeR. *et al.*, 2013). Electronic voting machines were intended to reduce errors and speed up the counting process. The advantages of e-voting over conventional systems or ballots according to (Kumar *et al.*, 2011) and (Riera and Brown, 2003) are:

- Eliminating the possibility of invalid and questionable votes, which in many cases are the causes of controversy in elections.
- Making the vote counting process much faster and more accurate than conventional systems.
- Reducing the amount of paper used is environmentally friendly
- Reducing printing, distribution and committee costs

We summarized the countries that carried out e-voting according to their status (Goretta *et al.*, 2019) as follows:

**Table 1: List of countries**

No.	Status	Country
1	Countries that have implemented e-voting completely	India, Brazil, Philippines, and Estonia
2.	Countries that have implemented e-voting partially	Argentina, United States, Belgium, Canada, Japan. Mexico, France and Peru
3	Countries that cancelled the implementation after conducting try outs of e-voting	Australia, Costa Rica, Finland, Guatemala, United Kingdom, Ireland, Italia, Kazakhstan, and Norwegian
4	Countries that did not continues the implementation of e-voting	Netherland, Germany and Paraguay
5	Countries that are in the process of Testing e-voting	Bangladesh, Bhutan, Ecuador, Mongolia, Switzerland, Nepal and Indonesia

In the table above, we can see that there are many countries which implemented e-voting only limited to trial or partial trials, even many of them cancelled the program or did not continue it. Many developed countries that carried out e-voting, but then did not continue it, like the United Kingdom, was claimed by the digital advocacy groups that the implementation of e-voting in their countries is not valid and cannot be trusted (Vassil *et al.*, 2016). Netherland faced widespread resistance from legislators and the public because the e-voting technology used was untrusted (Loeber, 2008). The possibility of privacy, verification, and confidentiality is part of important elements in the implementation of e-voting (Aljarrah, Elrehail and Aababneh, 2016).

We present the countries that were successfully implemented the e-voting below, they are:

### 2.1 India

India is the largest democratic country in the world, which began the experiment of the use of e-voting for its 16 states in 1989-1990 in Madhya Pradesh, Rajasthan and the Capital of Delhi. The e-voting pilot project in India actually has been started since 1982 on a limited basis (Wolchok *et al.*, 2010), but the Assembly in the State of Kerala canceled it, because it was not in accordance with the law. However, later on, India changed the state law that arrange and ratified the election using e-voting technology. Therefore, since 2003 in India, all states have already used e-voting technology for elections. In 2014, the voters in India were registered as 814 million and there were 930 thousand polling stations using Electronic Voting Machines (EVM). Initially, the e-voting machine in India consisted of two units, namely the voting machine and the control unit. The voting machine is stored in the voting booth and the control unit is kept within the authority of the voting officer. However, started from the 2014 elections, the voting machine has been added by the existence of a VVPAT (Voter Verifiable Paper Audit Trail) machine, in which this machine has the function to print the ballot papers chosen by the voters which can be counted manually if desired. All of the e-voting equipment do not depend on electricity supply, internet, WIFI



or USB. The pictures of EVM and VVPAT machines can be seen in Figure 1, taken from the election commission of India website ([eci.gov.in](http://eci.gov.in))



**Fig. 1: EVM and VVPAT Machine**

## 2.2 Brazil

Electronic elections in Brazil began partially in 2006 at local elections in the city of Santa Catarina, after the Supreme Court of Brazil approved it. Started in 2000, the Brazilian government began to convert the entire electoral process using e-voting, after conducting a feasibility study (Kumar *et al.*, 2011). At the time of the election, Brazil installed 400,000 e-voting machines in the form of kiosks, installed at the center of the crowd and offices. The machine consists of two parts: one part for the control unit installed in the officer's office, and the other part of the machine stored in the voting booth displaying candidates on the screen and voters vote with the help of an integrated keyboard (Everett *et al.*, 2008). For audit purposes, since the beginning Brazil used e-voting, the ballots will come out through a paper ballot machine (VVPAT). The forms of e-voting used in this country can be seen in Figure 2 below.



**Fig. 2: e-voting machine in Brazil**

## 2.3 Philippines

The Philippines is the closest neighboring country which have applied the technology and information in the electoral process, especially at the voting and counting stages. The Philippines first applied IT in the stages of voting and counting, in the 2010 elections. In preparation for the holding of the General Elections in May 2010, the Philippine election committee (COMELEC) issued general instructions on voting, vote counting, and sending process of the votes at the polling stations. Another procedure, including the regulation of disputes over the results of E-Voting, were also issued.

COMELEC chose PCOS (Filipino e-voting system) to be used in the 2010 elections. The PCOS system is a vote counting system based on OMR (Optical Mark Recognition) technology. Each PCOS machine was equipped with a memory card and i-Button, so that only certain ballots from a polling station can be scanned. Ballots marked by the voters were inserted into the PCOS machine to be scanned. This PCOS machine read the sign made by the voters, when the polling station was closed. The PCOS machine printed the voting report at the polling station with information about the number of votes of each candidate, and sent the results to the tabulation office at the city or district level, thus the election in the Philippines still used ballots or papers. Voters came to the polling station and were given a ballot, then, voters gave their choice marks on the ballots that have been provided.

The adoption of E-Counting with this PCOS machine was considered to be unsuccessful, by some people. In fact, one of the most influential election observers in the Philippines, AES, called the 2013 election as a "technological and political disaster" election, because of some controversy surrounding the holding of the 2013 elections.

## 2.4 Estonia

Estonia began using e-voting in its general elections in 2007. In fact, the e-voting project in the country began in 2003. Estonia was the first country that use the internet in e-voting, and in 2011, Estonia also used mobile phones in the conduct of e-voting (Tsahkna, 2013). The mobile phone is considered as an identity card with the SIM Card number as the voter's identification, and at the same time the voter must be in front of a computer that uses internet connection for the selection process (Mpekoa and Van Greunen, 2017).

## 3. Discussion

By the information presented in the literature above, we made the following table:

**Table 2: Comparison e-voting technology**

<b>Countries Technology</b>	<b>India</b>	<b>Brazil</b>	<b>Philippines</b>	<b>Estonia</b>
Hardware	EVM (Electronic Voting Machine)	GX-1 Integrated Processor	PCOS	None / Gadget voters /internet voting
Paper Audit Trail	VVPAT Machine	VVPAT Machine	Yes (conventional ballot)	Yes (Digital Receipt)
Internet connection	None	None	Yes (only for counting)	Yes
Wi-Fi / USB	None	None	Yes (only for counting)	Yes
Power	Battery	battery	Battery and electric	Battery and electric
Result	Success, No problem	Success, No problem	Success but many negative comments / claims from the public	Success but many negative comments / claims from the public

In the next step, we tried to compare the social, political, and economic studies of the countries that successfully carried out e-voting with the results as described below:

**Table 3: Social, politic and economic status**

<b>Countries Status</b>	<b>India</b>	<b>Brazil</b>	<b>Philippines</b>	<b>Estonia</b>
Economic Status	Developing country	Developing country	Developing country	Developed county
Sum of voters	814.000.000	140.000.000	54.000.000	176.000
e-voting constitution	Yes	Yes	Yes	Yes
Trial Process	Yes	Yes	Yes	Yes
Feasibility study	Yes	Yes	Yes	Yes

From the two tables above, it can be concluded that:

- Only Countries that used microcomputer devices without an internet connection that successfully carried out e-voting seamlessly (India and Brazil).
- Countries that used internet connections and successfully carried out the e-voting, but were not smoothly conducted it, got many negative comments from the people of the countries. It also created concerns among the people, especially about privacy, verification and confidentiality (Aljarrah, Elrehail and Aababneh, 2016).
- Most developing countries have successfully implemented e-voting.
- All countries that successfully carried out e-voting, have carried out trials, feasibility studies and have a strong legal support (Hapsara, 2013).

## 4. Conclusion

E-voting technology is an important factor in the implementation of e-voting in a country (Hapsara, 2016), but it is not the only thing that influences the success of its implementation. There are many other factors, such as: the readiness of voters and electoral committees, public trust, readiness of the constitution and others (Adeshina and Ojo, 2017), (Aljarrah, Elrehail and Aababneh, 2016), (Avgerou, 2013), (Alomari, 2016). In the future, it is better to conduct a review study on the countries that failed or cancelled in carrying out e-voting, because until now there is relatively a large gap of the ratio between the failing and the successful countries. Another studies that is no less important, is the necessity of having a framework study development (AboSamra *et al.*, 2017), (Hapsara, 2014) for the implementation of e-voting at the national level of all countries.

## 5. References

- AboSamra, K. M. *et al.* (2017) 'A practical, secure, and auditable e-voting system', *Journal of Information Security and Applications*. Elsevier Ltd, 36, pp. 69–89. doi: 10.1016/j.jisa.2017.08.002.
- AdelekeR., A. *et al.* (2013) 'Modeling and Evaluation of E-Voting System for a Sustainable Credible Election', *International Journal of Applied Information Systems*, 5(3), pp. 8–14. doi: 10.5120/ijais12-450862.
- Adeshina, S. A. and Ojo, A. (2017) 'Factors for e-voting adoption - analysis of general elections in Nigeria', *Government Information Quarterly*. Elsevier, (November 2015), pp. 0–1. doi: 10.1016/j.giq.2017.09.006.
- Aljarrah, E., Elrehail, H. and Aababneh, B. (2016) 'E-voting in Jordan: Assessing readiness and developing a system', *Computers in Human Behavior*. Elsevier Ltd, 63, pp. 860–867. doi: 10.1016/j.chb.2016.05.076.
- Alomari, M. K. (2016) "E-voting adoption in a developing country", *Transforming Government: People, Process and Policy*, *Emerald insight*, 10(4). doi: <http://dx.doi.org/10.1108/TG-11-2015-0046>.
- Avgerou, C. (2013) 'Explaining Trust in IT-Mediated Elections: A Case Study of E-Voting in Brazil.', *Journal of the Association for Information ...*, 14(8), pp. 420–451.
- Budurushi, J., Jöris, R. and Volkamer, M. (2014) 'Implementing and evaluating a softwareindependent voting system for polling station elections', *Journal of Information Security and Applications*, 19(2), pp. 105–114. doi: 10.1016/j.jisa.2014.03.001.
- Esteve, J. i, Goldsmith, B. and Turner, J. (2012) 'International Experience with E-Voting Norwegian E-Vote Project', (June), pp. 1–196. Everett, S. P. *et al.* (2008) 'Electronic voting machines versus traditional methods', p. 883. doi: 10.1145/1357054.1357195.
- Goretta, H. *et al.* (2019) 'Technology criteria analysis and e-voting adoption factors in the 2019 Indonesian presidential election', *2018 International Conference on Advanced Computer Science and Information Systems, ICACISIS 2018*. IEEE, pp. 143–149. doi: 10.1109/ICACISIS.2018.8618215.
- Hapsara, M. (2013) 'E-Voting Indonesia : A Safety-Critical-Systems model towards standard and framework for Indonesia ' s Presidential Election', (December), pp. 12–13.

- Hapsara, M. (2014) 'E-Voting Indonesia : A Safety-Critical-Systems Model Towards Standard and Framework for Indonesia ' s Presidential Election', *Australian Journal of Basic and Applied Sciences*, 8(4), pp. 301–308.
- Hapsara, M. (2016) 'Reinstating E-Voting as A Socio-Technical System', *2016 IEEE Region 10 Symposium (TENSYMP)*, pp. 282–287.
- Kumar, S. *et al.* (2011) 'Analysis of Electronic Voting', *International Journal on Computer Science and Engineering - IJCSE*, 3(5), pp. 1825–1830. doi: 10.1177/002076409604200204
- Liu, Y. and Zhao, Q. (2018) 'E-voting scheme using secret sharing and K-anonymity', *World Wide Web*. World Wide Web, (August 2017), pp. 1–11. doi: 10.1007/s11280-018-0575-0.
- Loeber, L. (2008) 'E-Voting in the Netherlands: from General Acceptance to General Doubt in Two Years', *Conference on Electronic Voting*, c, pp. 21–30. doi: 10.1109/MC.2007.271.
- Mpekoa, N. and Van Greunen, D. (2017) 'E-voting experiences: A case of Namibia and Estonia', *2017 IST-Africa Week Conference, IST-Africa 2017*, pp. 1–8. doi: 10.23919/ISTAFRICA.2017.8102303.
- Riera, A. and Brown, P. (2003) 'Bringing Confidence to Electronic Voting', *Electronic Journal of e-Government*, 1(1), pp. 43–50.
- Tsahkna, A.-G. (2013) 'E-voting: Lessons from Estonia', *European View*, 12(1), pp. 59–66. doi: 10.1007/s12290-013-0261-7.
- Vassil, K. *et al.* (2016) 'The diffusion of internet voting. Usage patterns of internet voting in Estonia between 2005 and 2015', *Government Information Quarterly*. The Authors, 33(3), pp. 453–459. doi: 10.1016/j.giq.2016.06.007.
- Wolchok, S. *et al.* (2010) 'Security analysis of India's electronic voting machines', *Proceedings of the ACM Conference on Computer and Communications Security*, pp. 1–14. doi: 10.1145/1866307.1866309.

## Model of Ubiquitous Precision Livestock System 4.0: A Technological Review

Irawan Afrianto<sup>1,2,\*</sup>, Sri Wahjuni<sup>1</sup> and Taufik Djatna<sup>3,1</sup>

<sup>1</sup> Department of Computer Science, Institut Pertanian Bogor (IPB), Bogor - INDONESIA

<sup>2</sup> Department of Informatics Engineering, Universitas Komputer Indonesia, Bandung - INDONESIA

<sup>3</sup> Department of Agro-Industrial Technology, Institut Pertanian Bogor (IPB), Bogor - INDONESIA

\* irawan.afrianto@email.unikom.ac.id

### Abstract

The main objective of this study is to propose a model Ubiquitous Precision Livestock 4.0 system that combines the ability of IoT and drones to monitor livestock biomass and herd cattle, wearable devices on livestock to provide location information and animal health, and utilize data communication networks using Long Range (LoRa) for coverage wider. The methods used in developing this model include collecting data and literature, analyzing technology needs, and developing the model. The results show that the model developed has a huge potential to be implemented to support the 4.0 livestock system which is faster, more accurate and precise in providing information to farmers.

*Keywords: IoT, drones, geofence, wearable devices, LoRa, Livestock 4.0.*

### 1. Introduction

Livestock are land animals that are raised in a regular agricultural environment to attract or produce these commodities such as meat, milk, eggs and skin. Livestock contribute to the diversity of the agri-food system globally and have many roles for various community groups (F.A.O, 2018) . IoT is a technology in which devices in an environment can communicate with each other through the internet network. IoT sensors used will facilitate the system in collecting data and will also improve data accuracy (Budiharto, 2019). One of the roles of IoT is widely used in agriculture (Muangprathub et al, 2019; Lakhwani, et al, 2019) and animal husbandry (Mitkari et al, 2019; Pratama et al, 2019). This is because the sensors contained in the IoT system can provide data that is faster, more precise and can be processed at a later stage (Khanna and Kaur, 2019). The application of IoT technology to animal husbandry led to the emergence of the term precision livestock 4.0. The technology used is increasingly developing. The need for extensive land for animal husbandry raises more accurate food, health and livestock monitoring issues. The need for technology that is able to provide data quickly on the condition and environment of livestock is needed.

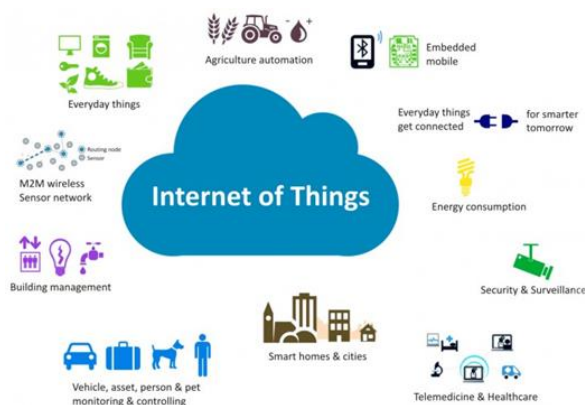
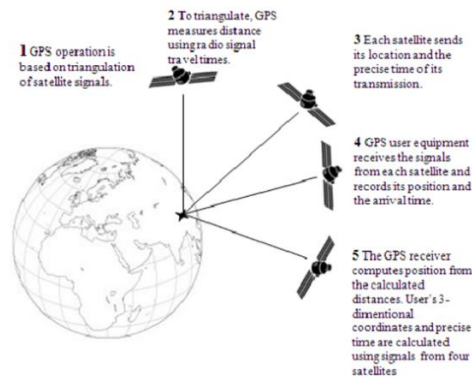


Fig. 1: IoT technology

Drones are unmanned aircraft that are controlled remotely using a radio control or autopilot system that is able to fly them automatically. Drones are very effectively used to carry out airborne monitoring of certain cases (Elliott et al, 2019). Likewise in a precision livestock environment 4.0, drones can be used as a solution to monitor the fertility of shepherds, because they have the ability to remote sensing to process the image of the land to then determine the elements contained in the land [Wahyuni et al, 2016; Yusandi, 2015), and monitor conditions and herding cattle (Barbedo and Koenigkan, 2018). In order to obtain precise data related to the location of livestock, the use of GPS technology installed on livestock and drones is proposed in the model to be developed. GPS is a technology that functions to determine the position on the surface of the earth using satellite signals (Hashim et al, 2011). This technology is supported by 24 satellites that send microwave signals to Earth. This signal serves to determine the position, speed, direction and time (Widyantara et al, 2015), so that it can monitor the location and presence of livestock in real time and precision.



**Fig. 2: GPS technology**

Wearable devices used in livestock, consisting of sensors to determine the condition (Haladjian et al, 2018) and the location of the livestock (Knight et al, 2018). While the GPS model on the drone was used for flight control (Oktaria et al, 2018), and found the cattle he had to lead. In order to localize large areas, geofencing technology was developed where there is a kind of virtual fence coordinated with GPS technology to monitor cattle inside or outside the fence. Geofencing is a feature in software programs that use a global positioning system (GPS) to determine geographical boundaries. The program that combines geofencing makes it possible to manage triggers, so that if an object using a certain device enters or exits specified limits, a notification will appear that will be sent to the user of the geofencing-featured application (Maiousak and Taleb, 2019; Muminov et al, 2019).

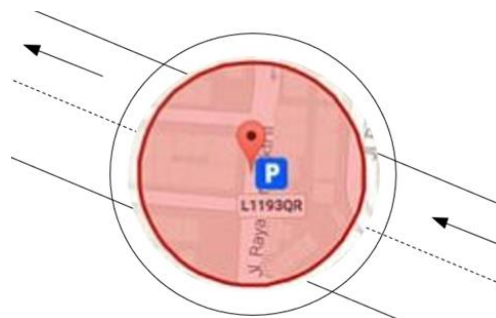


**Fig. 3: Geofence technology**

Data communication used in precision livestock system 4.0 is LoRa (Long Range) technology. LoRa is proposed because it has the right characteristics for developing an IoT-based system. LoRa is a wireless communication system for the Internet of Things, offering long distance communication (> 15 km in remote areas) and low power (5-10 years). LoRa has advantages compared to other types of communication such as cellular, BLE and WiFi. LoRa has long range communication capabilities such as cellular but low power like BLE, so its use is very suitable for sensor devices that are operated annually with battery resources and on a wide area. However, LoRa has limitations in data transmission speeds in the range of 0.3 -50 kbps (Augustin et al, 2016). However this is not a problem as long as the data sent by the sensor is relatively small (order 10-20 bytes). Such applications are very suitable for transmitting water meter sensor data, electricity meters, river water level sensors, temperature and humidity sensors, and etc (Sinha, et al, 2017).



Fig. 4: LoRa technology

## 2. Methodology

This research is a preliminary study to produce an architectural model of technology precision livestock system 4.0. The research flow that was developed included the following matters:

- Data collection and literature study: conducting data collection activities derived from studies and scientific articles relating to the research conducted.
- Technology needs analysis and evaluation: initiating and investigating data requirements, running business processes and technological requirements for precision livestock system 4.0, which will be used in the development of system architecture.
- Modeling technological architecture in precision livestock system 4.0., Based on theoretical studies and analysis at an earlier stage.

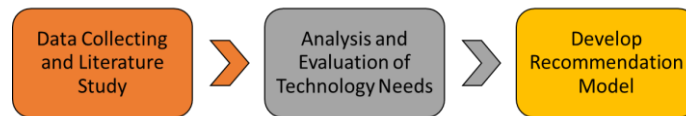


Fig. 5: Research methodology

## 3. Result and Discussion

The model of precision livestock 4.0. is a Cyber-Physical System (CPS) model that integrates technology and data to produce accurate and fast livestock information. IoT is the basis for the development of the model used because the input-process-output mechanism is carried out by various devices with the help of diverse communication and data networks. Multi-data analysis is performed to obtain information needed by farmers. As for the entities that are used in the model of precision livestock system 4.0 are drone, wearable device in livestock, and LoRa data communication network. While the software developed includes geofencing technology, object detection, location-based services, and data analysis.

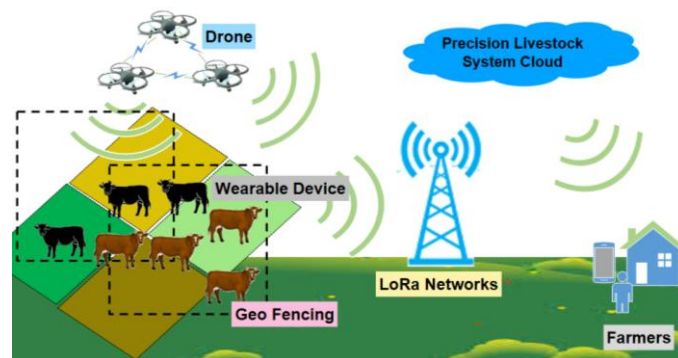


Fig. 6: Model of precision livestock system 4.0.

### 3.1. LoRa Technology in Precision Livestock Systems 4.0.



LoRa is used in the 4.0 Precision Animal Systems model. because of its wide range of capabilities making it suitable for shepherds and detect cattle at long distances with low power. LoRa is a lightweight protocol suitable for technology that develops IoT, controls drones over long distances and is able to transmit data in the form of data from sensors that are on wearable devices for livestock and drones.

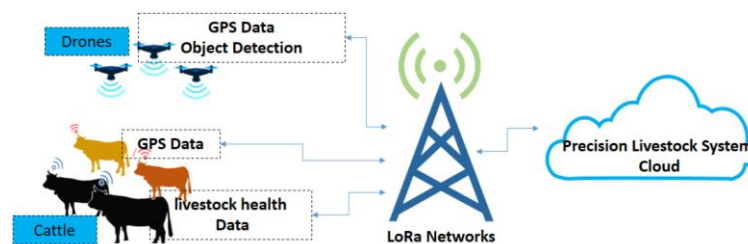


Fig. 7: Data communication for precision livestock systems 4.0 using LoRa.

### 3.2. Drone Technology in Precision Livestock Systems 4.0.

As an unmanned vehicle that has the ability to explore, the drone is used as a solution on model of precision livestock 4.0 (Figure 8). The role of the drone in the model of precision livestock 4.0, are:

As an entity that conducts surveillance of plant biomass, using image processing technology (Wahyuni et al, 2016; Yusandi, 2015), where the drones will work together / in groups using artificial intelligence (*swarm intelligence*), in order to sensing the shepherd by looking at the color composition of grass on the shepherd and map it in the form of a digital map in accordance with the calculation of biomass. The color composition is indicated as the size of the biomass contained in the land, which will be used to show the potential of grass biomass as feed from livestock in shepherds. The drone used has the intelligence swarm characteristics for speed and accuracy of measurement and detection which is more accurate, and has the ability to be adaptive to the environment. Apart from being a function of surveillance of plant biomass, drones are used to detect the color of objects (Arifin, 2014) and count the number of livestock in shepherds. The object to be tracked and detected is black bulls and brown cows and the system will calculate the number of cattle to be used as a parameter to analyze the availability of grass at a location with the number of cattle in the shepherds.

The drone functions as a shepherd. With the ability to adapt to the environment and the intelligence that is implanted in the drone, the drone can be used to herd cattle to pasture areas that still have a lot of grass. This is certainly based on the results of biomass data analysis and the number of livestock in one area. If the data show that biomass in the area is reduced, while the number of livestock in the area is still very large, the drone will use its function as a herder, to herd cattle to areas that have more grass (higher biomass).

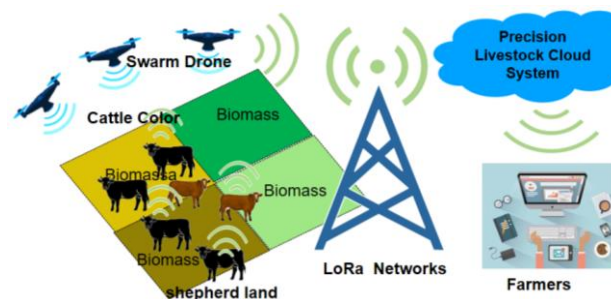


Fig. 8: Drones for grass biomass surveillance, cattle detection and cattle herder

### 3.3 Wearable Device Technology in Precision Livestock Systems 4.0.

Wearable devices can be interpreted as devices that are applied to an object or creature in order to detect, store data to make decisions from the data obtained. Wearable devices are usually in the form of sensors that have special functions for specific purposes (Haladjian et al, 2018).





Fig. 10: Wearable devices on model of precision livestock system 4.0.

In the model of precision livestock system 4.0. , livestock in the shepherd fields are fitted with wearable devices, in the form of GPS sensors, temperature sensors and other sensors to monitor the presence and health of these animals. The network used is LoRa, with transmitter mode to transmit data to the precision livestock system 4.0. by utilizing this wearble device, farmers can find out the location, position and health of their animals in real time. For data communication on precision 4.0 animal models, a LoRa network is used with modules placed on objects such as cattle and drones to send data, and modules to receive data (Liandana, 2019).

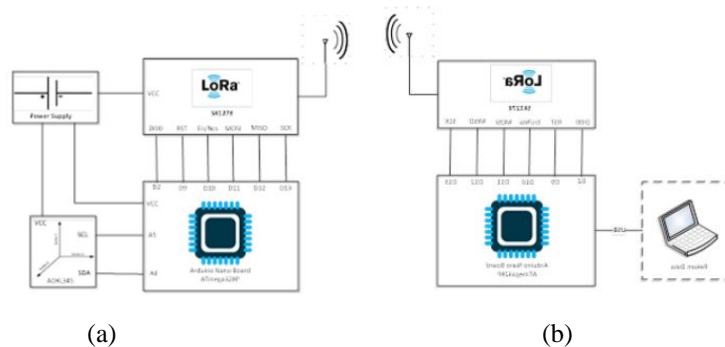


Fig. 11: Hardware architecture of the sender (a) and receiver (b) of data wearable devices using LoRa

### 3.4 GeoFencing Technology in Precision Livestock System 4.0.

The function of geofencing in the model of precision livestock system 4.0. is to ensure that the cattle are still in the herd (in geofence area). If the cattle leave the geofencing area, the system will notify the farmer that there are cattle outside the geofencing area, so that the farmer can lead them back to the geofencing area using drones to herd the cattle into the geofencing area.

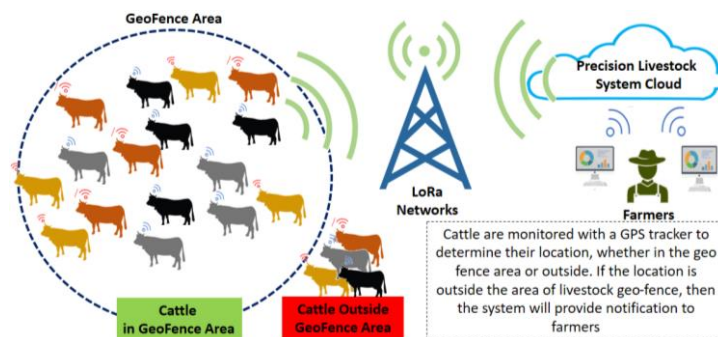


Fig. 12: Geofencing technology in the model of precision livestock system 4.0.

## 4. Conclusion

The results of the Precision Livestock 4.0 system model research show that the integration of input devices, data communication devices, servers to process and analyze data, can provide information easily, quickly and accurately that can be accessed at any time by farmers (ubiquitous system). IoT technology with the integration of drones, wearable devices, geofencing and LoRa can produce an integrated system to improve the quality and sustainability of livestock in the future.

## 5. References

- Arifin, F., Daniel, R.A. and Widiyanto, D., 2014. Autonomous detection and tracking of an object autonomously using ar. drone quadcopter. *Jurnal Ilmu Komputer dan Informasi*, 7(1), pp.11-17.
- Augustin, A., Yi, J., Clausen, T. and Townsley, W., 2016. A study of LoRa: Long range & low power networks for the internet of things. *Sensors*, 16(9), p.1466.
- Barbedo, J.G.A. and Koenigkan, L.V., 2018. Perspectives on the use of unmanned aerial systems to monitor cattle. *Outlook on Agriculture*, 47(3), pp.214-222.
- Budiharto, W., 2019. Inovasi Digital di Industri Smart Farming: Konsep dan Implementasi. In *Seminar Nasional Lahan Suboptimal* (No. 1, pp. 31-37).
- Elliott, K.C., Montgomery, R., Resnik, D.B., Goodwin, R., Mudumba, T., Booth, J. and Whyte, K., 2019. Drone Use for Environmental Research [Perspectives]. *IEEE Geoscience and Remote Sensing Magazine*, 7(1), pp.106-111.
- F.A.O., 2018. Shaping the future of livestock : Sustainably, responsibly, efficiently. 10th Global Forum for Food and Agriculture, Roma, p.1 [Online].. Available : <http://www.fao.org/publications/card/en/c/I8384EN/>. Accessed : June 25, 2019
- Haladjian, J., Haug, J., Nüske, S. and Bruegge, B., 2018. A wearable sensor system for lameness detection in dairy cattle. *Multimodal Technologies and Interaction*, 2(2), p.27.
- Hashim, R., Ikhmatiar, M., Karmin, M., & Herawan, T., 2011. Mosque Tracking on Mobile GPS and Prayer Times Synchronization for Unfamiliar Area. . *International Journal of Future Generation Communication and Networking*, 119, 237-246.
- Khanna, A. and Kaur, S., 2019. Evolution of Internet of Things (IoT) and its significant impact in the field of Precision Agriculture. *Computers and electronics in agriculture*, 157, pp.218-231.
- Knight, C.W., Bailey, D.W. and Faulkner, D., 2018. Low-Cost Global Positioning System Tracking Collars for Use on Cattle. *Rangeland ecology & management*, 71(4), pp.506-508.
- Liandana, M., 2019. Penerapan Teknologi LoRa Pada Purwarupa Awal Wearable Device. *RESEARCH: Computer, Information System & Technology Management*, 2(02), pp.40-46.
- Maiouak, M. and Taleb, T., 2019. Dynamic Maps for Automated Driving and UAV Geofencing. *IEEE Wireless Communications*, 26(4), pp.54-59.
- Mitkari, S., Pingle, A., Sonawane, Y., Walunj, S. and Shirsath, A., 2019. IOT Based Smart Poultry Farm. *system*, 6(03).
- Muangprathub, J., Boonnam, N., Kajornkasirat, S., Lekbangpong, N., Wanichsombat, A. and Nillaor, P., 2019. IoT and agriculture data analysis for smart farm. *Computers and electronics in agriculture*, 156, pp.467-474.
- Lakhwani, K., Gianey, H., Agarwal, N. and Gupta, S., 2019. Development of IoT for Smart Agriculture a Review. In *Emerging Trends in Expert Applications and Security* (pp. 425-432). Springer, Singapore.
- Muminov, A., Na, D., Lee, C.W. And Kang, H.K., 2019. Monitoring And Controlling Behaviors Of Livestock Using Virtual Fences. *Journal Of Theoretical And Applied Information Technology*, 97(18).
- Oktaria, E.R., Setyawan, G.E. and Kurniawan, W., 2018. Sistem Kendali Jarak Tempuh Quadcopter Menggunakan Metode Proportional Integral Derivative. *Jurnal Pengembangan Teknologi Informasi dan Ilmu Komputer* e-ISSN, 2548, p.964X.
- Pratama, Y.P., Basuki, D.K., Sukaridhoto, S., Yusuf, A.A., Yulianus, H., Faruq, F. and Putra, F.B., 2019. Designing of a Smart Collar for Dairy Cow Behavior Monitoring with Application Monitoring in Microservices and Internet of Things-Based Systems. In *2019 International Electronics Symposium (IES)* (pp. 527-533). IEEE.
- Sinha, R.S., Wei, Y. and Hwang, S.H., 2017. A survey on LPWA technology: LoRa and NB-IoT. *Ict Express*, 3(1), pp.14-21.

Wahyuni, S., Jaya, I.N.S. and Puspaningsih, N., 2016. Model for estimating above ground biomass of reclamation forest using unmanned aerial vehicles. *Indonesian Journal of Electrical Engineering and Computer Science*, 4(3), pp.586-593.

Widyantara, I.O., Warmayana, I.G. and Linawati, L., 2015. Penerapan Teknologi GPS Tracker Untuk Identifikasi Kondisi Traffik Jalan Raya. *Majalah Ilmiah Teknologi Elektro*, 14(1).

Yusandi, S., 2015. Model Penduga Biomassa Hutan Mangrove Menggunakan Citra Resolusi Sedang Di Areal Kerja BSN Group Kalimantan Barat. Bogor (ID): Institut Pertanian Bogor.

## Vulnerability Assessment for Basic Data of Education Website in Regional Government X – A Black Box Testing Approach

Atho' Novian Awlarijal<sup>1\*</sup>, Ahmad Almaarif<sup>2</sup>, and Avon Budiono<sup>3</sup>

<sup>1 2 3</sup> School of Industrial and System Engineering, Telkom University, Bandung - INDONESIA

Corresponding author email: [athonovian@student.telkomuniversity.ac.id](mailto:athonovian@student.telkomuniversity.ac.id),

[ahmadalmaarif@telkomuniversity.ac.id](mailto:ahmadalmaarif@telkomuniversity.ac.id), [avonbudi@telkomuniversity.ac.id](mailto:avonbudi@telkomuniversity.ac.id)

### Abstract

The development of technology in the current era is growing more rapidly. One example is the spread of information is no longer using the print media but uses web media. The Department of Education in Regional Government X uses the website to disseminate information to outside parties. The Department of Education uses the web to manage basic data of education (*Dapodik*). In the current era, information is very crucial. According to the Open Web Application Security Project (OWASP) in 2017 there are several vulnerabilities that often occur on websites such as injection flaws, sensitive data exposure, cross-site scripting (XSS), etc. This will impact the attacker in exploiting the system, retrieving information or important data on the web. Therefore, security must be ensured to maintain the integrity of the information on the website. One way to maintain the integrity of information on a website is by conducting vulnerability assessment. Vulnerability assessment is a series of actions to identify and analyze the possibility of security vulnerabilities in the system (ISACA, 2017). This paper provides a black box testing for vulnerability assessment of web application by mean of analyzing and using combined set tool to detect vulnerabilities. This black box testing using OWASP-ZAP dan OpenVAS for vulnerability scanning.

*Keywords: information, security, web application, vulnerability assessment, black box testing*

## 1. Introduction

Today, people have started to depend on the internet in everyday life. It can be concluded from increasing number of internet users in Indonesia. According to a survey conducted by the Indonesian Internet Service Providers Association (APJII 2017) internet users in Indonesia totaled 143.26 million people or around 54.68% of the total population of 262 million people. Internet users increased by around 10 million from 132.7 million the previous year. Internet users are predicted to continue to increase every year.

The government also uses the development of internet technology for basic data of education (*Dapodik*). Basic data of education (*Dapodik*) is a data collection system managed by the Ministry of Education and Culture which contains data on education units, students, educators, and education substance whose data is sourced from education units that are continuously updated online (Minister of Education and Culture 2015).

With the increase of internet users in Indonesia, more and more information will be obtained from the internet. This must be accompanied by a security system. Website security is needed to maintain the integrity of the information on the website. According to the Open Web Application Security Project (OWASP), there are ten vulnerabilities that often occur in web application (OWASP 2017). By taking advantage of these vulnerabilities, the attacker can exploit the system and retrieve sensitive information from system. One way to maintain the integrity of information on a website is by conducting a vulnerability assessment.

## 2. Literature review

### 2.1. Information Security

Information security is protecting information, data or other assets from access, disruption, or modification from unauthorized parties. In information security to ensure that information is said to be safe is known as the concept of Confidentiality, Integrity, and Availability, or commonly called the CIA Triad (Andress 2014)

Confidentiality is a part of information privacy that refers to the ability to safeguard information from irresponsible parties and only can be accessed by those who have access (Andress 2014). Confidentiality is protection of data from unauthorized access. In other words, only people who are authorized to do so can gain access to sensitive data. A failure to maintain confidentiality that means the secret data has been revealed and no way to un-reveal it.

Integrity is preventing the information or data from being change, modified or destroyed by unauthorized party and ensure the authenticity of information (Nieles, Dempsey and Pillitteri 2017). Data integrity is the content or property part of data that has not been illegally changed. Data integrity not only ensures that the data received is the same as the data sent, but also includes the process of sending from the sender and receiver, the data when stored in storage and processing on a computer. Maintaining data integrity can be done with authorization. Example of mechanism to control or maintaining data integrity are in the file system of Linux implement permission that restrict for preventing unauthorized changes.

Availability is ensuring information can be access reliable and timely (Nieles, Dempsey and Pillitteri 2017). In other words, availability is the ability to provide information when authorized party needs that information. Loss of availability may occur due to many reasons such as power loss, application or operating system problems, network attacks, or other problems.

## **2.2. Web Application Vulnerabilities**

Web application vulnerabilities are some of the most common flaws in website. This paper describes some of the most common web application vulnerabilities based on OWASP Top 10 2017. OWASP Top 10 is valuable document for web application security from collaboration of security expert who shared their expertise to produce top ten list web application vulnerabilities (OWASP 2017). The OWASP Top 10 2017 has listed ten vulnerabilities below:

- Injection
- Broken Authentication
- Sensitive Data Exposure
- XML External Entities (XXE)
- Broken Access Control
- Security Misconfiguration
- Cross-Site Scripting (XSS)
- Insecure Deserialization
- Using Components with Known Vulnerabilities
- Insufficient Logging & Monitoring

Injection, sensitive data exposure, and cross-site scripting (XSS) are the most popular vulnerabilities exploited by attacker. Injection flaws occurs when untrusted information or data sent to web application as part of command or query such command OS, query SQL, etc. Cross-site scripting (XSS) occur when web application input untrusted information or data without validation or update an existing web page with user supplied data like tag script html or JavaScript. XSS allow attacker to execute script in web browser. Sensitive data exposure occurs when there is no additional protection between client-server connections such as encryption.

## **2.3. Black Box**

Black box testing is technique of testing web application without knowledge of internal web application conditions. It only examines the basic of aspects of system and no relevance or has little relevance to internal logical structure of the system (Khan and Khan 2012). Black box approach can use a web vulnerability scanner tools or manual penetration testing.

## **2.4 Vulnerability Assessment**

A vulnerability is a weakness in an information system, system security procedures, internal controls, or implementation that could be exploited by a threat source (National Institute of Standards and Technology 2012). Vulnerability assessment is a series of actions to identify and analyze the possibility of security vulnerabilities in

the system. Vulnerability assessments are usually carried out using automated scanning tools to carry out discovery, testing, analysis and reporting of system vulnerabilities through network-based or host-based (ISACA 2017).

Weaknesses that are owned by the system can occur due to internal and external factors. Internal factors occur due to lack of administrator awareness in managing the system. While external factors due to the weakness of the system made so that the attacker can easily exploit the system. Risks due to internal or external effects cannot be eliminated but vulnerability assessment can reduce existing vulnerabilities or security holes. According to OWASP, there are three vulnerability assessment cycles, namely detection, report and remediation (OWASP 2019).

### 3. Methodology

As mentioned earlier, the methodology used is a black box test for vulnerability assessment of web applications using a set of combined tools to examine various security issues (Awang and Manaf 2013). This paper experimented web application testing uses a combination of OWASP-ZAP and OpenVAS. OWASP-ZAP and OpenVAS chosen because the software are free and easy to use. Using different tool to increase the probability of finding various types of vulnerability.



Fig. 1: Vulnerability Assessment Process

Fig. 1 explains process for vulnerability assessment test on web application target through four phases namely Information Gathering, Vulnerability Scanning, Result Analysis, and Reporting (Doshi and Trivedi 2015). Information Gathering – Define scope target and basic information about web application. Vulnerability Scanning – Begin with define tools uses for scanning, installing, and configure tool. After that, scanning web application target using vulnerability scanner tools. Result Analysis – After scanning complete with tools, analyze result of detection from tools and test manual to ensure result of detection from tools vulnerability scanning.

### 4. Test Result and Analysis

The focus on testing is to find vulnerabilities that may exist in educational basic data web applications. So that security recommendations will be given to improve the web application. The first step is to determine the target scope. After that using Nmap for gathering information.

```

Nmap scan report for dapo[redacted].id (2[redacted].[redacted].[redacted].[redacted])
Host is up (0.0040s latency).
rDNS record for 2[redacted].[redacted].[redacted].[redacted].id
Not shown: 996 filtered ports
PORT      STATE SERVICE      VERSION
21/tcp    closed ftp
80/tcp    open  http         Apache httpd 2.4.18 ((Ubuntu))
| http-cookie-flags:
| /:
|   PHPSESSID:
|   httponly flag not set
|_ http-favicon: Unknown favicon MD5: [redacted]
|_ http-methods:
|   Supported Methods: GET HEAD OPTIONS
|_ http-server-header: Apache/2.4.18 (Ubuntu)
|_ http-title: [redacted]
1723/tcp  open  ptp          linux (Firmware: 1)
8443/tcp  open  https-alt?
Device type: WAP|general purpose
Running: Actiontec embedded, Linux, Microsoft Windows XP
OS CPE: cpe:/h:actiontec:mi424wr-gen3i cpe:/o:linux:linux_kernel cpe:/o:microsoft:windo
ws_xp::sp3
OS details: Actiontec MI424WR-GEN3I WAP, Microsoft Windows XP SP3
  
```

Fig. 2: Nmap Information Gathering

Fig. 2 shows that the web application DNS Record with IPv4 2xx.xxx.xxx.xxx and several port are open such port 80 for http service, port 1723 for ptp service, etc. Other information from Nmap are like device type, OS details, etc. After get some information, begin vulnerability scanning with tools namely OWASP-ZAP and OpenVAS. The black box vulnerability testing using Kali Linux as operating system.

#### 4.1 Vulnerability scanner uses OWASP-ZAP

The Open Web Application Security Project Zed Attack Proxy (OWASP-ZAP) is one of popular open source free vulnerability security scanner tools and is actively development by an international team of volunteers. OWASP can find security vulnerabilities in web applications automatically. OWASP-ZAP is tool for penetration tester (pentester) to use for security testing. OWASP-ZAP also use while developing and testing a web application. Here is the result of vulnerability scanning basic educational data.

Table 1: Summary of detection on OWASP-ZAP

Risk Level	Total
High	1
Medium	2
Low	3
Informational	0

Table 1 shows the information after vulnerability scanning basic educational data web application using OWASP-ZAP. Total result of vulnerability scanning indicate that security system is insecure because there are many detected vulnerabilities and some of detection is high and medium level.

#### 4.2 Vulnerability scanner uses OpenVAS

The Open Vulnerability Assessment System (OpenVAS) is an open-source application that is used to scan for vulnerabilities. OpenVAS capabilities such as authenticated testing, various internet protocols, performance tuning, etc. OpenVAS was developed and managed by Greenbone Network since 2009. OpenVAS is open source under the GNU General Public License (GNU GPL) license.

Table 2: Summary of detection on OpenVAS

Risk Level	Total
High	2
Medium	29
Low	1
Informational	40

Table 2 shows the vulnerability information that was detected using OpenVAS. The vulnerability scanning results using OpenVAS more than OWASP-ZAP. These results indicate that web applications are not safe because there are many detected even many high and medium level vulnerabilities, including low and informational logs.

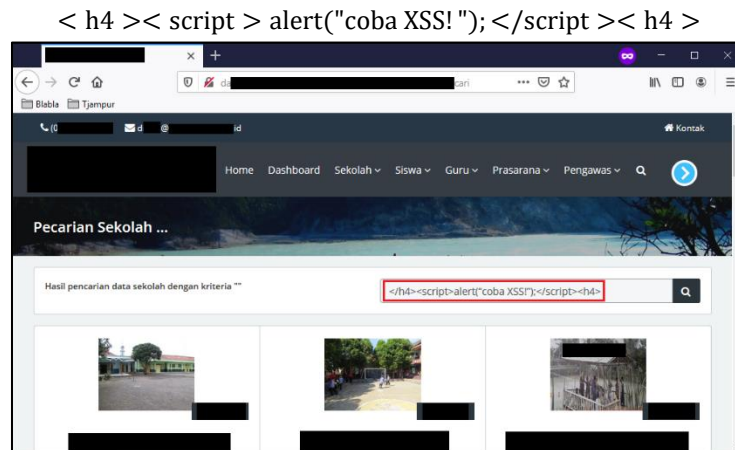
#### 4.3 Analysis Result

Table 3: Some Vulnerabilities Detected by The Application

Description	Nmap	OWASP-ZAP	OpenVAS
Cross-Site Scripting (Reflected)		✓	
Clear text transmission via HTTP			✓
Directory Browsing		✓	✓
Missing 'httpOnly' Cookie Attribute		✓	✓
Open Port	✓	✓	✓
Web Server Identification	✓		✓

Table 3 shows some vulnerability information detected through different applications. The result of vulnerability scanning can be used as parameter to minimize all forms attack from attacker. After get result from vulnerability scanning, next phase is result analysis. The analysis uses for validation that the detection from vulnerability scanner tools is valid. This paper analyzes several detections in high level not all detection result because too much. The first vulnerability detection found are cross-site Scripting (XSS), as a result of cross-site scripting injection, an attacker can bypass security on the client side, obtain sensitive information, and even insert dangerous

applications. So, the first step to validation is access the link that indicate XSS. After that, try inject with code in the search form, for example:



**Fig. 3: Try XSS**

After input inject code to search form, web application will respond by appearing in a pop up like figure 4 below.

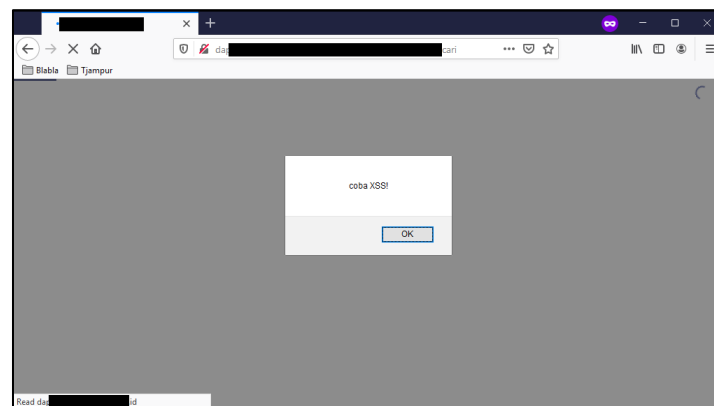


**Fig. 4: After submit XSS**

Another vulnerability detection found is clear text transmission. Clear text transmission is dangerous if accessed via public network such as café, airport, or others places that result in other parties can eavesdropping through a switch or router. So for first step is access the link that indicate clear text transmission. After that try to fill the form like figure 5 below

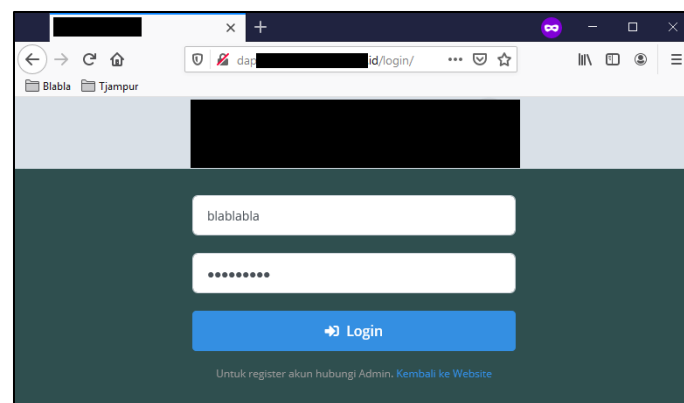


**Fig. 5: Login clear text**

Before submitting the form, start packet capture with Wireshark and see details in post method



4586	17.212790	1		1	HTTP	341 GET /msdownload/update/v3/static/trusted/en/disa...
4609	17.329079	1		1	HTTP	328 HTTP/1.1 304 Not Modified
4649	17.492618	1		1	TCP	1514 80 → 51946 [ACK] Seq=2030861 Ack=1 Win=55 Len=1460
5299	20.222946	1		1	HTTP	624 GET /linux/kali/dists/kali-rolling/main/binary-am...
8339	30.351564	1		2	HTTP	731 POST /login/login.php HTTP/1.1 (application/x-www...
8350	30.403426	2		1	HTTP	411 HTTP/1.1 200 OK (text/html)
8368	30.467545	1		2	HTTP	619 GET / HTTP/1.1
8464	30.636079	2		1	HTTP	702 HTTP/1.1 200 OK (text/html)
8488	30.715827	1		2	HTTP	572 GET /assets/img/slider/slider-1-cover.jpg?1570623...
8515	30.741669	1		2	HTTP	572 GET /assets/img/slider/slider-2-cover.jpg?1570623...
8736	31.019113	2		1	HTTP	1347 HTTP/1.1 200 OK (JPEG JFIF image)
9473	33.000041	2		1	HTTP	1367 HTTP/1.1 200 OK (JPEG JFIF image)

> Frame 8339: 731 bytes on wire (5848 bits), 731 bytes captured (5848 bits) on interface 0					
> Ethernet II, Src: Azurewaw_4c:17:93 (94:db:c9:4c:17:93), Dst: RuijieNe_4c:ad:c7 (58:69:6c:4c:ad:c7)					
> Internet Protocol Version 4, Src: 10.10.10.10, Dst: 203.113.1.1					
> Transmission Control Protocol, Src Port: 52056, Dst Port: 80, Seq: 1, Ack: 1, Len: 677					
> Hypertext Transfer Protocol					
▼ HTML Form URL Encoded: application/x-www-form-urlencoded					
> Form item: "user_id" = "blablalbla"					
> Form item: "sandi" = "123456789!"					

Fig. 6: Packet capture

## 5. Conclusion

This paper presents a black box testing approach for detection of vulnerabilities in web applications by selecting a set of tools in optimized and organized way. Based on the results of testing and analysis that has been done with the black box approach using a web vulnerability scanner tools shows that the basic data of education's website still has many vulnerabilities. The test results also show that scanning a web application using different tools will increase the probability of finding various types of vulnerability. High level of risks are found in this test, this indicate basic data of education website has high risk to be attacked. One solution for vulnerabilities found on this web application is by adding exception in source code in form section, such as login or search form. While the recommendations that can be done for Clear text transmission of sensitive information via HTTP is to use an SSL / TLS connection so that the communication between the client and the server is encrypted.

## 6. References

- Andress, Jason. 2014. *The Basics of Information Security Second Edition*. Waltham: Syngress.
- APJII. 2017. "Infografis Penetrasi & Perilaku Pengguna Internet Indonesia." APJII. Available at: <https://apjii.or.id/survei2017/download/brDi5U0PaVndoR9vfu8msNG1gEAzCQ> Accessed Desember 1, 2019.
- Awang, Nor Fatimah, and Azizah Abd Manaf. 2013. "Detecting Vulnerabilities in Web Applications Using and Automated Black Box and Manual Penetration Testing." *CCIS* 381, 230-239.
- Doshi, Jignesh, and Bhushan Trivedi. 2015. "Comparison of Vulnerability Assessment and Penetration Testing." *International Journal of Applied Information Systems (IJ AIS)* 8, 51-54.
- ISACA. 2017. *Vulnerability Assessment*. Rolling Meadows: ISACA.
- Khan, Mohd. Ehmer, and Farneena Khan. 2012. "A Comparative Study of White Box, Black Box and Grey Box Testing Techniques." *International Journal of Advanced Computer Science and Applications (IJACSA)*, 12-15.
- Minister of Education and Culture. 2015. *Peraturan Menteri Pendidikan dan Kebudayaan Nomor 79*. Jakarta: Minister of Education and Culture.
- National Institute of Standards and Technology. 2012. *NIST Special Publication 800-30 Revision 1 - Guide for Conducting Risk Assessments*. Gaithersburg: National Institute of Standards and Technology.
- Nieles, Michael, Kelley Dempsey, and Victoria Yan Pillitteri. 2017. *NIST Special Publication 800-12 Revision 1 - An Introduction to Information Security*. Gaithersburg: National Institute of Standards and Technohlogy.
- OWASP. 2017. "a" Category:OWASP Top Ten Project. Available at: [https://www.owasp.org/index.php/Category:OWASP\\_Top\\_Ten\\_Project](https://www.owasp.org/index.php/Category:OWASP_Top_Ten_Project). Accessed on December 1, 2019.
- . 2017. "b" "OWASP Top 10 2017." OWASP. Available at: [https://www.owasp.org/images/7/72/OWASP\\_Top\\_10-2017\\_%28en%29.pdf.pdf](https://www.owasp.org/images/7/72/OWASP_Top_10-2017_%28en%29.pdf.pdf). Accessed on December 1, 2019.
- OWASP. 2019. *Talk: OWASP Vulnerability Management Guide*. May 1. Available at: [https://www.owasp.org/index.php/Talk:OWASP\\_Vulnerability\\_Management\\_Guide#OWASP\\_Vulnerability\\_Management\\_Guide\\_v.1](https://www.owasp.org/index.php/Talk:OWASP_Vulnerability_Management_Guide#OWASP_Vulnerability_Management_Guide_v.1). Accessed on December 1, 2019.

# ANALYSIS OF POTENTIAL SECURITY ISSUES IN REGIONAL GOVERNMENT X WEBSITE USING SCANNING METHOD IN KALI LINUX

Jelita Putri Deviarinda<sup>1\*</sup>, Avon Budiyo<sup>2</sup>, and Ahmad Almaarif<sup>3</sup>

<sup>1 2 3</sup> Department of Information System, Telkom University, Bandung - INDONESIA

\* Corresponding author e-mail: [jelitaputrid@student.telkomuniversity.ac.id](mailto:jelitaputrid@student.telkomuniversity.ac.id),  
[avonbudi@telkomuniversity.ac.id](mailto:avonbudi@telkomuniversity.ac.id), [ahmadalmaarif@telkomuniversity.ac.id](mailto:ahmadalmaarif@telkomuniversity.ac.id)

## Abstract

The importance of website security is a top priority after data leakage or damage occurs. Website is a web page that is interconnected and contains a collection of information and can be accessed through the home page using a browser and internet network. According to the ministry of communications and information, 50% of the government's website is under threat from hacker attacks that can harm private information. Vulnerability assessment or process of identifying the weaknesses of a system can be an effective way to control and prevention against risks that occur. Given these problems, it is necessary to analyze the potential vulnerabilities on websites with vulnerability assessments aimed at preventing security vulnerabilities. In this study the analysis of potential website security loopholes was performed using scanning methods. The test is carried out with a vulnerability assessment using tools that are available on Linux and run on a virtual machine. Kali Linux is an operating system that has many tools including penetration testing, ethical hacking and network security assessment. This research was conducted using uniscan and nmap tools by scanning the target URL and assisted by using a web browser. The result of testing is to find a security vulnerability using a scanning method with tools and then giving the solution of the vulnerability it acquired.

*Keywords: Security, Website, Vulnerability Assessment, Scanning, Kali Linux*

---

## 1. Introduction

The development of technology in the current era is developing very rapidly. Information technology is a technology that can be used to process, obtain good data information, which is relevant, accurate information (Uno & Lamatenggo, 2011). The existence of information technology has enabled people to exchange information using Internet. Internet (Interconnected Network) is a network of computers that connect between networks globally, the Internet can also be called a natural network of a wide network (Sibero A. F., 2013). According to (APJII, 2018) Internet user in Indonesia has increased to 143.26 million people in 2017 or equivalent to 54.7 percent. The internet has a lot of information, one of which can be channeled through the website. Website is a web page that is interconnected and contains a collection of information and can be accessed through the home page using a browser and internet network. Based on the communication and Informatics White Book report in 2016 that a number of security incidents through Internet network in the domain of government is go.id often done cheating or data leakage (Iskandar, 2016). According to the Ministry of Communication and Informatics Office, 50% of Indonesia's government website is threatened by hacker attacks that can harm public personal data information.

Government is an agency to provide services to the community. There are many services provided by one of the online services which is a website that will facilitate the public in accessing information about the agencies in the government. Based on the report of the Communication and Informatics White Book year 2016 data obtained website with the domain go.id need a strong security to avoid attacks from outside Therefore, the purpose of this research is to find vulnerabilities and conduct analysis to prevent the occurrence of security vulnerabilities on government websites.

## 2. Literature review

### 2.1. Website

Website is a collection of information pages provided through Internet channels so that it can be accessed all over the world while connected to the Internet network without limited time and space (Suryayusra, 2014). According to Raharjo (Raharjo, 2011) website, is a service within the network of information space. As with Sibero (Sibero A. , 2013) website is a system related to documents and generally to display information in the form of text or images on the Internet network.

### 2.2. Website Security

Website security is important in building a website, good safety development is done at the beginning of the design of the website by the developer. Developers should follow the trend of attacks from hackers who always evolve with the development of Technology (Gultom & Mawaddah, 2015).

### 2.3. Vulnerability Assessment

Vulnerability Assessment (VA) is a process to identify or scan a system or software or network to find out defects and weaknesses. It also includes a series of systematic actions that are used to review and prioritize security vulnerabilities in network or communications systems or application services (Yaqoob, et al., 2017). Vulnerability Assessment is a systematic examination to determine the vulnerability to the information system and take precautions to minimize threats and reduce the risk of (Technology, 2013).

### 2.4. Technique of Vulnerability Assessment

Some of the Vulnerability Assessment techniques (Goel & Mehtre, 2015):

- Static Analysis

This technique do not run test cases or exploit. Static analysis is in this technique analyze the contents of the system and find out the types of vulnerabilities that exist and do not exploit the system. Weakness in this technique is requiring a lot of time for testing.

- Manual Testing

This technique do not require any tools or software to know the vulnerability. This technique tests by setting up a test plan manually or without a testing plan. On this technique do not use tools for testing and this technique is very less than on other techniques.

- Automated Testing

Automated testing technique uses automated vulnerability testing tool to determine vulnerabilities in the system. Accuracy in this technique is very good than other techniques. In this test use a scanner to test.

- Fuzz Testing

Known as fuzzing. Fuzz testing is done by inserting invalid data or any data into the system and then looking for crashes and failures. This technique can be used to determine the vulnerability of zero day.

### 4.1. Kali Linux

Kali Linux is a Linux security audit that is ready for companies based on Debian GNU or Linux. Security professionals usually use Linux times to do penetration testing, forensic analysis, and security audits. Kali Linux is a rolling distribution, meaning it will receive daily updates. The Menu on Kali Linux makes it easy to get tools for various tasks and activities including: Vulnerability analysis, Web application analysis, database assessment, password attack, sniffing and spoofing, forensics (Raphaël Hertzog & Aharoni, 2017).

## 3. Methodology

The research methods used in this study use testing method research (Hambling & Goethem, 2018), there are five phases in the study which is the cycle of testing. Start from Test Planning and Control, Test Analysis and Design, Test Implementation and Execution, Evaluating Exit Criteria and Reporting, and Test Closure Activities.

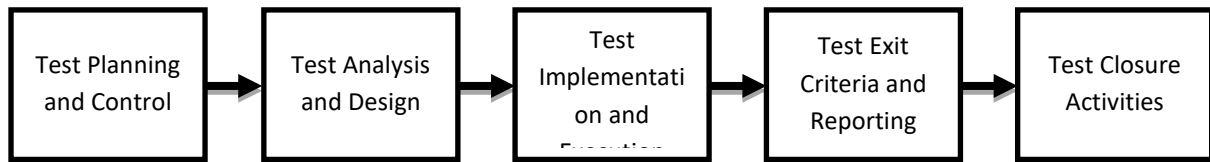


**Fig. 1: Testing Methodology (Hambling & Goethem, 2018)**

Fig. 1 explains the phase flow of the vulnerability testing methodology in research. Here is an explanation of each phase:

- **Test Planning and Control**  
Test planning is to create vulnerability criteria during testing. Criteria is when the testing process will end. The controls are what will be done if they do not match the plan as described in the test planning, after which the adjustments are made.
- **Test Analysis and Design**  
Test analysis and design focus on the details of what to test and how to combine it with a test case. Test analysis and Design is a bridge that connects between planning and execution.
- **Test Implementation and Execution**  
Implementation of testing and implementation involving test execution, and preparation before testing. This stage in execution using the uniscan and nmap tools and assisted by the Web browser.
- **Evacuating Exit Criteria and Reporting**  
At the stage of Evaluating Exit Criteria and Reporting will be evaluated on the outcome of the test execution, then it will be determined whether the testing expires or continues.
- **Test Closure Activities**  
The closure activity of the focus test to ensure that everything has been running well, the report is completed and bugs are closed.

This research will use all phases to test the vulnerability on target.

## 4. Experimental Result and Analysis

On this research focuses on the discovery of the vulnerabilities that exist on the target site X district and will provide recommendations to address the vulnerabilities found. The first step is test planning and control is planning the process will begin and expire. Next prepare the target website and test the vulnerability by using nmap, uniscan and assisted web browser tools that aim to get more information about the vulnerabilities that are on the website. The testing process is done on a virtual machine and uses operating system linux.

### 4.1. Vulnerability Assessment with Nmap Tools

Nmap is a port scanner that retrieves the IP address of the target machine or the hostname and then finds the basic information associated with it.

```

PORT      STATE SERVICE
53/tcp    open  domain
80/tcp    open  http
81/tcp    open  hosts2-ns
1723/tcp  open  pptp
2222/tcp  open  EtherNetIP-1
8443/tcp  open  https-alt

Read data files from: /usr/bin/./share/nmap
Nmap done: 1 IP address (1 host up) scanned in 62.01 seconds
Raw packets sent: 2042 (89.648KB) | Rcvd: 292 (11.704KB)
  
```

**Fig. 2: Scanning Nmap Port Result**

Fig. 2 is the result of the scanning of nmap on the target website. The following information that can be obtained:

- Port 53/tcp is a domain that has open port status.
- Port 80/tcp is a http that has open port status.
- Port 81/tcp is a hosts2-ns that has open port status.
- Port 1723/tcp is a pptp that has open port status.
- Port 2222/tcp is a EtherNetIP-1 that has open port status.
- Port 8443/tcp is a https-alt that has open port status.

```

PORT      STATE SERVICE      VERSION
113/tcp   closed ident
1723/tcp  open  pptp         linux (Firmware: 1)
8008/tcp  open  http         Fortinet FortiGuard block page
8443/tcp  open  https-alt?
Service Info: Host: local; Device: security-misc

```

Fig. 3: Scanning Nmap Port Result

Fig. 3 is Nmap port result scanning, in different command with Fig. 2 information that can be obtained is as follows:

- Port 113/tcp is a ident that has closed port status.
- Port 8008/tcp is a http Fortinet FortiGuard block page that has open port status.

## 4.2. Vulnerability Assessment with Uniscan Tools

Uniscan is an open-source penetration testing tool. Uniscan can scan vulnerabilities on target websites, folders, and security issues. Meanwhile, the administrator panel of the target website can be found through a directory check with Uniscan.

```

Directory check:
[+] CODE: 200 URL: .id/api/
[+] CODE: 200 URL: .id/assets/
[+] CODE: 200 URL: .id/file/
[+] CODE: 200 URL: .id/image/

```

Fig. 4: Directory Check Uniscan Result

Fig. 4 is the result of scanning Uniscan that displays the directory check on the target website it is .id/api, .id/assets, .id/file, .id/image.

```

File check:
[+] CODE: 200 URL: .go.id/error_log
[+] CODE: 200 URL: .go.id/home.php
[+] CODE: 200 URL: .go.id/index.php
[+] CODE: 200 URL: .go.id/login.php

```

Fig. 5: File Check Uniscan Result

Fig. 5 is the result of scanning Uniscan that displays the file check on the target website it is .id/error\_log, .id/home.php, .id/index.php, .id/login.php.

## 4.3. Directory Check and File Check Uniscan in the Web Browser

Web browsers are software to receive and present information over the Internet. At this stage the Web browser used chrome to check directories and files that have been testing on Uniscan tools.



**Fig. 6: Directory Check File**

Fig. 6 is a test in Web browser based testing on Uniscan that is in the Directory Check file section. In the Directory Check file section there is a file contents manual book.

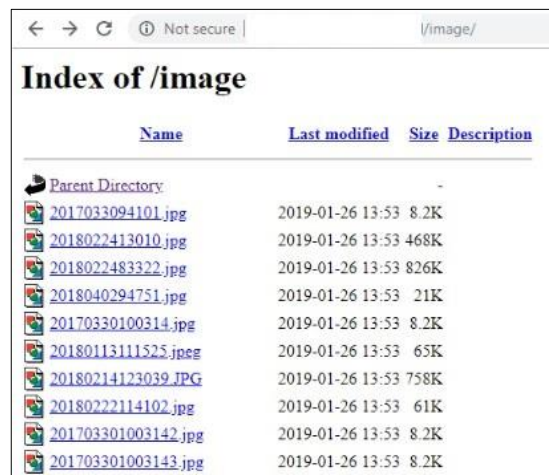


**Fig. 7: Directory Check Image**

Fig. 7 is a test in Web browser based testing on Uniscan that is in the directory check the image section. In the directory check the file section there are all images available on the target website and the size and last modified.



**Fig. 8: File Check Error Log**

Fig. 8 is a test in Web browser based testing on Uniscan that is in the file check error log. In the file check this section there are user information used with access time and modification.

## 5. Conclusion

Based on testing using different tools resulting in various kinds of vulnerabilities such as when conducting testing using uniscan tools and assisted with Web browsers is information obtained is found directory and files. Hackers can find out the information that is on the directory and files that are already in scanning. This information will be used by hackers in data retrieval. Testing using NMAP tools can show both open and closed ports and there are ports that need to be closed to avoid hackers use open ports to perform hacker and exploitations against the website. Website analysis by testing using Web browser is Google Chrome. The conclude on testing this hacker can find out the information the user name used. This information will be used by hackers in conducting tests using SQL Injection. Therefore it is recommended to immediately handle and upgrade the vulnerability because to minimize the occurrence of threats from outside.

## 6. References

- APJII, A. P. (2018, March 22). *Penetrasi Internet di Indonesia Capai 143 Juta Jiwa*. Retrieved from <https://apjii.or.id/download/file/BULETINAPJIIEDISI22Maret2018.pdf>
- Goel, J. N., & Mehtre, B. (2015). 3rd International Conference on Recent Trends in Computing 2015 (ICRTC-2015). *Vulnerability Assessment & Penetration Testing as a Cyber Defence Technology*, 712-713.
- Gultom, L. M., & Mawaddah, H. (2015). Analisis Celah Keamanan Website Instansi Pemerintah Di Sumatera Utara. *Teknovasi*, 1.
- Hambling, & Goethem. (2018). Testing Methodology. In L. J. Siagian, *Software Testing Automation* (pp. 6-8). Yogyakarta: Deepublish.
- Iskandar, B. Y. (2016). *BUKU PUTIH KOMUNIKASI DAN INFORMATIKA 2016*. Jakarta: Badan Litbang, SDM Kementerian Komunikasi dan Informatika.
- Raharjo, B. (2011). *Belajar Pemrograman Web*. Bandung: Modula.
- Raphaël Hertzog, J. O., & Aharoni, M. (2017). *Kali Linux Revealed Mastering the Penetration Testing Distribution*. USA: Offsec Press .
- Sibero, A. F. (2013). *Web Programming Power Pack*. Yogyakarta: MediaKom.
- Suryayusra. (2014). Analisis Web Vulnerability pada Portal Pemerintahan Kota Palembang menggunakan Acunetix Vulnerability.
- Technology, N. I. (2013). VULNERABILITY ASSESSMENT AND PENETRATION TESTING IN THE MILITARY AND IHL CONTEXT. *Security and Privacy Controls for Federal Information Systems and Organizations*, 53.
- Uno, H. B., & Lamatenggo, N. (2011). *Teknologi Komunikasi dan Informasi*. Jakarta: PT Bumi Aksara, cet 2 .
- Yaqoob, I., Hussain, S. A., Mamoon, S., Naseer, N., Akram, J., & Rehman, A. u. (2017). Penetration Testing and Vulnerability Assessment. 10-11.



## Design of Auto Height Check Machine Control System Based on PLC to Improve Quality the Complete Piston Rod Assembly Process

Syahril Ardi<sup>1</sup>, Chandra Kirana Kaomu<sup>2</sup>

<sup>1</sup>Mechatronics Department, Politeknik Manufaktur Astra, Jakarta, Indonesia

<sup>2</sup>Engineering Production & Manufacturing, Politeknik Manufaktur Astra

\* Corresponding author e-mail: Syahril.ardi@polman.astra.ac.id

### Abstract

This paper discusses research on improving the quality of the complete piston rod assembly process which is part of the OCU (Oil Cushion Unit) or rear assembly process. The complete piston rod functions to regulate fluid circulation when OCU experiences compression and rebound. The complete piston rod assembly process is a process of combining piston rods, dust seals, oil seals, rod guides, sub springs, valve stopper, leaf springs, non-return valves, leaf valves, special washer, pistons, and piston rings. A non-return valve, leaf valve, and special washer are thin circular plates. The part that has been assembled is checked in number and composition according to the standard. The problem in the complete piston rod assembly process is when the operator counts the number of non-return valves, leaf valves, and special washer according to the required amount. This is because of its very thin size and stickiness. Errors in the number of non-return valves, leaf valves, and special washer assembled will cause the complete piston rod to reject. Therefore, this study aims to provide a solution to these problems, namely designing an auto height check machine. This machine functions to check the number of non-return valves, leaf valves, and a special washer that has been assembled accurately. The auto height check machine control uses the Omron CJ1M-CPU11 PLC (Programmable Logic Controller) that is communicated with the Omron NS5-SQ10B-V2 HMI (Human Machine Interface). Input devices used are pushbuttons, selector switches, state switches, reed switches, emergency stops, and smart sensors. The output devices used are tower lamps and solenoid valves. Checking the number of non-return valves, leaf valves, and special washer using smart sensors. The result obtained after the existence of the auto height check machine is the reduction in the number of the complete piston rod which rejects from 5 pieces per day to 0 pieces per day.

*Keywords : non-return valve, leaf valve, a special washer, mesin auto height check, PLC*

---

### 1. Introduction

This research was conducted at one of the manufacturing industry companies in the field of automotive components with the main product being a shock absorber. The shock absorber is one component in two-wheeled vehicles and four-wheeled vehicles that function as vibration dampers. In two-wheeled vehicles, shock absorber can be divided into two types, namely: Front Fork (front) and Oil Cushion Unit (rear).

In the OCU assembly process, several stages occur, namely: sub assembly, assembly damper and mounting assy. Sub assembly is a line where the internal components of OCU are assembled. One of the processes contained in the line sub assembly is the complete piston rod assembly process. The complete piston rod functions to regulate fluid circulation when OCU experiences compression and rebound. The complete piston rod assembly process is a process of combining piston rods, dust seals, oil seals, rod guides, sub springs, valve stopper, leaf springs, non-return valves, leaf valves, special washer, pistons, and piston rings. A non-return valve, leaf valve, and special washer are thin circular plates. The part that has been assembled is checked in number and composition according to standard. When checking the operator has difficulty in calculating the number of the non-return valve, leaf valve, and special washer according to the amount needed because of its very thin size and stickiness. Errors in the number of non-return valves, leaf valves, and special washer assembled will cause the complete piston rod to reject.



Based on a request from the customer to replace the non-return valve, leaf valve, and special washer checking process which is still manual and to avoid mistakes in the complete piston rod (human error) checking process, so an auto height check machine is made. This machine functions to check the number of non-return valves, leaf valves, and a special washer that has been assembled accurately.

Some studies and research related to the design of this control system, namely the use of PLCs for various control systems, including (Alexander Fay, et.all, 2015); (Gökhan Gelena, Murat Uzamb, 2014). In addition, he has conducted various researches related to the use of PLCs as a control system and HMI, for various systems and machinery, especially in the area of manufacturing and automotive industries, including: (Ardi, S .; Defi, W.Y, 2018); (Ardi, S., Cascarine, L.T, 2018); (Ardi, S., Tommy, M.I., Afianto, 2018); (Ardi, S., Nugraha, Z.A, 2018); (Ardi, S., Ardyansyah, D, 2018); (Ardi, S., Ponco, A., Latief, R.A. 2017); (Ardi, S., Abdurrahman, H, 2017); (Ardi, S., Al-Rasyid, A, 2016). Furthermore, this research is focused on the design of a system that can control the machine auto height check on the complete piston rod assembly process. With the PLC controller and communicate with the HMI (Human Machine Interface).

## 2. Methodology

### 2.1 Product Introduction

The shock absorber or shock absorber is a tool to reduce vibrations that occur in two-wheeled vehicles or four-wheeled vehicles so that motorists are easier and more comfortable in controlling their vehicles. Fig. 1 shows the shock absorber.



**Fig. 1: Shock absorber (a) SA Standard (b) OCU (c) Strut (d) Front Fork**

In two-wheeled vehicles, shock absorber (SA) can be divided into 2 types, namely Oil Cushion Unit (OCU) and Front Fork. OCU is used at the rear of the vehicle and Front Fork is used at the front of the vehicle. Whereas in four-wheeled vehicles, there are types of SA Standard and Strut. In the shock absorber system on four-wheeled vehicles, the SA Standard type shock absorber is used at the rear of the vehicle and Strut type is used at the front of the vehicle. Besides functioning as a silencer, OCU and Strut shock absorbers also function as a vehicle body support.

### 2.2 Problem Solution

Based on the problems that exist in the complete piston rod checking process and the request from the customer to replace the non-return valve, leaf valve, and special washer checking process that is still manual, the solution to solve the problem, namely: made a machine that can check the number of non-return valve, leaf valve and special washer that has been assembled accurately.

Expected Machine Specifications are:

- The machine must be able to check the number of non-return valves, leaf valves, and a special washer that has been assembled accurately.
- The non-return valve, leaf valve, and special washer checking system uses the smart sensor type inductive sensor. Smart sensors are used to check the number of non-return valves, leaf valves, and a special washer that has been assembled. The checking method is carried out by measuring the thick dimensions of the number of non-return valves, leaf valves, and a special washer that has been assembled.
- The machine must be equipped with HMI. This aims to facilitate the user in monitoring.
- The machine must be equipped with a tower lamp. This is to find out the results of checking good or not good.
- The machine must be equipped with an emergency stop button. This button is used to stop the machine immediately. This is to avoid work accidents on the operator and the machine.

### 3. Design and Testing

#### 3.1 Auto Height Check Machine Design

Fig. 2 shows the auto height check machine design. The location of the actuator, input device, and output device are used more clearly can be seen in area 1, area 2, and area 3

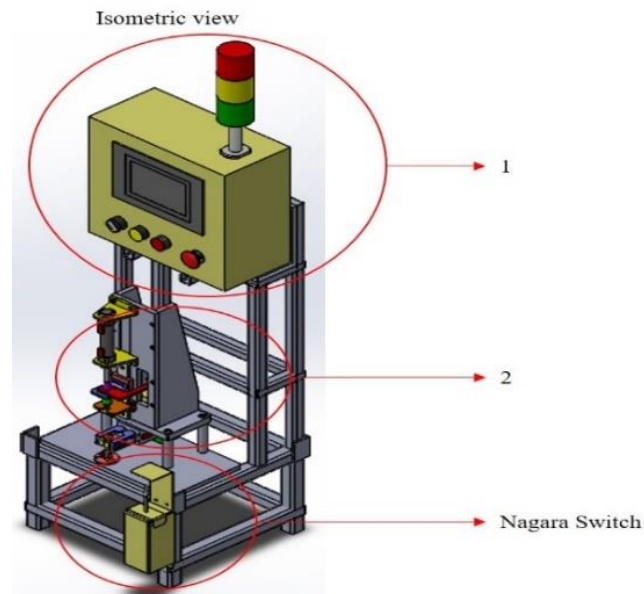


Fig. 2: Auto height check machine

#### 3.2 Electrical System Design: PLC wiring, HMI, and power supply with power supply

Fig. 3 shows the wiring of PLC, HMI, and power supply. The main voltage source used is AC 220V. This voltage source is then connected to the PLC and power supply. The power supply will change the AC voltage to 220V to DC 24V. The 24V DC voltage is then used to turn on the HMI.

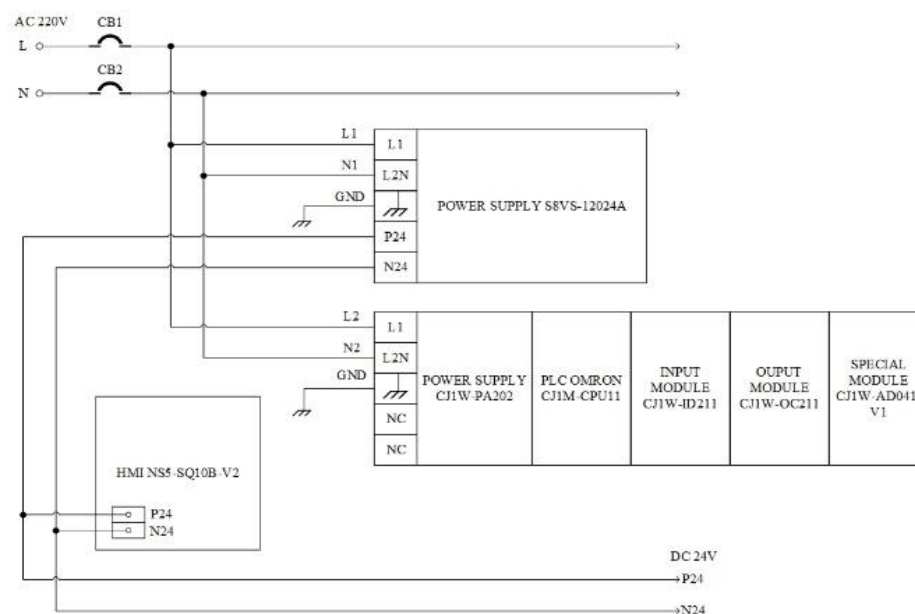


Fig. 3: Wiring of PLC, HMI, and power supply

### Wiring input components with PLC

It is a process of connecting input components with PLC. Input components that function to provide input will be connected to the PLC with certain addresses through the CJ1W-ID211 input module.

### Wiring the output component with PLC

It is a process of connecting the output components with a PLC. The output component will be connected to the PLC with certain addresses via the CJ1W-OC211 output module. The output component is an embodiment of the program algorithm.

### Smart sensor wiring with PLC

The smart sensor used is a smart sensor with an inductive sensor type. Smart sensors are activated with a voltage of DC 24V from the power supply. The way to connect a smart sensor with a PLC is to use the special module CJ1W-AD041-V1. Special module functions to convert analog data into binary data that can be processed by a PLC processor. Fig. 4 shows the wiring between the smart sensor and the PLC special module.

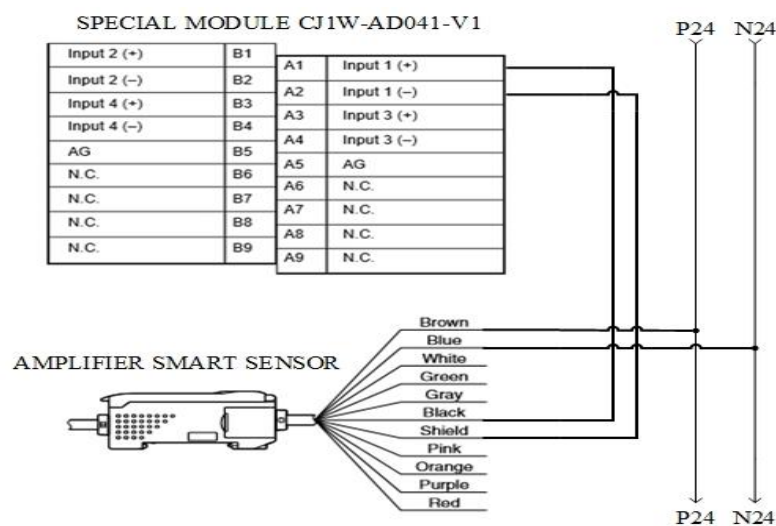


Fig. 4: The wiring between the smart sensor and the PLC special module

## 3.3 Testing

### PLC input Testing

How to test the PLC input can be done in 2 ways, namely by connecting the PLC with a personal computer (PC) through monitoring mode or can see directly through the status of LEDs that are on the PLC. Testing is done by pressing the push button, rotating the selector switch and activating the smart sensor. The OK parameter when testing the input is if the sensor, push button, selector switch, or another input device that is given a trigger or pressed will turn on the input contacts in the CX-Programmer monitoring mode according to the address of the input device respectively. OK, when the Input component is activated and the input contact is in active monitoring mode. NG parameter, i.e. when the Input component is activated and the input contact in monitoring mode is inactive.

### PLC output Testing

How to test the PLC output can be done by connecting the PLC with a personal computer (PC) through monitoring mode and can see directly through the status of LEDs that are on the PLC and by seeing changes or movement of the actuator used. The OK, when the output of the contacts in monitoring mode is activated and the output component is active. The NG parameter, i.e. when the Contacts output in monitoring mode is activated and the output component is inactive.

## 4. Results

The results obtained from the manufacture of auto height check machines include a decrease in the time of the complete piston rod assembly process, from 11 seconds to 9 seconds; a decline in the number of rejecting the complete piston rod from 5 pieces a day to 0 pieces per day. This data is taken based on OCU assembly production data and test results. The making of an auto height check machine gives good results to the complete piston rod checking process so that the results obtained from the checking process are more accurate.

## 5. Conclusion

In this paper, the design and manufacture of an automatic height check machine control system have been used using the Omron CJ1M-CPU11 PLC which is communicated with the Omron NS5-SQ10B-V2 HMI. Input devices used are push-buttons, selector switches, state switches, reed switches, emergency stops, and smart sensors. While the output devices used are tower lamp and solenoid valve. PLC as the brain of the auto height check machine regulates the input and output devices to produce a machine that can check the number of non-return valves, leaf valves, and a special washer that has been assembled accurately. Checking the number of non-return valves, leaf valves, and special washer uses smart sensors. The result obtained after the existence of an auto height check machine is the reduction in the number of the complete piston rod which rejects from 5 pcs per day to 0 pcs per day. For further research, this auto height check machine can add a buzzer alarm, so in the event of an error, an operator can immediately find out.

## 6. Acknowledgment

We would like to acknowledge the support of Mechatronics Department, Politeknik Manufaktur Astra, and an Astra Group Company in this research paper for their helping in the elaboration of this work.

## 7. References

- SMC. 2007. Reed Switch AutoSW Band Mounting Style.
- Yves dan Fiset J. 2009. Human-Machine Interface Design for Process Control Applications.
- Alexander Fay, et.al. 2015. Enhancing a model-based engineering approach for distributed manufacturing automation systems with characteristics and design patterns. *The Journal of Systems and Software* 101, 221–235.
- Gökhan Gelena, Murat Uzamb. 2014. The synthesis and PLC implementation of hybrid modular supervisors for real time control of an experimental manufacturing system. *Journal of Manufacturing Systems* 33, 535–550.
- Ardi, S.; Defi, W.Y. 2018. Control Systems Modification of Loading and Unloading in Oil Filling Machine Based on Programmable Logic Controller at Manufacturing Industry. *AIP Conference Proceedings* 2021, 060029.
- Ardi, S., Cascarine, L.T. 2018. Design Control System of Auto Air Remaining Machine based on Programmable Logic Controller in the Automotive Manufacturing Industry. *MATEC Web Conf.*, Volume 197, 2018, The 3rd Annual Applied Science and Engineering Conference (AASEC 2018).
- Ardi, S., Tommy, M.I., Afianto. 2018. Automation of Waste Treatment on the Washer Machine Based on PLC Control System in the Manufacturing Industry. July 2018.
- Ardi, S., Nugraha, Z.A. 2018. Design Control System of Washing Oil Pan Machine Based on PLC in the Automotive Manufacturing Industry. Published in: 2018 International Conference on Electrical Engineering and Informatics (ICEITICs) Date of Conference: 19-20 Sept. 2018, Date Added to IEEE Xplore: 29 November 2018, INSPEC Accession Number: 18290112.
- Ardi, S., Ardyansyah, D. 2018. Design Control Systems of Human Machine Interface in the NTVS-2894 Seat Grinder Machine to Increase the Productivity. *IOP Conference Series: Materials Science and Engineering*, 306 (1), 012112, (2018).
- Ardi, S., Ponco, A., Latief, R.A. 2017. Design of integrated SCADA systems in piston production manufacturing case study on the conveyor, the coolant, the hydraulic, and the alarm systems using PLC. *IEEE Xplore*, 187 – 191.
- Ardi, S., H Abdurrahman. 2017. Design of pokayoke systems to increase the efficiency of function check oxygen sensor machine using programmable logic controller in manufacturing industry, *IEEE Xplore*, 192 – 196.
- Ardi, S., Al-Rasyid, A. 2016. Design of Pokayoke Sensor Systems in Drill Oil Hole Machine to Detect the Presence of Drill using Programmable Logic Controller. *Advanced Science Letters* 22(7), pp. 1813-1816.

## The Usage of Quick Response Code and Captive Portal for Wi-Fi Security and Bandwidth

Muhammad Adam Nugraha<sup>1</sup>, Nyoman Bogi Aditya Karna<sup>1</sup>, and Ridha Muldina Negara<sup>1</sup>

<sup>1</sup> Department of Electrical Engineering, Telkom University (Tel-U), Bandung - INDONESIA

\* Corresponding author e-mail: adamanugraha@student.telkomuniversity.ac.id

### Abstract

Internet of Things (IoT) allows different devices to communicate with each other without the compulsion to use outdated-fashioned communication styles such as data cables, external flash drives, and disks. Nowadays, people connect their smartphones to Wi-Fi in the public area by manually inputting a Wi-Fi password on their smartphones, which is regarded as a problem, mainly when the password is complex and confusing. This research demonstrates the feasibility of using the Quick Response (QR) code and the Captive Portal featured in router Tenda W15E AC1200, to guard the Wi-Fi password and to avoid unwanted users from exploiting the Wi-Fi public area. Simulation by using an open source QR code generator software to acquire the Wi-Fi QR code and experimentation from both qualitative and quantitative approaches are therefore necessary. As a result, the safety of the Wi-Fi public area is protected as the password is not revealed to the user.

*Keywords: QR code, Wi-Fi, IoT, Captive Portal, Tenda W15E AC1200.*

---

### 1. Introduction

Currently, wireless technology is the world's leading competitor of wired technology and has become the world's first selling point for transmission technology. The primary reason for this is the simplicity of accessing the Internet of Things (IoT) and smartphones using Wi-Fi to make it effective for people to connect their devices to the Web so that they can access online media, education and social networking with various people around the world. Wi-Fi hotspots are an important part of the wireless infrastructure and are designed to improve user experience. Wi-Fi hotspots are no longer confined to regular top sites, such as airports or hotels, and move quickly to local retail stores, parks, restaurants and shopping centers [1].

Most customers who go to a restaurant just buy one or two cheap foods or drinks to get the restaurant's free Wi-Fi service. Subsequently, these customers take it for granted and end up staying in the restaurant for more than the average stay duration of typical restaurant customers. Although complicated numerical alphabetical letters are possible to be saved by the Wi-fi for its password, they are still insufficient. In research [2], Quick Response (QR) code is used to provide an efficient and secured way of locker loaning services.

The preventative solution proposed by this research is the introduction of a QR code and bandwidth limitation done by Captive Portal. The QR code is a technology that uses two-dimensional (2D) barcode for smartphones scanning to provide faster action [3]. It can deliver the restaurant's Wi-Fi password securely to customer's smartphones. Currently, the QR code is used by huge number of people daily due to its simplicity [4]. Captive Portal's bandwidth limitation is intended for those customers who remain in restaurant for too long to discourage them from exploiting the internet connection speed that reduces other customer's internet connection speed. As a result, the utilization of QR code and Captive Portal can greatly reduce losses for public area Wi-Fi businesses.

### 2. System design

In this research, QR code is used as it is the most efficient amongst the others barcodes with its ability to store embedded information and to provide smooth reading to the QR code scanner [4]. The Captive Portal feature is available inside the router Tenda W15E AC1200. This feature gives the authentication code to the customers along with bandwidth limitation, time session, and also to prevent any customer from abusing the Wi-Fi speed [5]. It is also capable to remove the access of any verified customers when a certain specified time has passed [6].

The configuration of the Captive Portal for bandwidth limitation and limit time session is shown in the Fig. 1. ZXing barcode scanner able to scan and decode QR code via the device by using the smartphones' camera [7]. However, not all smartphones are able to install the ZXing barcode scanner as it only supports android version 5 (Lollipop) and above [8].

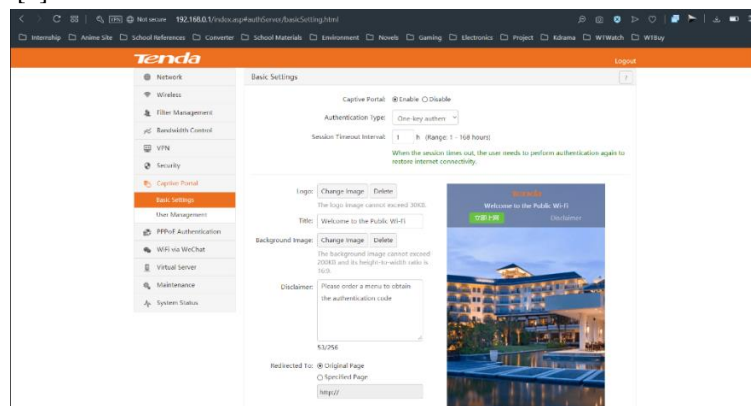


**Fig. 1: Configuration of Captive Portal in Tenda W15E AC1200 to Limit Bandwidth and Time Session.**

The Fig. 2 represents the block diagram of the system. The system starts when the customer is provided with a QR code. The customer uses a smartphone that has a QR code reader application installed to scan the QR code and obtain the password. The customer is then redirected to the Captive Portal web for the process of authentication done through the router Tenda W15E AC1200. If the verification is successful, the customer is then granted the Wi-Fi internet access with the provided bandwidth speed. If the verification via Captive Portal failed, the customer's smartphone is rejected from connecting to the public Wi-Fi.

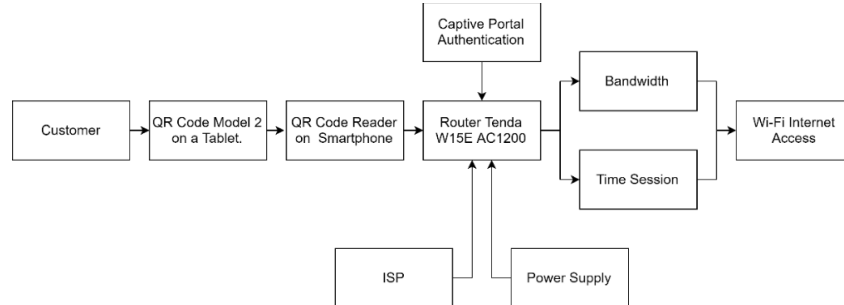


**Fig. 2: Block Diagram System.**

Fig. 3 shows the flowchart of the system. In this case, there are two situations; customer buys Wi-Fi service and customer does not buy Wi-Fi service.

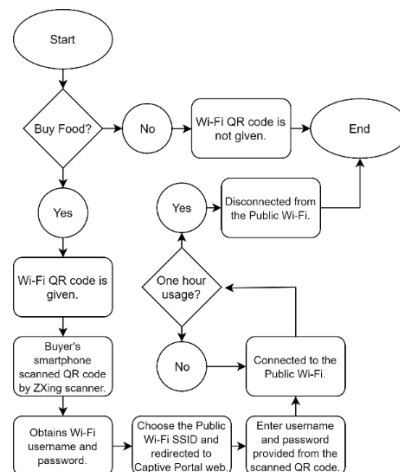


**Fig. 3: Flowchart of QR code and Captive Portal Implementation.**

### 3. Testing Results and Analysis

#### 3.1. Survey for the Effectiveness of QR Code and Captive Portal Implementation

The testing experiment is done to find out the qualitative measurement surveys from the public place users. The success criterion in this experiment is reached when the survey result shows that most of the survey takers are satisfied with the system proposed in this thesis. Based on Fig. 4, the results obtained are satisfactory as the percentage of the survey takers who are happy and satisfied with the implementation of these technologies are  $\geq 80\%$  in response to thirty-six number of respondents.

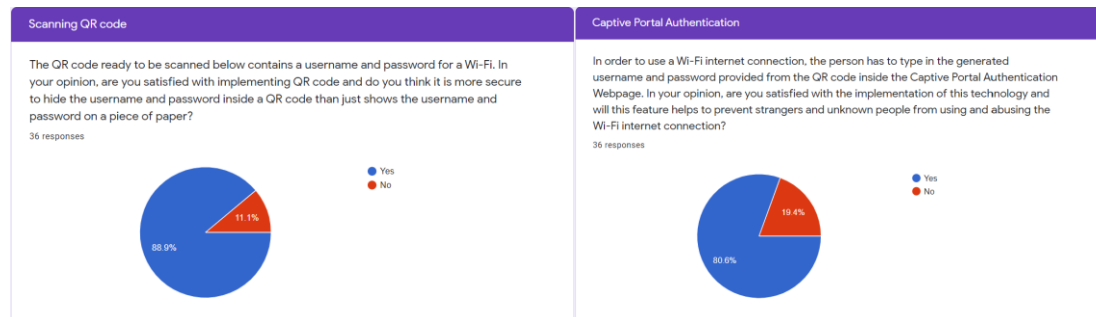


Fig. 5: Survey for the Implementation of QR code and Captive Portal.

#### 3.1. Optimal Distance and Average Time Taken

The testing to find the optimal distance of scanning the QR code is done by providing a range of distance from 0 cm to 200 cm. Meanwhile, the average time taken is earned after the sum of a repetition of three times of taking the time taken to scan the QR code in every tested distance divided by three. The Fig. 5 shows the setup of the devices during the testing experiment of finding the optimal angle and average time taken. The Tab. 1 shows the data obtained after testing the implementation of scanning the QR code through a range of distance and average time taken by a smartphone with ZXing Barcode Scanner installed. The result of scanning the QR code from range 0 cm to 15 cm is unsuccessful due to the location of the QR code is too closed with the smartphone used to scan. Meanwhile, from the range distance of 20 cm to 140 cm, the testing is successful. When the distance is made further than 140 cm, the QR code scanning failed due to its long distance. Based from the Tab. 1, the optimal distance to scan the QR code is at 20 cm with an average time taken of 145.5 ms for scanning the QR code.



Fig. 5: Optimal Distance and Average Time Taken Testing Experiment.

Table 1: The Successfulness of Scanning QR Code to Find the Optimal Distance and Average Time Taken.

Distance (cm)	Time Taken 1 (ms)	Time Taken 2 (ms)	Time Taken 3 (ms)	Avg Time Taken (ms)	Successfulness
0 - 19	-	-	-	-	No
20	157	145	134	145.4	Yes
30	161	165	138	154.7	Yes



40	141	264	148	184.4	Yes
50	204	143	160	169	Yes
60	148	173	145	155.4	Yes
70	211	151	135	165.7	Yes
80	172	173	195	180	Yes
90	160	155	195	170	Yes
100	178	195	196	189.7	Yes
110	232	190	200	207.4	Yes
120	437	611	512	520	Yes
130	342	150	202	231.4	Yes
140	1201	943	2301	1481.7	Yes
141 - 200	-	-	-	-	No

### 3.2. Optimal Angle Horizontally and Vertically

The testing experiment finding the optimal angle of scanning the QR code is done by providing a range of angle horizontally (X-Axis) and vertically (Y-Axis) from 0° to 360°, respectively. The Fig. 6 shows the setup of the devices to obtain the optimal angle in horizontal X-Axis. Based on the Tab. 2, the optimal angles to scan the QR code within the distance 20 cm are from range 0° to 50° and 310° to 360° horizontally and vertically. Other than these mentioned angles, the result of scanning the QR code is unsuccessful.

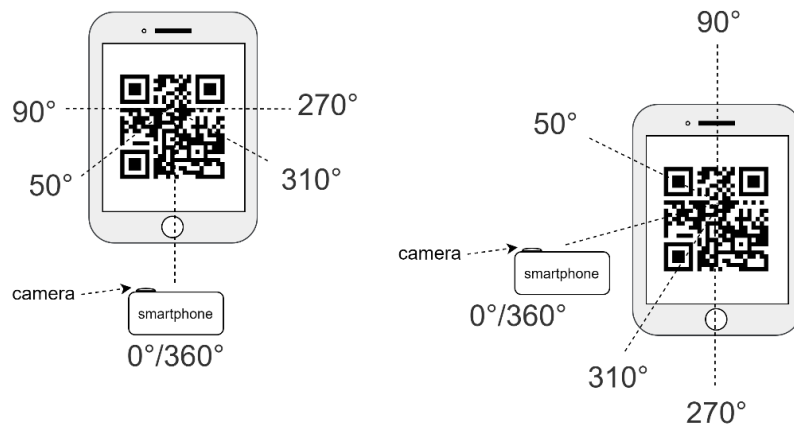


Fig. 6: Optimal Angle in Vertical Y-Axis Testing Experiment.

Table 2: The Successfulness of Scanning QR Code to Find the Optimal Vertical Y-Axis Angle.

Angle in Horizontal and Vertical (°)	Successfulness
0 – 50	Yes
51 – 309	No
310 - 360	Yes

### 3.3 Captive Portal Authentication

The testing experiment is required to make sure that the username and password generated by the QR code are possible to be used by the customers for login. In the Fig. 7, the customer failed to login through the Captive Portal authentication as the authentication is incorrect. The customer has to buy the service first such as food or drink. Then the customer gets a generated QR code containing the username and password that is to be scanned by the application ZXing barcode scanner. While, in the Fig. 8, the customer is able to login through the Captive Portal



authentication since the customer uses the provided and correct username and password generated by the QR code after scanning it with the ZXing QR code. The customer then gains an internet access for browsing, downloading, and uploading from the public area Wi-Fi for an hour long duration. After one hour of Wi-Fi usage, the customer gets disconnected from the Wi-Fi as the customer exceeded the time limit set from the configuration of the Captive Portal in the Tenda router. To obtain the internet access again, the customer has to buy the service again.

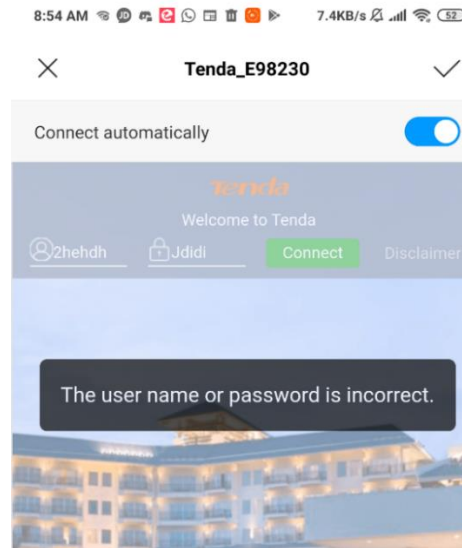


**Fig. 7: Failed Captive Portal Authentication During Testing Experiments.**

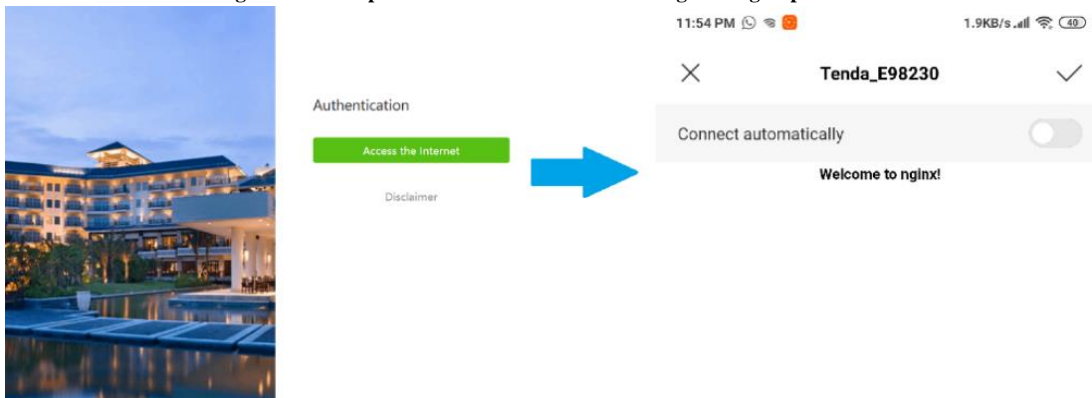


**Fig. 8: Succeeded Captive Portal Authentication During Testing Experiments.**

### 3.4 Internet Speed and Devices Connected

The testing to find the behavior of the Wi-Fi internet speed after the bandwidth is limited to 700 KB/s for downloading and 300 KB/s for uploading, and after the number of devices connected is increased. The testing is divided into two scenarios; download speed comparison during browsing only and when downloading a file and upload speed comparison during browsing only and when uploading a file. When the Wi-Fi is only served for browsing only, the internet speed remains the same of 700 KB/s regardless of the number of devices connected. However, when the Wi-Fi is used for downloading, the internet speed of the Wi-Fi decreases as the number of devices connected increases. When the number of devices connected is  $\leq 10$ . The average download speed for downloading remains  $\approx 700$  KB/s. But when the number of devices connected is 50, the average download speed is 269.5 KB/s as shown in the Tab. 3. When the Wi-Fi is only served for browsing only; not uploading, the internet speed remains the same of 300 KB/s regardless of the number of devices connected. However, when the Wi-Fi is used for uploading, the internet speed of the Wi-Fi decreases as the number of devices connected increases. When the number of devices connected is  $\leq 10$ . The average upload speed for uploading remains  $\approx 300$  KB/s. But if the number of devices connected is 50, the average upload speed is 240.8 KB/s as shown in the Tab. 4.

**Table 3: The Average Download Speed with Respect to the Number of Devices Connected.**

<b>Download Speed = 700 KB/s</b>		
<b>Number of Devices</b>	<b>Average Download Speed (KB/s) Browsing only</b>	<b>Average Download Speed (KB/s) Downloading</b>
0	700	700
10	700	700.5
20	700	632.3
30	700	479.4
40	700	343.8
50	700	269.5

**Table 4: The Average Upload Speed with Respect to the Number of Devices Connected.**

<b>Download Speed = 300 KB/s</b>		
<b>Number of Devices</b>	<b>Average Upload Speed (KB/s) Browsing only</b>	<b>Average Upload Speed (KB/s) Uploading</b>
0	300	301.2
10	300	301.2
20	300	288.5
30	300	273.4
40	300	343.8
50	300	269.5

## 4. Conclusion

The Wi-Fi username and password for Captive Portal authentication are given to the customer via the generated QR code. Captive Portal effectively prevents unknown people from connecting to Wi-Fi and limiting the Wi-Fi bandwidth internet speed. Based on the qualitative approach taken, more than 80% of the 36 respondents agreed and satisfied with the implementation of QR code and Captive Portal. Based on the quantitative approach taken, the optimal distance and angle to scan the QR code via ZXing barcode scanner are 20 cm with an average time taken of 145.4 ms, and 0° - 50° and 290° - 360° horizontally and vertically, respectively. The Wi-Fi internet speed is inversely proportional to the number of devices connected when the Wi-Fi is used actively for downloading and uploading.

## 5. References

- D. Arora, S. W. Neville and K. F. Li, "Mining WiFi Data for Business Intelligence," *2013 Eighth International Conference on P2P, Parallel, Grid, Cloud and Internet Computing*, Compiegne, 2013, pp. 394-398.
- R. M. Negara, R. Tulloh, N. Hadiansyah, and R. T. Zahra, "My locker : Loaning locker system based on QR code," *IJEAT*, 2019.
- C. Aktas, *The Evolution and Emergence OF QR Codes*. Cambridge Scholars Publishing, 2017.
- S. Tiwari, "An Introduction to QR Code Technology," *2016 International Conference on Information Technology (ICIT)*, Bhubaneswar, 2016, pp. 39-44.
- Tenda, AC1200 Wireless Hotspot Router W15E User Guide, available at: <https://gzhls.at/blob/ldb/e/e/9/8/407d3ed2892923da607ab50c4335c3029b1b.pdf>, accessed on November 5, 2019.
- B. Fleck and B. Potter, *802.11 Security*. O'Reilly, 2002.
- M. Zaslavsky, About ZXing, available at: <https://stackoverflow.com/tags/zxing/info>, accessed on April 1, 2019.
- R. Tulloh, R. M. Negara, Y. E. Y. Prasetya and S. Saputra, "HERO: Maximizing Student Potential to Mobilize Community Empowerment Activities Around Campus," *2019 International Conference of Artificial Intelligence and Information Technology (ICAIIIT)*, Yogyakarta, Indonesia, 2019, pp. 431-436.

## Design of IoT-Based Manufacturing Quality Control Systems with Exponentially Weighted Moving Average Chart

Bintang Wibawa Mukti\*, Cahyadi Nugraha and Fadillah Ramadhan

Department of Industrial Engineering, Institut Teknologi Nasional (Itenas), Bandung - INDONESIA

\* Corresponding author e-mail: bintangwibawamukti@yahoo.co.id

### Abstract

Quality control is needed for each manufacturing industry, so that product quality remains stable. Product variation is one of the factors that can reduce product quality, so quality control is needed. Control chart is one of the tools in statistical quality control that can be used to detect changes in product variations. One of the control charts that has a high sensitivity to the average shift is Exponentially Weighted Moving Average (EWMA) control chart. But in its implementation, the company still uses a manual process, starting from the process of data collection, data entry, to data processing into a control chart. Manual process can cause data collection errors and delays in quality decision. For EWMA control chart, the complicated calculation contributes additional difficulties for quality control implementation. The Internet of Things (IoT) is a concept that combines a device with other devices using internet connectivity, so that the distribution of data and information flow becomes faster and more accurate. Based on the IoT concept, a quality control design system is proposed that integrates data retrieval, data processing, control chart computation, and data display so that it can improve speed and accuracy in the process of making EWMA control chart. Based on testing, this system has been able to improve the accuracy of data retrieval and processing, speed up the process of making control charts, and integrate data collection, recording, and processing activities.

*Keywords: statistical process control, internet of things, exponentially weighted moving average, digital caliper, web-based system.*

### 1. Introduction

Product variation is a state when one product is not identical with another. Variations are caused by differences in treatment during the production process such as the condition of the equipment used or the way the operator processes the product. Large variations indicate that the quality of the product is low, because the product does not meet the standards desired by the enterprise. This causes the enterprise needs quality control to reduce these variations. Control chart is one of the tools in statistical process control to detect if the variations is out of control, so that corrective action can be taken to stabilize the process (Mitra, 2008).

There are several control charts, one of which is the Exponentially Weighted Moving Average (EWMA) control chart. The EWMA control chart is used to see variations based on the average shift in a production process. The EWMA control chart is used to analyze products that have variable data characteristics. The process of creating an EWMA control chart is different from other control charts. The EWMA control chart does not ignore data that has been previously plotted, so the latest data will always be influenced by previous data. This causes the EWMA control chart to have a higher sensitivity than other control charts in detecting average shifts (Montgomery, 2009).

The implementation of the monitoring process using the control chart is carried out through several processes such as measurement of product dimensions, recording, data entry, calculation, and making a control chart. Commonly in most mid-small companies the process is done manually. Starting from product measurement, product size recording, product data entry, to making control charts. Manually processing takes a long time and can cause delays in taking action. In addition, the chance of an error in data entry is quite high. Data entry errors can result in decreased accuracy of data processing on the control chart. So that it causes errors of action in quality control efforts (Ćwikła, 2013)

One way to overcome this is to utilize the concept of the Internet of Things (IoT) in the process of making a control chart. The concept of IoT can help the process of taking data, recording data, and processing control chart data. IoT helps integrate these activities more quickly and efficiently by using the internet network. In general, IoT is defined as a global network infrastructure where physical and virtual attributes in manufacturing systems are seamlessly integrated into the information network (Xu et al., 2014). According to Lee (2015), IoT is recognized as one of the most important fields of future technology and receives wide attention from various industries. IoT is an internet-based system that can connect other entities. The concept is that IoT can send and access data in real-time, thus speeding up the process of information dissemination. IoT in the manufacturing industry is used for various purposes, such as monitoring the state of the machine, taking data from sensors so as to assist companies in carrying out quality control (Mishra et al., 2018). Examples of uses such as using sensors to monitor product quality results. The sensor accepts data criteria on the product (size or color), after which the data is sent to the operator via the internet network. The data is received by the operator into computer software, so the operator can take action based on the data obtained.

Based on these problems, this research was conducted to designing a quality control system with a system that can integrate the measurement process, data entry, data calculation, and appearance of an IoT-based control chart with an output in the form of an EWMA control chart. System testing is carried out on Small Scale Manufacturing Laboratory (SSML) which is a manufacturing company. The resulting product has a critical value on the dimensions (variables) of the product. SSML still applies quality control in a conventional process. The process of archiving data size and data entry is still done manually by operators at SSML.

## 2. Exponentially weighted moving average control Chart

The EWMA control chart is able to detect if there is a cause of variability in the production floor. The cause of variability is detected through a shift in the average occurring in a process. That is because the EWMA control chart takes into account previous observation data, so that small shifts can be detected. The EWMA control chart is defined as follows:

$$Z_i = \lambda x_i + (1 - \lambda) Z_{i-1}, \quad (1)$$

$$UCL = \mu_0 + L\sigma \sqrt{\frac{\lambda}{(2-\lambda)} (1 - (1 - \lambda)^{2i})} \quad (2)$$

$$LCL = \mu_0 - L\sigma \sqrt{\frac{\lambda}{(2-\lambda)} (1 - (1 - \lambda)^{2i})} \quad (3)$$

In equations (1)  $Z_i$  is EWMA value, where the  $x_i$  is the observation value and  $\lambda$  is the smoothing value, the value ranges from  $0 < \lambda \leq 1$ . (2 and 3) UCL is upper control limit and LCL is lower control limit,  $\mu_0$  is the target value or observation mean,  $\sigma$  is the standard deviation, and  $L$  is the width of the control limits (Montgomery, 2009). The examples of EWMA control chart charts can be seen in Figure 1.

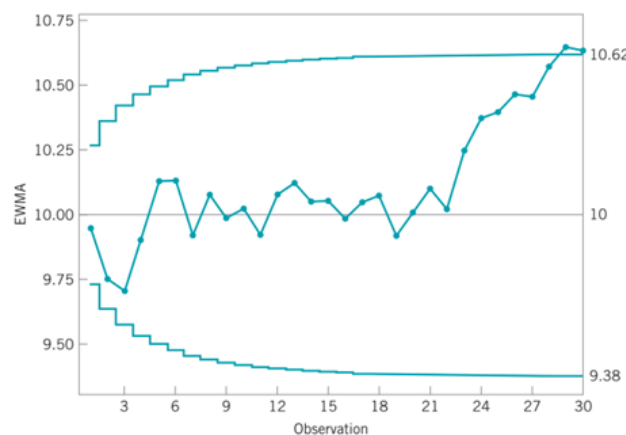


Fig. 1: Examples of EWMA Control Chart

### 3. Basic Concept of The System

The system design will be described in the form of architecture diagrams, information systems, and data flow diagrams. The system design is as follows.

#### 3.1 Architecture Diagrams

Computer architecture can be seen in Figure 2. The scheme of the tool designed is divided into three parts, namely client tier, logic tier, and database tier. Client tier shows how the system interacts directly with user and operator. Object measurement is using digital caliper Mitutoyo. Microcontroller is used to take the record data from digital caliper, and sending the measurement data to web application. Application tier shows applications that are on the system. The application will process measurement data received from the microcontroller. Tier database is a place to store measurement data. Measurement data is stored in a database so that the data is more organized and efficient if you want to use the data.

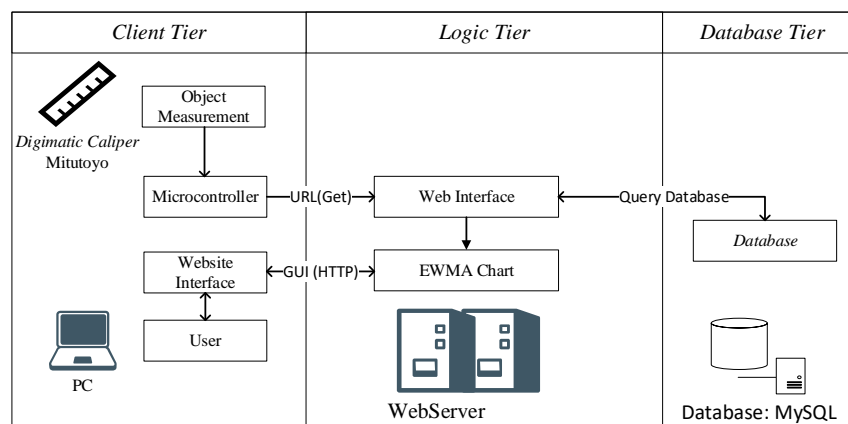


Fig. 2: Architecture Diagram

#### 3.2 Information Systems Flow

The flow of information systems is used as a description of the flow of logic that occurs in a system. The information system is depicted in a visual form in the form of a chart containing symbols. There are several entities that interact with the system, including measuring devices, microcontrollers, websites, users, and operators. The design of information system flow can be seen in Figure 3.

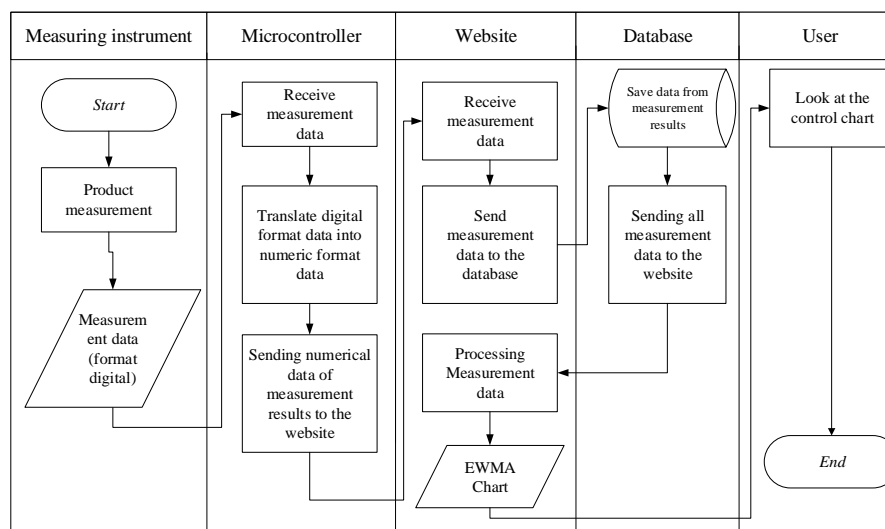
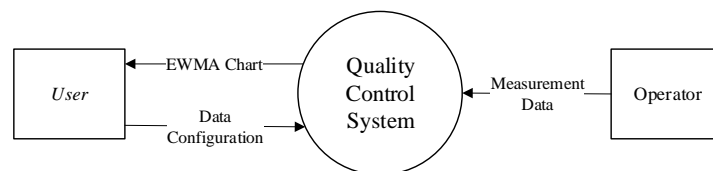


Fig. 3: Information Systems Flow

### 3.3 Data Flow Design

Data flow in the quality control system design is described in the form of Data Flow Diagrams (DFD). DFD has several diagrams, namely Context Diagrams, DFD level 1, and DFD level 2. Context diagrams are used as a preliminary description of the system before the DFD is described. Context diagrams illustrate how the system interacts with external entities. Context Diagrams can be seen in Figure 4.

DFD on this system contains two external entities, has five processes, and one data store. Entities in this system are operators and users. The processes contained in the system are data translation, data transmission, data processing, and data display. Data storage performed by the system is the measurement of numerical data from measurement results. DFD level 1 in the design of this quality control system can be seen in Figure 5. There is a more detailed description of the data flow from DFD level 1, namely DFD level 2. DFD level 2 in the design of this quality control system can be seen in Figure 6.



**Fig. 4: Context Diagrams**

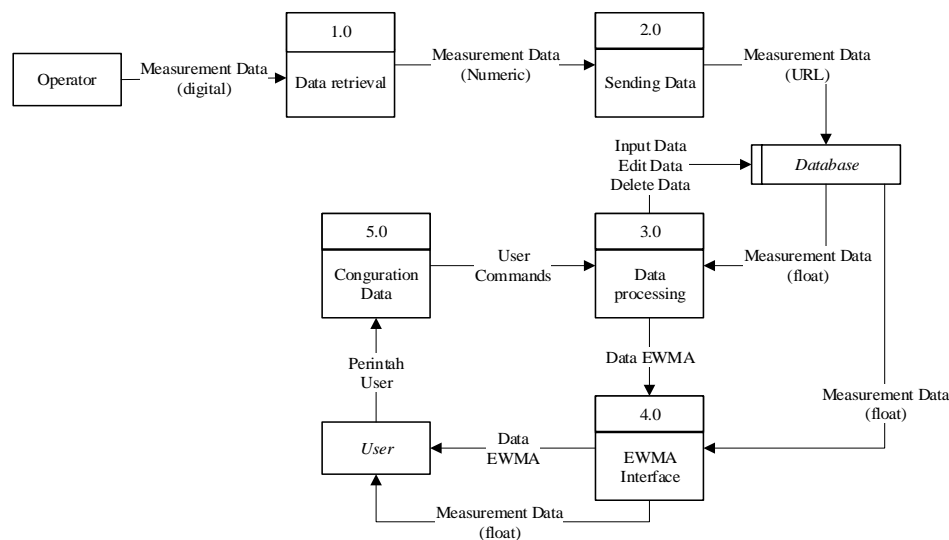


**Fig. 5: DFD Level 1**

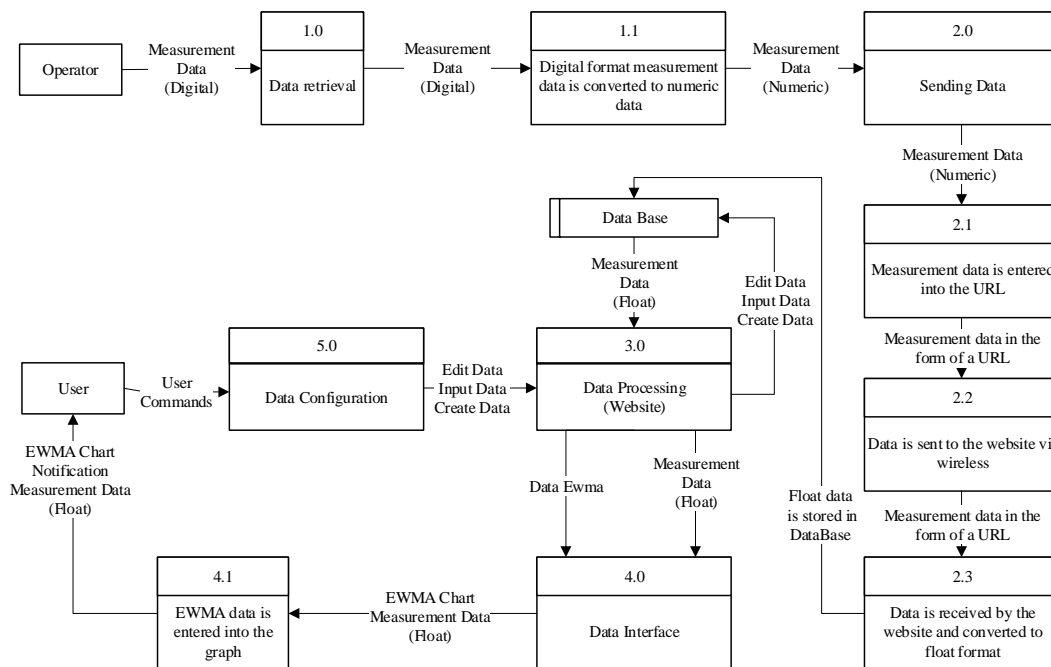


Fig. 6: DFD Level 2

## 4. System Prototype and Testing

The prototype system in this paper has been made and the system will be tested. The appearance of EWMA control chart in the website system can be seen in Figure 7. System testing is performed using measurement data on the Front Cover sub-product in Small Scale Manufacturing Laboratory and the output will be an EWMA control chart of the observed production system. Testing is done by taking 25 subgroup data, each of which contains 1 sample. Based on Figure 7 that there is data out of control, so the company needs to take corrective action on the production system. The results of EWMA control chart data processing from the system are in accordance with the results of data processing in the Minitab application, so it can be said that the accuracy of data processing on this system has been accurate.

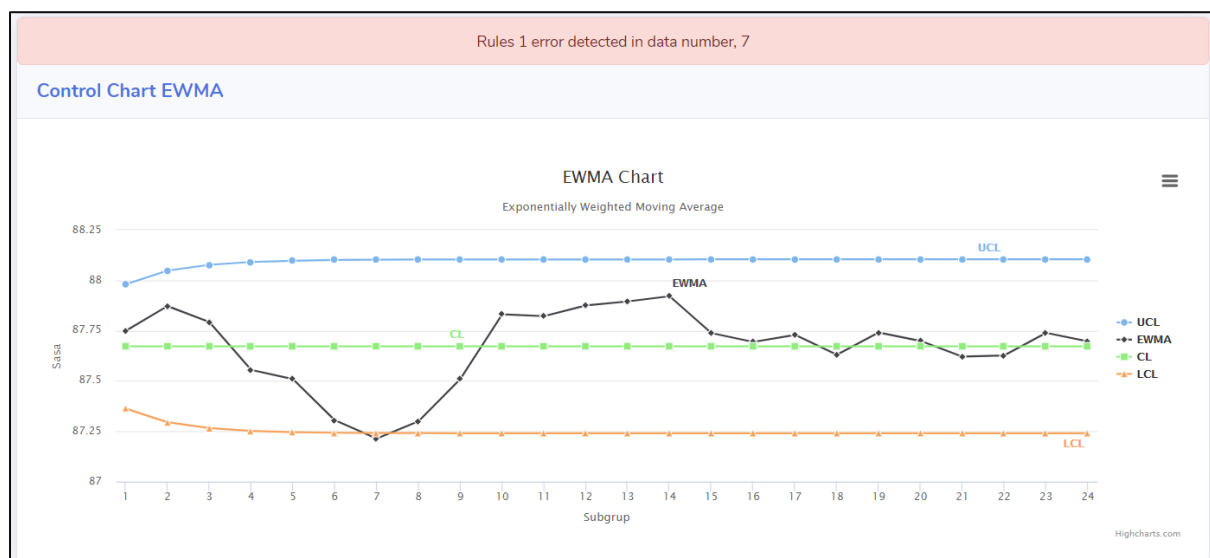


Fig. 7: EWMA Control Chart on System

After that, a comparison is made between the quality control process manually and the process using the system. This is to see whether the system can minimize time and improve data accuracy. The comparison between system and manually process can be seen in Table 2.

**Table 2: Comparison between System and Manually of Measurement Data and Recording Speed**

Measurement Data			Process Time		
No	Measurement Manually (mm)	Measurement Using Proposed System (mm)	No	Process Time Manually (seconds)	Process Time Using Proposed System (seconds)
1	87.93	87.93	1	192.1	4.53
2	88.16	88.16	2	196.8	5
3	87.61	87.61	3	196.72	5.2
4	87	87	4	197.18	4.6
5	87.4	87.4	5	200.15	5.33
6	86.83	86.83	6	201.75	4.2
7	87	87	7	197.13	4.75
8	87.5	87.5	8	199.24	4.79
9	88	88	9	197.54	5.02
10	88.58	88.58	10	199.41	5
11	87.8	87.8	11	193.12	4.92
12	88	88	12	195.11	5.74
13	87.94	87.94	13	200.68	5.35
14	87.98	87.98	14	218.14	5.6
15	87.31	87.31	15	214.12	4.45
16	87.59	87.59	16	201.67	4.8

**Table 2: Comparison between System and Manually of Measurement Data and Process Time (Continued)**

Measurement Data			Process Time		
No	Measurement Manually (mm)	Measurement Using Proposed System (mm)	No	Process Time Manually (seconds)	Process Time Using Proposed System (seconds)
17	87.81	87.81	17	208.48	5.12
18	87.4	87.4	18	210.7	4.63
19	88	88	19	208.88	3.21
20	87.6	87.6	20	220.51	4.25
21	87.44	87.44	21	232.07	5.22
22	87.64	87.64	22	230.4	4.62
23	88	88	23	217.1	5.74
24	87.68	87.6	24	215.41	3.37
25	87.17	87.17	25	232.83	4.13
Average				207.09	4.78

Based on Table 2 above, the time required in the measurement process, recording data to the database, and processing the EWMA control chart data with a manual process is 207.09 seconds. The time needed to carry out the process of measuring, recording data to the database, and processing the EWMA control chart data by the system is an average of 4.78 seconds for each measurement. Based on Table 2 above, it is shown that from 25 measurements, the measurement data results in the system are in accordance with the measurement data manually. This indicates that the accuracy of the data obtained from the measuring instrument is very good.



## 5. Conclusion

Based on the system that has been designed, the accuracy of the data obtained is accurate both for data collection and data processing. The system can reduce the possibility of errors in data collection, recording, and processing. Based on system testing, the time needed for the measurement, taking, and processing to become an EWMA control chart is only 4.78 seconds, compared to 207.09 seconds using manual process. This system has minimized the time needed to carry out EWMA-chart process control activities, making it easier and faster for the quality control section to detect out-of-control condition due to the shifting of process variations. The proposed system integrates process control activities, including: data measurement activities, data entry, data processing, and computational result display.

## 6. References

- Ćwikła, G. (2013) 'Methods of Manufacturing Data Acquisition for Production Management - A Review', *Advanced Materials Research*, 837, pp. 618–623. doi: 10.4028/www.scientific.net/amr.837.618.
- Lee, I. and Lee, K. (2015) 'The Internet of Things (IoT): Applications, investments, and challenges for enterprises', *Business Horizons*. 'Kelley School of Business, Indiana University', 58(4), pp. 431–440. doi: 10.1016/j.bushor.2015.03.008.
- Mishra, D. *et al.* (2018) 'A review on sensor based monitoring and control of friction stir welding process and a roadmap to Industry 4.0', *Journal of Manufacturing Processes*, 36, pp. 373–397. doi: 10.1016/j.jmapro.2018.10.016.
- Mitra, A. (2008) *Introduction to quality control and improvement*. 3rd ed. A John Wiley Sons Inc., New Jersey.
- Montgomery, D. (2009) *Introduction to Statistical Quality Control*. 6th edn. John Wiley & Sons, New York.
- Xu, L. Da, He, W. and Li, S. (2014) 'Internet of things in industries: A survey', *IEEE Transactions on Industrial Informatics*, 10(4), pp. 2233–2243. doi: 10.1109/TII.2014.2300753.

# Implementation Of The Internet of Things for $\bar{X}$ and R Control Chart in Quality Control

Aldi N. Firdaus\* , Cahyadi Nugraha and Fadillah Ramadhan

Departement of Industrial Engineering, Institut Teknologi Nasional (Itenas), Bandung – INDONESIA

e-mail: [aldinahlafirdaus@gmail.com](mailto:aldinahlafirdaus@gmail.com)

## Abstract

Quality control is one of the important things in an industrial enterprise, but in carrying out the process the enterprise is constrained by the speed, and accuracy produced by the quality control process. A set of basic quality control tools are  $\bar{X}$  and R control charts. These basic charting is sometimes face speed and accuracy problem due to the required measurement, data recording, and calculation processes. Considering these problems, an appropriate, fast and accurate quality control system is proposed and prototyped for computing the quality control process with the assistance of the Internet of Things. This system's prototype uses digital calliper, microcontroller-based wireless data recorder, database, and web-based application environment. System test is comprised of accuracy verification, speed comparison for quality control process, and process integration evaluation. System test has shown that this quality control system has the accuracy and speed in calculating the quality control process with an accuracy rate of 100% and a calculation speed of 4.731 seconds, significantly compared to manual system, so that it can overcome existing quality control problems.

**Keywords :** *Internet of Things (IoT), Statistical Process Control, Digital Caliper,  $\bar{X}$  and R Control Chart, Web Based System*

## 1. Introduction

Increasing the quality and productivity of a product has become an important element for all companies. All companies compete to produce high quality products (Zhang *et al.*, 2015), but in making this happen sometimes the companies forget to carry out a quality control process, according to Bakhtiar (2013), quality control is activities to ensure whether the policies made at the beginning in terms of quality or standards can be reflected in the final results produced, while according to Nastiti (2015), the notion of quality control is the number and attributes or characteristics as described in the product concerned. From these notions can be interpreted in other words that quality control is an activity carried out in order to maintain and direct the quality of the products produced in accordance with the plan that was determined at the beginning of production.

Changes in the world that are currently entering the industrial era 4.0 or the fourth industrial revolution are driving the rapid development of information technology in every industrial activity (Rohida, 2019). Industry 4.0 is also a promising thing for the development of the production control process, which in technical aspects will apply a concept called the Internet of Things (IoT) and Cyber Physical System (CPS) industry to run the company's production system (Xu *et al.*, 2014). Manufacturing industry and IoT are two inseparable things in the development of industry 4.0 in the current era. With the IoT all things that are in a manufacturing industry can be connected, so the company can receive information about the company's condition in real time (Mahdavi, 2007). This information can contain data regarding the execution of production orders, the effectiveness of machinery and equipment, the circulation of finished and semi-finished materials, and the quality of the products produced (Ćwikła, 2013).

Quality control is one of the important things in a company, there are a lot of methods and ways to control the quality of a product, but for companies that are starting to develop there is one quality tool that is often used in companies and is quite easy to do that is the control chart  $\bar{X}$  and R (Hidayatullah, 2018). The control chart is useful for monitoring the average size of the product produced, and can see how much variation in the size of the product produced, the data will be used as material for the analysis of the production process, to produce a stable product quality (Abdullah, 2010).

Companies that are starting to develop basically assume that the process for carrying out quality control requires quite a long time and requires additional experts who understand the quality control process, so the production control process is often missed (Gilchrist, 2016). However, with the current industry advances that have entered Industry 4.0, these constraints are very likely to be overcome. So that with the development of Industry 4.0, a quality control system can be carried out quickly, precisely, and accurately (Ferreira, 2018).

## 2. Design of the information flow system

The design of the information flow system describes the quality control system information flow that will be created, starting from the process of taking data to display data that will be presented on the web. This information flow starts from the measurement process which will be data in the form of digital measurement data which will later be sent to the microcontroller for processing. The following is a picture of the Design Of The Information Flow System, can be seen in Figure 1.

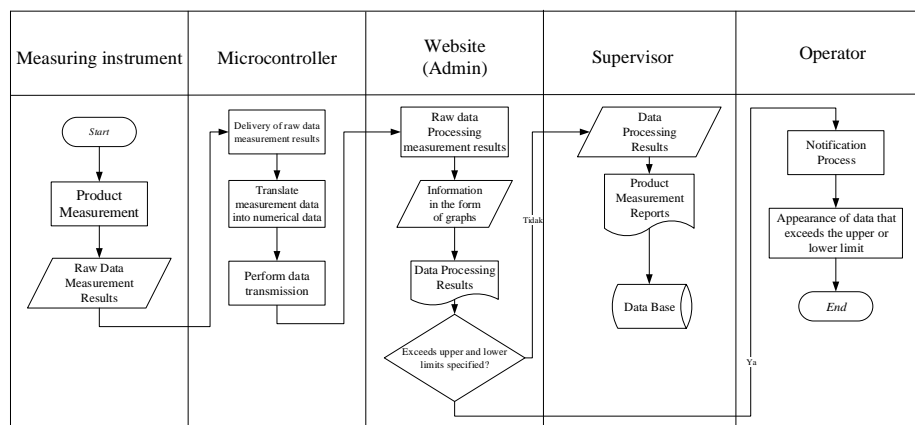


Fig. 1: Design Of The Information Flow System

### 2.1 Architecture Diagrams

This architectural system design is a picture of the entire quality control system that will be created starting from data retrieval to data appearance and storage in the database. The following is a picture of the architecture diagrams, can be seen in Figure 2.

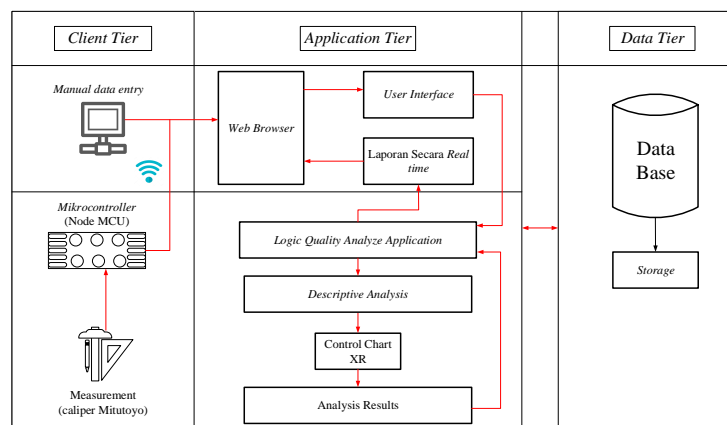


Fig. 2: Architecture Diagrams

## 2.2 Context Diagram

This context diagram draws all the inputs that enter the quality control system to be made, as well as all the outputs that are issued by the quality control system. Inputs that enter the system are the measurement data carried out by the operator and the management of the system by the admin who is the maker and manager of the web. As for the output released by the system, the information display will be used by the user to analyze the problems that occur in the production process. The following is a picture of the context diagram, can be seen in Figure 3.

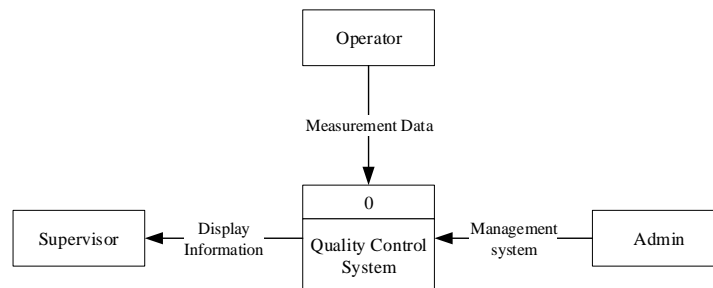


Fig. 3: Context Diagram

## 2.3 Data Flow Diagram Level 0 and level 1

Data Flow Diagram (DFD) level 0 is a more detailed development of the context diagram that has been made, which consists of operators, admins, and users. In level 0 DFD, the process that occurs between the system and the users of the system will be described again. Data Flow Diagram (DFD) level 1 is developed in more detail from DFD level 0, in DFD level 1 it will explain in more detail the data flow of each user starting from sending data to be displayed. The following is a picture of DFD level 0 and DFD level 1, can be seen in Figure 4a and 4b.

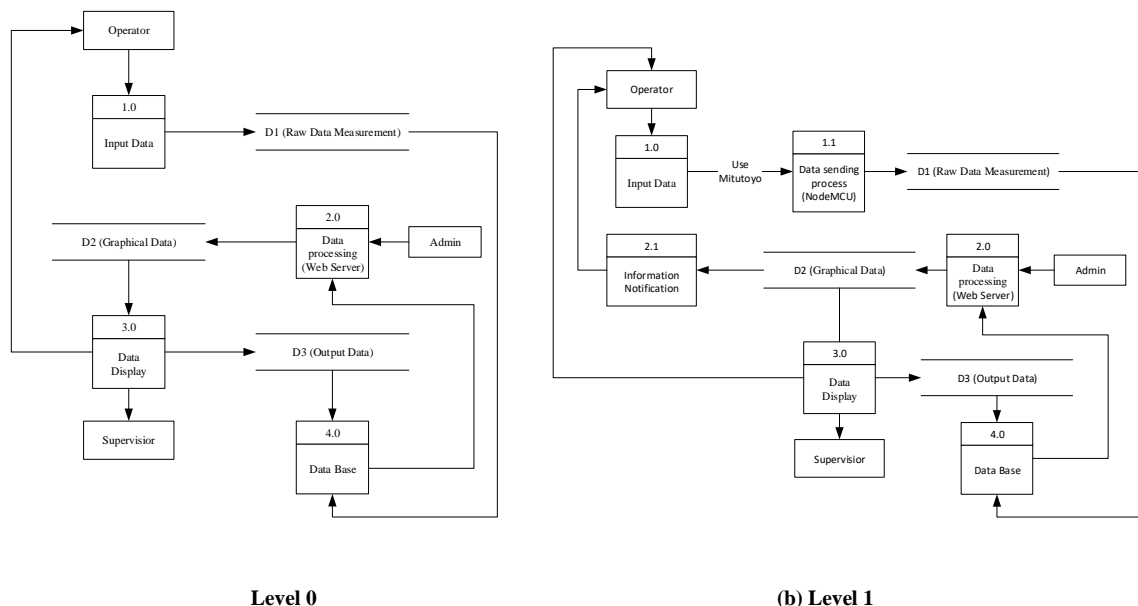


Fig. 4: Data Flow Diagram

### 3. Flowcharts of the data delivery

The design of this delivery system aims to explain how the system that is done by NodeMCU in sending dimensional data from digital signals sent by Mitutoyo until it can be received by the web server and entered into the database. The process of sending data is assisted with a push button that is useful for giving orders to send measurement results produced by the caliper mitutoyo. The following is a picture of the data delivery scheme, can be seen in Figure 5.

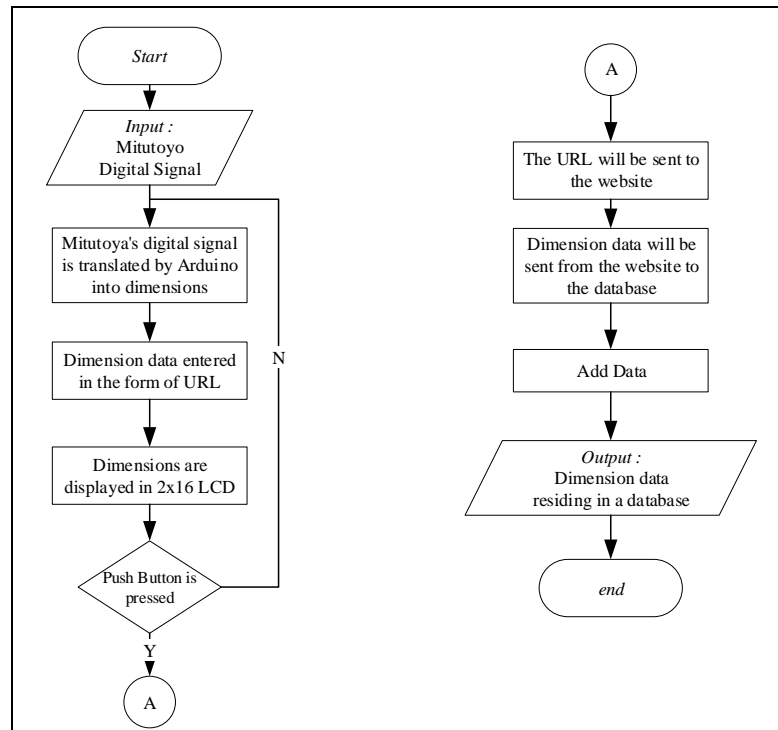


Fig. 5: Data Delivery scheme

### 4. Flowcharts of the data processing

This data reception design explains the next process after the measurement data has been received by the website and entered into the database. The measurement data will be processed into  $\bar{X}$  control chart data processing and R control chart. The following is a picture of the data processing scheme, can be seen in Figure 6.

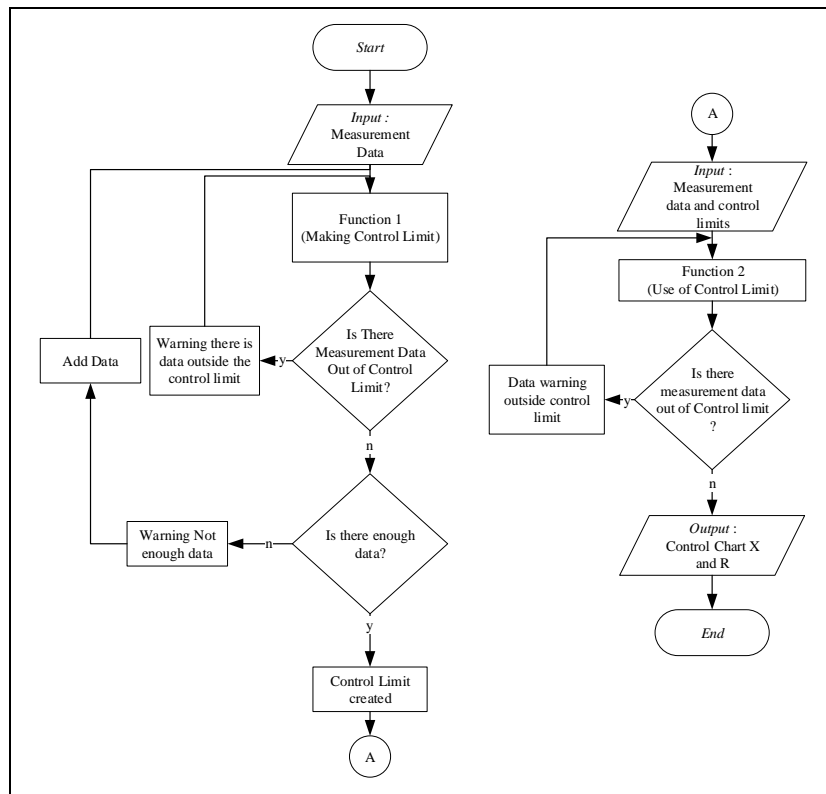


Fig. 6: Data Processing scheme

## 5. Program display design

This data appearance design will explain the data display from measurement data that has been received. The measurement data that has been received will be processed into a quality control tool in the form of  $\bar{X}$  and R control charts. The purpose of this data display system design is to make it easier for users to get information about  $\bar{X}$  and R control charts. The following is a picture of the program display design, can be seen in Figure 7.

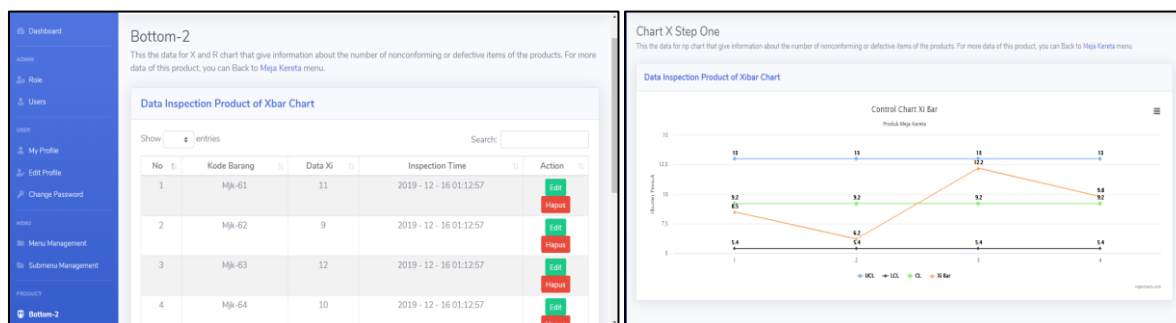


Fig. 7: Page Display

## 6. System testing

This system test is divided into several tests: accuracy testing and speed testing, the following is the result of that test. The following is a table of the comparison of measurement result and table of the comparison of counting speed, can be seen in Table 1 and 2.

Table 1: Comparison of Measurement Results

No	System Measurement Results (mm)	Digital Measurement (mm)	No	System Measurement Results (mm)	Digital Measurement (mm)
1	56.51	56.51	11	56.51	56.51
2	56.42	56.42	12	56.53	56.53
3	56.55	56.55	13	56.43	56.43
4	56.55	56.55	14	56.53	56.53
5	56.53	56.53	15	56.53	56.53
6	56.52	56.52	16	56.41	56.41
7	56.51	56.51	17	56.52	56.52
8	56.51	56.51	18	56.56	56.56
9	56.52	56.52	19	56.53	56.53
10	56.52	56.52	20	56.53	56.53

Table 2: Comparison of Counting Speed

No	Manual Counting Speed (seconds)	System Counting Speed (seconds)
1	181.32	4.38
2	179.67	5.23
3	185.45	3.66
4	175.44	4.67
5	180.65	5.11
6	177.68	5
7	189.01	5.06
8	175.01	4.34
9	177.33	5.43
10	178.45	4.43
Average	240.001	4.731

Based on the results of system testing that has been done, it is found that the accuracy of product size readings contained in the measuring instrument is the same as that displayed on the web page, this can show that the level of accuracy of sending data from the measuring tool to the web page is very accurate, so with a high level of accuracy this can help in the quality control process that will be applied.

However, in the time of sending data from measuring devices to web pages takes about 4.731 seconds before measurement data can be received by the web page. This causes the company to regulate the speed of its production so that there is no excess product buildup when conducting quality control processes.

## 7. Conclusion

The system that has been made has a fairly fast speed  $\bar{X}$  and R control charts. This is evidenced from the results of the comparison of the speed of calculating the system with manual calculations, where the proposed system's speed in on the average of 4.7 seconds while the manual process produces an average time of 240 seconds.

The system that has been made has high accuracy in reading measurement results, this can be proven from the results of comparison of measurement systems that have been done, where the results of reading the measurement system with digital measurements have the same results while the results of manual measurements have some differences with the measurements using digital tool. So that the system that has been created can produce an appropriate, fast and accurate quality control system in carrying out the quality control process by using the  $\bar{X}$  and R control charts.

## 8. References

- Abdullah, M.A (2010) Application of statistical control maps in controlling the production results of a company. (69).
- Bakhtiar, S., Tahir, S. and Hasni, R. A. (2013) 'Quality Control Analysis Using Statistical Quality Control (SQC) Methods', *Miej*, 2(1), pp. 29–36.
- Cwikla, G. (2013) Methods of Manufacturing Data Acquisition for Production Management - A Review. *Advanced Materials Research*, 837, pp. 618–623.
- Ferreira, F., & Guerra, H. (2018). The coordinate measuring machines, essential tools for quality control of dimensional and geometrical specifications of technical components, in the context of the industry 4.0. *Journal of Physics: Conference Series*, 1044(1), 0–6. <https://doi.org/10.1088/1742-6596/1044/1/012065>
- Gilchrist, A. (2016). Industry 4.0: The Industrial Internet of Things. In *Apress*. <https://doi.org/10.1007/978-1-4842-2047-4>
- Hidayatullah Elmas, M.S. (2018) Quality Control By Using Statistical Quality Control (Sqc) Methods To Minimize Failed Products At Barokah Bakery. *Wiga : Jurnal Penelitian Ilmu Ekonomi*, 7(1), pp. 15–22.
- Mahdavi, I., Shirazi, B., & Cho, N. (2007). A Framework of E-Based Quality Management for Distributed Manufacturing System. *Contemporary Management Research*, 3(2), 103–118.
- Nastiti, H. (2015) Analysis of Product Quality Control Using Statistical Quality Control Methods (Case Study: PT "X" Depok ). Pp. 414–423.
- Rohida, L. (2019) 'Pengaruh Era Revolusi Industri 4.0 terhadap Kompetensi Sumber Daya Manusia', *Jurnal Manajemen dan Bisnis Indonesia*, 6(1), pp. 114–136. doi: 10.31843/jmbi.v6i1.187.
- Xu, L. Da, He, W. and Li, S. (2014) 'Internet of things in industries: A survey', *IEEE Transactions on Industrial Informatics*, 10(4), pp. 2233–2243. doi: 10.1109/TII.2014.2300753.
- Zhang, Y., Wang, W., Liu, S. and Xie, G. (2014) 'Real-time shop-floor production performance analysis method for the internet of manufacturing things', *Advances in Mechanical Engineering*, 2014. doi: 10.1155/2014/270749.



## Design of Monitoring and Control of SCADA Systems on Curing Machine using PLC and HMI Wonderware InTouch

Syahril Ardi<sup>1\*</sup>, Nanda Indah Angger Lestari<sup>2</sup>

<sup>1</sup>Mechatronics Department, Politeknik Manufaktur Astra, Jakarta, Indonesia

<sup>2</sup>Engineering Production & Manufacturing, Politeknik Manufaktur Astra

\* Corresponding author e-mail: Syahril.ardi@polman.astra.ac.id

### Abstract

In this era, IoT applications in the manufacturing industry, especially in developing industry 4.0 continues to develop widely and rapidly. In this case, research related to the design and application of the Industrial Internet of things in the world of automotive manufacturing industry that produces tires for 2-wheeled vehicles. In the process of making a marketable tire, the process that is passed is the process of mixing, topping, extruding, bead wire, tire assembly, spraying, gimlet, and curing tire. In the last process, namely the curing tire, there is a process of collecting counter data which is carried out by the operator EBS (E-business switch), where the counter data collection is still done manually. After the data is retrieved, the EBS operator will input data into the EBS system. This process is considered inefficient because it is quite a time consuming, and the level of human error is quite high. This paper discusses the design and application of the SCADA System (Supervisory Control and Data Acquisition) on 6 curing machines using HMI Wonderware InTouch application, which functions for monitoring and control systems. In the PLC control system, it utilizes the Mitsubishi QJ71E71-100 Ethernet module as its communication module and uses Microsoft Access as a database. By designing this system, the level of accuracy produced is much higher. While EBS operators can monitor production results via a PC (Personal Computer) both in the interface, as well as data acquisition recorded in Microsoft Access.

*Keywords: Curing tire, PLC, SCADA, HMI Wonderware InTouch, Microsoft Access*

### 1. Introduction

This research was conducted at a manufacturing company that manufactures tires in a motorcycle. The process of making a tire in going through the following processes: the process of mixing, topping, extruding, bead wire, tire assembly, spraying, gimlet, and curing tire. In the tire curing process, there is a curing machine used to print a tire. Tire printing has raw materials in the form of green tires that have been made in the previous process. The raw material will be printed at a temperature of 175 °C for approximately 500 seconds, and the production results will be calculated with a digital counter that has been displayed on the machine's HMI. On each curing machine, there are 4 cavities, so that in one production will produce 4 tires at once.

In this process, there is a data retrieval activity of the amount of production of each cavity on the curing machine which is carried out by an EBS operator (E-business switch) every 45 minutes periodically. After the data is collected, the operator must then enter the data into the EBS system. This activity is considered inefficient because it takes a long time.

Furthermore, a SCADA system was designed on 6 curing machines, so that it can monitor and carry out the data acquisition process of the process that occurs. In this case, the interface designed for HMI Wonderware InTouch application, communication between the PLC and HMI via Ethernet, and testing the SCADA system.

Some studies and research related to the design of this control system, including (Owned, A, 2015); (G. Valencia-Palomo, J.A. Rossiter, 2011); (Wang, R., Song, X., Zhu, J., Gu, M, 2011); (Alexander Fay, et.all, 2015); (Gökhan Gelena, Murat Uzamb, 2014). Also, various studies have been conducted related to the use of PLCs as a control system and HMI, for various systems and machinery, especially in the area of manufacturing and automotive industries, including (Ardi, S. ; Defi, W.Y, 2018); (Ardi, S., Cascarine, L.T, 2018); (Ardi, S., Tommy, M.I., Afianto, 2018); (Ardi, S., Nugraha, Z.A, 2018); (Ardi, S., Ardyansyah, D, 2018); (Ardi, S., Ponco, A., Latief, R.A.

2017); (Ardi, S., Abdurrahman, H, 2017); (Ardi, S., Al-Rasyid, A, 2016); (Ardi, S., Wibowo, B, 2017); (Ardi, S., Kusuma, R, 2016); (Ardi, S., Hidayat, A. 2015) through 4 stages, namely connection testing, interface testing, program testing, and database testing.

This system has increased the accuracy of data counter retrieval (E-business Switch). Also, this SCADA system can be applied to other machines, i.e. with some address adjustments.

## 2. Methodology

### 2.1 Product Introduction

The company where this research was carried out, producing outer tires and inner tubes. Tires are devices that cover the wheels. Tires are an important part of land vehicles and are used to reduce vibrations caused by road surface irregularities, protect wheels from wear and damage, and provide stability between the vehicle and the ground to increase acceleration and facilitate movement. Fig. 1 shows the process of making an outer tire, which is mixing (the process of mixing raw material), extruding (the process to refine a compound), callendering (making material ply & steel belt, JLB & cap ply). Cutting bias is the process of cutting nylon cord from the callendering process diagonally at a certain angle to a sheet called ply with a width according to the desired specifications. Building tire assembly is all core material forming Tire such as Bead wire, Ply cord, Thread, which are combined into one. Curing is the process of cooking a green tire into a finished tire. The final inspection is the process of checking a tire, the tire is visually inspected for defects or not.

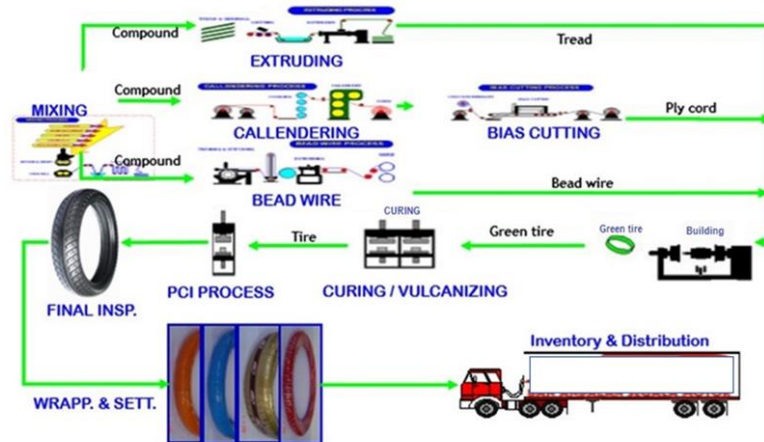


Fig.1: The process of making an outer tire

### 2.2 Curing Machines

The curing process is cooking or vulcanizing green tires into finished tires. Curing process or this cooking requires very hot temperatures and a very high amount of steam pressure. The green tire will be placed on the mold with the desired temperature for production. Fig. 2 shows an illustration a curing machine.



Fig. 2: an illustration a curing machine

### 2.3 Problem Analysis

The curing machine starts operating from the insertion of a green tire into the machine until it is finished cooking, then produces a finished tire, then sent to the next process. This process carried out continuously which is divided into 3 shifts in a day and the counter counts occur every time cooking and reset every shift. In this process, there is also an EBS Operator whose job is to retrieve the data counter manually. Data retrieval is done every 45 minutes for 1 shift, the operator will take as much as 8 times the data. Data retrieval is still done using a check-sheet and the operator goes around to each machine.

### 2.4 System criteria

The following are the required system criteria: creating a system that can be monitored remotely; on the interface, displays the counter, timer, and indication that the curing machine is on operated or not; interface that is easily understood by the user; have a security system so that not everyone can access the database; it can record production data on the curing machine for 3 shifts (24 hours); it can record accurate data.

### 2.5 Network Topology

Each curing machine is controlled by a Mitsubishi FX3U PLC, then the data from the PLC. It will be transferred to the PLC master, the Mitsubishi Q02U PLC via CC-Link. Fig. 3 shows the network topology. The curing process is cooking or vulcanizing green tires into finished tires. Curing process or this cooking requires very hot temperatures and a very high amount of steam pressure. The green tire will be placed on the mold with the desired temperature for production.

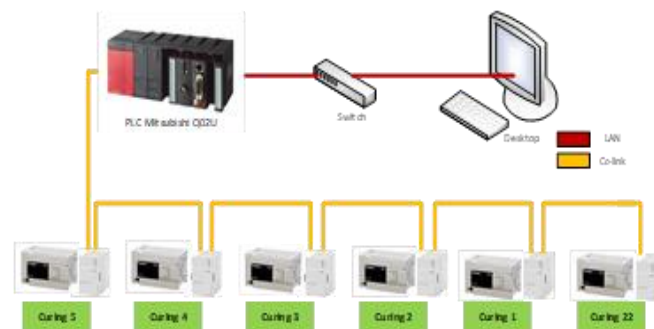


Fig. 3: Network topology

### 2.6 Interface design

From the pre-existing criteria, the following windows will be created, namely: Window log in, Window counter, Window chart counter, Window chart timer, and Window record

### 2.7 Program Design

When the user starts the system, the first window that will appear in the login window, after logging in, the next window that opens is the main window, the window counter on the curing machine. Two types of users can access this page, namely operator and guest. A striking difference between the two users is the range of access, the operator can open up to a database and graphics, but for guests can only monitor the main page. In this window, there are several other options (if the operator logs in), namely, the timer graph button, counter graph, and record. When the operator selects the timer graph button, it will display the timer graph screen of each curing machine historically, or this graph records the time data from the curing machine. When the operator selects the counter graph button, it displays a graph of the results of the curing machine. And when the operator selects a button to record, it will display a window for the operator to activate the connection between Wonderware and Microsoft access.

## 2.8 Database Design

In creating a database, Microsoft Access is used. The table to be displayed is a table that contains the main data needed by the EBS operator, namely the date of data retrieval, the time of data retrieval, the results of production of each cavity on each machine, and the total production results of each machine. The database will record the results every minute.

## 3. Results and Discussion

### 3.1 SCADA System Design

#### Design of Connections Between Applications

In this case, the System Management Console software is used as a protocol between PLCs Mitsubishi Q02U with Wonderware InTouch. The communication module used on the PLC is the Ethernet module QJ71E71-100, because it uses the Ethernet module, the communication used is DASMTEthernet. In making connections there are several stages, the first is to create new channels and devices, this channel functions in configuring each of the existing games on objects on InTouch. Next is to set the PLC id and module. The order of determining the ID for the SMC is (255.255.255.255: N <Net Number>: <PC Number>). In the first part, 255.255.255.255 is replaced by the IP address of the Ethernet module used and the last is to create a new device group.

#### Design of the Interface

Several types of windows exist, the first is the login window, where the user must log in first. Window counter all serves to display the main data needed by the operator such as cavity lights, cavity counters, curing timers, manual-auto indicators, exhaust indicators and curing indicators on-off. Fig. 4 displays the counter window and Table 1 shows the tag name on one of the machines, namely curing machine number 1.



Fig. 4: Counter all window

Table 1: Tag name on Curing machine 1

No	Name	Tag name	Tag Type
1	Lamp of cavity 1	Lamp1	I/O Discrete
2	Counter cavity 1	C1A	I/O Real
3	Lamp of cavity 2	Lamp2	I/O Discrete
4	Counter cavity 2	C1B	I/O Real
5	Lamp of cavity 3	Lamp3	I/O Discrete
6	Counter cavity 3	C1C	I/O Real
7	Lamp of cavity 4	Lamp4	I/O Discrete
8	Counter cavity 4	C1D	I/O Real
13	Timer Curing	C1Timer	I/O Real
14	Indicator of man-auto	LampPower1	I/O Discrete
15	Indicator of exhaust	Exhaust1	I/O Discrete
16	Curing on/off	Power1	I/O Discrete

The third window is the counter graph window, this window serves to display the amount of curing machine production in real-time.

The next window is the timer graph window, where this window contains historical graphs, the purpose of historical here is that the previous time graphs can be saved to the system. Figure 4 shows an example of the graphic display in curing choice number 1.

In making the Interfaces that can be run as desired, there are several compiler objects, namely, historical trend charts, legend trends. The last is the close button, this button allows you to close the window and return to the timer graph window. The last window is the record window, this window serves to display a button to activate the connection between Wonderware and the database that is on Microsoft Access.

### **Input-Output Configuration**

A new device and channel have been created in the System Management Console application before, the name of the device group is "mits" with an interval of 100 milliseconds. At each tag name when the type of the tag name is changed to type Input-Output, be it real Input-Output, discrete Input-Output, or analog Input-Output, the access name section will appear, in this section, the name of the device group will be added. was made. The first thing in making an access name is to create a new access name. Select the menu dictionary game, and select the access name button, then a list view will appear from the existing access name.

The next step is to open the device item in the System Management Console. After successfully opening device items, then 2 parts must be input, namely the name and the item reference section. The name part is the game that has been created in the Wonderware InTouch, while the item reference is the source of data that is in the PLC program.

### **Design of Database**

Design of database consists of 3 main stages, namely creating a table on Microsoft access, then uploading the table that has been made to the ODBC data source and after uploading it, the wonder software intouch is made a bindlist. Bindlist functions to connect between a label in a Microsoft access table and a tagname in a Wonderware InTouch. For example, the C1A tagname will be displayed in column 1A, C1B will be displayed in column 2A, and so on. After creating a bindlist, settings in the script window must also be done because this will affect the retrieval of data that will later be stored in the database.

### **3.2. Testing**

Testing on this system is done after making connections, interfaces, and databases. This process is carried out to determine whether the design to manufacture has been functioning properly and as expected. Testing is divided into 4 parts, namely connection testing, interface testing, program testing, and database testing. Connection testing is done by ascertaining whether Wonderware InTouch can communicate with PLC or not. Communication between PLC and Wonderware InTouch uses the System Management Console software. Interface testing is done by running the program on Wonderware InTouch, various objects exist in each window. This test is done to see whether all components on the interface are running by the target. After testing the interface, it continues with the program testing. This test is done by aligning the active address on the PLC and the existing indicators on the Wonderware InTouch. In this experiment, a program reading from the PLC must be carried out, to monitor the program directly so that the test will give accurate results. When testing the program has been carried out, then the next is to test the database. This test is carried out to see whether the database is in line with expectations or still, has shortcomings that must be added.

### **3.3 Discussion**

After doing various kinds of tests, such as connection testing, interface testing, program testing, and database testing. It can be concluded that the results are quite by the objectives of the author. The window counter all can display the data needed and display accurate data. Experiments are conducted at the beginning of shift 1, where at the beginning of every shift, the operator will reset the counter, and the calculation of production will start at 0.

After Wonderware has successfully displayed data, the next thing is to activate the connection between the database and Wonderware. The results obtained are Wonderware successfully communicating with Microsoft Access, this is marked in the error message section in the record window will display the results "no error

occurred" and the data in Wonderware InTouch can be recorded in Microsoft Access. If previously the operator is still doing data retrieval by visiting curing machines one by one, then with this system, the operator does not need to directly retrieve data. Operators only log in to InTouch Wonderware and retrieve records that are already in Microsoft Access. Human error is reduced by 100% because the data is taken directly from the PLC without manually retrieving it. Some additional features can also help the operator in analyzing work performance or problems that exist on the curing machine. Like when on one shift, if the production target is not reached, then the operator can see whether each cavity is working continuously, or there is one cavity that is not working. In Figure 5 the left shows the overall curing machine timer graph. Whereas in Fig. 5 the right shows the timer graph on the curing machine no. 3.

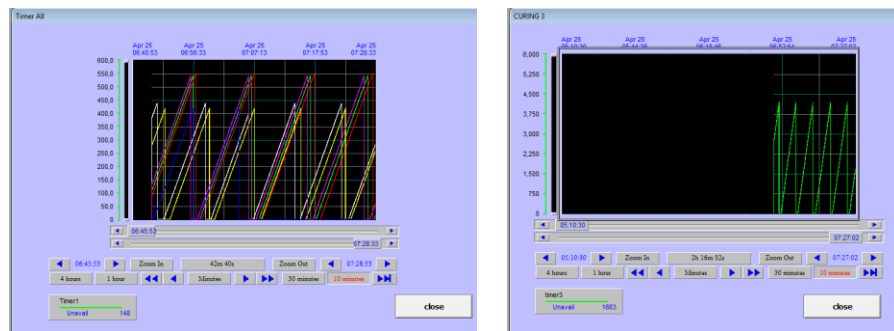


Fig. 5: The timer graph on the curing machine

## 4. Conclusion

The SCADA system design on 6 curing machines was made using HMI Wonderware InTouch application. The PLC utilizes the Mitsubishi QJ71E71-100 Ethernet module as a communication module and uses Microsoft Access as a database. The interface design of HMI Wonderware InTouch is quite simple because it uses an existing library, this library is obtained from the wizard menu, and every object in the wizard must be added a tag name, this tag name functions for addressing of each object to which the address of the Input-Output PLC to be displayed is added. The communication design between PLC and HMI Wonderware InTouch utilizes the Ethernet module QJ71E71-100 using DASMT Ethernet communication in the System Management Console application. This system testing is carried out through 4 stages, namely connection testing, interface testing, program testing, and database testing. This system has increased the accuracy of data counter retrieval (E-business Switch). Also, this SCADA system can be applied to other machines, i.e. with some address adjustments.

## 5. Acknowledgment

We would like to acknowledge the support of Mechatronics Department, Politeknik Manufaktur Astra, and an Astra Group Company in this research paper for their helping in the elaboration of this work.

## 6. References

- Milik, A. 2015. On PLCs Control Program Hardware Implementation Selected Problems of Mapping and Scheduling. IFAC-PapersOnLine 48-4, 354-361.
- G. Valencia-Palomo, J.A. Rossiter. 2011. Programmable logic controller implementation of an auto-tuned predictive control based on minimal plant information. ISA Transactions 50, pp. 92-100.
- Rullan, A. 1997. Programmable Logic Controllers versus Personal Computers for Process Control. Computers ind. Engineering, Nos 1-2, pp. 421-424.
- Alexander Fay, et.all. 2015. Enhancing a model-based engineering approach for distributed manufacturing automation systems with characteristics and design patterns. The Journal of Systems and Software 101, 221-235.
- Gökhan Gelena, Murat Uzamb. 2014. The synthesis and PLC implementation of hybrid modular supervisors for

real time control of an experimental manufacturing system. *Journal of Manufacturing Systems* 33, 535–550.

Ardi, S.; Defi, W.Y. 2018. Control Systems Modification of Loading and Unloading in Oil Filling Machine Based on Programmable Logic Controller at Manufacturing Industry. *AIP Conference Proceedings* 2021, 060029; <https://doi.org/10.1063/1.5062793>

Ardi, S., Cascarine, L.T. 2018. Design Control System of Auto Air Remaining Machine based on Programmable Logic Controller in the Automotive Manufacturing Industry. *MATEC Web Conf.*, Volume 197, 2018, The 3rd Annual Applied Science and Engineering Conference (AASEC 2018).

Ardi, S., Tommy, M.I., Afianto. 2018. Automation of Waste Treatment on the Washer Machine Based on PLC Control System in the Manufacturing Industry. July 2018, DOI: 10.1109/ICISCE.2018.00140

Ardi, S., Nugraha, Z.A. 2018. Design Control System of Washing Oil Pan Machine Based on PLC in the Automotive Manufacturing Industry. Published in: 2018 International Conference on Electrical Engineering and Informatics (ICELTICS)

Date of Conference: 19-20 Sept. 2018, Date Added to IEEE Xplore: 29 November 2018, INSPEC Accession Number: 18290112, DOI: 10.1109/ICELTICS.2018.8548819

Ardi, S., Ardyansyah, D. 2018. Design Control Systems of Human Machine Interface in the NTVS-2894 Seat Grinder Machine to Increase the Productivity. *IOP Conference Series: Materials Science and Engineering*, 306 (1), 012112, (2018), doi:10.1088/1757-899X/306/1/012112

Ardi, S., Ponco, A., Latief, R.A. 2017. Design of integrated SCADA systems in piston production manufacturing case study on the conveyor, the coolant, the hydraulic, and the alarm systems using PLC. *IEEE Xplore*, 187 – 191.

Ardi, S., H Abdurrahman. 2017. Design of pokayoke systems to increase the efficiency of function check oxygen sensor machine using programmable logic controller in manufacturing industry, *IEEE Xplore*, 192 – 196.

Ardi, S., Al-Rasyid, A. 2016. Design of Pokayoke Sensor Systems in Drill Oil Hole Machine to Detect the Presence of Drill using Programmable Logic Controller. *Advanced Science Letters* 22(7), pp. 1813-1816.



## Overview of Graphene-Like-Graphite (GLG) Synthesis Technology from Green Petroleum Coke (GCP) as a High Capacity Anode Material for Lithium-Ion Batteries

Nugroho Adi Sasongko<sup>1</sup>, Ulya Qonita<sup>2</sup>, Riza Murniati<sup>2</sup>, Cepi Kurniawan<sup>2</sup>

<sup>1</sup>Centre for The Assessment of The Process and Energy Industry (PPIPE), Agency for The Assessment and Application of Technology (BBPT), Serpong, Tangerang Selatan, Indonesia

<sup>2</sup>Chemistry, Semarang State University (UNNES), Semarang, Jawa Tengah, Indonesia

### Abstract

This study examines the use of graphite anodes as an anode material on lithiumion batteries (LiBs). Graphite synthesized from Green Petroleum Coke (GPC) residue. GPC is used as raw material because it is more environmentally friendly and cheaper, so it can reduce production costs. Graphite synthesis is carried out by GPC graphitization at 2700°C. Graphene like graphite (GLG) uses the Brodie method, which is known to have a large capacity and is fast chargeable. SEM characterizes the morphology and crystal structure of GLG, and its electronic properties are tested in half and or in one battery cell. From the analysis results, it knows that GLG has the most capacity high compared to raw material (GPC) and graphite.

*Keywords: Anode Lithium-ion Battery, Green Petroleum Coke (GPC), Graphite, Graphene like Graphite (GLG).*

### 1. Introduction

The use of fossil fuels by industry used to produce and drive production machinery has been carried out for years. As in China, the total primary energy consumption in 2016 was 1,437 x 1020 J and more than 88.3% used came from fossil fuels (Wang et al., 2019). Apart from being limited in number, the use of fossil fuels also produces combustion emissions in the form of carbon dioxide gas (CO<sub>2</sub>) and toxic pollutants. These emissions can cause climate change due to global warming (Perera, 2017).

One effort that can be done to minimize the impact of climate change and air pollution is the use of Rechargeable Lithium Batteries in moving production machines (Tomaszewska et al., 2019). Lithium battery production has increased since it was produced in 1991. The higher demand is due to lithium batteries having specific energy, energy density, specific power, efficiency, and high life span (Horiba, 2014). In addition, the high efficiency of Lithium batteries enables their use in power generation, namely to maximize the quality of the use of renewable energy such as wind, solar, geo-thermal, and other renewable energy (Nitta et al., 2015). Commercially, Lithium batteries must meet several criteria, namely high energy density, fast charging capability, long life cycle, and low production costs (Scrosati et al., 2011).

Carbon is an attractive candidate in making anodes from lithium batteries. This is because the cost is relatively cheap, its stability, and high reversibility to enter Li ions. In addition, carbon anodes are easier to make because their components are stable in the air (Tran et al., 1995). Another advantage of using carbon as an anode is a carbon structure that can reversibly absorb and release lithium ions at low electrochemical potential. This results in only slightly increased energy density, so batteries have an increased life cycle and safety (Flandrois & Simon, 1999).

Graphite is the most suitable material used to make anode lithium-ion batteries. The choice of graphite as an anode is due to its relatively high specific capacity, high efficiency, and low irreversible capacity. Petroleum coke is the main precursor material in the manufacture of synthetic graphite. Petroleum coke has a medium electronic conductivity and pores that can easily diffuse in and out of lithium ions. Coke itself is a high potential anode material.



Green Petroleum Coke (GPC) is an artificial carbon product produced from residues that are heated at temperatures around 900 K to remove the mild fraction of hydrocarbons until polymerization occurs which forms solid carbon that does not melt. GPC has a lower economic value of around 2-3% compared to the economic value of gas, oil and other refinery products. (Edwards, 2014). Therefore, so far 100% of GPC produced by Pertamina RU Dumai has been exported abroad. On the other hand, recently many countries in the world have used GPC as fuel to be able to save costs. (Zhan et al., 2011). For example China and India which use GPC as fuel in power generation and cement production (Zou et al., 2007).

## 2. Method

**Grafitization Process.** To remove the impurities from the soot collected from the petroleum coke boiler and improve crystallization, annealing was performed in an ultra-high-temperature electric furnace under an argon gas flow (4 L/min) at two temperature conditions of 2000 °C and 2700 °C. The heating rate was set at 10 °C/min until 1800 °C, and 5 °C/min until 2700 °C. After maintaining the two temperature conditions (2000°C, 2700°C) for 2 hours, the electric furnace was naturally cooled to the ambient temperature.

**Synthesis of GLG.** We synthesized GO from natural graphite (Z-5F, Ito Graphite) by oxidation with KClO<sub>3</sub> in fuming HNO<sub>3</sub> for 3 h at 60 °C based on Brodie's method<sup>37,38</sup>. The obtained GO was then heat treated in a step heating process. Specifically, GO was heated under vacuum from room temperature to 170 °C at a temperature-increasing rate of 1 °C/min then heated to 250 °C at 0.1 °C/min. After that, the temperature-increasing rate was changed to 1 °C/min until it reached 800 °C. The temperature was kept at 800 °C for 5 h, then a small amount of air (ca. 15 kPa) was introduced in the reactor and naturally cooled. The obtained sample was used without any further treatment.

**Characterization.** To analyse the element composition of the residue according to the annealing temperature, the composition ratios of elements were measured using a carbon, hydrogen, nitrogen, and sulfur (CHNS) analyser.

**Electrochemical Measurement.** The electrochemical test of petroleum coke was performed using 2032-coin type (Wellcos Corp.) half-cells. The slurry for electrode fabrication was produced with petroleum coke (80 wt %), carboxymethyl cellulose (CMC) / styrene-butadiene rubber (SBR) (10 wt %) as binder, Super P (10 wt %) as conductive material, and distilled water as solvent. The fabricated slurry was coated on the Cu-foil substrate using the doctor blade coater, and the solvent was removed by drying at 40°C for 12 h under vacuum (−700 mmHg). Next, it was pressed to a thickness of 35 µm using a roll press and the typical mass loading for the electrodes was 0.0039 g/cm<sup>2</sup>. Lithium coin chips were used for counter and reference electrodes, and Celgard 2400 for separation membrane. The electrolytes were obtained by dissolving 1 M LiPF<sub>6</sub> in a solvent made by adding 20 wt % of fluoroethylene carbonate (FEC) in ethylene carbonate (EC)/diethyl carbonate (DEC) (1:1 v/v). The FEC additive was used to prevent the instability of SEI film formed at the edge of the ring surface due to shrinkage and expansion during charging and discharging. The coin was produced in a glove box filled with Ar. The electrochemical test was performed in the voltage range of 0.01–3 V (vs Li / Li<sup>+</sup>) using the BCS-805 biologic battery test system (Biologic, France).

## 3. Result and Discussion

The CHNS elements are analyzed to determine the composition of residual impurities in soot, which can affect electrochemical performance; the results are listed in Table 1. Large amounts of sulfur were detected in soot before annealing, while the amounts of hydrogen and nitrogen were less. The quantity of hydrogen is less in petroleum coke soot because the composition of petroleum coke is more similar to a lump of pure carbon than a hydrocarbon. The amount of impurities decreases significantly after annealing, and no nitrogen is detected.

**Table 1.** CHNS elements of petroleum coke before and after graphitization process

Sample	Carbon	Hydrogen	Nitrogen	Sulphur
Raw	68,03	0,75	0,43	7,32
2000 °C	85,59	0,42	Not detected	3,08
2700 °C	<b>96,77</b>	0,45	Not detected	<b>1,99</b>

To evaluate the electrochemical performance of petroleum coke soot as an anode of active ingredients, a galvanostatic charge / discharge experiment was carried out. Figure 1a shows the measurement data of reversible capacity using soot annealed at 2000 °C and 2700 °C as an anode. When annealed at 2000 °C, it exhibits lower cycle performance and capacity than commercial graphite anodes, but when annealed at 2700 °C, exceptional performance is observed with a capacity of 250 mAh/g even for more than 300 cycles at a rate 1 C. Consistent with previous results, when the annealing temperature increases, better performance is obtained because the soot structure is very crystallized. Experimental results confirm that when annealed at high temperatures of 2700 °C, soot shows performance comparable to commercial graphite anodes.

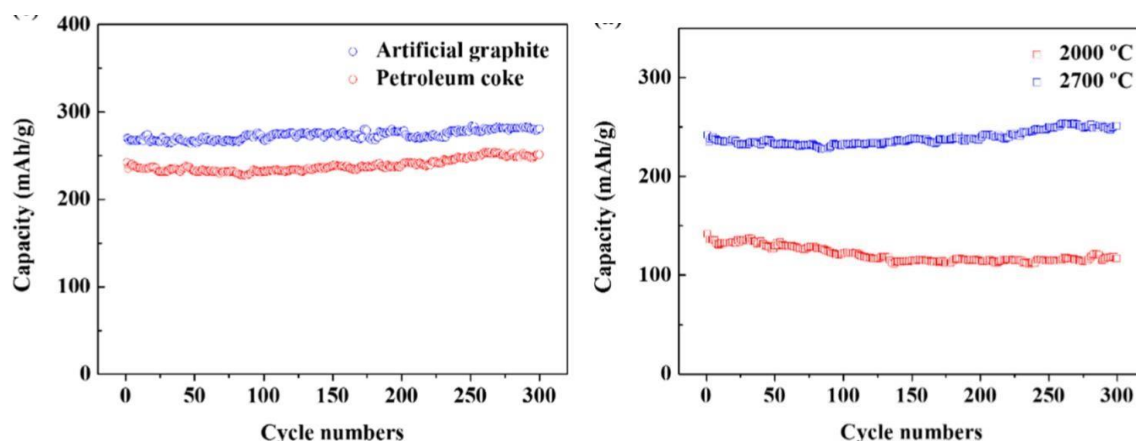
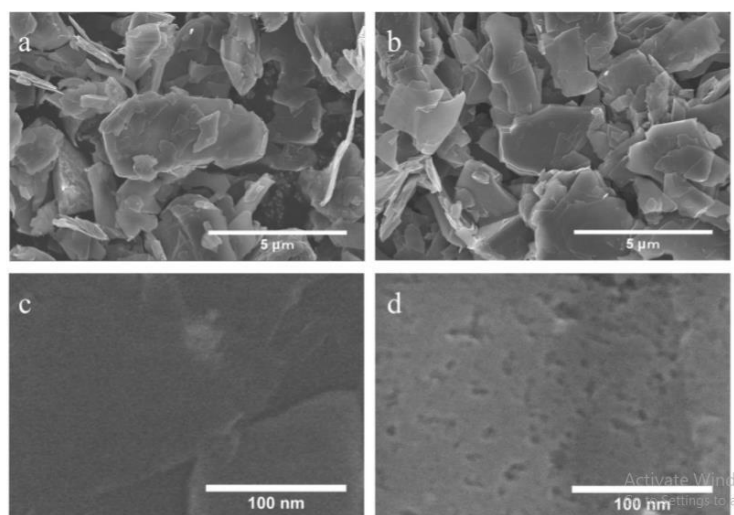


Figure 1. the measurement data of reversible capacity using soot annealed at 2000 °C and 2700 °C as an anode (a), the initial Coulomb efficiency values of annealed soot (b).

Figure 1b shows the initial Coulomb efficiency values of annealed soot, namely 82.2% and 92.3%. Coulomb efficiency improvements were observed because basal plane fields increased when crystal rings were produced during the grafting process.

**Material characterization.** The morphology of carbon material is shown in Fig. 2. Figure 2 is a SEM image of pure graphite. Flake type graphite of about 5  $\mu\text{m}$  was used for this experiment. Figure 1b is an SEM image of GLG at the same magnification to compare it with that shown in Figure. 2a GLG material has a morphology and size that is almost the same as pure graphite. As a result, GLG is compatible with current graphite anode electrode fabrication processes. Currently, researchers are trying to control graphite, which is used as an anode material for Li-ion batteries, with a relatively small specific surface area to have an acceptable initial coulombic efficiency and cycle. This is because no solvent can survive without reduction at very low potential when filling to 0 V vs Li / Li<sup>+</sup>, and SEI will be formed on the surface of the anode material, which consumes Li from one of the cathodes or electrolytes (Zou *et al.*, 2007). In addition, the amount of binder needed is proportional to the specific surface area of the electrode material. Anode materials with high surface area, such as graphene (4001200 m<sup>2</sup>/g), require 15% binder to make electrodes, which makes it difficult to make batteries with high energy densities (Bryers *et al.*, 1995). As a result, GLG with an unchanging size is sufficiently compatible with the current process to make Li-ion battery electrodes. Figure 2c is an SEM image of a pure graphite surface, and Figure. 1d is a surface morphology at the same magnification of GLG. 3-5 nm micropore is revealed in GLG, while there are no pores on the surface of pure graphite. The pores should have formed during the process of thermal reduction, where O functional groups containing O react with C atoms to form CO or CO<sub>2</sub>. Surface nanopores increase specific surface area. So the anode surface area of GLG material is slightly larger than pure graphite. GLG material is expected to have good initial coulombic efficiency because of the specific surface area smaller than graphene.



**Figure 2.** SEM images of graphite and GLG. (a) SEM image of graphite (b) SEM image of GLG. (c) High resolution image of natural graphite surface. (d) High resolution image of GLG surface.

Figure 3 shows the XRD pattern of GLG. Peak (002) GLG has a shift to a lower angle of  $2\theta = 26.26^\circ$  ( $d = 0.339$  nm) compared to graphite  $2\theta = 26.57^\circ$  ( $d = 0.3354$  nm), which is an interlayer space larger than GLG. Peaks (004) and (110) were also observed at  $2\theta = 54.18^\circ$  ( $d = 0.1693$  nm) and  $77.93^\circ$  ( $d = 0.1226$  nm). The size of the crystals along the a and c (La and Lc) GLG axes was estimated from the width of the peaks (002) and (110), and obtained 16.3 and 23.1 nm, respectively. They decreased dramatically from graphite (573 and 118 nm) after being converted to GLG. However, surprisingly, together with the peaks above, they were separated (100) and (101), and (112) peaks at  $2\theta = 42.64^\circ$  ( $d = 0.2120$  nm),  $44.38^\circ$  ( $d = 0.241$  nm) and  $84.9^\circ$  ( $d = 0.1142$  nm)) was observed. This means that the three-dimensional arrangement of the carbon layer is still maintained in GLG, as in graphite. These results indicate that it is appropriate to mention this GLG material.

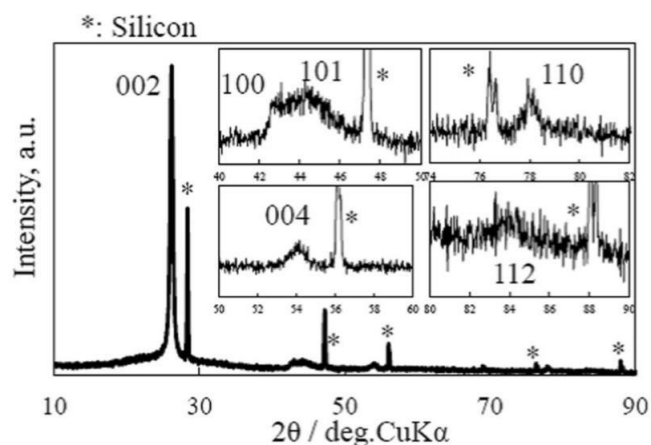


**Fig. 3:** the XRD pattern of GLG.

**Electrochemical properties of GLG Anode.** Figure 4 plots the initial GLG filling and emptying curve.

During the charge, a plain around 0.7 V is observed, the electrode potential gradually decreases. During disposal, the plateau increases almost linearly to 2 V. This behavior is similar to that reported for graphene-based materials (Yoo *et al.*, 2008; Wang *et al.*, 2009). The filling and emptying capacity is 1033 and 608 mAh/g, respectively. This GLG release capacity is far greater than graphite. The greater capacity is thought to originate from the greater number of oxygen atoms in GLG materials. graphenebased anodes show greater release capacity, even exceeding 1000 mAh/g (Yoo *et al.*, 2008; Wang *et al.*, 2009); However, they show a higher average discharge potential than GLG-based anodes, which is 0.92 V. The coulombic efficiency of GLG is 56%, which is much higher compared to graphene(Yoo *et al.*, 2008; Wang *et al.*, 2009). Lower coulombic efficiency can be attributed to 1) higher

specific surface area ( $11.9 \text{ m}^2/\text{g} \rightarrow 31.3 \text{ m}^2/\text{g}$ ) and nanopore structure (Figure 4d) compared to pure graphite and 2) strong interactions between ions Li and O-containing functional groups, which are associated with capacity in high discharge potential ( $> 1.5 \text{ V}$ ). Many Li ions may still be trapped by functional groups even in 2-V release.

The ability to fill and empty the half-cell rate of pure graphite and measured GLG is shown in Figure 5. Figure 5a is the ability to fill rate (lithiation) of graphite and GLG. The cells were charged (Li-ion intercalation) to 0 V vs. Li metal at 0.1, 0.2, 0.5, 1, 2, 3, 5 and 10 C then discharged (Li-ion deintercalation) to 1.5 V vs. Li metal at 0.1 C from 1.5 to 0 V. The capacity at every C-rate is plotted. The GLG material exhibited much larger capacity at 0.5 C or higher, and even at 10 C, 30% of capacity was still delivered, which means that it has a better charge-rate capability.

Figure 10b plots the discharge (delithiation)-rate capability of pristine graphite and GLG. The cells are charged (intercalating Li-ion) to 0 V vs Li metal at 0.1, 0.2, 0.5, 1, 2, 3, 5 and 10 C then discarded (Li-ion deintercalation) to 1.5 V vs Li metal at 0.1 C from 1.5 to 0 V. The capacity at each C-rate is plotted. GLG material shows a much greater capacity at 0.5 C or higher, and even at 10 C, 30% of the capacity is still being delivered, which means that it has a better rate capability. the extraordinary performance of the GLG rate is related to the following things. 1) Surface nanopores, which are characterized by SEM (Figure 2d), provide extra intercalation or deintercalation sites for Li ions. 2) Internal pores, marked by TEM, from exfoliated GLG can facilitate the rate of diffusion of Li-ion. 3) Greater space between layers facilitates better diffusion rates during filling and application. 4) The smaller crystal size reduces the intercalation/deintercalation pathway for Li ions. As a result, GLG shows superior level performance than pure graphite.

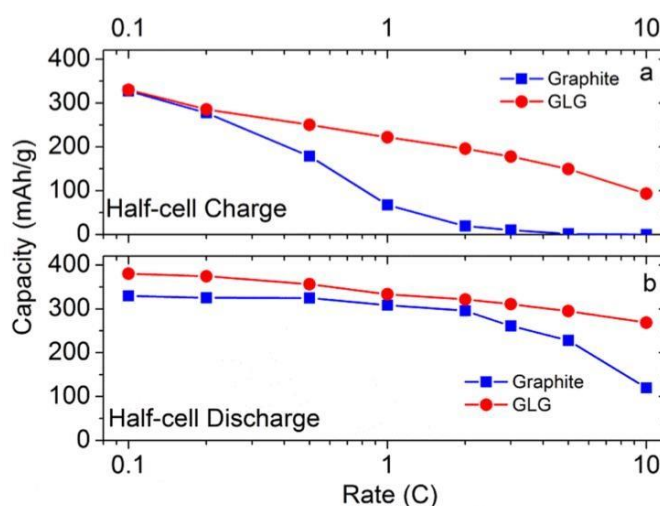


Figure 5. Half-cell (a) charge- and (b) discharge-rate capability of GLG in comparison with those of graphite.

## 4. Conclusion

Changing the structure of carbon to be denser allows the existence of more unpaired orbitals, so that the capacity of electricity that can be accommodated increases.

## 5. References

- Edwards, L. (2014). The History and Future Challenges of Calcined Petroleum Coke Production and Use in Aluminum Smelting. *Jom*, 67(2), 308-321. doi:10.1007/s11837-014-1248-9
- Flandrois, S., & Simon, B. (1999). Carbon materials for lithium-ion rechargeable batteries. *Carbon*, 37(2), 165-180. doi:10.1016/s0008-6223(98)00290-5
- Horiba, T. (2014). Lithium-Ion Battery Systems. *Proceedings of the IEEE*, 102(6), 939-950. doi:10.1109/jproc.2014.2319832
- Nitta, N., Wu, F., Lee, J. T., & Yushin, G. (2015). Li-ion battery materials: present and future. *Materials Today*, 18(5), 252-264. doi:10.1016/j.mattod.2014.10.040

- Perera, F. (2017). Pollution from Fossil-Fuel Combustion is the Leading Environmental Threat to Global Pediatric Health and Equity: Solutions Exist. *Int J Environ Res Public Health*, 15(1). doi:10.3390/ijerph15010016
- Scrosati, B., Hassoun, J., & Sun, Y.-K. (2011). Lithium-ion batteries. A look into the future. *Energy & Environmental Science*, 4(9), 3287. doi:10.1039/c1ee01388b
- Tomaszewska, A., Chu, Z., Feng, X., O'Kane, S., Liu, X., Chen, J., Ji, C., Endler, E., Li, R., Liu, L., Li, Y., Zheng, S., Vetterlein, S., Gao, M., Du, J., Parkes, M., Ouyang, M., Marinescu, M., Offer, G., & Wu, B. (2019). Lithium-ion battery fast charging: A review. *eTransportation*, 1, 100011. doi:10.1016/j.etrans.2019.100011
- Tran, T., Feikert, J., Song, X., & Kinoshita, K. (1995). Commercial carbonaceous materials as lithium intercalation anodes. *Journal of the Electrochemical Society*, 142(10), 3297-3302.
- Wang, Q., Mao, B., Stoliarov, S. I., & Sun, J. (2019). A review of lithium ion battery failure mechanisms and fire prevention strategies. *Progress in Energy and Combustion Science*, 73, 95-131. doi:10.1016/j.pecs.2019.03.002
- Zhan, X., Jia, J., Zhou, Z., & Wang, F. (2011). Influence of blending methods on the co-gasification reactivity of petroleum coke and lignite. *Energy Conversion and Management*, 52(4), 1810-1814. doi:10.1016/j.enconman.2010.11.009
- Zou, J. H., Zhou, Z. J., Wang, F. C., Zhang, W., Dai, Z. H., Liu, H. F., & Yu, Z. H. (2007). Modeling reaction kinetics of petroleum coke gasification with CO<sub>2</sub>. *Chemical Engineering and Processing: Process Intensification*, 46(7), 630-636. doi:10.1016/j.cep.2006.08.008

***D. Information System, Business Management &  
Industrial Engineering, Education Technology***

## The Role of Technology and social transformation challenge in Industrial Revolution 1.0 – 4.0.

**Fred Soritua Rudiyanto<sup>1,\*</sup>, Agus Sachari<sup>2</sup>, Setiawan Sabana<sup>3</sup>, Yannes Martinus Pasaribu<sup>4</sup>**

<sup>1,2,3,4</sup> Faculty of Visual Art and Design, Institut Teknologi Bandung (ITB), Bandung - INDONESIA

\* Corresponding author e-mail: fredsaritua1975 @gmail.com

### Abstract

The Industrial Revolution has been permanent related to technology society and human readjustment to the technology. The changed of technology society and human adaptation are impulse and reaction as a social being that sometimes conflicting each other so, therefore, need to look for the best solution to the clash and the social problems that emerged. Further understanding of the industrial revolution required a brief historical knowledge related to the industrial revolution. This article explains the background of several technology histories and the social life as supporting or the impact of the industrial revolution. Facing the challenges from the future need to be considered and forecast especially related to the present industrial revolution, particularly to the social impact that might be happened, that allowing generate pre solution to eliminate the friction among human.

*Keywords: Challenged, History, Industrial Revolution, Social life, Technology*

## 1. Introduction

To understand the industrial revolution 4.0 or the nowadays industrial revolution required comprehensive and knowledge why the industrial revolution ensued and drive of it. The depiction hereunder are a few parts that relevant to the concatenation major swoop in the industrial revolution which can break concerning the role of technology and social changed because an invention or technology improvement sustainability. This article is prepared as rumination to the social life prediction that might be occurred in the nowadays industrial revolution or 4.0.

Secondary data of heuristic, the sorting of importance occurrence and author preferences were used to composing the series if industrial revolution history, especially interpretation which related to the technological invention that will applied in automotive or vehicle development. For data selection related to the occurrence's, author utilize the documentary video from trusted media, that shown physical evidence, proconsul ship, that has been reprinted from the era of industrial revolution and also international or local article journal which then was cited, rephrase to construct this article, so it has histography plot or timeline, and structural sequence.

## 2. Discussion

### 2.1. Strive and Survive Before Industrial Revolution 1.0

The end of the medieval century was a great invention era of the historical human dimension, and it was known as the first era of the industrial revolution in European. Scientists and Engineers at those time try to look the alternative energy that could drive system such as hydraulic, machine, besides the energy who come from wind, or ebttide ocean energy. In the 10th and 13th centuries are resurrection and the huge technology invention (Gimpel, 1976). Afterward, Gimpel also told the story about the huge boom of invention from the scientist and the engineer, and then slowly reduced as an industrial revolution consequence since 1750 and also occurring at several places in United Stated, and it was known as the first industrial revolution. In the medieval century, machinery was built manually, daunting and involves numerous workers. Machinery is a common thing for the farmers or factory owners, because they tackling and built the system on their own, also on water and wind energy conversion system to support their work, such as corn grinding, olive pondering, weaving cloth, leather tanning, and paper-making. A report from the 12th century the Cistercian monastery or in French it referred to as Clairvaux

monastery, suggested that mechanization became a crucial thing and major for the European economy. It was described that technology became a loud hymns, and there were 742 reviewed about that story and it was a real condition that revealed by one of the Cistercian monastery.

The abbeys were built in many countries in Europe with the distance almost thousands of miles between one and others. The abbeys places and locations were in Portugal, Sweden, Scotland until Hungary. All the parish has the same building design and water power as a source energy, and there was a story about the monk activity, if in the parish there were a blind monk and were transferred to another parish, therefore that monk specifically known his position in the room that he was (Gimpel, 1976).

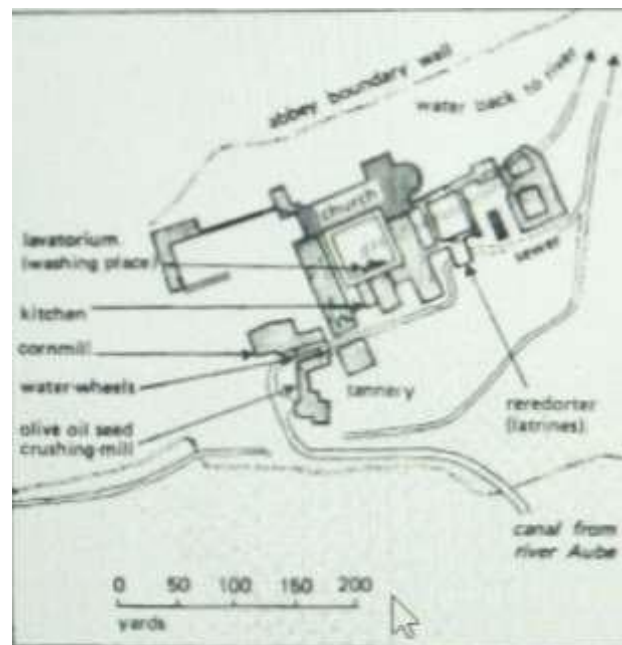


**Fig. 1: Spatial Planning of Parish Clairvaux (Cistercian).** Source: Holmes & Meier Publisher

Various way of life as discipline was implemented to the monk activity, e.g. for the monk in Saint Bernard, such as the arrangement for very tight schedule, so if there were any violation and deviation by the monk to the rules, and it would be getting a penalty or punishment, latter it becomes as Henry Ford rationale to follow the system and applied the punishment when he was built his assembly line in Ford Company. Except doing the spiritual activities, the monks at that era also involve to the production system to preserve the parish or daily necessities, and it was done by the monks over the European, by processing various natural resources which is available on the area, for example olive raw materials was only in stock in Provence area and it could not found in north of France, thereby in Provence carried out the process and built the mechanism to pondering and milling to produced olive oil. Another example if an area was found the iron ore, so mechanism for forged production was built, and if they were failed planting and harvest the grape, the other things that they will be doing is built a production place to produce beer. The report exposed by parish Clairvaux describe the presence of water was so important as apart from conversion energy and mechanism for processing from resources of water, for example, was water conversion energy to produce fire and warm atmospheric that used to keep the temperature of beer that has been produced by the monk and put in to the barrels. The water usage beside for domestic the monks, it was also used to support the production system in those parishes (Gimpel, 1976). Article from Lubna Sungkar (Sungkar, 2007) describe of concerning French urbanization. French people were moved from their belongs and decide to stay and lived near the road and the river edge, and later have a better life enhancement, so that led to the emerge of villages that evolved in to a new city called "*Bourg*" even though the exposure was not made a clear note about the amount of the population in the occupied areas. The community system in those era was a feudal or based on dissimilarity concept, disaggregated by 3 main community categories, such as the nobility people (*Ordre de Noblesse*), comprising the derivative nobility and the new class of nobility, who get the nobility title from the King, the



ecclesiastic class (*Ordre du Clerge*) consist of the *régulier* and *séculier*, as a clergy who lives in the parish and the clergy who lives with the society or the commoners people (*Ordre du tiers Etats*), who became dairy cows for two top-class community (Carpentier, 1987). The social trends, many commoners' people improve their life by serving the country as military troops, and that was the only way to show loyalty to the emperor and later described as *de facto* nobleman, which the duty was as an officer. The continuously succeed in the officer and achievement to the high level of rank causes that the officer could be got facilities to attend on the royal party and have a right to seat close to the King, and also get a special facility to avoid the taxes (Eddy Kristiyanto, 2005).

## 2.2. Secure and The Born of Industrial Revolution 1.0

The feudal system disaggregated the occupation certainly between the landlord (*séigneur*) that have task as a leader, protect the land, for the clergyman they have function for pray dan teaching, meanwhile the farmers and craftsman's have a duty to ensure all the life needs in material (Sungkar, 2007). The trouble then, that will be faced by the farmers and the craftsmen are overpressure from the landlord and the circumstances of unsupported climate, also the emerging of the outbreaks that causing the crop failure. Most of the farmers and craftsmen were immigrating and wandering and the result was a huge urbanization to the new villages and evolve as a city and was known as *Bourg*, as a trading city, therefore, bring out the word of "*bourgeois*". The reality at that time, was the movement of the society to the area's or places which the resource of energy became the main factor to support the production or human occupation, so that water resources as a origin energy could raise the economic level for drive all the mechanism ( Salzman B.A, 1913). The other thing that usually happens at that time was the large number of wars. The war requires enormous logistics related to the readiness of war equipment, mobilization by using the horses and walking troops, all these activities required food and clothing. The war Logistic emerged the trading between the royal, nobleman and gave the auspicious for the community or *Bourg* that had been through by the soldier. For sure, the church and the monks at those eras could not get involved, as a consequences of their functions and mission as a clergy, this opportunity was taken by certain societies to provide all the demand of warfare, then resulting the wealthy community or new bourgeois outside the overpower royal area (Sugiharto, 2018).

The feudal system disaggregated the occupation certainly between the land lord (*séigneur*) that have task as a leader, protect the land, for the clergyman they have function for pray and teaching, meanwhile the farmers and craftsman's have a duty to ensure all the life needs in material. The trouble then, that will be face by the farmers and the craftsman's are overpressure from the landlord and the circumstances of unsupported climate, also the emerging of the outbreaks that causing the crop failure. Most of the farmers and craftsman's were immigrate and wandering and the result was a huge urbanization to the new villages and evolve as a city and was known as *Bourg*, as a trading city so therefore bring out the word of "*bourgeois*". The reality at that time, was the movement of the society to the area's or places which the resource of energy became the main factor to support the production or human occupation, so that water resources as a origin energy could raise the economic level for drive all the mechanism. The other thing that usually happens at that time was the large number of wars. The war requires enormous logistics related to the readiness of war equipment, mobilization by using the horses and walking troops, all these activities required food and clothing. The war Logistic emerged the trading between the royal, nobleman and gave the auspicious for the community or *Bourg* that had been through by the soldier. For sure, the church and the monks at those era could not get involved, as a consequences of their functions and mission as a clergy, this opportunity was taken by certain societies to provide all the demand of warfare, then resulting the wealthy community or new bourgeois outside the overpower royal area.

The rise of *bourgeois* increasing the social gap among them, based on the acquisition of material and punctilious to execute the property. Webner Sombar describe that the wealthy could be achieved not only from the work hard to earn the money or get a high amount of wages but it depends on how to press the expenses and accumulate more asset. Meanwhile the nobleman tends to squandered the money and giving the charity, as a way to show the opulence and do the things that excessive indulgence than to help and with a vengeance, and while the *bourgeois* has a frugal lifestyle and prefer to be parsimonious, all the things related to the assets should be calculated, so sometimes people called them as an egoistical social class, which was they step always based on the extrapolated of the assets, moreover the marriage was a part of business and unification the social class and also contributed to gain the assets, who became a main drive to other aspect of life (Sungkar, 2007).

The *bourgeois* has struggled to achieve the success in materialistic because the mindset among them, which the dignity, prosperity could be achieved and admitted if became a rich man. The gap between the wealthy people and poor became wider as well as the shape of new feudal system between the employee and the labor classes, then also the emerging conflict and competition among the *bourgeois*, the nobleman and the clergy, after the privilege was given to the *bourgeois* class, e.g. in education field, who initially exclusive for clergy or monk, nobleman and limited for peasants and craftsman's. Parish and cathedral school are main institution that develop and effectuate the education even it was constrained, to reduced illiteracy in particular area, and it was responsibility of the priest or family through the trivium subjects ( grammar, Rhetoric and logic), in the future it was evolve and establishment as university all around the Europe in 14<sup>th</sup> and 15<sup>th</sup> century, during that period the clergy in addition has the religious knowledge also getting knowledge such as archeology, anthropology, natural sciences, physics, astronomy, biology, art, languages and other's, as a consequences of absolute power and church financial capability to develop, moreover to negated the knowledge and science cause high dependency from the clergy to the church and King, an example, the scientist in 19<sup>th</sup> century describe, the impact of church absolut power there was no Christ scientist in the medieval century admitted that the earth is not round, moreover the scientist like Lindberg and Ronald Numbers stated that the scientist from medieval century has been estimating and calculating the length of circumference of earth, although it was Ronald Numbers quote as a myth that widespread and regarded as the true history without the support from the newest historical studies (Numbers, 2009).

Lubna Sungkar (Sungkar, 2007) described, in the 16th century the bourgeois started to penetrate the Laws carrier when on the time, The king concerned all the opinions from the legal experts. Getting an expert in Law science become one of the bourgeois ambitioned, they directed their children to learned about it so their children might have a role in government for Law degree were highly respected and had important parts in government posts. This lifestyle did not occur on aristocrats' hedonic lifestyle. Bourgeois engender Industry generations, bankers, entrepreneurs and professionals services groups of doctors, notaries and lawyers.

Those bourgeois professions related to the establishment of the Academies, Oxford University in the 12th century and Cambridge University in the 13th century, for example, these were mentioned and proved by the lecturers and documentation in Oxford in early 1096 and the university around Parish Church on early 1100. Later on, Henry II-restricted England students to study at the University of Paris around 1167, in 1188 a historian named Gerard visited Oxford University from Wales, and met the deans to admit students from overseas and two years later Emo University of Friesland became the first university who admitted overseas students. Around 1200, Oxford become after Paris and Bologna which developed as an education center in West Europe, whilst constrained of aristocratic rights and immunities feud with the other residents, which increased the rent housing, soaring goods costs and loans (Lawson J., Silver H, 1973), therefore Oxford students change over Cambridge around 1209. In 1300 Oxford gained 1500 students when they provided a dormitory to answer the problems, afterward it become Oxford College and Oxford University (for Theology master science) and Cambridge University which possess 500 students (Gillard, 2018).

England formed an institution such as *The Royal for Improving Natural Knowledge* (1662) and French formed *The French Academy of Science* (1666) by King Louis XIV and advised by Jean- Baptist Colbert for built and protect scientific research in French.

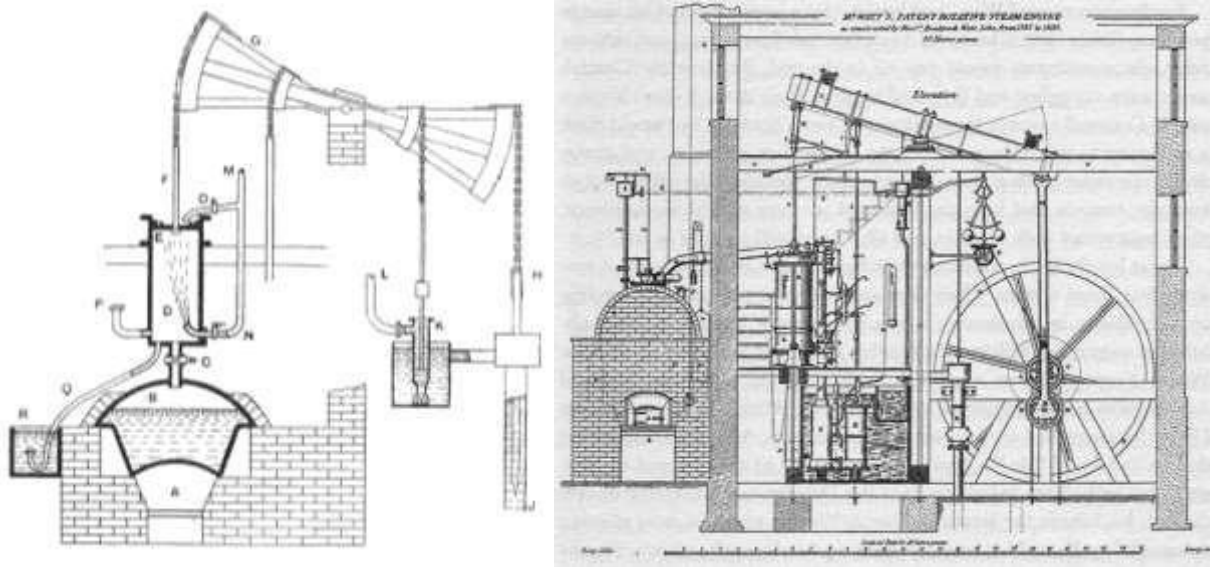


**Fig. 2: Thomas Newcomen and James Watt Steam Engine Design. Source: Chronozoom.com**

Emma Griffin an England historian who studied specifically the history of workers and their social activity explained how their life in England Industry Revolutions, e.g. in Quarry mills factory (*quarry bank*) in 1800. England's income sources in 1825–1830 were from products made from cotton material and hold 95% of the commodity markets by cotton spinning to yarns and fabrics. There are 900 similar industry in England areas, to increase the productions and to compete among the factories, Samuel Greg, Quarry mills owner whom called as the Cotton King and assisted by Peter Ewart (Trust, 2001), started to applied the propulsion from steam engine in 1810 to reduce the bondage from water which frequently lack in summer and other factories around quarry mills usage. Dr. William J. Asworth from University of Liverpool stated that the revolution started from the Steam Engine utilization, more specific, Industry revolutions was Water Energy utility. Quarry mills industries at the beginning using the giant wheel which called “Great Wheel” with a weight of 44 tons and produced 100 horsepower was the biggest factory in England with water streaming as a driving force source.



**Fig. 3: Great Wheels**

**Source: Power at Quarry Bank, Nationaltrust.org.uk**

Hundreds of workers consist of children and female workers invited to operate all the machine and textile equipment, kids have 12 hours workhour or more in a day, in charge to clean the dust and the fallen out cotton or other work. The workers prefer *Quarry mills* because the textile factory offered more amount of wages than as Hodge, and *Quarry mills* also prepare the shelter, cloth and food as long as they work at the factory, and it was known as *Apprentice system*, related to *parish system*, which is a system for looking labor with the parish church support, to round up the poor and displaced children then they will hired at the factory with food, cloth and place to stay as mutual when they work at the factory. One of the requirements for the children worker is the capability for 12 long hour's works, and if they could not be made, the factory owner will send the kids back to the parish.

The Patriarchal System was made for foodstuff selling monopolized by the factory owner to the workers and their family who lived in the factory area, worker bought their needs from the local market that running by the factory, therefore the money that was given by the factory as wages will return to the factory owner, or by using voucher (tommy voucher system), and it was given to the workers and could be exchange with the foodstuff based on the worker level (Documentary, 2018).

A letter in 1796, was revealed from the *Quarry mills* archives in a documentary movie that was produced by Chanel 4 United Kingdom, it describes an agreement between Samuel Greg and Job Rowley as an overseer, concerning to the orphan and the name is Jane Lamb, they consist of the agreement was about working hours for 12 hour a day and 6 day in a week, the documentary film also describe the average age of workers, start from 9 years old until 21 years old, the archive also describe about conflict the age of contention, causing Jane Lamb should work for one years longer as a result of the date of birth forgery that where numbered one year younger and Jame Lamb fight the owner of *Quarry mills* for her problem. To the increasing production, in 1866, the adult worker was brought from north area to achieve 250 workers, and placed on housing with 50 meters distance from *Quarry mills*. For mold the work ethic, the work system at *Quarry mills* was built by the doctrine of Sunday Service that embrace by Samuel Greg, through Unitarianism based on civility, self-improvement and hardworking ( "thinking is the hardest" or Unitarianism character is interpreting the bible by using historical, difference with orthodox approach, without finding the meaning in the bible text and accept the meaning from the utterance of Jesus, very critical to the bible and as a the absolute of truth, holding fast to the unity of Allah and reject the Trinitarian).

Problem regarding the time of work continued and resulting the friction between workers and factory owners around the United Kingdom, struggling with circumstances could not be heard by the Royal by the small number political right or 2 % of vote in parliament, incurring a huge workers movement on 16 August 1819, approximately 60.000 people congregating around the Manchester in *Peter Street* area and became a important history record and very known in United Kingdom, with the aim to demand the right to vote for poor people and life betterment. The event also caused 15 people were killed and 600 people were injured due to the clashed with the cavalry troops and known as the accident of *Paterlo Massacre*. The United Kingdom parliament at the end produced reformation action which allowed more people vote the parliament, event it was limited to the middle to hi-class community, and it raises the new restlessness for the worker in city area, in contrast to the rural area such as *Quarry mills*, the workers were placit condition because the Unitarianism doctrine who develop by the church and the factory owner. Other than mentioned above, *Quarry mills* also undertook the concept of Paternal system as an opportunity that gave by the factory owners to the workers for doing the social activity and the responsibilities of the factory owner to protect the workers environmental, by affording them shelter and education. In the *Quarry mills*, education imparted to the adult workers and the children, specialty for adult was taught the history knowledge, science, astronomy, and agricultural science, while the children taught how to read and counting (Logic). This system was so famous around of *Quarry mills* until drew the attention and visited by John Audubon an anthologists and famous painter from America, to saw and attest the education system, and the education core were taught not only for leisure, but it was conceived for mold the mental discipline, hard worker, and gave the tranquility, allowing to control the worker behavior pattern, and shaping them became an ideal worker. The other system that introduced in *Quarry mills* was the distinction of worker cloth and the owner, for the worker they used collars with a simple design, without an ornament studs, using the plain pattern and square collars, so that form a functional working cloth.



The surge of work time was kept on fought with a purpose to restrictive the work time, specially for the children, which conduct by John Daugherty, until in 1833 the United Kingdom parliament unleashed *Factory Act*, to restrict the working time for the children, and gave the opportunity for education, and celebrate the Christmas and Good Friday before the Easter. The surge because the *Factory Act* decision lead the factory to the fluctuated condition. The reduction and restriction of working time for 10 hours cause the production decline, therefore Robert Greg wrote a book titled: *Factory Question*, about how the government should interfere with the labor problems. Finally, to keep the production balances, the factory authorities start to use the steam engine and the automaticmechanic machine. At the end of 1850, British was industrialized by utilizing the steam engine technology and established automation for yard production and cloth from cotton material right up to 20 times more productive than human.

### 2.3. Industrial Revolution 2.0: From Mechanization to the Electronic and Materialistic

The second industrial revolution generally known start in 1870 until 1914, although in detail the years start of second revolution industry was predicted around in 1850, in line with the slowing the famous invention after years 1825, thereby steam engine was the biggest and known invention until last 3 decade, and the following invention of technology in next year were not too much known as consequences of focus on the product development and product improvement. The known invention in the era of the second revolution industry was energy, material, chemist, and medicare which gave a huge impact on production as a result of the effectivity improvement toward the researches and the development activity on research on micro things. At the end the inventions could reduce the product marginalization, except on the invention who did the breakthrough thus reveals the new vision (Mokyr, 2003).

The entanglement of second industrial revolution in Indonesia ascertainable from the Dutch colonial history that associated to the exploration activity and mineral mining tied with machine mechanization as a result from the technology development at that era, Nusantara was undergone on mineral exploration under the authority of Hindia Dutch colony were established from the Dutch company as known VOC (*Vereenigde Oostindische Compagnie*). The second industrial revolution in Indonesia caused the transformation, or more accurately called the exploitation transformation, from agriculture to the development mineral mining industry, so therefore, there were famous idioms regarding: “*Molukken is het verleden, Java is het heden, en Sumatera is de toekomst*” which mean Molukken or Maluku island is passed, Jawa or Java island is known and Sumatra island is the future. This provoking was famous around the 19th century among the Hindia Dutch colonials (Sitompul, 2018), as a result of the totality mastery to the spices and the beginning industrialization of mineral mining mobilization. The progression of mineral drilling and petroleum in Indonesia also related to the development mining technology in other countries, especially pertaining to the globalization production of petroleum as a result from technology transformation in 19th century to the 20th century, that is the invention of internal combustion engine (ICE) diesel or petrol engine, and then applied to mining industry. The first initiation in the used of ICE for well drilling carried out in 1870. The engineer and constructor in many places in Russia develop the drilling technology by using the energy hydraulic pump which then replaced the electric power source. In 1873, H.G Cross from Amerika obtaining patent for “single-stage turbine” and built a construction of internal combustion engine drilling and put it under the well mine in 1883, although there were several problems when they try to applicate the invention. In 1890, technician and engineer from BAKU, K.G Simchenko develop a turbo drilling machine or rotary machine that can move down by the assistance of hydraulic motor that spinning during the drilling, and five years later the others BAKU engineers received the patent for drilling turbo engine development which notch by using the electrical wire power drill (Mir Yusif Mir., 2012). (Mir Yusif Mir., 2012).

The second industrial revolution well known on emphasis to the value transformation aspect in production organization, second industrial revolution became a witness for a great growth of industry and economic scale also output (Alfred Chandler term), highly regarded factor to the economy in a part of manufacture activity and caused some of the industry growth and became larger than before, especially the industry who develop objects or product and industry chemical material. E.g. the cost of production for container structure, and related to the cylinder volume which comparable to the surface area and volume capacity. In the beginning, it depended on the form of a cube and the volume, and also the cost of production per unit including the amount of unit production.

Quality inspections of the completed were growth due the chemical industry progression, oil refinery, and as the

start of development the container or pack industry, thereby could be developed automatic vending machine with the ability to accommodate various potables container with the same dimensions, and it caused consideration to the dimensions when developing a product in order could be able to store by various type vending machine. Economic value has become a serious concern and it was well organized by producing with the term of mass production with the ability using the similarity component or parts and interchangeable to it. To increase profit, and to support sales activity, therefore the industry conduct the monopoly such as Carnegie Steel, DuPont, Ford Motor and General Electric were located in America by created representative company and partners in Europe, and perpetually to hired as little as possible of labor amount so that known as character for industry in 1914, others characteristic is developing specific of niche market, which mold the industry became flexible and could serve specific services and localized (Scranton, 1997).

## Steel

1850 is the beginning era of the use of steel material, although wrought iron was mostly used than steel. The usage of wrought iron for engine part and railway needs a huge cost, including for other usage as iron material for machinery or as a construction material. The weakness of iron at that time was elastic and the lack of strength. Another trouble was how to mold the iron material at a lower cost. The solutions were developed and solved by Henry Bessemer in 1856 (Mokyr, 2003). The steel process in Bessemer converter used pig iron, extracted from the iron process on high temperatures. Steel could be produced from iron ore and scrap iron, and need purification to remove the manure or excessive element such as phosphor, silicon, sulfur and carbon or oxygen, nitrogen to produce certain steel specifications. Bessemer method was the control of carbon contents that contained in iron material, perpetrated by oxidation and spout the air into the converter liquid containing iron through an aperture Tuyer in the bottom of steel cylinder, the steel converter has 6 meter high and beforehand were covered by refractory which was containing silica thereby enrichment of oxygen in the converter will be reacted to the manure or a nonmetallic element that might be not necessary for the reaction of oxide carbon, and also lees iron were consist silicon and manganese. After the oxide separation has been done, therefore, produce steel rough (ingot), then the steel were ready to process or further manufactured into different kind shape according to the needs or ordered (Wijaya, 2015).

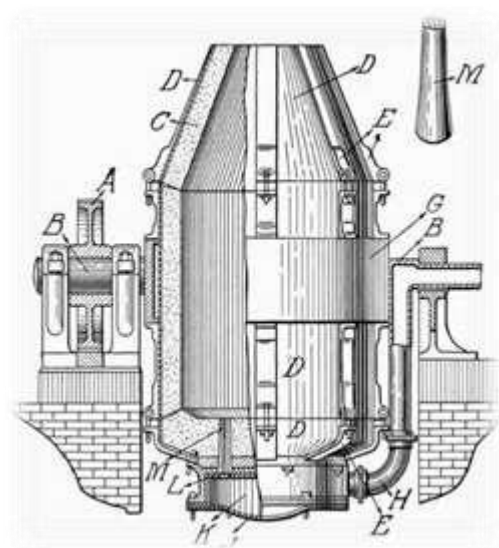


Fig. 4: Konstruksi Konverter Bessemer

Source: [chestofbooks.com](http://chestofbooks.com)

## Chemicals

On 1840, Justus Von Liebig, a Germany Organic Chemist published his book Organic Chemistry in its Application to Agriculture and Physiology, which discussed about every aspects related physiology with Agriculture Physiology and later known as Minimum Liebig Law. His reviews about Humus Theory stated that Mineral required from the Soil, Carbon dioxide, Hydrogen and Oxygen. Liebig also discuss about The Nitrogen which

cultivated from the Oxygen, even though this was not suitable for the majority of the plants, the theory applied for plants from the family of Fabceae ), therefore Liebig revealed that Soil nutrition's which came from plants, substitutable with fertilizer given (Mustaqin, 2018).

1856 William Henry Perkin started his experiment with Quinine synthetic, a malaria medicine from charcoal tar. In the experiment, Perkin oxidized Aniline by using gallium dichromate and toluidine, as an impurity which reacted with aniline and produce a solid element in color black which assumed as a fail synthetic organic. While cleansing the beaker with alcohol, Perkin saw there is a violet part of the solution as a side result of the experiment. The violet part become the base of the synthetic color industry. The aside result become very influential in Chemistry Industry in rears later. As an example, a large company such as BASF produces thermoplastic, sponges, urethanes, polystyrene, acrylonitrile butadiene styrene (ABS) which uses in home appliances products.

#### Motor Fuel, Car and Transportation

In 1885, Gotieb Daimler with his partner Wilhem Maybach developed 4 steps motor fuel machine which invented by Otto in 1876, therefore they produce an engine with advanced technology and they have the patent rights for the modern fuel motor prototype. Daimler was a Technical Director of Deutz Gasmotorenfabrik where Otto was the owner, which stood since 1872. Later then, there was a controversial about whose the inventor of the two wheels motor engine between Daimler and Otto.

Daimler – Maybach invented a small size, lighter and fast motor engine which already using carburetor as a device to exhale the fuel. The form of the engine machine of Daimler- Maybach is a machine with a vertical structure. The specification of the machine become a motor design revolutionary case. On 8 March, 1886 Daimler applicate the machine by designing the four-wheel vehicle in the world. In 1889, Daimler invented a two cylinders machine with V configuration. Later on Daimler – Maybach built an automobile industry together by building the vehicles and produced from the bottom part to top part by piece to piece. The vehicle they built reaches 10 miles per hour velocity with 4 parts of speed accelerations (Ratiu, 2003).

In America, Henry Ford with his team successfully created T model Ford vehicle, which built based on observation and organizing teamwork in the production system. In building their line production, Henry Ford consulted with Frederick Taylor, a management expert for testing the efficient production methods and form. Hendy Ford observed on the production lines of the Midwest factories which already use a conveyor belt (Wilson, 2014). Bill Ford (great-grandson of Henry Ford) said, Henry Ford had ideas for the point productions which he received from the frozen packaging site in Illinois. Henry Ford scanned that each worker have their certain tasks when the meat passing through the conveyor belt.

Henry Ford applied the observation result to build his Ford Motor industry production lines system (Reynoald, 2013). Henry Ford hiring Norval Hawkins a smart accountant who leads the sales division which enforced advertising campaigns that influent the market (Bob Casey, 2010). The consequences from the line production system, T-Model Ford produced efficiently and reduced production cost of the vehicles, from 800 US dollars to 280 US dollars each vehicle, thereby the vehicles become affordable for the public.



**Fig. 5: Ford line production & Model-T.**

Source: mtf.com

In its progress, transportation mode become massive and even greater parallel with technology development. Transportation mode start to using Fuel engine or gas turbine, as an example, Titanic vessel which using 3 main engine, consist of 4 step pistons engine, triple multiple expansion engines and one low tension parson turbine, which made the vessel cruises away even with its enormous size, cargoes and passengers. Titanic had 69 meters of height, 82 meters in width and 260 meters in length with 6000 tons of weight. Another Transportation mode that increased by the invention of steel with Bessemer method was the Train industry. It defined by the appearance of various intercity train track, interurban or street railway which using diesel and electricity power rail with low voltage were 500 to 600 V DC and intercity busses.

Sky transportation mode or airplane develop from many inventors, Wright brothers was one of the inventors. As assumed, Santos Dumont who enhanced ailerons as a control instrument which hanging on an airplane and become the first production of airplane series which reach a velocity of 120miles/hour. As a war facility, Italy was the first country who produced the airplane as one that applied upon war on Libya areas in 1911. The airplane engines were *inline engine*, the phenomenal *V-type engine*, and the legendary H-engine and Rotary engine from Rolls Royce Merlin (Gibbs., 1985).

The first commercial airline's company is DELAG which using Zeppelin (Iatrou, 2014). In heir first year, they accommodate 34.000 passengers in 15.000 flights (Dan Grossman, 2017). The history recorded that 30 June until 12 July 1914 the Second Industry Revolutions period, a pilot named Sikorsky Ilya Muromets, achieved flying record from Saint Petersburg to Kieve, Via Versa with 1200 distances miles. The first flight took 14 hours and 38 minutes with refuel in Orsha and the return trip took 13 hours with refuel stop at Novosokolniki.

#### **2.4. Industry Revolution 3.0: Network Ascendant Era**

Three main aspects that delivered the Industry Revolution are Vacuum tube, Transistor, and integrated circuit. Based on Thomas Alva Edison's invention, electron might devolve from one conductor to another in vacuum space, which was called as Edison Effect. John Fleming implements Edison effect through two electrons tubes or diode and named as valve, it works as a signals detector, alike Radio Marconi Telegraph (J. Bata, 2014). Vladimir Zworykin in 1920 using an iconoscope tube which is a vacuum tube as the basis of television camera. It conceived the electro-mechanics television era. Bell Laboratories produces them the first time in 1927. The Following development is the discovery of computer. In the early years, it develops by using an electron tube and caused the dimension size, it become very impractical. John Barden, Walter H. Brattain, and William Shockley invented transistor in 1948 which made from semiconductor material such as arsenide gallium crystal, sulfide cadmium, cadmium telluride, indium antimonite and substitute the triode tube function, with smaller size and lower power which therefore made them could manufacture in cheaper and mass production. Transistor components connected through PCB (printed circuit board) with brazing techniques. Transistor development finally delivered Integrated Circuit Concept which developed by Geoffrey W.A in 1952. And in 1958 J.S Kilby invented an integrated chain in form as a fragment (chip), single silicone in micro dimension, which contains of defused and settling electronic circuits. Texas Instrument produced them at the first time (Rosadi, 2004). Further development is the quantities of the components that inserted in the chip and knowns as small, medium, large and very large scale integration that delivered IC microprocessor as the brainpower of the Computer, and it produced by Intel.Inc United States in 1971(J.Bata., 2014). To perform the components and communicate inter devices, the computer uses a binary language using numbers 0 and 1. Number 0 means it disintegrated with the signal or electricity voltage. Number 1 is the contrary. The binary data group always consists of 8 bit or 1 byte.

Computer smaller size development become more personal and affordable not only for big institutions like it before. The Computer with simpler software simplifies to write, basic calculation, games and programming code such as BASIC, COBOL. Software and hardware development moves as the activities and humans need, such as picture processing, vector and image graphics, calculating and processing data and complex data algorithm, also simulations which demands to approach the reality. As an example computer substitute architectural manual drawing techniques, design techniques, and engineering techniques. It also used in vehicles designing and or buildings, that allowing small scale calculating and rapid actual size afterward. Drawing table, rulers, calculator and ink pen substituted with software and printer, which also operated by single operator that made a designer task even simpler and multitasking as a creator and computer operator to provisions of all the ideas.



For sharing data and accelerate the other area tasks, computer users were getting connected. The connection is through cables from one to another computer. Analog data start transforming and switching to digital and stored on a hard disk. Connection technologies extern computer initiated by United States government which called ARPANET program on an internet known by now. In the beginning, the program connects only four university website for military necessities.

In 1971 is the invention of e-mail (electronic mail) by Ray Tomlinson who presented '@' icon which defines 'at', and he start to expand the computer network to abroad United States, and on March 26<sup>th</sup> 1976, Queen of England succeed to sent her first e-mail. The consequences of the rapid network development caused regulated protocol required.

Transmission Control Protocol or Internet Protocol established in 1982. Network computer rivalry emerged in Europe continent named EUNET which consists of countries, Dutch, England, Denmark and Swedish, knowledge as e-mail service and USENET Newsgroup. To simplify and homogenize the network usage, agreement created through Domain Name System (Stewart, 2000). Further invention which enlarge international network usage is Internet Relay Chat (IRC) as a facilitator 'chat' (conversation) between computer users, founded by Jarko Oikarinen in 1988, which connecting more than 100.000 computers in one network. 1994 internet development reach 3.000 website address and rapidly enlarged by the online buying system from the network computer (Barry M Leiner et al, 1997).

Internet of thing (IOT) is a network which connect everything with internet base through protocol stipulation to collect information and using sensors element to exchange information and communication which generate certainty, position, searching, observing and administration comprehension (Keyur K Patel, 2016). Intersection with IOT phase product development recently is avoiding repeat innovation from one opponent or itself and the company kept. Innovation could be developed to produce ideas and concepts which manifested through a new product (Sundaram, 2016). Ideas are considerations through observations and analyses process which produce a solution. Concepts are subconscious thought which shaped by experiences got, and it was 'intuitive'.

The advantages of using IOT in developing program is simplifying data complex mapping that made data group analyzed. For example, consumer data tendency in money consumption, through IOT, we can collect the money traffic digital banking data, therefore which restaurant who have multitude visitor in town, and even consumer tendency for a product could be known in detail. This is an important data for a designer to develop a product. The other examples, coolant and lighting product, users could control remotely as there is a network connection between the user and the room which to be controlled.

IOT can also be used in searching for preferences or inclination about consumer expectations. News's, statements and pictures uploaded on social media are priceless information about a condition of a community, are in the wider section. The big data recorded in a social media bank data server where the social media companies are. And the data separated in criteria and keywords made. Other examples, for a presidential election, data from social media can be processed through keywords made, which made mapping tendencies and voting quantities probabilities of a candidate could be done.













Observation survey taken regarding a consumer with IOT technology could be done in remote, details, massive, rapid and highly supported for the team design who will be analyzing and resuming data despite the expensive material or sett-up system.

## ***2.5. Industry Revolution 4.0: Significant, Legacy, Sharing***

The word of Industry 4.0 introduced by The Germany government in 2011 at Hannover Fair, which is the initial action for manufacture based on digitalize and exploitation for new technologies industry (Rojko, 2017). Therefore the production of industrial products determined by global competition and rapid necessity of production, to adapt from the market changing condition which integrating business and manufactures process, as also implemented on the integration of industry player and company, which connected with supply chain value (supplier and customer) and technical aspects which require general concepts of Cyber-Physical System (CPS) and Industrial Internet of Things (IIOT) implementation on industry production system.

Industry Revolution 4.0 era is the supremacy of The Artificial Intelligent Supremacy era and the enormous development of IOT. Machines which developed in accordance to 4.0 code industry were machines with autonomous system, therefore it would conduct independent decision based on algorithm acquisition which implemented on and the ability to record real-time data. It also could performed analyzing processes and recording previous data activities (Rojko, 2017). One of the Industry Technology 4.0 implementation is on Transportation Industry. The autonomous system which require connectivity and capability from various system to integrate, or the system ability to perform and applicable by different system.

Autonomous vehicles divided into grades, as shown on the table below.

	0	1	2	3	4	5
DRIVER	 Control remains with the driver.	 The driver must leave the drive and be ready to resume full control immediately.	 The driver must observe the drive and be ready to resume full control immediately.	 The driver does not need to observe the drive but must be ready to resume control at any time.	 No driver needed.	 No driver needed.
VEHICLE	 The driver must control the vehicle.	 The vehicle can operate under driver's control.	 The vehicle can operate under driver's control.	 The vehicle can operate under driver's control.	 The vehicle can operate under driver's control.	 The vehicle can operate under driver's control.
	No automation Driver only	Driver only No automation Driver only	Assisted Driver assistance Assisted	Partially automated Partial automation Partially automated	Highly automated Conditional automation Highly automated	Fully automated High automation Fully automated

Picture 7. Autonomous Grade

Source: ecnmag.com

At the supreme level of autonomous, the driver is no longer necessary. The vehicle can operate in varieties situation and circumstance. In order to runs perfect, autonomous vehicle requires infrastructures design which consist of road infrastructure, server, provider, wireless network, real-time shipping and acceptance data network, layered security system to secure data and software, sensors that acts to collect activities and situations inside and outside of the vehicle, simple and understandable user friendly application, complex algorithms, with nearly 100% synchronize with simulation situation, and the ability to renew, maintain and enhancing to the new versions. As the example of autonomous usage is online driver service, known as *ojek online* in Indonesia. Autonomous vehicle distinguished present in front of the customer without driver and able to deliver goods to a destination with the order input through the application. Transportation Autonomous Technology development solved various migrate transportation problems with significant differentiation from non-autonomous technology. Autonomous vehicle develop from electric vehicle which then integrate with Computer capability, network, and artificial intelligence which allowing the non-human drive vehicles, in other words, an intelligence machine substitute the driver. A customer could utilize the vehicle through the application provided by an autonomous service company, or equally with the application for ordering an *ojek online*. The certain differentiation or transformation in autonomous vehicles is the vanishing of interaction between passenger and driver which is only focusing on delivering to the destination or uninterruptable. Transportation activity centralized in reaching to single destination point ‘one-stop point’ and finished. Autonomous concepts could vanishing personal vehicle ownership, and transformed to sharing vehicles or whomever order and owned by autonomous vehicle company. Personal vehicle ownership would be quite expensive due to parking lot limitation and trait of personal ownership which forbid other people to use. Vehicle touring activity for relaxation activity would be vanished and decreased for it would provoke conflict between the systematic and regulated machine with the unpredictable human. A philosophy technology advocate, Martin Heidegger stated that ontologically, technology has changed the essential manner of human existence (Heidegger, 1977).

### 3. Conclusion

Industry revolution correlates with how human solving, searching for the opportunity and moreover in sustaining their lives from their issues through technology and how to fulfilled every necessary. Industry Revolution also conceived personal and team success story, therefore every opinion and thoughts regarding the daily lifetime insight implementation of the figure became a role model and transformed people's previous outlook. Clashes between a group of people to the point of inter-nation in the form of economy value raises Human's life irregularities. The irregularities occurred tried to resolve by the rules, agreements and partnership cooperation. For every phase generates a gap between the beneficial side and exploited side. Strategies made to find the intersection agreement for making all things run in organized, despite it would never satisfy both sides. Gap between machines, as an invention from technology rapid development which probably overcome human intelligence. The Social nature of humanity could be replaced by machines, and in one-day machines would have more sensitiveness, more sentiment and more romantic then human. Machine might be even more humanist then human being, which made humans as machines creators, more concerned and fussed about invent complicated and sophisticated machines. Industry revolution 4.0 is the newest and so now phase from the industrial revolution. Technology created to contribute opportunities for human beings to comprehended significant things, that living life is not only for self, that money and objects are not everything.

For sharing, human beings should not merely accomplished economic enlightenment for the first time, in other words, technologies delivered forethought that sharing and advocate might start from the lower social level. Generate legacy for human beings to share and advocate in pursuing happiness, are the responsibilities of the Industrial revolution.

### 4. Acknowledgements

We are really grateful because we managed to complete our article The Role of Technology and social transformation challenge in Industrial Revolution 1.0 – 4.0 assignment within the time given by Agus Sachari. The assignment cannot be completed without the effort and co-operation from Setiawan Sabana, Yannes Martinus Pasaribu. We also sincerely thank to National Institute of Technology, especially FoITIC team as the organizer the international congress for Towards industry 4.0: Challenges and Opportunities for Industrial Technology and Other Sectors.

### 5. References

- Barry M.Leiner et all. (1997). Brief history of the internet 1997. -: Internet society.
- Salzmann B.A. (1913). English industries of the middle ages. London: Constable and Company LTD.
- Bob Casey., H. D. (2010). Henry Ford Innovation : From Curators. Illionis: The Henry Ford Education.
- Carpentier, J. e. (1987). Histoire de France. Paris: Seuil.
- Dan Grossman, P. R. (2017). Zeppelin Hindenburg : an illustrated History of LZ-129. China: Britihs Library.
- Documentary, C. 4. (2018). Private life of the industrial revolution ; steam engine ; history documentary; real thruth history. Belfast: Chanel 4.
- Eddy Kristiyanto, O. (2005). Absolutisme negara dan lembaga agama: pasca aufklarung di eropa barat. M lintas, 216.
- Gibss., S. (1985). Aviation. London: The Stationery Office.
- Gillard, D. (2018). Education in England : a history. Scotland: Queen's Printer For Scotland.
- Gimpel, J. (1976). The medieval machine, the industrial revolution of the middle ages. Victoria: Penguins Book.
- Iatrou, K. (2014). 100 Years of Commercial Aviation. Hamburg: Hermes Air Transport Club.
- J.Bata, W. (2014). Elektronika dasar, sejarah perkembangan dan komponen elektronika. Science of world, 1-19.
- Keyur K Patel, S. M. (2016). Internet of Things-IOT: Definition, Characteristics, Architecture, Enabling

Technologies, Application & Future Challenge. IJESC, 6(5), 6122-6131.

Lawson J., Silver H. (1973). A social History of education in England. London: Methuen & Co.Ltd.

Mir Yusif Mir., B. (2012). A brief History of oil and gas well drilling. Azerbaijan: Visions of Azerbaijan  
<http://www.visions.az/en/news/366/4ca556e3/>.

Mokyr, J. (2003). The Second Industrial Revolution, 1870-1914. In R. H. Joel Mokyr, The lever of Riches (pp. 219-245). Illinois, Evanston: Northwestern University.

Mustaqim, W. A. (2018). Hukum minimum Liebeg - sebuah ulasan dan aplikasi dalam biologi kontemporer. Jurnal Bumi Lestari, 28-32.

Numbers, R. L. (2009). Miths and thruth in science and religion ; a historical perspective. Actualizacao Rapida, 250-256.

Ratiu, S. (2003). The History of the internal combustion engine. TImisaora: Faculty Of Engineering Hunedoara.

Reynoald, D. (2013). Henry Ford's Assembly line : How it's still rolling along 100 years later. CBS news:  
<https://www.cbsnews.com/news/henry-fords-assembly-line-how-its-still-rolling-along-100-years-later/>.

Rojko, A. (2017). Industry 4.0 Concept: Background and Overview. ECPE European Center for Electronics, 7790.

Rosadi, R. (2004). Sejarah Komputer dari Generasi pertama hingga sekarang. Bandung: Acedemia Edu.

Scranton, P. (1997). Endles novelty : specialty production and American industrialization, 1865-1925. Princeton: Princeton University Press.

Sitompul, M. (2018). Mendulang Sejarah Tambang Nusantara.  
<https://historia.id/politik/articles/mendulangsejarah-tambang-nusantara-P4WOp>.

Sugiharto, B. (2018). Materi Kuliah Filsafat Ilmu . Bandung: Program Doktoral S3-ITB.

Sundaram, K. (2016). The Internet of things and the changing landscape of product design. Dimensions, 1(1), 14.

Sungkar, L. (2007). Peranan golongan borjuis pada revolusi Prancis tahun 1789. Citra Lekha Jurusan Sastra Inggris Fakultas Sastra Universitas Diponegoro, 1-7.

Trust, N. (2001). Powerful Partnership : Greg, Ewart and the first engine. London: National Trust.

Wijaya, W. P. (2015). Steel converter Bessemer. Malang: Universitas Negeri Malang.

Wilson, J. M. (2014). Henry Ford Vs. Assembly line balancing. Internaltional Journal of Production Research, 757-765.

## Design of Information System for the Protection of Indonesian Migrant Workers

Leonardi Paris Hasugian<sup>1,\*</sup>, Deden Abdul Wahab<sup>2</sup>, Yeffry Handoko Putra<sup>3</sup>, Rangga Sidik<sup>4</sup>, and Yusrila Yeka Kerlooza<sup>5</sup>

<sup>1,4</sup> Sistem Informasi, Universitas Komputer Indonesia, Bandung - INDONESIA

<sup>2</sup> Magister Manajemen, Universitas Komputer Indonesia, Bandung - INDONESIA

<sup>3,5</sup> Magister Sistem Informasi, Universitas Komputer Indonesia, Bandung - INDONESIA

\* Corresponding author e-mail: leonardiparishasugian@unikom.ac.id

### Abstract

Indonesian Migrant Workers, called PMI, are Indonesian workers working overseas. The existence of PMI abroad is far from the control and monitoring of the government. Various cases that are often exposed in the mass media on PMI issues involved in killings, persecution, and so on are indicators that the involvement of various parties including the government has not been maximized. These issues should ideally be minimized if there is a form of communication, and the continuation of that is the response. Communication and response become one of the media for Indonesian Migrant Workers working abroad. Providing fast and accurate information needs to be designed. For that reason, the author designs website and mobile-based information systems by proposing hardware, software, brainware, and network design. The purpose of this research is to get a blueprint or design of information system to provide protection for PMI so that it can be manifested in hardware, software, brainware, and network development later.

*Keywords: Indonesian Migrant Workers, Protection, Design of Information System*

### 1. Introduction

Government institutions that specifically handle PMI is Badan Nasional Penempatan dan Perlindungan Tenaga Kerja Indonesia (BNP2TKI) accompanied by the presence of various laws, one of which is Law No. 18/2017 concerning Protection of Indonesian Migrant Workers (Pekerja Migran Indonesia - PMI), which is that state adapted by Suradiansyah. This underlines that the government is actively involved in serving PMI. However, this foundation only shades PMI in terms of regulations and laws. Real form through Standard Operational Procedure (SOP) made by the government in the Departemen Ketenagakerjaan has not been ideally implemented, for example: A PMI must report periodically so that the existence and condition of PMI can be known. If a problem occurs, the government will also help it related to work problems (SOP for Work, Salary, Form of Work Violence, etc.). This explains that PMI when working will definitely find a problem, both small and large scale. The tendency, the continuation of this problem can be fatal if the handling is not immediately resolved. So it is not surprising that several cases of maltreatment and murder involving PMI were exposed by the mass media because they stem from handling problems that are not holistic and fast. Then for this situation, conclusion from the results of various research from Adha, Pawestri, Taufik, Sejati, and Palebang refers to problems that require an ideal solution.

There are quite a lot of cases involving PMI in various countries where PMI works. Veenstra stated, the case will be resolved when it is known to other people or raised in a mass media and social media that is categorized as citizen journalism. A question "what about the persecution and murder cases involving PMI but not exposed?", It became a homework for all parties. It is undeniable that cases of crime and violence involving PMI are like the iceberg phenomenon. According to Hasugian research, some statements that became the findings of PMI involvement with certain cases were obtained from the BNP2TKI report for 2011-2018 which stated that: 1) Malaysia, Taiwan, Hong Kong, and Saudi Arabia were the countries with the largest PMI objectives compared to other countries, 2) Complaints to data centers on PMI issues via email, SMS, telephone, underutilized social

media, 3) undocumented PMI, illness, inappropriate salary, layoffs, and repatriation are problems that often occur, and 4) The number of PMI complaints from Saudi Arabia and Malaysia is in line with the Death rates of PMI working in that country.

Basically efforts to protect workers in various countries already exist such as efforts to protect migrant workers in the ASEAN country environment such as in the country; Malaysia built the Foreign Workers Centralized Management Systems (FWCMS) known as MIGRAMS, the Philippines with the Foreign Labor Operations Information System (FLOIS), and Singapore which utilized the Geographical Information System, where this system had become the discourse of the Indonesian government for adopted into the PMI monitoring system and manifested by the presence of SIPMI, similar efforts were also made by Rismanto with the utilization of location base service technology for PMI monitoring systems abroad. Barry and Hager stated, the role and existence of Information Technology should have functioned in resolving various cases affecting PMI. When Information Technology becomes a "weapon" for PMI, they will feel safe and comfortable when working. Simply put Information Technology that is built bridges information from PMI to the government. When the government gets information from PMI, the response is to contact or meet with the PMI. This makes PMI trust and believe that they are actively protected by the government. Information technology in the form of information systems which will be integrated with existing systems within the BNP2TKI. The provision of services in the form of an integrated information system will be built by building a PMI (repository) information portal on the side of the PMI and the BNP2TKI administration environment. Mobile-based applications will be provided to PMI as a medium for sending information on the whereabouts and condition of PMI on a regular basis, while website-based applications will be built as a medium to monitor PMI for BNP2TKI. As a whole the development of digital media services is used to provide services to PMI and assist BNP2TKI in monitoring PMI. In general, the design of these media includes hardware, software, brainware, and network. That scope is a blueprint in the construction of PMI control and monitoring. For this reason, the author will design an information system which can give protection for PMI in order to obtain a design in the development of the information system later.

## 2. Research method

The phase of research refer to Figure 1. The research phase that the author does is mapping the needs of designing computer components in the system, namely hardware, software, brainware, and network. The design that the author builds is modeled with the Unified Modeling Language tool by translating the entire procedure into a use case. For the user interface layout built with the appearance of a mobile application that generally expresses the operational use of the system. Whereas brainware is translated into access that can be done by each stakeholder. For the network is designed by simulating using a computer network simulation tool to get the network design scheme that is connected in the system.

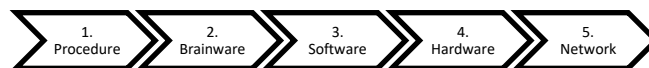


Fig. 1: Research Method

## 3. Result and Discussion

### 3.1. Procedure Design

The design procedure is carried out to obtain the pattern of activities that will work in the Indonesian Migrant Workers Protection Information System. There are seven procedures that form the basis of the system which are translated into use cases that are built based on our research before in Figure 2, namely (1) Reporting; This procedure describes the provision of the latest PMI state data through the input process based on absences, attendance photos, and questions which are the personal attributes of each PMI. Afterwards, PMI status will be assessed and mapped whether it is in a normal or emergency situation. Shortly after entering the system, the system will display three main menus namely Attendance, Emergency, and History. In the Reporting section, the system will display an Attendance menu where PMI will fill in the attendance list, provide a selfie photo, and answer a series of questions (around 5-10 questions) whose answers are PMI's personal attributes known only to PMI and BNP2TKI. For example like; a) Mother's maiden name, b) Name of the area where grandfather and grandmother are, 3) First pet name, etc. (2) Panic; Basically the same as the reporting procedure, but the

differentiator in this section is that PMI can provide reporting with direct verification without going through absences, selfies, and questions by displaying Emergency PMI notifications and current PMI locations. Thereafter, PMI Status will be mapped in an emergency and can be followed up immediately by other stakeholders, (3) PMI Status; This procedure explains the determination of PMI Status whether in a normal or emergency situation related to follow-up by the Embassy and the Authorities. PMI status is obtained from calculations based on the Analytical Hierarchy Process through three attendance variables, selfies, and questions about PMI attributes in the Verification section. Based on the calculations, the main focus is on these three variables: a) Attendance will be assessed based on how often PMI reports itself to the system, whether full absent, half absent, or absent at all, b) Selfie photos will recognize symptoms that are not appropriate, whether in accordance with the default data by using face recognition support by AWS Rekognition according to Santhoshkumar, whether PMI is in good condition or not good by photographing itself, accompanied by certain codes known only to PMI and BNP2TKI and or other stakeholders, and c) Questions originating from PMI's personal attributes known to PMI and BNP2TKI must PMI was answered with a minimum validation limit above 80%. If the values of the three variables are met then the PMI Status will be "Green" in the sense of Safe and Controlled. If one of them has a value that is not met then PMI Status will be "Yellow" in the sense of Safe and Needs Further Confirmation. Whereas if all the variable values are not met then the PMI Status will be "Red" in the sense of Requiring Serious Attention or Requiring Responsive Response, (4) Verification; In the Verification section. The system will assess the calculation process using the Analytical Hierarchy Process as explained in the PMI Status procedure. In this section the system will independently process the input data from PMI in the form of absences, photo suitability, and answer questions and produce output in the form of information about PMI status related to whether PMI falls into the category of: a) Green, b) Yellow, or c) Red, ( 5) Response; This procedure explains the process of follow-up by the Embassy and the Authorities in responding to the PMI Status case. If "Green" then the stakeholders do not need further response. If "Yellow" then the stakeholders must reconfirm PMI to receive valid data through other means (contact by telephone, email, social media, etc.), so that when it is found it can be entered into the "Green" or "Red" category means a different response. Whereas if "red" then the stakeholders must respond immediately through direct visit or visit in an immediate time to find out the condition and whereabouts of PMI directly, (6) Actions; Procedure Actions provide access to all stakeholders to respond responsibly (without giving administrative documents). Each stakeholder will be given authority to convey who is involved in responding to the "Red" category. Specifically, full authority rests with BNP2TKI, who is directly aware of this information by the Embassy and / or Third Parties (for example the local police, the country where the PMI works), and can subsequently be followed up with real action so that the response can be faster and on target, and (7) Report; A report that indicates every activity in the system. Existing reports in the form of: a) Data of each stakeholder in the system (PMI, BNP2TKI, Indonesian Embassy, Third Parties, and PMI Families), b) PMI Reports that do Reporting, c) Verification calculation reports, d) PMI Status Reports (Green, Yellow and Red), e) Panic Report (Emergency), and f) Response Report that has the attributes: i) Who responds, ii) Who goes to PMI, and iii) PMI under what conditions. In general, the above procedure is modeled on the use case diagram based on Figure 2. The diagram shows that actors and cases are inclusive of various activities in utilizing information system components, namely hardware, software, brainware, network, data and procedures.

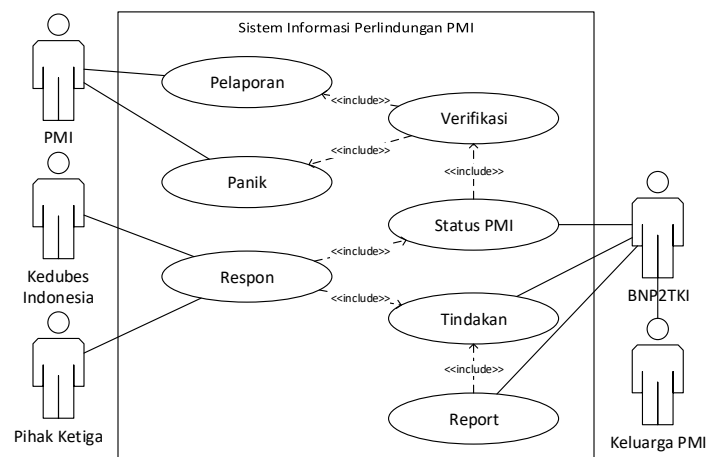


Fig. 2: Use Case of PMI Protection Information System

The procedure above discusses the activities carried out by all stakeholders. In detail in each activity there are inputs and outputs carried out by stakeholders. Based on this procedure, it can be mapped class diagrams that are manifested into the data needed in database design. Broadly speaking, the database design has PMI, BNP2TKI, Indonesian Embassy, Third Party and Family identity tables as well as response tables and actions taken by BNP2TKI, Indonesian Embassy, and Third Party.

### 3.2. Brainware Design

Based on the development of a PMI protection information system use case, the roles and activities of the brainware involved in the PMI protection information system are found. Table 1 describes the access and activities performed by each brainware. Each brainware has its own access (limited).

**Table 1: Brainware of PMI Protection Information System**

Brainware Access	Menu that can be accessed	Activities on the Menu
(Indonesia Migrant Workers) PMI	(Reporting) Pelaporan	Reporting by filling in the status form, taking selfies, and answering questions then submitting them
	(Panic) Panik	Access the panic button as an instant reporting that PMI is in an emergency by providing the latest location data
BNP2TKI	(PMI Status) Status PMI	See PMI categories whether their status is red, yellow, or green which is related to the action whether emergency, further response, or normal
	(Action) Tindakan	Checking as a form of final verification to proceed to the response of the Indonesian Embassy and Third Parties by providing information in the form of information and attachments
	(Report) Laporan	Final Report whether the PMI responded whether it has been completed or not yet finished
(Indonesia Embassy) Kedubes Indonesia	(Response) Respon	Following up on information provided by BNP2TKI by responding (visiting) and providing reports on photos and response results that are relevant to third parties
(Third Parties) Pihak Ketiga	(Response) Respon	Following up on information provided by BNP2TKI by responding (visiting) and providing reports on photos and response results in accordance with the Indonesian Embassy
(PMI Family) Keluarga PMI	(Report) Laporan	Get the latest reports on the status of PMI through downloadable documents

### 3.3 Software Design

Figure 3.a - 3.f refers to the design of input and output on the software to be built. The design of the software user interface is specifically built for mobile platform, besides the web platform. The context of software user interface presented will be the same on all platforms.

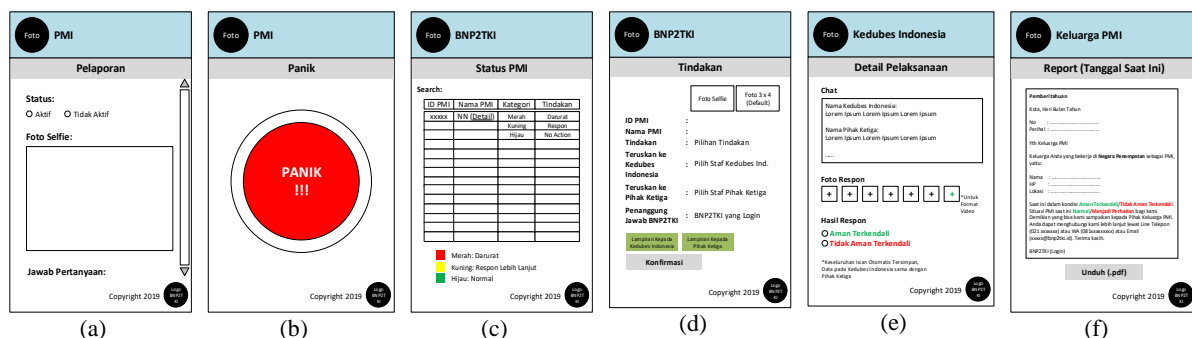


**Fig. 3: Software User Interface of PMI Protection Information System (a) PMI Reporting, (b) PMI Panic, (c) PMI Status, (d) BNP2TKI Action, (e) Indonesia Embassy Response, dan (f) Report for PMI Family**

In general, Figure 3.a states the display for PMI when reporting by displaying active / inactive status, selfies, and answering questions. From this the system will be about whether there is an appropriate or not based on attendance parameters, the suitability of selfie photos with photos stored on the database server, and 10 (ten) answers to



questions whose conformity value is above 80%. Even so, according to Figure 3.b, PMI can report critical situations by pressing Panic access where PMI can be identified through the location of the device PMI is using. After that based on Figure 3.c the status of PMI will be identified to immediately proceed to assignment in Actions in Figure 3.d which will be forwarded to the Indonesian Embassy and Third Parties in accordance with Figure 3.e. Basically information and other statements will be attached with the same statement and subsequently the Indonesian Embassy and Third Parties will follow up by visiting the places that PMI has reported and they will coordinate and provide integrated reports (enter and update data together). After that the report from them will be forwarded to BNP2TKI into a report that will be forwarded back to the PMI Family in accordance with Figure 3.f.

### 3.4 Hardware Design

Hardware design based on minimum server and client specifications. The design is obtained based on consideration of minimum needs so that it can be later implemented. The design for servers is focused on desktop devices while for clients on desktop and mobile devices. Table 2 below is the minimum specifications of hardware used.

**Table 2: Hardware Specifications of PMI Protection Information System**

Server/ Client	Device Category	Minimum Specifications
Server	Desktop	Platform: Dual CPU Rack Server, O/S Provided: Optional, PSU: 550 W, Optical Drive: Optional, 1 <sup>st</sup> Processor Onboard: Intel® Xeon® Processor Silver 4114 (10 Cores, 2.20 GHz, 13.75M Cache), 2 <sup>nd</sup> Processor Onboard: Optional, Input Device Type: Optional, Dimension (W x H x D): 59 x 21 x 100 Cm, Standard Bays: 8 x 2.5" SAS/SATA HDD, Slot Provided: 6 Gbps SATA, Onboard SATA AHCI (non-RAID), 12 Gbps SAS/6 Gbps SATA, RAID 0/1/10/5/50 with RAID 530-8i, RAID 730-8i 1 GB Cache atau RAID 930-8i 2GB Flash, Chipset: Intel C622, Networking: 2 x 1 GbE Network, Video Type: Integrated Matrox G200, Chasis Form Factor: 1U Rackmount Chassis, Monitor: Optional, Standard Memory: 1 x 8GB RDIMM, Processor Type: Intel Xeon Processor, Weight: 20 Kg, 1 <sup>st</sup> Hard Drive: Optional, Keyboard Type: Optional, Max. Memory: Up to 12 DIMM sockets.
Client	Desktop	Processor: Intel Core 2 Duo 2.0 GHz, Mainboard: Ampttron G41, HDD: 80 Gb, RAM: DDR3 2 GB, VGA Card: GT 210 1 GB, DDR3, DVD RW: LG, Casing: Castello Moluca, Power Supply: 450 Watt, Keyboard: Optional, Mouse: Optional, Monitor: Optional.
	Mobile	Processor: Qualcomm® Snapdragon™ 430 with 64bit Quadcore, Screen: 5.45" 18:9 Ultrawide display in 5' compact size, Camera: 5 MP + 13 MP, Jaringan: 2G/3G/4G, RAM: 2 GB, Memory: 16 GB.

### 3.5 Network Design

Domain name that can be access by the stakeholder is <http://pmiprotection.id>. The domain is accessed through a network which is simulated mapped based on Figure 4. Where, the server will be in contact with each host through various desktop and mobile devices. Network topology design using star topology with wide area network coverage. For the range of IP addresses use Class C with IP address 192.0.0.0. Figure 4 shows a simulation of the PMI protection information svstem.

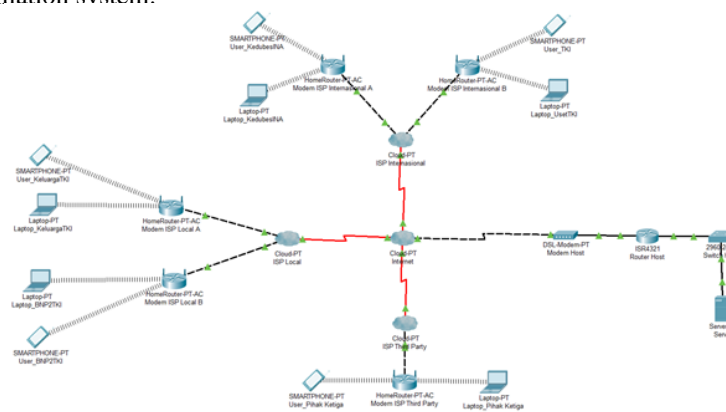


**Fig. 4: PMI Protection Information System Network Simulation**

## 4. Conclusion

Indonesian Migrant Workers problems are followed up by build the design of procedures and data, brainware, hardware, software, and networks. Based on that, blueprint is made to prepare for development information system. The design purpose is become a standard in the development of information system that able to protect Indonesian migrant workers. This design will continue to build the whole information system and do testing and evaluating to get a fit overall system.

## 5. Acknowledgements

The authors thank the various parties involved in this research, specifically for friends of Indonesian Migrant Workers who contributed in providing data, information, and suggestions. This research is funded by a research grant from Kementerian Riset, Teknologi dan Pendidikan Tinggi.

## 6. References

- Adha, L. Hadi. 2015. Perlindungan Hukum Tenaga Kerja Indonesia (TKI) yang Melebihi Batas Masa Tinggal (Overstay). Jurnal Hukum Jatiswara. Universitas Mataram. Jatiswara.
- Barry, B. W. 1986. Strategic Planning Workbook for Public and Nonprofit Organizations. St. Paul, MN: Amherst Wilder Foundation.
- FLOIS. Foreign Labor Operations Information System (FLOIS) for the protection of migrant workers. [http://www.ilo.org/dyn/migpractice/migmmain.showPractice?p\\_lang=en&p\\_practice\\_id=131](http://www.ilo.org/dyn/migpractice/migmmain.showPractice?p_lang=en&p_practice_id=131)
- Hager, M.A, dan Tyler Curry. 2009. Models of Collaboration: Non Profit Organizations Working Together, ASU Lodestar Center.
- Hasugian, L.P., and Rahayu, T.M. 2018. Requirement Analysis of Monitoring Information System for Indonesian Migrant Workers Protection. In Proceedings of the INCITEST International Conference on Informatics Engineering, Science, & Technology (Bandung, May 9, 2018).
- Indonesia, Undang-Undang No. 18/2017 tentang Perlindungan Pekerja Migran Indonesia.
- Kementerian Tenaga Kerja. Kemnaker Modernisasi Sistem Monitoring TKI dan TKA Berbasis Digital. <http://infopublik.id/read/164698/kemnaker-modernisasi-monitoring-tenaga-kerja-berbasis-digital.html>
- Migrams. Migrant Management System. <https://www.migrams.com>
- Palebang, Herson. 2014. Koordinasi dalam Pemulangan Ternaga Kerja Indonesia (TKI) di Kabupaten Nunukan. eJournal Ilmu Pemerintahan. 2, 3, 2980-2991.
- Pawestri, Anindhita Okta. 2014. Fungsi Kartu Tenaga Kerja Luar Negeri (KTKLN) dalam Upaya Perlindungan Hukum bagi Tenaga Kerja Indonesia. Universitas Atma Jaya Yogyakarta.
- Rismanto S., Solihin H. Hanafiah. 2017. Pemanfaatan Teknologi Location Base Service untuk Sistem Monitoring Tenaga Kerja Indonesia di Luar Negeri. Jurnal Infotronik. 2, 2.
- Santhoshkumar, G.S., et al. 2019. Face-track : Smart Attendance System using Face Recognition. International Research Journal of Engineering and Technology (IRJET). 6, 5 (May, 2019), 6580-6582.
- Sejati, Satriyo Pringgo. 2015. Perlindungan Tenaga Kerja Indonesia di Luar Negeri. Tesis. Pasca Sarjana Universitas Muhammadiyah Yogyakarta. Yogyakarta.
- Suradiansyah, Jeffri. 2016. Peran Dinas Tenaga Kerja dalam Perlindungan dan Pengawasan Ketenagakerjaan di Kota Samarinda. eJournal Ilmu Pemerintahan. 4, 2, 947-960.
- Taufik, Soraya, Dewa Gede Rudy, I Made Dedy Priyanto. 2012. Peran Dinas Tenaga Kerja dalam Mencegah Terjadinya Masalah TKI di Luar Negeri. Fakultas Hukum. Universitas Udayana. Bali.
- Tribunnews. Kemnaker Luncurkan Aplikasi SIPMI untuk Pekerja Migran. <http://www.tribunnews.com/nasional/2018/12/27/kemnaker-luncurkan-aplikasi-sipmi-untuk-pekerja-migran>
- Veenstra, A. S., Iyer, N., Delwar, M., & Park, J., 2014. Computers in Human Behavior Time, Place, Technology: Twitter as an information source in the Wisconsin labor protests. Computers in Human Behavior. 31, 65–72.

## Clustering Emotional Features using Machine Learning in Public Opinion during the 2019 Presidential Candidate Debates in Indonesia

Agus Sasmito Aribowo<sup>1,2</sup>, Yuli Fauziah<sup>1</sup>, Halizah Basiron<sup>2</sup>, Nanna Suryana Herman<sup>2</sup>,  
and Siti Khomsah<sup>3</sup>

<sup>1</sup> Department of Information Engineering, Universitas Pembangunan Nasional “Veteran” Yogyakarta,  
Yogyakarta - INDONESIA

<sup>2</sup> Fakulti Teknologi Maklumat dan Komunikasi, Universiti Teknikal Malaysia Melaka - MALAYSIA

<sup>3</sup> Department of Information Engineering, Institut Teknologi Telkom Purwokerto, Purwokerto -  
INDONESIA

Corresponding author e-mail: sasmito.skom@upnyk.ac.id, siti@itttelkom-pwt.ac.id

### Abstract

This research has produced a description of the emotions of streaming-video viewers of presidential candidate debates broadcasted on Youtube. In the first presidential candidate debate, the emotions of viewers were still neutral and tended to be feelings of pleasure and happiness. In the second to fifth presidential candidate debates, the dominant emotions were happy, angry, and sad. This research is known as emotion analysis, using comments from viewers of presidential candidate debates on Youtube as the data. Those comments were downloaded and pre-processed for data cleaning, emotion feature extraction, and clustering using K-Means based on six basic types of emotions: anger, sadness, happiness, fear, surprise, and disgust. The aims to be achieved are to determine a more homogeneous cluster for each opinion in the presidential candidate debate videos and to provide an emotional label for each cluster formed. The results of the research are five clusters that have distinctive homogeneity, namely happiness, anger, neutral, surprise-angry-disgust, and sadness. Each cluster member was labeled according to its characteristics. After being divided for each stage of the presidential candidate debate, it can be seen that the journey from the first debate to the next debate period tended to increase the emotion of anger and reduce the emotion of neutral.

*Keywords: Emotion Analysis, Clustering, K-Means, Basic Emotion*

### 1. Introduction

Indonesia entered the political year in 2019. Political parties make use of social media as a means of political communication by posting political news, comments and videos. Youtube as the largest video-based news portal is used as a means of political communication. Comments on Youtube videos related to the presidential election represent public response to the political figures, campaign programs, and political promises. Analysis of sentiment is needed to analyze and assess public opinion on a video, conversation, or certain topics on social media. Sentiment analysis is the extraction of information which aims to extract information about the feelings of authors both positively and negatively by analyzing many documents (Mukherjee & Bhattacharyya, 2013). Sentiment analysis can be considered as a combination of text mining and natural language processing. Basically, the work process of text mining adopts many data-mining studies, but the difference is that the patterns used by text mining are taken from a group of unstructured natural languages whereas in data mining, the pattern is taken from structured data (Han & Kamber, 2012). An important feature of analysis sentiment is the emotion feature. Emotion analysis is also a field of study that analyzes emotions towards entities such as products, organizations, individuals, information services, issues, events, topics, and attributes. The emotion analysis is computational research of emotions expressed textually (Liu, 2012). Many of English emotion analysis researches classify documents or opinions based on Ekman's 6 (six) basic emotions: surprise, happiness, anger, fear, disgust, and sadness (Ekman, 1992).

It is difficult to classify public opinion on Youtube videos, that are available in large numbers, into several groups of emotions. In addition, related research is still limited. Then, this research is about how to recognize emotions so as to expand the level of existing sentiments. The aim is to describe public emotions better so that it can be known at what level they are considered harmful.

One of the methods for unsupervised grouping of data is clustering method. This method can be used as a first step to group opinion data based on emotional features that have been extracted previously. Then, the most dominant characteristics in each cluster produced can be observed and labeled. The label will be used as a label for every data in the cluster. The results of the clustering will be visualized, and it functions as a description of the emotions of netizens in each presidential candidate debate.

## 2. Literature review

Research on sentiment and emotion analysis includes predicting the results of gubernatorial or presidential election (Mochamad Ibrahim, Abdillah, Wicaksono, & Adriani, 2015) (Joyce & Deng, 2017) (Budiono,

Nugroho, & Doewes, 2017) (Attarwala, Dimitrov, & Obeidi, 2017) (Kušen & Strembeck, 2018), predicting the results of parliamentary elections (Smailovic, Kranjc, Gracar, Znidarsic, & Mozetic, 2015) (Castro & Vaca, 2017), political party market share (Sharma & Moh, 2016) (Wicaksono, Suyoto, & Pranowo, 2016), political figures (Razzaq, Qamar, & Bilal, 2014) and general political conditions in countries (Charalampakis, Spathis, Kouslis, & Kermanidis, 2015) (Filho, Almeida, & Pappa, 2015). If emotion analysis is applied to public opinion on the 2019 presidential candidate debate video, it is expected that public emotions toward the content of the presidential candidate debate videos can be known. This certainly gives positive contributions to politics in Indonesia. Emotion features are needed to determine the power of sentiment and are divided into six basic emotions according to Ekman, namely anger, sadness, disgust, happiness, fear, and surprise. It is necessary to specify how negative an opinion is because of the fact speaking, especially negative sentiment. There are often incidents in social media. Social media is often used for negative political communication, such as black campaigns, negative sentiment, hate speech, and opinion warfare. Social media is often used for hate speech between supporters of political figures against others. Many incidents of political fanaticism on social media cause broken friendships, broken brotherhood, destroying family and community relations (BBC News, 2014). There are cases of political fanaticism on social media causing murders (Flo, 2018).

## 3. Methodology

### 3.1 Research Steps

Based on the background of the problem, the research steps are shown in Fig 1. The research went through 6 (six) steps and was carried out sequentially. This sequence of steps were carried out to group political opinions in an unsupervised way on social media related to the presidential candidate debates to display the results in graphical form.

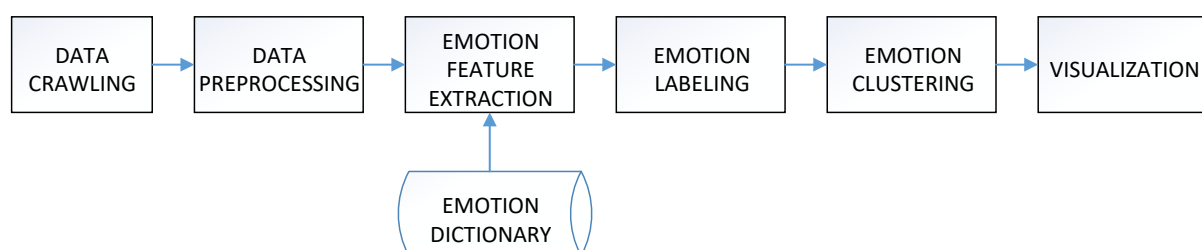


Fig. 1: Research Steps

### 3.2 Data Crawling

Public opinion on the videos of the presidential candidate debates was obtained from the official video of the television stations that broadcasted the debates live using streaming media on Youtube. Not all channels were selected in the data collection. The debate schedule, topics, and Youtube channel that is the source of the data are in Table 1:

**Table 1: Debate Schedule and Youtube Channel**

Debate Number	Topic	Channel	Record Number
I	Law, Human Rights, Corruption and Terrorism	Kompas TV IDN Times	715
II	Energy and Food, Natural Resources and the Environment, and Infrastructure	MNC TV CNN Indonesia	715
III	Education, Health, Employment, Social and Culture	Kompas TV IDN Times	715
IV	Ideology, Governance, Defense and Security, International Relations	Kompas TV IDN Times	715
V	Economy and Social Welfare, Finance and Investment, Trade and Industry	TV One News CNN Indonesia	715
	TOTAL		3575

Two Youtube channels were chosen in every presidential candidate debate. Youtube channel selection is based on the largest number of viewers, video length, completeness of video content, and the highest number of comments. The data retrieval process was done with Youtube Comment Scrapper software, and all comments from the videos could be downloaded and saved in csv format. The csv file had a good structure, containing comments and comment replies, date, users' identities, and several other attributes. Selection of comments in csv file was done manually, so that only opinion comments related to the videos of presidential candidate debates would be included in the next process. There are 715 opinions chosen randomly in each debate.

### 3.3 Data Preprocessing

Data preprocessing activities are removing unstructured text, converting text into words that are easily processed by machine learning, and deleting unimportant text data. Pre-processing is crucial in sentiment analysis because social media mostly contains unstructured words. The purpose of preprocessing is to clean and make the word uniform so that the word is ready for extraction to the next stage (Haddi, Liu, & Shi, 2013). There are several sub-tasks of pre-processing such as tokenizing, removing punctuation, removing username, removing hashtag, cleaning number, cleaning one character, removing URL, removing RT i.e. the symbol "@" before a username in question, converting non-standard words and emoticons. Preprocessing is useful for experts to facilitate the labeling of emotions so that preprocessing does not eliminate punctuation, word affixes, and letter case.

### 3.4 Emotion Feature Extraction

After the opinions were cleaned in the data cleaning stage, the emotional features of the opinions were removed from each sentence. The process of extracting emotional features from each sentence was done by matching each word in the opinion sentence with the NRC-Emotion-Lexicon dictionary downloaded from the internet (Mohammad, 2017). This dictionary contains a list of keywords along with the dominant types of emotions that apply to those keywords. Each sentence can contain several emotional features, and each emotional feature can have different strengths. However, the emotional features produced by matching with this dictionary are not the final justification for each opinion sentence. This research involves experts who manually test every sentence feature generated using the dictionary.

### 3.5 Emotion Labeling

Emotion is divided into 6 types according to Ekman's 6 (six) basic emotions such as happiness, surprise, anger, disgust, fear, and sadness (Ekman, 1992). In this research, every type of emotion has 4 (four) levels of polarity as shown in Table 2.

**Table 2: Level and Weight of Emotion**

Level of Emotion	Weight	Information
High	3	The emotion value on the text approximately 100%-67%
Average	2	The emotion value on the text approximately 66%-34%
Low	1	The emotion value on the text approximately 33%-1%
None	0	No emotion on the text

Emotion labeling for each opinion sentence that has been cleaned and extracted using a dictionary was done by experts. Experts provided justification for emotional judgment in each sentence using the emotional assessment form as in Fig. 2

No	Comment	Angry	Fear	Disgust	Sadness	Surprise	Happiness
1	semoga bpk prabowo menang di pilihan presiden 2019...Aamiin..	Tidak Ada	Tidak Ada	Tidak Ada	Tidak Ada	Tidak Ada	Sedang
2	Saya dr Bondowoso Jawa timur tetap dukung Prabowo-Sandi	Tidak Ada	Tidak Ada	Tidak Ada	Tidak Ada	Tidak Ada	Sedang
3	Kalau ada yang cinta pada rakyat indonesia... dialah Pak Prabowo..	Tidak Ada	Tidak Ada	Tidak Ada	Tidak Ada	Tidak Ada	Sedang
4	Tak ada yang bisa megganti seorang jokowi, jngan berharap lebih ya no x?	Lemah	Lemah	Tidak Ada	Tidak Ada	Tidak Ada	Tidak Ada
5	cuma orang goblok yg milih nmr x	Sedang	Tidak Ada	Lemah	Tidak Ada	Tidak Ada	Tidak Ada
6	Dari dulu tetap jokowi tidak pernah berubah #jokowi2periode	Tidak Ada	Tidak Ada	Tidak Ada	Tidak Ada	Tidak Ada	Sedang

**Fig. 2: Form to determine the type of emotion**

### 3.6 Clustering

The clustering process starts by converting each emotion label into a number. The conversion number is obtained from the weight in Table 2. For positive emotions, the weight is positive (happiness and surprise). For negative emotions, the label will be given a negative value (anger, sadness, fear and disgust). Some of the results of the conversion of emotion labels into emotion weight are in Fig. 3.

No	Comment	Angry	Fear	Disgust	Sadness	Surprise	Happiness
1	semoga bpk prabowo menang di pilihan presiden 2019...Aamiin..	0	0	0	0	0	2
2	Saya dr Bondowoso Jawa timur tetap dukung Prabowo-Sandi	0	0	0	0	0	2
3	Kalau ada yang cinta pada rakyat indonesia... dialah Pak Prabowo..	0	0	0	0	0	2
4	Tak ada yang bisa megganti seorang jokowi, jngan berharap lebih ya no x?	1	1	0	0	0	0
5	cuma orang goblok yg milih nmr x	2	0	1	0	0	0
6	Dari dulu tetap jokowi tidak pernah berubah #jokowi2periode	0	0	0	0	0	2

**Fig. 3: Converting from an emotion label into an emotion weight**

The clustering process was carried out using K-Means method with a configuration of a K value of 5 because it was desired to produce 5 clusters. The results of the clustering process are a table containing the centroid values of the results of the clustering process in the opinion data in Fig 3. Each centroid cluster becomes the midpoint of more homogeneous emotion groups. The emotion values for each cluster center point are in Table 3. Based on Table 3, this research concludes that each cluster has specific emotion characteristics. Clustering also manages to divide data into 5 large groups that are more homogeneous. The numbers in the highlighted table cell are the most dominant type of emotion in cluster 1 is anger (-2,36). Cluster 2 is happiness (2,19). Cluster 3 is surprise (2,68), anger (-2,027), and sadness (-1,19). Cluster 4 is sadness (-2,14). Negative number in Table 3 indicates the type of negative emotion and positive numbers indicate the type of positive emotion. The summary characteristics of each cluster are in Table 4. The dominant emotion characteristics in each cluster are the label for all data bound to the cluster. Thus, there are 5 data groups.

Table 3: Centroit Table

Emotion	Cluster				
	0	1	2	3	4
Happiness	0.29	0.09	2.19	0.33	0.07
Disgust	-0.13	-0.66	-0.02	-1.86	-0.09
Surprise	0.03	0.06	-0.02	2.68	0.06
Anger	-0.23	-2.36	-0.06	-2.03	-0.24
Sadness	-0.14	-0.21	-0.02	-1.19	-2.14
Fear	-0.14	-0.21	-0.04	-0.92	-0.09

Table 4: Emotion Characteristics of each Centroit

Cluster	Emotion Characteristics Domination of each Cluster
0	Neutral
1	Anger
2	Happiness
3	Surprise, Anger, and Disgust
4	Sadness

### 3.7 Data Labeling

Each sentence in the dataset is labeled as a cluster number. Then each presidential debate is recapitulated based on the number of members of each cluster as in table 5.

Table 5: The number and percentage of each cluster in each presidential debate

Debate I			Debate II			Debate III			Debate IV			Debate V		
Clus ter	Rec. Num	%	Clus ter	Rec. Num	%	Clus ter	Rec. Num	%	Clus ter	Rec. Num	%	Clus ter	Rec. Num	%
0	465	65,3	0	402	56,4	0	232	32,7	0	252	35,7	0	301	42,1
1	33	4,6	1	86	12,0	1	95	13,3	1	226	31,7	1	174	24,3
2	200	28,0	2	226	31,6	2	353	49,3	2	234	32,7	2	239	33,6
3	2	0,0	3	2	0,0	3	2	0,0	3	3	0,0	3	1	0,0
4	14	2,0	4	0	0,0	4	33	4,7	4	0	0,0	4	0	0,0

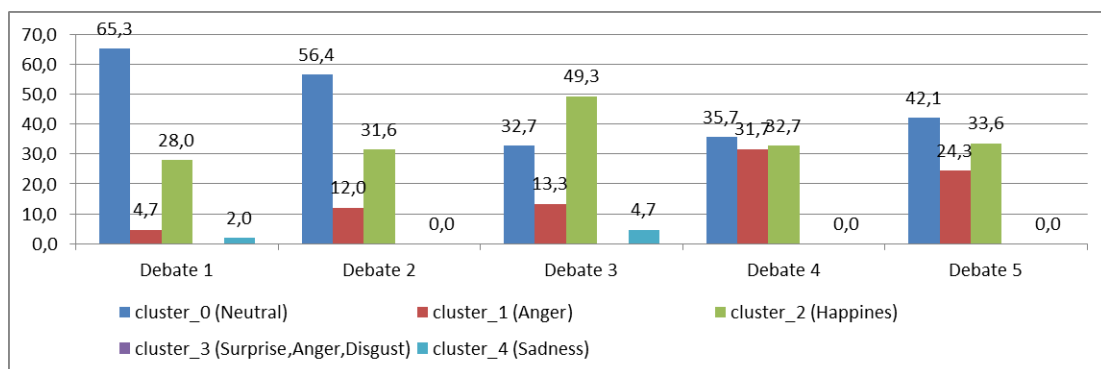


Fig. 4: The percentage of clusters at each presidential candidate debate

Fig 4 show than in the first presidential candidate debate, the dominant cluster was cluster 0, meaning that the audience was still neutral (65.3%) and did not show significant emotions. In the second presidential candidate debate, viewers began to show the emotion of anger (12%) and happiness (31.6%). In the third presidential candidate debate, viewers showed increasingly diverse emotions, ranging from anger (13.3%), happiness (49.3%) and sadness (4.7%). In the fourth debate, viewers showed only two kinds of emotions, namely anger (31.7%), and this was the peak of the emotion of anger, and happiness (32.7%). In the fifth presidential candidate debate, anger decreased (24.3%), and the emotion of happiness increased slightly (33.6%).

## 4. Conclusion

This research produces a description of emotions of viewers of presidential candidate debates on Youtube using K-Means machine learning methodology. The description of the emotions of the viewers shows that the most dominant types of emotions are happiness and anger. These emotions generally begin to emerge in the second presidential candidate debate. This description can be used to monitor interactions between viewers of presidential candidate debates. If negative emotions tend to strengthen or increase in frequency, this monitoring can be an early warning towards conditions that threaten national security.

## 5. References

- Attarwala, A., Dimitrov, S., & Obeidi, A. (2017). How Efficient is Twitter - Predicting 2012 U.S. Presidential Elections using Support Vector machine. In *Intelligent Systems Conference 2017*.
- BBC News. (2014). Putus Pertemanan Gara-Gara Pilpres. *BBC News*.
- Budiono, D. F., Nugroho, A. S., & Doewes, A. (2017). Twitter Sentiment Analysis of DKI Jakarta's Gubernatorial Election 2017 with Predictive and Descriptive Approaches. In *International Conference on Computer, Control, Informatics and its Applications Twitter*.
- Castro, R., & Vaca, C. (2017). National Leaders' Twitter Speech to Infer Political Leaning and Election Results in 2015 Venezuelan Parliamentary Elections. In *International Conference on Data Mining Workshops National*.
- Charalampakis, B., Spathis, D., Kouslis, E., & Kermanidis, K. (2015). Detecting Irony on Greek Political Tweets : A Text Mining Approach. *16th EANN Workshops*.
- Ekman, P. (1992). An Argument for Basic Emotions. *Cognition and Emotion*, 6(3–4), 169–200.
- Filho, R. M., Almeida, J. M., & Pappa, G. L. (2015). Twitter Population Sample Bias and its impact on Predictive Outcomes. In *International Conference on Advances in Social Networks Analysis and Mining*.
- Flo, E. (2018). Fanatisme Dukung Capres Berujung Pembunuhan, Ini Tanggapan Presiden Jokowi. *MerahPutih.Com*.
- Haddi, E., Liu, X., & Shi, Y. (2013). The Role of Text Pre-processing in Sentiment Analysis. *First International Conference on Information Technology and Quantitative Management*, 17(December 2014), p.26–32.
- Han, J., & Kamber, M. (2012). Data Mining: Concepts and Techniques Jiawei. In *Data Mining: Concepts and Techniques Jiawei*.
- Joyce, B., & Deng, J. (2017). Sentiment Analysis of Tweets for the 2016 US Presidential Election. *IEEE*, 5–8.
- Kušen, E., & Strembeck, M. (2018). Politics, Sentiments , and Misinformation : An Analysis of the Twitter Discussion on The 2016 Austrian Presidential Elections. *Online Social Networks and Media* 5, 5, 37–50.
- Liu, B. (2012). *Sentiment Analysis and Opinion Mining*. Morgan & Claypoll Publisher.
- Mochamad Ibrahim, Abdillah, O., Wicaksono, A. F., & Adriani, M. (2015). Buzzer Detection and Sentiment Analysis for Predicting Presidential Election Results in a Twitter Nation. In *15th International Conference on Data Mining Workshops Buzzer*.
- Mohammad, S. M. (2017). NRC Word-Emotion Association Lexicon.
- Mukherjee, S., & Bhattacharyya, P. (2013). *Sentiment Analysis : A Literature Survey*. Indian Institute of Technology, Bombay.
- Razzaq, M. A., Qamar, A. M., & Bilal, H. S. M. (2014). Prediction and Analysis of Pakistan Election 2013 based on Sentiment Analysis. In *International Conference on Advances in Social Networks Analysis and Mining (ASONAM 2014)*.
- Sharma, P., & Moh, T.-S. (2016). Prediction of Indian Election Using Sentiment Analysis on Hindi Twitter. In *IEEE International Conference on Big Data (Big Data) Prediction*.
- Smailovic, J., Kranjc, J., Grcar, M., Znidarsic, M., & Mozetic, I. (2015). Monitoring the Twitter sentiment during the Bulgarian Elections. *IEEE*.
- Wicaksono, A. J., Suyoto, & Pranowo. (2016). Proposed Method for Predicting US Presidential Election by Analysing Sentiment in Social Media.pdf. In *2nd International Conference on Science in Information Technology (ICSITech)*.



# AN INNOVATION CAPABILITY MODEL TO INCREASE MICRO, SMALL AND MEDIUM ENTERPRISES (MSMEs) COMPETITIVENESS IN INDONESIA: A CONCEPTUAL MODEL

Roosdiana Noor Rochmah<sup>1</sup>

<sup>1</sup> Faculty of Industrial Engineering, Telkom University, Bandung - INDONESIA

\* Corresponding author e-mail: diananr@telkomuniversity.ac.id

## Abstract

Globalization and the fourth Industrial Revolution have presented various opportunities but also disruption in the economy and social life. Although Indonesia's performance among ASEAN countries is very good, in 2019, Indonesia has experienced a decline in globally competitiveness. One of the low aspects is the innovation capability. As the main driver of the nation's economy, MSMEs must have the innovation capability to create innovation and make valuable contributions to the nation's competitiveness. It is very important to identify the factors that show the innovation capability. This paper present the key constructs of Innovation capability and the developed conceptual model which shows an innovation capability model through a conclusive research. The model identifies three key innovation capability constructs, namely knowledge & technology output, knowledge utilization for product innovation, and innovation fund generation and other important factors to explain the constructs. The first two constructs constitute the technical aspect and the third construct indicate the financial aspect of innovation capability.

*Keywords: innovation capability, competitiveness, MSMEs, conceptual model*

## 1. Introduction

Globalization and the fourth Industrial Revolution have presented various opportunities but also disruption in the economy and social life. Business competition forces business owners to have competitive advantages and strategies to maintain their business. Greater opportunities to attract consumers are owned by those who can deliver superior products through entrepreneurial orientation and innovation ability (Mohammad et al, 2019). At present, innovation is a major driver of long-term business success (Enzing et al., 2011), so it is a major challenge for all types of organizations (Andreeva and Kianto, 2011).

### 1.1 Global Competitiveness

Competition strategy is defined as all decisions and behaviors that provide competitive advantage through creating value and having basic capabilities for customers in certain markets (Porter, 2004). According to Porter, the company must determine its strategic position to maintain their presence in an intensive competition environment. The strategy a company must provide an opportunity to suggest values that are different from its competitors or present various benefits. The World Economic Forum (WEF) conducted survey data to measure global competitiveness, which was set out in the Global Competitiveness Index (GCI) Report. In the 2019 GCI report, Indonesia ranks 50<sup>th</sup>, down five places from last year. Among ASEAN countries, Indonesia ranks fourth after Singapore (1<sup>st</sup>), Malaysia (27<sup>th</sup>), and Thailand (40<sup>th</sup>). Indonesia's main strengths are its market size and macroeconomic stability. Apart from performance on other pillars, the quality of access remains relatively low. In the innovation ecosystem pillar, Indonesia gets the lowest score of all indicators for innovation capability and ranks 74<sup>th</sup>. On the other hand, Indonesia ranks 85<sup>th</sup> in the 2019 World Intellectual Property Organization (WIPO) on Global Innovation Index Report.

### 1.2 Creative Economy

Conceptual age is identical with creative economy era, whereas the core of economy is creative industry (Suhendra, 2017). The creative economy began to increase in Indonesia since 2017. The contribution of the creative economy to the Gross Domestic Product (GDP) has continued to increase in recent years. According to the Creative Economy Agency report, the GDP of the creative economy in 2018 will reach Rp. 1102 Trillion (Bekraf, 2019). Creative industries are part or subsystem of the creative economy. In general, the creative industries that have emerged in Indonesia are in the form of Micro, Small and Medium Enterprises (MSMEs), usually a form of business that is established independently by the owner. Recognizing the importance of MSMEs for economic growth and their ability to provide employment opportunities for the community, especially in rural areas (Abdullah & Mustapha, 2009; Ismail, 2013;

Mohamad, Rashed, & Rahman, 2008), many researchers have studied MSME factors to gain excellence competitiveness. Some researchers suggest that the main determinant of MSMEs to gain competitive advantage is the ability of MSMEs to develop unique products, and their flexibility in adopting new technologies (Williams & Hare, 2012). Saunila (2014) stated that MSMEs could get more benefits if they develop and explore an innovation orientation. Innovation is defined as a mental process that leads to the creation of new phenomena in the form of new material or new services or new techniques (Abou-Moghli, Abdallah, & Muala, 2012). Innovation has a strong positive impact on competitive advantage. Aziza & Samad (2016) said that innovation contributed 73.5% in competitive advantage.

### 1.3 Research Problem

Innovation has a strong positive impact on competitive advantage. It is very important to identify the factors that show the capability of innovation and then develop an innovation capability model to improve the competitiveness of MSMEs. That is the purpose of this research.

## 2. Literature review

### 2.1 Innovation Capability

The ability of innovation can be described as the ability to continuously change knowledge and ideas into new products, processes and systems for the benefit of the company and its stakeholders (Mohammad et al, 2019). Not only does it refer to the ability to be successful in managing new business flows, the ability of innovation is also related to the ability to synthesize the operating paradigm (Lawson and Samson, 2001). Romijn and Albaladejo (2002) refer to the ability of innovation as the skills and knowledge needed to effectively absorb, master and improve existing technologies to create new ones. Meanwhile, innovative capabilities are also described as the capacity to gain access to develop and implement innovative technologies for design and manufacturing (Xu, Lin, and Lin, 2008).

The 2019 World Intellectual Property Organization (WIPO) on Global Innovation Index divides the variables to measure innovation into two categories, namely the innovation input sub-index and the innovation output sub-index. Innovation input sub-index consists of 5 variables, namely institutions, human capital and research, infrastructure, market sophistication and business sophistication. While the innovation output sub-index consists of two variables, namely knowledge and technology outputs and creative outputs. Meanwhile Valaei et al (2017) describe innovation into four processes: exploitative learning, explorative learning, improvisational creativity, and compositional creativity.

Tesyafe and Kitaw (2018) mentioned in their journal that the variables forming the innovation capability are knowledge accumulation, knowledge application and innovation fund generation.

**Table 1. Innovation Capability Constructs in Literature**

No	Authors	Constructs addressed
1.	Azabadi et al. (2012)	Knowledge acquisition, knowledge creation, knowledge utilization
2.	Sobanke et al. (2013)	Internal factors (education, relevant prior experience, training efforts, use of ICT), external factors (technical/management/ financial support received) technological innovation
3.	Bo (2015)	Knowledge transfer, knowledge storage
4.	Cheng et al. (2016)	Knowledge acquisition, knowledge sharing
5.	Zou et al. (2016)	Establishing networking, external knowledge source, knowledge storage, absorptive capacity, technology innovation achievements
6.	Tesfaye et al (2018)	Knowledge accumulation, knowledge utilization, and innovation fund generation
7.	WEF on Global Competitiveness Index (2019)	Diversity and collaboration, Research and development, Commercialization
8.	WIPO on Global Innovation Index Report (2019)	Knowledge and technology outputs (Knowledge creation, knowledge impact, knowledge diffusion) and Creative outputs (Intangible assets, Creative goods and services, Online creativity)

## 2.2 MSMEs

The Indonesian Ministry of Cooperatives and SMEs reports that in terms of units, MSMEs have a share of around 99.99% (62.9 million units) of the total number of business operators in Indonesia (2017), while large businesses are only 0.01% or around 5400 units. Micro Business absorbs around 107.2 million workers (89.2%), Small Business 5.7 million (4.74%), and Medium Enterprises 3.73 million (3.11%); while Large Enterprises absorbed around 3.58 million people. This means that combined MSMEs absorb around 97% of the national workforce. SMEs are considered to be significantly important to contributors to economic development, particularly in regards to providing jobs and employment opportunities; and generating income for many households (Kongolo, 2010, Saerang et al, 2018). SMEs have a tendency to use entrepreneurship principles to focus on exploitation of opportunities and adopt innovative approaches to attract customers and increase profitability (Mohammad et al, 2019).

## 2.3 The existing innovation capability model's relevance to the MSMEs

Tesfaye et al (2018) using three key constructs such as knowledge accumulation, knowledge utilization, and innovation fund generation. The proposed conceptual model defines the whole process of Innovation capability.

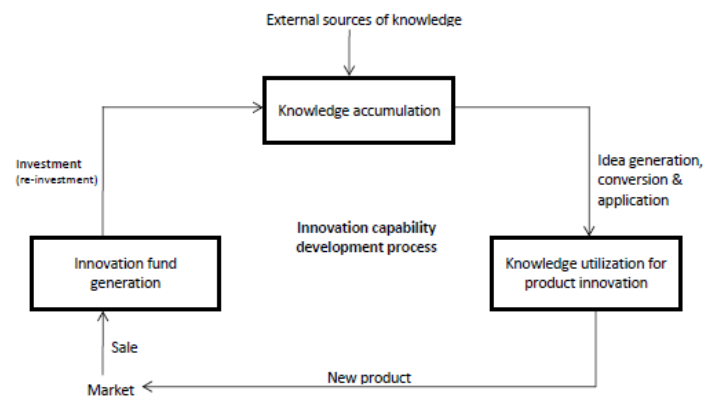


Fig. 1: Innovation Capability Model (Tesfaye, 2018)

The WEF on Global Competitiveness Index (2019) using three constructs which is diversity& collaboration, research&development and commercial.

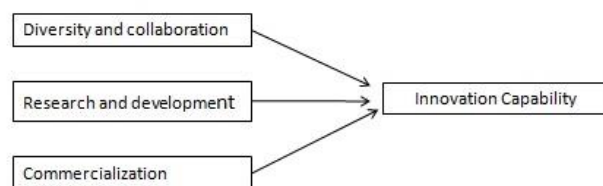


Fig. 2: Innovation Capability Mode (GCI, 2019)

The last conceptual model is from WIPO on Global Innovation Index Report (2019). The report using two construct which is knowledge & technology outputs and creative outputs. The variables for knowledge &technology outputs are Knowledge creation, knowledge impact, knowledge diffusion. The creative outputs variables are Intangible assets, creative goods and services, online creativity.

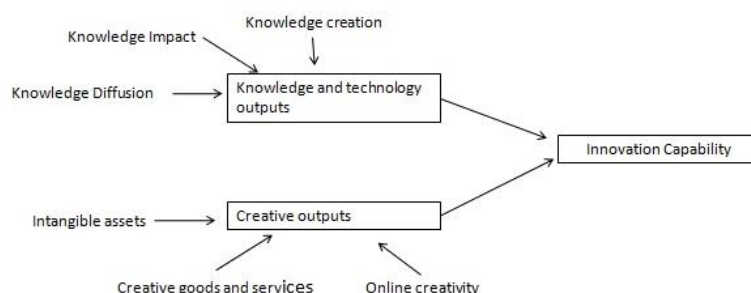


Fig. 3: Innovation Capability Mode (GII, 2019)

## 2.4 Gaps in the literature as advocacy of a new innovation model for MSMEs

Tesfaye et al (2018) noted that based on the literature review, either the most commonly used innovation measures or the innovation capability models are not sufficient to develop innovation capability for the innovation capability. This is because; innovation in the developing countries is challenged by barriers that are not found in the advanced economies (Cirera & Maloney, 2017). MSMEs in emerging markets may see MSMEs innovation as critical as they are dealing with unprecedented competition and abundant business opportunities. Therefore, it is imperative for SMEs including those from emerging market economies to benefit from innovation even if it is not an easy task (Games,2019). This research finds the gap of integrating the aspects of Innovation capability into the nature of MSMEs as a remarkable deficiency in the literature.

## 3. Methodology

This research is designed into two core parts using conclusive research type. The first part is to find the key constructs of Innovation capability. In the existing literature, these constructs are addressed in different contexts and aspects. The second part of the research is the developed conceptual model which shows an innovation capability model.

## 4. Result and Discussion

### 4.1 Building The innovation Capability Model for MSMEs

As modeled in figure 4, there's three main constructs identified: knowledge & technology output, knowledge utilization for product innovation and innovation fund generation. MSMEs use the accumulated knowledge&technology to generate and apply new ideas. The second construct is knowledge utilization for product innovation. Through a dynamic process of diversity&collaboration, research&development and commercialization the product, MSMEs will increase its competitiveness to compete globally. When the new products are commercialized successfully in the market, innovation can generate income for the MSMEs (innovation fund generation). According to this research, the first two constructs (knowledge & technology output, knowledge utilization for product innovation) constitute the technical aspect and the third construct (innovation fund generation) indicate the financial aspect of innovation capability.

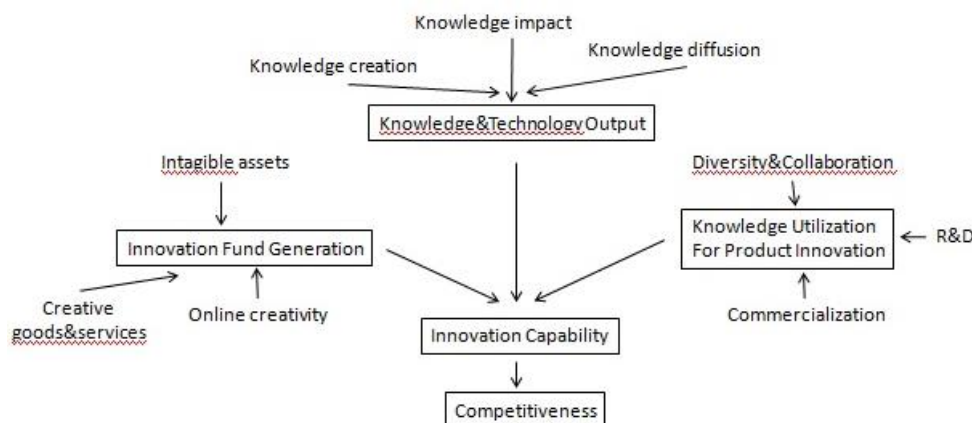


Fig. 4 : Proposed conceptual model for Innovation Capability in MSMEs in Indonesia

## 5. Conclusion

As the main driver of the nation's economy, MSMEs must have the capability of innovation to create innovation and make valuable contributions to the nation's competitiveness. Nevertheless, the lack of references to the innovation capability model makes MSMEs, especially in Indonesia, difficult to improve their performance, especially to compete internationally. The majority of literature discusses the technical aspects which are the initial phase of innovation. Research that discusses the technical and financial aspects is still rarely done.

To avoid this gap, this research develops a continuous and dynamic conceptual model of innovation capability. The model identifies three key innovation capability constructs, namely knowledge & technology output, knowledge utilization for product innovation, and innovation fund generation and other important factors to explain the constructs. The first two constructs constitute the technical aspect and the third construct indicate the financial aspect of innovation capability.

Technical aspects namely knowledge & technology output and knowledge utilization for product innovation require knowledge from external sources. The knowledge and information obtained from external sources has been analyzed, processed and interpreted to be transformed and utilized to generate innovations. On the other hand, MSMEs capability of generating financial returns from innovation will enhance their capability to re-invest in the MSME development and expansion.

Finally, the proposed conceptual model can place a great understanding of the key constructs and the nature of their relationships to enhance the MSMEs practices to develop their innovation capability.

## 6. Reference:

- Abdullah, N. C., & Mustapha, R., 2009. Kajian Kes Usahawan Tani Industri Kecil Sederhana ( IKS ) Bumiputera Di Negeri Terengganu ( A Case Study Of SMI Bumiputera Agropreneurs In Terengganu ). *Jurnal Pendidikan Malaysia*, 34(2), 143–165.
- Abou-Moghli, A. A., Abdallah, G. M. Al, & Muala, A. Al., 2012. Impact Of Innovation On Realizing Competitive Advantage In Banking Sector In Jordan . *American Academic & Scholarly Research Journal*, 4(5).
- Andreeva, T. And Kianto, A. (2011), “Knowledge Processes, Knowledge-Intensity And Innovation: A Moderated Mediation Analysis”, *Journal Of Knowledge Management*, Vol. 15 No. 6, Pp. 1016-1034.
- Azabadi, J.H., Noorossana, R., Jafari, M., Owlia, M.S., & Saryazdi, M.D. (2012). *Knowledge Management Analysis: A System Dynamics Approach*. Paper Presented At International Conference On Innovation And Information Management (ICIIM 2012).
- Aziza, N.N.A ., Samad, S. (2016). Innovation And Competitive Advantage: Moderating Effects Of Firm Age In Foods Manufacturing Smes In Malaysia. *Procedia Economics And Finance* 35 ( 2016 ) 256 – 266.
- Bekraf. (2019). *Ekonomi Kreatif Outlook*.
- Bo, Y. (2015). Modeling Of Knowledge Transfer In Logistics Supply Chain Based On System Dynamics. *International Journal Of U- And E- Service, Science And Technology*, 8(12), 377-388.
- Cheng, C.J., Yang, C., & Sheu, C. (2016). Effects Of Open Innovation And Knowledge-Based Dynamic Capabilities On Radical Innovation: An Empirical Study. *Journal Of Engineering And Technology Management*, 41, 79-91.
- Cirera, X., & Maloney, W.F. (2017). *The Innovation Paradox, Developing Country Capabilities And The Unrealized Promise Of Technological Catch-Up*. Washington, DC: International Bank For Reconstruction And Development / The World Bank.
- Enzing, C.M., Batterink, M.H., Janszen, F.H. And Omta, S.O. (2011), “Where Innovation Processes Make A Difference In Products’ Short-And Long-Term Market Success”, *British Food Journal*, Vol. 113 No. 7, Pp. 812-837.
- Games, Donard. (2019). Can SME Benefit From Innovation In An Emerging Market Economy?. *Academy Of Entrepreneurship Journal*: Volume 25, Issue 1, 2019
- Ismail, M. D., 2013. Learning Orientation And Trust In Small And Medium Enterprise (SME) Export Competitive. *Asian Academy Of Management Journal*, 18(2), 153–179.
- Kongolo, M. 2010. Job Creation Versus Job Shedding And The Role Of Smes In Economic Development. *African Journal Of Business Management* 4(11): 2288-2295.
- Lawson, B., & Samson, D. (2001). Developing Innovation Capability In Organizations: A Dynamic Capabilities

Approach. *International Journal Of Innovation Management*, 5(3), 377–400.

Mohamad, A. N. A., Rashed, Z. N., & Rahman, R. A., 2008. Potensi, Cabaran Dan Hala Tuju Industri Kecil & Sederhana. *Prosiding Perkim III*, 1,662–674.

Mohammad, I.N. Massie, J.D.D., Tumewu F.J. (2019). The Effect Of Entrepreneurial Orientation And Innovation Capability Towards Firm Performance In Small And Medium Enterprises. *Jurnal EMBA Vol.7 No.1 Januari 2019*, Hal. 1 – 10

Porter, M.E. (2004). *Competitive Strategy: Techniques For Analyzing Industries And Competitors*. Free Press, New York, NY

Romijn, H., & Albaladejo, M. (2002). Determinants Of Innovation Capability In Small Electronics And Software Firms In Southeast England. *Research Policy*, 31(7), 1053–1067.

Saerang, D. P. E., Tulung, J. E., & Ogi, I. W. J. (2018). The Influence Of Executives' Characteristics On Bank Performance: The Case Of Emerging Market. *Journal Of Governance & Regulation*, 7(4), 13-18.

Saunila, M., 2014. Innovation Capability For SME Success: Perspectives Of Financial And Operational Performance. *Journal Of Advances In Management Research*, 11(2), 163–175.

Sobanke, V., Adegbite, S., Ilori, M., & Egbetokun, A. (2013). Determinants Of Technological Capability Of Firms In A Developing Country. *Procedia Engineering*, 69, 991-1000.

Suhendra, A.A. (2017). Strategic Review On Indonesia Development Plan For Creative Economy. *Developing Country Studies*. Vol.7, No.5.

Tesfaye, G., Kitaw,D. (2018). An Innovation Capability Development Process For Firms In Developing Countries: A Theoretical Conceptual Model. *Journal Of Entrepreneurship, Management And Innovation (JEMI)*, Volume 14, Issue 3, 2018: 87-110

Williams, D., & Hare, L., 2012. Competitiveness Of Small Hotels In Jamaica: An Exploratory Analysis.: Ebscohost

Valaei, N., Rezaei, S., Ismail, W.K.W.(2017). Examining Learning Strategies, Creativity, And Innovation At Smes Using Fuzzy Set Qualitative Comparative Analysis And PLS Path Modeling. *Journal Of Business Research* 70 (2017) 224–233.

World Economic Forum. (2019). *The Global Competitiveness Index Report 2019*. Geneva.

World Intellectual Property Organization. (2019). *The Global Innovation Index Report 2019: Creating Healthy Lives—The Future Of Medical Innovation*.

Xu, Z., Lin, J., & Lin, D. (2008). Networking And Innovation In Smes: Evidence From Guangdong Province, China. *Journal Of Small Business And Enterprise Development*, 15(4), 788–801.

Zou, B., Gou, F., & Guo, J. (2016). Absorptive Capacity, Technological Innovation, And Product Life Cycle: A System Dynamics Model. *Springerplus*, 5, 2-25.

# **Determination Of The Shortest Route of Electrical Scooters Maintenance Patrol in Bandung Using Nearest Neighbor and Genetic Algorithm Approaches**

**Sely P. Oktaviani, Rispianda**

Department of Industrial Engineering, Institut Teknologi Nasional (Itenas), Bandung - INDONESIA

e-mail: selyoctavian@gmail.com

## **Abstract**

The increasing number of parking spot locations has increased the number of Electrical Scooters fleet maintenance patrols. For this reason, it is necessary to determine the shortest route for maintenance crew for patrolling through all parking spots. In this study, the determination the number of routes is done using the Nearest Neighbor approach and the shortest route path using the Genetic Algorithm approach. Based on the results of calculations, the best number of routes that can be used is 3 routes with each patrol time of 460, 414, and 417 minutes. With this research, it is expected that company can minimize patrol time and shortest mileage.

*Keywords: Electrical Scooters, Nearest Neighbor, Genetic Algorithm*

---

## **1. Introduction**

Electric scooters are one of the modes of transportation that are in demand in the city of Bandung both as a short distance transportation or as a means of recreation. The number of electric scooter parking spots is 35 location points. From each location point there are 5 electric scooters. It is necessary that this electric scooter needs to be checked and maintained periodically to ensure that the electric scooter engine is safe to drive.

Increasing number of parking spot locations makes increasing maintenance patrol locations also. This resulted in the number of patrol routes possibly increasing. To minimize patrol time, it is necessary to find a route or the shortest path to minimize time and distance. Problems such as optimal route search are commonly referred to as Vehicle Routing Problems.

Many methods or approaches can be used to solve Vehicle Routing Problems, one of which is using the Nearest Neighbor approach. In general this approach is to sort each existing location point based on the shortest distance to the furthest distance. The advantage of this method is the simplicity of efficient and effective analytical techniques in the fields of pattern recognition, text categorization, subject recognition, etc., but has limitations on memory requirements and computational complexity (Bhatia and Vandana, 2010). The aim of using Genetic Algorithm is to improve the solution obtained by the Nearest Neighbor (NN). It is expected that the use of Genetic Algorithms makes the results of completion of the shortest route more optimal.

## **2. Literature Review**

Our work is mainly related to the issue of extended Vehicle Routes Problem (VRP) and the shortest route determination approach, we review some of the most relevant studies in this section.

### **2.1. Vehicle Routes Problem (VRP)**

Vehicle Routing Problem (VRP) according to Miller (1999) is a matter of determining the delivery route which involves a set of vehicle routes that are centered on one depot or more to serve customers scattered in various shipping areas with their respective requests.

Vehicle Routing Problems (VRP) have important applications in the field of distribution management, so they are one of the examples of problems that are widely studied in the combinatorial optimization literature and are recognized as one of the most successful experiences in operations research. The VRP type is generally described as a case where a number of vehicles with a certain capacity must send a number of goods from a depot assuming

the distance between customers is known so the purpose of this problem is to minimize vehicle mileage so that vehicle operating costs are minimal with various constraints (Arvianto et al, 2018).

## 2.2. Saving Matrix

Saving Matrix is a method used to determine the distance, route, time or cost in the delivery of goods from companies to consumers. This method aims to deliver goods according to customer orders can be done in an effective and efficient manner, so that companies can save costs, labor, and delivery time (Istantiningrum, 2010 in Suparjo, 2017).

The Saving Matrix method consists of several steps. According to Istantiningrum (2010) in Suparjo (2017) the steps in the saving matrix method are as follows:

### 1. Determining the Distance Matrix

In determining the distance matrix, the distance data between the company and location and location to other locations is very necessary. After knowing the coordinates of each location, the distance between the two locations can be calculated using the following formula:

$$j(1,2) = \sqrt{(x_1 - x_2)^2 + (y_1 - y_2)^2} \quad (1)$$

However, if the distance between the two the coordinates are known, then calculations using formulas not used and use existing distance.

### 2. Determine the Savings Matrix

After knowing the overall distance between the plant and one location and another, then in this step it is assumed that every location will be bypassed one truck exclusively. The meaning will be there are several different routes that are will be bypassed for each destination. As such there will be savings if there are merging routes that are considered one-way with the other route. For looking for a savings matrix can The following formula is used:

$$S(x, y) = J(x, y) + J(x, y) - J(x, y) \quad (2)$$

$S(x, y)$  is distance savings that is, from the combination of route x by route y.

### 3. Vehicle and Route Allocation Based on Location

After the savings matrix is known, then the next step is the allocation of locations to the route or vehicle. Meaning in this step will be determined route new shipping based on the above merging routes in step second above. The result is delivery location 1 and location 2 will done using 1 route.

### 4. Sorting Destination Locations Within A Route

This step determines the order visit.

## 2.3. Nearest Neighbour

The nearest neighbor algorithm is a search method with the concept of adding the closest point to the previous point until all points in one path are exhausted (Hutasoit et al, 2014). At this stage, the Warehouse is set as the starting point ( $t_0$ ) of travel. The nearest location is searched and added then considered as the end point ( $t_1$ ).  $t_1$  is assumed as  $t_0$ , then the above procedure is repeated until all points are exhausted and returned to the warehouse as the end of the journey.

## 2.4. Genetic Algorithm

Genetic algorithms were first developed in 1975 by John Holland of Michigan University (Randy, 2004). Genetic algorithm is an algorithm that utilizes the natural selection process known as the evolutionary process proposed by Charles Darwin. In the process of evolution, individuals continually undergo changes in genes to adapt to their environment. "Only strong individuals can survive." Genetic algorithms may not always achieve the best results, but often solve problems quite well. Genetic algorithms represent a solution to the problem as chromosomes. There are several important aspects in genetic algorithms, including the definition of fitness function, definition and implementation of genetic representations, definition and implementation of genetic operations.



Some important terms in genetic algorithms (Prayoga, 2016) include genes, chromosomes, generation, mutation, crossover, and fitness value. A gene is a value that expresses the basic unit that forms a certain meaning and a gene unity is called a chromosome. generation is a one-unit cycle of the evolutionary process. Mutation is an operator function to change the genetic information of an individual so that new individuals are generated by mutations based on the probability of mutations that have been determined. Crossovers are function operators for combining genetic information between two individuals to produce new individuals. Fitness value is a value that states how good the value of an individual or the solution obtained.

### 3. Problem Formulation

#### 3.1. Problem Definition

The process flow that will be carried out in this study can be seen in Fig. 1.

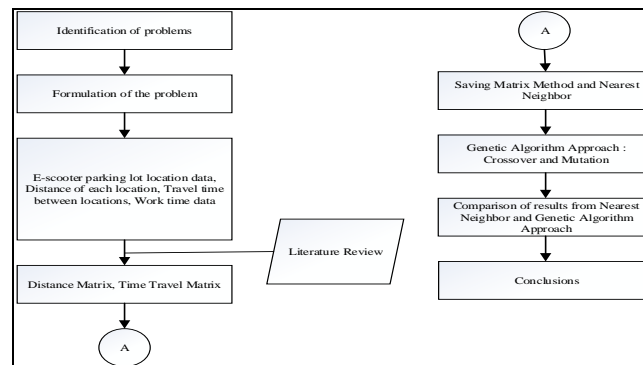


Fig. 1: Process Flow Diagram

The number of electric scooter parking spots is 35 location points. From each location point there are 5 electric scooters. The starting point of the patrol departure location is in the company office at Pasirkaliki street. Data of distance obtained from the Google Earth application. The following is a distance matrix obtained assuming the distances a to b and b to a are the same:

Table 1: Distance Matrix

NO	Distance (km)	P0	PP	UR	UB	SE	UK	ND
0	P0	-	5,500	5,300	...	...	...	6,000
1	PP	5,500	-	2,300	...	...	...	5,700
2	UR	5,300	2,300	-	...	...	...	4,100
...	UB	5,000	3,100	0,750	...	...	...	3,500
34	UK	3,900	4,000	2,300	...	...	...	2,800
35	ND	6,000	5,700	4,100	...	...	...	-
		P0	PP	UR	UB	SE	UK	ND

The following is a time allocation matrix for each location and assumptions:

Table 2: Time Matrix

NO	Time (minutes)	P0	PP	UR	UB	SE	UK	ND
0	P0	-	...	...	...	...	...	...
1	PP	55,0	-	...	...	...	...	...
2	UR	48,0	36,0	-	...	...	...	...
...	UB	47,0	38,0	28,0	-	...	...	...
34	UK	43,0	43,0	33,0	35,0	32,0	...	...
35	ND	49,0	50,0	41,0	40,0	41,0	34,0	...
		P0	PP	UR	UB	SE	UK	ND

**Table 3: Assumptions**

Electric Scooters/ parking spot	5	Unit
Regular Patrol Team	1	Team
Assumptions		
Time check/ scooters	5	Minutes
Time check/ parking spot	25	Minutes
Road Conditions	weekend	
Work Time	8	Hours
Work Time	480	Minutes/ Days

### 3.2. Saving Matrix Between Distance and Time

The following is the result of saving the distance matrix over time:

**Table 4: Distance Vs Time Matrix**

Distance Vs Time	PP	UR	UB	...	UK	ND
PP	-					
UR	8,500	-				
UB	7,400	9,550	-			
...	8,200	7,800	6,800	-		
UK	5,400	6,900	6,900	5,300	-	
ND	5,800	7,200	7,500	5,200	7,100	-
	PP	UR	UB	...	UK	ND

**Table 5: Results Order of Saving Matriks**

No	Location Pairs	Saving
1	SS & WUB	12,590
2	WUB & BCC	11,800
3	TU & SS	11,550
4	BCC & KKIC	11,400
...	KB & WUP	4,650
34	XP & HS	1,300

### 3.3. Nearest Neighbour

The Nearest neighbor approach is based on the results of the largest order of saving matrix. This is done so that the distance from the resulting route has a large saving value. Determination of the number of routes is influenced by the work time limit which is assumed to be 480 minutes.

**Table 6: Results of Nearest Neighbour**

Route	Location Pairs	Time (Minutes)
Route 1	P0 - WUS - WUD - EC - TU - SS - WUB - BCC - KKIC - CR - UB - NB - HS - SE - P0	460
Route 2	P0 - Ecc - HBS - BD - DC - AH - WUR - UR - HoA - XDB - XGB - PP - P0	458
Route 3	P0 - WUP - KB - XBC - SP - BBC - SBC - SPN - XP - GC - ND - UK - P0	387
Total		1305

Calculation example for Route 1:

Make a comparison of the distance between the points P0 with the location that has the largest saving matrix value. Select the location with the closest distance and calculate the travel time between the selected locations (WUS). Comparison of distance values, location determination, and time calculations are repeated until the time travel total of all location from the last point to the starting point P0 is  $\leq 480$  minutes.

### 3.4. Genetics Algorithms

Genetic algorithm approach is used to make the optimal route solution at Nearest Neighbor. Genetic algorithms may not always achieve the best results, but usually used to try to solve problem well. The aim of using Genetic Algorithm is to improve the solution obtained by the Nearest Neighbor (NN).

**Table 7: Parameters and Assumptions Genetics Algorithm**

Population Size	35
Crossover Probability	0,5
Mutation Probability	0,5
Generation Minimum	8

#### 3.4.1 Determination of the parent chromosome

The determination of the route Genetic Algorithm is based on the fitness value. Route 2 is made a parent based on a random value that is smaller than the value of the selection probability. For individual crossover pairs, only route 3 is chosen because the random selection crossover value is smaller than the crossover probability value.

**Table 8: Determination of Parent Individuals**

Individu	Time Fitness (minutes)	Selection Probability (Pi)	Selection Probability Cumulative (Qi)	Random Selection (ri)
1	460	0,352	0,352	0,545
2	458	0,351	0,703	0,141
3	387	0,297	1,000	0,616
Total	1305	1		

**Table 9: Determination of Individual Crossover Pairs**

Individu	Time Fitness (minutes)	Selection Probability (Pi)	Selection Probability Cumulative (Qi)	Random Crossover (rc)
1	460	0,352	0,352	0,791
2	458	0,351	0,703	0,148
3	387	0,297	1,000	0,401

#### 3.4.2 Crossover

Exchange genes by combining the same number of genes as the minimum number of generations. The selected crossover result is a pair of routes that have the smallest total fitness value. From 8 trials, the 6th trial was chosen.

**Table 10: 6th Trial of Crossover**

Individu	Gen/ Parking Spot	Time Fitness (minutes)
2	P0 - WUP - KB - XBC - SP - BBC - SBC - SPN - XP - GC - ND - PP - P0	414
3	P0 - Ecc - HBS - BD - DC - AH - WUR - UR - HoA - XDB - XGB - UK - P0	417
Total		831

### 3.4.3 Mutation

Each individual has a gene mutation with a mutation probability determined. Mutated genes are genes that have a smaller random probability than mutation probabilities. mutated genes are WUB and BD so the results as shown here are obtained:

**Table 11: Mutation**

Individu	Gen/ Parking Spot	Time Fitness (minutes)
1	P0 - WUS - WUD - EC - TU - SS - <b>BD</b> - BCC - KKIC - CR - UB - NB - HS - SE - P0	476
2	P0 - Ecc - HBS - <b>WUB</b> - DC - AH - WUR - UR - HoA -XDB - XGB - PP - P0	475
3	P0 - WUP - KB - XBC - SP - BBC - SBC - SPN - XP - GC - ND - UK - P0	387
Total		1338

### 3.4.4 Results

The following is the result of the calculation of Nearest Neighbor (NN) and Genetic Algorithm (GA).

**Table 12: Results**

Methods	Fitness (minutes)
NN	1305
CO	1291

## 4. Conclusion

Based on the results of the calculation of the nearest neighbor obtained 3 routes that can be used with a total travel time of 1,305 minutes. To maximize this solution a review of the route results is carried out using a genetic algorithm approach. The genetic algorithm itself consists of a crossover process with travel time of 1,291. From these results it can be concluded that the route results from the genetic crossover algorithm approach were chosen because they have a smaller total travel time. The best number of routes that can be used from is 3 routes with the shortest path P0 - WUS - WUD - EC - TU - SS - WUB - BCC - KKIC - CR - UB - NB - HS - SE - P0, P0 - WUP - KB - XBC - SP - BBC - SBC - SPN - XP - GC - ND - PP - P0, P0 - Ecc - HBS - BD - DC - AH - WUR - UR - HoA -XDB - XGB - UK - P0 with each patrol time of 460, 414, and 417 minutes. With this research, it is expected that company can minimize patrol time and shortest mileage. For further research can be developed with other methods that are more flexible and computerized (software programs) for the number of locations might change.

## 5. References

- Arvianto et al., 2018. Application of Simulation And Reliability In The Vehicle Model Problem Routing (VRP) With Probabilistic Demand. SIMETRIS Journals, Vol.9 No. 1 April 2018. ISSN: 2252-4983.
- Bhatia, N., & Vandana., 2010. Survey of Nearest Neighbour. International Journal of Computer Science and Information Security, Vol. 8, No. 2.
- Hutasoit et al., 2014. Beam Distribution Route Determination Using Nearest Neighbor Algorithm and Local Search (Case Study of PT. X). Journal of the National Institute of Technology, Vol. 2. Available at <https://ejurnal.itenas.ac.id/index.php/rekaintegra/article/view/428/593>, accessed on December 28, 2019.
- Miller et al., 1999. A Capacitated Vehicle Routing Problem For Just In The Time Delivery, ITE Transactions, 31, 1083-1092.
- Prayoga, R., 2016. Route of Crystal Ice Distribution Using Genetic Algorithm And Branch & Bound Method At PT Atlas Tube Ice. Department of Industrial Engineering - National Institute of Technology in Bandung.
- Randy, L, Haupt., & Sue, E, Haupt., 2004. Practical Genetic Algorithms. A John Wiley & Sons, Inc., Hoboken, New Jersey, pp. 22-23.
- Suparjo., 2017. Saving Matrix Method as an Alternative Method For Efficiency of Distribution Costs (Empirical Study In Log Timber Transport Companies In Central Java). Faculty of Economics and Business - University of 17th August 1945 in Semarang.

## Economic Simulation of Indonesia's Clean Energy Policy: Shifting from LPG to Induction Stove

Dzikri Firmansyah Hakam<sup>1,2,\*</sup>, Meiri Triani<sup>1</sup>, I Putu Wirasangka<sup>1</sup>, and Siti Aisyah<sup>1</sup>

PT. PLN (Persero) Research Institute, Jakarta, - INDONESIA

School of Business and Management, Institut Teknologi Bandung (ITB), Bandung - INDONESIA

\* Corresponding author e-mail: dzikri@pln.co.id

### Abstract

Indonesian government is facing the burden increase of state budget from the energy subsidy, especially Liquefied Petroleum Gas (LPG) subsidy. According to state budget plan of Indonesia (RAPBN) year 2019, the LPG subsidy (3 kg tube) year 2019 was estimated more than 70 Billion Rupiah. The subsidy nominal for LPG 3 kg tube is fluctuated because influenced by the uncertainty of world crude oil price where the LPG is the refinery product of crude oil. The increase of crude oil price in the global market could significantly increase the LPG subsidy of Indonesia's government. In the other hand, PLN as Indonesia's state-owned electricity company currently constructing new power plant approximately 35,000 MW that lead to the increasing of reserve margin in the power system that should be absorbed by the consumers. Recently, induction stove emerges by the Indonesia's government as a solution for those two issues above. However, the literature review regarding the economics and policy of the development of induction stove in Indonesia's electricity market is still limited. This research provides the economic valuation of induction stove compared to the utilization of LPG stove for each electricity and LPG tariff, i.e. subsidy and non-subsidy tariff. This research could serve as an academic reference for energy sector stakeholders in Indonesia in objective to implementing the clean energy policy to shift cooking technology from LPG stove to induction stove.

*Keywords: Induction stove, LPG, energy subsidy, economic valuation, clean energy policy*

### 1. Introduction

Indonesian government is facing the burden increase of state budget from the energy subsidy, especially Liquefied Petroleum Gas (LPG) subsidy. According to state budget plan of Indonesia (RAPBN) year 2019, the LPG subsidy (3 kg tube) year 2019 was estimated more than 70 Billion Rupiah. The subsidy nominal for LPG 3 kg tube is fluctuated because influenced by the uncertainty of world crude oil price where the LPG is the refinery product of crude oil. The increase of crude oil price in the global market could significantly increase the LPG subsidy of Indonesia's government. In the other hand, PLN as Indonesia's state-owned electricity company currently constructing new power plant approximately 35,000 MW that lead to the increasing of reserve margin in the power system that should be absorbed by the consumers.

Recently, induction stove emerges by the Indonesia's government as a solution for those two issues above. Induction stove program increases the household access to clean energy source, increases the public health, has an adverse effect of climate change compared to the CO<sub>2</sub> emission from LPG stove, increases energy efficiency and security (Brown et al. 2017; Quinn et al. 2018). However, the literature review regarding the economics and policy of the development of induction stove in Indonesia's electricity market is still limited. This study determines the economics of induction stove compared to LPG stove for each electricity and LPG tariff, i.e. subsidy and non-subsidy tariff. This research could serve as an academic reference for energy sector stakeholders in Indonesia in objective to implementing the clean energy policy to shift cooking technology from LPG stove to induction stove. Therefore, this research contributes to the academic literature review of clean energy policy in Indonesia.

This study provides economic valuation, strategy, and policy implementation for induction stove development in Indonesia. This research focuses in the utilization of induction stove for household consumer that comprises of electricity tariff 450-900 VA and > 1,300 VA. The structure of this paper is as follows: The first section provides the introduction, research gap, research objective, research structure, and research novelty of the study. The second section shows the research methodology of economic valuation of induction stove compared to LPG stove. The third chapter is the economic simulation and analysis of induction stove for each electricity tariff. Chapter four is the conclusion of the study.

## 2. Research methodology

This research has an objective to determine the economic valuation and policy implication of induction stove compared to LPG stove for each electricity tariff. To address research objective above, this study applied descriptive analysis and economic valuation methodology. Economic simulation was performed by comparing the cost of cooking of induction stove and LPG stove to determine the cooking cost saving. The efficiency assumption of induction stove in this simulation is based on the reference from (PLN Puslitbang, 2017) where PLN Research Institute performed efficiency study and cooking time experiment using different type kind of stove, i.e. LPG stove, electricity stove, and induction stove. There are three types of electricity tariff applied in (Puslitbang, 2017):

- Electricity tariff with subsidy of 605 Rp/kWh for 450 VA and 900 VA household
- Electricity tariff non-subsidy of 1,352 Rp/kWh for 900 VA household
- Electricity tariff non-subsidy of 1,467 Rp/kWh for 1,300 VA and 2,200 VA

This study using LPG price assumption of 6,666 Rp/kg for LPG price with subsidy and 12,083 Rp/kg for LPG price with non-subsidy based on (PLN Puslitbang, 2017).

The result of efficiency and cooking time comparison for each type of stove could be seen in Table 11. According to Table 11, the LPG stove 1,800 Watt has the highest efficiency of 81.78% and the lowest cooking time of 3.6 %. The greater the power from the induction cooker, the higher the resulting efficiency, and the shorter the cooking time. For the 2,200 VA electric power tariff group, the lowest cooking cost (Rp 152) was generated by a 1,800 Watt induction stove. Due to the power installation limitation for households with 900 VA electricity tariff rates, the lowest cooking costs generated by the 500-Watt induction stove was Rp 166. For the 450 VA electric power tariff group, the lowest cooking cost (Rp 74) generated by 300-Watt induction stove. When compared to LPG stoves, LPG stoves have cooking costs of Rp. 161 for the price of non-subsidized LPG and Rp. 89 for the price of subsidized LPG.

The economic simulation in this study applies three types of subsidized LPG (3 kg) prices based on the delivery point, namely:

- The delivery point at LPG agent with LPG price Rp 4,250 / kg or Rp 12,750 / tube
- The retail delivery point is based on the Highest Retail Price (HET) of Rp. 17,900 / tube
- The retail delivery point for households is IDR 22,000 / kg

It is important to note that the retail sale price of households for 3 kg LPG can vary according to the LPG scarcity in each province, where the selling value of subsidized LPG to the consumers can reach Rp 40,000 / kg.

## 3. Economic Simulation of Induction stove

The economic simulation in this study is divided into 4 scenarios. The first scenario calculates cooking cost savings made by households by comparing the cost of cooking using induction stoves subsidized tariffs (605 Rp / kWh) with LPG stove subsidized tariff (Rp 4,250 / kg at LPG agent). In this scenario, it is assumed that the induction stove used is of low efficiency, i.e. 300-Watt induction cooker. Based on table 1, the energy utilization of 1 kg LPG on an LPG stove is equivalent to 10.7 kWh on a 300-Watt induction stove. Based on the financial calculations in table 2, there was a savings in cooking costs per month amounting to Rp 10,344 per month for the 12 kg LPG/ month usage pattern. If there is a scarcity of LPG cylinders in the field, the price of 3 kg LPG could

risers to Rp 40,000 per tube, then the savings in cooking costs also increase up to Rp 82,344 per month. The electricity tariff group assumption in this scenario applies 605 Rp / kWh tariff with the consideration that this scenario can be done by low-income households, with subsidized electricity tariff groups of 450 VA and 900 VA, who make the cooking behavior transition from 3 kg LPG stove to induction stove without having to make changes in the electrical installation of the household. Things to consider from this scenario are the availability and manufacturing of 300-watt scale induction stoves where induction stoves usually have relatively larger power nominal than 300-watt.

**Table 1: Volume and power equivalents between LPG and induction cookers**

Type of Stove	Nominal	Cost	Volume	Equivalency
Induction stove	300 Watt	210.3	0.14333 kwh	10.696 kwh
	500 Watt	180.51	0.12302 kwh	9.181 kwh
	1000 Watt	165.75	0.11296 kwh	8.430 kwh
	1400 Watt	159.11	0.10844 kwh	8.093 kwh
	1800 Watt	152.3	0.1038 kwh	7.746 kwh
LPG Stove	LPG 3 kg	89.33	0.0134 kg	1 kg
	LPG 12 kg	161.92	0.0134 kg	1 kg

The second scenario calculates cooking cost saving made by household by comparing the cost of cooking induction stove subsidized tariff (500 Watts stove at electricity tariff of 605 Rp / kWh) with LPG stove subsidized tariff (Rp 4,250 / kg at an agent) with. Unlike the first scenario, this second scenario can only be done by household group of 900-watt subsidized electricity tariff rate. Based on table 1, the energy utilization of 1 kg LPG is equivalent to 9.18 kWh on a 500-Watt induction stove. Based on the calculations in table 3, there was a saving in cooking cost per month of Rp 21,344 per month for the 12 kg LPG / month usage pattern. If there is a scarcity of LPG cylinders in the field, the price of 3 kg LPG could rise to Rp 40,000 per tube, therefore the cooking cost savings will also increase to Rp 93,344 per month. It can be compared with the first scenario, that with the increase in induction stove power from 300 Watt to 500 Watt, the cooking cost saving has doubled. In line with the first scenario, this second scenario can be done if the household gets access to a 500-Watt induction cooker.

The third scenario is carried out with the assumption that household subsidized electricity tariffs received a facilities access to increase the electricity installation capacity so that the household can use the high-efficiency induction stoves such as the 1,800-Watt induction stove. Based on the conversion energy in the table 1, 1 kg of LPG is equivalent to 7.74 kWh of 1,800-Watt induction stove. Based on the cost saving calculation in table 4, there is a saving in cooking cost per month of Rp 31,761 per month for the 12 kg LPG/month usage pattern. If there is a scarcity of LPG cylinders in the field and the price of 3 kg LPG rises to Rp 40,000 per tube, the saving in cooking cost also increase up to Rp 103,761 per month. This third scenario has an economic saving that is more than three times greater than the saving in the first scenario. This scenario is specifically intended for low-income households because the electricity tariff applied is the subsidized electricity tariff (605 Rp/kWh). Therefore, it should be remembered that this scenario needs to consider the investment costs that need to be undertaken by the government / PLN to increase the low voltage electricity installations so that the low-income households can use induction cookers and other power tools with high efficiency.

The fourth scenario calculates the cooking cost saving that can be made for middle and high-income households by comparing the cost of cooking of non-subsidized LPG stoves (1,800-Watt) induction stove with induction stove with non-subsidized electricity tariffs. Similar with the subsidized LPG tariff, the price of non-subsidized LPG also varies depending on the delivery point. At the agent delivery point, LPG has a price of Rp 156,000 / 12 kg while at the retail delivery point, the LPG has a price of Rp 180,000/ 12 kg. Based on the calculation in table 5, there is an economic saving in cooking costs per month in the amount of Rp 43,606 per month for the 12 kg LPG/month usage pattern. From all the scenarios carried out, it can be analyzed that the biggest cooking cost savings occur in the middle and high-income households who change their cooking behavior and migrate the cooking technology from non-subsidized LPG stove to high-efficiency induction stove with non-subsidized electricity tariffs.

Tables 2-5 shows the evaluation results based on simulation.

**Table 2: Scenario 1 Economic simulation of LPG stove with subsidized LPG tariff and 300-Watt induction stove with 605 Rp / kWh electricity tariff**

	LPG						Induction stove	
Consumption (per Household)	1 gas tube/ 7 days	1 gas tube/ 10 days	1 gas tube/ 7 days	1 gas tube/ 10 days	1 gas tube/ 7 days	1 gas tube/ 10 days	32.09 kwh / 7 days	32.09 kwh / 10 days
Consumption (per household per month)	4 gas tube = 12 kg	3 gas tube = 9 kg	4 gas tube = 12 kg	3 gas tube = 9 kg	4 gas tube = 12 kg	3 gas tube = 9 kg	128.36 kwh / month	96.27 kwh / month
Delivery point	Agen		Retail (HET)		Household retail		Lov voltage network	
Price	12,750	Rp/tube	17,900	Rp/tube	22,000	Rp/tube	605 Rp/kwh	605 Rp/kwh
Cost per household per month	51,000	38,250	71,600	53,700	88,000	66,000	77,655.87 Rp	58,241.90 Rp
Energy saving per household per month							10,344.13 Rp	7,758.10 Rp
Energy saving per household per month on scarcity							82,344.13 Rp	61,758.10 Rp

**Table 3: Scenario 2 Economic simulation of LPG stove with subsidized LPG tariff and 500-Watt induction stove with 605 Rp / kWh electricity tariff**

	LPG						Induction stove	
Consumption (per Household)	1 gas tube/ 7 days	1 gas tube/ 10 days	1 gas tube/ 7 days	1 gas tube/ 10 days	1 gas tube/ 7 days	1 gas tube/ 10 days	27.54 kwh / 7 days	27.54 kwh / 10 days
Consumption (per household per month)	4 gas tube = 12 kg	3 gas tube = 9 kg	4 gas tube = 12 kg	3 gas tube = 9 kg	4 gas tube = 12 kg	3 gas tube = 9 kg	110.17 kwh / month	82.63 kwh / month
Delivery point	Agen		Retail (HET)		Household retail		Lov voltage network	
Price	12,750	Rp/tube	17,900	Rp/tube	22,000	Rp/tube	605 Rp/kwh	605 Rp/kwh
Cost per household per month	51,000	38,250	71,600	53,700	88,000	66,000	66,655.55 Rp	49,991.66 Rp
Energy saving per household per month							21,344.45 Rp	16,008.34 Rp
Energy saving per household per month on scarcity							93,344.45 Rp	70,008.34 Rp

**Table 4: Scenario 3 Economic simulation of LPG stove with subsidized LPG tariff and 1,800-Watt induction stove with 605 Rp / kWh electricity tariff**

Consumption (per Household)	1 gas tube/ 7 days	1 gas tube/ 10 days	1 gas tube/ 7 days	1 gas tube/ 10 days	1 gas tube/ 7 days	1 gas tube/ 10 days	23.24 kwh / 7 days	23.24 kwh / 10 days
Consumption (per household per month)	4 gas tube = 12 kg	3 gas tube = 9 kg	4 gas tube = 12 kg	3 gas tube = 9 kg	4 gas tube = 12 kg	3 gas tube = 9 kg	92.96 kwh / month	69.72 kwh / month
Delivery point	Agen		Retail (HET)		Household retail		Lov voltage network	
Price	12,750	Rp/tube	17,900	Rp/tube	22,000	Rp/tube	605 Rp/kwh	605 Rp/kwh
Cost per household per month	51,000	38,250	71,600	53,700	88,000	66,000	56,238.66 Rp	42,178.99 Rp
Energy saving per household per month							31,761.34 Rp	23,821.01 Rp
Energy saving per household per month on scarcity							103,761.34 Rp	77,821.01 Rp

**Table 5: Scenario 3 Economic simulation of LPG stove with non-subsidized LPG tariff and 1,800-Watt induction stove with 1,467 Rp / kWh electricity tariff**

	LPG				Induction stove			
Consumption (per Household)	1 gas tube/ 7 days	1 gas tube/ 10 days	1 gas tube/ 7 days	1 gas tube/ 10 days	23.24 kwh / 7 days	23.24 kwh / 10 days		
Consumption (per household per month)	4 gas tube = 12 kg	3 gas tube = 9 kg	4 gas tube = 12 kg	3 gas tube = 9 kg	92.96 kwh / month	69.72 kwh / month		
Delivery point	Agent		Household retail		Lov voltage network			



Price	39,000	Rp/gas tube	45,000	Rp/gas tube	1,467	Rp/kwh	1467	Rp/kwh
Cost per household per month	156,000	117,000	180,000	135,000	136,393	Rp	102,295	Rp
Energy saving per household per month					43,606.85	Rp	32,705.14	Rp

## 4. Conclusion

This study has conducted the economic simulations of induction stoves compared to LPG stoves under various scenarios. The simulations carried out in this study consider various possibilities that can occur in the field.

- For various possible economic scenarios conducted in this study, the application of induction stoves for cooking are more economical when compared to LPG stoves.
- In the existing condition (without electrical installation uprating) for low-income households, the transition of cooking behavior from LPG (subsidized) stove to 300-Watt induction stove provides monthly cooking savings per household of Rp 10,344. The application of 500-Watt induction stove provides savings in cooking costs of Rp. 21,344 per month per household. These scenarios need to consider the availability of low power induction stoves, in this case the induction stove with the scale of 300 Watt and 500 Watt.
- In the existing conditions for the middle- and high-income household group, the cooking cost savings obtained will be even greater of Rp 43,606 per month per household. This economic scenario is carried out by considering the use of an 1,800 Watt high-efficiency induction stove.
- If the electrical installation rating for a low-income household is upgraded so that the household can apply a high-efficiency induction cooker (1,800 Watt), the cooking cost saving gained will increase significantly of Rp. 31,761 per month per household.
- The economic saving for low-income households will increase significantly if there are a scarcity of 3 kg LPG tubes in the field.

## 5. Acknowledgements

This research is supported by PT. PLN (Persero)

## 6. References

- Brown, Ed, Jon Leary, Gillian Davies, Simon Batchelor, and Nigel Scott. 2017. "ECook: What Behavioural Challenges Await This Potentially Transformative Concept?" *Sustainable Energy Technologies and Assessments* 22 (2017): 106–15. <https://doi.org/10.1016/j.seta.2017.02.021>.
- Quinn, Ashlinn K., Nigel Bruce, Elisa Puzzolo, Katherine Dickinson, Rachel Sturke, Darby W. Jack, Sumi Mehta, Anita Shankar, Kenneth Sherr, and Joshua P. Rosenthal. 2018. "An Analysis of Efforts to Scale up Clean Household Energy for Cooking around the World." *Energy for Sustainable Development* 46: 1–10. <https://doi.org/10.1016/j.esd.2018.06.011>.

# STUDY OF COMPANY REVENUE BASED ON PRODUCTION PLANNING CONFIGURATION USING GOAL PROGRAMMING METHOD

Fajar Azhari Julian<sup>1,\*</sup>, Rispianda<sup>2</sup>

<sup>1,2</sup> Department of Industrial Engineering, Institut Teknologi Nasional (Itenas), Bandung – INDONESIA

\* Corresponding author e-mail: fajarazharijulian@gmail.com

## Abstract

Production planning in company management is very important to manage. Production planning needs to consider various aspects. Starting from optimizing profits, minimizing production costs, maximizing the available resources. A Goal Programming Method is one method that can be used to optimize production planning, being able to solve problems to be optimal with more than one objective (multi-objective). UD. Lotus is a textile company, which aims to increase sales revenue, decrease production costs by maximizing regular work hours and optimize the use of available resources. The purpose of this study is to make an appropriate discussion to count the number of clothes produced and multiply the cost of production using the Goal Programming method. The results of the research determine the product combination optimization results from programming objectives increase more funds with the policies made by the company so far. The company's profit with a programming objective solution is exceed the company's profit target.

*Keywords: Goal Programming, Multi Objectives, Production Planning*

---

## 1. Introduction

Nowadays, the world of fashion is high in demand by the market. Therefore, many companies offer a variety of products and promote them as well as possible. This causes a high demand, so the company must meet these demands to dominate the market. UD. Lotus is required to meet the number of requests from consumers. therefore, the company strives to maximize existing production, to meet the number of consumer demand by making optimal production planning. In practice, a company's production planning does not only pay attention to consumer demand, but the company must also pay attention to other aspects, including consumers, available resources, and the manufacturing process.

So far UD. Lotus only orientates the production planning to fulfill the number of demands. This causes production planning to be less efficient. Overtime is done by the company to reach the amount of production. However, this overtime makes production costs at UD. Lotus increased, and the worker performance in carrying out its production is less than optimal. For this reason, companies need to maximize regular work hours so that overtime can be minimized or eliminated.

Goal Programming is a method that can optimize multiple goals (multi-objective). Goal programming is

the outcome of a linear programming model, the difference is in the final result. In Linear Programming, the final result defines the maximum or minimum value, whereas in Programming Goal the final result is something that has been agreed upon. Goal Programming tries to minimize the (total) deviation between the goals set and what can be achieved with a certain agreement.

## 2. Related works

Goal Programming have been used by many controlled system in industries. The application of programming system is explained in some other research, table 1 is some research which using Goal Programming.

**Table 1. Application of Goal Programming In Previous Research**

No.	Year and Place	Researhers	Research	Result
1.	America	(Qu, J. et al. 2019)	<i>A goal programming approach for balancing diet costs and feed water use under different environmental conditions</i>	The results of this model are based on the feeds, production level of model animals, and prices adopted, and these inputs can be easily modified. The proposed model provides a conceptual framework for the study and evaluation of irrigation water usage in the field of dairy production and a technique for potential use with other livestock systems.
2.	America	(Mcallister et al. 2000)	<i>Goal Programming Applications In Multidisciplinary Design Optimization</i>	The configurations from the traditional formulation to the bi-level goal programming formulations are the improved effectiveness and speed of the Undersea Vehicle Design

According to (Mcallister et al. 2000), from Research “Goal Programming Applications in Multidisciplinary Design Optimization”, A goal programming is to extend multi-objective system-level analysis to the subsystem level. Goal programming is exceptionally well suited to these design problems because, through deviation variables, the approach automatically captures information about the relative attainment of goals. Therefore, the reported optimal solution can be constrained to a feasible design while incorporating secondary performance measures that are desirable but not required.

## 3. Methodology explanation and reasoning

Methodology of this research devided on several steps with the reasoning, these are the following steps:

### 3.1. System Observation

The existing system in this company still using own perception based on the demand from markets to determine production planning. This production planning leads to not achieve the revenue targets, incur more cost, because of the overtime, and the used of available resource id not optimized. A solution is needed to help stakeholders to make a decision for production planning.

### 3.2. Modelling Goal Programming

(Chowdary & Slomp, 2002), Production planning is a complicated task that requires cooperation among multiple functional units in any organization. In order to design an efficient production planning system, a good understanding of the environment in terms of customers, products and manufacturing processes is a must. Before forming the model, calculating the value of unknown parameters is needed, which the value will be used in the model later.

Table 2 shows the entity and performance measure which is need to be determined.

**Table 2. Planning Production Performance Measures**

Entity	Performance Measure
Consumer	Fulfill the Demand
Product	Volume of Production
Manufacturing Process	Revenue Cost Optimizing Resource

Table 3 shows the total raw material costs, used raw materials, demand, and available resource used for calculate the selling price. The total of raw material cost is a simple equation which raw material cost multiplied with raw material used per dozen.

**Table 3. Type, Raw Material Cost, Demand, and Available Resources**

Product	Product Name	Raw Material Used per Dozen (Kg)	Raw Material Cost	Total Raw Material Cost	Demand* (Dozen)	Available Resources (Kg)
X <sub>1</sub>	Futsal Shirt	4	Rp 50,000	Rp 200,000	500	3700
X <sub>2</sub>	Tracksuit	10	Rp 55,000	Rp 550,000		
X <sub>3</sub>	Cotton Shirt	4.5	Rp 80,000	Rp 360,000		

\*Demand is based from the last month order.

To calculate the selling price, company has a term. The selling price is a simple equation which terms of the selling price multiplied by total raw material cost. The term and selling price is shown by table 4.

**Table 4. Terms of Selling Price and Selling Price**

Product	Product Name	terms of the selling price* (x 1.8)	Selling Price
X <sub>1</sub>	Futsal Shirt	1.8	Rp360,000
X <sub>2</sub>	Tracksuit		Rp990,000
X <sub>3</sub>	Cotton Shirt		Rp648,000

\*Terms is from the company policy.

To calculate the cost of production, company has a term. The cost of pproduction is a simple equation which terms multiplied by selling price. The term and cost f productin is shown by table 5.

**Table 5. Terms of the Cost and Cost of Production**

Product	Product Name	Selling Price	Terms Of The Cost* (x 15%)	Cost of Production
X <sub>1</sub>	Futsal Shirt	Rp 360,000	15%	Rp 54,000
X <sub>2</sub>	Tracksuit	Rp 990,000		Rp148,500
X <sub>3</sub>	Cotton Shirt	Rp 648,000		Rp 97,200

\*Terms is from the company policy.

This company is targeting the cost of production is below 65.000.000 and the total revenue is above 300.000.000 with the maximum of productions is 500 pcs per month because the labor limitations. Table 6 shows the number of productions, revenue, and cost of production.

**Table 6. Number of Production, Total Revenue, and Total Cost of Production**

Product	Product Name	Number of Production	Revenue	Cost of Production
X <sub>1</sub>	Futsal Shirt	150	Rp 54,000,000	Rp 54,000
X <sub>2</sub>	Tracksuit	150	Rp 148,500,000	Rp 148,500
X <sub>3</sub>	Cotton Shirt	200	Rp 129,600,000	Rp 97,200
Total		500	Rp 332,100,000.00	Rp 49,815,000.00

### 3.3. Modelling Goal Programming

The formulation of goal programming model is the determination of the optimal product combination. The decision variable is the number of each type of product to be made. The number of each type of product are X<sub>1</sub> = Futsal Shirt, X<sub>2</sub> = Tracksuit, and X<sub>3</sub> = Cotton Shirt.

The objectives to be achieved by UD. Lotus in sequence is fulfill product demand, maximize sales revenue, minimize production costs, optimize the available resources. The following formulation model according from (Anis & Nandiroh, 2007) to achieve the goals of UD. Lotus is as follows:

1. Objective is to maximize the volume of production to fulfill demand :

$$X_i + d_i^- - d_i^+ = P_i \quad \dots (1)$$

Where :

X<sub>i</sub> = number of products i produced P<sub>i</sub> = demand of product i d<sub>i</sub><sup>-</sup> = the value of the deviation is below P<sub>i</sub> d<sub>i</sub><sup>+</sup> = the value of the deviation above P<sub>i</sub> the value of d<sub>i</sub><sup>-</sup> and d<sub>i</sub><sup>+</sup> need to be minimized, then the function of Z will be :

$$\text{Min } Z = \sum (d_i^- + d_i^+) \quad \dots (2)$$

2. Determine the function of constraints on the use of raw materials and the availability of raw materials

Determination of the constraint function for the use of raw materials and the availability of raw materials is obtained from the number of raw materials used in and the number of available raw materials

$$R_1 + R_2 + R_3 \leq 3700 \quad \dots (3)$$

Where :

R<sub>i</sub> = number of raw material used per dozen

3. The value of production constraints

As mentioned previous, the demand is an estimate of previous month's demand, due to the absence of demand archiving every month. Constraints on the amount of production are assumptions from research. That the production is at least 50 per type per month and maximum total production is 500 per month.

$$X_1 \geq 50 \quad \dots (4)$$

$$X_2 \geq 50 \quad \dots (5)$$

$$X_3 \geq 50 \quad \dots (6)$$

$$X_1 + X_2 + X_3 \leq 500 \quad \dots (7)$$

4. Objective is to maximize the revenue, then the function of Z will be :

$$\text{Max } Z = \sum_{i=1}^m S_i X_i \quad \dots(8)$$

Where :

$S_i$  = selling price per unit of

product i  $X_i$  = number of products i

produced m = types of products

From the equation (8) company wants to maximize the revenue, sales revenue can be achieved if product sales can be maximized. these are the following functions to maximize revenue :

$$\text{Max } Z = 360.000X_1 + 990.000X_2 + 648.000X_3 \quad \dots(9)$$

5. Objective is to minimize the cost, then the function of Z will be :

$$\text{Min } Z = \sum_{i=1}^m C_i X_i \quad \dots(10)$$

Where :

$C_i$  = selling price per unit of product i  $X_i$

= number of products i produced m

= types of products

From the equation (10) company wants to minimize cost of production, minimizing the cost of production can be achieved if cost of production is below the target. These are the following functions to maximize revenue:

$$\text{Min } Z = 54.000X_1 + 148.500X_2 + 97.200X_3 \quad \dots(11)$$

## 4. Validation and Result

The validation is comparing between optimized result from this research with the target of company. This result is done by running solver in excel, these following tables are the result of the maximizing, revenue, minimizing cost, and fulfill the demand.

**Table 7. Comparison Between the Optimized Solution Number of Production and Previous Production**

Goal Number of Productions	Optimized Solution	Previous Production	Company Target
Futsal Shirt	75	150	≤ 500 Pcs / Month
Tracksuit	250	150	
Cotton Shirt	175	200	
Total	500	500	

With using the optimized solution from number of productions, that make the revenue increased. This following table show the comparison from the optimized solution with previous production.

**Table 8. Comparison Between the Optimized Solution and Previous Production of each Goals**

Goal	Optimized Solution	previous Production	Company Target
Maximize Gross Profit	Rp 387,900,000	Rp 332,100,000	-
Minimizing cost	Rp 58,185,000	Rp 49,815,000	Rp 65.000.000
Total Revenue	Rp 329,715,000	Rp 282,285,000	Rp 300.000.000

From the data table can be analyzed there is the difference between the optimized solution with the previous production. The total revenue from previous production is Rp 282,285,000, this is 5.9% lower than the company target. However, the result from the optimized solution shows Rp 329,715,000 which 9.9% higher from the company target. Even though the cost of optimized solution is 12.9% higher from previous production this cost is still below the company's target.

## 5. Conclusion

The result of this study is to reduce the stake holders subjectivity in configuring a number of production. The validation from the result of goal programming has 9.9% higher value from the company target. Although the value of the cost from the optimized solution is higher than the previous production, stakeholder should take this configuration from optimized solution because the total revenue is exceed the company target.

## 6. References

- Anis, M., & Nandiroh, S. (2007). Optimasi perencanaan produksi dengan metode Goal Programming. *Jurnal Ilmiah Teknik Industri*, 5, 133–143.
- Chowdary, B. V., & Slomp, J. (2002). Production Planning under Dynamic Product Environment: A Multiobjective Goal Programming Approach.
- Mcallister, C. D., & Simpson, T. W. (2000). Goal Programming Applications In Multidisciplinary Design Optimization. *Symposium on Multidisciplinary Analysis and Optimization*, 8(c).
- Qu, J., Hsiao, T. C., Depeters, E. J., & Zaccaria, D. (2019). A goal programming approach for balancing diet costs and feed water use under different environmental conditions, 11504–11522. <https://doi.org/10.3168/jds.2019-16543>

## **Detection of Decreased Kidney And Lung Function Through the Iris of the Eye Using the Method Convolutional Neural Network (CNN)**

**Juwairiah<sup>1</sup>, Herry Sofyan<sup>2</sup>, Vincentius Dian Asa Putra<sup>3</sup>, Herlina Jayadianti<sup>4</sup>**

<sup>1,2,3,4</sup> Information System Program study, Informatic Department  
Universitas Pembangunan Nasional Veteran Yogyakarta  
Yogyakarta, Indonesia

*E-mail:* juwairiah@upnyk.ac.id, herrysofyan@gmail.com, vincentiusdap@gmail.com,  
herlinajayadianti@gmail.com

### **Abstract**

Iridology is a scientific study of the shape and structure of the iris that can provide an overview of every organ in the human body. Research on computerized iridology has been carried out. Cases of decreased organ excretion through iridology that are commonly found are the organs of the lungs and kidneys. The purpose of this research using a deep learning approach namely Convolutional Neural Network to detect decreased organ function in the lungs and kidneys through the iris of the eye. The study of iridology and iris image obtained from iridologists. The cropping method is used to extract the identified part of the eye image. The cropping method consists of a median filter to remove noise, a hough circle transforms to get an iris circle and a region of interest to get the identified part. Image cropping results are used as training data and test data. The Convolutional Neural Network training process uses the VGG16 model with 2 classes, normal and not normal. The results of Convolutional Neural Network research can detect decreased organ function in excretion through the iris of the eye. From 40 testing data with details of 20 right eyes and 20 left eyes, the accuracy is 90%.

*Keywords:* Iridology, Human Iris, Excretion, Convolutional Neural Network, deep learning

---

## **1. Introduction**

In recent years, naturopathic practitioners have renewed interest in a disease recognition method that is based on detailed characteristics of the human iris. Iridology represents the study of carefully mapped sections of the iris and the assigned organ systems represented by those areas. There is much research looking for a relation between disease and human iris.

One case that is quite commonly identified through the iris is an organ in the excretion system. The excretory system organ that has decreased function such as kidneys, lungs, liver, and skin have identical patterns and colors on the iris of the eye. Cases of decreased organ excretion through iridology that are commonly found are the organs of the lungs and kidneys. The rapid development of technology gave rise to a method with a high degree of recognition of patterns that is the Convolutional Neural Network (CNN). CNN is one method that can be used to detect and recognize an object in a digital image. Deep Learning is one of the sub-areas of Machine Learning. Basically, Deep Learning [3] is the implementation of the basic concepts of Machine Learning which implements the ANN algorithm with more layers. The number of hidden layers that are used between the input layer and the output layer, then this network can be said to be a deep neural net. In the last few years, Deep Learning has shown outstanding performance. This is largely influenced by stronger computational factors, large data sets, and techniques for training deeper networks [1]. CNN's ability is claimed as the best model for solving object detection and object recognition problems.

## **2. State of the art**

Research on the detection of the condition of the pancreatic organs through the iris with the title "Detection of the Condition of the Pancreas Organs Through the Eye Iris Using Artificial Neural Networks (ANN) Back Propagation Method by Characterizing the Gray-Level Arum Co-Occurrence Matrix" [1]. The image is then



performed by the process of localizing the iris, the organ making pancreatic ROI, and extracting the GLCM feature. The feature extraction results are used as input data (training data and test data) for the back propagation neural network method and then used to diagnose the condition of the pancreas, which is normal or abnormal. The feature extraction results are used as input data (training data and test data) for the back propagation neural network method and then used to diagnose the condition of the pancreas, which is normal or abnormal. Based on the results of the test training data, the program can make a correct diagnosis on the data entered with a 95.8% success rate. While based on test results of test data with a 75% success rate.

Research on the identification of the decline in kidney organ function conditions through the iris with the title "Identification of the Reduction in Functioning of the Kidney Organs through the Iris Eye using the Learning Vector Quantization Artificial Neural Network Method" This study was conducted to making software support modules to detect the deterioration in the function of kidney organs in the human body using the principle of iridology. Iris data is processed using canny edge detection feature extraction to obtain matrix or vector images as an input of artificial neural networks. The method in this study uses a learning vector quantization artificial neural network to recognize the pattern of kidney organs. The results of the network training achieved 100% accuracy with training data, while testing achieved an accuracy of 93.75% with test data.

Research on identification of colon disorders based on iris image with the title "Identification of Colon Disorders based on Iris Eye Image Using the Naïve Bayes Method" [2]. The method used in this software is the Bayesian Method. This method processes the iris image pixels according to the largest frequency, then calculates the probability of each category. This method will produce the probability value of each pixel of the iris image of the eye that has been previously trained to be used in the test image. The iris image database used is Uiris V.1. This image database is a collection of grayscale images with a size of 200x150 px. Research on the detection of disorders of the gastric organs through iris images with the title "Detection of Disturbances in the Gastric Organs through Iris Eye Images using the Backpropagation Artificial Neural Network (ANN) Method" [1]. This study created a system that can detect the presence or absence of interference with the gastric organs in a person's body. Then the system can perform feature extraction with the Principal Component Analysis (PCA) method and classify it using Back propagation Artificial Neural Networks.

Research on the iris segmentation of kidney disease sufferers [6] requires 4 general stages, namely segmentation, normalization, extraction, and matching. In this study, researchers conducted a study of kidney disease datasets using the hough transform and integrodifferential methods by only focusing on the segmentation stage. From the 19 iris images tested, the accuracy rate obtained was 5.26%, while the integrodifferential operator method was 42.10%.

Research on the identification of disease patterns in iris images with RBF neural network [4] recognizes patterns that appear on the iris can be identified with the help of artificial neural network technology, one of which is the RBF method used in this study. The results found in this study are the use of the RBF method can recognize patterns in the iris of the eye, and can provide the results of recognition of complex diseases and stress with an accuracy that is practically still average (around 50%).

### 3. Iridology

Iridology or commonly referred to as iris diagnosis is a medical method that states that each part of the body can be represented by the region contained in the iris (the colored part of the pupil) [5]. The real originator of Iridology was a Hungarian physicist named Ignatz von Peczely. Iridology is science and practice that can reveal inflammation (inflammation), accumulation of toxins in tissues, glandular dams (congestion), where it is located (in which organs), and what is the severity of the condition (acute, subacute, chronic and degenerative) [6] By observing the iris, through a person's body condition can be known, for example, the status is weak or strong, the level of health and the transition to the severity or healing process. The following chart is Dr. Iris's eye map Bernard Jensen, D.C., Ph.D. with an update from Ellen Jensen, Ph.D., D.Sc., commonly used today.

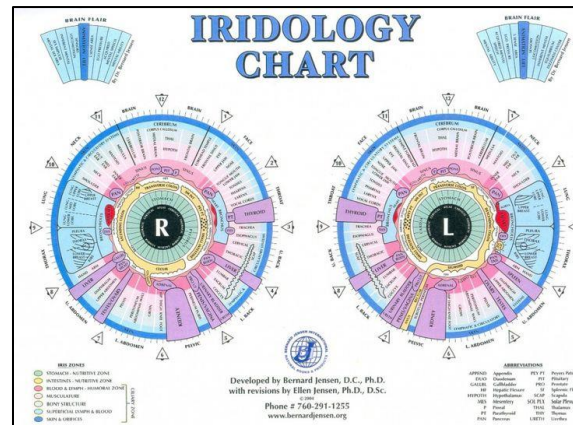


Fig. 1: Iridology Chart

Iridology charts are drawn in a clockwise area. Right-sided iris area showing the kidney was found at 17:30. The right iris area showing the condition of the lungs is at 20:50. The iris area of the left eye that shows the condition of the kidney organ is found in the area of the clock at 18:36. The left iris area showing the condition of the lungs is at 2:15.

## 4. Result and discussion

The data that has been obtained is classified into right eye iris and left-right eye iris. Modeling iridology patterns with 200 iris images divided by 100 iris irregular images showing abnormalities and 100 iris images normal. From each modeling, the data will be divided into training and test data. The ratio of training and test data comparison for each model is 80:20.

Table 1: Training and testing dataset

Image data	Training Data	Testing Data
Normal iris	80	20
Abnormal iris	80	20

Normal iris with an iris that has damage there is a difference in the structure of the surface layer of the iris. From the color, texture, and location of patches of pigment in the iris, a person's health condition can be analyzed. Iris eye that is damaged (abnormal) there are patches of pigment.

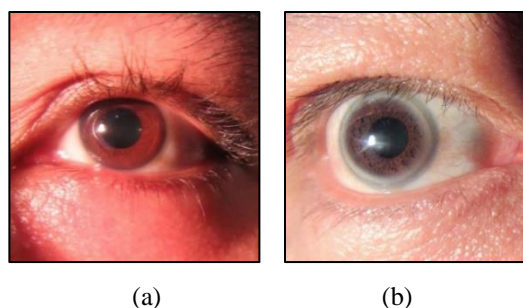


Fig. 2: Normal Iris (a), Abnormal Iris (b)

### 4.1 Image Processing

Image processing is used to get the location of the iris area that shows a decline in organ function in accordance with the data sought. Image processing is designed using the median filter method, hough circle transformation and region of interest (ROI).

(i) Median Filter

The initial iris image is made into a grayscale image, then read the value at each pixel of the grayscale image value. The calculation is done by sorting the pixel intensity value group and then changing the pixel value processed by the average value of the sequence results. The filter used is 5x5 in size.

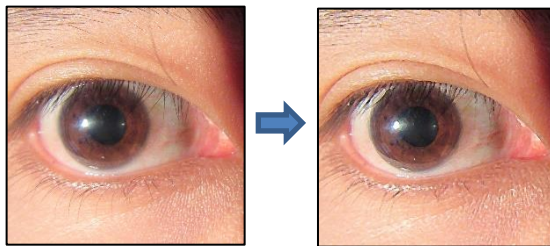


**Fig. 3: Median Filter of Iris Image**

### (ii) Hough Circle Transform

The image of the median filter results will be detected edges then transformed to the accumulator (a b space) using  $a = x - \theta \cos \theta$  and  $b = y - R \sin \theta$ . Variables a and b = circle points on the accumulator, x and y = coordinates of the points in the transformed image  $\theta$  = angle from 0o to 360°. The results of this transformation will produce a new circle on the accumulator. Some of the circles on the accumulator will intersect at a certain point. Then vote and cell that has the largest value will be detected as the actual center of the circle. Hough circle transform process to get the perfect iris.

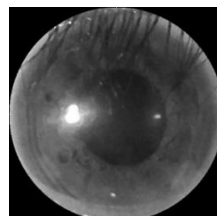


**Fig. 4: Hough Circle Transform of Iris Image**

### (iii) Region of Interest (ROI)

ROI is used to find points in the kidney or lung area to be detected. The strategy of taking the area of the lungs or kidneys, the iris image will be divided into 32 parts as shown in figure a for right eye iris ROI and image b for left eye iris ROI

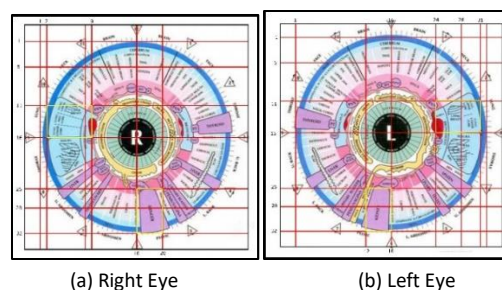


**Fig. 5: Hough Circle Transform of Iris Image**

The results of image processing are used as training and test data. Example of iris image resulting from image processing:

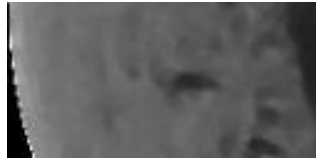


Fig. 6: Result of Image Processing

## 4.2 Model Making

Following are the steps in making an iridology model:

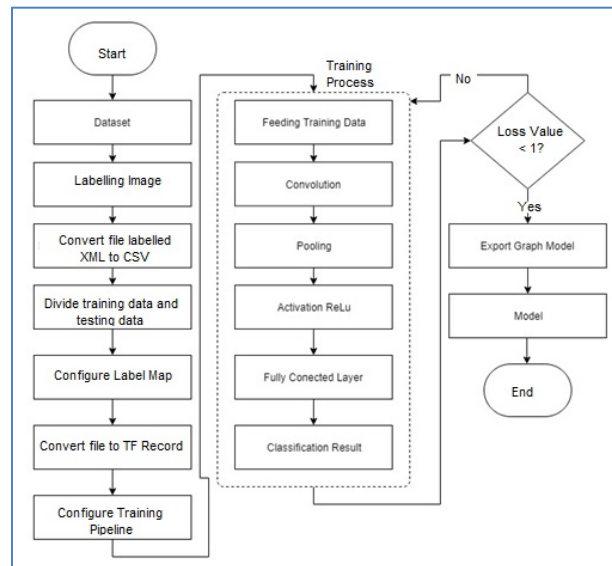


Fig. 7: Iridology Model Making

In this study, a single shot detector (SSD) with a convolutional neural network architecture is used which is VGG16. SSD models using MobileNet can run with light computing [11]. In this study, the SSD model using MobileNet underwent a modification in the clarification process to get the appropriate output.

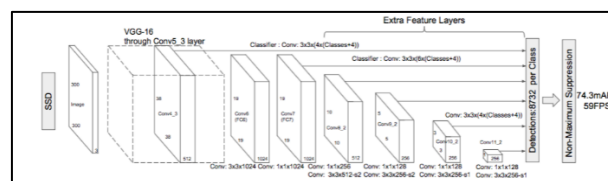


Fig. 8: VGG16 Architecture

This architecture has 13 convolution layers and five max-pooling layers. All convolution layers have a filter width of 3 x 3 with the number increasing in each block. All of these layers have the ReLU activation function. While the max-pooling layer has a filter width of 2 x 2. There is also a global average pooling layer before entering the two fully connected layers. Both fully connected layers have 512 hidden units and a dropout of 0.5. The output from this set of processes will be classified with the classifier. The classifier used is a fully connected layer with a softmax activation function. This layer is needed so that the training process with backpropagation can be carried out.

### 4.3 Model Testing

Following are the steps in making an iridology model testing:

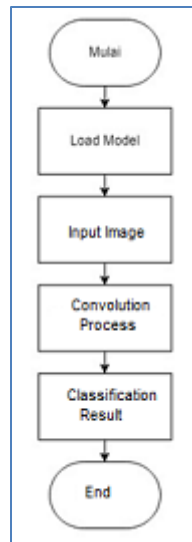


Fig. 9: Flowchart of Model Testing

Accuracy is one of the parameters in this study. Accuracy is obtained after the model testing process in the form of a percentage. Accuracy calculations are performed on each part of the iris of the left or right eye which has decreased organ function in the lungs or kidneys. Calculation formula:

$$\text{Percentage of Accuracy} = \frac{\text{Amount of test data image is correct}}{\text{Total amount of test image data}}$$

From the above calculation, it can be seen the level of accuracy of the Convolutional Neural Network method in identifying decreased organ function in the lungs or kidneys through the iris of the eye.

The training process starts by calling the training library from TensorFlow. The data training process with steps totaling 50,000 requires approximately 2 days. The output that will be generated during the training process data will be included in the training folder. The loss value is a quantitative measure of how much the predictions differ from the actual output (label). The value of the loss is inversely proportional to the accuracy of the model. The greater the loss value, the less accurate the model is made. The loss value in this training process is following the research target of 0.8504. The iridology model created was tested with input data in the form of 10 right eye iris data and 10 left eye iris data. One iris image has 2 tests to identify decreased lung and kidney function according to ROI. Model testing is made in the form of a desktop application. The following are examples of test results:

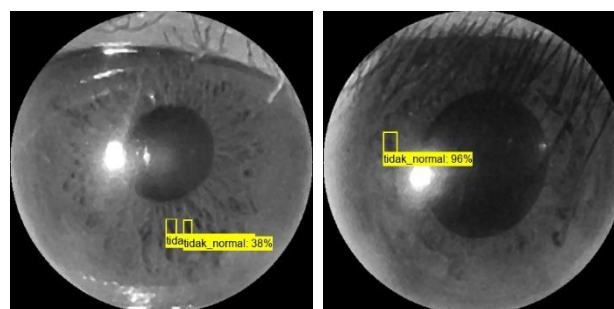


Fig. 10: Right Eye Testing



**Fig. 11: Left Eye Testing**

From the result of these tests, the calculation of accuracy:

$$\frac{36}{40} \times 100\% = 90\%$$

Accuracy obtained by 90%, with details of 10 data decline in function of the right iris kidney organ is true, 9 data decline in function of the right iris pulmonary organ is true, 8 data decline in kidney function of the left iris is true and 9 data decline in organ function left iris lung is true. Incorrect data are 1 data decline in function of the right iris pulmonary organ, 2 data decrease in function of the left iris kidney organ and 1 data decrease in function of the left iris lung organ. Incorrect data is not detected because noise and light in shooting make parts undetectable

## 5. Conclusion

Convolutional Neural Network using VGG16 architecture can recognize well the pattern of decreased organ function excretion through the iris with an accuracy of 90% from 40 testing data. Future studies can develop by examining the noise and light factors in the iris in the iris image processing

## 6. References

- Li Xu , Jimmy SJ Ren, Ce Liu, Jiaya Jia, 2014, "Deep convolutional neural Network for Image deconvoluton", Advances in Neural Information Processing Systems 27 (NIPS 2014)
- NS Sarode, 2015, Iris Recognition using LBP with Classifiers-KNN and NB, International Journal of Science and Research (IJSR) ISSN (Online): 2319-7064 Index Copernicus Value (2013)
- Goodfellow, I., Bengio, Y, and Courville, A. 2016. Deep Learning (Adaptive Computation and Machine Learning Series). The IMT Press.
- GB Huang, 2005, P Saratchandran "A generalized growing and pruning RBF (GGAP-RBF) neural network for function approximation", IEEE, <http://www.eng.buffalo.edu/~psingla/Teaching/MAE502/ReadingPapers/MRANPapers.pdf>
- Saccharin, Farida. 2005, Iridology: A Complete Guide To Diagnosing Through the Iris And To Related Forms of Treatment, New York, USA
- Smereka, Marcin & Duleba, Ignacy. (2008). Circular Object Detection Using a Modified Hough Transform. Applied Mathematics and Computer Science. 18. 85-91. 10.2478/v10006-008-0008-9.
- Sherif E.Hussein,Osama A.Hassan,Malcolm H.Granat,"Assessment of the potential iridology for diagnosing kidney disease using wavelet analysis and neural networks , Biomedical Signal Processing and Control journal, Volume 8, Issue 6, November 2013, Pages 534-541
- Liu, Tianyi, Shuangshang Fang, Yuehui Zhao, Peng Wang dan Jun Zhang. 2015. Implementation of Training Convolutional Neural Networks. <https://arxiv.org/ftp/arxiv/papers/1506/1506.01195.pdf>.

## DESICION SUPPORT SYSTEM USING TOPSIS METHOD FOR SMARTPHONE SELECTION

Mira Musrini<sup>1</sup>, Sofia Umaroh<sup>1,\*</sup> and Alvin Al Arifin<sup>3</sup>

<sup>1</sup>Department of Information System, Institut Teknologi Nasional (Itenas), Bandung - INDONESIA

<sup>1</sup>Departement of Information System, Institut Teknologi Nasional (Itenas), Bandung - INDONESIA

<sup>2</sup>Departement of Informatics, Institut Teknologi Nasional (Itenas), Bandung - INDONESIA

\* Email: sangkuriang26@itenas.ac.id, sofia.umaroh@gmail.com

### Abstract

Nowadays smartphone has developed rapidly, within days and months, they will build many smartphones and with so many differences feature such as more powerful processors, wider screen, more powerful front and back camera etc. Sometimes buyer has difficulties in determining which smartphone that most suitable with their needs. In this research, we implement TOPSIS method to support buyer in choosing the most appropriate smartphone, based on its feature and brands. TOPSIS, stand for Technique for Order of Preference by Similarity to Ideal Solution, is one of Decision support method based on calculation of positive ideal distance solution and negative ideal distance solution. Final output of TOPSIS calculation is order of priority of recommended smartphone's brand. TOPSIS was also applied in Decision Support System, where the output of this application was compared with the result of manual TOPSIS calculation.

*Keywords TOPSIS, positive ideal distance solution, negative ideal distance solution weighted normalized decision matrix*

### 1. Introduction

Decision Support system is Based Computer system used to make decision for organization. Decision Support Systems can be either fully computerized or human powered or combination of both. Decision Support System are used as a support tools for users or managers to solve specific problems. Database of the decision support system can be used to generate periodically reports, or to produce information as result of simulation of one or more components.[6][7]

One of the technics that's is used for simulation of decision support system models Multi-criteria Decision Making Methods. . The development of computer technology is very beneficial for the development of MCDM science. The development of MCDM is closely related to the development of computer technology. With advanced computer technology, it is very helpful in conducting systematic analysis of complex MCDM problems.[3]

One method of MCDM is TOPSIS Method, TOPSIS is stand for Technique for Order Preference by Similarity to Ideal Solution. The TOPSIS method was first introduced by Yoon and Hwang in 1981. This method is one method that is widely used to resolve practical decision making. TOPSIS has a concept where the chosen alternative is the best alternative that has the shortest distance from the ideal positive solution and the farthest distance from the negative ideal solution.[2][4] The more factors that must be considered in the decision-making process, the more difficult it is to take.

According to [Petr Průša, Stefan Jovčić] "Alternatives of TOPSIS methods are evaluated based on their distance in relation to the ideal and anti-ideal solution. The alternative is considered best if there is a minimum distance in relation to the ideal solution and the greatest distance from the anti-ideal solution".

Nowadays, many brands of smartphones with various specifications sold in the market. This situation makes it difficult for users to make choices according to their wishes and budget. The rapid development and sales of smartphones on the market are increasing within short time. With all kinds of features available and with so many prices, consumers are often faced problems of difficulties in choosing a smartphone.

Related to these problems, a decision support system is built to help consumers to determine a type of smartphone are most appropriate based on their needs, features, and budget. Hopefully, this TOPSIS method in the decision support system can help customers to solve their problems.



## 2. Methodology

Technique for Order Preference by Similarity to Ideal Solution (TOPSIS) is a multi-criteria decision-making method. First introduced by Yoon and Hwang in 1981 [10]. TOPSIS uses the principle that the chosen alternative must have the closest distance from the positive ideal solution and the longest distance from the negative ideal solution to determine the relative proximity of an alternative with the optimal solution [11][12]. The TOPSIS method is based on the concept that the best-chosen alternative not only has the shortest distance from the positive ideal solution, but also has the longest distance from the negative ideal solution

TOPSIS methods consists of these steps:

Step 1. Let us consider the decision matrix  $D$ , which consists of *alternatives* and *criteria*, described by:

$$D = \begin{matrix} & C_1 & \dots & C_n \\ \begin{matrix} A_1 \\ \vdots \\ A_m \end{matrix} & \begin{pmatrix} x_{11} & \dots & x_{1n} \\ \vdots & \ddots & \vdots \\ x_{m1} & \dots & x_{mn} \end{pmatrix} \end{matrix} \quad (1)$$

Where  $A_1, A_2, \dots, A_m$  are alternatives and  $C_1, \dots, C_n$  are criteria. In our case study,  $A_i$  are brands of smart phone, and  $C_i$  are features of each brands.  $x_{ij}$  are value of criteria  $C_j$  of alternatives  $A_i$  which are given by survey. Each criteria  $C_j$  it's weight value  $W_j$  which satisfy :

$$\sum_{j=1}^n W_j = 1 \quad (2)$$

In general, the criteria is classified into two types, those are Benefits and Costs. Benefit criterion means, the higher value the better, while Cost criterion means the opposite.

Step 2, Since the data comes from differences resources, it is necessary to normalize it in order to transform it into a dimensionless matrix. The normalized decision matrix can be determined as follows:

$$r_{ij} = \frac{x_{ij}}{\sqrt{\sum_{i=1}^m x_{ij}^2}} \quad \text{with } i=1..m, j=1..n \quad (3)$$

Thus, normalized decision matrix can be represented as  $r = [r_{ij}]_{m \times n}$  with  $i=1..m$ , and  $j=1..n$

Step 3, After normalization, we calculate the weighted normalized decision matrix  $R = [b_{ij}]_{m \times n}$  with  $i=1..m, j=1..n$  by multiplying the normalized decision matrix by its associated weights ( $w_i, i=1..n$ ). The weighted normalized value  $b_{ij}$  can be calculated as

$$y_{ij} = w_i \cdot r_{ij} \quad i=1..m, j=1..n \quad (4)$$

Step 4, calculate the positive ideal solution  $A^+$  and Negative ideal solution  $A^-$  as follows:

$$A^+ = (Y_1^+, Y_2^+, \dots, Y_m^+) \quad (5)$$

$$A^- = (Y_1^-, Y_2^-, \dots, Y_m^-) \quad (6)$$

Where

$$Y_j^+ = (\max_i y_{ij}, j \in J_1: \min_i y_{ij}, j \in J_2)$$

$$Y_j^- = (\min_i y_{ij}, j \in J_1: \max_i y_{ij}, j \in J_2)$$

Step 5, calculate Euclidean distance from positive ideal Solution ( $A^+$ ) to each value  $A_i$ , and Euclidean distance from negative ideal Solution ( $A^-$ ) to each  $A_i$  follows:

$$d_i^+ = \sqrt{(Y_i^+ - y_{ij})^2} \quad (7)$$

$$d_i^- = \sqrt{(Y_i^- - y_{ij})^2} \quad (8)$$

where:

- $Y_i^+$  is value of ideal positive solution of  $A^+$ , with  $i=1, \dots, m$



- $Y_i^-$  is value of ideal negative solution of  $A_i^-$ , with  $i=1, \dots, m$
- $y_{ij}$  is value of weighted normalized matrix, with  $i=1, \dots, m, j=1, \dots, n$

Step 6, Calculate the relative closeness  $V_i$  for each alternative  $A_i$ , with respect to positive ideal solution as given by:

$$V_i = \frac{d_i^-}{d_i^+ + d_i^-} \quad \text{with } i=1, \dots, m \quad (9)$$

### 3. Case study

In our case study, several brands smartphones were chosen, those are ASUS Zenfone MAX PRO M1, Xiaomi Redmi Note 5A, Samsung Galaxy J6, Oppo A3s and Vivo Y69. Each of alternatives has its own criteria, those are prosessor, RAM, internal memory, Camera, screen size and battery capacity. Those datas were input in the DSS. Input table can be seen in the table 1, as follows:

Table 1: Input table

Alternatif/ Kriteria	ASUS Zenfone MAX PRO M1	Xiaomi Redmi Note 5A	Samsung Galaxy J6	Oppo A3s	Vivo Y69
Prosesor	Qualcomm SDM636 Snapdragon 636	Qualcomm Snapdragon 435	Exynos 7870 Octa	Qualcomm SDM450 Snapdragon 450	Mediatek MT6750
RAM	3 gb	3 gb	3 gb	3 gb	3 gb
Internal Memory	32 gb	32 gb	32 gb	32 gb	32 gb
Camera	Primary Dual: 13 MP (f/2.2, 1.12m) + 5 MP (f/2.4, 1.12m),	Primary camera 13 MP, f/2.2	Primary 13 MP (f/1.9, 28mm)	Primary Dual: 13 MP, f/2.2, AF, 2 MP, f/2.4	Primary 13 MP, AF, f/2.2
Screen size	5.99 inches, 93.1 cm <sup>2</sup> (~77.0% screen-to-body ratio)	5.5 inches (~71.5% screen- tobody ratio)	5.6 inches, 80.1 cm <sup>2</sup> (~76.5% screen-to-body ratio)	6.2 inches, 95.9 cm <sup>2</sup> (~81.2% screen-to-body ratio)	5.5 inches, 83.4 cm <sup>2</sup> (~71.4% screen-to-body ratio)
Bateray capacity	5000 mah	3080 mah	3000mah	4230 mah	3000mah

One person as a decision maker was asked to determine the decision value of all criteria from each alternative. Based on that decision value matrix is obtained. Entry of decision value matrix considered as  $x_{ij}$ , where  $i$  is equal to index of criteria, and  $j$  is equal to index of alternatives. The decision value matrix can be seen in the table 2 bellows.

**Table 2 : Decision value Matrix**

Kode	K1	K2	K3	K4	K5	K6
A1	4	4	3	3	4	5
A2	2	3	3	3	4	3
A3	3	3	3	4	3	3
A4	2	3	3	4	5	5
A5	2	3	3	3	4	3

Weight values of all alternatives were obtained from a survey. Weight value of criteria, that is  $w_1, w_2, w_3, \dots, w_6$ , can be seen in table 3 bellows. As can be seen, the attributes of all criteria, considered as benefit.

**Table 3: Weight criteria value Matrix**

code	Name	Attribute	weight
K1	Processor	Benefit	5
K2	RAM	Benefit	3
K3	Memory Internal	Benefit	4
K4	Camera	Benefit	4
K5	screen size	Benefit	4
K6	Battery capacity	Benefit	5

Step 1, the normalized decision value is calculated, based on equation (3), and we have matrix of normalizes decision value Entry of this matrix is considered as  $r_{ij}$ , where  $i$  is index of alternative, and  $j$  is index of criteria.

Step 2, the normalized decision value is multiply by weight criteria value, based on equation (5). We have matrix of weight normalizes decision value, Entry of this matrix is considered as  $y_{ij}$ , where  $i$  is index of alternative, and  $j$  is index of criteria.

Step 3, Determine positive ( $A^+$ ) ideal solution and negative ideal solution ( $A^-$ ). Since all weight criteria is considered as benefit, thus equation of positive ideal solution is described in the equation 10:

$$A^+ = (y_1^+, y_2^+, y_3^+, \dots, y_5^+), \text{ where } y_i = \max (y_{ij}), \text{ } i \text{ is index of alternative, and } j \text{ is index of criteria} \dots \dots \dots (10)$$

Equation of negative ideal solution is described in the equation 11:

$$A^- = (y_1^-, y_2^-, y_3^-, \dots, y_5^-), \text{ where } y_i = \min (y_{ij}), \text{ } i \text{ is index of alternative, and } j \text{ is index of criteria} \dots \dots \dots (11)$$

Step 4, Determine Euclidean distance of negative ideal solution ( $D^-$ ) and positive ideal solution ( $D^+$ ) based on equation (7) and (8). .

Step 5. determine preference value  $v_i$  based on equation (9). This  $V_i = (V_1, V_2, \dots, V_6)$  was sorted descendant. If  $V_i$  has biggest value, then alternative of brand of smartphone is the best choice according to the individual decision maker. The rank of  $V_i$  is  $V_1 > V_4 > V_3 > V_2 > V_5$ . Those values can be seen in the table 5 bellows:

**Tabel 4. Preference value of each alternative**

Alternative	Preference value	Ranking
A <sub>1</sub>	0.754	1
A <sub>4</sub>	0.475	2
A <sub>3</sub>	0.363	3
A <sub>5</sub>	0.170	4
A <sub>2</sub>	0.170	5

#### 4. Decision Support System using TOPSIS method

Criteria form is displayed and the user can enter criterion data. as can be seen in the figure 1.

The screenshot shows a web browser window with the URL 127.0.0.1/TOPSIS/index.php?m=kriteria\_tambah. The page title is 'SPK TOPSIS'. The main heading is 'Tambah Kriteria'. The form contains the following fields: 'Kode \*' with the value 'KD1', 'Nama Kriteria \*' with the value 'Prosesor', 'Atribut \*' with a dropdown menu showing 'Benefit', and 'Bobot \*' with the value '5'. At the bottom, there are two buttons: 'Simpan' (Save) and 'Kembali' (Back). The footer text is 'TOPSIS - Alvin Al Arifin - 2018'.

**Fig. 1: form input of criteria's data**

After user finish input criteria, then alternative form is displayed as can be seen in the figure 2.

The screenshot shows a web browser window with the URL 127.0.0.1/TOPSIS/index.php?m=alternatif\_tambah. The page title is 'SPK TOPSIS'. The main heading is 'Tambah Alternatif'. The form contains the following fields: 'Kode \*' with the value 'A01', 'Nama Alternatif \*' with the value 'ASUS Zenfone MAX PRO M1', and 'Keterangan' which is an empty text area. At the bottom, there are two buttons: 'Simpan' (Save) and 'Kembali' (Back). The footer text is 'TOPSIS - Alvin Al Arifin - 2018'.

**Fig. 2: form input of alternative's data**

A decision maker can input all entry of decision value of all alternative and criteria, later on known as decision value matrix ( $X_{ij}$ ). The matrix of decision value in DSS can be seen in the figure 3

Kode	Nama Alternatif	K01	K02	K03	K04	K05	K06	Aksi
A01	ASUS Zenfone MAX PRO M1	4	4	3	3	4	5	<a href="#">Cetak</a>
A02	Xiaomi Redmi Note 5A	2	3	3	3	4	3	<a href="#">Cetak</a>
A03	Samsung Galaxy J6	3	3	3	4	3	3	<a href="#">Cetak</a>
A04	Oppo A3s	2	3	3	4	5	5	<a href="#">Cetak</a>
A05	Vivo Y69	2	3	3	3	4	3	<a href="#">Cetak</a>

Fig. 3: Matrix of decision value ,  $x_{ij}$

Equation 3,4,5 until equation 9 is implemented in the system. Final result of DSS are preferences values,  $V_i$ , where  $i$  is equal 1 to 6. All Value of  $V_i$  will be displayed in descendant order. The alternative with the highest value of  $V_i$ , is the best choice. Rank of  $V_i$  as output of DSS, can be seen in figure 4:

5

Perangkingan		
	Total	Rank
A01 - ASUS Zenfone MAX PRO M1	0.754	1
A04 - Oppo A3s	0.475	2
A03 - Samsung Galaxy J6	0.363	3
A05 - Vivo Y69	0.17	4
A02 - Xiaomi Redmi Note 5A	0.17	5

Fig. 4: preferences value or relative closeness value

The result of the system is exactly the same as result value in the table 9.

## 5. Conclusion

Based on research conducted, a decision support system using the TOPSIS method has been successfully created and can provide recommendations for smartphone brand selection based on selected criteria, namely processor, ram, internal memory, camera, screen size, and battery capacity. In the final stage, the calculation of preference value is conducted and those value are ranked. Those rank of preference value are Asus Zenfone Max Pro M1 (0.753764224), A2 - Xiaomi Redmi Note 5A (0.170158058), A3 - Samsung Galaxy J6 (0.362518271), A4 - Oppo A3s (0.474802777), A5 - Vivo Y69 (0.170158058).

This Decision Support System can be developed to be Group DSS in the future.

## 6. References

- Petr Průša, Stefan Jovčić, Vladimír Němec, Petr Mrázek, "Forklift Truck Selection Using Topsis Method," *International Journal for Traffic and Transport Engineering*, 2018, 8(3): 390 - 398
- Srikrishna S, Sreenivasulu Reddy. A, Vani S1, "A New Car Selection in the Market using TOPSIS Technique," *International Journal of Engineering Research and General Science Volume 2, Issue 4, June-July, 2014* ISSN 20912730.
- Ewa Roszkowska, "MULTI-CRITERIA DECISION MAKING MODELS BY APPLYING THE TOPSIS METHOD TO CRISP AND INTERVAL DATA,"

- Renato A. Krohlinga , André G. C. Pachecob, “A-TOPSIS – An approach Based on TOPSIS for Ranking Evolutionary Algorithms”, *Procedia Computer Science* ,55 ( 2015 ) 308 – 317
- Davood Sabaei, John Erkoyuncu, and Rajkumar Roy , “A review of multi-criteria decision making methods for enhanced maintenance delivery” *Procedia CIRP* 37 ( 2015 ) 30 – 35
- Vasiliki Balioti, Christos Tzimopoulos and Christos Evangelides, “Multi-Criteria Decision Making Using TOPSIS Method Under Fuzzy Environment. Application in Spillway Selection,” *Proceedings . International Conference on “Insights on the Water-Energy-Food Nexus”, Lefkada Island, Greece, 27–30 June 2018*. Published: 31 July 2018
- M. Socorro García-Cascales, M. Teresa Lamata , “On rank reversal and TOPSIS method,” *Mathematical and Computer Modelling* 56 (2012) 123–132
- Xing Zhongyou, “Study on the Application of TOPSIS Method to the Introduction of Foreign Players in CBA Games”, *Physics Procedia* 33 ( 2012 ) 2034 – 2039
- Rubayet Karim<sup>1</sup>, C. L Karmaker, “Machine Selection by AHP and TOPSIS Methods,” *American Journal of Industrial Engineering*, 2016, Vol. 4, No. 1, 7-13
- Kambiz Shahroudi, S.Maryam Shafaei TONEKABONI, “APPLICATION OF TOPSIS METHOD TO SUPPLIER SELECTION IN IRAN AUTO SUPPLY CHAIN,” *Journal of Global Strategic Management*, Vol 6 , No2 , December 2012, pp 123-131.
- Robbi Rahim<sup>1</sup>, S Supiyandi<sup>2</sup> et al, “TOPSIS Method Application for Decision Support System in Internal Control for Selecting Best Employees” *IOP Conf. Series: Journal of Physics: Conf. Series* 1028 (2018) 012052

## Safety Integrity Level (SIL) Study for HIPPS

**Dzulfikar Ali Hafizh<sup>1\*</sup>, Dani Rusirawan<sup>2</sup>, Ahmad Taufik<sup>3</sup>, Deddy Nugraha<sup>3</sup>**

<sup>1</sup> Under Graduate Student of Mechanical Engineering, Iitenas, Bandung – INDONESIA

<sup>2</sup> Dept. of Mechanical Engineering, Iitenas Bandung – INDONESIA

<sup>3</sup> Indonesian Society for Reliability (ISR)

\*Corresponding author e-mail: dzulfikarahafizh@gmail.com

### Abstract

A safety analysis is a type of study that examines system-level and related assets to determine loss of containment scenarios, identify risk levels, decide whether a safety instrumented system (SIS) is required, and define the provisions that protect against, or mitigate, loss of containment. Safety analysis is a key component of integrity management. Other components of integrity management include process design, alarm identification and management, protective devices, and community and plant emergency response plans. Together, these actions form a layer of protection around critical systems.

*Keywords: safety integrity level, layer of protection, A high-integrity pressure protection system (HIPPS)*

### 1. Introduction

James Reason's Swiss cheese model for process safety illustrates how major accidents and catastrophic system failures actually uncover multiple, smaller failures leading to an actual hazard. In the model, each slice of cheese represents a safety barrier for a particular hazard and that no single barrier is fool proof, each having 'holes.' When the holes align a catastrophic failure occurs, which can result in serious consequences. To protect ourselves from these holes, systems need to be properly managed, inspected and tested to verify their ongoing reliability. The procedure for defining this process needs to be documented and designs reviewed. A safety instrumented function (SIF) study assesses system risk, defines risk mitigation or elimination actions required to return the system to a safe state when conditions such as pressure or temperature reach a threshold level. An SIF detects a specific hazard and brings the process to a safe state. It provides a defined level of risk reduction or safety integrity level (SIL) for a specific hazard by automatic action using instrumentation.

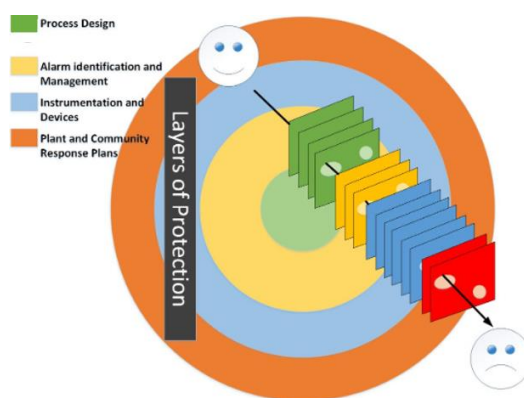
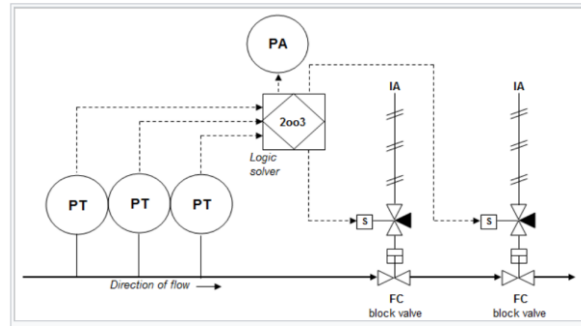


Fig. 2 Swiss Cheese Model

A high-integrity pressure protection system (HIPPS) is a type of safety instrumented system (SIS) designed to prevent over-pressurization of a plant, such as a chemical plant or oil refinery. The HIPPS will shut off the source of the high pressure before the design pressure of the system is exceeded, thus preventing loss of containment through rupture (explosion) of a line or vessel. Therefore, a HIPPS is considered as a barrier between a high-pressure and a low-pressure section of an installation.

HIPPS is a complete functional loop consisting of:

- sensors, (or initiators) that detect the high pressure
- a logic solver, which processes the input from the sensors to an output to the final element
- final elements, that actually perform the corrective action in the field by bringing the process to a safe state. In case of a HIPPS this means shutting off the source of overpressure. The final element consists of a valve, actuator and solenoids.



**Fig. 3: HIPPS Configuration**

The scheme above presents three pressure transmitters (PT) connected to a logic solver. The solver will decide based on 2-out-of-3 (2oo3) voting whether or not to activate the final element. The 1oo2 solenoid panel decides which valve to be closed. The final elements consist here of two block valves that stop flow to the downstream facilities (right) to prevent them from exceeding a maximum pressure. The operator of the plant is warned through a pressure alarm (PA) that the HIPPS was activated. This system has a high degree of redundancy:

- failure of one of the three pressure transmitters will not compromise the HIPPS functionality, as two readings of high pressure are needed for activation.
- failure of one of the two block valves will not compromise the HIPPS functionality, as the other valve will close on activation of the HIPPS.

## 2. Standards and Design Practices

### 2.1 IEC 61508 & IEC 61511

The International Electrotechnical Commission (IEC) has introduced the IEC 61508 and the IEC 61511 standards in 1998 and 2003. These are performance based, non-prescriptive, standards which provide a detailed framework and a life-cycle approach for the design, implementation and management of safety systems applicable to a variety of sectors with different levels of risk definition. These standards also apply to HIPPS.

The IEC 61508 mainly focuses on electrical/electronic/programmable safety-related systems. However, it also provides a framework for safety-related systems based on other technologies including mechanical systems. The IEC 61511 is added by the IEC specifically for designers, integrators and users of safety instrumented systems and covers the other parts of the safety loop (sensors and final elements) in more detail.

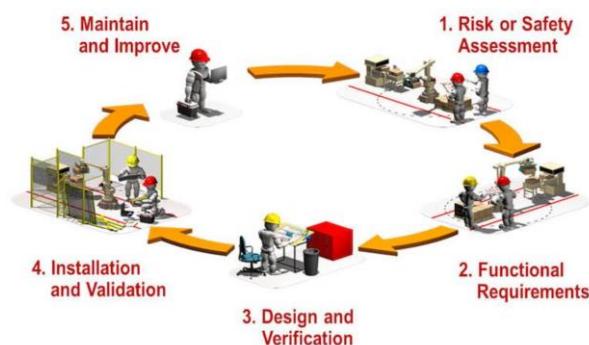


**Fig. 4: Safety Life Cycle**

The basis for the design of your safety instrumented system is the required Safety Integrity Level (SIL). The SIL is obtained during the risk analysis of a plant or process and represents the required risk reduction. The SIS shall meet the requirements of the applicable SIL which ranges from 1 to 4. The IEC standards define the requirements for each SIL for the lifecycle of the equipment, including design and maintenance. The SIL also defines a required probability of failure on demand (PFD) for the complete loop and architectural constraints for the loop and its different elements.

In laymen terms, SIL basically classifies your plant by its probability to detect dangerous failures that might lead to injuries, fatalities or a catastrophic disaster.

SIL1 your plan could fail to detect danger once in 10 times to 100 times. (0.1% to 0.01% fail on demand)

SIL2 your plan could fail to detect danger once in 100 to 1000 times (0.01% to 0.001% fail on demand)

SIL3 your plan could fail to detect danger once in 100 to 1000 times (0.001% to 0.001% fail on demand)

SIL4 your plan could fail to detect danger once in 100 to 1000 times (0.0001% to 0.00001% fail on demand)

**Table 6 Relation Between SIL, PFD, and RRF**

Safety Integrity Level	Risk Reduction Factor	Probability of Failure on Demand
SIL 4	100,000 to 10,000	$10^{-5}$ to $10^{-4}$
SIL 3	10,000 to 1,000	$10^{-4}$ to $10^{-3}$
SIL 2	1,000 to 100	$10^{-3}$ to $10^{-2}$
SIL 1	100 to 10	$10^{-2}$ to $10^{-1}$

## 2.2 Layer of Protection Analysis (LOPA)

Layer of Protection Analysis (LOPA) is a risk management technique commonly used in the chemical process industry that can provide a more detailed, semi-quantitative assessment of the risks and layers of protection associated with hazard scenarios.

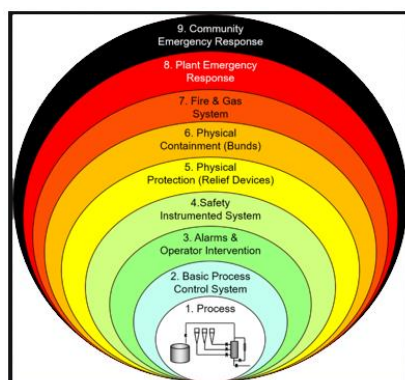


**Fig. 5: Layer of Protection Analysis (LOPA)**

LOPA combines both qualitative and quantitative elements of hazard evaluation and risk assessment to analyze and judge the adequacy of existing or proposed safeguards against process deviations and accident scenarios. A key to the success of LOPA is its rules for judging if protection layers are truly independent. Because of these rules, LOPA helps the analysts make consistent judgments of if the risk of scenarios are “as low as reasonably practical (ALARP)”.



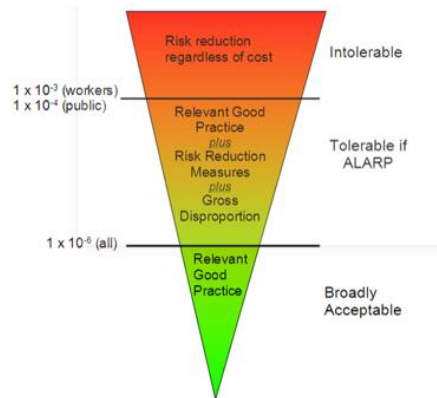


Fig. 6: As Low as Reasonably Practical (ALARP)

### 3. Methodology

In this model, it is assumed that a control system controls some equipment that has associated high-level safety requirements. These high-level requirements generate two types of more detailed safety requirements that apply to the protection system for the equipment:

- Functional safety requirements that define the safety functions of the system
- Safety integrity requirements that define the reliability and availability of the protection system. These are based on the expected usage of the protection system and are intended to ensure that it will work when it is needed. Systems are classified using a safety integrity level (SIL) from 1 to 4. Each SIL level represents a higher level of reliability; the more critical the system, the higher the SIL required.

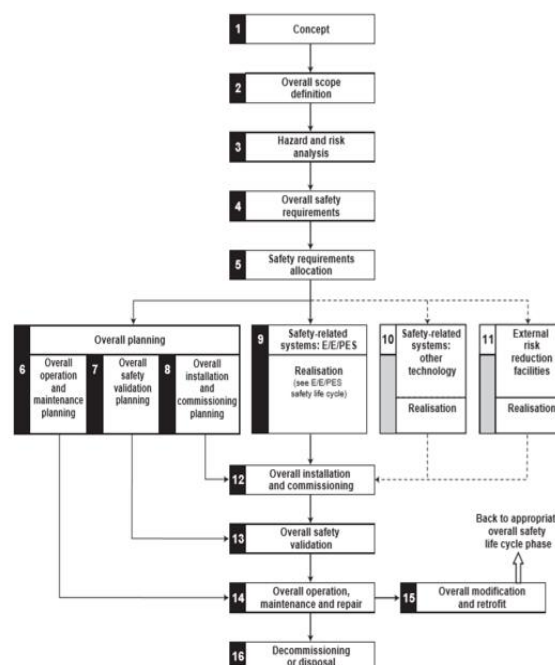


Fig. 7: Safety Life Cycle Based on IEC 61508

The first stages of the IEC 61508 safety life cycle define the scope of the system, assess the potential system hazards and estimate the risks they pose. This is followed by safety requirements specification and the allocation of these safety requirements to different sub-systems. The development activity involves planning and implementation. The safety-critical system itself is designed and implemented, as are related external systems that may provide additional protection. In parallel with this, the safety validation, the installation, and the operation

and maintenance of the system are planned.

#### 4. Verification HIPPS

Overall safety requirement system HIPPS defined SIL 3

SIF configuration refer to figure 2 HIPPS

$$PFD_{avg} \text{ sensor } (1001) = 1.6206 \times 10^{-4} \text{ (in 1 year)}$$

$$PFD_{avg} \text{ sensor } (2003) = 2.431 \times 10^{-5} \text{ (in 1 year)}$$

$$PFD_{avg} \text{ logic solver} = 5 \times 10^{-4} \text{ (in 1 year)}$$

$$PFD_{avg} \text{ actuator } (1001) = 9.417 \times 10^{-4} \text{ (in 1 year)}$$

$$PFD_{avg} \text{ actuator } (1002) = 4.743 \times 10^{-5} \text{ (in 1 year)}$$

$$PFD_{avg} \text{ valve } (1001) = 4.038 \times 10^{-8} \text{ (in 1 year)}$$

$$PFD_{avg} \text{ valve } (1002) = 2.02 \times 10^{-9} \text{ (in 1 year)}$$

$$\begin{aligned} PFD_{avg} \text{ system} &= PFD_{avg} \text{ sensor} + PFD_{avg} \text{ logic} + PFD_{avg} \text{ final element} \\ &= 5.243 \times 10^{-4} \text{ (in 1 year)} \end{aligned}$$

This value presented that probability of failure on process will occur once per 5204 years. Therefore, with minimum required system SIL 3 for HIPPS, this configuration meet the requirement that said  $PFD_{avg}$  must be in range  $10^{-4} - 10^{-3}$ . In this study, we can conclude that HIPPS is qualified for SIL 3 as required.

#### 5. Conclusions

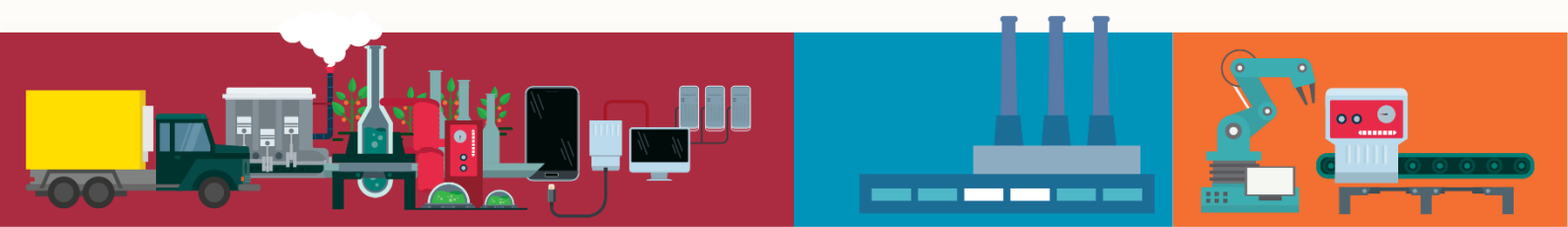
This study is aimed to implement safety integrity level on safety instrumented function based on IEC 61508/61511. In this study, we can conclude that:

- HIPPS met the minimum required SIL 3 because it lays within the determined range.
- To maintain HIPPS consistantly on SIL 3, inspection and test or maintenance activity should be conducted every 3 years align with re-certification program set up by Indonesian Oil & Gas Authority (MIGAS).

#### 6. References

- Marszal, E.M., & Scharpf, E.W. (2002) *Safety Integrity Level Selection: Systematic Methods Including Layer of Protection Analysis*. New York: ISA–The Instrumentation, Systems, and Automation Society
- Gulland, W.G. (2004, Februari) *Methods of Determining Safety Integrity Level (SIL) Requirements - Pros and Cons*. Article posted on *International Symposium on Safety Science and Technology*, Boston: Elsevier.
- Ingre, A., Lerévérend.P (2005) *SIL IEC 61508/61511 Edition 2005, Manual Safety Integrity Level*
- Willey, J.R. (2014, Desember) *Layer of Protection Analysis*. Artikel dipublikasi dalam *The Proceedings of the Safety-Critical Systems Symposium*, London, Springer-Verlag London Ltd.





ISBN 978-623-7525-37-0



9 786237 525370

Organized by:  
Faculty of Industrial Technology, Institut Teknologi Nasional (Itenas) Bandung, West Java Indonesia.